

UNIVERSAL
LIBRARY



119 707

UNIVERSAL
LIBRARY

TRANSACTIONS

OF THE

AMERICAN INSTITUTE OF MINING AND METALLURGICAL ENGINEERS

(INCORPORATED)

Volume 152

INSTITUTE OF METALS DIVISION 1943

PAPERS AND DISCUSSIONS PRESENTED BEFORE THE DIVISION AT MEETINGS HELD AT
CLEVELAND, OCTOBER 12-14, 1942, AND NEW YORK,
FEBRUARY 15-18, 1943

PUBLISHED BY THE INSTITUTE
AT THE OFFICE OF THE SECRETARY
29 WEST 39TH STREET
NEW YORK 18, N. Y.

Notice

This volume is the seventeenth of a series constituting the official proceedings of the Institute of Metals Division of the American Institute of Mining and Metallurgical Engineers. It deals with nonferrous metals and includes papers presented at the Cleveland Meeting, Oct. 12-14, 1942, and the New York Meeting, Feb. 15-18, 1943. The complete list of publications and proceedings, including the present volume, is as follows:

- 1908-1911 *Transactions* of the American Brass Founders' Association: 1908, Vols. 1 and 2; 1909, Vol. 3; 1910, Vol. 4; 1911, Vol. 5.
- 1912-1916 *Transactions* of the American Institute of Metals, Vols. 6-10.
- 1917-1918 *Journal* of the American Institute of Metals, Vols. 11-12.
- 1919-1926 TRANSACTIONS of the American Institute of Mining and Metallurgical Engineers, Volumes 60, 64, 67, 68, 69, 70, 71 and 73.
- 1927-1928 PROCEEDINGS of the Institute of Metals Division of the American Institute of Mining and Metallurgical Engineers, two volumes, of which the later is now designated Vol. 78 of the A. I. M. E. TRANSACTIONS.
- 1929-1943 TRANSACTIONS of the American Institute of Mining and Metallurgical Engineers, Volumes 83, 89, 93, 99, 104, 111, 117, 122, 124, 128, 133, 137, 143, 147 and 152, Institute of Metals Division.

COPYRIGHT, 1943, BY THE
AMERICAN INSTITUTE OF MINING AND METALLURGICAL ENGINEERS
(INCORPORATED)

PRINTED IN THE UNITED STATES OF AMERICA

THE MAPLE PRESS COMPANY YORK, PA.

FOREWORD

This is the thirty-sixth annual volume to contain in one form or another a record of the scientific and technical activity of the Institute of Metals Division, or its parent and grandparent, the American Institute of Metals and American Brass Founders' Association, respectively. On looking through the early volumes, one sees, as in any contemporary representative record of human thought and activity, some pages of considerable importance, others of a trivial nature, and still others reflecting the amusing stupidities and errors of the times. The papers included in the present volume probably fall into similar categories, though to the reader in 1943 they seem all to be of a high calibre and to be either of direct importance to the science and art of metallurgy or to be of secondary but fundamental value as material likely to initiate a productive train of thought in the mind of a receptive reader.

The divisional Program Committee, under the guidance of E. E. Schumacher, Chairman, and E. A. Anderson, Vice-chairman, has done its work well in selecting fields for emphasis, and the Institute's Papers and Publications Committee, under the chairmanship of Dr. A. B. Kinzel until its reorganization in 1942, has exercised its customary care in selecting the best from the papers that were submitted to it.

An increasingly important divisional activity that is not as yet well represented in this volume is the publication of papers given at division symposia; two of which were held in the past year, one on rare metals, organized by Mr. E. M. Wise for the Rare and Precious Metals Committee, which was the high point of the Cleveland meeting, and one on secondary metals held at the New York meeting in February. Some of the papers for the rare metals symposium are included in this volume, and the proceedings of the secondary metals symposium will probably be published *in toto* in the 1944 Transactions.

As in previous volumes of this series, the practical metallurgist will find some papers of immediate use to him, while others, perhaps a majority, will not seem valuable until they are interpreted for him. The eventual practical value of "highbrow" papers is unquestionable, and readers who, owing to the pressure of executive, sales or production duties, have been unable to keep in touch with recent scientific advances should feel that the fraction of their dues that goes into publications is well spent, even though the direct application of some of the research papers to dollars and cents metallurgy is not immediately apparent. It is a professional privilege and a professional duty to support such publications, if for no other reason than that they help to assure the profits of future years, just as today's profits are partly based on similar scientific research and publication of earlier years.

The Annual Lecture of the Division has become an important event in American metallurgical circles. The electron microscope has been known for some years as a potentially useful tool, but it has now reached the thoroughly practical stage where even those who are inexpert in electronics can operate it and get useful information.

FOREWORD

is, therefore, particularly timely to have Dr. Zworykin describe so interestingly some forms of the instrument and show how it may be applied to industrial problems.

With an organization such as ours composed of committees, individuals and groups who need some counsel and much prodding, someone must be responsible for the coordination of their activity. As Chairman one comes more than ever to realize how important are the services of our secretary, Mr. Frank T. Sisco, to the functioning of the Division. The readers of this volume and the authors whose work is included herein should also know their indebtedness to Mr. E. J. Kennedy, Jr., and Miss K. S. Lovell, who see a manuscript safely through the long and occasionally bulk-reducing path between its first receipt and its final appearance in print.

CYRIL STANLEY SMITH, *Chairman*,
Institute of Metals Division.

SANTA FE, NEW MEXICO

July 21, 1943.

CONTENTS

	PAGE
Foreword. By CYRIL STANLEY SMITH	3
A.I.M.E. Officers and Directors.	7
Institute of Metals Division Officers and Committees	8
Annual Award Certificate	10
Institute of Metals Division Lectures and Lecturers	11
Photograph of V. K. Zworykin, Institute of Metals Division Lecturer	12

PAPERS

Institute of Metals Division Lecture

Applications of the Electron Microscope in Metallurgy. By V. K. ZWORYKIN. (<i>Metals Technology</i> , June 1943).	13
--	----

Physical Metallurgy

Phase Diagram of the Copper-iron-silicon System from 90 to 100 Per Cent Copper. By A. G. H. ANDERSEN and A. W. KINGSBURY. (<i>Metals Technology</i> , Sept. 1942).	38
Constitution of the Iron-rich Iron-nickel-silicon Alloys at 600°C. By EARL S. GREINER and ERIC R. JETTE. (<i>Metals Technology</i> , April 1943.) (With discussion)	48
Constitution of Lead-rich Lead-antimony Alloys. By W. S. PELLINI and F. N. RHINES. (<i>Metals Technology</i> , Sept. 1942.) (With discussion)	65
The Hardness of Certain Primary Copper Solid Solutions. By J. H. FRYE, JR. and J. W. CAUM. (<i>Metals Technology</i> , Feb. 1943)	75
Hardness and Lattice Stress in Solid Solutions. By J. H. FRYE, JR., J. W. CAUM and R. M. TRECO. (<i>Metals Technology</i> , April 1943.) (With discussion).	83
Hardening Effects Resulting from the Formation of Both a Precipitate Phase and a Superlattice. By M. R. PICKUS and I. W. PICKUS. (<i>Metals Technology</i> , April 1943.) (With discussion)	94

Copper and Brass

Effect of Certain Fifth-period Elements on Some Properties of High-purity Copper. By J. S. SMART, JR. and A. A. SMITH, JR. (<i>Metals Technology</i> , June 1943.) (With discussion)	103
Internal Friction of an Alpha-brass Crystal. By CLARENCE ZENER. (<i>Metals Technology</i> , Sept. 1942)	122
Effect of Antimony on Some Properties of 70-30 Brass. By DANIEL R. HULL, H. F. SILLIMAN and EARL W. PALMER. (<i>Metals Technology</i> , February 1943.) (With discussion).	127
Hardness Changes Accompanying the Ordering of Beta Brass. By CYRIL STANLEY SMITH. (<i>Metals Technology</i> , Oct. 1942.) (With discussion)	144

Alloys of Aluminum and Magnesium		PAGE
Recent Developments in the Formation of Aluminum and Aluminum Alloys by Powder Metallurgy. By G. D. CREMER and J. J. CORDIANO. (<i>Metals Technology</i> , June 1943.) (With discussion)		
		152
Rate of Precipitation of Silicon from the Solid Solution of Silicon in Aluminum. By LAWRENCE K. JETTER and ROBERT F. MEHL. (<i>Metals Technology</i> , Sept. 1942.) (With discussion)		
		166
Aging in the Solid Solution of Silver in Aluminum. By A. H. GEISLER, C. S. BARRETT and R. F. MEHL. (<i>Metals Technology</i> , Feb. 1943.) (With discussion)		
		182
Mechanism of Precipitation from Solid Solutions of Zinc in Aluminum, Magnesium in Aluminum and of Some Magnesium-base Alloys. By A. H. GEISLER, C. S. BARRETT and R. F. MEHL. (<i>Metals Technology</i> , Feb. 1943.) (With discussion)		
		201
Slip and Twinning in Magnesium Single Crystals at Elevated Temperatures. By P. W. BAKARIAN and C. H. MATHEWSON. (<i>Metals Technology</i> , April 1943.) (With discussion).		
		226
 Miscellaneous Heavy Metals and Alloys		
Preliminary Spectrographic and Metallographic Study of Native Gold. By WELTON J. CROOK. (<i>Metals Technology</i> , Feb. 1939).		
		255
Embrittlement of Silver by Oxygen and Hydrogen. By D. L. MARTIN and E. R. PARKER. (<i>Metals Technology</i> , April 1943.) (With discussion).		
		269
Sulphides in Nickel and Nickel Alloys. By A. M. HALL. (<i>Metals Technology</i> , June 1943.) (With discussion)		
		278
Time-to-fracture Tests on Platinum, 10 Per Cent Iridium-platinum and 10 Per Cent Rhodium-platinum Alloys. By H. E. STAUSS. (<i>Metals Technology</i> , April 1943).		
		286
The Metallurgy of Fillet Wiped Soldered Joints. By E. E. SCHUMACHER, G. M. BOUTON and G. S. PHIPPS. (<i>Metals Technology</i> , Feb. 1943.) (With discussion).		
		291
 Nonferrous Reduction Metallurgy		
New Electrolytic Zinc Plant of the American Zinc Company of Illinois. By L. P. DAVIDSON. (<i>Metals Technology</i> , Aug. 1942.) (With discussion).		
		298
Relative Rates of Reactions Involved in Reduction of Zinc Ores. By E. C. TRUESDALE and R. K. WARING. (<i>Metals Technology</i> , April, 1941.) (With discussion)		
		303
Direct Production of Metallic Zinc by the Electrothermic Process. By GEORGE F. WEATON and CARLETON C. LONG. (<i>Metals Technology</i> , Feb. 1939.) (With discussion).		
		316
Adherence of Electrodeposited Zinc to Aluminum Cathodes. By H. R. HANLEY and CHARLES Y. CLAYTON. (<i>Metals Technology</i> , Oct. 1938)		
		328
An Investigation into Anode-furnace Refining of High-nickel Blister Copper. By FREDERIC BENARD. (<i>Metals Technology</i> , Feb. 1938)		
		336
Recovery of Selenium and Tellurium at Copper Cliff, Ontario. By FREDERIC BENARD. (<i>Metals Technology</i> , Feb. 1938).		
		341
Recovery of Precious Metals and Production of Selenium and Tellurium at Montreal East. By C. W. CLARK and J. H. SCHLOEN. (<i>Metals Technology</i> , Oct. 1938.) (With discussion)		
		350
Index		
		377
Contents of 1943 Iron and Steel Volume		
		383

A.I.M.E. OFFICERS AND DIRECTORS

For the year ending February 1944

PRESIDENT AND DIRECTOR

C. H. MATHEWSON, New Haven, Conn.

PAST PRESIDENTS AND DIRECTORS

JOHN R. SUMAN, Houston, Texas
EUGENE McAULIFFE, Omaha, Nebraska

TREASURER AND DIRECTOR

H. T. HAMILTON, New York, N. Y.

VICE-PRESIDENTS AND DIRECTORS

ERLE V. DAVELER, New York, N. Y.	HARVEY S. MUDD, Los Angeles, Calif.
CHESTER A. FULTON, New York, N. Y.	LEROY SALSICH, Duluth, Minn.
PAUL D. MERICA, New York, N. Y.	L. E. YOUNG, Pittsburgh, Pa.

DIRECTORS

HOLCOMBE J. BROWN, Boston, Mass.	WILBER JUDSON, New York, N. Y.
CHARLES CAMSELL, Ottawa, Ont., Canada	RUSSELL B. PAUL, New York, N. Y.
J. TERRY DUCE, San Francisco, Calif.	LEO F. REINARTZ, Middletown, Ohio
C. A. GARNER, Jeddo, Pa.	FRANCIS A. THOMSON, Butte, Mont.
WILLIAM B. HERoy, Washington, D. C.	J. R. VAN PELT, Jr., Chicago, Ill.
CHARLES H. HERTY, Jr., Bethlehem, Pa.	H. Y. WALKER, New York, N. Y.
O. H. JOHNSON, Denver, Colo.	F. A. WARDLAW, Jr., Salt Lake City, Utah
IRA B. JORALEMON, San Francisco, Calif.	CLYDE E. WILLIAMS, Columbus, Ohio
FELIX E. WORMSER, New York, N. Y.	

SECRETARY

A. B. PARSONS, New York, N. Y.

DIVISION CHAIRMEN—Acting as Advisers to the Board

CYRIL STANLEY SMITH (Institute of Metals), Waterbury, Conn.
C. A. WARNER (Petroleum), Houston, Texas
HERBERT W. GRAHAM (Iron and Steel), Pittsburgh, Pa.
CADWALLADER EVANS, Jr. (Coal), Scranton, Pa.
A. F. GREAVES-WALKER (Education), Washington, D. C.
HOWARD I. SMITH (Industrial Minerals), Washington, D. C.

STAFF IN NEW YORK

Assistant Secretaries
EDWARD H. ROBIE
CHESTER NARAMORE
FRANK T. SISCO
Assistant Treasurer
H. A. MALONEY

Assistant to the Secretary
E. J. KENNEDY, JR.

Business Manager
“Mining and Metallurgy”
WHEELER SPACKMAN

INSTITUTE OF METALS DIVISION

Established as a Division April 26, 1918

(Bylaws published in the 1939 TRANSACTIONS Volume of the Division.)

Officers and Committees for Year ending February 1944

Chairman, CYRIL STANLEY SMITH, Waterbury, Conn.
Past Chairman, CARL E. SWARTZ, Cleveland, Ohio.
Vice-chairman, ARTHUR PHILLIPS, New Haven, Conn.
Vice-chairman, E. E. SCHUMACHER, Murray Hill, N.J.
Treasurer, H. A. MALONEY, New York, N.Y.
Secretary, FRANK T. SISCO, A.I.M.E., 29 W. 39 St., New York, N.Y.

PAST CHAIRMEN

W. M. CORSE, 1918, 1919
W. H. BASSETT, 1920, 1921
W. B. PRICE, 1922, 1923
G. K. ELLIOTT, 1924, 1925
P. D. MERICA, 1926, 1927
S. SKOWRONSKI, 1928, 1929

ZAY JEFFRIES, 1930
SAM TOUR, 1931
C. H. MATHEWSON, 1932
T. S. FULLER, 1933
J. L. CHRISTIE, 1934
W. M. PEIRCE, 1935
E. H. DIX, JR., 1936

A. J. PHILLIPS, 1937
R. F. MEHL, 1938
R. H. LEACH, 1939
EDMUND M. WISE, 1940
D. K. CRAMPTON, 1941
CARL E. SWARTZ, 1942

Executive Committee

1944
WILLIAM C. ELLIS, New York, N.Y.
ALAN MORRIS, Bridgeport, Conn.
KENT R. VAN HORN, Cleveland, Ohio

1945
C. S. BARRETT, Pittsburgh, Pa.
T. A. WRIGHT, New York, N.Y.
L. L. WYMAN, Schenectady, N.Y.

1946
H. L. BURGHOFF, Waterbury, Conn.
GERALD EDMUNDS, Palmerton, Pa.
A. A. SMITH, JR., Barber, N.J.

Finance

JOHN L. CHRISTIE, *Chairman*
JEROME STRAUSS, *Vice-chairman*
L. W. KEMPF
W. M. PEIRCE
KENT R. VAN HORN

Data Sheet

LYALL ZICKRICK, *Chairman*
F. N. RHINES
GERALD EDMUNDS
CARL E. SWARTZ
KENT R. VAN HORN
E. W. PALMER

Mining and Metallurgy

W. A. DEAN, *Chairman*
B. W. GONSER, *Vice-chairman*
E. O. KIRKENDALL
F. N. RHINES
FRANCES H. CLARK
S. E. MADDIGAN
T. E. KIELGREN
D. O. NOEL
J. S. SMART, JR.

Programs

E. A. ANDERSON, *Chairman*
A. A. SMITH, JR., *Vice-chairman*

J. D. HANAWALT
W. A. JOHNSON
T. A. READ

F. N. RHINES
GEORGE SACHS

A. U. SEYBOLT
D. W. SMITH
CARL E. SWARTZ

Publications

E. E. SCHUMACHER, *Chairman*
E. A. ANDERSON, *Vice-chairman*

O. B. J. FRASER
E. W. PALMER

ARTHUR PHILLIPS

G. M. ROLLASON
A. A. SMITH, JR.

Membership

J. S. SMART, JR., *Chairman*
A. G. ZIMA, *Vice-chairman*

J. F. CERNES
MORRIS COHEN
J. B. CUNNINGHAM
H. I. DIXON
GERALD EDMUNDS
F. R. HENSEL

W. R. HIBBARD
W. D. HOLLAND
R. R. HULTGREN
T. C. JARRETT
K. V. KING
E. O. KIRKENDALL
S. P. LINDAU

C. R. LOW
A. S. NICHOLS
J. F. OESTERLE
A. U. SEYBOLT
E. N. SKINNER, JR.
D. W. SMITH

Rare and Precious Metals

E. M. WISE, *Chairman*
C. B. SAWYER, *Vice-chairman*

P. H. BRACE
F. E. CARTER
G. H. CHAMBERS

FRANCES H. CLARK
F. R. HENSEL
G. M. HICKEY
C. M. HOKE

HANS OSBORG
A. J. PHILLIPS
C. H. SAMANS

Annual Lecture

ARTHUR PHILLIPS, *Chairman*
R. F. MEHL, *Vice-chairman*

E. H. DIX, JR.

LOUIS JORDAN
J. T. NORTON

CARL E. SWARTZ

Annual Award

L. W. KEMPF, *Chairman*
E. E. SCHUMACHER, *Vice-chairman*

R. M. BRICK

A. B. GRENINGER
A. J. PHILLIPS

C. S. SMITH

Nominating

CARL E. SWARTZ, *Chairman*
E. M. WISE, *Vice-chairman*

R. F. MEHL

A. J. PHILLIPS

W. M. PEIRCE

ANNUAL AWARD CERTIFICATE OF THE INSTITUTE OF METALS DIVISION

In 1933, the Institute of Metals Division of the American Institute of Mining and Metallurgical Engineers established its annual award of an engraved certificate to the author or authors of the paper that in the opinion of the award committee represents the most notable contribution to metallurgical science among the papers that have been accepted by the Division for presentation at one of its meetings and have been published by the Institute within the three years preceding the date of award. The award is made by the Division each February. There are no restrictions with respect to nationality, age or occupation of the author or authors.

Awards have been made as follows:

- 1934 Robert F. Mehl and Charles S. Barrett: Studies upon the Widmanstätten Structure, I—Introduction. The Aluminum-silver System and the Copper-silicon System. TRANSACTIONS (1931) 93, 78-110.
- 1935 E. A. Anderson, M. L. Fuller, R. L. Wilcox and J. L. Rodda: The High-zinc Region of the Copper-zinc Phase Equilibrium Diagram. TRANSACTIONS (1934) 111, 264-292.
- 1936 Cyril S. Smith and W. Earl Lindlief: A Micrographic Study of the Decomposition of the Beta Phase in the Copper-aluminum System. TRANSACTIONS (1933) 104, 69-105.
- 1937 Arthur Phillips and R. M. Brick: Effect of Quenching Strains on Lattice Parameter and Hardness Values of High-purity Aluminum-copper Alloys. TRANSACTIONS (1934) 111, 94-112.
- 1938 William L. Fink and Dana W. Smith: Age-hardening of Aluminum Alloys, I—Aluminum-copper Alloy. TRANSACTIONS (1936) 122, 284-293.
- 1939 Frederick N. Rhines and Robert F. Mehl: Rates of Diffusion in the Alpha Solid Solutions of Copper. TRANSACTIONS (1938) 128, 185-221.
- 1940 Alden B. Greninger: Martensite Transformation in Beta Copper-aluminum Alloys. TRANSACTIONS (1939) 133, 204-221.
- 1941 S. E. Maddigan and A. I. Blank: Recovery and Recrystallization in Long-time Annealing of 70-30 Brass. TRANSACTIONS (1940) 137, 170-190.
- 1942 F. N. Rhines: A Metallographic Study of Internal Oxidation in the Alpha Solid Solutions of Copper. TRANSACTIONS (1940) 137, 246-288.
- 1943 J. D. Hanawalt, C. E. Nelson and J. A. Peloubet: Corrosion Studies of Magnesium and Its Alloys. TRANSACTIONS (1942) 147, 273-298.

THE INSTITUTE OF METALS LECTURE

An annual lectureship was established in 1921 by the Institute of Metals Division, which has come to be one of the important functions of the Annual Meeting of the Institute. In 1934 the Division established the custom of presenting a certificate to each lecturer.

A number of distinguished men from this country and abroad have served in this lectureship. The roll is quoted below:

- 1922 Colloid Chemistry and Metallurgy. By Wilder D. Bancroft.
- 1923 Solid Solution. By Walter Rosenhain.
- 1924 The Trend in the Science of Metals. By Zay Jeffries.
- 1925 Action of Hot Wall: a Factor of Fundamental Influence on the Rapid Corrosion of Water Tubes and Related to the Segregation in Hot Metals. By Carl Benedicks.
- 1926 The Relation between Metallurgy and Atomic Structure. By Paul D. Foote.
- 1927 Growth of Metallic Crystals. By Cecil H. Desch.
- 1928 Twinning in Metals. By C. H. Mathewson.
- 1929 The Passivity of Metals, and Its Relation to Problems of Corrosion. By Ulick R. Evans.
- 1930 Hard Metal Carbides and Cemented Tungsten Carbide. By S. L. Hoyt.
- 1931 X-ray Determination of Alloy Equilibrium Diagrams. By Arne Westgren.
- 1932 The Age-hardening of Metals. By Paul D. Merica.
- 1933 Present-day Problems in Theoretical Metallurgy. By Georg Masing.
- 1934 Ferromagnetism in Metallic Crystals. By L. W. McKeekhan.
- 1935 Gases in Metals. By C. A. Edwards.
- 1936 Diffusion in Solid Metals. By Robert F. Mehl.
- 1937 Refractories. By R. S. Hutton.
- 1938 The Nature of Metals as Shown by Their Properties under Pressure. By P. W. Bridgman.
- 1939 The Creep of Metals. By D. Hanson.
- 1940 Acceleration of Rate of Corrosion by High Constant Stresses. By Edgar H. Dix, Jr.
- 1941 Some Fundamentals of the Flow and Rupture of Metals. By George Sachs.
- 1942 Notes on the History, Manufacture, and Properties of Wrought Brass. By Wm. Reuben Webster.
- 1943 Applications of the Electron Microscope in Metallurgy. By V. K. Zworykin.



V. K. ZWORYKIN

Institute of Metals Division Lecturer, 1943

Applications of the Electron Microscope in Metallurgy

By V. K. ZWORYKIN*

(Institute of Metals Division Lecture†)

THROUGHOUT its development the science of electronics, like so many other branches of science and industry, has been indebted to the metallurgist. Metallurgy has provided the electronic engineer with conductors to furnish passage for electrons outside of his evacuated tubes; it has developed tungsten and tantalum wires for emitting electrons and various refractory metals and alloys suitable for electrodes, which receive them and guide them within the tube; finally it has supplied ferromagnetic materials both for shielding electronic apparatus from magnetic fields and for forming highly concentrated fields for deflecting electron. Today I hope to show you that electronics has not been altogether ungrateful for this assistance. More specifically, I wish to indicate the role that the electron microscope, a relatively recent product of electronic engineering, is playing even now in the study of metals.

Every metallographer is aware that his standard metallographic microscope will not reveal structural detail involving separations smaller than a certain fraction—at the very best a tenth—of a micron. This limitation, he knows, is a consequence of the fact that the wave length of the light employed for forming the image has this order of magnitude. It is, thus, a property of all light microscopes. To overcome it, a different imaging medium must be

employed. The existence of such a medium became evident when it was demonstrated¹ that electrons were affected by magnetic and electric fields with axial symmetry just as light is affected by glass lenses; these fields, or “electron lenses,” curve the paths of electrons reaching them from an object located on the axis of symmetry in such a manner that, at some distance from the lens, a true image of the object is formed. Furthermore, although a wave length may be ascribed to electron beams just as to light, this wave length is much shorter; for electrons accelerated through a difference of potential of 50 kilovolts, the wave length is only about one hundred-thousandth of that of visible light. Actually, the electron microscopes of today resolve detail one hundred times as fine as light microscopes; if the maximum useful magnification of the latter is taken to be a thousand, that of electron microscopes is one hundred thousand.

THE ELECTRON MICROSCOPE

Since electrons are readily scattered and absorbed by matter, specimens to be observed in the electron microscope must be prepared to be less than one micron in thickness; furthermore, the interior of the microscope must be carefully evacuated to prevent collisions between the electrons and the molecules of the air. Finally, as already mentioned, the lenses are formed by axially symmetric magnetic or electric fields, and not by any material medium such as glass. Apart from these basic differences, the electron microscope closely

* Associate Director, RCA Laboratories, Radio Corporation of America, Princeton, N. J.

† Presented at the New York Meeting, February 1943. Twenty-second Annual Lecture. Manuscript received at the office of the Institute Jan. 11, 1943. Issued in METALS TECHNOLOGY, June 1943.

¹ References are at the end of the paper.

resembles the light microscope in plan, as is brought out by the diagrams in Fig. 1.

Electrons leaving a hot tungsten filament are concentrated, by a condenser lens, on

fluorescent screen, for direct viewing, or on a photographic plate, for permanent record. The image on the plate, in general, is so sharp that an optical enlargement

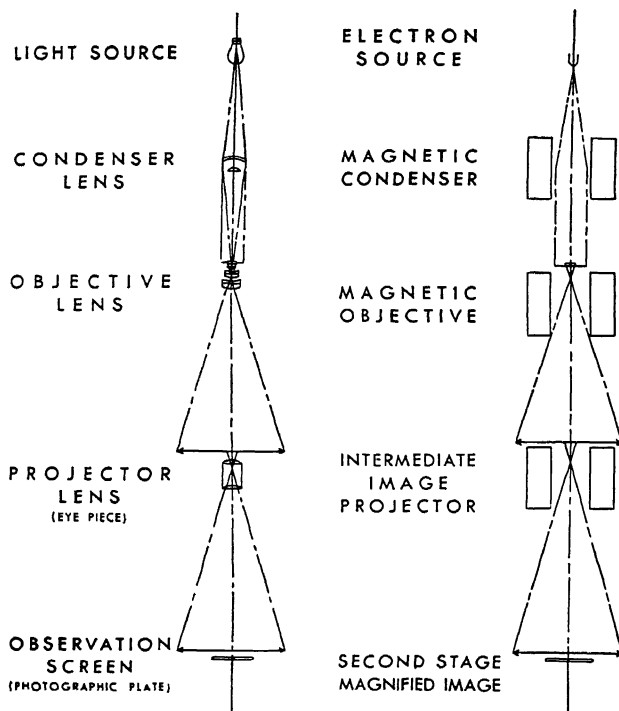


FIG. 1.—COMPARISON OF LIGHT MICROSCOPE AND ELECTRON MICROSCOPE.

the object, placed just above the objective lens. The object scatters these electrons, the degree of scattering depending on the thickness and density of the object portion considered. Only electrons that are either unscattered or deflected but slightly are able to pass through the objective, and thus to contribute to the formation of the intermediate image of the object. The electron density distribution in this image is related to the distribution of mass thickness in the original object. A small central section of the intermediate image, which usually itself has a magnification of the order of one hundred, is magnified by a further, similar, factor by the projector lens, which forms the final image either on a

must be prepared from it to make all of the detail present on it visible to the unaided eye.

The first attempts at realizing instruments of this general character took place about ten years ago. At the present time a degree of performance, compactness, and ease and certainty of operation has been achieved, which make the electron microscope a valuable accessory for any research laboratory. Thus, by now, RCA Electron Microscopes are currently operated in some 50 institutions of widely varying character in the United States alone. The lenses in these instruments—and, in fact, in all electron microscopes achieving very high resolutions—are magnetic, formed by suit-

ably designed pole pieces excited by iron-encased coils. An example of an electrostatic electron microscope with relatively low magnification was recently demonstrated by the General Electric Co. Here the lens action is exercised by the electrostatic fields between apertured electrodes at different potentials.

The RCA electron microscope² is shown in Fig. 2. The instrument as a whole occupies 5 sq. ft. of floor space and is about 7 ft. high. The cabinet in the rear accommodates the transforming, rectifying, and stabilizing equipment for providing the high voltage, as well as the current for heating the filament and for exciting the three magnetic lenses. All the electrical controls of the instrument are mounted on a panel behind the microscope proper and may thus be reached by the observer in a seated position. The microscope is focused by adjusting the objective current, its magnification varied by changing the projector current.

The sectional diagram (Fig. 3) indicates details of construction more clearly. At the top of the instrument is the insulated electron source *A*, to which the high voltage is applied. Sets of adjustment screws permit the perfect alignment of the beam issuing from the source with the optics of the instrument. These are the three magnetic lenses *B*, *C*, and *D*; that is, the condenser, objective, and projector lenses. Between the condenser and the objective is the object chamber. This is provided with an airlock mechanism which permits the introduction of the object, placed in a suitable cartridge, without breaking the vacuum. Just above the projector lens is a small fluorescent screen, on which the intermediate image may be observed through a port in the microscope column. Below the projector lens is the viewing chamber, with six ports for binocular observation of the final image by three persons simultaneously. The fluorescent screen, on which the final image is observed, serves at the same time as a shutter for exposing a

photographic plate placed below it. As for the object, an airlock is provided for the introduction of photographic plates into the instrument without admitting air into the microscope column.

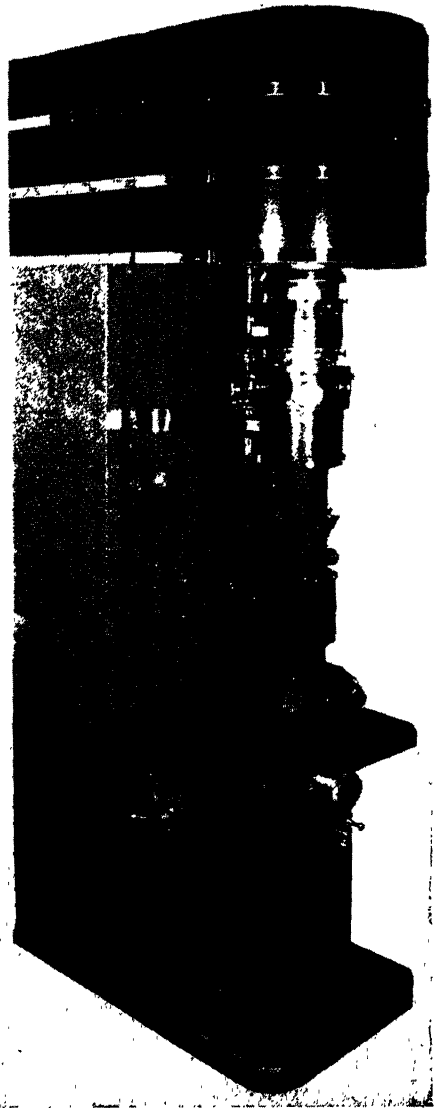


FIG. 2.—RCA ELECTRON MICROSCOPE.

The object, most commonly in the form of a thin film or a suspension placed on a

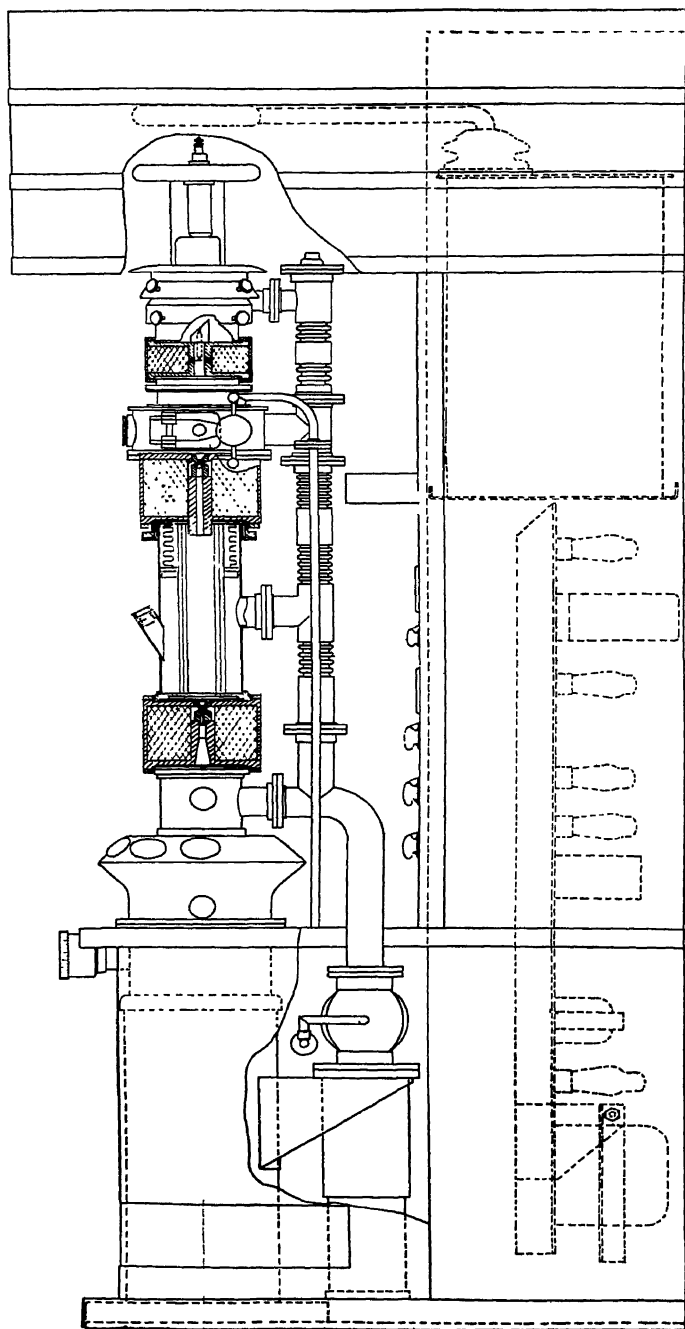


FIG. 3.—SECTION THROUGH RCA ELECTRON MICROSCOPE.

structureless film, is mounted on a disk of fine-mesh wire screen. This disk is inserted in a small cartridge, which may be introduced into the object chamber as shown in

between 20 and 30 Ångstrom units have been demonstrated—but is characterized, in addition, by extraordinary versatility. Thus, with the aid of a special specimen

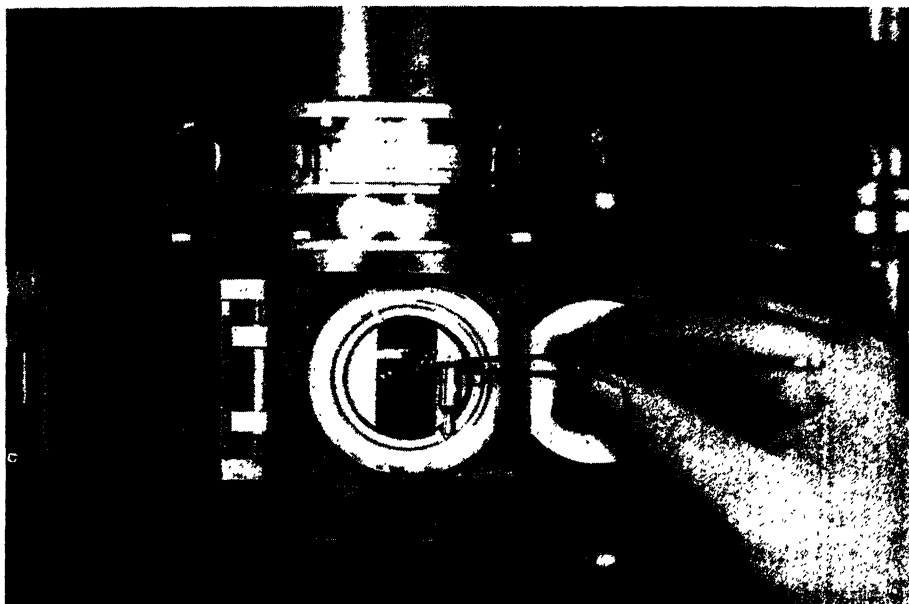


FIG. 4.—INTRODUCING OBJECT CARTRIDGE INTO RCA ELECTRON MICROSCOPE.

Fig. 4. A simple manipulation of the air-lock mechanism brings the specimen into place above the objective lens. Thus the exchange of the specimen need interrupt the process of observation by only about one minute. Similarly, the time required to exchange photographic plates—each of which accommodates a series of pictures—is reduced to a minimum by the application of the airlock principle. The electron-optical magnification of the pictures recorded on the plates can be varied, at an operating voltage of 60 kv., between 1000 and 30,000, the low magnifications permitting convenient comparison with light micrographs of the same specimen.

Versatility of Electron Microscope

The electron microscope described not only excels in performance—resolutions

holder, which tilts the specimen successively in opposite directions with respect to the optic axis, stereomicrographs may be prepared, which, when viewed in an ordinary stereoscope, present a three-dimensional image of the specimen to the eye. Such pictures, revealing the relative depth of different parts of the specimen, are very helpful in interpreting the minute structures observed.

Again, if the standard projector coil is replaced by a special unit, incorporating, in addition to the projector coil, a secondary specimen chamber and a weak focusing lens, the RCA electron microscope may instantly be converted into a high-precision electron diffraction camera.³ The ray paths in the latter are indicated in Fig. 5. The objective lens now serves merely to form an exceedingly fine point source of electrons,

which is imaged by the focusing lens on the fluorescent screen or photographic plate; the projector lens is rendered inactive. All rays diffracted through a fixed angle by the

the crystal, or, with the aid of published tables,⁴ the identity of the compounds composing the specimen. A typical diffraction pattern is that of zinc oxide (Fig. 6). The

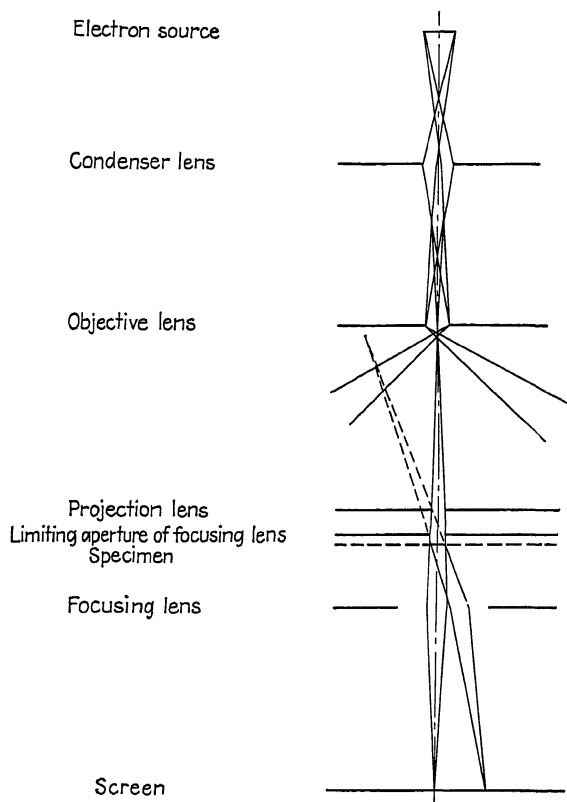


FIG. 5.—RAY DIAGRAM OF RCA ELECTRON MICROSCOPE USED AS DIFFRACTION CAMERA.

crystalline material of the specimen are brought to focus at a different point of the screen. If the microcrystals of the specimen are oriented randomly, the magnitudes of the angles of diffraction, being functions of the lattice spacings in the crystal, take on a series of discrete values, while their directions are random. Thus the luminous points on the screen arrange themselves in circles about the point of incidence of the undiffracted beam. From their diameters the analyst is capable of deducing the shape and dimensions of the elementary cell of

sharpness of the diagram and the stability of the voltage and current supplies are such that an accuracy of measurement of one tenth of one per cent is attained over long periods of time even without recalibration. The specimen holder of the diffraction unit is designed to permit rotation of the specimen both about a normal to its surface and about an axis lying in the surface. It is thus adapted for the study of thick, opaque specimens as well as of those that can be examined directly in the electron microscope. The specimen is then arranged to be

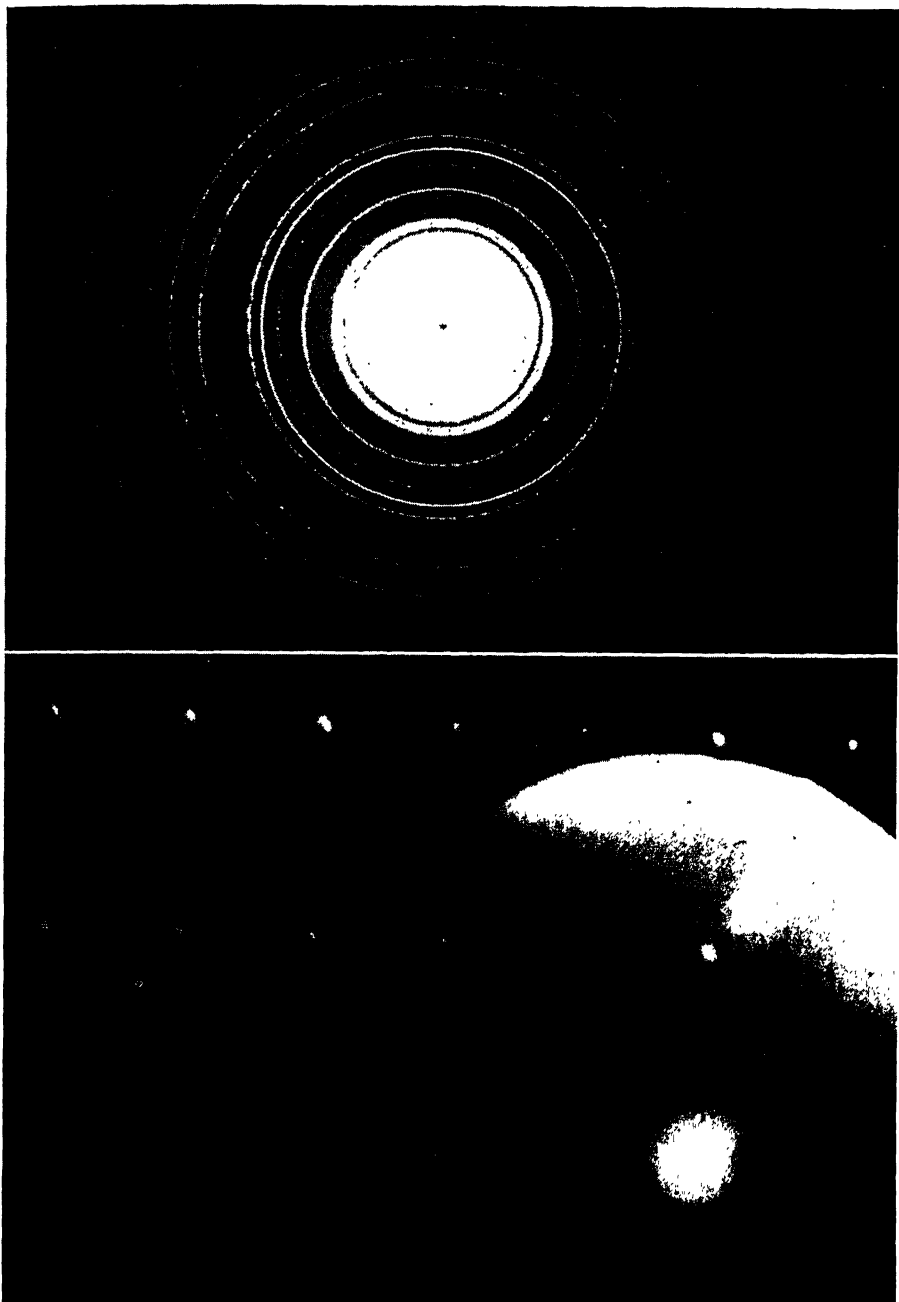


FIG. 6.—DIFFRACTION PATTERN OF ZINC SMOKE (ZnO).
FIG. 7.—DIFFRACTION PATTERN OF SILICON SINGLE CRYSTAL.

struck by the electrons at grazing incidence. The pattern of a single crystal of silicon (Fig. 7) illustrates the results obtained with such specimens.

corresponding quantities of the standard instrument, photomicrographs obtained on fine-grained photographic materials at this relatively low magnification may usefully

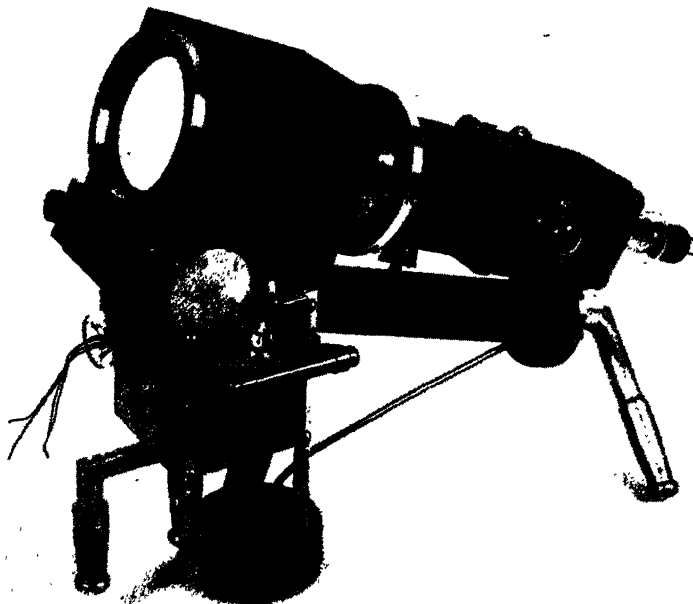
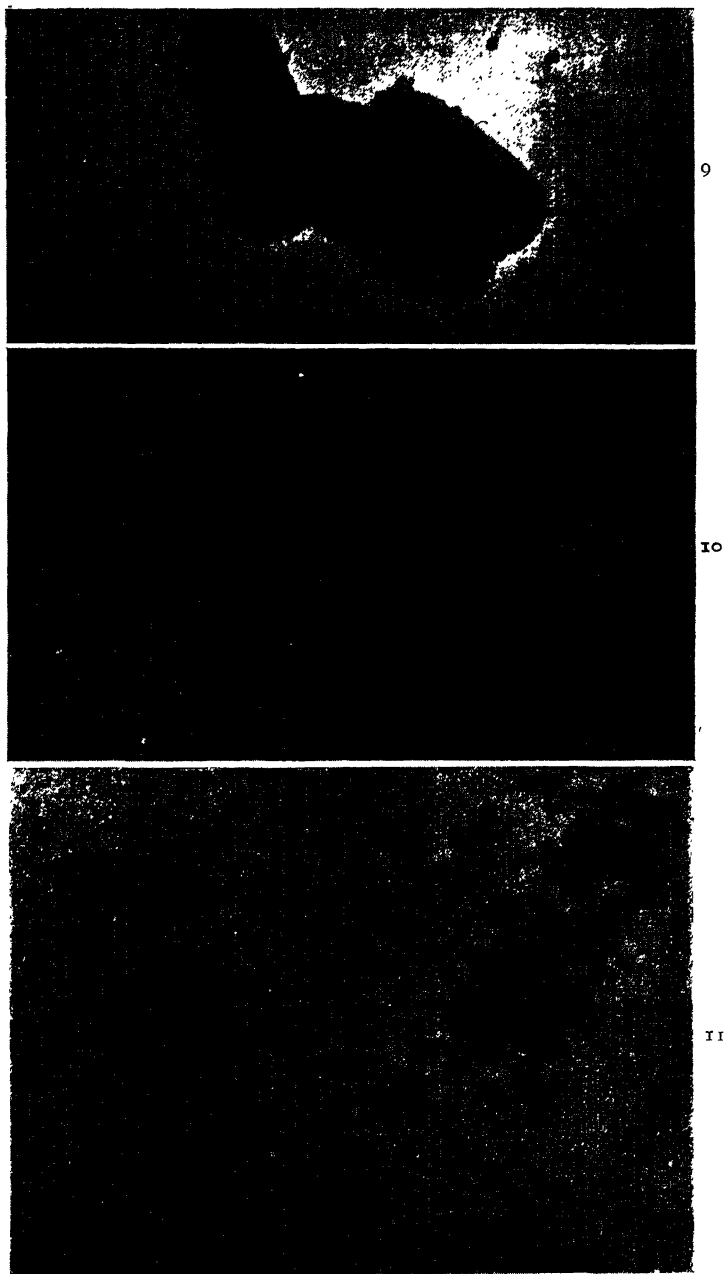


FIG. 8.—SMALL RCA ELECTRON MICROSCOPE.

All these possibilities are of great value to the researcher. Yet there are many fields of application of the electron microscope that require neither these secondary functions of the instrument nor the wide latitude in magnification and operating voltage permitted by the standard design. An extremely compact electron microscope, constructed specifically to meet such purposes, is shown in Fig. 8. The length of the microscope column, which is inclined so as to present to the observer the final image on the transparent viewing screen at a convenient angle, is only 16 in. The objective and projector lenses form part of the same magnetic circuit and are excited by a single coil. The magnification of the instrument is 5000. Since, however, its limiting resolution, and hence its useful magnification, are of the same order as the

be enlarged by a factor of about 20. Lower magnifications than 5000 may be obtained by changing the mechanical setting of the lenses. The operating voltage remains fixed at 30,000 volts. Focusing is accomplished by adjusting the coil current. Since the total volume of the microscope is only about one liter, it can be evacuated in about two minutes, so that no airlocks are required in either the specimen or the photographic chamber. Mounted on a standard desk, the compactness and simplicity of construction of this small electron microscope make it extremely easy to manipulate and render it particularly favorable for routine observations.

The great increase in resolving power attained with the electron microscope was quickly applied by bacteriologists and medical researchers to further their investi-



FIGS. 9-11.—BACTERIOPHAGES AND COLI BACILLI CULTURES.

Fig. 9. In contact 5 minutes. Original magnification 42,000; reduced $\frac{1}{2}$ in reproduction.

Fig. 10. In contact 15 minutes. Original magnification 52,000; reduced $\frac{1}{2}$ in reproduction.

Fig. 11. In contact 24 minutes. Original magnification 34,000; reduced $\frac{1}{2}$ in reproduction.

gations. Innumerable minute organisms and organic reactions, whose existence had been inferred from indirect evidence, became visible. The action of bacterio-

determination of the characteristic shapes and the size distribution of finely divided matter. This plays an important role in all kinds of reagents, catalysts, pigments,



FIG. 12.—ZINC OXIDE SMOKE.
Original magnification 40,000; reduced $\frac{1}{2}$ in reproduction.

phages, bacterial parasites much too small to be seen with the light microscope, on *Coli* bacilli forms a good example. In the first picture (Fig. 9), obtained after five minutes' contact between the bacterial culture and the suspension of bacteriophage, the bacteriophages appear to move up to a group of three bacteria. A few have already attached themselves to the bacterial cells. In the second picture (Fig. 10), after 15 minutes' contact, the cell walls are practically covered with the minute parasites. The last picture (Fig. 11), taken after 24 minutes of interaction between the two cultures, shows two bacterial cells which have been completely disintegrated by the action of the bacteriophages.

In the chemical field, also, the electron microscope has found wide application. It has proved particularly valuable for the

insecticides, drugs, etc. Only rarely are the particles in question large enough to permit a determination of size and shape with the light microscope. The beauty and complexity of these simple "dusts" is well illustrated by the starlike particles of zinc oxide smoke (Fig. 12).

ELECTRON MICROSCOPE IN METALLURGY

Turning to the utilization of the electron microscope in metallurgy, we are confronted by a new difficulty: The typical metallographic specimens are far too thick to be penetrated by either light or electrons. The metallographic light microscope circumvents this difficulty by illuminating the specimen either through the objective or from the side, and utilizing the light reflected by the surface to form the image. The same procedure is possible, in principle,

with the electron microscope (Fig. 13*a*). However, the electrons reflected by the surface are highly inhomogeneous in velocity and hence are incapable of forming

successful with aluminum. The oxide film is formed by anodic oxidation and is removed from the parent metal by immersing the specimen in saturated mercuric chloride

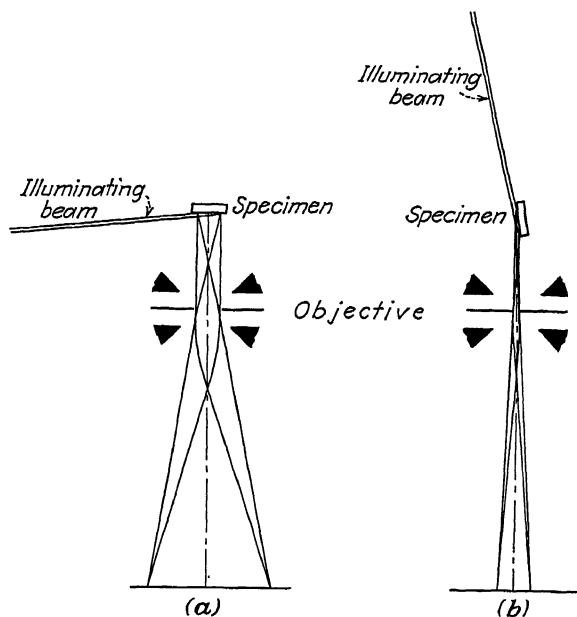


FIG. 13.—OBSERVATION OF SOLID OBJECTS WITH THE AID OF REFLECTED ELECTRONS.

images of great sharpness.⁵ The inhomogeneity of the image-forming electrons can be greatly reduced by placing the specimen at a glancing angle with respect to the illuminating beam and the optic axis of the microscope⁶ (Fig. 13*b*). This leads, however, to greatly distorted pictures and poor resolution in a direction normal to the axis of tilt, so that it, also, presents no satisfactory solution to the electron-microscopic observation of etched metal surfaces.

Such a solution was found, however, in the preparation of thin replicas of the surface which then could be examined directly in the electron microscope. The first suggestion of such a procedure was made by Mahl,⁷ who proposed to form oxide layers on the metal surface, which were then removed by chemically dissolving the metal underneath. This procedure has proved

solution, the film having previously been scratched in several places to admit the solution to the metal. Mahl also formed a thin lacquer film on the aluminum surface and obtained, in this manner, a lacquer film replica after dissolving the aluminum.⁸

Replicas for Observation

While the latter work was in progress, we undertook, at the RCA Laboratories, to develop more general methods for preparing replicas for electron microscope observation, which did not necessitate the destruction of the original specimen.⁵

Silver-collodion Process.—The most successful of these methods was the silver-collodion process. Here a fairly thick layer of silver is evaporated in a vacuum onto the specimen surface. This thick silver layer, with an exact imprint of the surface on one

side, is readily stripped from its base. A drop of collodion solution is permitted to spread over the surface of contact of the silver film. After drying, the latter is immersed in weak nitric acid, which dissolves the silver without attacking the collodion. The remaining collodion film, which constitutes a positive replica of the original surface, may then be washed and examined in the electron microscope.

Formvar Process.—One of the other methods examined consisted in forming a collodion or vinylite film directly on the etched metal surface and removing this mechanically, lifting off first a thickened edge of the film. This technique, which originally gave relatively imperfect negative replicas, was perfected to the point of yielding excellent results by Schaefer and Harker at the laboratories of the General Electric Co.^{10,11} Schaefer and Harker employed polyvinyl formal or "formvar" dissolved in dioxane for forming the replica. They found it essential that the replica be prepared immediately after etching. After the film has been formed on the specimen surface, it may either be stripped off mechanically, with the specimen immersed in water, or by placing a suitable gelatin solution on the surface and drying or freezing the solution. In the second method differential expansion or contraction causes the gelatin, with the replica attached to it, to split off the surface. The gelatin may be removed subsequently by washing the replica in distilled water.

Polystyrene-silica Method.—A method that yields positive replicas of excellent quality is the polystyrene-silica method developed by Heidenreich and Peck¹² of the Dow Chemical Co. laboratories. Here a polystyrene molding of the specimen is prepared, at a temperature of 160°F., in a molding press, pressures between 2000 and 5000 lb. per sq. in. being employed. After cooling the sides of the mold are sawed off and the original specimen is either lifted off or dissolved in acid or caustic. The molded

surface is now exposed to silica evaporating in vacuum from a spiral tungsten filament containing some quartz splinters. Since the silica molecules have the property of migrating readily both on the polystyrene and on the silica that has already been deposited, a uniform silica film is formed on the surface. This may be removed and utilized as a positive replica by dissolving the polystyrene base in ethyl bromide.

Types of Replicas

Before exhibiting some of the results of these replica techniques, a diagram may help to show the relation between the intensity distribution in the image and the actual surface contours (Fig. 14). For convenience of representation it is assumed that the photographic density in the image is proportional, in each case, to the scattering power, or mass per unit area normal to the optic axis, of the replica.

First of all, the oxide-film process of Mahl leads to a replica that we assume at first is everywhere of equal thickness. This gives an image in which level portions of the original surface appear light, whether they are high or low with respect to the mean level of the surface. Sharply sloping surface elements, on the other hand, appear dark. The general appearance of the image is reminiscent, to some degree, of a light photomicrographic negative obtained with oblique illumination. However, since the rate of oxidation for different planes of crystals may vary, the film is not likely to be of uniform thickness in practice. This introduces further differences in density, which makes the interpretation of the picture somewhat more complicated; but if the angles of crystal planes are taken into consideration, the picture gives still more valuable information.

With the positive replica, such as is obtained with the silver-collodion and polystyrene-silica processes, the surface tension of the replica material causes one side of the replica to be flat. The thickness

of the replica and the density of the image in the electron microscope are thus given simply by the height of the surface element in question above some constant level,

and by supplying us with suitable specimens, our own efforts at developing electron microscope techniques in metallurgy.

Fig. 15 shows a silver-collodion replica of

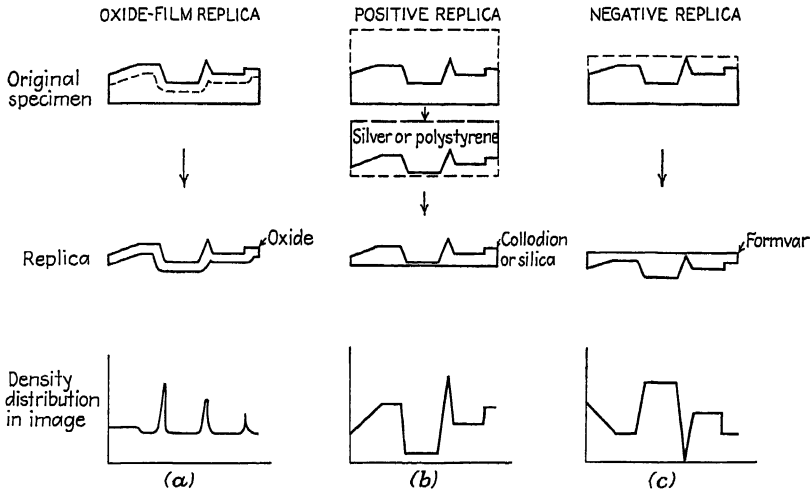


FIG. 14.—THREE TYPES OF SURFACE REPLICAS.

which is determined by the amount of replica material applied to the secondary (silver or polystyrene) surface. Ridges appear dark, valleys light.

The density values in the images obtained with a negative replica, finally, are given, conversely, by the depth of any part of the original surface below some level in space above the specimen. Thus, ridges appear light and valleys dark. On the other hand, the negative obtained with this process closely resembles the positive image obtained with a positive replica.

Metal Specimens

For the electron microscope pictures of metal specimens that follow, I am largely indebted to Mr. Heidenreich, of the Dow Chemical Co.; Mr. Schaefer, of the General Electric Co.; and Dr. Mehl, of the Carnegie Institute of Technology. Dr. Mehl first applied the electron microscope to the study of steels. In addition, he has furthered, from the start, both by his counsel

fine pearlite. A different section of the same specimen shows a region in which the lamellae are largely broken up (Fig. 16). While in both of these pictures the sheets of iron carbide are substantially normal to the plane of the figure, others show them almost parallel to the surface. Fig. 17 shows a polystyrene-silica replica of pearlite that shows some degree of nodulation. A very good example of a pearlite picture, obtained by Dr. Barrett, of the Carnegie Institute of Technology, by Mr. Schaefer's formvar stripping process is shown in Fig. 18.

By examining a very large number of electron photomicrographs of fine pearlite, Dr. Mehl¹³ was able to show that the unresolved structure frequently referred to as nodular troostite consisted, in fact, of lamellar pearlite, the spacings of the lamellae going down to 300 Å.

Negative replica pictures of hardened eutectoid and hypereutectoid steels are shown in Figs. 19 and 20. Bainite tends to exhibit, in the light microscope, a needle-

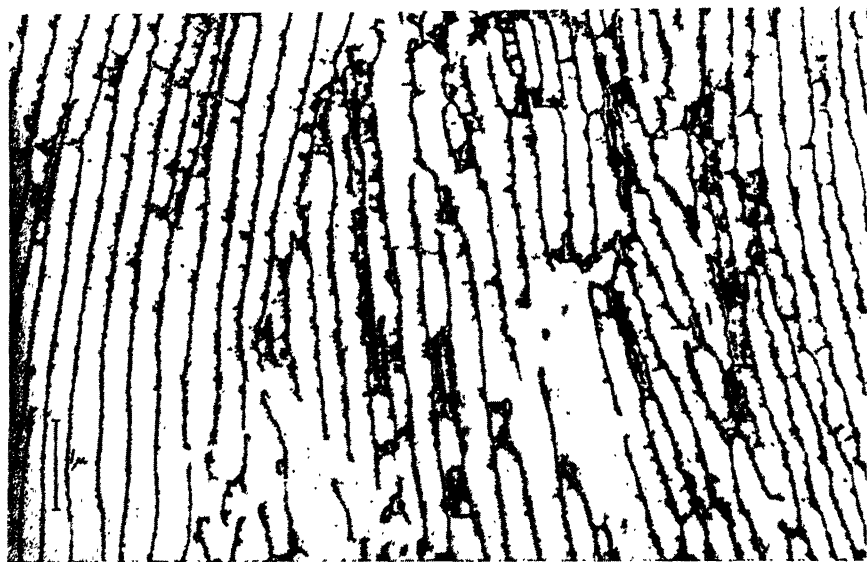


FIG. 15.—FINE PEARLITE, PICRAL ETCH. SILVER-COLLODION REPLICA.

Original magnification 25,000; reduced $\frac{1}{2}$ in reproduction.

Specimen supplied by Dr. R. F. Mehl, Metals Research Laboratory, Carnegie Institute of Technology.



FIG. 16.—FINE PEARLITE. CEMENTITE LAMELLAE LARGELY BROKEN UP. PICRAL ETCH. SILVER-COLLODION REPLICA.

Original magnification 60,000; reduced $\frac{1}{2}$ in reproduction.

Specimen supplied by Dr. R. F. Mehl.

like structure. Two silver-collodion replica micrographs show its appearance in the electron microscope (Figs. 21 and 22).

Turning to nonferrous materials, etched

structure of the metal is clearly outlined. The remaining pictures were almost all prepared by Mr. Heidenreich by the polystyrene-silica method. The first, Fig. 24,



FIG. 17.—PEARLITE, PARTLY SPHEROIDIZED. POLYSTYRENE-SILICA REPLICA.
Original magnification 37,000; reduced $\frac{1}{3}$ in reproduction.
Courtesy of Mr. R. D. Heidenreich, Dow Chemical Co.

aluminum obtained by Mr. Heidenreich from an oxide film by the method devised by Mahl is shown in Fig. 23. The cubic

shows a rolled magnesium-manganese alloy having fine grain size and exhibiting precipitation of manganese. Lines due to

working are also visible. Next, lamellar precipitate in a Dowmetal magnesium-aluminum alloy is shown (Fig. 25). The orientation of the structure may be made

ELECTRON SCANNING MICROSCOPE

Apart from the highly successful replica method, a second procedure has been developed for utilizing the high resolving

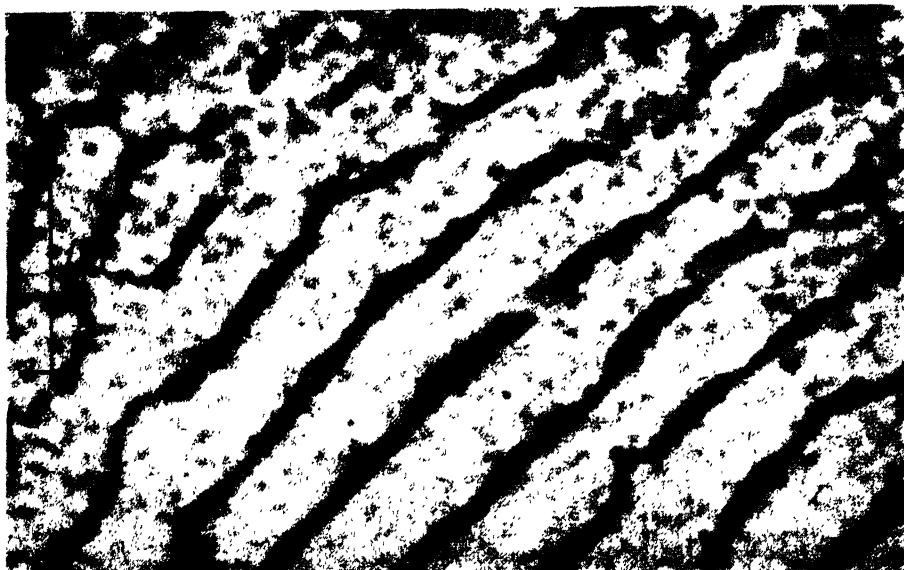


FIG. 18.—PEARLITE. FORMVAR REPLICA. $\times 27,000$.

Courtesy of Dr. C. S. Barrett, Metals Research Laboratory, Carnegie Institute of Technology.

more evident by viewing a stereo pair of pictures, as described earlier. Two fine pictures (Figs. 26 and 27) of aged copper-beryllium alloy show the precipitation of beryllium along the lattice planes of the copper on the one hand and a characteristic etch structure similar to that found in copper and brass, on the other. These alloys were furnished by Dr. Harker, of the General Electric Co. and also were imaged by the formvar negative-replica method (Figs. 28 and 29). The excellent resolution of the polystyrene-silica method is well demonstrated, finally, by a picture of a freshly cleaved calcite surface (Fig. 30). From it Mr. Heidenreich is able to deduce that this method of observing surfaces with the electron microscope is capable of a resolution of at least 50 Å.

power attainable with electrons for the observation of surfaces. This, exemplified by the electron scanning microscope,¹⁰ produces a picture of the surface directly. Briefly, an electron-optical system resembling an inverted electron microscope forms an extremely fine electron probe, which is made to scan the surface to be studied (Fig. 31). Wherever incident, this probe liberates secondary electrons; since their number is a function of the condition of the surface at the point in question, their number may be regarded as a measure of the "brightness" of the surface at that point. These secondary electrons are accelerated toward a fluorescent screen and generate there a light signal, which is reconverted into an electrical signal by the photocathode of an electron multiplier.

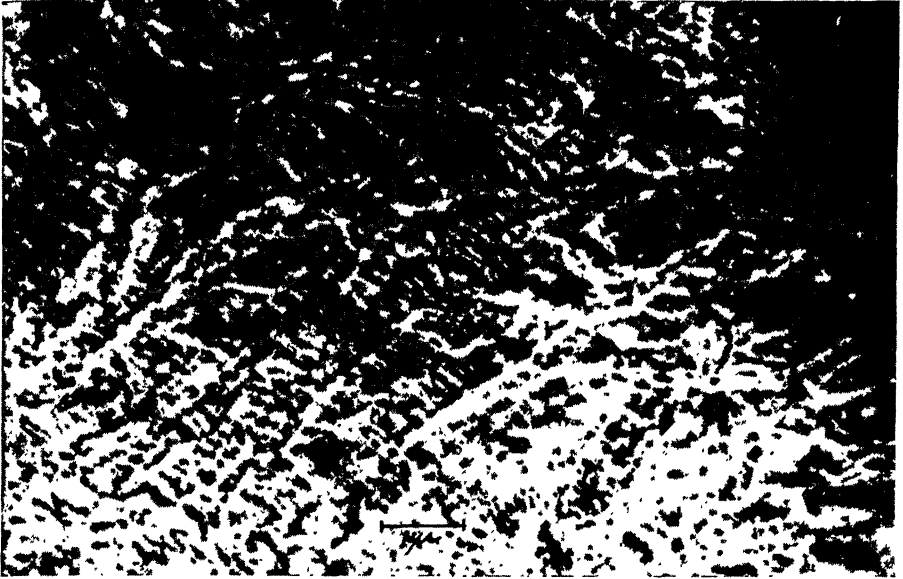


FIG. 19.—WATER-QUENCHED EUTECTOID STEEL. NITAL ETCH. FORMVAR REPLICA.
Original magnification 15,000; reduced $\frac{1}{3}$ in reproduction.
Courtesy of Mr. V. Schaefer, General Electric Co.

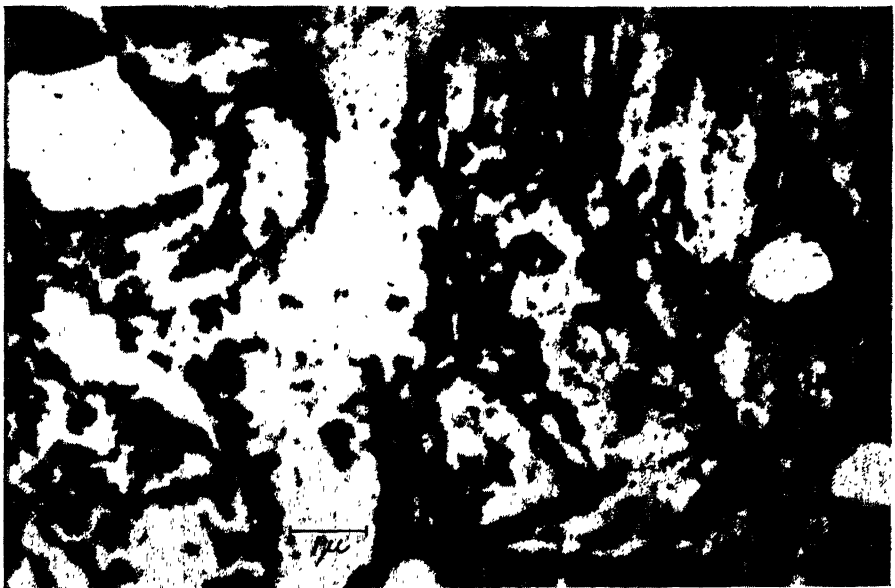


FIG. 20.—WATER-QUENCHED HYPEREUTECTOID STEEL. NITAL ETCH. FORMVAR REPLICA.
Original magnification 14,000; reduced $\frac{1}{3}$ in reproduction.
Courtesy of Mr. V. Schaefer, General Electric Co.

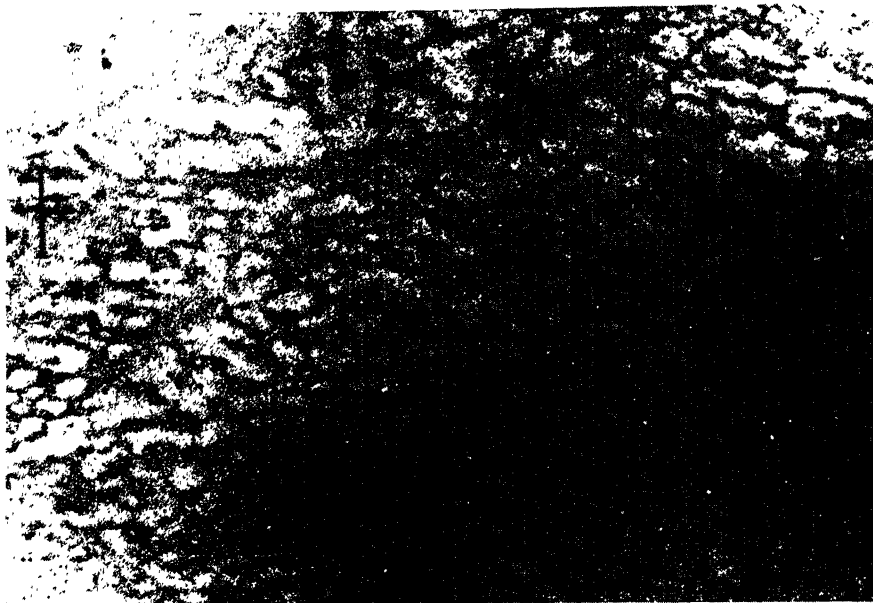


FIG. 21.—BAINITE. SILVER-COLLODION REPLICA.
Original magnification 25,000; reduced $\frac{1}{2}$ in reproduction.
Specimen supplied by Dr. R. F. Mehl.



FIG. 22.—BAINITE. SILVER-COLLODION REPLICA.
Original magnification 28,000; reduced $\frac{1}{2}$ in reproduction.
Specimen supplied by Dr. R. F. Mehl.

Enormously amplified by electronic means, this signal actuates the printer bar of a facsimile receiver in unison with the electron probe scanning the specimen and

visible on the photograph (Fig. 32). Pictures obtained so far with this device exhibit a resolution of 500 Å.—several times better than a light microscope. A



FIG. 23.—ETCHED SHEET ALUMINUM. ALUMINUM OXIDE REPLICA.
Original magnification 25,000; reduced $\frac{1}{2}$ in reproduction.
Courtesy of Mr. R. D. Heidenreich, Dow Chemical Co.

thus prints out a picture of the specimen surface. The time required to record a single micrograph is about 8 minutes. The relatively great complexity of the apparatus results, primarily, from the extreme fineness of the electron probe—it must be only some hundred Ångstrom units in diameter—and the corresponding smallness of the signal currents. Only the use of the electron multiplier as a pre-amplifier and the increase of recording time to several minutes prevent the random voltage fluctuation that occurs in conventional amplifier systems from causing a deterioration of the image.

The complete apparatus, including a power unit, the vacuum chamber and control board, and the facsimile recorder, are

typical example is the photomicrograph of etched, slightly annealed, brass (Fig. 33). The individual scanning lines can barely be discerned. A specimen of somewhat different character is formed by carbonyl iron particles cast in Bakelite (Fig. 34). Although it is to be expected that the resolving power of the scanning microscope will always remain somewhat lower than that of the standard electron microscope, it may perform valuable services in the study of specific objects.

CONCLUSION

It is obvious that I have been able to give you only a glimpse of the role which the electron microscope is now playing in metallurgy. Much of the work is, of neces-



FIG. 24.—MAGNESIUM-MANGANESE ALLOY (DOWMETAL M ALLOY). POLYSTYRENE-SILICA REPLICA.
Original magnification 10,000; reduced $\frac{1}{2}$ in reproduction.
Courtesy of Mr. R. D. Heidenreich, Dow Chemical Co.



FIG. 25.—MAGNESIUM-ALUMINUM ALLOY (DOWMETAL C ALLOY). POLYSTYRENE-SILICA REPLICA.
Original magnification 10,000; reduced $\frac{1}{2}$ in reproduction.
Courtesy of Mr. R. D. Heidenreich, Dow Chemical Co.

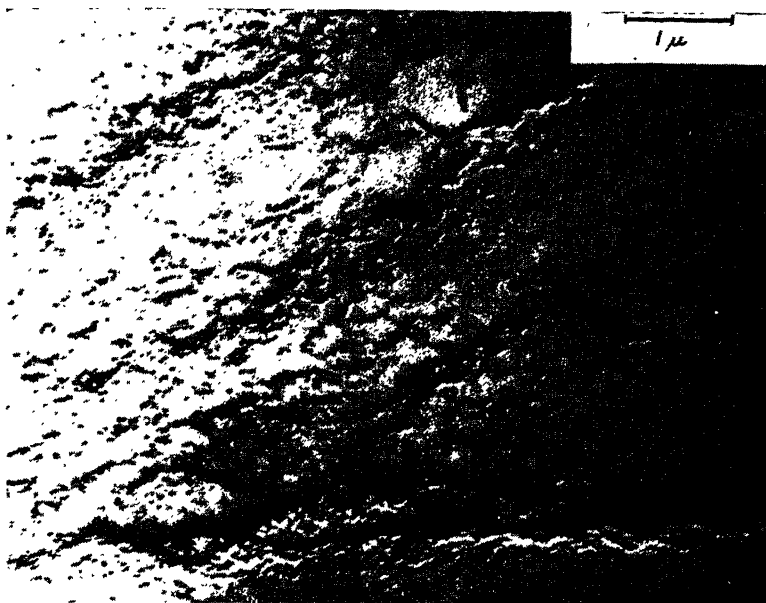


FIG. 26.—COPPER-BERYLLIUM ALLOY. POLYSTYRENE-SILICA REPLICA.
Original magnification 25,000; reduced $\frac{1}{2}$ in reproduction.
Courtesy of Mr. R. D. Heidenreich, Dow Chemical Co.

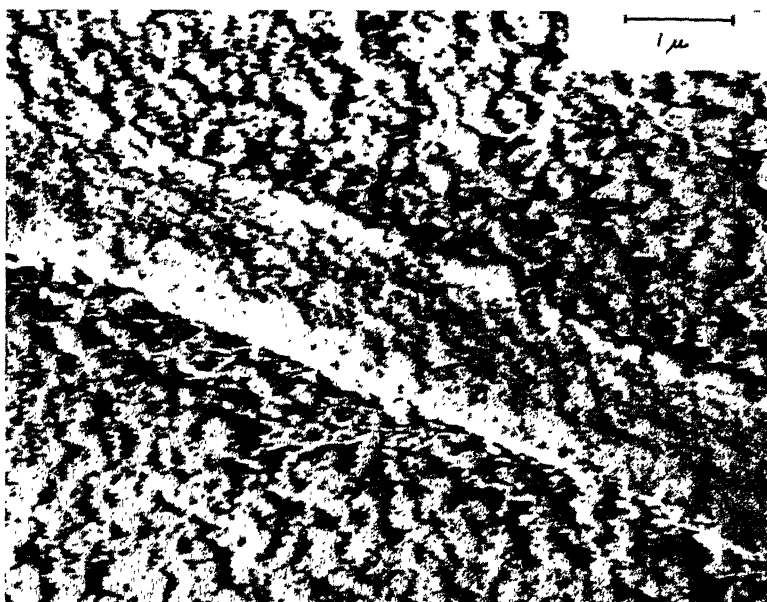


FIG. 27.—COPPER-BERYLLIUM ALLOY. POLYSTYRENE-SILICA REPLICA.
Original magnification 25,000; reduced $\frac{1}{2}$ in reproduction.
Courtesy of Mr. R. D. Heidenreich, Dow Chemical Co.



FIG. 28.—COPPER-BERYLLIUM ALLOY. FORMVAR REPLICA.
Original magnification 14,000; reduced $\frac{1}{3}$ in reproduction.
Courtesy of Mr. V. Schaefer, General Electric Co.



FIG. 29.—COPPER-BERYLLIUM ALLOY. FORMVAR REPLICA.
Courtesy of Mr. V. Schaefer, General Electric Co.

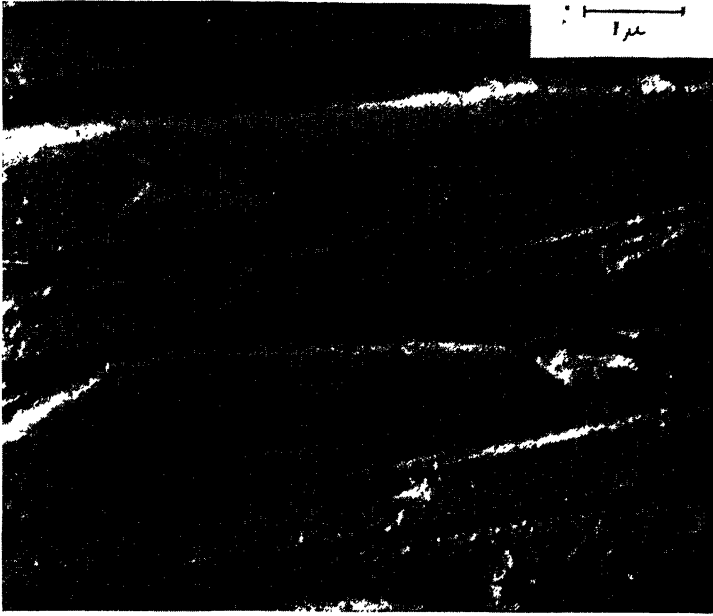


FIG. 30.—FRESHLY CLEAVED CALCITE. POLYSTYRENE-SILICA REPLICA.
Original magnification 24,000; reduced $\frac{1}{2}$ in reproduction.
Courtesy of Mr. R. D. Heidenreich, Dow Chemical Co.

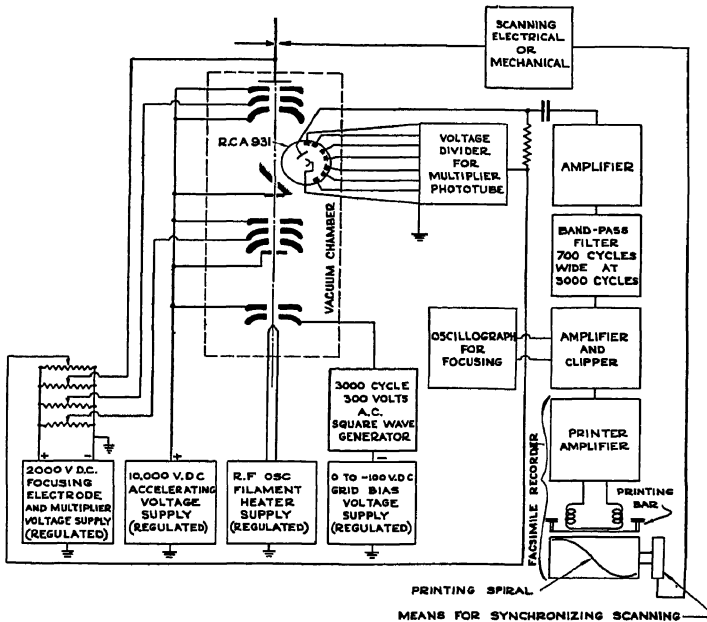


FIG. 31.—SCHEMATIC DIAGRAM OF SCANNING MICROSCOPE FOR SURFACE STUDIES.



FIG. 32.—SCANNING MICROSCOPE FOR SURFACE OBSERVATION.

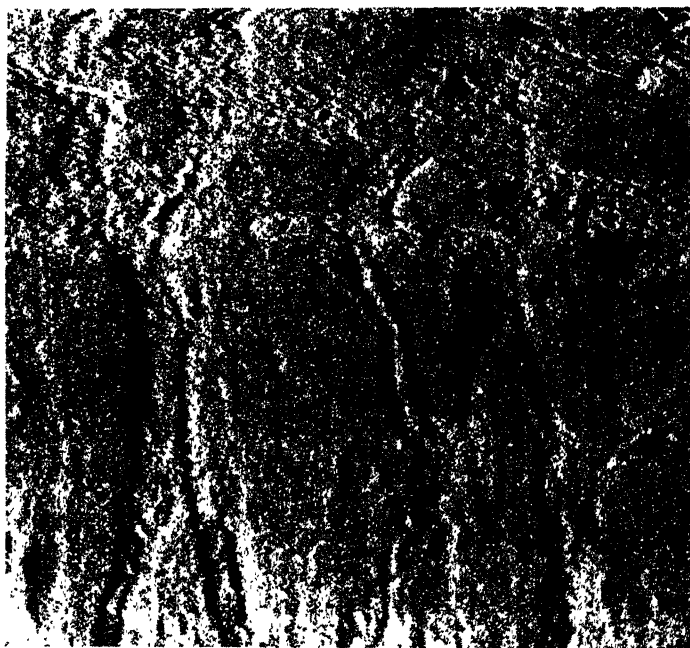


FIG. 33.—SCANNING PHOTOMICROGRAPH OF ETCHED, SLIGHTLY ANNEALED BRASS.
Original magnification 6000; reduced $\frac{1}{2}$ in reproduction.

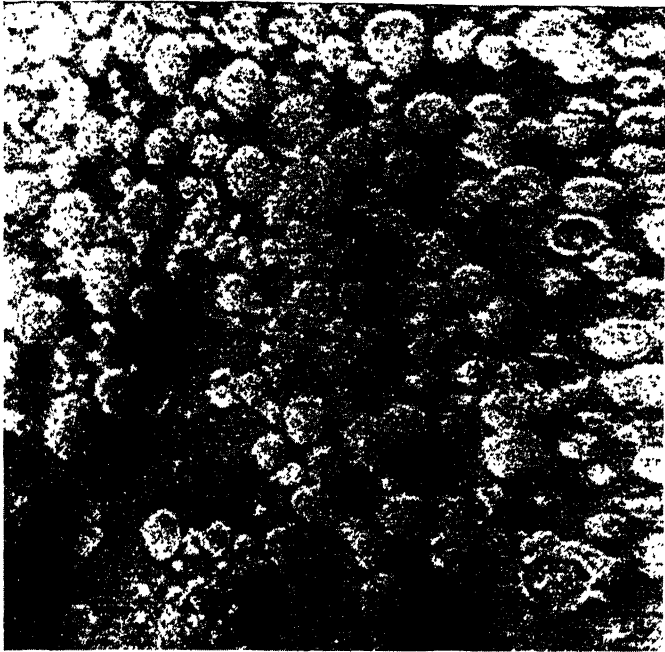


FIG. 34.—SCANNING PHOTOMICROGRAPH OF CARBONYL IRON IN BAKELITE.
Original magnification 6000; reduced $\frac{1}{2}$ in reproduction.

sity, unavailable. There can be no question that valuable techniques have been developed of which we are not even aware. Yet, even the material that has been presented will, I hope, convince you that, in the electron microscope, researchers have acquired a tool that will deepen their insight in the structure, formation, and physical properties of metals and alloys.

ACKNOWLEDGMENTS

The author wishes to acknowledge the part played in this work by Dr. James Hillier and Dr. E. G. Ramberg, of the RCA Laboratories.

REFERENCES

1. H. Busch: On the Operation of the Concentration Coil in the Braun Tube. *Archiv Elektrotechnik* (1927) **18**, 583-594.
2. J. Hillier and A. W. Vance: Recent Developments in the Electron Microscope. *Proc. Inst. Radio Engrs.* (1941) **29**, 167-176.
3. J. Hillier, R. F. Baker and V. K. Zworykin: A Diffraction Adapter for the Electron Microscope. *Jnl. Appl. Phys.* (1942) **13**, 571-577.
4. J. D. Hanawalt, H. W. Rinn and L. K. Frevel: Chemical Analysis by X-ray Diffraction. *Ind. and Eng. Chem. (Anal. Ed.)* (1938) **10**, 457-512.
5. E. Ruska and H. O. Müller: *Ztsch. Phys.* (1940) **116**, 336.
6. B. C. Borries: *Ztsch. Phys.* (1940) **116**, 370.
7. H. Mahl: Metallurgic Studies with the Electrostatic Supermicroscope. *Ztsch. tech. Phys.* (1940) **21**, 17-18.
8. H. Mahl: A Plastic Printing Process for the Study of Metal Surfaces with the Supermicroscope. *Metallwirtschaft* (1940) **19**, 488-491.
9. V. K. Zworykin and E. G. Ramberg: Surface Studies with the Electron Microscope. *Jnl. Appl. Phys.* (1941) **12**, 692-695.
10. V. J. Schaefer and D. Harker: Surface Replicas for Use in the Electron Microscope. *Jnl. Appl. Phys.* (1942) **13**, 427-433.
11. V. J. Schaefer: New Methods for Preparing Surface Replicas for Microscopic Observation. *Phys. Rev.* (1942) **62**, 495-496.
12. R. D. Heidenreich and V. G. Peck: Electron Microscope Study of Surface Structure. *Phys. Rev.* (1942) **62**, 292-293.
13. R. F. Mehl: The Structure and Rate of Formation of Pearlite. *Trans. Amer. Soc. Metals* (1941) **813-862**.

Phase Diagram of the Copper-iron-silicon System from 90 to 100 Per Cent Copper

By A. G. H. ANDERSEN,* MEMBER, AND A. W. KINGSBURY,† JUNIOR MEMBER A.I.M.E.
(Cleveland Meeting, October 1942)

SILICON bronzes containing iron are used to a considerable extent in industry, under the trade name of P.M.G. alloys. Various classes of wrought alloys fall in the composition range 1.5 to 3.5 per cent silicon, and 0.5 to 2.5 per cent iron. Castings may contain as much as 6 per cent silicon and 3 per cent iron at present.

The constitutional diagrams of these alloys are thus of considerable practical importance. Copper-silicon-binary alloys have been thoroughly investigated by a number of workers, the latest reports being those of C. S. Smith¹ and of A. G. H. Andersen.²

Although much work has been done on iron-copper alloys,³ recorded investigations on the copper-rich copper-iron binary constitutional diagram are not numerous. Tammann and Oelsen⁴ determined the solubility limits of iron in copper by means of magnetic measurements, and found that the solubility of iron in copper amounts to a fraction of one per cent at 400°C., increasing slowly to one per cent at 800°C. From 800°C., the solubility increases rapidly and attains 4 per cent at 1100°C.

Hanson and Ford,⁵ using electrical resistivity measurements and the microscope, determined a somewhat different solubility limit.

Of earlier X-ray works on the copper-iron system, very little has been published. The work by Bradley and Goldschmidt⁶ on copper-iron-aluminum alloys includes some information on the copper-iron binary. These investigators conclude that substitution of iron in the copper lattice decreases the spacings, which is contrary to the evidence of the present work.

Hanson and West⁷ have investigated the ternary alloys of copper with iron and silicon. Although their diagrams are valuable contributions to the understanding of these alloys, they did not recognize the kappa phase,^{1,2,7,8} and their diagrams do not everywhere conform to the phase rule.

The present work contains a check by means of X-rays of the solid solubility limit of iron in copper, and an X-ray investigation of the ternary-phase diagram, which, owing to present conditions, it became necessary to curtail considerably.

PREPARATION OF SAMPLES

Castings weighing about 75 grams were melted under vacuum. The charges were made up of ingot iron, copper cathodes from Laurel Hill, and refined silicon supplied by the Electrometallurgical Co. Alundum crucibles were generally used. The exceptions were alloys 77 and 78, which were melted in graphite crucibles. The ingots were annealed at 800°C. for one week, then samples were cut for chemical analysis. Longitudinal sections of the binary alloy ingots were hammered into plates $\frac{1}{8}$ in. thick. Wherever possible, these plates were homogenized at temperatures ensuring

Manuscript received at the office of the Institute Dec. 1, 1941; revised July 1, 1942. Issued in METALS TECHNOLOGY, September 1942.

* Metallurgist, Oakdale, N. Y.

† Research Metallurgist, Phelps Dodge Corporation, Maspeth, N. Y.

¹ References are at the end of the paper.

single-phase alloys. The heat-treatments consisted generally of one to four days heating at 800° to 1025°C., followed by quenching. Powder samples from the annealed and quenched plates were sealed in evacuated silica tubes and heated for periods ranging from 20 days for some of the lower temperatures to a couple of hours for the highest temperatures. Many of the powders sintered after a few hours heating. Small solid samples were then heat-treated at or closely above the final quenching temperature. Powders taken from the quenched solid samples were reheated at the exact final quenching temperature for periods as short as 20 min., in order to relieve any strains caused by filing off the powder. Even after this treatment, it was not possible to get satisfactory photograms above 1000°C.

The ternary alloys were treated in the same way as the binary alloys except that for most of them pretreatments on solid plate before treatment on powders were not used. Identification of phases and measurement of the lattice parameters were made on filings from the alloys wherever possible. However, the reflections of the iron constituents do not register on the photograms unless the iron content amounts to several per cent. Positive identification of the iron phases was made on powders obtained by dissolving away the copper phases of certain alloys having 5 to 6 per cent iron. Filings from the alloys were heated in warm 10 per cent nitric acid overnight. The iron phases were then obtained as relatively insoluble residues. These were heated with hot caustic soda, to remove adhering silica gel, washed and dried.

Chemical Analysis.—Both copper and iron were determined in nearly all alloys, and silicon determinations were made on all ternary alloys. Copper was determined electrolytically, silicon by the perchloric acid evaporation method, and iron volumetrically.

TABLE I.—*Chemical Analysis of Alloys*

Alloy No.	Weight, Per Cent		
	Copper	Silicon	Iron
1	98.64	0.43	0.73
2	97.89	1.54	0.66
3	97.71	0.97	1.32
4	96.82	2.53	0.83
5	97.00	1.93	1.35
6	95.68	3.53	0.81
7	95.54	3.12	1.44
8	95.67	2.53	1.82
9	94.52	4.52	0.95
10	94.88	3.58	1.60
11	94.78	3.10	2.04
12	93.47	5.51	1.05
13	93.90	4.78	1.21
14	92.40	6.47	1.16
15	91.91	7.55	0.48
16	91.92	6.90	1.15
17	92.43	7.06	0.51
25	99.52		0.56
26	98.88		1.08
35	79.70	10.18	10.02
36	98.08		1.94
37	98.41		1.58
38	92.94	5.06	1.93
39	91.95	6.16	1.90
40	92.67	5.17	2.14
41	98.42	0.98	0.61
42	98.35	0.44	1.27
43	97.71	0.41	1.97
44	97.03	1.41	1.52
45	96.25		3.69
46	96.88	0.41	2.65
48	97.10		2.87
50	96.98	2.87	6.15
51	96.40	3.91	5.89
52	89.08	5.01	5.91
53	88.15	5.77	6.18
58	94.50	0.87	4.60
69	93.02	1.86	5.07
70	97.27	2.16	0.53
71	96.68	2.77	0.35
72	96.11	3.71	0.25
73	98.22	0.24	1.55
74	98.10	0.73	1.14
75	97.63		2.39
76	96.72		3.22
77			0.49
78			0.25
79			0.12
80			0.24

X-ray Analysis.—The line patterns of the phases were identified by means of a Debye-Scherrer-type camera of 10-cm. radius, using iron radiation. All the films used for measuring the lattice constant were taken in a focusing camera of high dispersion designed by E. R. Jette. The camera temperature was thermostatically controlled within 1°C. Cobalt-iron radiation was used for the alpha-copper phase, and chromium-iron radiation for the alpha-iron and the FeSi phase. The line spacings were measured to the nearest 0.1 mm. on a glass scale ruled to 1/2-mm. divisions, and

corrected for film shrinkage. Cohen's method^{20,21} of calculation was used. No corrections were made for refraction. The individual lattice-constant measurements

correction for refraction. A value of 3.6077 was obtained in this laboratory in 1938 for the lattice constant of annealed copper at 25°C. This figure was checked recently

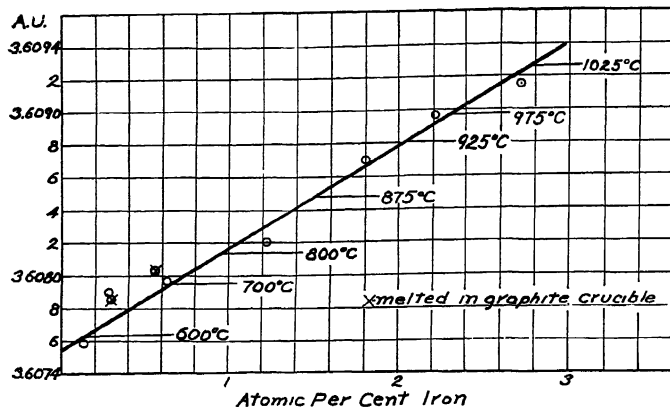


FIG. 1.—LATTICE CONSTANTS OF COPPER-IRON ALLOYS.

of the alloys are probably correct within ± 0.00015 Å. The wave lengths used were those given by Siegbahn in 1933.

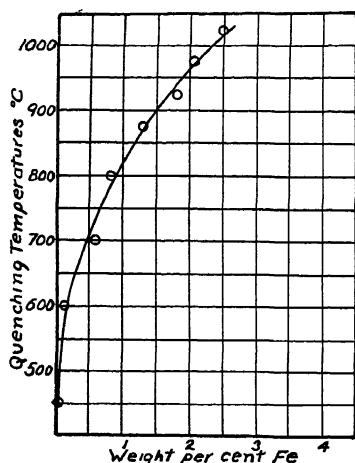


FIG. 2.—SOLUBILITY OF IRON IN COPPER.

Lattice Constant of Copper.—The lattice constant of pure copper has been determined by E. A. Owen and V. W. Rowland.¹⁰ They give $a_0 = 3.60745$ Å. Foote and Jette¹⁹ obtained 3.60778 at 25°C. with a

and a value of 3.6076 Å. obtained. The copper used was P.D.C.P. coalesced bar. One sample was annealed for 20 min. at 800°C. and 100 min. at 600°C., and gave a value of 3.60752 Å. A second sample was annealed at 600°C. for 13 days and gave 3.6077 Å.

Lattice Constants and Solid Solubility of Copper-iron Alloys.—Fig. 1 shows a diagram of the lattice constants as functions of composition in atomic per cent iron. Lattice constants of two-phase alloys are indicated by a horizontal line for each particular temperature, and represent average values from several alloys. The intersections between the horizontal lines and the lattice-parameter line then give the solubility limits at the various temperatures marked on each line. The solubility limits thus determined are given in Fig. 2. The presently determined limit between 1000° and 600°C. runs very close to that determined by Tammann and Oelsen⁴ and deviates somewhat from the limit determined by D. Hanson and G. W. Ford.⁵

Lattice Constants of Ternary Alloys.—Table 2 shows the parameters of the alpha-

TABLE 2.—*Lattice Parameters at 25°C. on Quenched Specimens of Copper-iron-silicon Alloys, Alpha Copper*

Alloy No.	Quenching Temperatures, Deg. C.					
	1025	1000	975	925	875	800
	Lattice Parameters, Å.					
73		3.60882	3.60873 ^a	3.60860	3.6084	
1	3.6080		3.60827		3.60823	
42	3.6081		3.6081	3.60855		3.60844
43	3.60839		3.60816	3.60856		3.60858
74		3.60851	3.6087	3.6090	3.60867	3.60847
41	3.60928		3.6090			3.60855
3	3.6086		3.6090	3.60935		3.60836
44	3.60909		3.60905	3.60905		3.60922
2			3.61007	3.6100	3.60986	3.6100
5	3.61022		3.61028	3.61064	3.61036	3.61069
70			3.6109	3.61101		
4			3.61148	3.61129		3.6112
8						3.61116
71				3.61197	3.61196	3.61154
7						3.61223
11						3.6127
6						3.6129
72				3.61283		

^a Alloys left of the partition line were used for obtaining isoparametric surface.

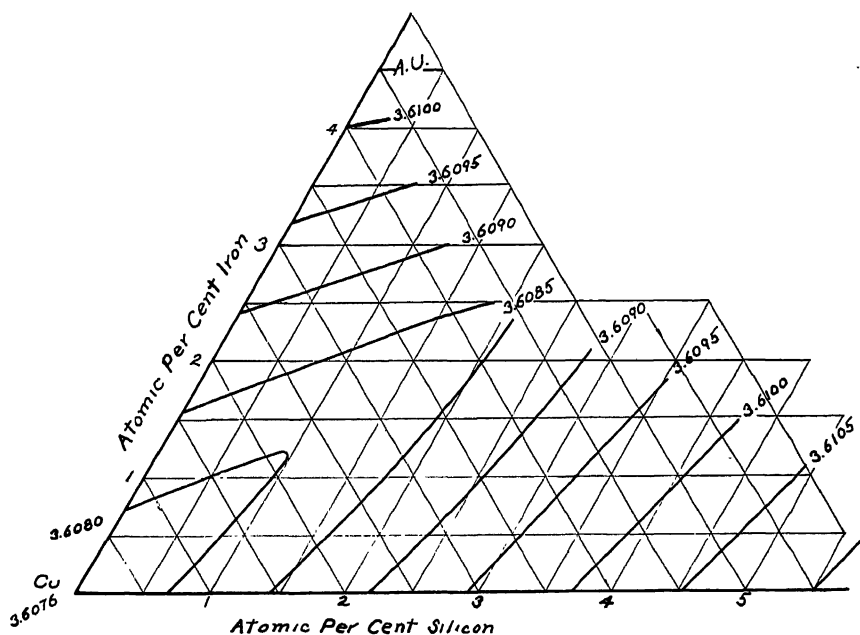


FIG. 3.—LATTICE PARAMETERS OF COPPER-IRON-SILICON ALLOYS.

TABLE 3.—Phases Identified by Diffraction Patterns

Alloy No.	Quenching Temperatures, Deg. C.									
	1025	975	925	900	875	800	700	600	500	400
	Phases									
1	a 2 $\frac{3}{4}$ hr.	a 16 hr. a 16 hr. a 17 hr. a 16 hr.	a 96 hr. a 18 hr. a 18 hr.		a 60 hr. a 168 hr.	a 72 hr. a 200 hr. a 24 hr.	a 72 hr. a 72 hr.	a 60 hr. a 60 hr. a 60 hr.	a 72 hr. a 72 hr.	
2					$a + F$ 96 hr.	$a + F$ 24 hr. a 24 hr.	$a + F$ 24 hr. a 20 hr. a 24 hr.	a 117 hr.		a 51 hr.
3						a 50 hr. $a + k$ 16 hr.	a 24 hr. a 26 hr.	a 67 hr. a 117 hr.	a 44 hr.	a 51 hr.
4	a 1 $\frac{3}{4}$ hr.					a 20 hr. $a + k$ 16 hr.	a 26 hr. $a + k$ 24 hr.	$a + y$ 147 hr. $a + y + kw$ 69 hr.		$a + y + kw$ 66 hr.
5						$a + FeSi$ 115 hr.	$k + y$ 113 hr. $k + y$ 137 hr. $k + k + y$ 50 hr.	$k + y + FeSi$ 142 hr. $a + y$ 147 hr. $k + y + FeSi$ 147 hr.		
6										
7										
8										
9										
10										
11										
12										
13										
14										
15										
17										
35										
38										
39										
41	a 2 hr.	a 99 hr.	a 16 hr.	$a + F$ 72 hr. a 72 hr.						
42	a 4 hr.	a 3 hr.	a	a 168 hr.						
43	a 3 $\frac{1}{2}$ hr.	a 96 hr.	a 114 hr.	$a + Fe$ 72 hr. $a + Fe + FeSi + FeSi_2$ 96 hr.						
44	a^* 2 hr.	a 70 hr.		$a + FeSi + FeSi_2$ 96 hr.						
50				$a + FeSi + FeSi_2$ 96 hr.						
51				$a + FeSi + FeSi_2$ 96 hr.						
52				$a + FeSi + FeSi_2$ 96 hr.						
53				$a + Fe$ 264 hr. $a + Fe$ 264 hr.						
68				$a + Fe$ 264 hr.						
69				$a + Fe$ 264 hr.						
70		a 17 hr. $a + F$ 22 hr.	a 90 hr.							
71										
72		a 72 hr.	a 20 hr.							
73	a^* 16 hr.	a 72 hr.	a 93 hr.							
74	a^* 18 hr.	a 72 hr.	a 143 hr.		a 169 hr. a 171 hr.					

a , alpha copper.
 F , faint unidentified lines.
 k , Kappa phase.

w , weak lines, unstable phase.
 $FeSi$, $FeSi$ phase.
 Fe , solid solution with Fe lattice.

$FeSi_2$, $FeSi_2$ phase.
 γ , gamma phase.
 $*$ 1000 C.

copper lattice measured on the actual alloys. It does not, however, include the results of such measurements on alloys from which acid-treated powder residues were also prepared. The latter are given in Table 3.

Isoparametric Surface.—The isoparametric surface was developed from the data on the copper-iron binary (Fig. 1), the previously published data on the copper-silicon binary² and the data given in Table 2. The general methods used have been described elsewhere.¹¹ Table 2 shows that generally there is a small change in the lattice constants of any alloy with temperature, and that this value tends to become constant at the higher temperatures. The values at the higher temperatures, before a definite change takes place, thus correspond closely to the single-phase lattice constants, and were used as such for obtaining the isoparametric surface. In Table 2 these alloys are indicated on the left side of the partition line.

If the alloy compositions are spotted in on the diagram of Fig. 3, most parameter values fit in within about 2×10^{-4} Å. It may be seen from the isoparametric surface and the manner in which the parameters change with temperature that in the alpha-copper plus alpha-iron region the tie lines must run approximately parallel to the iron-copper axis.

BINARY AND TERNARY PHASES

In Table 3 are listed the phases identified at various temperatures. Many of the alloys in which only the alpha-copper phase was identified undoubtedly also contain one or more of the iron phases, which give very weak or no reflections unless present to an amount of 2 per cent or more. The kappa phase is not stable when found in these alloys at 500°C. and 400°C. Although the data presented would indicate a drop in the temperature of the kappa \rightarrow alpha plus gamma horizontal from the temperature of 560°C. in the binary, the

fact that a four-phase equilibrium is involved makes the temperature invariant. The phase fields containing the iron phases were ascertained from powder residues on alloys 68, 69, 50, 51, 52 and 53, as described on page 2 and from alloys of still higher iron content, Nos. 35, 38 and 39, without resorting to isolation of the phases. Parallel identifications were made from the alloys themselves for the copper phase and from the residues for the iron phases. In this manner it was possible not only to identify the phases beyond a doubt, but also to determine the lattice parameters of both phases in binary fields, and of all three phases in a ternary field.

TABLE 4.—*Determination of Conjugate Lattice Constants in Binary and Ternary Fields*

Alloy No.	Cu, CoFe Radiation	Fe, CrFe Radiation	FeSi, CrFe Radiation	FeSi ₂ , CrFe Radiation
11 days at 500°C.				
68	3.60763	2.83045	None	None
69	3.60873	2.82067	None	None
50	3.60943	2.81914	None or faint	None
51	3.61027	2.81842	4.47828	None
52	3.61128	None	4.47824	None
53	3.61185	Tr.	4.47802	None
4 days at 700°C.				
68	3.60803	2.83140	None	None
69	3.60846	2.82101	None	None
50	3.61045	2.82011	None or faint	None
51	3.61136	2.81846	4.47796	None
52	3.61128	None	4.47825	None
53	3.61183	None	4.47822	None
3 days at 900°C.				
68	3.60825	2.8314	None Tr.	None None
69	3.60898	2.82291		
50	3.6105	2.82070	Very weak Present	Present Present
51	3.6118	2.81815		
52	3.6134	Very weak	4.4791	Present
53	3.6130	None		

Table 4 gives a summary of these determinations. It is to be noted that four phases are found in alloys 51 and 52 at 900°C. Unless this is an invariant temperature plane separating two ternary regions, and this is very unlikely, one of the silicide phases is unstable in those cases.

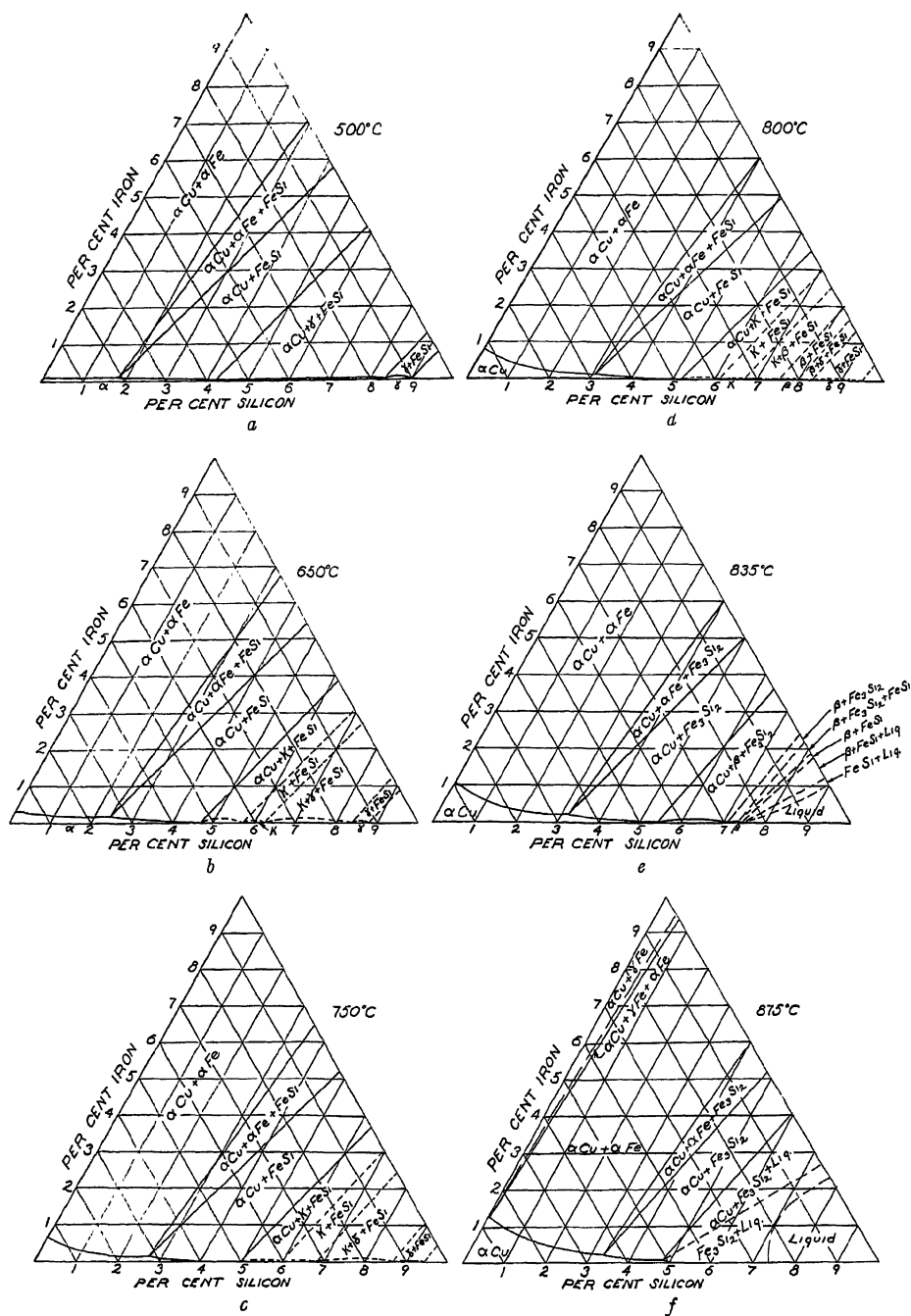


FIG. 4.—ISOTHERMAL SECTIONS OF TERNARY CONSTITUTION DIAGRAMS, WEIGHT PER CENT.

According to Greiner and Jette,¹² the FeSi phase in the iron-silicon binary is unstable between 825° and 1030°C., when the iron-silicon ratio of the alloy is above

sponding pure binary, it is found that considerable changes have taken place, indicating that this phase takes copper in solid solution. At the same time, there is

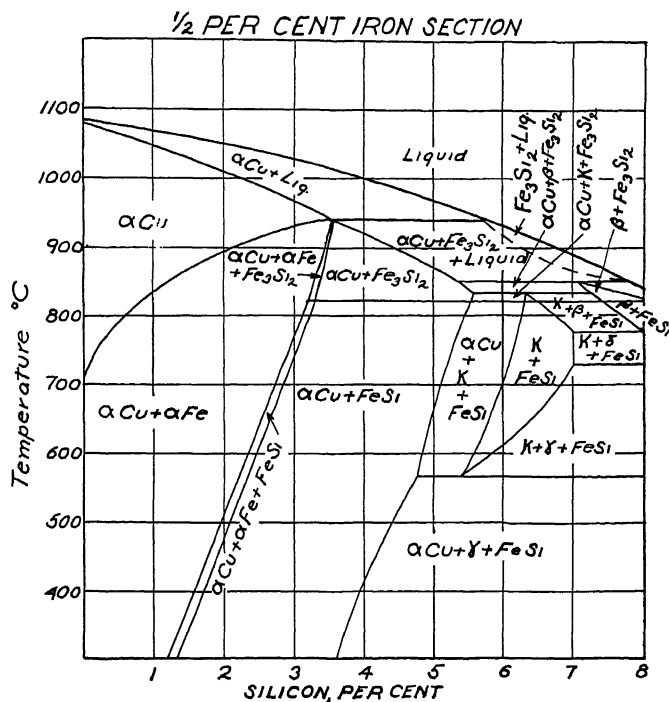


FIG. 5.—COPPER-IRON-SILICON DIAGRAM, WEIGHT PER CENT, $\frac{1}{2}$ PER CENT IRON SECTION.

certain values (6:1 and 4:1 by weight, respectively, for the limiting temperatures); but the FeSi and the Fe₃Si₂ phases coexist in this temperature range when the iron-silicon ratio falls below 4:1. Applying the phase rule and Guertler's principle¹³ in drawing the phase boundary according to these facts, it becomes highly improbable that the FeSi phase is stable in preference to the Fe₃Si₂ phase in alloys 51 and 52 as well as in 53, at 900°C.

The structure of the Fe_3Si_2 phase has never been determined. Its lines therefore are identified by direct comparison with standard films.

In comparing the lattice spacings of the alpha-iron phase with those of the corre-

taking place a change in the lattice spacing of the alpha-copper phase with temperature.

Alloy 51 contains the alpha-iron phase at 500°C., 700°C., and 900°C., in three-phase fields. The lattice constant changes from 2.8185 Å. at 700°C. to 2.8182 Å. at 900°C. In the binary phase, according to Greiner and Jette,¹² the limiting lattice constant of alpha iron at 700°C. is 2.8776 Å. and at 900°C., 2.8133 Å. The lattice constant at 900°C. of the alpha iron in the ternary alloy thus is larger than the corresponding ones in the binary alloys, a fact that hardly can mean anything but that copper has entered into the iron-silicon phase in the ternary alloy. In the two-phase alloys (alpha iron plus alpha

copper), the lattice parameters of the ternary alpha-iron phase decrease sharply with increasing silicon content, as is to be expected from comparison with the behav-

attained and four phases are present. The lattice constant of the binary FeSi phase is given by Wyckoff¹⁴ as 4.467 Å. and in the ternary phase it is of the order of 4.478

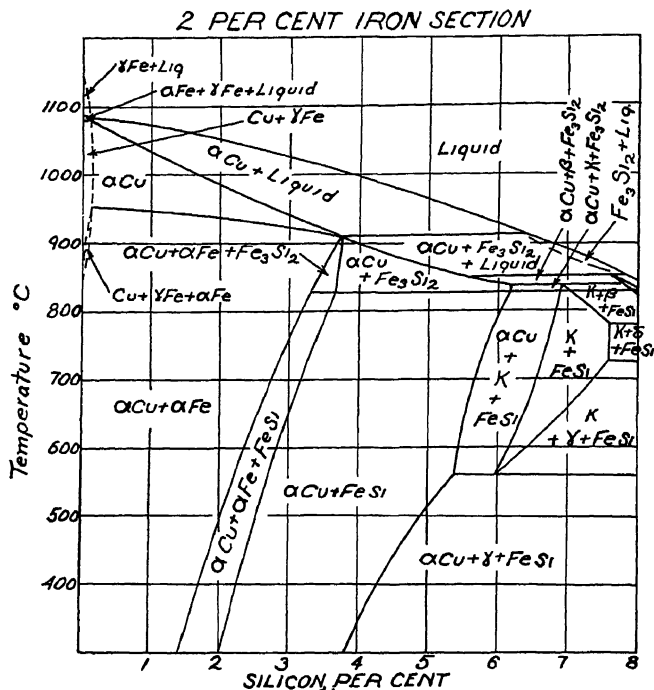


FIG. 6.—COPPER-IRON-SILICON DIAGRAM, WEIGHT PER CENT, 2 PER CENT IRON SECTION.

ior of the corresponding binary phase. In these alloys—Nos. 68, 69 and 50—the lattice constants of the alpha-iron phase in each alloy increases with increasing temperature. Simultaneously, the lattice parameters of the alpha-copper phase increases. Hence, the tie lines in the alpha-copper plus alpha-iron field in the environment of these alloys undergo a counterclockwise rotation as the temperature increases. Moreover, the density of alloys in this range must simultaneously decrease, since there is an increase in the atomic volumes of both coexisting phases. In the three-phase alloy No. 51, the lattice parameter of the FeSi phase remains virtually unchanged between 500° and 700°C. At 900°C., equilibrium was not

attained and four phases are present. The lattice constant of the binary FeSi phase is given by Wyckoff¹⁴ as 4.467 Å. and in the ternary phase it is of the order of 4.478

Å. The latter is essentially the same value as that given by Phragmén,¹⁸ and accordingly FeSi probably does not take up considerable amounts of copper. Thus, though dimensionally small, profound changes are taking place in these alloys upon heating and cooling, with changes in densities of the phases which can be estimated from the changes in the compositions of phases and their lattice spacings.

PHASE DIAGRAMS

From the data presented, a number of isothermic sections of the ternary-phase diagram have been prepared (Fig. 4). Use has been made as far as possible of the methods described by Andersen and

Jette.¹⁵ Few lattice-parameter measurements below 800°C. were obtained, since conditions made it necessary to curtail the work. Thus, excepting the limiting binaries, the diagrams (Figs. 5 and 6) were drawn up relying mainly on phase identifications in combination with Guertler's principle,¹³ although some guidance was obtained from the measured lattice constants. All included information on the liquid-phase boundaries was obtained from the work of Hanson and West⁹ on the ternary diagram, and that of Smith^{1,16,17} on the copper-silicon binary. It is to be remembered that there is a $\alpha\text{Fe} \rightleftharpoons \gamma\text{Fe}$ reaction taking place in the iron-silicon binary and in the copper-iron binary. In alloy No. 68, however, no evidence was found of the presence of gamma iron, which probably therefore does not exist in ternary alloys of more than 1 per cent silicon. On one of the diagrams such reactions in the ternary have been tentatively indicated by broken lines.

ACKNOWLEDGMENT

The authors wish to express their thanks to the executives of the Phelps Dodge Corporation for permission to have this work published. They are indebted to Mr. William H. Osborn, Director of the Phelps Dodge Research Laboratory, and his staff for continuous collaboration. Thanks are due to Dr. S. B. Tuwiner and Mr. W. Upchurch for the chemical analysis of the samples. Mr. J. S. Marsh has kindly discussed the diagrams, and given valuable suggestions.

REFERENCES

1. C. S. Smith: Constitution and Microstructure of Silicon-copper Alloys. *Trans. A.I.M.E.* (1940) **137**, 31.

2. A. G. H. Andersen: The Alpha-solubility Limit and the First Intermediary Phase in the Copper-silicon System. *Trans. A.I.M.E.* (1940) **137**, 333.
3. J. L. Gregg and B. N. Daniloff: The Alloys of Iron and Copper. Eng. Foundation *Monograph*, 1934. McGraw-Hill Book Co. New York.
4. Tammann and Oelsen: Dependence of Concentration of Saturated Mixed Crystals on Temperature. *Zisch. anorg. Chem.* (1930) **186**, 257.
5. D. Hanson and G. W. Ford: Effect of Iron on Copper. *Jnl. Inst. Metals* (1924) **32**, 335.
6. A. F. Bradley and H. F. Goldschmidt: X-Ray Study of Slowly Cooled Iron-Copper Aluminum Alloys. *Jnl. Inst. Metals* (1939) **65**, 384.
7. T. Isawa: On the Constitutional Diagram of the Copper-rich Copper-silicon Alloys. *Nippon Kinzoku, Gakukai-Si* (Aug. 2, 1938) **2**, 400. Abst. in *Metals and Alloys* (Jan. 1939) **10** MA 50.
8. M. Okamoto: On the Kappa Phase Adjacent to the Alpha Phase in the Copper-silicon System. *Sci. Repts. Tohoku Imp. Univ.* (1938) **27** (1), 155.
9. D. Hanson and E. G. West: The Constitution of Copper-Iron-Silicon Alloys. *Jnl. Inst. Metals* (1934) **54**, 229.
10. E. A. Owen and V. W. Rowland. *Jnl. Inst. Metals* (1940) **66**, 361.
11. A. G. H. Andersen and E. R. Jette: X-Ray Investigation of the Iron-Chromium-Silicon Phase Diagram. *Trans. Amer. Soc. for Metals* (1936) **24**, 375.
12. E. S. Greiner and E. R. Jette: X-ray Study on Constitution of Iron-silicon Alloys. *Trans. A.I.M.E.* (1937) **125**, 473.
13. W. Guertler: Zur Fortentwicklung der Konstitutionsforschungen bei Ternaren Systemen. *Zisch. anorg. allg. Chem.* (1926) **154**, 439.
14. R. W. G. Wyckoff: The Structure of Crystals. Amer. Chem. Soc. *Monograph*, 2d Ed. New York, 1931. Chem. Catalog Co.
15. A. G. H. Andersen and E. R. Jette: X-Ray Methods for Ternary Systems. Amer. Soc. for Metals (1936) **24**, 519.
16. C. S. Smith: The Constitution of the Copper-silicon System. *Trans. A.I.M.E.*, (1929) **83**, 414.
17. C. S. Smith: The Alpha-Phase Boundary of the Copper-Silicon System. *Jnl. Inst. Metals* (1928) **40**, 359.
18. G. J. Phragmén: *Jnl. Iron and Steel Inst.* (1926) **114**, 397.
19. F. Foote and E. R. Jette: *Phys. Rev.* (1940) **58**, 81.
20. M. U. Cohen: *Zisch. Kristallographie* (1936) **94**, 288.
21. F. Foote and E. R. Jette: *Jnl. Chem. Physics* (1935) **3**, 605.

Constitution of the Iron-rich Iron-nickel-silicon Alloys at 600°C.

BY EARL S. GREINER* AND ERIC R. JETTE,† MEMBERS A.I.M.E.

(New York Meeting, February 1943)

ALTHOUGH the mechanical and chemical characteristics of certain iron-nickel-silicon alloys have been investigated,¹ the available literature shows no results of a systematic investigation of the constitution of this system. This paper describes the results of an X-ray investigation of the constitution of the iron-rich iron-nickel-silicon alloys at 600°C. Data on the constitution of the included binary systems obtained in other investigations have been correlated with the structure of the ternary alloys.

Jette and Foote² have presented a tentative constitutional diagram of the iron-nickel system following X-ray studies on quenched specimens. This diagram shows that the alloys at 600°C. containing from zero to approximately 4 atomic per cent nickel consist of a body-centered cubic (alpha) phase, the alloys containing 4 to 24 atomic per cent nickel consist of body-centered cubic (alpha) and face-centered cubic (gamma) phases, and the alloys containing from 24 to 100 atomic per cent nickel consist of a face-centered cubic (gamma) phase. These investigators recognized that it was not possible to retain the gamma phase in equilibrium by quenching alloys containing less than approximately 25 atomic per cent nickel and that high-temperature X-ray methods were

desirable to determine the gamma-phase solubility limit. In a later investigation of the iron-nickel alloys, Owen and Sulley³ determined the alpha-phase solid solubility limit to be 3.5 atomic per cent nickel at 600°C. High-temperature X-ray methods showed the solid solubility limit of the gamma phase to be 14 atomic per cent nickel at 600°C. Since the high-temperature X-ray method should reveal equilibrium conditions in these alloys better than the quench method of other investigators, the results of Owen and Sulley pertaining to the gamma-phase boundary are to be preferred.

As the result of an X-ray investigation of quenched iron-silicon alloys, Greiner and Jette⁴ have shown these materials to consist of a body-centered cubic (alpha) phase containing from 0 to 26.4 atomic per cent silicon at 600°C. The alloys containing from 26.4 to approximately 50 atomic per cent silicon consist of two phases at 600°C.; namely, alpha and eta. The eta phase corresponds to the stoichiometrical formula FeSi (33.4 wt. per cent Si).*

The literature pertaining to the constitution of the nickel-silicon alloys has been reviewed by Ackerman,⁵ who found disagreements in the results of various investigators on several parts of the system. Subsequent data on the constitution of the nickel-silicon alloys were reported by Osawa and Okamoto.⁶

Manuscript received at the office of the Institute Dec. 1, 1942. Issued in METALS TECHNOLOGY, April 1943.

* Graduate student in Metallurgy, Columbia University, New York, N. Y.

† Professor of Metallurgy, Columbia University, N. Y.

¹ References are at the end of the paper.

* The phase corresponding to the formula FeSi₂ (25.1 wt. per cent Si) was found to be unstable below 825°C.

TABLE I.—Composition, Heat-treatment and X-ray Data on Alloys

Alloy No.	Location of Alloy in Ternary Plot, Area No.	Fe, Wt. Per Cent	Ni, Wt. Per Cent	Si, Wt. Per Cent	Ni, At. Per Cent	Si, At. Per Cent	Temperature of Heating, Deg. C.	Period of Heating, Days Except Where Noted	Lattice Constant of Alpha Phase, Å.	Phases Observed	X-ray Reflections from Superlattice
15	I	90.3	2.4	7.3	2.1	13.5	595	30	2.8436	α	Absent
16	I	86.5	2.3	11.2	2.0	20.0	595	30	2.8292	α	Present
19	I	89.2	4.8	6.0	4.3	11.3	595	30	2.8492	α	Absent
20	I	86.1	4.6	9.3	4.1	17.0	600	28	2.8483	α	Absent
21	I	83.2	4.5	12.3	3.8	21.7	600	28	2.8368	α	Absent
60	I	82.9	9.2	7.9	8.2	14.7	600	28	2.8262	α	Present
61	I	77.7	8.5	13.8	7.1	24.2	595	56	2.8232	α	Absent
							600	28	2.8239	α	Present
74	I	76.1	13.4	10.5	11.6	19.0	1000	1 hr.	2.8355	α	Present (?)
85	I	79.3	11.5	9.2	10.1	16.9	595	28	2.8369	α	Present
89	I	81.1	8.9	10.0	7.7	18.2	595	30	2.8324	α	Present
							600	33	2.8317	α	Present
95	I	79.5 ^a	13.4 ^a	6.7 ^a	12.0 ^a	13.3 ^a	890	3 hr.	2.8447	α	
96	I	82.4	11.2	6.4	10.1	12.0	895	2 hr.	2.8447	α	Present
97	I	79.8	11.1	9.1	9.7	16.7	595	56	2.8370	α	Present
98	I	76.7	11.7	11.6	10.0	20.8	595	56	2.8286	α	Present
100	I	79.4	12.9	7.7	11.5	14.3	1000	2 hr.	2.8403	α	Present
101	I	77.3	13.5	9.0	11.9	16.6	1000	2 hr.	2.8363	α	Present
102	I	73.2	13.6	13.2	11.5	23.3	1000	2 hr.	2.8199	α	Present
93A	II	76.2 ^b	21.5 ^b	2.4 ^b	20.0 ^b	4.5 ^b	600	3	$\alpha + \gamma$		
94A	II	73.8 ^b	21.8 ^b	4.5 ^b	20.0 ^b	8.5 ^b	600	3	$\alpha + \gamma + \lambda$		
52	IV	62.2	30.5	7.3	27.4	13.7	595	56	2.8526 ^c	$\alpha + \gamma + \lambda$	
							600	12	2.8513	$\alpha + \lambda$	
43	V	74.0	18.6	7.4	16.6	13.9	600	28	2.8535	$\alpha + \lambda$	
51	V	62.8	24.9	12.3	21.4	22.0	595	28	2.8265	$\alpha + \lambda$	
73	V	71.8	18.1	10.1	15.8	18.4	600	28	2.8387	$\alpha + \lambda$	
74	V	76.1	13.4	10.5	11.6	19.0	600	28	2.8364	$\alpha + \lambda$	
81	V	69.9	19.4	10.7	16.8	19.4	600	21	2.8354	$\alpha + \lambda$	
82	V	65.1	23.0	11.9	19.8	21.4	600	28	2.8311	$\alpha + \lambda$	
88	V	79.9 ^a	13.4 ^a	6.7 ^a	12.0 ^a	12.5 ^a	600	33	2.8249 ^c	$\alpha + \lambda$	
95	V	79.5	13.4	7.1	12.0	13.3	595	21	2.8510 ^d	$\alpha + \gamma$	
									2.8431 ^d	$\alpha + \lambda$	
									2.8513 ^d	$\alpha + \gamma$	
95	V	79.5 ^a	13.4 ^a	7.1 ^a	12.0 ^a	13.3 ^a	595	56	2.8451 ^d	$\alpha + \lambda$	
									2.8530 ^d	$\alpha + \lambda$	
95	V	79.5 ^a	13.4 ^a	7.1 ^a	12.0 ^a	13.3 ^a	600	168	2.8514	$\alpha + \lambda$	
96	V	82.4	11.2	6.4	10.1	12.0	595	21	2.8443	$\alpha + \lambda$	
96	V	82.4	11.2	6.4	10.1	12.0	595	56	2.8446 ^d	$\alpha + \lambda$	
									2.8490 ^d	$\alpha + \lambda$	
96	V	82.4	11.2	6.4	10.1	12.0	600	168	2.8457 ^d	$\alpha + \lambda$	
									2.8488 ^d	$\alpha + \lambda$	
100	V	79.4	12.9	7.7	11.5	14.3	600	28	2.8410	$\alpha + \lambda$	
101	V	77.5	13.5	9.0	11.9	16.6	600	28	2.8376	$\alpha + \lambda$	
83	VI	56.2	30.2	13.6	25.6	24.1	600	28	2.8266	$\alpha + \epsilon + \lambda$	
							595	28	2.8239	$\alpha + \epsilon$	
44	VII	69.1	17.1	13.8	14.4	24.3	605	1	2.8241	$\alpha + \epsilon$	
							600	28	2.8193	$\alpha + \epsilon$	
50	VII	62.2	22.4	15.4	18.6	26.8	605	6	2.8201	$\alpha + \epsilon$	
							595	28	2.8216	$\alpha + \epsilon$	
72	VII	66.3	18.6	15.1	15.5	26.3	610	13	2.8214	$\alpha + \epsilon$	
							600	28	2.8197	$\alpha + \epsilon$	
76	VII	72.1	12.7	15.2	10.5	26.4	610	13	2.8202	$\alpha + \epsilon$	
102	VII	73.2	13.6	13.2	11.5	23.3	600	28	2.8234	$\alpha + \epsilon$	
36	VIII	73.2	8.0	18.8	6.4	31.6	600	7	2.8190	$\alpha + \epsilon + n +$	
									(Fe ₃ Si ₂ -trace) ^e		
37	VIII	64.8	16.1	19.1	13.0	32.2	585	6	2.8185	$\alpha + \epsilon + n$	
							595	28	2.8184	$\alpha + \epsilon + n$	
38	VIII	56.1	24.2	19.7	19.5	33.1	595	28	2.8193	$\alpha + \epsilon + n$	
48	VIII	68.4	7.6	24.0	5.8	38.7	595	28	2.8193	$\alpha + \epsilon + n +$	
									(Fe ₃ Si ₂ -trace) ^e		
49	VIII	68.9	11.9	19.2	9.6	32.2	595	56	2.8190	$\alpha + \epsilon + n$	
							600	28	2.8184	$\alpha + \epsilon + n$	
55	VIII	59.8 ^a	15.5 ^a	24.7 ^a	12.0 ^a	39.3 ^a	595	28	2.8188	$\alpha + \epsilon + n$	
58	VIII	49.3 ^a	25.9 ^a	24.8 ^a	20.1 ^a	39.9 ^a	595	28	2.8192	$\alpha + \epsilon + n$	
							600	28	2.8190	$\alpha + \epsilon + n$	
63	VIII	67.1	16.5	16.4	13.6	28.2	605	6	2.8184	$\alpha + \epsilon + n$	
17	IX	82.4	2.3	15.3	1.9	26.4	595	30	2.8178	$\alpha + n^* +$ (Fe ₃ Si) ^f	
22	IX	80.4	4.3	15.3	3.5	26.5	595	30	2.8180	$\alpha + n^* +$ (Fe ₃ Si, trace) ^g	
62	IX	77.1	4.1	18.8	3.3	31.6	595	28	2.8188	$\alpha + n$	
							610	7	2.8177	$\alpha + n$	
84	IX	80.4	3.6	16.0	2.9	27.5	595	28	2.8184	$\alpha + n +$ (Fe ₃ Si) ^h	
56		32.7 ^a	34.4 ^a	32.9 ^a	25 ^a	50 ^a	600	3	n		

^a Not analyzed.^b Not analyzed; prepared with carbonyl iron, shot nickel and a ferrosilicon alloy (80 per cent Si).^c Not in equilibrium.^d Not in equilibrium; two body-centered cubic lattices present in same alloy.^e There was only a trace of the n -phase present in the X-ray pattern.

MATERIALS AND METHODS

Most of the alloys used in this investigation were prepared of carbonyl iron, electrolytic nickel and specially purified silicon (99.79 per cent Si). For seven alloys (Nos. 19, 20, 21, 22, 100, 101 and 102), however, electrolytic iron was used instead of carbonyl iron. Alloys Nos. 93A and 94A, prepared from materials less pure, were used only for qualitative evaluation. The impurities in the carbonyl iron are: 0.007 per cent C, 0.004 Si, trace Mn, 0.004 S; those in the electrolytic iron, 0.01 per cent C,* 0.01 Cu,* 0.000 Al,* 0.001 Si,* 0.01 Mn,* 0.005 Sn,* 0.01 S,† 0.03 P†; those in the nickel, trace Si, 0.11 per cent Co, trace S, 0.013 Fe; those in the silicon, 0.004 per cent C, 0.008 Al, 0.014 Ca, 0.027 Fe, 0.002 O₂, 0.10 N₂, trace H₂.

The required quantities of the respective materials to prepare 30 or 50-gram ingots were placed in alundum crucibles and melted in vacuum by means of a high-frequency induction furnace. The compositions of the alloys are given in Table 1. The ingots were homogenized by heating in vacuum or hydrogen at 1000°C. for about one week. Powders for the X-ray analysis were obtained by grinding the ingots with an alundum wheel. The metallic powder was separated magnetically from the alundum. These powders were sealed in evacuated quartz, Pyrex or Jena glass tubes and heated according to the conditions given in Table 1. The specimens treated in the region of 600°C. were heated in horizontal tubular electric resistance furnaces and then quenched in water. The high-temperature heat-treatments were in vertical furnaces with a drop-quenching device, which has been described previously.⁸

CHEMICAL ANALYSIS AND X-RAY TECHNIQUE

The alloys were analyzed for iron and either nickel or silicon; the third element was determined by difference. The iron contents were determined by the silver reductor method, using standardized ceric sulphate solutions for titration with ferrous phenanthroline as an indicator.⁹ Nickel was determined by titrating prepared solutions of the alloys with potassium cyanide, and the silicon contents were obtained gravimetrically.¹⁰

The X-ray diffraction patterns were obtained in focusing cameras designed by Phragmén. Radiation from an iron target was used throughout the investigation; the wave lengths were those assigned by Siegbahn (1931). The $K\alpha_1$ and $K\alpha_2$ X-ray reflections from the (211) and (220) planes and, in some cases, the $K\beta$ reflections from these and the (310) planes, were used for determining the lattice constants of the body-centered cubic (alpha) phase. The error in determining the lattice constants may be set at ± 0.0005 Å.

STRUCTURES OF PHASES

From the X-ray diffraction patterns of the ternary alloys prepared in this investigation and the results on the binary iron-nickel and iron-silicon alloys obtained in

TABLE 2.—*Phases in the Iron-rich Iron-nickel-silicon Alloys*

AREA IN FIG. 1	PHASES PRESENT
I	α
II	γ
III	$\alpha + \gamma$
IV	$\alpha + \gamma + \lambda$
V	$\alpha + \lambda$
VI	$\alpha + \lambda + \epsilon$
VII	$\alpha + \epsilon$
VIII	$\alpha + \epsilon + \eta$
IX	$\alpha + \eta$

other investigations,^{2,3,4} the phases existing in the iron-rich iron-nickel-silicon alloys are given in Table 2 and located in the 600°C. isothermal section as shown in Fig. 1 (atomic per cent) and Fig. 2 (weight per cent).

* From spectroscopic analysis.

† Estimated from chemical analysis of iron-silicon alloys No. 25 and No. 32, reference 7.

The alpha phase has a body-centered cubic and the gamma phase a face-centered cubic atomic lattice. The eta phase has the same structure as the intermetallic com-

cubic structure with an edge length of 6.131 Å. The observed and calculated $\sin^2 \theta$ of the corresponding Fe-K α_1 reflections are given in Table 3. The shifting

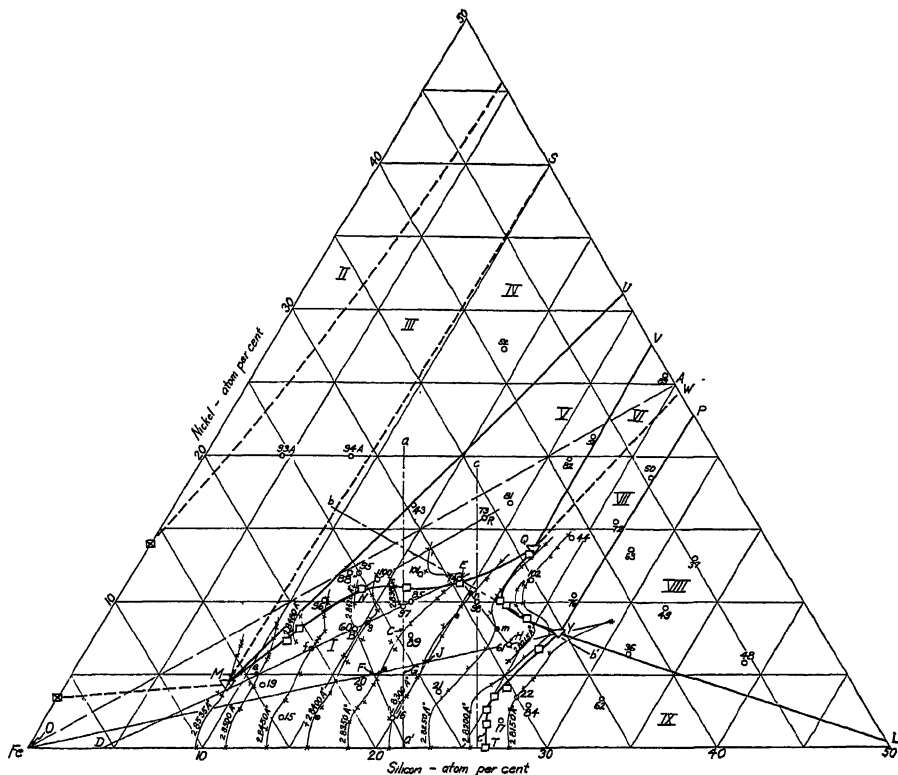


FIG. 1.—ALLOY LOCATIONS, ISOPARAMETER LINES AND PHASE BOUNDARIES OF IRON-RICH IRON-NICKEL-SILICON ALLOYS AT 600°C., ATOMIC PER CENT.

Points designated \boxtimes are from Owen and Sulley.

pound FeSi (33.4 wt. per cent Si) which, according to Phragmén¹¹ belongs to the tetartohedral class of the cubic system.

No alloy containing only the lambda phase was prepared. It was possible, however, to determine the structure of this phase in the two-phase alloy No. 51 after heating at 595°C. for 28 days and quenching. X-ray diffraction patterns of this alloy showed the presence of the alpha and lambda phases. After eliminating the lines associated with the alpha phase, the remaining lines could be accounted for by a

of the lambda-phase diffraction lines shows that the unit cell size increases as the composition changes from the boundary MU to OV in Fig. 1.

A similar situation arose with regard to the epsilon phase. In this case the two-phase alloy No. 50, heated at 605°C. for 6 days and quenched, was used to determine the structure of the epsilon phase. After elimination of the diffraction lines associated with the alpha phase, it was found that the remaining lines could be reasonably well accounted for by a tetrag-

onal structure with $a = 8.308$ Å. and $c = 9.012$ Å. The observed and calculated Fe- $K\alpha_1$ reflections are given in Table 4. With a large structure of this type, con-

ternary alloys is to construct surfaces whose vertical distances above an equilateral triangle (representing composition) are proportional to the lattice constants of

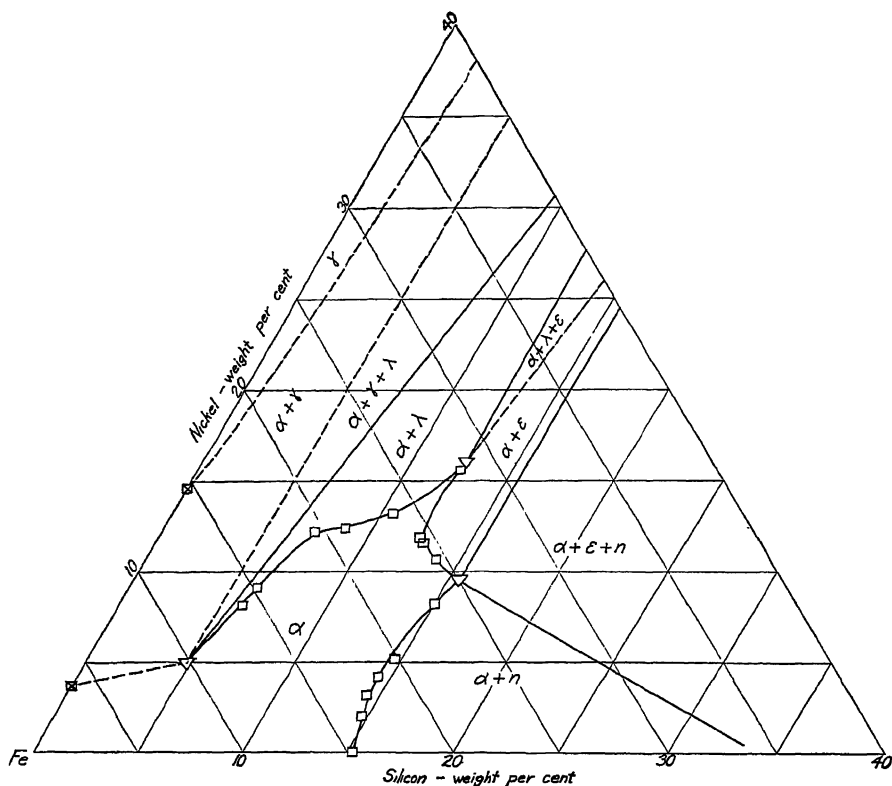


FIG. 2.—CONSTITUTION OF IRON-RICH IRON-NICKEL-SILICON ALLOYS AT 600°C., WEIGHT PER CENT. Points designated \square are from Owen and Sulley.

firmation by Laue or rotating-crystal methods is essential. These methods require single crystals, which could not be obtained in the alloys prepared.

Because of the uncertainties arising from conditions imposed by the nature of the alloys, the structures proposed for the lambda and epsilon phases are to be regarded as *tentative*.

METHOD OF DETERMINING ALPHA-PHASE SOLUBILITY LIMIT AT 600°C.

One method for determining the solid solubility limits of a single-phase area in

the single phase in the single and polyphase areas, respectively. Then the intersections of the single-phase surface with the polyphase surfaces, corresponding to certain temperatures, are the solid solubility limits at these temperatures. This method involves working with a three-dimensional model, which is inconvenient. If, however, the traces formed by the intersections of various vertical planes with the lattice constant or parametric surfaces are projected on suitable reference planes, it is possible to evaluate the data in two-dimensional diagrams.

Such a method of orthographic projection for evaluating X-ray data in the determination of solid solubility limits in ternary alloys has been described by Anderson and Jette.¹² This method is particularly suited

(p. 530 of ref. 12) but in its application appears more confusing.

For systems with a large number of different phases, resulting in many restricted one-phase and two-phase areas, it is not

TABLE 3.—Data on Structure of Lambda Phase Obtained from Alloy No. 51, Heated at 595°C. 28 Days and Quenched (Fe-K α_1 Radiation)

Intensity ^a	Sin ² θ Observed	Indices of Reflecting Planes	Sin ² θ Calculated ^b
m	0.147	(211)	0.149
vs	0.221	(300)	0.223
vs	0.251	(310)	0.248
s	0.274	(311)	0.273
sm	0.450	(330)	0.447
m	0.498	(420)	0.497
sm	0.645	(510) (431)	0.646
m	0.670	(511) (333)	0.670
sm	0.7199	(520) (432)	0.720
m	0.7442	(521)	0.745
mw	0.8690	(531)	0.869
mw	0.8934	(600)	0.894

^a vs, very strong; s, strong; sm, strong to medium; m, medium; mw, medium to weak.

^b On basis of cubic system, the lattice constant is 6.131 Å.

to ternary alloy systems involving only a few phases and with relatively large one-phase and two-phase areas in the isothermal sections. In the iron-rich iron-nickel-silicon alloys, however, it was found that the one-phase and two-phase areas are restricted and the parametric surface corresponding to the single-phase area is folded irregularly near the solid solubility limit. Consequently the systematic procedures used for the iron-chromium-silicon alloys (ref. 12, Figs. 4, 8, 9, 10, pp. 391 et seq.) are not applicable to the data on the iron-nickel-silicon alloys. The method used in evaluating the data for the latter alloys involves the orthographic projection of sections through the alloy compositions, which are neither parallel to the sides nor pass through the corners of the equilateral triangle representing composition. Fundamentally, this method is the same as that with the section lines described previously

TABLE 4.—Data on Structure of Epsilon Phase Obtained from Alloy No. 50 Heated at 605°C. 6 Days and Quenched (Fe-K α_1 Radiation)

Intensity ^a	Sin ² θ Observed	Indices of Reflecting Planes	Sin ² θ Calculated ^b
sm	0.121	(221)	0.120
		(300)	0.122
s	0.176	(320)	0.176
sm	0.215	(400)	0.216
sm	0.230	(410)	0.230
vs	0.267	(402)	0.262
sm	0.271	(420)	0.270
vs	0.314	(115)	0.315
		(422)	0.316
m	0.332	(413)	0.334
m	0.411	(305)	0.409
sm	0.445	(441)	0.445
vs	0.489	(600)	0.486
m	0.497	(601)	0.498
m	0.514	(444)	0.517
m	0.619	(207)	0.618
		(631)	0.620
w	0.629	(406)	0.630
w	0.674	(701)	0.674
		(710) (550)	0.675
mw	0.7353	(008)	0.735
sm	0.7628	(118)	0.763
mw	0.8793	(810) (740) (11,3,0)	0.879

^a vs, very strong; s, strong; sm, strong to medium; m, medium; mw, medium to weak; w, weak.

^b On basis of tetragonal system, $a = 8.308$ Å., $c = 9.012$ Å.

possible to secure data sufficient to set up the parametric surfaces without making a very large number of alloys. The simpler procedure using X-ray diffraction patterns only for phase identification becomes more convenient here. This method has been described in some detail by Bradley and his associates.¹³ The iron-rich corner of the iron-nickel-silicon system is an intermediate case for which neither the method of orthographic projections nor that of phase identification alone suffices. It was necessary therefore to use a combination of these two procedures.

The X-ray methods, like the classical microscopic methods, depend upon the assumption that equilibrium has been

attained by suitable heating and (except for the thermal contraction) retained by quenching until the examination has been completed.

For evaluating the data obtained in this investigation, the atomic compositions of the alloys were plotted on equilateral triangular coordinate paper with a scale of one centimeter per atomic per cent. In the plots of lattice constant against relative positions of the alloys (to be described later), 0.0020 Å. is equivalent to one centimeter.

LATTICE CONSTANTS OF ALPHA-PHASE ALLOYS (AREA I).

It has previously been shown⁷ that the lattice constants of the iron-silicon alloys containing from 0 to 9 atomic per cent silicon decrease at the rate of 0.00065 Å. per atomic per cent silicon, while the lattice constants of alloys containing from 9 to 26 atomic per cent silicon decrease at the rate of 0.00209 Å. per atomic per cent silicon. Around 9 atomic per cent silicon the change of slope in the lattice constant vs. composition curve shown in Fig. 3 is very great and appears to be a sharp break. In the iron-nickel system it has been shown² that nickel increases the lattice constant of alpha iron. Since the nickel atom is smaller than the iron atom, the effect of nickel on the alpha-iron lattice constant should reach a maximum and the form of the curve should be generally similar to that of the gamma phase in the iron-nickel system. On the other hand, unpublished results obtained in this laboratory indicate that the effect of silicon on the lattice constant of nickel is extremely small and has not been measured with certainty.

Since it was inconvenient to work with the parametric surface directly, lines of constant lattice parameters as functions of composition were set up (Fig. 1). The first step in constructing these isoparameter lines was to draw the projections on con-

stant nickel sections of lattice constant vs. composition traces of the alloys in area I, Fig. 1. In order to construct these projections shown in Fig. 4, a reference line aa' was drawn in Fig. 1, perpendicular to the side of the equilateral triangle representing the compositions of the binary iron-silicon alloys. The process for the construction of these traces will be illustrated by using the data for alloy No. 60. The perpendicular distance from the location of alloy No. 60 to line aa' in Fig. 1, was measured with dividers. This distance (BC) was then transferred to Fig. 4 and measured off as the abscissa of a point having 2.8413 Å. (the lattice constant of alloy No. 60) as the ordinate. The process was repeated for each alloy in area I. Then in Fig. 1, the alloys in area I were connected by straight lines which are traces of sections; e.g., section DBE . The lattice constants of alloys on these respective sections were then connected by lines in Fig. 4; e.g., $D'B'E'$, which represents the lattice constants of the alloys on section DBE in Fig. 1.

In preparing these sections of lattice constant vs. composition in Fig. 4, it should be noted that each section contains at least three experimentally determined points. In a few instances, one of the points on the individual sections was determined by interpolating along another intersecting section; e.g., point K , on the section $B'KG$ in Fig. 4 was derived by interpolating along FKH . Sometimes one of the points on the sections was taken from the lattice constant vs. composition curve of the binary iron-silicon alloys shown in Fig. 3.

Each curve on Fig. 4 covers a limited range of lattice constants, so that by reversing the process certain points having arbitrarily chosen values of the lattice constant can be located on the original section lines in Fig. 1. Thus the points e , f and g , with lattice constants respectively 2.8500, 2.8450 and 2.8400 Å. on line DBE

on Fig. 1, were found by interpolation along line $D'B'E'$ of Fig. 4. Similarly, points h and m on line EH in Fig. 1 were found from line $E'H'$ in Fig. 4.

In order to use more effectively the lattice-constant data for the ternary alloys, a second procedure in the construction of the isoparameter lines was introduced by determining the lattice constants of alloys along sections having constant atomic ratios of nickel to silicon, from the data in Fig. 4. The lattice constant vs. composition traces of the alloys along sections having constant atomic ratios of nickel to silicon (area I) are shown in Fig. 5 as projections on constant iron sections. In order to construct these projections, it was necessary to draw traces of sections in Fig. 1 having constant nickel to silicon ratios. These traces were passed through the point O and the respective composition points of the single-phase alloys. The reference line OA in Fig. 1 was drawn perpendicular to the constant iron sections. The method for determining the points for the curves shown in Fig. 5 from data shown in Fig. 4 will be illustrated by deriving the point F' in Fig. 5. This is the lattice constant of the alloy at the point F in Fig. 1, at the intersection of sections OF and BF . The distance FG perpendicular to aa' in Fig. 1 was measured with dividers, and then transferred to Fig. 4. Since point F is on section BF in Fig. 1, which contains alloys Nos. 60 and 16, the curve $B'F'$ in Fig. 4 is followed until this distance FG (from Fig. 1) exactly spans the distance between $B'F'$ and aa' on the left side of line aa' , as at $F'G'$. The point F' on $B'F'$ in Fig. 4 corresponds to the lattice constant (2.8361 Å.) of the alloy having the composition of F in Fig. 1. In Fig. 1, the perpendicular distance F to OA was measured with dividers. This distance was then measured perpendicular to $O'A'$ in Fig. 5 as the abscissa of the point F' , having the ordinate 2.8361 Å. Thus, by taking various points on the traces shown in Fig. 4, and transferring the data to Fig. 5

in the manner just described, it was possible to obtain for each of the sections of fixed nickel to silicon ratio a series of points, marked x in Fig. 5. The line connecting the points for any section gives the lattice constants of alloys on that section. It may be noted that each of these lattice constant vs. composition traces can be extrapolated linearly to a lattice constant of 2.8740 Å. at 100 per cent iron, which is the value obtained by extrapolating to zero per cent silicon the 9 to 25 atomic per cent silicon portion of the plot for the lattice constants of the binary iron-silicon alloys in Fig. 3. This value of the lattice constant (2.8740 Å.) at 100 per cent iron, obtained by extrapolation, is larger than the experimental value of 2.8604 Å. because of the marked contraction of the lattice at silicon contents above 9 atomic per cent.⁷

As the final step in constructing the isoparameter curves shown in Fig. 1, it was necessary to transfer the lattice-constant data shown in Fig. 5 to Fig. 1. The transferring process will be described by use of the data for alloys having the same nickel to silicon ratio as alloy No. 61 (Fig. 1). In this case, it was desirable to determine the intersection of the 2.8300 Å. isoparameter line with section OH (which contains alloy No. 61) in Fig. 1. In Fig. 5 the horizontal distance ($J'K'$) from $O'A'$ to the line $O'J'$ at 2.8300 Å. was measured with dividers. Then, on a perpendicular to OA in Fig. 1, the position of distance $J'K'$ between OA and OH was determined. The intersection of this line at J with OH in Fig. 1 was the composition of an alloy on the OH section which had a lattice constant of 2.8300 Å. This process was repeated to obtain each of the isoparameter lines in area I of Fig. 1; the points so determined were designated x . The agreement between the method just described and the one based directly on Fig. 4 is shown by the way test points designated by encircled crosses in Fig. 1, obtained from Fig. 4,

fall on the isoparameter lines derived from Fig. 5.

As noted in Table 1, alloys Nos. 95 and 96, quenched from 890° or 895°C., and

BOUNDARY BETWEEN ALPHA AND ALPHA + LAMBDA PHASES

The ternary alloys containing alpha and lambda phases are listed in Table 1 and

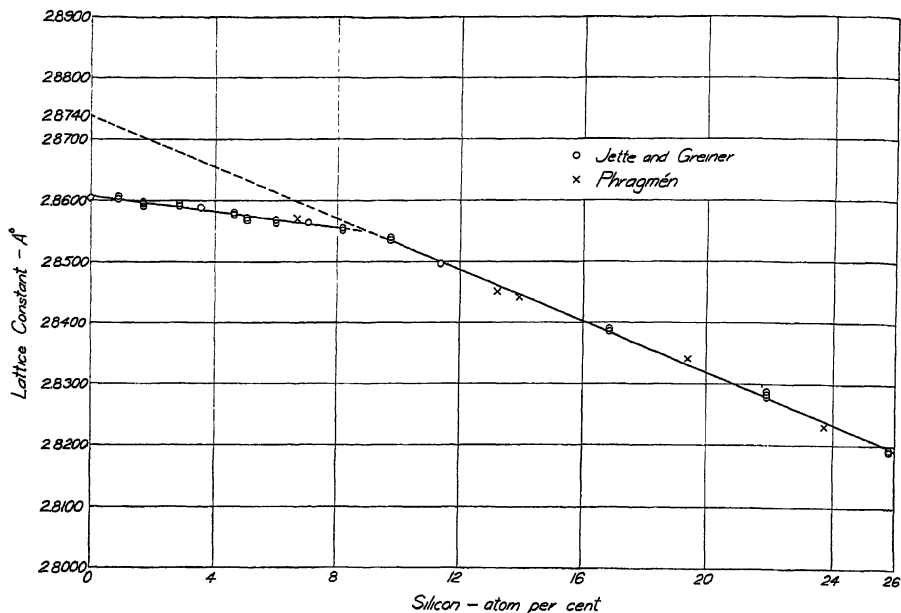


FIG. 3.—LATTICE CONSTANTS OF IRON-RICH IRON-SILICON ALLOYS.⁷

alloys Nos. 74, 100, 101 and 102, quenched from 1000°C., contain only the alpha phase. If these alloys are quenched from 600°C., however, their structures consist of alpha and either lambda or epsilon phases. The data for the alloys containing only the alpha phase were used in establishing the single-phase parametric surface.

In using these isoparameter lines for determining the solid solubility limit of the alpha phase, long extrapolations are questionable and may be made only when supported by data that show the phases present in alloys close to the boundaries of the phase areas being investigated.

The alpha-phase alloys in area I that gave X-ray reflections from a superlattice of the type observed in the binary iron-silicon alloys⁷ are noted in Table 1.

located in area V of Fig. 1. In order to determine the boundary line at 600°C. between area V and the single-phase area I, it was necessary to determine the intersection between the lattice-constant surface of the alpha-phase alloys in area V heat-treated at 600°C. with the lattice-constant surface of the alpha phase in area I.

The method of determining the points on the boundary *MNEQ* in Fig. 1 is as follows. The reference line *bb'* was drawn through the location of alloy No. 74 and perpendicular to the constant silicon sections. Then on the perpendiculars to *bb'* the distances between the locations of the various alloys in the two-phase area and line *bb'* were measured. These distances were the abscissas of points in Fig. 6, whose ordinates

were the alpha-phase lattice constants of the respective alloys.

The point N at the solid solubility limit of the alpha phase on section RN , Fig. 1,

the distances of points from bb' , where the trace RN intersects the 2.8400 and 2.8420 Å. isoparameter lines, were measured on perpendiculars to bb' . These distances were

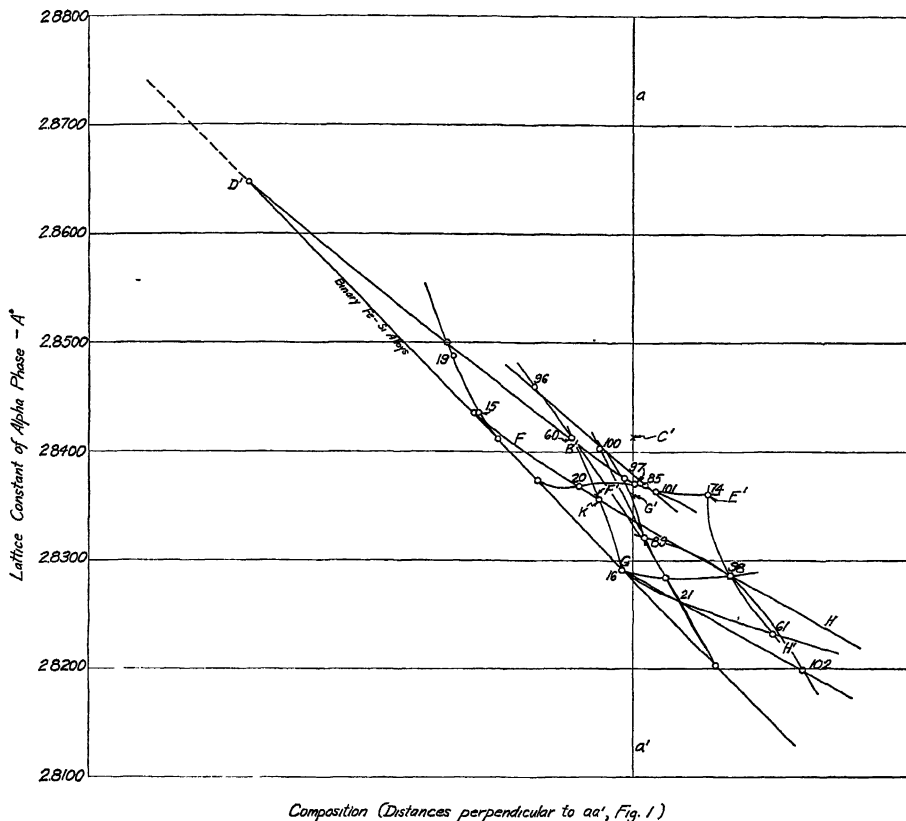


FIG. 4.—PROJECTIONS, ON CONSTANT NICKEL SECTION, OF TRACES OF LATTICE CONSTANT VS. COMPOSITION FOR ALLOYS IN AREA I.

was determined in the following manner. The line $R'N'$ in Fig. 6 represented the projection of the trace resulting from the intersection of a vertical section at RN in Fig. 1 with the lattice-constant surface of the alpha phase in the two-phase area. The projection is on a constant silicon section. Then to obtain the projection of the trace formed by the intersection of the vertical section at RN (Fig. 1) with the single-phase (alpha) lattice-constant surface,

plotted as abscissas on Fig. 6, while the corresponding values of the isoparameter lines were the ordinates; the points are designated E' and F' . A line connecting the points E' and F' will be the projection of the trace formed by the lattice-constant surface of the single-phase alloys intersecting the vertical section along NR (Fig. 1). The point N' in Fig. 6 represents the intersection of the projection of the trace of the lattice-constant surface of the alpha

phase in the alpha plus lambda-phase area with the trace of the lattice-constant surface of the single-phase (alpha) area. The horizontal distance from N' to bb' in

point N , designated by a square, in Fig. 1 is a point at the solid solubility limit of the alpha solid solution at 600°C.

The other points (designated by squares)

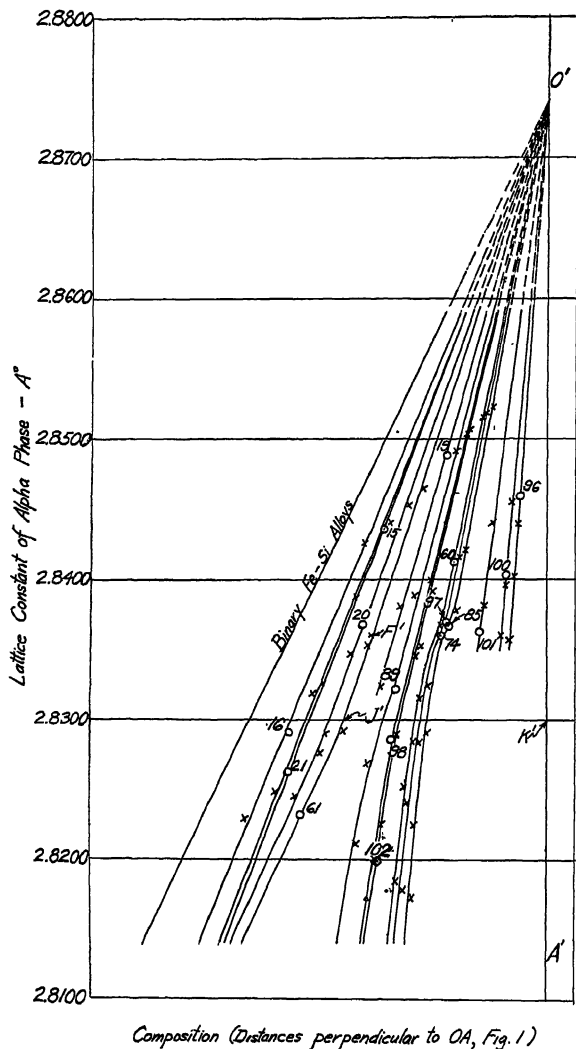


FIG. 5.—PROJECTIONS, ON CONSTANT IRON SECTION, OF TRACES OF LATTICE CONSTANT VS. COMPOSITION DERIVED FROM FIG. 4.

Fig. 6 ($N'T'$) was determined by means of dividers. Then, on a perpendicular to bb' in Fig. 1, the position of distance $N'T'$ between NR and bb' was determined. Thus

on the solid solubility limit between areas I and V were determined similarly and are shown in Figs. 1 and 2. The traces for the alpha phase in the two-phase area (Fig. 6)

contain two points designated by numbers, while the traces of the alpha phase in the single-phase area are drawn between points designated α .

was probably caused by the failure of the structure to reach equilibrium and the deviation of alloy No. 95 may be due to an error in estimating the composition, since

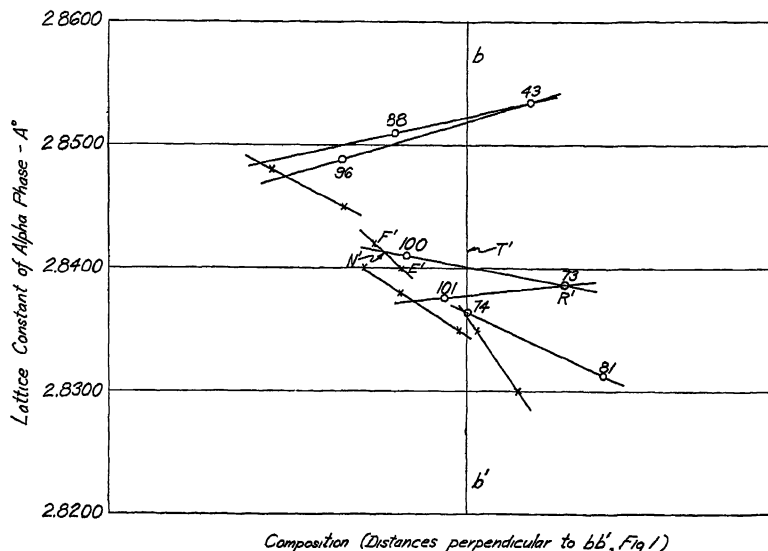


FIG. 6.—PROJECTIONS, ON CONSTANT SILICON SECTION, OF TRACES OF LATTICE CONSTANT VS. COMPOSITION FOR ALLOYS IN AREAS I AND V.

It may be noted that the solid solubility limit between areas I and V in Fig. 1, derived by the method just described, is supported by qualitative X-ray data that show the presence of the alpha and lambda phases in alloys Nos. 96, 100, 101 and 74 (quenched from 600°C.) which are close to the boundary $MNEQ$ in Fig. 1. Furthermore, alloys 85 and 97, which lie reasonably close to the boundary $MNEQ$ on the single-phase side, contain only the alpha phase.

From the shape of area V, Fig. 1, and the resulting directions of the tie lines, the lattice constants of the 11 alloys in this area should fall in the following order of increasing magnitude as the tie lines are crossed from QV to MU : Nos. 51, 82, 74, 81, 73, 101, 100, 95, 96, 88, 43. The data in Table 1 show that the lattice constants of alloys 82, 81, 73 and 95 would not permit them to be in that order. The deviation of alloy No. 82

it was not analyzed. The deviation of alloy No. 73 is within the experimental errors of the chemical analysis and lattice-constant determination. Fig. 6 shows that the deviations in the results for alloys 73 and 81 would cause little change in the positions of the points on the solubility limit determined with these alloys.

Some of the alloys in the iron-nickel-silicon system apparently are difficult to bring to equilibrium at 600°C. This was shown by the presence of two body-centered cubic phases in addition to the lambda phase in alloy No. 95 when heated at 595°C. for 21 days and quenched. The lattice constants of the body-centered cubic phases were 2.8431 and 2.8513 Å., respectively. When this alloy was heated at 595°C. for 56 days, the lattice constants of the body-centered cubic phases changed to 2.8451 and 2.8530 Å., respectively. After heating at 600°C. for 168 days, however,

only one body-centered cubic phase was present (in addition to the lambda phase) and this had a lattice constant of 2.8514 \AA . The latter was assumed to be the equilibrium value for the lattice constant of the body-centered cubic (alpha) phase in alloy No. 95 when quenched from 600°C .

A similar difficulty in attaining equilibrium was experienced in the case of alloy No. 96, whose composition is in the region of that of alloy No. 95. It was found that if alloy 96 is heated at 595°C . for 21 days and quenched it consists of two phases; namely, alpha and lambda. The alpha or body-centered cubic phase has a lattice constant of 2.8443 \AA . After this alloy is heated at 595°C . for 56 days and quenched, two body-centered cubic phases and the lambda phase are present. The lattice constants of the body-centered cubic phases are 2.8446 and 2.8490 \AA ., respectively. If alloy No. 96 is heated at 600°C . for 168 days and quenched, the lattice constants of the body-centered cubic phases are 2.8457 and 2.8488 \AA ., respectively. Apparently the latter heat-treatment did not bring the alloy to equilibrium at 600°C ., but since the body-centered cubic phase having the larger lattice constant was not observed in the material heated for 21 days, but was observed in the material heated for 56 and 168 days at 600°C ., it may be assumed that this phase was nearer to equilibrium than the body-centered phase having the smaller lattice constant. Furthermore, the value of 2.8488 \AA . is in agreement with the lattice constants used for the other determinations of points on the boundary between areas I and V.

THE THREE-PHASE AREAS IV AND VI

Figs. 1 and 2 show that the alpha plus lambda phase area V is bounded on the left by a three-phase area IV, containing the alpha, gamma and lambda phases. For equilibrium conditions at 600°C ., this three-phase area is necessarily bounded by straight lines. The structure of alloy No. 52 heat-treated at 600°C . for 3 days, or at

595°C . for 56 days (Table 1), shows the presence of these phases. The lattice constant of the alpha phase of this alloy when treated at 595°C . for 56 days was 2.8535 \AA . This is the lattice constant of the single-phase (alpha) alloy in equilibrium with three-phase alloy No. 52 at 595°C . The point *M* in Fig. 1 (designated by triangle) was located at the intersection of the isoparameter line 2.8535 \AA . with the solid solubility line *MNEQ* (determined above). The position of the line *MS* was determined approximately by correlation of the present results with those of Osawa and Okamoto⁶ on the binary nickel-silicon alloys. The position of line *MU* was determined from the various phases observed in the alloys, and also the position of point *M*. Since the lattice constant of the alpha phase in the two-phase alloy No. 43 quenched from 600°C . is 2.8535 \AA ., the tie line containing this alloy must be on or near the boundary *MU*.

Likewise, the alpha plus lambda phase area V, Figs. 1 and 2, is bounded on the right side by the three-phase area VI, containing the alpha, epsilon and lambda phases. Alloy No. 83 is in this area and contains the three phases when heat-treated at 600°C . for 28 days. The lattice constant of the alpha phase of this alloy is 2.8266 \AA . This is also the lattice constant of the single-phase (alpha) alloy point *Q*, Fig. 1 (designated by triangle), in equilibrium with alloy No. 83 at 600°C . The positions of lines *QV* and *QW* in Fig. 1 were determined from the various phases observed in the alloys noted near these lines. Since the lattice constant of the alpha phase in the two-phase alloy No. 51 quenched from 595°C . is 2.8265 \AA ., the tie line containing this alloy must be on or near the boundary *QV*.

BOUNDARY BETWEEN ALPHA AND ALPHA + EPSILON PHASES

The alloys in area VII of Fig. 1 contain two phases, designated alpha and epsilon.

These alloys are listed in Table 1. The solid solubility limit of the alpha phase between areas I and VII at 600°C. was determined by the method described in

eta and epsilon phases, are listed in Table 1. The average value of the lattice constants of the alpha phase of these alloys heat-treated at 600°C. is 2.8190 Å., which is the

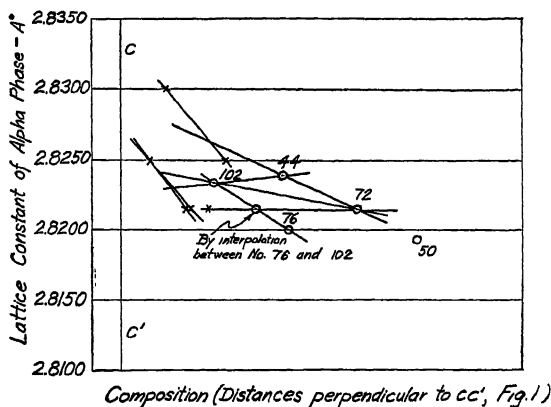


FIG. 7.—PROJECTIONS, ON CONSTANT NICKEL SECTION, OF TRACES OF LATTICE CONSTANT VS. COMPOSITION FOR ALLOYS IN AREAS I AND VII.

connection with areas I and V. The reference line cc' was used to derive the points on the intersection of the lattice-constant surface of the single-phase (alpha) alloys with the lattice-constant surface of the alpha phase in the two-phase alloys. The construction details are shown in Fig. 7. The traces of the lattice constants of the alpha in the two-phase area are drawn through at least one alloy point designated by a number, while the traces for the lattice constant of the alpha in the single-phase area are drawn between points designated x .

The X-ray diffraction patterns of alloys 44 and 102 (quenched from 595° and 600°C., respectively) which lie close to the boundary of area VII, Fig. 1, show the presence of the alpha and epsilon phases. Likewise the X-ray diffraction pattern of alloy No. 98 (quenched from 505°C.), which lies in area I close to the boundary, shows the presence of only the alpha phase.

THE THREE-PHASE AREA VIII

The compositions of the alloys in area VIII of Fig. 1, which contains the alpha,

lattice constant of the single-phase (alpha) alloys at point Y in Fig. 1, in equilibrium with the three-phase alloys in area VIII.

The alloys Nos. 36 and 48 contain a phase having the structure of Fe_3Si_2 in addition to the alpha, eta, and epsilon phases. The Fe_3Si_2 phase, however, was found to be unstable at 600°C. in the binary alloys,⁴ although its decomposition to alpha and $FeSi$ (eta) is sluggish. Consequently, the Fe_3Si_2 phase in these alloys probably formed because the materials were not in equilibrium.

The position of line YP in Fig. 1 was determined from the structures of the alloys located near it. Since the X-ray reflection lines of the eta phase show approximately the same lattice spacing as the eta of the binary iron-silicon alloys, the composition of the eta of the three-phase alloys is probably near that of the eta in the binary alloys. Therefore, the line YL in Fig. 1 was drawn to show a small solid solubility of nickel in the eta phase. The position of YL was further confirmed by the location and phases present in alloy No. 36.

BOUNDARY BETWEEN THE ALPHA AND ALPHA + ETA PHASES

The alpha plus eta-phase area (IX) borders the binary iron-silicon alloys as

SUMMARY

The constitution of the iron-rich iron-nickel-silicon alloys at 600°C. has been studied by X-ray crystal structure meth-

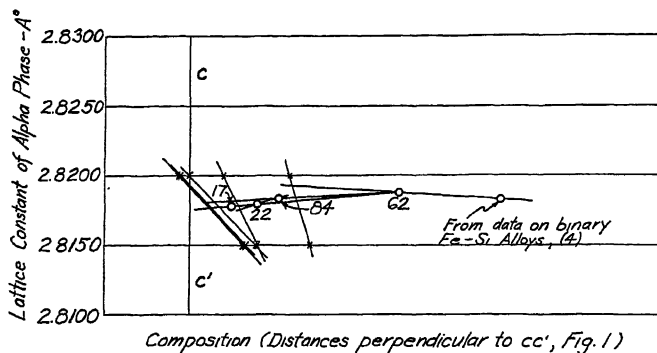


FIG. 8.—PROJECTIONS, ON CONSTANT NICKEL SECTION, OF TRACES OF LATTICE CONSTANT VS. COMPOSITION FOR ALLOYS IN AREAS I AND IX.

shown in Figs. 1 and 2. The solid solubility limit YT (Fig. 1) at 600°C. was determined by the method described above for the areas I and V; the construction details are shown in Fig. 8. The traces for the lattice constants of the alpha phase in the two-phase area pass through points designated by alloy numbers, while the traces for the lattice constants of the alpha in the single-phase area are drawn between points designated x . The results in Fig. 1 show that the alpha-phase solid solubility limit at 600°C. changes from 26.4 atomic per cent silicon in the binary alloys to 26.8 atomic per cent silicon, 7.9 atomic per cent nickel in the ternary alloys.

The X-ray diffraction patterns of alloys 17, 22 and 84, heated at 595°C. for at least 28 days and quenched (see Table 1), show the presence of the alpha, eta and Fe_3Si_2 phases. The Fe_3Si_2 phase in these alloys is probably caused by the failure of the structures to reach equilibrium, as with alloys 36 and 48, area VIII. The results of evaluating the lattice-constant data for alloys 17, 22 and 84 indicate that their structures should consist of the alpha and eta phases.

ods. The body-centered cubic (alpha) phase in a ternary plot is bounded by four two-phase areas. Three three-phase areas separate the respective two-phase areas. Three of the phases in these polyphase areas have the same structures as corresponding phases in the binary iron-nickel or iron-silicon alloys. In addition, two new phases, whose structures have been tentatively identified, have been observed.

The isoparameter lines in Fig. 1 show that the surface representing the lattice constants of the single-phase (alpha) alloys is not a plane. This indicates that the alloys do not follow Vegard's rule.

The solid solubility limit of the alpha phase at 600°C. has been determined from lattice-constant data by a method of orthographic projection. The points on this boundary obtained in this and other investigations are tabulated in Table 5 and plotted in Fig. 1 (atomic per cent) and in Fig. 2 (weight per cent). The solubility of nickel in the alpha phase changes from 3.5 atomic per cent in the binary iron-nickel alloys to 13.6 atomic per cent in the ternary alloys containing 22.4 atomic per cent

silicon. From the latter composition, the solubility of nickel in the alpha phase changes to 7.9 atomic per cent at 26.8 atomic per cent silicon, and of course is zero at 26.4 atomic per cent silicon in the binary iron-silicon alloys. The solid solubility limits determined from the lattice-constant data have been confirmed by the disappearing-phase criterion.

TABLE 5.—Points on Alpha-phase Boundary at 600°C. Determined from Lattice-constant Data

Phase Boundary between Areas	Nickel		Silicon	
	Atomic Per Cent	Wt. Per Cent	Atomic Per Cent	Wt. Per Cent
I-III	3.5 ^a	3.7 ^a	0.0	0.0
I-IV	4.5	5.0	0.2	4.8
I-V	7.3	8.1	11.2	5.9
I-V	8.2	9.1	11.5	6.1
I-V	10.9	12.2	13.7	7.3
I-V	10.9	12.4	16.1	8.7
I-V	11.4	13.2	19.0	10.5
I-VI	13.6	16.0	22.4	12.6
I-VII	13.3	15.6	22.3	12.5
I-VII	10.1	11.9	22.2	12.5
I-VII	9.8	11.6	22.7	12.8
I-VII	8.9	10.6	24.4	13.9
I-VIII	7.9	9.5	26.8	15.5
I-IX	6.8	8.2	26.1	15.0
I-IX	4.2	5.1	25.5	14.7
I-IX	3.5	4.2	25.1	14.4
I-IX	2.6	3.1	25.1	14.4
I-IX	1.7	2.0	25.6	14.7
I-IX	0.0	0.0	26.4 ^b	15.3 ^b

^a Owen and Sulley.³

^b Greiner and Jette.⁴

ACKNOWLEDGMENTS

The authors are indebted to Mr. Frank Schnettler, Research Assistant in Metallurgy at Columbia University, for his cooperation on many occasions during the course of this work.

The highly purified silicon was obtained from the Electro-Metallurgical Company through the courtesy of the late Dr. F. M. Becket.

REFERENCES

1. E. S. Greiner, J. S. Marsh and B. Stoughton: The Alloys of Iron and Silicon, 273-281. Engineering Foundation, New York, 1933. McGraw-Hill Book Co.
2. E. R. Jette and F. Foote: X-ray Study of Iron-nickel Alloys. *Trans. A.I.M.E.* (1936) 120, 259.

3. E. A. Owen and A. H. Sulley: The Equilibrium Diagram of Iron-nickel Alloys. *Phil. Mag.* (1939) 71, 27, 614.
4. E. S. Greiner and E. R. Jette: X-ray Study of the Constitution of Iron-silicon Alloys Containing from 14 to 33.4 Per Cent Silicon. *Trans. A.I.M.E.* (1937) 125, 473.
5. D. E. Ackerman: The Constitution of Nickel-silicon Alloys. *Metals Handbook* (1939) 1634. Amer. Soc. Metals.
6. A. Osawa and M. Okamoto: The Nickel-silicon System. *Sci. Repts. Tohoku Imp. Univ.* (1939) 27 (3), 326. Also see *Metal Progress* (1939) 489.
7. E. R. Jette and E. S. Greiner: An X-ray Study of Iron-silicon Alloys Containing from 0 to 15 Per Cent Silicon. *Trans. A.I.M.E.* (1933) 105, 259.
8. E. R. Jette, V. H. Nordstrom, B. Queneau and F. Foote: X-ray Studies on the Nickel-chromium System. *Trans. A.I.M.E.* (1934) 111, 373.
9. G. H. Walden, Jr., L. P. Hammett and S. M. Edmonds: *Jnl. Amer. Chem. Soc.* (1934) 56, 350.
10. G. B. F. Lundell, J. I. Hoffman and H. A. Bright: Chemical Analysis of Iron and Steel. New York, 1931. John Wiley and Sons.
11. G. Phragmén: Om järn-kisellegeringarnas byggnad. *Jernkontorets Ann.* (1923) 107 (78), 121-131.
12. A. G. H. Andersen and E. R. Jette: X-ray Investigation of the Iron-chromium-silicon Phase Diagram, and X-ray Methods for Ternary Systems, *Trans. Amer. Soc. Metals.* (1936) 24, 375-419, 519-540.
13. A. J. Bradley, H. J. Goldschmidt, H. Lipson, A. Taylor: Investigation of Equilibrium Diagrams of Ternary Alloys by X-rays. *Nature* (1937) 140, 543.

DISCUSSION

(John T. Norton presiding)

F. M. WALTERS,* Anacostia, D. C.—I would like to have Mr. Greiner tell us some more about the giant tetragonal.

E. S. GREINER (author's reply).—The X-ray diffraction data on the structure of the epsilon phase, referred to by Dr. Walters, were obtained from powder patterns of alloys containing the alpha and epsilon phases. Because of the large dimensions of the tetragonal cell and since no single crystals were available for Laue or rotating-crystal patterns, we have proposed a tentative structure for the epsilon phase.

R. M. BRICK,† New Haven, Conn.—How did the authors assure themselves that the different phases, analyzed at room temperatures, represent the phases as they were present

* Naval Research Laboratory.

† Hammond Metallurgical Laboratory, Yale University.

at 600°? Is there any assurance, for example, that the tetragonal phase found to be tetragonal at room temperature had the same structure at the high temperature? It seems possible that a change might have occurred during quenching.

E. S. GREINER.—It has been stated in the text of this paper that the present results are given on the assumption that equilibrium structures in the alloys were attained by

suitable heating and (except for the thermal contraction) retained by quenching until the examination was completed. This assumption is similar to that used in evaluating the results of microscopic investigations of the constitution of alloy systems. In the present investigation, however, the satisfactory quality of the X-ray diffraction patterns indicated that structural changes did not occur during the quenching procedure.

Constitution of Lead-rich Lead-antimony Alloys

By W. S. PELLINI* AND F. N. RHINES,† MEMBER A.I.M.E.

(Cleveland Meeting, October 1942)

IN many of the otherwise well established alloy phase diagrams the solidus curves (temperatures at which liquid first appears upon melting) have not been located accurately, chiefly because the experimental techniques that have been most popular for determining solidus temperatures have been both cumbersome and subject to large errors. C. E. Homer and H. Plummer¹ have described a sensitive and at the same time a very simple technique for locating the solidus curves in a number of alloys of tin. Their method consists simply in noting the temperature at which a specimen of the alloy ruptures under the influence of a light bending force.

Although this method is not new, it has been little used for this purpose in the past; nevertheless, it appears so attractive in its possibilities of speed, simplicity, and precision that the investigations presently to be described were undertaken to verify its merits. The redetermination of the solidus and eutectic temperatures of the lead-antimony system was employed as a medium of experimentation. New values obtained in this way are believed to be sufficiently precise to warrant a revision of the currently accepted lead-antimony phase diagram (Fig. 1).

This paper was presented in partial fulfillment of the requirements of the degree of Bachelor of Science in Metallurgical Engineering at the Carnegie Institute of Technology. Manuscript received at the office of the Institute March 9, 1942. Issued in METALS TECHNOLOGY, September 1942.

* Research Assistant, Metals Research Laboratory, Carnegie Institute of Technology, Pittsburgh, Pa.

† Member of Staff, Metals Research Laboratory; Assistant Professor of Metallurgy, Carnegie Institute of Technology.

¹ References are at the end of the paper.

Determinations of the solidus of the lead-rich lead-antimony alloy series have been published by R. S. Dean² and by E. E. Schumacher and F. C. Nix.³ Their points are represented in Fig. 1. In their work the solidus was not located at antimony concentrations greater than 2 per cent; the curve was presumed to meet the eutectic horizontal at an antimony concentration of about 2.5 per cent. In the present studies the solidus has been traced to 3.5 per cent, where the eutectic horizontal is intersected (Table 1 and Fig. 1). Within the range investigated by Dean and by Schumacher and Nix the agreement with their values is good. H. Seltz and B. De Witt,⁴ on the basis of activity measurements, have calculated that the intersection of the solidus and the eutectic reaction horizontal should lie at 3.86 per cent of antimony.

The following determinations of the eutectic temperature have been reported: Roland-Gosselin,⁵ 228°C.; Ewen,⁶ 228°C.; J. E. Stead,⁷ 247°C.; Campbell,⁸ 228°C.; W. Gontermann,⁹ 245° to 252°C.; R. Loebe,¹⁰ 245°C.; E. Heyn and O. Bauer,¹¹ 245°C.; H. Endo,¹² 250°C.; R. S. Dean,² 247° to 258°C.; E. Abel, O. Redlich, and J. Adler,¹³ 245°C.; W. Broniewski and L. Sliwowski,¹⁴ 250° to 252°C.; H. Seltz and B. De Witt,⁴ 250°C.

A temperature of 247°C. appears to have been generally accepted in recent years; it is the value most frequently obtained by the method of cooling curves. Values below 247°C. have usually been obtained by inferior cooling-curve techniques; those above 250°C., by the method of heating

curves. In a very careful measurement by means of cooling curves using metal of high purity and a cooling rate of $0.25^{\circ}\text{C. per min.}$, the present authors found the eutectic

appraising the results to observe at this point that an alloy of high purity (No. 63) containing 12 per cent of antimony was held for 30 min. at a carefully controlled and

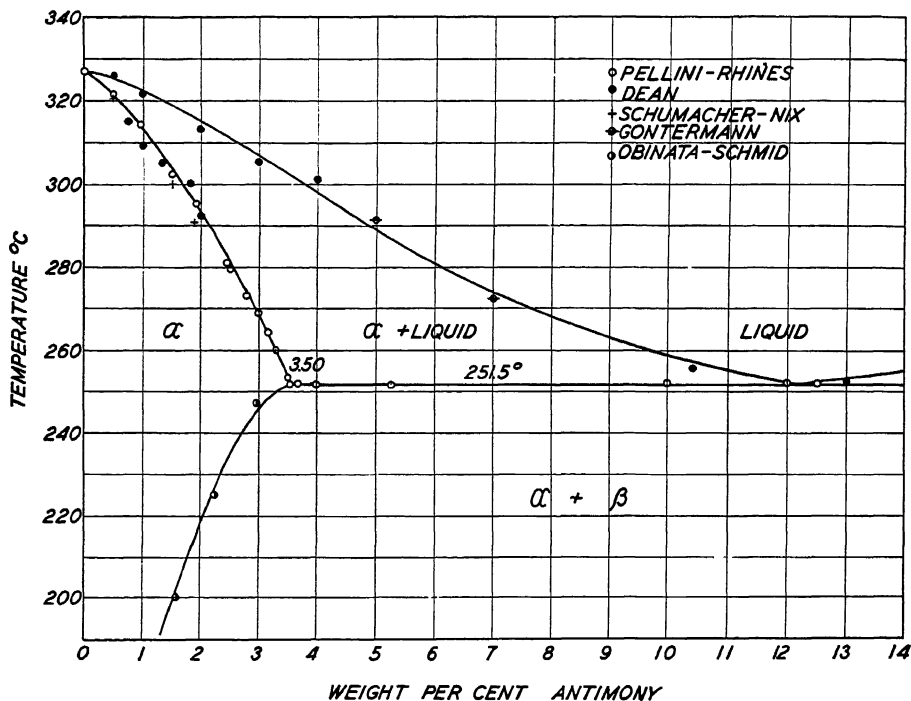


FIG. 1.—REVISED LEAD-ANTIMONY PHASE DIAGRAM.

arrest at 249.8°C. At another laboratory,¹⁵ by a similar technique, a temperature value of 249°C. was found recently. Probably the commonly accepted figure, 247°C. , is too low; this is the expected direction of error in measurements of this kind, and it is to be anticipated, furthermore, that undercooling should be pronounced in a reaction at so low a temperature.

Applying the technique of Homer and Plummer to this measurement, values between 251.5° and 252.5°C. were consistently obtained over a concentration range of 3.52 to 12.5 per cent of antimony (Table 1). The nature of the errors that may be expected of this method will be described presently, but it will be useful in

measured temperature of 251°C. without showing any signs of softening, and that melting occurred quite suddenly at 251.8°C. when the temperature was raised at a rate of $0.05^{\circ}\text{C. per min.}$ The expected error lies in the direction of a high temperature reading in this type of measurement, but it is inconceivable that the melting temperature could lie below 251°C. without melting having occurred in 30 min. It is concluded, therefore, that the true eutectic temperature is $251.5^{\circ} \pm 0.5^{\circ}\text{C.}$

In order to present a complete phase diagram (Fig. 1) within the range of compositions covered, the liquidus curve determined by R. S. Dean² is included, as well as the solidus curve established by I.

TABLE I.—*Data on Alloys Studied*

Specimen No.	Composition (Per Cent Sb)	Heat-treatment, Days	Temperature of Rupture, Deg. C.
1	None added	None	327.7 ^a
2	None added	None	326.8
3	None added	None	326.8
4	None added	None	326.7
5	None added	None	327.1 ^b
6	None added	None	327.1 ^b
7	None added	None	326.8 ^b
8	0.50	9 at 240°C., 10 at 250°C., 7 at 300°C.	322.2
9	0.50	9 at 240°C., 10 at 250°C., 7 at 300°C.	321.3
10	0.50	9 at 240°C., 10 at 250°C., 7 at 300°C.	321.8
11	0.95	9 at 240°C., 10 at 250°C., 7 at 300°C.	314.8
12	0.95	9 at 240°C., 10 at 250°C., 7 at 300°C.	313.9
13	0.95	9 at 240°C., 10 at 250°C.	314.6
14	1.50	5 at 240°C., 5 at 285°C.	302.2
15	1.50	5 at 240°C., 8 at 285°C.	302.4
16	1.50	None	300.2
17	1.50	5 at 240°C., 3 at 285°C.	302.4
18	1.50	5 at 240°C.	301.9
19	1.90	9 at 240°C., 9 at 250°C.	295.6
20	1.90	9 at 240°C., 10 at 250°C.	294.6
21	1.90	9 at 240°C., 10 at 250°C.	295.7
22	2.42	10 at 240°C.	280.0
23	2.42	10 at 240°C.	279.8
24	2.42	10 at 240°C., 5 at 250°C., 5 at 270°C.	281.0
25	2.42	10 at 240°C., 5 at 250°C., 5 at 270°C.	281.2
26	2.43	None	278.7 ^b
27	2.47	12 at 240°C., 12 at 250°C.	279.1
28	2.47	12 at 240°C., 12 at 250°C.	279.6
29	2.47	12 at 240°C., 18 at 250°C.	279.0
30	2.77	12 at 240°C., 12 at 250°C.	273.1
31	2.77	12 at 240°C., 12 at 250°C.	272.3
32	2.77	12 at 240°C., 18 at 250°C.	273.9
33	2.98	None	264.1 ^b
34	2.98	10 at 250°C.	269.5 ^b
35	2.98	10 at 250°C.	269.3 ^b
36	3.15	12 at 240°C., 12 at 250°C.	265.2
37	3.15	12 at 240°C., 12 at 250°C.	263.9
38	3.15	12 at 240°C., 18 at 250°C.	264.5
39	3.28	12 at 240°C., 12 at 250°C.	259.6
40	3.28	12 at 240°C., 12 at 250°C.	260.1
41	3.28	12 at 240°C., 18 at 250°C.	260.6
42	3.50	12 at 248°C.	253.3
43	3.50	12 at 248°C.	254.0
44	3.52	25 at 248°C.	253.1
45	3.52	12 at 248°C.	252.0
46	3.52	12 at 248°C.	252.4
47	3.66	12 at 248°C.	251.3
48	3.66	12 at 248°C.	251.4
49	3.66	12 at 248°C.	252.5
50	4.00 ^c	25 at 248°C.	252.0
51	4.00	12 at 248°C.	251.6
52	4.00	25 at 248°C.	252.6
53	4.00	25 at 248°C.	251.8
54	4.00	25 at 248°C.	252.0
55	5.25 ^c	12 at 248°C.	251.5
56	5.25	12 at 248°C.	251.9
57	10.00 ^c	None	251.3
58	10.00	None	252.3
59	12.50 ^c	12 at 248°C.	251.5
60	12.50	12 at 248°C.	252.3
61	12.00 ^c	None	252.0 ^b
62	12.00	None	251.8 ^b
63	12.00	None	252.2 ^b
			251.8 ^b

^a Fast heating rate, 3° to 4°C. per minute.^b Made from high-purity metals.^c Not analyzed.

Obinata and E. Schmid.¹⁶ At temperatures lower than those represented on the diagram (Fig. 1), the solidus curve may be extended by the use of the values of E. E. Schumacher and G. M. Bouton.¹⁷

EXPERIMENTAL PROCEDURE

The measurements described were made with an apparatus embodying a number of

couple placed very close to the center of the sample. In operation the furnace temperature is increased at a diminishing rate, while the temperature of the oil bath is read continually with a sensitive potentiometer. Thus the potentiometer is balanced at all times so that a reading can be made without delay when the rupture of the sample is indicated by the drop of the

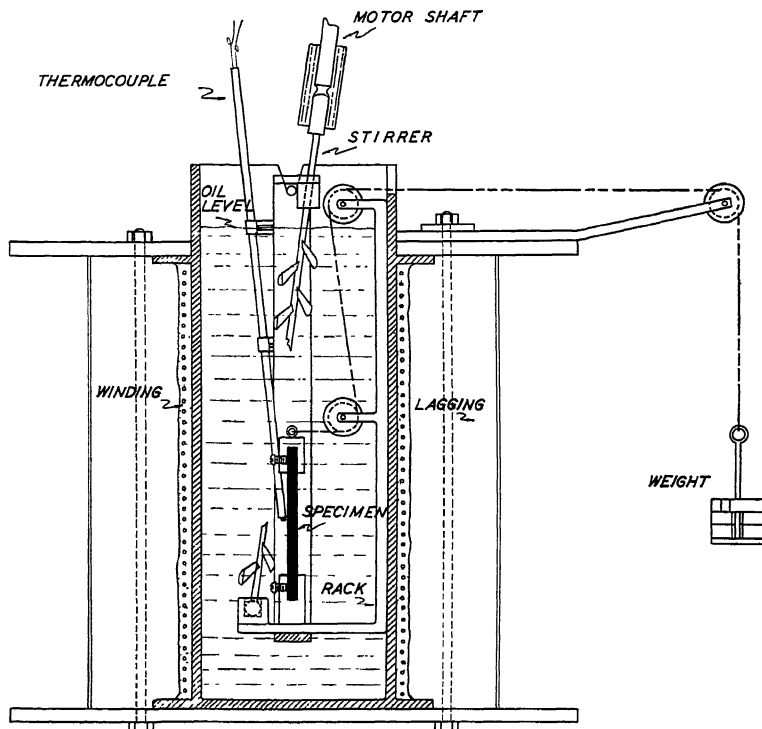


FIG. 2.—APPARATUS FOR MEASURING SOLIDUS TEMPERATURE OF LOW-MELTING ALLOYS.

improvements over the very simple equipment used by Homer and Plummer (Fig. 2). The specimen, consisting of a bar $\frac{1}{4}$ by $\frac{3}{8}$ by 3 in., is held vertically between two clamps, the lower clamp being fixed in position while the upper clamp is attached only to a wire, which, when loaded with a weight, applies a bending force to the sample. By means of a rapidly circulated oil bath, a uniform temperature is maintained. Temperatures are read with a thermo-

weight. It was found convenient to raise the temperature rapidly to a point about 50°C. below that of the expected reading and then at a rate of 0.25° to 0.5°C. per min. until rupture occurred.

The lead-antimony alloys used in this investigation, with the exceptions noted below, were made from Omaha pig lead and technical antimony. A master alloy containing 5 per cent of antimony was used in making all alloys containing less

than 4 per cent of antimony; at higher concentrations direct additions were made. A list of analyses is included in Table 1. Alloys numbered 5, 6, 7, 24, 31, 32, 33, 60, 61, 62, and 63, Table 1, were made from Cerro de Pasco lead of selected high purity and Kahlbaum antimony. These were melted in heats of 300 grams each (100 grams of the high-purity alloys) in pure graphite crucibles under a cover of lamp-black. The alloying temperature in all cases was $450^{\circ}\text{C}.$, at which temperature each alloy was held for 3 hr. with frequent stirrings with a graphite rod. After casting in iron chill molds, the resulting ingots were reduced 85 per cent by rolling to a thickness of $\frac{1}{4}$ in. Bars $\frac{3}{8}$ in. wide and 3 in. long cut from the rolled slabs were first homogenized for a minimum of 9 days at $240 \pm 1^{\circ}\text{C}.$ in an electric drying oven; the temperature was then generally raised to $250 \pm 1^{\circ}\text{C}.$ for periods ranging from 5 to 18 days, the longer treatments being applied to the alloys with a higher antimony content. Immediately after quenching in water from the final homogenizing treatment, the samples were tested in the apparatus described above. All treatments and measurements are recorded in detail in Table 1.

DISCUSSION OF ERRORS

Errors introduced into the measurements are probably to be ascribed to one or more of the following: (1) inaccuracy in the measurement of temperature, (2) influence of the rate of heating, (3) presence of inhomogeneity in the alloy, (4) influence of the grain size, (5) inaccurate chemical analysis, and (6) rupture due to causes other than melting. The precautions that were taken to avoid errors from these sources will be described.

Temperature.—The thermocouples were made from a specially selected lot of Chromel and Alumel wire, the reliability of which had been assured in the course of earlier constitutional studies made in this

laboratory. In addition, the calibration of the thermocouples was frequently checked against the melting points of pure lead and Chempur tin and the boiling point of water. It was found, moreover, that cast bars of pure lead broke upon heating at 0.4 to $0.2^{\circ}\text{C}.$ below the accepted value of $372.3^{\circ}\text{C}.$; cold-rolled pure lead ruptured at about $0.2^{\circ}\text{C}.$ above the freezing temperature. Similar results were obtained with pure tin and indium. It is presumed that the occurrence of concentrations of impurities at the grain boundaries accounts for the low results with the cast metals. Some overheating ($0.2^{\circ}\text{C}.$) is indicated by the wrought samples. It may be concluded that the temperature measurement is correct to about $\pm 0.2^{\circ}\text{C}.$

Rate of Heating.—In preliminary tests, speeds of heating up to $4^{\circ}\text{C}.$ per min. were tried in experiments with both pure metals and alloys; the increase in the apparent temperature of rupture over measurements made at $0.5^{\circ}\text{C}.$ per min. was $1^{\circ}\text{C}.$ in the most extreme case found. An error of this kind and magnitude would be expected to result from a temperature lag between the specimen and the bath and from the increased difficulty of keeping the potentiometer in balance. All reported readings were made at heating rates of not more than $0.5^{\circ}\text{C}.$ per minute.

Inhomogeneity.—It is evident from the work of Homer and Plummer that cast alloys in the alpha range, owing to concentrations of eutectic constituents at the grain boundaries, frequently rupture at the eutectic temperature. In order to avoid this, the alloys used in the present studies were all cold-worked and homogenized. It has already been pointed out, for pure lead, tin, and indium, that working alone tends to prevent rupture through the melting of undissolved impurities. Cold-rolled alloys not homogenized were found to rupture not more than $5^{\circ}\text{C}.$ below the breaking temperature found after a long period of homogenization. The times of homogeniza-

tion used were all greatly in excess of those necessary to produce constant ($\pm 0.5^{\circ}\text{C}.$) readings.

Grain Size.—In all cases the fractures of the ruptured samples were found to be

tion, several alloys were analyzed at a laboratory experienced in this kind of determination, and no disagreement greater than 0.05 per cent of antimony was found. The correspondence between the analyses



FIG. 3.—FRACTURE SURFACE OF ALLOY CONTAINING 1.5 PER CENT ANTIMONY BROKEN IN A SOLIDUS TEMPERATURE DETERMINATION.

Notice that grain-boundary rupture below fractured surface can be seen on side of specimen.

intergranular (Fig. 3). (This could be observed only when the samples were removed from the oil bath immediately, 5 to 10 sec. after breaking.) Such being the case, it is evident that the least overheating prior to rupture should occur when the disposition and size of the grains requires a minimum volume of liquid to form a complete film across the sample; thus a large grain size should suppress apparent overheating; that is, a smaller total quantity of liquid will be required, consuming less heat, and causing less lag of the sample temperature below that of the bath. All the alloys in the alpha range had a very large grain size (Fig. 3) especially after long homogenizing treatments. Rather smaller grain sizes were found in the near-eutectic alloys. It is believed that errors resulting from differing grain size are insignificantly small.

Chemical Analysis.—With the exception of the alloys starred in Table 1, all were analyzed by standard procedures. In addi-

and the intended composition lends confidence to the concentration values reported for the six alloys that were not analyzed.

Other Causes of Rupture.—It is well known that intercrystalline fracture at temperatures slightly below the melting points of metals is common. This type of failure appears in creep tests and has been reported also under conditions of rapid loading. It is important, therefore, to establish that true melting was the cause of rupture in the present experiments. Aside from the convincing observation that the new measurements are in fair agreement with those made by other methods, it is noteworthy that the loads used in the present experiments were so low that no yielding was observed at temperatures more than a fraction of a degree below the temperature of the final rupture; Homer and Plummer found that tin alloys would withstand an indefinitely large number of bends at a temperature of $0.5^{\circ}\text{C}.$ below the melting temperature; the eutectic

sample, No. 63 of Table 1, held for 60 min. at 250°C. and 30 min. at 251°C., showed no signs of failure until the melting temperature, 251.8°C., was reached; the results were self-consistent and wholly reproducible throughout this work.

SUMMARY

The solidus and eutectic temperature of the lead-rich alloys of the lead-antimony system have been redetermined by observing the temperature at which rupture occurs when a slightly loaded specimen is slowly heated.

The solid solubility limit at the eutectic temperature is found to lie near 3.5 per cent of antimony; the eutectic temperature is $251.5 \pm 0.5^\circ\text{C}$.

An improved apparatus for this type of determination is described, and the sources of error inherent in the method are discussed.

REFERENCES

1. C. E. Homer and H. Plummer: Embrittlement of Tin at Elevated Temperatures. *Jnl. Inst. Metals* (1939) 64, 169.
2. R. S. Dean: The System Lead-antimony. *Jnl. Amer. Chem. Soc.* (1923) 45, 1683.
3. E. E. Schumacher and F. C. Nix: The Solidus Line in the Lead-antimony System. *Trans. A.I.M.E.* (1927) 77, 195.
4. H. Seltz and B. De Witt: A Thermodynamic Study of the Lead-antimony System. *Jnl. Amer. Chem. Soc.* (1939) 61, 2594.
5. Roland-Gosselin: Recherches sur la Fusibilité des Alliages Métalliques. *Bull. Soc. Encour. Ind. Nat.* (1896) 5, 1301.
6. O. Ewen: Shrinkage of the Antimony-lead Alloys and of the Aluminum-zinc Alloys during and after Solidification. *Jnl. Inst. Metals* (1910) 4, 130.
7. J. E. Stead: Micro-Chemical Examination of Lead-antimony, Tin-antimony, Tin-arsenic Alloys, etc. *Jnl. Soc. Chem. Ind.* (1897) 16, 200.
8. W. Campbell: Upon the Structure of Metals and Binary Alloys. *Jnl. Franklin Inst.* (1902) 154, 205.
9. W. Gontermann: Über Antimon-Bleilegerungen. *Ztsch. anorg. Chem.* (1907) 55, 419.
10. R. Loebe: Über die Konstitution der ternären Legierungen von Blei, Zinn und Antimon. *Metallurgie* (1911) 8, 7.
11. E. Heyn and O. Bauer: Untersuchungen über Lagermetalle. Beiheft Verh. Ver. Gewerbef. (1914) 224.
12. H. Endo: On the Relation between the Equilibrium Diagram and the Magnetic

- Susceptibility in Binary Alloys. *Sci. Repts. Tohoku Imp. Univ.* (1925) 14, 503.
13. E. Abel, O. Redlich and J. Adler: Das ternäre System Blei-Antimon-Cadmium. *Ztsch. anorg. allgem. Chem.* (1928) 174, 270.
 14. W. Broniewski and L. Sliowski: Sur les Alliages Antimoine-étain. *Rev. de Mét.* (1928) 25, 397.
 15. E. E. Schumacher, Bell Telephone Laboratories, New York, private communication.
 16. I. Obinata and E. Schmid: X-ray Investigation of Antimony-lead and Tin-lead Alloys. *Metallwirtschaft* (1933) 12, 101.
 17. E. E. Schumacher and G. M. Bouton: The Solid Solubility of Antimony in Lead as Determined by Conductivity Measurements on Cold-worked Alloys. *Jnl. Amer. Chem. Soc.* (1927) 49, 1667.

DISCUSSION

(Dana W. Smith presiding)

E. E. SCHUMACHER* AND G. M. BOUTON,* New York, N. Y.—This paper constitutes a valuable contribution to the study of alloy equilibria by focusing attention on the Homer-Plummer technique and by advancing the knowledge of the lead-antimony system in particular. We believe this method gives precise results for the lower end of the melting range of alloys containing peritectics or eutectics, or for pure metals. When a solid solution is involved, the method may give high results, since the breaking temperature indicated must be that at which a finite quantity of liquid exists sufficient to extend in a nearly complete film across the section of the material being tested. Such a temperature must necessarily be somewhat above that at which the first liquid is present. It is, of course, quite possible that the difference between these temperatures is less than the error normally encountered in most thermal methods for determining the solidus.

To aid in interpreting the results obtained by the breaking technique, we are showing the accompanying photomicrographs (Figs. 4 to 6), taken some years ago and presented before this Institute in connection with a determination of the solidus in the lead-antimony system by the Heycock-Neville method. The samples photographed were made of high-purity materials and had been worked and homogenized before being tested. The thermocouples were calibrated against Bureau of Standards temperature standards after each specimen was tested. The series of pictures gives some insight

* Bell Telephone Laboratories, Inc.

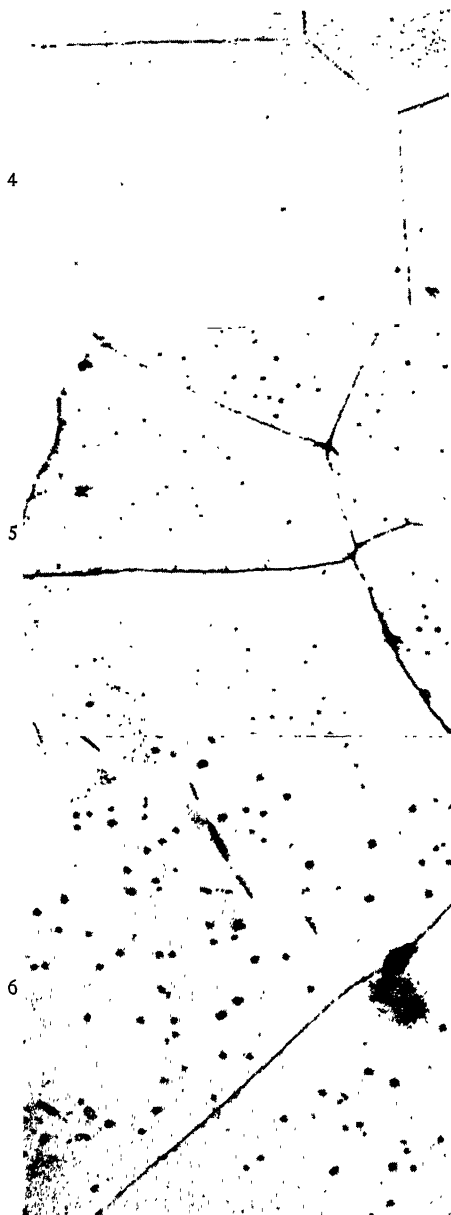


FIG. 4.—ALLOY OF LEAD AND 1.5 PER CENT ANTIMONY SHOWS NO MELTING AT 299°C. $\times 200$.

FIG. 5.—LEAD AND 1.5 PER CENT ANTIMONY SHOWS EVIDENCE OF MELTING BOTH AT BOUNDARIES AND WITHIN GRAINS AT 301°C., WHICH IS 1.5°C. BELOW THE SOLIDUS SHOWN BY THE

as to the manner in which lead-antimony alloys melt. Fig. 4 shows no melting. Fig. 5 shows evidence of melting at 301°C., which is about 1.5° below the temperature shown by the hot-shortness method for this composition. It is significant that appreciable evidence of melting is present within the grains that presumably would not be detected by the Homer-Plummer technique. It is not surprising that worked and homogenized materials should not show preferential grain-boundary melting, since coring and segregation of impurities are characteristic of cast materials. Fig. 6 shows evidence of melting at 292°, which is about 3° below that shown by the newer method.

For a good many years we have used a similar but somewhat simpler fracture technique for determining incipient melting. It consists of horizontally suspending a sample of the material to be tested in a beaker of heated oil. A thermocouple is placed near the sample and thorough stirring is employed. To suspend the specimen two or three turns of 0.01-in. diameter wire are wrapped around one of its ends. In this way the weight of the specimen itself supplies the bending force, which the present authors produce by means of a string and pulley device. The breaks obtained by us are generally coarsely crystalline in appearance, similar to those described in the paper. Our method has the advantage of being extremely simple and having no heavy clamps possessing appreciable heat capacity, which might introduce a lag in the temperature change of the sample by heat conduction. By using a hydrogenated oil such as Crisco, temperatures slightly over 300°C. can be reached without appreciably decreasing the transparency of the oil. Thus visual observation of the sample during the period of test is possible. This method can be used to good advantage when higher temperatures are involved, by conducting the test in inert atmospheres. Furnaces with transparent windows make possible direct observation.

Several years ago a practical problem involving embrittlement presented itself in connection with the repair of splices on telephone cable. The incident is cited here to emphasize the im-

NEW METHOD. $\times 200$.

FIG. 6.—LEAD AND 1.82 PER CENT ANTIMONY SHOWS EVIDENCE OF MELTING AT 292°C., WHICH IS ABOUT 3°C. BELOW THE SOLIDUS SHOWN BY THE NEW METHOD. $\times 200$.

portance of homogenization. In such splices a cylindrical lead sleeve over the joined copper wires is beaten down and sealed to the ends of the two cable sheaths by wiped solder joints. Common repair practice is to pour molten solder over the joint until the old solder has softened and can be wiped off. A tool is then inserted under the beaten-in end of the sleeve, to pry it open. Lead sleeving containing 0.8 per cent antimony frequently cracked during this operation. Studies made under heated oil showed that when this material was bent, at temperatures slightly above the eutectic but considerably below the solidus, soon after the sample was immersed, cracking took place. When, on the other hand, the sample was allowed to remain unstressed at this intermediate temperature for two or three minutes, it did not crack unless heated to the solidus temperature. Our repair men now either let the sleeve cool to below the lead-antimony eutectic temperature before attempting to pry it open or keep it hot for an appreciable period of time by repeated applications of molten solder.

We would be interested to know the weight employed by the authors in applying the bending stresses to the specimens and whether or not any experiments were conducted to show the effect of different bending stresses upon the breaking temperature of specimens of a given composition.

The authors refer to the grade of lead used in most of their alloys as "Omaha." This does not constitute a descriptive term in lead parlance; for example, Omaha lead may contain as little as 0.001 per cent bismuth or as much as 0.25 per cent. We believe that the composition should be stated more exactly.

In summation, we are glad that attention has again been focused on the fracture method. When judiciously and properly used, it is a good procedure; however, if used with incompletely homogenized or impure materials, errors far greater than those obtained with conventional methods may result.

G. EDMUNDS,* Palmerton, Pa.—The shape of the specimen was not described other than by saying that it was a rectangular cross-section bar of regular section. I wonder if in that case the breaks did not occur at the lower grip, cor-

responding to the most highly stressed region of the cantilever. A point was made of the fact that the thermocouple was placed at the center of the specimen. Would it not be preferable to have the couple at the point of breakage, or did the specimen break in the middle?

There would seem to be the possibility of interference by oxide films in this type of determination. Probably it is not serious in lead alloys. On zinc alloys, however, frequently there is present a rather tenacious and strong oxide film. Conceivably this film would cause relatively high values to be obtained by using the method under discussion. I should like to hear this point discussed by Mr. Pellini or Mr. Schumacher.

W. S. PELLINI (author's reply).—We have varied the weights applied to the sample from $\frac{3}{4}$ lb. and less to one pound or slightly more, and have not noted any effect of this change. Most of the specimens did not break at the grip; they broke in the middle, and they did not break into two pieces but into three or more pieces. Embrittlement was quite definite, as is shown by the fact that breakage occurred in three or four places at once. The openings were rectangular in cross section; we did not make an investigation of the effect of the shape. Incidentally, some cylindrical samples were tested and no difference was observed, but we did not make any particular effort to notice whether the shape had an effect upon the breakage.

F. N. RHINES (author's reply).—I should like to thank Messrs. Schumacher and Edmunds for commenting on the method so thoroughly. Bringing out the possible defects in any technique is very important. I am inclined to agree that the method is more sensitive where one would expect to get large amounts of liquid at the beginning than where relatively little liquid occurs, as near the pure metal side of the system.

Perhaps it should be pointed out that the break does occur in a very short time after the liquid first forms, whereas in the quenching method considerable time must elapse before the structure is fixed by quenching. Thus a true grain-boundary segregation of liquid may spheroidize into isolated puddles before it is observed, giving the impression that no grain-

* New Jersey Zinc Company.

boundary rupture would have appeared. If we could see the liquid at once, it is possible that we might see only a very thin film at grain boundaries before anything becomes apparent within the grains where the nucleation of liquid is slow. The observation that the quenching method actually gives lower temperatures is interesting and important, I think. We have no analysis of the Omaha pig. Instead, the work was checked with high-purity lead.

With regard to Mr. Edmunds' very interesting suggestion about the possible effect of oxides, it is my impression that there would be a real effect of oxide skins on metals like

aluminum (probably zinc too) where a fairly tough oxide film forms. Lead oxide, on the other hand, is characteristically soft, and I would not think that it would have an appreciable effect on the apparent strength of the metal. However, I am inclined to believe that this method is subject to a related error. Certain materials can oxidize very rapidly at the grain boundaries at temperatures slightly below the eutectic or where melting occurs. I think that one might encounter cases where low readings were obtained by the formation of low-melting oxide liquids at the grain boundaries. I believe that something of that sort has been encountered in trying the method on steels.

The Hardness of Certain Primary Copper Solid Solutions

By J. H. FRYE, JR.,* MEMBER A.I.M.E. AND J. W. CAUM†

(New York Meeting, February 1943)

ONE of the most important methods of increasing the hardness of metals is alloying. In spite of the widespread use of alloys, the fundamental mechanism of alloy hardening is little understood. This is true even of the simplest form of alloy, the primary substitutional solid solution in which solute atoms substitute for solvent atoms at random in the crystal lattice of the latter. A fundamental understanding of the mechanism of solid-solution hardening would be important, both because of the widespread use of alloys of this type and because of the light that might be thrown on the mechanism of hardening in more complicated alloys.

The present investigation covers the hardness of primary substitutional solid solutions of zinc, gallium, germanium, and arsenic in copper. All of these are B sub-group elements from the third period of the periodic table. Cu, Zn, Ga, Ge, and As are in groups I, II, III, IV, and V, respectively, and lie just to the right of the transition elements. Because of their cost, it is unlikely that Ga-Cu and Ge-Cu solutions will ever be of commercial importance, but the intent of this study has been to discover some of the fundamentals of solid-solution hardening and it has been demonstrated that such a study is far more likely to be fruitful if alloys are made up on the basis of position of the constituent elements in the periodic table than if commercially important alloys are used.

Manuscript received at the office of the Institute Nov. 2, 1942. Issued in METALS TECHNOLOGY, February 1943.

* Assistant Professor of Metallurgy, Lehigh University, Bethlehem, Pa.

† Lehigh University, Bethlehem, Pa.

Many investigations have been made of the hardness of substitutional solid solutions, but lack of attention to purity of the metals, infrequent grain-size control, and the use of varying testing techniques have virtually invalidated any comparisons. The purpose of most investigations has been to solve immediate problems and not to solve the primary problem: Why do solid solutions usually have a greater hardness than pure metals?

PREVIOUS WORK

Theories have been advanced to account for the hardness of solid solutions, but relatively little experimental work has been done. Perhaps the first experimental work of merit was that of Norbury¹ on copper alloys. He showed that for several alloys there was a correspondence between the hardness of one atomic per cent solutions and atomic volume of the solutions. More recently Brick, Martin, and Angier² have investigated the effect of various solute elements on the hardness of copper. They concluded that the hardening effect of these solutes depended "primarily on the difference in atomic volume of solute and solvent or, relatedly, upon the parameter change of the solvent or the extent of solid solubility." They also observed the effect of these elements on hardness and texture developed by rolling and by annealing of rolled material. Austin³ examined the hardness and response to heat-treatment of various iron solid solutions. Frye and Hume-Rothery⁴ measured the hardness of a number of silver solid solutions containing approximately

¹ References are at the end of the paper.

2.5 and 5 atomic percentages of solute. They found that the hardness of these solid solutions depended on at least four factors. These were plastic deformation produced by the hardness indenter, concentration of solute, the row of the periodic table from which the solute was taken, and the increase in the lattice parameter of the solvent produced by the solute. By holding the first three of these variables constant, it was possible to show a relation between hardness and lattice parameter.

EXPERIMENTAL PROCEDURE

Increases in the hardness of copper produced by the solutes used in this investigation are small. Therefore, considerable stress has been placed on accuracy. All measurements have been made as carefully as possible and an attempt has been made to keep impurities in the metal at a minimum.

Hardness measurements were made by means of the Meyer analysis.⁵ This method of testing was selected for three reasons: (1) results of high accuracy can be secured; (2) much previous work on other alloys has employed this method and comparison could be made with this work only by using the same test; (3) the Meyer analysis permits an evaluation of rate of work-hardening.

The specimens used for the hardness test followed standards outlined by O'Neill.⁶ They were at least 19 mm. in diameter and 17 mm. in depth. The actual Meyer analysis consisted of applying a load for a minimum of 15 sec. to a 4-mm. ball and then measuring the diameter of the recovered impression produced. The ball was next centered in the previous impression and a larger load applied for 15 sec. Again the diameter of the recovered impression was measured. And so the Meyer analysis proceeded, increasing loads and measuring impression diameters within the limits $0.1 < \frac{d}{D} < 1$ where d indicates

diameter of impression and D , diameter of ball.

With the data thus collected, a straight-line graph of $\log L - \log d$ may be plotted according to the relation shown by Meyer:

$$L = ad^n \text{ or } \log L = \log a + n \log d.$$

L = applied load.

a = constant.

d = impression diameter in mm.

n = constant (slope of line).

This straight line is extrapolated to $\log d = 0.602$, ($\log 4$), and $\log d = 0$, ($\log 1$), to read the load, L_u , necessary to produce a 4-mm. impression, and the load, L_a , producing a 1-mm. impression. Two Meyer hardness numbers are calculated from these loads and diameters, one corresponding to a slight amount of plastic deformation, the other to the ultimate amount of plastic deformation that can be obtained in testing with the 4-mm. ball:

$$P_a = \frac{L_a}{\sqrt[3]{4\pi d^2}} \quad (d = 1) \quad [1]$$

$$P_u = \frac{L_u}{\sqrt[3]{4\pi d^2}} \quad (d = 4) \quad [2]$$

The Meyer hardness test may be used to obtain a type of stress-strain curve for the specimen under analysis. This arises from the fact that the Meyer hardness increases with impression diameter because of work-hardening, which increases with penetration of the ball. This relation can be investigated by the following development of the Meyer equation:

$$\begin{aligned} P &= \frac{L}{\sqrt[3]{4\pi d^2}} & (L = ad^n) \\ P &= \frac{ad^n}{\sqrt[3]{4\pi d^2}} \\ P &= \frac{4ad^{n-2}}{\pi} \end{aligned}$$

The constant n may be evaluated by obtaining the slope of the $\log L - \log d$ curve. The constant a is evaluated as follows:

When

$$\begin{aligned}d &= 1 \\L_a &= ad^n \quad (d = 1) \\L_a &= a\end{aligned}$$

Thus having obtained values for a and n , it is only necessary to substitute any value for d in Eq. 3 and p may be calculated for that impression diameter (within the limits of 1 mm. $< d < 4$ mm.).

The purities of the metals used to make up the alloys studied were Cu, 99.991 per cent; Ga, 99.9; Ge, 99.5+; Zn, 99.99+; As, 99.5. The pure copper and alloys of gallium and germanium with copper were melted in graphite molds, which were enclosed in an evacuated silica tube. Power for melting was supplied by an Ajax-Northrup induction furnace. The graphite molds had an ash content of less than 0.75 per cent, and a separate mold was used for each alloy. Alloys of zinc and arsenic with copper were melted in graphite molds under a covering of fused borax.

The vacuum obtained during melting was 3 mm. of mercury. This was considered quite sufficient to eliminate oxidation in the metals, as Mr. J. G. Thompson, of the National Bureau of Standards, wrote: "We have thus deoxidized 10 lb. of tough-pitch copper in 1 to 2 hr., when the pressure in the furnace never was lower than 3 or 4 mm. of mercury."

The resulting ingots were examined for gravity segregation, by making Rockwell hardness measurements along their length. If any segregation was found, they were remelted until none could be detected by this method. These ingots were 1 in. in diameter and about 5 in. long.

When no gravity segregation could be observed, the ingots were squeezed in a compression machine and annealed in an evacuated Pyrex tube at not less than 650°C. for two days, to eliminate cored structure. They were squeezed again nearly to a square shape in order to break up the grain structure; the ingots were turned

down to a 3/4-in. rod and 20-mm. lengths were cut from each. The faces of the 20-mm. specimens were made parallel to within 2° and one face was polished to a final step of levigated alumina and selvvyt cloth. The surfaces polished on specimens from the same ingot faced one another in the original ingot. This was done to eliminate, as much as possible, any difference in solute concentration if it was necessary to make more than one Meyer analysis on the same alloy.

These specimens were annealed at various temperatures in evacuated Pyrex glass tubes, in order to obtain definite grain sizes. The annealing temperatures were varied, so that at least one specimen of each alloy or pure copper had a grain diameter of 0.074 mm., or was very near to this diameter. When the one grain size was only near the standard, one other specimen was annealed at such a temperature as to give another grain size within the same range as the first, so that a correction for the variation of Meyer hardness with grain size could be made to the standard grain diameter.

The hardness testers used for applying the loads were a Brinell and a Diamo-Brinell. The Brinell was calibrated against a proving ring at the Tinus Olsen Manufacturing Company's plant in Philadelphia, and the Diamo-Brinell was calibrated against dead weights supplied to Fritz Laboratory at Lehigh University by the Tinus Olsen Manufacturing Co. After calibrations were complete, the testers were checked against one another by hardness tests and were found to be in good agreement. At the end of the research the testers were recalibrated against a proving ring that had been calibrated at the National Bureau of Standards. Calibrations at the beginning and end of the research agreed within one per cent.

The impression diameters were read by means of a traveling microscope accurate to ± 0.002 mm. Before each use it was checked against a line standard obtained from the

National Bureau of Standards. Four different diameters, equally spaced around the impression, were measured, and the value of d plotted on the $\log L - \log d$ graphs was an average of these.

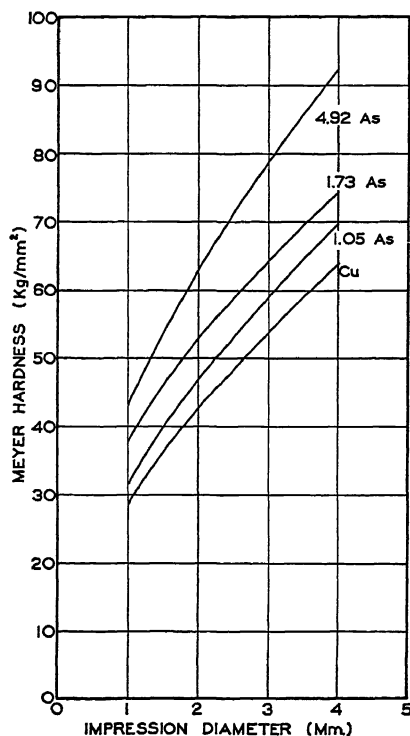


FIG. 1.—VARIATION OF MEYER HARDNESS WITH IMPRESSION DIAMETER FOR PURE COPPER AND FOR COPPER CONTAINING VARIOUS ATOMIC PERCENTAGES OF ARSENIC.

After the Meyer analysis was completed, the specimens were cut vertically down through the hardness impression. One half was polished and the grain size was measured by the traveling microscope. The cross hairs were set at a grain boundary just below the plastically deformed portion around the hardness impression and the vernier reading was taken. One hundred grains were crossed and another reading was taken. The difference divided by 100 gave the average grain diameter. This was

done four times beneath the impression and the four results were averaged to give the average diameter of grains in the specimen. The hardnesses of the alloys are all compared at an average grain diameter of 0.074 mm., which corresponds to 59 grains per sq. millimeter.

The remaining halves of the hardness specimens were sent to the American Brass Co. for chemical analyses. Drillings for the analyses were taken from directly below the hardness impression. Spectrographic analyses also were made on the alloys, and the following was reported:

"In each instance spectrographic examinations showed the samples to be of good purity. The spectrographs showed absence of metals other than copper and arsenic and copper and zinc in the arsenic-copper and zinc-copper specimens. In the gallium-copper specimens there was a small amount of silver, a slight amount of antimony, and a slight amount of lead. Samples of germanium-copper carried a small amount of silver, a slight amount of iron, and a very slight amount of lead."

"Our spectrographer says that the line intensity is less than in N.E.C. copper and thinks the silver is certainly less than 0.009 per cent, the lead less than 0.0009 per cent in all samples. However, you realize that line intensity is unreliable with the absence of standards of the same base composition."

HARDNESS AND PLASTIC DEFORMATION

One of the variables influencing the hardness of a pure metal is the amount of previous deformation. It is known that solutes usually produce hardness increases when their atoms replace atoms of a solvent metal in primary substitutional types of alloys. These hardness increases, due to various solutes, might be expected to depend in part on the plastic deformation created by penetration of the testing ball. This can be investigated by examining the variation of P with d , since any increase in

P with d is due to work-hardening. Such graphs for As-Cu are shown in Fig. 1.

In this graph it is shown that (dP/dd) , which is a measure of rate of work-hardening,

Owen and Roberts.⁷ These data are in fair agreement with those of Hume-Rothery, Lewin, and Reynolds,⁸ but they were used because the last-named workers did not

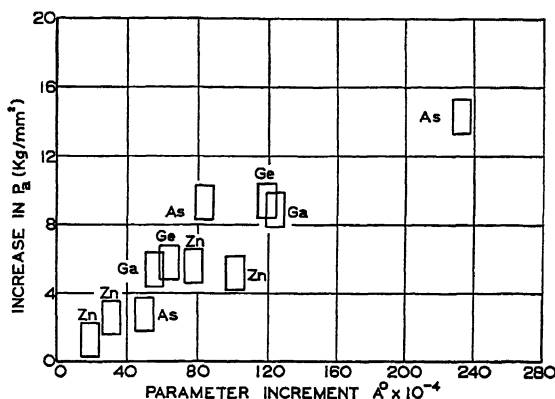


FIG. 2.—INCREASE IN MEYER HARDNESS P_a WITH INCREASE IN LATTICE PARAMETER OF COPPER PRODUCED BY VARIOUS CONCENTRATIONS OF DIFFERENT SOLUTES.

ing, is greater for the alloys than for pure copper. This is also true for Ge-Cu, and for the more concentrated Ga-Cu. On the other hand, 2 per cent Ga and all the zinc alloys differ little from pure copper in this respect. In general the rate of work-hardening appears to increase with concentration and with subgroup number of the solute element in the periodic table.

It must be concluded that plastic deformation is one of the variables affecting the increase in hardness produced by various solutes.

HARDNESS, COMPOSITION AND LATTICE PARAMETER

Next was investigated the relation between hardness increases produced by the solutes zinc, gallium, germanium and arsenic and the increase in lattice parameter of copper produced by these solutes. All hardness values are based on a grain diameter of 0.074 mm.

In Table 1 hardnesses and increases in parameter for the various compositions have been listed. Increases in parameter have been calculated from the data of

measure the parameters of arsenic-copper alloys.

TABLE 1.—Hardnesses and Increases in Parameter

Atomic Per Cent Solute	a	n	P_a	P_u	$\Delta S, \text{\AA.}$
1.93 Ge.....	26.43	2.523	33.63	69.53	0.0064
3.60 Ge.....	30.06	2.527	38.27	79.41	0.0119
2.08 Ga.....	26.85	2.503	34.19	68.69	0.0056
4.45 Ga.....	29.65	2.488	37.75	74.29	0.0124
0.90 Zn.....	23.66	2.563	30.13	65.77	0.0019
1.60 Zn.....	24.66	2.547	31.40	66.97	0.0031
4.02 Zn.....	27.04	2.488	34.42	67.75	0.0078
5.11 Zn ^a	26.73	2.500	34.04	68.06	0.0102
1.05 As.....	24.83	2.573	31.62	69.97	0.0050
1.73 As.....	29.92	2.487	38.08	74.84	0.0084
4.92 As.....	33.89	2.550	43.15	92.45	0.0233
Vacuum-melted Cu.	22.65	2.575	28.84	63.96	

^a Average grain diameter, 0.120 mm.

Hardness increment and parameter values have been plotted in Figs. 2 and 3. The actual points have been surrounded by rectangles, which represent experimental error. Whereas it is improbable that definite limits can be set on the experimental error, undoubtedly the majority of the values are accurate within the limits indicated by the

rectangles. These graphs show that there is no simple relation between hardness and lattice parameter for alloys of various concentrations.

in Figs. 4 and 5, a clear relationship between the two is revealed. These graphs are based on the data of Table 2. Fig. 4 shows the relation between the Meyer hardness P_a ,

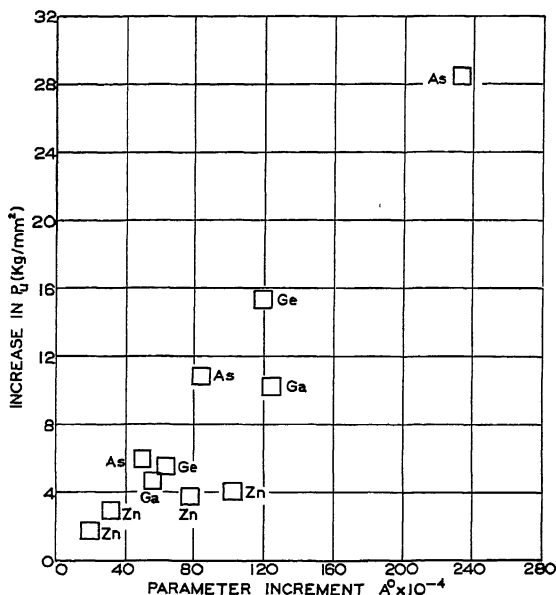


FIG. 3.—INCREASE IN ULTIMATE MEYER HARDNESS P_u WITH INCREASE IN LATTICE PARAMETER OF COPPER PRODUCED BY VARIOUS CONCENTRATIONS OF DIFFERENT SOLUTES.

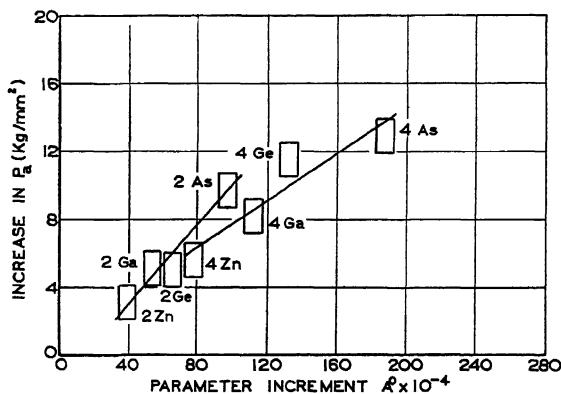


FIG. 4.—INCREASE IN MEYER HARDNESS P_a WITH INCREASE IN LATTICE PARAMETER OF COPPER PRODUCED BY TWO AND FOUR ATOMIC PERCENTAGES OF VARIOUS SOLUTES.

On the other hand, if hardness increment is plotted against parameter increment for equiatomic compositions, as has been done

($d = 1$), and parameter increment for two and for four atomic percentages of solute. Fig. 5 shows the relation between the

ultimate Meyer hardness P_u , ($d = 4$), and parameter increment for the same solutes.* Hardnesses corresponding to intermediate values of impression diameters have not

are plastic deformation, concentration of solute, and expansion of the solvent crystal lattice. This is in full agreement with results on silver alloys.⁴

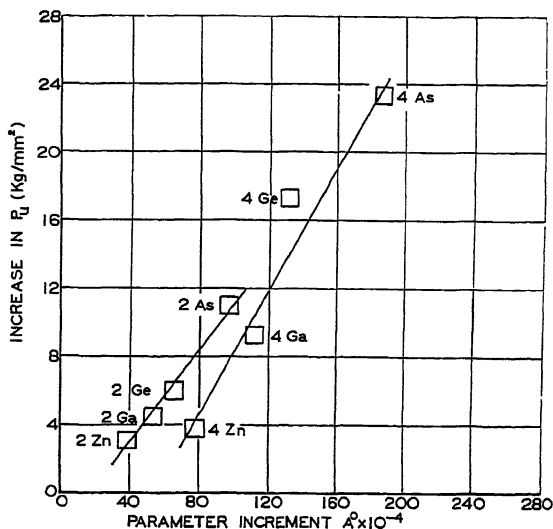


FIG. 5.—INCREASE IN ULTIMATE MEYER HARDNESS P_u WITH INCREASE IN LATTICE PARAMETER OF COPPER PRODUCED BY TWO AND FOUR ATOMIC PERCENTAGES OF VARIOUS SOLUTES.

been plotted, but these may be expected to show the same relation. These curves clearly show that, for equal concentration and equal plastic deformation, the hardness increases produced by these solutes are proportional to expansion of the copper lattice produced by them.

CONCLUSIONS

With reference to the alloys discussed herein, the following conclusion may be drawn: At least three variables control the hardness increases produced in copper by elements in dilute solid solution. These

ACKNOWLEDGMENTS

The authors wish to thank Mr. John H. Frye, Sr., for supplying the fellowship that made this work possible; Prof. Gilbert E.

TABLE 2.—*Relationship between Hardness and Parameter Increment*

Atomic Per Cent Solute	P_s	P_u	$\Delta S, \text{\AA.}$
2 Ge.....	33.8	69.9	0.0066
4 Ge.....	40.3	81.3	0.0132
2 Ga.....	34.0	68.5	0.0054
4 Ga.....	37.1	73.3	0.0112
2 Zn.....	31.9	67.1	0.0039
4 Zn.....	34.4	67.8	0.0078
2 As.....	38.5	75.0	0.0097
4 As.....	41.7	87.4	0.0187
Vacuum-melted Cu.....	28.8	64.0	

* The points for 4 atomic per cent Ge in Figs. 4 and 5 are in poor agreement with the others. Very erratic results were obtained from the chemical analyses. From one hardness specimen, samples were analyzed to contain 4.62 per cent Ge by The American Brass Co.; 4.86 per cent Ge by Butts and Mcikle at Lehigh, and 4.72 per cent Ge by The American Brass Co. This scatter may have been due to segregation and work on this alloy would have been repeated but for the pressure of war work.

Doan, Prof. Allison Butts, and Mr. Martin Sheska, of Lehigh University, for encouragement, advice, and help with the experimental work, respectively, and the New Jersey Zinc Co. for several grams of gallium.

The assistance of the American Brass Co., and of Messrs. C. S. Smith and R. P. Nevers, of that company, has been invaluable. They supplied all the copper used and made all chemical and spectrographic analyses.

REFERENCES

1. Norbury: *Jnl. Inst. Metals* (1923) **29**, 407, 423; *Trans. Faraday Soc.* (1923-24) **19**, 586.
2. R. M. Brick, D. L. Martin and R. P. Angier: *Amer. Soc. Metals Preprint* 37 (Oct. 1942).
3. C. R. Austin: *Amer. Soc. Metals Preprint* (Oct. 1942).
4. J. H. Frye, Jr. and W. Hume-Rothery: *Proc. Roy. Soc.* (1942) **181-A**, 1.
5. E. Meyer: *Ztsch. Ver. Deut. Ing.* (1908) **52**, 645.
6. H. O'Neill: *The Hardness of Metals and Its Measurement*. London, 1934. Chapman and Hall, Ltd.
7. Owen and Roberts: *Phil. Mag.* (1939) [7] **27**, 294-327.
8. Hume-Rothery, Lewin, and Reynolds: *Proc. Roy. Soc.* (1936) **157-A**, 167.

Hardness and Lattice Stress in Solid Solutions

By J. H. FRYE, JR.,* MEMBER A.I.M.E., J. W. CAUM† AND R. M. TRECO†

(New York Meeting, February 1943)

It has been suggested that: "Insofar as the hardening due to a solute depends upon the increase of lattice parameter produced by it, it is reasonable to suppose that this hardening might be related to the resistance which the pure solvent would offer to increase in its parameter."¹ It was further suggested that this hypothesis might be examined by comparing the hardnesses of analogous silver and copper alloys, since the stress necessary to produce a given lattice expansion is quite different in the two metals. Suitable data^{2,3,4} are now available on these alloys, and we shall proceed to an examination of the hypothesis quoted above.

HARDNESS, LATTICE PARAMETER AND IONIC OVERLAP

Increase in ultimate Meyer hardness has been plotted against increase in lattice parameter in Figs. 1 and 2. It is believed that most of the values are accurate within the limits indicated by the rectangles. These data are also presented in Table 1. Ultimate Meyer hardness, P_u , is defined by the equation:

$$P_u = \frac{4L}{\pi D^2}$$

where L = load,

D = diameter of an impression having the same diameter as the

testing ball, which in this case is 4 mm. Increase in lattice parameter is defined as the difference between the lattice parameter of the solid solution and that of the pure solvent. The curves in Figs. 1 and 2 are based on equal solute concentration and an equal degree of plastic deformation produced by the testing ball. Hardnesses are corrected to a constant grain size for copper and silver alloys, respectively, and these two grain sizes are approximately equal. Furthermore, all solutes are from the same period of the B subgroup of the periodic table as their solvent.

TABLE 1.—Increase in Ultimate Meyer Hardness and in Lattice Parameter

Alloys, Per Cent	ΔP_u Kg. per Sq. Mm.	ΔS , Å.	Lattice Stress, Kg. per Sq. Mm.
2 Cd-Ag.....	0.6	0.0035	27.1
2 In-Ag.....	2.2	0.0060	44.7
2 Sn-Ag.....	3.6	0.0077	57.4
2 Sb-Ag.....	9.2	0.0116	86.4
2 Zn-Cu.....	3.1	0.0039	45.1
2 Ga-Cu.....	4.5	0.0054	62.4
2 Ge-Cu.....	6.0	0.0066	76.3
2 As-Cu.....	11.0	0.0097	112.1
4 Cd-Ag.....	3.5	0.0075	55.9
4 In-Ag.....	7.3	0.0121	90.2
4 Sn-Ag.....	13.2	0.0162	120.7
4 Sb-Ag.....	19.2	0.0236	175.8
4 Zn-Cu.....	3.8	0.0078	90.1
4 Ga-Cu.....	9.3	0.0112	129.5
4 Ge-Cu.....	17.3	0.0132	151.6
4 As-Cu.....	23.4	0.0187	216.2

Manuscript received at the office of the Institute Nov. 2, 1942. Issued in METALS TECHNOLOGY, April 1943.

* Assistant Professor of Metallurgy, Lehigh University, Bethlehem, Pa.

† Lehigh University, Bethlehem, Pa.

References are at the end of the paper.

The question arises as to whether or not lattice parameter is the only factor controlling the hardness of these alloys. There

is at least one other variable present that might reasonably be expected to affect the hardness of these solutions, which is not

distance from the center of the ion. In this figure r is one half the distance between ions that are nearest neighbors. There is a con-

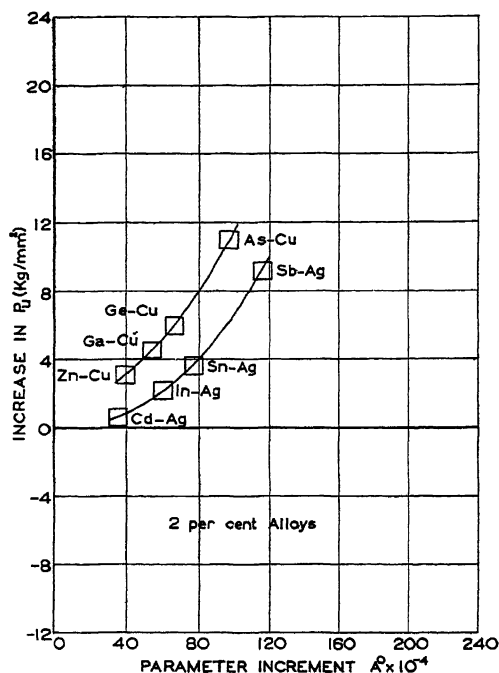


FIG. 1.—INCREASE IN ULTIMATE MEYER HARDNESS, P_u , WITH INCREASE IN LATTICE PARAMETER OF COPPER OR SILVER PRODUCED BY TWO ATOMIC PERCENTAGES OF VARIOUS SOLUTES.

taken into account in these curves. This is ionic overlap, or overlap of the electron clouds of the ions. This factor is treated here in a qualitative way in the hope of eliciting discussion and further investigation along these lines.

Ionic overlap will be discussed in terms of copper and copper alloys, but the discussion is also applicable in a general way to silver and its alloys. The copper lattice may be thought of as consisting of ions with a charge of $+1$ held together by valency electrons.⁵ These copper ions do not have discrete boundaries, but extend indefinitely into space. This is shown graphically in Fig. 3,⁶ which shows the variation of the charge density of the 3d electron shell (outermost shell) of the copper ion with

siderable overlap of the outer shells of the ions in a copper crystal.

This overlap accounts for well over half of the elastic resistance to shear in a copper crystal.⁵ It is reasonable to expect that the elastic resistance to shear will affect the resistance to shear in a work-hardened lattice, and it has been suggested that this is true.⁶ Therefore it seems reasonable to consider the effect on this ionic overlap of substituting an atom of zinc, gallium, germanium or arsenic for a copper atom to form a solid solution.

First, each of these elements expands the copper lattice and thus diminishes the overlap of the ions. Second, the radial extension into space of the ions of any one of these solutes is less than that of the copper ion.

This is seen in an examination of the ionic radii by Pauling,⁷ listed in Table 2. These ionic radii give a comparative measure of the radial extension of the charge densities

Because the curve of Fig. 3 drops with extreme rapidity at first and then tends to flatten out, it might be expected that the substitution of zinc for copper would be

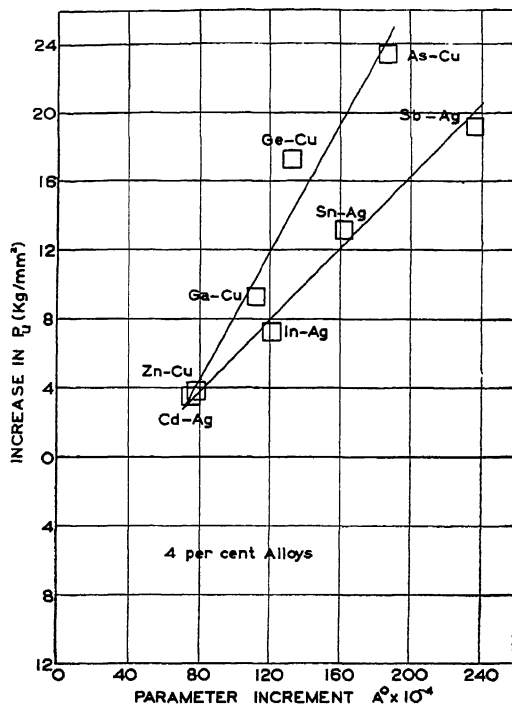


FIG. 2.—INCREASE IN ULTIMATE MEYER HARDNESS, P_u , WITH INCREASE IN LATTICE PARAMETER OF COPPER OR SILVER PRODUCED BY FOUR ATOMIC PERCENTAGES OF VARIOUS SOLUTES.

of these ions. Thus both the lattice expansion produced by these solutes and the replacement of copper ions by smaller solute ions decrease the ionic overlap that existed in the solvent. This decrease in ionic overlap may be expected to lessen any hardness increase due to stresses arising from the lattice expansion produced by the solutes.

Since the lattice expansions produced in copper by equal atomic percentages of the solutes—zinc, gallium, germanium and arsenic—increase in that order and the ionic radii of these solutes decrease in the same order, it follows that the ionic overlap in the crystals will decrease in the order Cu, Zn-Cu, Ga-Cu, Ge-Cu, and As-Cu.

more serious in its effect on ionic overlap and hence in the effect of that on hardness than would be the replacement of the zinc by Ga, Ga by Ge or Ge by As.

TABLE 2.—Ionic Radii

Ion	Ionic Radii, C.N. 6, Å.	Ion	Ionic Radii, C.N. 6, Å.
Cu ⁺¹	0.96	Ag ⁺¹	1.26
Zn ⁺²	0.88	Cd ⁺²	1.14
Ga ⁺³	0.81	In ⁺³	1.04
Ge ⁺⁴	0.76	Sn ⁺⁴	0.96
As ⁺³	0.71	Sb ⁺³	0.89

If this be correct, the effect of ionic overlap would be mitigated and a true relation

between hardness and lattice parameter would be more nearly approached in curves such as those of Figs. 1 and 2 by taking Zn-Cu and Cd-Ag as the origin rather than

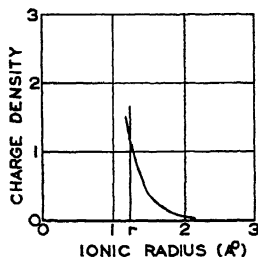


FIG. 3.—VARIATION IN CHARGE DENSITY OF A COPPER ION WITH DISTANCE FROM ITS CENTER.

The midpoint between neighboring ions in the copper crystal is indicated by the vertical line at r .

Cu and Ag. For this reason, in considering the relation between hardness and lattice stress, we shall compare increases in hardness with increases in lattice stress, which arise when the zinc atom in solid solution in copper or the cadmium atom in solid solution in silver is replaced by another solute.

HARDNESS AND LATTICE STRESS

This section will present an empirical relation between increase in hardness and increase in lattice stress when cadmium in silver is replaced by indium, tin or antimony or when zinc in copper is replaced by gallium, germanium or arsenic. For purposes of this discussion lattice stress will be defined as the stress that would be necessary to expand the lattice of pure silver or copper by any given amount.

The stresses necessary to produce in these pure metals the same lattice parameters as are found in the copper and silver alloys mentioned above will be estimated. This will be done by use of Bridgman's equation⁸ for the hydrostatic compression of a metal. The relation between hydrostatic pressure and change in volume of a metal is given as

$$-\frac{\Delta V}{V_0} = mp - np^2$$

in which

V_0 = original volume,
 ΔV = change in volume,
 p = pressure,
 m = a constant,
 n = a constant,

Since our data are in terms of lattice parameter rather than volume, we shall convert the volume term of this equation to a parameter term.

Let S indicate original parameter and s , change in parameter. Then:

$$\frac{\Delta V}{V_0} = \frac{(S+s)^3 - S^3}{S^3}$$

By substitution in the equation above,

$$-\frac{(S+s)^3 - S^3}{S^3} = mp - np^2$$

Differentiate this equation with respect to s , and find that

$$\left(\frac{dp}{ds}\right)_{s=0} = -\frac{3}{mS}$$

The only interest here is in absolute values, so the negative sign may be disregarded, making

$$\left(\frac{dp}{ds}\right)_{s=0} = \frac{3}{mS}$$

Although in all probability $(dp/ds)_{s=0}$ is applicable to both expansion and contraction of a lattice, it has been derived from an equation for compression and conveniently may be termed the incompressibility. Taking values of the constant m from Bridgman⁸ and lattice parameters from Hume-Rothery,⁹ we find that the incompressibility of copper is 11,560 kg. per sq. mm. per Å., and that of silver is 7450 kg. per sq. mm. per Å. Although these figures give some measure of the resistance of these metals to expansion over a range of lattice parameter, it must be emphasized that they are strictly applicable only to the initial resistance of the lattice to expansion.

These values of $(dp/ds)_{s=0}$ have been used to attempt an estimate of the stress necessary to produce in the pure silver or copper the lattice expansions produced in

parameter and incompressibility. In Fig. 6, increase in hardness has been plotted against increase in lattice stress for both 2 and 4 atomic percentages of solute. To a

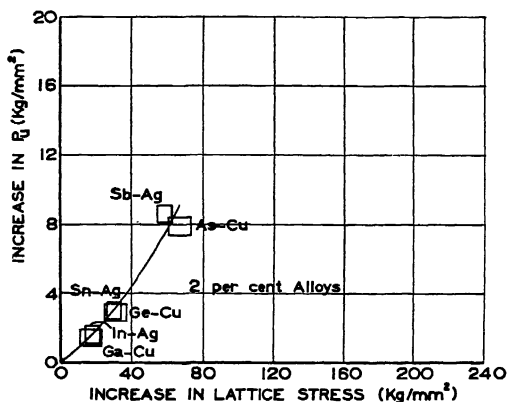


FIG. 4.—INCREASE IN ULTIMATE MEYER HARDNESS, P_u , WITH INCREASE IN LATTICE STRESS WHEN ZINC IN COPPER OR CADMIUM IN SILVER IS REPLACED BY ANOTHER SOLUTE.

silver or copper by the various solutes. This has been done by multiplying the lattice expansion by $(dp/ds)_{s=0}$ for copper or silver, as the case might be.* Values of the estimated lattice stress are listed in Table 1. It is noteworthy that the copper solutions show the more rapid increase of hardness with lattice expansion and that copper is more incompressible than silver.

In Table 3 are listed increases in hardness and in lattice stress when Zn in Cu is replaced by Ga, Ge, or As and when Cd in Ag is replaced by In, Sn, or Sb. These data are plotted in Figs. 4 and 5 for 2 and 4 atomic percentages of solute, respectively. Most of the points lie on a single curve within limits of experimental error as indicated by the rectangles, and these limits of error do not allow for any error arising in the estimation of lattice stress from lattice

first approximation points lie on a single curve.

DISCUSSION OF RESULTS

The relation between increase in hardness and increase in lattice stress presented in Figs. 4, 5 and 6 is essentially empirical. Nevertheless, a discussion of some of the factors involved might be useful.

TABLE 3.—Increases in Hardness and in Lattice Stress by Chemical Replacements

Alloys, Per Cent	ΔP_u , Kg. per Sq. Mm.	Increase in Lattice Stress, Kg. per Sq. Mm.
2 Cd-Ag.....	0	0
2 In-Ag.....	1.6	17.6
2 Sn-Ag.....	3.0	30.3
2 Sb-Ag.....	8.6	59.3
2 Zn-Cu.....	0	0
2 Ga-Cu.....	1.4	17.3
2 Ge-Cu.....	2.9	31.2
2 As-Cu.....	7.9	67.0
4 Cd-Ag.....	0	0
4 In-Ag.....	3.8	34.3
4 Sn-Ag.....	9.7	64.8
4 Sb-Ag.....	15.7	119.9
4 Zn-Cu.....	0	0
4 Ga-Cu.....	5.5	39.4
4 Ge-Cu.....	13.5	61.5
4 As-Cu.....	19.6	126.1

* Although lattice stress is estimated from the average lattice expansion throughout the crystal, there is no implication that a uniform change in lattice parameter would increase the hardness. In fact, experimental evidence is at hand indicating that hardness increases are due not to an average change in lattice but to localized expansions or contractions in the neighborhood of the solute atoms.²

The most straightforward approach to the problem of hardness and lattice stress would be to calculate the stress produced in the lattice by the solute and then to calcu-

the stress and strain distribution in a metal about the penetrating ball during a hardness test.

An alternative method of attack was

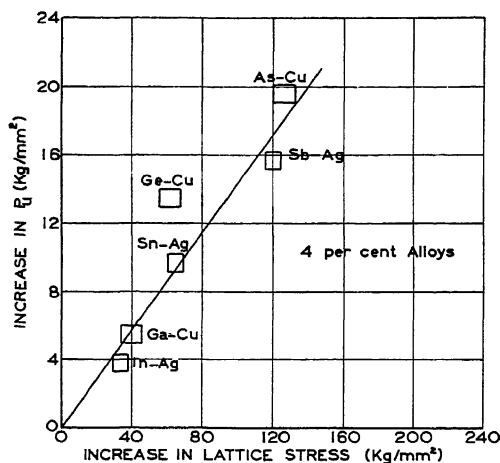


FIG. 5.—INCREASE IN ULTIMATE MEYER HARDNESS, P_u , WITH INCREASE IN LATTICE STRESS WHEN ZINC IN COPPER OR CADMIUM IN SILVER IS REPLACED BY ANOTHER SOLUTE

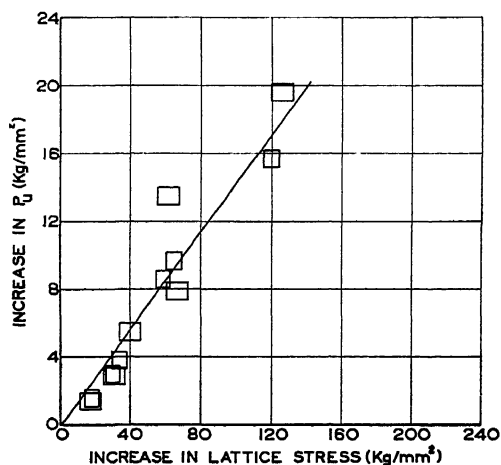


FIG. 6.—INCREASE IN ULTIMATE MEYER HARDNESS, P_u , WITH INCREASE IN LATTICE STRESS WHEN ZINC IN COPPER OR CADMIUM IN SILVER IS REPLACED BY ANOTHER SOLUTE. Points are for both 2 and 4 atomic percentages of solute.

late the increase in hardness that should arise from this stress. There are many difficulties in the way of such a calculation. One of these is the impossibility, in our present state of knowledge, of analyzing

selected, essentially as follows: The silver and copper alloys considered here are quite analogous. Copper and silver are both in group I of the B subgroups of the periodic table and have face-centered cubic lattices.

Furthermore, all solutes are from the same period of the B subgroups as their solvent. Increase in hardness was plotted against lattice stress for the silver alloys and a simple but not necessarily significant relation was revealed between the two. If this relation were significant, it should also hold for the closely analogous copper alloys. This was found to be true, as indicated in Figs. 4 and 5, where the relation between increase in hardness and increase in lattice stress is shown to be the same for both copper and silver alloys. That a single simple relation exists between hardness and lattice stress for two series of solid solutions differing both as to solvents and solutes is evidence in favor of the validity of the relation.

There are two points of uncertainty in the present work which are worthy of further investigation. The discussion of ionic overlap has been purely qualitative and it is not certain that the correction made for it is justified.

Lattice stress is defined as the stress necessary to produce a given lattice expansion in the pure solvent metal. The exact relation between lattice stress and the actual stress existing in the solid solution lattice is not known. X-ray measurements give only the mean value of the lattice parameter, but it is recognized that large variations may occur from point to point throughout the lattice. In the absence of this knowledge, any calculation of the actual stress in the solid solution lattice would appear to be difficult.

The relation between hardness and lattice stress has been presented as an empirical one. Some indication has been given, however, of the reasoning that led to this relation, and this has been done in the hope of stimulating discussion and further work along these lines.

SUMMARY

It was suggested some years ago that a simple relation should exist between hard-

ness and lattice stress in solid solutions of different solvent metals provided all other factors were held equal. Data have been accumulated to enable this hypothesis to be examined for copper and silver solid solutions. In these data all known variables affecting hardness have been held constant. In addition, an attempt has been made to mitigate the effect of another probable variable; namely, ionic overlap. It is found that there is a single, simple relation between increase in hardness and increase in lattice stress for both copper and silver alloys when zinc dissolved in copper is replaced by gallium, germanium or arsenic and cadmium dissolved in silver is replaced by indium, tin or antimony.

ACKNOWLEDGMENT

Grateful acknowledgment is made of the financial assistance of John H. Frye, Sr., without which this work would not have been possible.

REFERENCES

1. Frye: The Hardness of Certain Primary Metallic Solid Solutions. Thesis presented for the degree of Doctor of Philosophy in the University of Oxford.
2. Frye and Hume-Rothery: *Proc. Roy. Soc.* (Sept. 1942) A, 1.
3. Frye and Caum: Page 75, this volume.
4. R. M. Treco: Senior Thesis, Lehigh University, 1942.
5. Mott and Jones: *Properties of Metals and Alloys*. Oxford, 1936.
6. G. I. Taylor: *Proc. Roy. Soc.* (1934) 145-A, 362.
7. L. Pauling: *The Nature of the Chemical Bond*, 326. Cornell Univ. Press, 1939.
8. Bridgman: *The Physics of High Pressure*, 160-162. New York, 1931. Macmillan Co.
9. Hume-Rothery, Lewin, and Reynolds: *Proc. Roy. Soc.* (1936) 157-A, 167.

DISCUSSION

(Robert F. Mehl presiding)

R. F. MEHL,* Pittsburgh, Pa.—This paper goes to the question of the reasons for hardness of solid solutions, and therefore it is of very great fundamental interest. Some of you may remember that in 1923 Rosenhain came here and lectured on the hardness of solid solutions as determined by lattice stresses, originating

* Director, Metals Research Laboratory, Carnegie Institute of Technology.

in differences in atomic volume. This was a little oversimple, but in the intervening 20 years a good deal has been learned about other factors that contribute to the hardness in solid solutions. I think it is unusual that the authors should have had as much success as they have had with a problem as complicated as this. Is there any discussion?

J. T. NORTON,* Cambridge, Mass.—I should like to ask Dr. Frye if he will discuss a little further the reasons why he thinks there should be a relation between the hardness and the hypothetical lattice stress he has calculated. It seems obvious from the data presented that there is a relation between the two.

J. H. FRYE, JR. (author's reply).—In seeking an answer to this question it is important to consider the meaning of hardness. The ultimate Meyer hardness used here gives a measure of the resistance to plastic deformation of a crystal in the plastically deformed and work-hardened condition. This work-hardening is due to and increases with penetration of the testing ball. Thus it is possible in the Meyer analysis to observe the effect of this work-hardening on the increase in hardness due to various solutes. This has been done in earlier work^{2,3} and it has been demonstrated that increases in hardness produced by solute elements are strongly dependent on this plastic deformation. It is clear therefore that we have to do with the properties of a plastically deformed crystal and that no complete explanation of the relation between hardness and lattice stress can be given without understanding the nature of such a crystal. Although a great deal of excellent work has been done recently in an attempt to learn the nature of a plastically deformed crystal and explain its properties, our knowledge is still far from complete. For this reason it has seemed wise to present the relation between hardness and lattice stress as an empirical one.

F. E. CARTER,† Newark, N. J.—When you add to a metal another element in the same group of the periodic table, do you expect to obtain an effect on the hardness greater or less than if a corresponding amount

of an element in a different group is added? I had thought that an element of the same group would have a smaller effect, but note that Dr. Frye has always kept to elements of the same group in the alloys reported in this paper. Perhaps a little information on this point might be given.

J. H. FRYE, JR.—The hardness of silver containing roughly 2.5 and 5 atomic per cent of Mg and Al from the second short period, zinc from the first period of the B subgroups and Cd, In, Sn, and Sb from the second period of the B subgroups has been measured. If the solutes are all taken from the same period as Ag, as in the case of the solutes Cd, In, Sn, and Sb considered in this paper, there is found to be a certain relation between hardness and change in lattice parameter. If one of these solutes is replaced by a solute from another period a greater hardening effect may be produced for the same change in parameter. For example, Mg and Al harden Ag more per unit change in lattice parameter than do Cd, In, Sn, or Sb. This is in qualitative agreement with results on copper alloys. These have been investigated by Norbury in England and by Brick, Martin, and Angier in this country. They found that Si, which is in the fourth group of the second short period, and which therefore might be expected to be somewhat electronegative relative to copper, hardened copper much more than would have been expected from the lattice distortion produced by it.

F. E. CARTER.—Did you say anything about palladium?

J. H. FRYE, JR.—I am unable to say anything about palladium.

R. F. MEHL.—As I remember it, Norbury believed that the anomalous hardening caused by silicon is caused by the formation of molecules in solid solutions.

Do you think compressibilities measured on solid solutions will have any chance of throwing light on these problems, particularly in attempting to approximate stress? I know what a difficult question that is.

J. H. FRYE, JR.—We have thought about that problem, but have not been able to find any data in the literature that are directly

* Associate Professor, Physics of Metals, Massachusetts Institute of Technology.

† Physical Metallurgist, Baker Platinum Works.

applicable to these solid solutions. Bridgman¹⁰ has made measurements of the compressibility of various intermediate alloy phases (so-called intermetallic compounds). In the systems of Ag with Cd and Sn, and Cu with Cd and Sn,¹ he found that the compressibilities of the intermetallic compounds were appreciably greater than those of the pure solvent metals, Ag and Cu. This is rather indirect evidence, but it appears that we have an increase in hardness accompanying an increase in compressibility in some cases.

G. EDMUNDS,* Palmerton, Pa.—The data given in Fig. 1 are represented by curves which, if continued, might pass through the origin of coordinates. Why are the same data represented in Fig. 5 of the authors' second paper† by a straight line?

The straight lines used in Fig. 2 of the paper just presented would not, if continued, pass through the origin. I wonder why they would not, as they would then indicate no hardness increase for zero parameter increment.

J. H. FRYE, JR.—In each of the graphs referred to in Mr. Edmund's first question, curves and straight lines agree with the experimental data within the probable limits of accuracy as indicated by the rectangles that surround the points. The reason for drawing curves in one case and straight lines in the other is, I fear, a rather personal one. These graphs apparently were drawn at different times and were drawn while the authors were busy on war research.

The second question brings up what I think is a very interesting point. If the straight lines of Fig. 2 were extrapolated to zero parameter increment they would cut the hardness axis below the origin. This suggests the possibility that the various solute elements produce a hardening effect due to their distortion of the solvent lattice and a softening effect due to some other cause. There is a factor present in these alloys that could conceivably produce a softening effect. In the copper lattice positive ions are held together by valency electrons. The boundaries of these ions are not discrete and there is a finite probability of finding an

electron at any distance from the center of its ion. In the copper crystal there is a considerable overlap of the closed shells of the ions. The elastic resistance to shear in copper has been calculated and found to be in agreement with experiment. This calculation indicates that well over half of the elastic resistance to shear is due to this overlap. In the alloys considered in this paper the overlap between solute and solvent ions is probably less than that between ions in the pure solvent. Thus replacing a solvent by a solute ion results in a decrease in overlap of the cores of the ions. We should expect this to reduce the resistance to elastic shear and it would not be surprising to find that it also reduced the resistance to plastic shear or hardness.

The decrease in overlap that occurs will depend upon what element has been added as a solute to silver or copper. For example, there is a much greater decrease for As than for Zn in Cu. It is possible, however, that in all cases the overlap has decreased to such a point as to make a negligible contribution to the hardness. Ionic overlap is smaller in a sodium than in a copper crystal. In the former it accounts for roughly one tenth of the elastic resistance to shear while in the latter it accounts for nearer two thirds of this resistance. This hypothesis as to the effect of overlap on the hardness of these alloys therefore is consistent with the concept that the relation between hardness and stress depicted in Fig. 2 is linear and that these lines do not pass through but below the origin.

This discussion of ionic overlap is qualitative and highly speculative. In view of the great importance of this factor in elastic resistance to shear, the possibility cannot be overlooked that it may also be a factor of importance in the hardness of solid solutions. This question should be investigated quantitatively.

C. S. BARRETT,* Pittsburgh, Pa.—It seems likely that the hardening of solid solutions is associated more with localized stresses around dissolved atoms than with homogeneous expansion of the lattice. The correlation shown here between hardening and homogeneous lattice expansion may mean, therefore, that a simple relation exists between homogeneous

¹⁰ P. W. Bridgman: *Proc. Amer. Acad. Arts and Sci.* (1935) 70, 285.

* New Jersey Zinc Company.

† See page 81, this volume.

* Physicist, Metals Research Laboratory, Carnegie Institute of Technology.

expansion and local, "microscopic," stresses. There has been a long history of X-ray research directed toward an understanding of the microscopic stresses in cold-worked metal, and it should be profitable to apply the conclusions of this research to the problem treated in the present paper.

If we assume that it is the local stresses, varying from point to point in the metal, that account for solid solution hardening, one is tempted to suggest that the widths of X-ray diffraction lines should correlate with hardening. But studies of line width that have been made on cold-worked metals have failed to account for more than one-thousandth of the total energy that is known to be left in metals after cold-working. The current thought on this result is that the strain energy is distributed in areas so highly localized that they do not diffract to form diffraction lines, even wide ones. The diffracted X-rays, on the other hand, go into the background between the lines and act like the distortions caused by heat waves in the metal, which have their principal effect on the *intensities* of the diffracted lines. Analysis of line intensities has succeeded quite well in accounting for the residual strain energy from cold-work.

Accordingly, I would like to suggest that the data in this paper be compared with diffracted line intensities (i.e., atomic scattering factors) to see whether local distortions can be detected, and perhaps measured, that would account for the hardening effect of alloying. Experiments of this kind would appear to be more profitable than studies of line widths, and more directly related to the cause of hardening than studies of homogeneous lattice expansion.

J. H. FRYE, JR.—The authors agree with Dr. Barrett that change in lattice parameter is an indirect means of evaluating distortion in the neighborhood of a solute atom and appreciate his suggestion that this might be done more effectively by means of line-intensity measurements. Should such an investigation be made by Dr. Barrett or others, we would suggest that a similar study should also be made of the pure metals and solid solutions after plastic deformation. It cannot be emphasized too strongly that rates of work-hardening due to penetration of a testing ball during the Meyer hardness test varies widely

with composition.^{2,3} It is possible that the differences in hardness found among the various alloys may be attributable to differences in rates of work-hardening. It would therefore be of the greatest interest to evaluate the relative lattice distortions in the pure metals and alloys after a constant amount of plastic deformation. Such an investigation should include a measurement of the size of the small crystallites produced by plastic deformation. We had hoped to make an X-ray investigation of plastically deformed solid solution alloys and pure metals at Lehigh, but research on solid solutions has had to be discontinued because of the pressure of war work.

S. L. HOYT,* Columbus, Ohio.—This paper contains subject matter of considerable scientific interest, and it is interesting to note that the authors departed from usual hardness-testing practice for their correlations.

I feel, however, that their selection of the "ultimate Meyer hardness" was unfortunate, since it does not provide a basic hardness value. Having made the necessary determinations for the Meyer analysis, I would suggest the use of the constant a , or similar constant, corresponding closely to the resistance to penetration of the virgin material. This is the only point on the P - d relationship that is significant, for the reason just stated. All other points reflect work-hardening, and that includes the ultimate Meyer hardness number, so that the correlations reported in the paper relate to the effects of the various solute atoms in the solid solutions plus a considerable and indeterminate amount of cold-work. In other words, it would appear preferable to unscramble the effects of lattice hardening by solid solution and work-hardening by indentation. Cannot the authors reproduce their relationships using the hardness constant a ?

Incidentally, it is difficult to see what special significance, if any, attaches to the ultimate Meyer hardness number, since it merely represents resistance to penetration at one load. Meyer's work shows that a complete representation of hardness cannot be given by a reading for one load except for the case of $n = 2.00$.

J. H. FRYE, JR.—The Meyer constant a to which Dr. Hoyt refers may be defined as the

* Battelle Memorial Institute.

load necessary to produce an impression having a diameter of 1 mm. when a testing ball of a given diameter is used. In earlier publications²⁻⁴ from which the data of the present paper are taken, values of the Meyer hardness, P_a , corresponding to a 1-mm. impression, have been presented. The Meyer hardness P_a is related to the constant a by the equation $P_a = 4a/\pi = 1.27a$. Thus P_a and a are essentially equivalent and the discussion that follows is applicable to both.

In silver and copper alloys the experimental error involved in measuring P_a is roughly twice that involved in measuring P_u . Furthermore, increases in hardness are very much less for P_a than for P_u . In silver alloys this results in so high a ratio of experimental error to hardness increment that the data were not suitable for the quantitative investigation of the relation between hardness and lattice parameter made in an earlier paper,² and for this reason have not been included in the present paper. Hardness increase per unit of lattice-parameter increase is greater for copper alloys than for silver alloys, as would be expected from the higher incompressibility of copper, and this is in qualitative agreement with the conclusions of this paper.

Undoubtedly it would be very interesting to know the effect of the various solutes on the initial resistance to shear of copper and silver in the absence of any work-hardening. This information is not given by P_a (or a). When a 1-mm. impression has been produced in the metal or alloy, plastic deformation, and therefore work-hardening, has taken place and P_a indicates the resistance to further plastic deformation of this work-hardened metal. One might, of course, attempt to measure the stress necessary to produce the first permanent impression, but the Meyer

equation is not applicable to such small indentations. Furthermore, it would seem that the resistance of unworked metal to plastic deformation is best investigated by measuring rates of flow under very small stresses.

The Meyer analysis does permit one to evaluate to some extent the importance of work-hardening in determining the ultimate Meyer hardness of these solid solutions. Work-hardening has been discussed in earlier papers,^{2,3} but perhaps some comment here is in order. Since the Meyer hardness increases with impression diameter due to work-hardening, a plot of hardness against impression diameter gives what is in effect a stress-strain curve. By use of Meyer constants a and n , which have been corrected for grain size, it is possible to construct such curves and thus obtain an insight into the effect of work-hardening. The writer and co-workers have constructed 24 of these curves for various copper and silver-rich solid solutions.^{1,11} These covered the range of strain from a 1-mm. to a 4-mm. impression, which was the range over which the data could be safely used. The slopes of these P - d curves have been found in a few cases to be roughly equal to and in the great majority of cases to be greater than those for the respective pure solvents. Furthermore, rates of work-hardening for equal solute concentrations have been found to increase with lattice distortion for both the silver and the copper alloys considered in this paper. It is therefore clear that the hardness differences observed here are attributable in part, if not entirely, to variation in rates of work-hardening.

¹¹ J. W. Caum: The Hardness of Certain Solid Solutions of Copper. Thesis presented in partial fulfillment of the requirement for the degree of Master of Science at Lehigh University.

Hardening Effects Resulting from the Formation of Both a Precipitate Phase and a Superlattice

By M. R. PICKUS* AND I. W. PICKUS,* JUNIOR MEMBERS A.I.M.E.

(New York Meeting, February 1943)

ORDINARILY age-hardening is thought of as being associated with a limited solubility of one metal in another. Much less has been written about the type of age-hardening that attends the formation of superstructures. Solid solutions generally have a disordered or random arrangement of atoms; that is to say, in a unit cell, such as that of the face-centered cubic lattice, there is no distinction between atomic sites. Atoms of a given metal may occupy cube corners or face centers. Under certain conditions, however, some alloys develop what is known as an ordered structure. In this case, cube corners would be occupied by only one type of atom and face centers by another type. Associated with this ordering process are many interesting changes in physical and electrical properties. Moreover, in many instances the alloys become susceptible to age-hardening. From the evidence now to be described, it appears that age-hardening in 14-carat gold alloys is due to the formation of both a superstructure and a precipitate.

Alloys of the metals gold, silver and copper were known in antiquity. The available knowledge regarding their constitution has been ably summarized and extended by Sterner-Rainer,¹ Jänecke,² Carter,³ Wise,⁴ and Coleman.⁵ Despite the long familiarity with these alloys and the numerous investigations of their properties that have been

made, there is still much that remains unexplained.

It has been known for a long time that the hardness of these alloys is closely related to the rate of cooling. Similar changes have been observed in the binary gold-copper system,⁶ one alloy of which corresponding to the formula Cu_3Au , has been the subject of a careful and competent report by the English investigators, Sykes and Evans.⁷ They have established the fact that the shift of atoms from the ordered to the disordered condition takes place in some critical temperature range. At temperatures above the critical range the structure is random, and at temperatures below it the structure is ordered. No difference between these two structures is revealed by the microscope. Both have a face-centered cubic lattice and complete solubility, so that there is no evidence to suggest that the changes in properties are associated with a phase change. The more slowly the alloy is cooled, the higher is the degree to which the ordering process proceeds and the more marked is the increase in hardness.

As experimental data were accumulated on 14-carat gold alloys, several contradictions arose. Certain observations tended to confirm the existence of a superstructure, while other observations seemed to be inconsistent with such a transformation.

PRESENT INVESTIGATION

As a focal point about which to develop this subject, it is expedient to consider first

Manuscript received at the office of the Institute Dec. 1, 1942. Issued in METALS TECHNOLOGY, April 1943.

* The Parker Pen Co., Janesville, Wis.

¹ References are at end of paper.

the alloy containing 58.33 per cent gold, 30.00 per cent copper, and 11.67 per cent silver. This alloy was chosen for two reasons: first, as will be shown later, its

in a high-frequency furnace and cast into ingots approximately $\frac{1}{2}$ in. thick. The ingots were soaked at 1200°F. and then quenched into water. Slowly cooled alloys

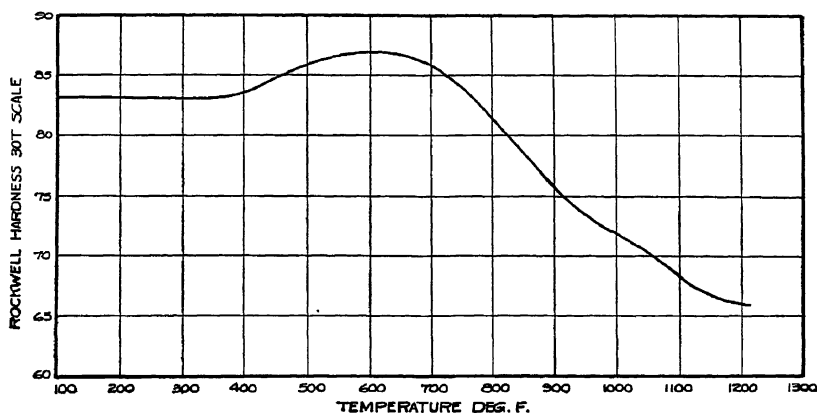


FIG. 1.

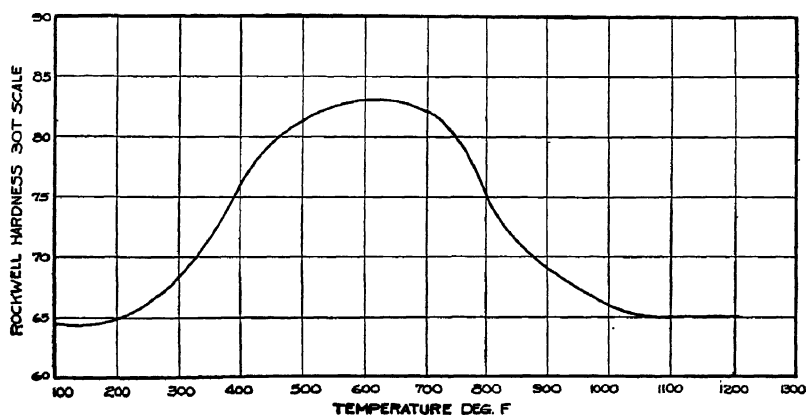


FIG. 2.

FIGS. 1 AND 2.—HARDNESS CHANGES FOR GOLD-SILVER-COPPER ALLOY.
58.33 per cent gold, 30.00 per cent copper and 11.67 per cent silver.

FIG. 1. Quenched from 1200°F., rolled to a reduction in thickness of 43 per cent and then heated for $\frac{1}{2}$ hour at various temperatures.

FIG. 2. Quenched from 1200°F. and annealed $\frac{1}{2}$ hour at various temperatures.

properties are typical of all the 14-carat gold alloys in the gold, silver, copper system; and second, it is used by the Parker Pen Co. in the manufacture of its gold nibs for fountain pens. The specimens were prepared in the following manner. The respective proportions of fine gold, fine silver, and electrolytic copper were melted

are too brittle to roll. All the rolling was done cold, with approximately 50 per cent reductions between anneals. The annealing was done in furnaces with controlled atmosphere.

The recrystallization characteristics of this alloy are for the most part what would be expected, except, possibly, that the

increase in hardness immediately preceding recrystallization is rather more pronounced than is usual. The recrystallization data are summarized in Fig. 1. The specimens

cold-rolled specimens. In Fig. 2 are summarized the hardness data obtained on specimens that were quenched from 1200°F. and then reheated for ½-hr. periods at



FIGS. 3 AND 4.—GOLD-SILVER-COPPER ALLOY. $\times 100$.
(58.33 per cent gold, 30.00 per cent copper and 11.67 per cent silver.)
FIG. 3. Quenched from 1200°F. and reheated ½ hour at 600°F.
FIG. 4. Quenched from 1200°F. and reheated ½ hour at 990°F.

employed in obtaining these data were quenched from 1200°F., cold-rolled to a reduction in thickness of 43 per cent, and then reheated for ½-hr. periods at various

temperatures. In attempting to account for these peculiar hardness changes, one must consider that, according to the best information available, the constitution of the 14-carat gold-silver-copper alloys

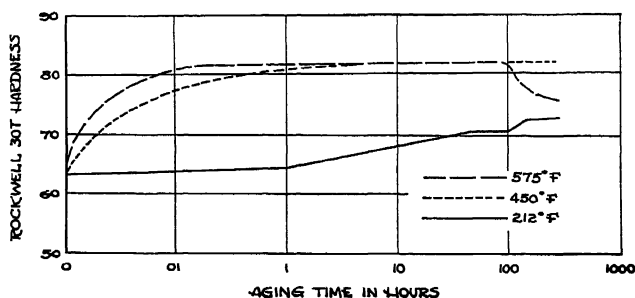


FIG. 5.—AGE-HARDENING OF A GOLD-SILVER-COPPER ALLOY.
58.33 per cent gold, 30.00 per cent copper, 11.67 per cent silver.

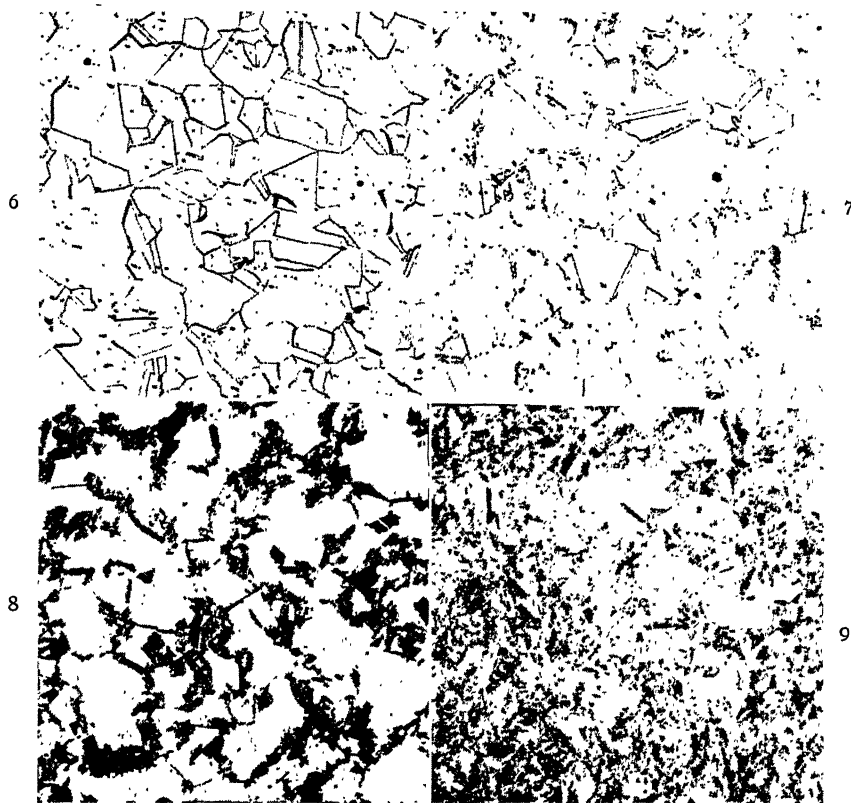
The anomalous behavior of this alloy becomes apparent when specimens previously annealed at 1200°F. are reheated after quenching. Specimens reheated at 600°F. become nearly as hard as severely

conforms to a typical unlimited solid-solubility system, except for the formation of the ordered phase CuAu. According to Sykes and Evans, there is some critical temperature at which the transition from

the disordered to the ordered state commences on cooling. They showed that the slower the rate of cooling through this critical temperature, the more closely is

METALLOGRAPHIC INVESTIGATION

Attempts to explain the hardness changes metallographically were unsuccessful at first, for indeed, there appeared to be no



FIGS. 6-9.—GOLD-SILVER-COPPER ALLOY. QUENCHED FROM 1200°F. AND AGED AT 575°F. $\times 100$.
58.33 per cent gold, 30.00 per cent copper, 11.67 per cent silver.

Fig. 6. Aged 1 hour.

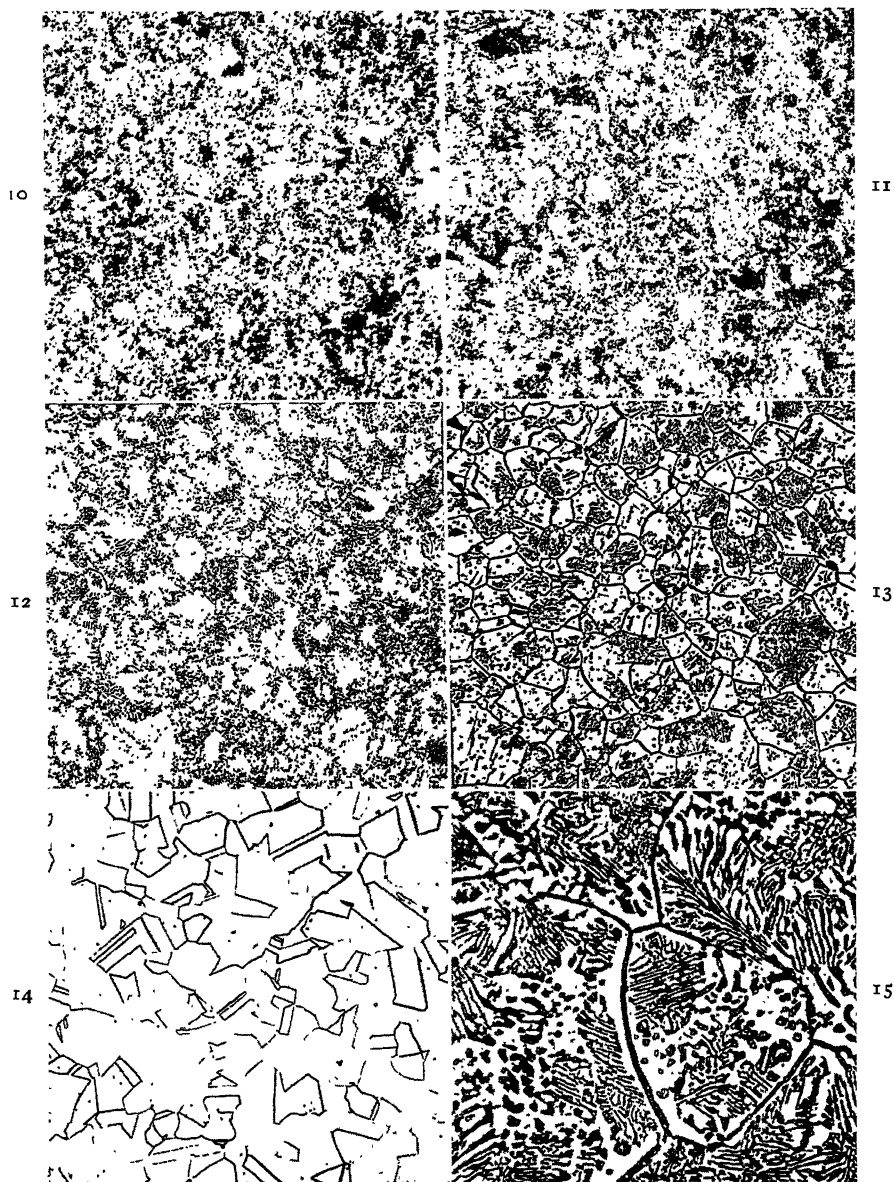
Fig. 7. Aged 16 hours.

Fig. 8. Aged 115 hours.

Fig. 9. Aged 354 hours.

the equilibrium degree of ordering approached. When an attempt was made in this investigation to determine the critical temperature for the 14-carat gold alloy under discussion, it was observed that very slow rates of cooling resulted in lower hardness values than did intermediate rates of cooling. This suggested the possibility of some agency other than a simple order-disorder transformation.

phase change. The first clue was obtained when specimens were reheated at temperatures between 850° and 1000°F. Gold alloys, because of their nobility, ordinarily are somewhat difficult to etch satisfactorily, but for specimens heated in this temperature range it seemed especially difficult to avoid a smudge. As the technique in preparing these specimens improved, the smudge became more suggestive of a



FIGS. 10-15.—GOLD-SILVER-COPPER ALLOY.

58.33 per cent gold, 20.84 per cent copper and 20.83 per cent silver.

Fig. 10. Heated 24 hours at 900°F. and quenched. $\times 100$.

Fig. 11. Heated 24 hours at 1000°F. and quenched. $\times 100$.

Fig. 12. Heated 24 hours at 1050°F. and quenched. $\times 100$.

Fig. 13. Heated 24 hours at 1100°F. and quenched. $\times 100$.

Fig. 14. Heated 1 hour at 1200°F. and quenched. $\times 100$.

Fig. 15. Slowly cooled from 1200°F. $\times 500$.

precipitate.* The results of some of the later experiments are shown in Figs. 3 and 4. If the photomicrographs of these figures are compared with the graph of Fig. 2, it

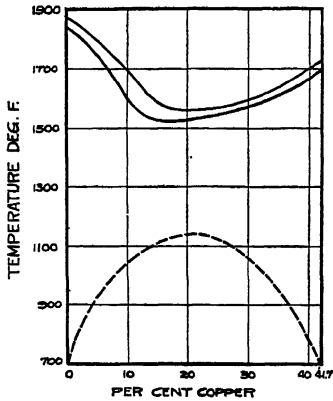


FIG. 16.—LIQUIDUS AND SOLIDUS CURVES FOR 14-CARAT GOLD-SILVER-COPPER ALLOYS (58.33 PER CENT GOLD) AFTER STERNER-RAINER¹ WITH TENTATIVE DOMAIN OF LIMITED SOLID SOLUBILITY INDICATED BY BROKEN CURVE.

will be seen that the peak in the hardness curve is accompanied by no apparent change in microstructure. However, if the temperature is maintained long enough, the microstructure undergoes marked changes. The results of some aging experiments are shown in Fig. 5 and the corresponding metallographic changes for the 575°F. curve are shown in Figs. 6 to 9. It is believed that this is the first evidence of the formation of a precipitate in 14-carat gold-silver-copper alloys.

The work was extended to cover the range of compositions having 58.33 per cent gold and the balance various proportions of silver and copper. Age-hardening has been observed in all the alloys except

the binary gold-silver alloy. In the binary gold-copper alloy, while age-hardening was observed, no precipitate phase was detected. Specimens were prepared from six compositions (0, 6, 12, 21 and 42 per cent copper) and heated for 24 hr. at various temperatures, with the object of surveying, approximately, the domain of limited solid solubility. As an example of the results, the photomicrographs for the alloy containing equal proportions of silver and copper are reproduced in Figs. 10 to 15. Here may be seen the progressive coarsening of the precipitate and the decrease in the relative amount as the temperature is raised. The temperature at which the precipitate disappears is different for each of the various compositions, and in Fig. 16 an attempt has been made to summarize the metallographic data in relation to the liquidus and solidus curves of Sterner-Rainer. The boundary of the limited solid-solubility region is represented by a broken line, to represent its tentative nature. It is not intended to represent true equilibrium conditions, the heating period being too short for that purpose. The curve does, however, serve to represent the data and to indicate the nature of the system.

The properties of these alloys may be changed by interesting combinations of aging and deformation. Specimens that have been aged and cold-rolled acquire greater hardness than is possible by either aging or rolling alone. The final hardness is the same, whether the aging or the rolling is done first.

SUMMARY AND CONCLUSIONS

While age-hardening in the binary 14-carat gold-copper alloy was observed in this investigation it was not found possible to detect the presence of a precipitate phase in this alloy. Therefore it must be assumed that the hardness changes are due solely to the formation of a superstructure. In all the other cases, however, a precipitate phase was observed: there-

* After much experimentation, it was found that a mixture containing equal proportions of 25 per cent ferric chloride solution and 3 per cent hydrogen peroxide solution darkens the precipitate phase without attacking the matrix. For specimens not containing the precipitate phase, a mixture containing equal proportions of 10 per cent ammonium persulphate solution and 10 per cent potassium cyanide solution was employed.

fore it is reasonable to suppose that the property changes are at least partly due to the formation of a precipitate. Moreover, since only in the binary gold-copper and gold-silver alloys is no precipitate phase observed, it appears that the simultaneous presence of both silver and copper are necessary for its formation. At this point it seems appropriate to consider briefly the interesting paper published by Hultgren and Tarnopol,⁸ which discussed the effect of silver on the gold-copper superlattice AuCu and concluded that the addition of silver has the effect of lowering the critical temperature of the order-disorder transformation. With no intention of questioning the validity of this conclusion—for we have no data to justify this—one wonders whether these experiments were not complicated by the formation of a precipitate phase. It would be interesting, if their specimens are still available, to subject them to a careful metallographic examination.

Some specimens have been prepared for X-ray diffraction studies and the authors hope to carry this investigation further.

ACKNOWLEDGMENT

The authors desire to express their gratitude to Mr. Kenneth S. Parker, President of the Parker Pen Co., for his interest in research, and to Dr. C. H. Mathewson, for his comments on the manuscript.

REFERENCES

1. L. Sterner-Rainer: *Die Edelmetall-Legierungen in Industrie und Gewerbe*. Leipzig, 1930. Wilhelm Diebener G.M.B.H.
2. E. Jänecke: *Metallurgie* (1911) **8**, 597.
3. F. E. Carter: *Trans. A.I.M.E.* (1928) **78**, 786.
4. E. M. Wise: *Trans. A.I.M.E.* (1929) **83**, 384, Inst. of Metals Div.
5. R. L. Coleman: *Nat. Bur. Stds. Research Paper No. 32* (1928).
6. N. S. Kumakow, S. F. Zemczuzny and M. Zasedatelev: *Jnl. Inst. Metals* (1916) **15**, 305.
7. C. Sykes and H. Evans: *Jnl. Inst. Metals* (1936) **58**, 255.
8. R. Hultgren and L. Tarnopol: *Trans. A.I.M.E.* (1939) **133**, 228.

DISCUSSION

(Robert F. Mehl presiding)

J. T. EASH,* Bayonne, N. J.—The authors have presented some useful data on the hardening of 14-carat gold-silver-copper alloys, and their Fig. 16, showing the tentative limited solid solubility, is a very interesting contribution toward establishing the domain of the AuCu phase in the ternary system; it does, however, need further explanation.

There are a few additional points that would deserve consideration. The authors have failed to mention that the structural transformation on cooling of alloys of the AuCu composition involves not only a change from a random distribution of the atoms to an ordered state, but also results in the formation of a tetragonal structure in the latter. There can be little doubt that the formation of this tetragonal phase plays an important part in the hardening of these alloys. It has been shown by Asher⁹ that gold-copper alloys containing AuCu, the ordered tetragonal phase, age-harden very remarkably but gold-copper alloys containing AuCu₃, the ordered face-centered cubic phase, age-harden only mildly.

Work described in a paper¹⁰ presented before this society in 1933, which dealt with the structure and mechanism of hardening of dental alloys, is related to the present subject. One alloy investigated contained 70.8 per cent gold, 15.5 per cent silver and 13 per cent copper, which is close to those considered by the Messrs. Pickus. Results obtained by metallographic and X-ray diffraction confirm the presence of a precipitated phase in the overaged alloy. After quenching from the solid solution temperature, 700°C., the specimen contained one phase that was face-centered cubic with random arrangement. Upon aging for 15 min. at 300°C., the alloy attained its highest observed tensile strength, and contained a single phase that was face-centered tetragonal and in the ordered state. After aging for 624 hr. at the same temperature, a precipitate was observed under the microscope and X-ray patterns showed the presence

* The International Nickel Company.

⁹ H. H. Asher: *Jnl. Dental Research* (1934) **14**, 349.

¹⁰ E. M. Wise and J. T. Eash: *Trans. A.I.M.E.* (1933) **104**, 276.

of a new face-centered cubic structure in addition to the tetragonal phase. Judging from our work, it was the formation of tetragonal AuCu that caused the useful age-hardening and the precipitate was the result of a secondary reaction that took place on overaging.

R. VINES,* Long Island City, N. Y.—The authors, from the title of their paper, set out to show that the hardening obtained on aging certain 14-carat gold-silver-copper alloys is due to the formation of *both* a precipitate phase and a superlattice, it being implied that the superlattice is based upon AuCu or AuCu₃. Their paper establishes beyond question that the supersaturated solid solution type of age-hardening does occur in these alloys. However, the contribution, if any, of the order-disorder transformation to the observed hardening was either not investigated or not reported.

Although little exact information on the gold-silver-copper system is available, a wealth of qualitative data permit construction of a working diagram. The constitution of this ternary system can best be pictured by building it upon the silver-copper base. In the silver-copper system, which is a eutectic, the duplex region at the solidus temperature extends from about 9 to 91 per cent copper. As gold, which is soluble in both silver and copper, is added, this duplex region is narrowed, but it is not eliminated at the solidus temperature until about 50 per cent gold is added. As in the binary silver-copper system, this duplex region broadens with decreasing temperature owing to the decomposition of the unstable solid solution. Evidence indicates that below about 200°C. the solid solution is unstable up to about 80 per cent gold at equal copper-silver contents.

The authors' work supports this suggested constitution, which, if correct, would explain the observed hardening effects without recourse to superimposed superlattice transformations. Undoubtedly, the gold-copper order-disorder transformations do intrude into the ternary system but evidence thus far presented indicates that they have very limited domains. In addition, if superimposition is found, it is unlikely that the ordering and precipitation temperatures will coincide. It is noted that the authors plan to continue their investigation

and it is hoped that they will examine the contribution of the order-disorder transformation to the hardening of the ternary alloys. The palladium-silver-copper system investigated by Glander¹¹ and data given in a paper by E. M. Wise and the writer¹² may prove useful in continuation of the study.

Further data on the degree of hardening obtained on the binary gold-copper alloy and the other ternary alloys would be welcomed. In addition, justification would be appreciated for the statement "The more slowly the alloy is cooled, the higher is the degree to which the ordering process proceeds and the more marked is the increase in hardness."

F. E. CARTER,* Newark, N. J.—I should like to suggest that for a paper like this, where discussion of physical properties is all based on one particular alloy series, that series should be mentioned in the title. Such a custom would be very helpful to abstracters and later investigators.

Up to the present, jewelers mostly have been interested in these gold-silver-copper alloys. They have known that the colors of the alloys can be varied from green to yellow to red simply by changing the proportions of silver and copper. They also have known by experience that a quench after annealing softens the alloys, and slow cooling hardens them. The authors of the present paper claim that very slow cooling renders them soft. I am skeptical and would like further confirmation.

Dozens of papers have been written on the subject of order-disorder in the binary gold-copper series. In the ternary gold-silver-copper alloys, it has been well known that there was precipitation hardness due to the formation of the compounds AuCu and AuCu₃. The authors assert that both phenomena—namely, lattice change and compound formation—occur, and, in my opinion, have given sufficient proof of the correctness of their view.

In Fig. 2, I noted the maximum hardness obtained by the reheating of this particular alloy to 600°F. (325°C.), so I looked up some results I had obtained with other similar alloys. The same phenomenon was observed.

¹¹ *Metallwirtschaft* (1939) 17, 357.

¹² Age Hardening of Metals. Amer. Soc. for Metals (1940).

* Physical Metallurgist, Baker Platinum Works.

* Ford Instrument Co., Inc.

For example, an alloy of 58.33 per cent gold, 10.42 per cent copper and 31.25 per cent silver quenched from 1472°F. (800°C.) and re-annealed at various temperatures for one hour, gave a similar maximum at 450°F. (230°C.). Also an alloy of 75 per cent gold, 6 per cent copper and 19 per cent silver gave a very sharp maximum at 400°F. (200°C.). The former alloy was then reheated for 24 hr. at 450°F. (230°C.) and no change in hardness was obtained. This is understandable because the temperature at which the heating was done is below the maximum temperature (about 750°F.) at which the Au-Cu can form. In this connection it is difficult to see why, in Fig. 5, there should be a drop in hardness on long continued heating at 575°F. (300°C.), which is still well below this point.

In addition to the etchants mentioned, we have used: (1) potassium iodide in alcohol, (2) dilute aqua regia plus 1 per cent of a 5 per cent solution of ferric chloride, (3) potassium cyanide with the alloy as anode.

With reference to the increased hardness of a slowly cooled alloy over that obtained when quenched, I checked over figures in a paper of mine (reference 3 in this paper) and found that other alloys in the ternary series showed a much larger increase when the copper-silver proportion was different from that of the alloy examined by the present authors. If the authors would examine metallographically the alloy that showed the greatest increase, perhaps the photomicrographs would show the changes even more distinctly.

While jewelers have known about these hardness changes for a long time and have made use of them in their fabrication, the phenomena are of still more importance to pen manufacturers. The publication of a scientific paper on the subject is welcomed and the results of the promised X-ray diffraction investigation are anticipated with interest.

M. R. PICKUS AND I. W. PICKUS (authors' reply).—The discussion, for the most part, is self-explanatory; however, it may be of interest in view of some of the questions that were raised to amplify somewhat the remarks on the nature of the order-disorder type of transformation. On cooling, the alloy passes from the disordered state to the ordered state in such a manner that at each temperature below the given temperature there exists a certain equilibrium degree of order. At any given temperature the equilibrium degree of order may be approached either by cooling very slowly, so that equilibrium exists during the cooling, or alternatively, the alloy may be maintained at the given temperature until the equilibrium degree of order is obtained. In order to maintain equilibrium, the rate of cooling must be very slow, of course.

Dr. Carter has raised a question about the effect of very slow rates of cooling. For the alloy containing 58.33 per cent gold, 30.00 per cent copper and 11.67 per cent silver, a Rockwell hardness of 84(30T) was obtained after furnace cooling from 1200°F.; when the alloy was cooled from 1200°F. to room temperature over a period of one week, the hardness was 66(30T).

Effect of Certain Fifth-period Elements on Some Properties of High-purity Copper

By J. S. SMART, JR.* AND A. A. SMITH, JR.,* MEMBERS A.I.M.E.

(New York Meeting, February 1943)

THE elements silver, cadmium, tin, antimony and tellurium either are found as impurities in commercial coppers or are intentionally added to produce coppers for special uses. When present in small quantities, each of these metals exerts a significant effect on the properties of copper, but despite considerable experience and investigation much remains to be learned about their specific behavior.

The presence of extraneous elements, particularly oxygen, complicates the study of individual additions of impurities in the range 0 to 0.05 per cent, and the use of high-purity copper has been found extremely helpful in circumventing these difficulties. It has also been found that individual behavior can be satisfactorily determined from measurements of two commercially important properties, conductivity and softening temperature, according to methods that have been described previously.^{1,2} Data of this type, obtained in the course of a general investigation of the effects of impurities on the properties of both oxygen-bearing and oxygen-free copper are presented herewith.

All samples except those containing cadmium were prepared as $\frac{3}{8}$ -in. continuously cast oxygen-free rod from pure copper and weighed amounts of a similarly

synthesized master alloy. Composition was checked by chemical methods, which in every case verified the calculated analyses. Test wires were cold-drawn one B. and S. number per pass on a string-up machine using four 30-min. 600°C. anneals at 0.3125, 0.257, 0.204 and 0.162 in. and a final cold reduction of 75 per cent to 0.081 in. Some oxygen-bearing samples were produced directly from the $\frac{3}{8}$ -in. oxygen-free rods by diffusion from a surface scale at 850°C. and drawn to size as listed above, but most of the alloys were remelted in pure graphite and cast through air into a 1-in. round mold. The slugs were then hot-rolled to $\frac{5}{16}$ in., drawn to 0.162 in., annealed as listed above, and drawn to 0.081 inch.

Conductivity wires were annealed for 1 hr. at 100°C. intervals between 300° and 800°F., using a hydrogen atmosphere for oxygen-free samples and purified nitrogen for the oxygen-bearing type. All samples were quenched from the annealing temperature in 10 per cent H₂SO₄ and conductivity was measured on a Hoopes bridge that had been checked against a Kelvin bridge. The softening temperatures represent the half-hard stage of the annealing curve as determined by a standard procedure.¹

EFFECT OF SILVER

Numerous excellent studies of the argentiferous coppers are found in the literature, and these have been adequately

Manuscript received at the office of the Institute Dec. 1, 1942. Issued in METALS TECHNOLOGY, June 1943.

* Central Research Laboratory, American Smelting and Refining Co., Barber, N. J.

¹ References are at the end of the paper.

reviewed by Gregg.³ It is well known that silver does not react with the Cu_2O present in tough-pitch coppers; that it has but a minute effect on the conductivity, and is widely used in amounts up to 30 oz. per

ton. As previously recorded by Gregg and others, the effect of silver on the conductivity is exceedingly small and is difficult to detect when less than 10 oz. per ton is present.

TABLE I.—*Alloys of Silver and Pure Copper*

Sample No.	Ag. Oz. per Ton	Ag. Per Cent	O ₂ Per Cent	Hard Drawn	Conductivity, Per Cent I.A.C.S., Annealed at						Softening Temperature, Deg. C.
					300°C.	400°C.	500°C.	600°C.	700°C.	800°C.	
229M	Nil	Nil	Nil	100.25	102.25	102.25	102.3	102.3	102.3	102.3	140
230M	0.25	0.00086	Nil	100.15	102.2	102.15	102.2	102.25	102.2	102.25	151
231M	0.50	0.0017	Nil	100.15	102.15	102.2	102.1	102.2	102.3	102.3	148
232M	1.0	0.0034	Nil	100.25	102.3	102.25	102.3	102.3	102.3	102.25	155
233M	2.0	0.0068	Nil	100.2	102.25	102.25	102.3	102.25	102.15	102.25	186
234M	10.0	0.0343	Nil	99.8	100.7	102.0	102.15	102.15	102.25	102.1	301
234MO	10.0	0.0343	0.026	99.65	100.65	101.9	102.05	102.05	102.05	101.95	295

ton in coppers where high softening temperature is desired. The present study is of interest primarily because of the opportunity provided for exploration of the very low concentration range where solid solubility is presumed.⁴

In general, the softening-temperature data agree with those of previous investigators although the variety of test methods used renders the comparisons somewhat speculative. The shape of the softening-temperature curve of Fig. 1 is of particular

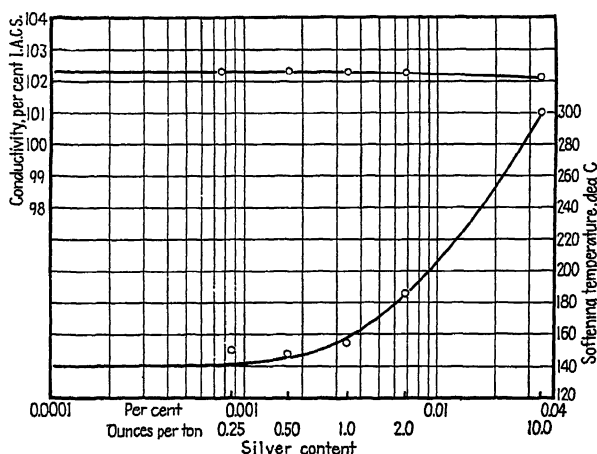


FIG. 1.—EFFECT OF SILVER ON CONDUCTIVITY AND SOFTENING TEMPERATURE OF HIGH-PURITY COPPER.

The measurements were obtained primarily from oxygen-free alloys (Table I); only one oxygen-bearing sample was prepared for check purposes, inasmuch as the accuracy is somewhat affected by the necessary corrections for the oxygen

interest, especially in the region of low concentration, showing that 1.0 oz. per ton Ag has but a very small effect and approximately 2.6 oz. per ton Ag is required to raise the softening temperature of pure copper to 200°C., which is in the

commercial wirebar range. Since the various impurity effects on this property are not additive, except in a very few cases, it is apparent that the small amounts of silver in commercial coppers contribute little to their annealing behavior.

When high softening temperatures are required, silver is an ideal alloying element

behavior and other qualities as influenced by the reaction of antimony with oxygen. In the range of commercial impurity, the proportion of oxygen to antimony is relatively high, and in the present investigation considerable attention has been directed to their mutual behavior.

The synthesized oxygen-free samples

TABLE 2.—*Alloys of Antimony and Pure Copper*

Sample No.	Sb, Per Cent	O ₂ , Per Cent	Hard Drawn	Conductivity, Per Cent I.A.C.S., Annealed at						Softening Temperature, Deg. C.		
				300°C.	400°C.	500°C.	600°C.	700°C.	800°C.	$\frac{1}{2}$ Hr. 600°C. ^a	1 Hr. 850°C. ^a	15 Hr. 500°C. ^a
79M	Nil	Nil	100 3	102.15	102.2	102.25	102 3	102.3	102.3	138		
74M	0.0013	Nil	99.8	102.05	102.05	102.1	102.05	102.05	102.05	170		
76M	0.0018	Nil	99.9	101.9	101.8	101.95	101.85	101.9	101.85	185		
77M	0.0058	Nil	99.4	100.05	101.3	101.35	101.35	101.35	101.25	293		
78M	0.0194	Nil	96.9	97.7	99.1	99.1	99.05	99.1	99.1	331		
75M	0.060	Nil	91.0	92.0	92.6	92.7	92.75	92.75	92.7	337		
76MO	0.0018	0.03	99.6	101.9	101.95	101.8	102.0	101.9	101.8	175		
77MO	0.0058	0.13	99.05	101.4	101.75	101.25	101.4	101.25	101.15	270		
78MO	0.0194	0.13	97.85	100.75	101.05	100.85	100.65	99.40	99.0	290	291	208
83M	0.062	0.028	91.3	93.2	93.85	96.1	99.75	98.5	93.85	337	325	240

^a Denotes heat-treatment at 0.162 in. before cold-drawing to 0.081 in. All samples quenched from indicated temperatures.

if used within its limitations, but it will be recognized that the curve of Fig. 1 flattens out rapidly above 10 oz. per ton Ag (Gregg³) and that the unit effect of further additions decreases rapidly when high percentages of silver are added. Where very high softening temperatures are desired, other elements may be added with considerable advantage, as will be discussed later.

EFFECT OF ANTIMONY

The solid solubility of antimony in copper increases from 2 per cent at 200°C. to over 11 per cent at 650°C., according to the diagram of Mertz and Mathewson.⁵ Additions of antimony raise the strength, fatigue limit, and softening temperature, and lower the conductivity, as previously summarized and discussed by Archbutt and Prytherch.⁶ Almost all of the earlier work was carried out in the presence of varying amounts of oxygen, resulting in a confusion of observations on the rolling

were investigated as outlined, with the results set forth in Table 2 and Fig. 2. In the absence of oxygen, solid solubility is ensured and the effect on both conductivity and softening temperature is pronounced. The conductivity losses determined by Skowronski⁷ and by Archbutt and Prytherch are in good agreement with the present results; the deviations that do exist are relatively minor and are due to the presence of oxygen in the copper used by the earlier investigators. Up to 0.06 per cent Sb, the loss in conductivity is a linear function of antimony content and amounts to 0.16 per cent I.A.C.S. for each 0.001 per cent Sb by weight present in solid solution.

The softening-temperature curve is especially interesting with regard to both the large quantitative effects and the characteristics of the phenomenon in general. The softening temperature is influenced only slightly by the initial additions of antimony in the range in which this element occurs as an impurity in commercial electrolytic

coppers. This stage is followed by a limited concentration zone of high effectiveness, which, in turn, is terminated by a rapidly diminishing zone. This behavior is typical

increase in conductivity was found to be prohibitively slow. Consequently, the samples were prepared by remelting three of the oxygen-free rods, and compounding a

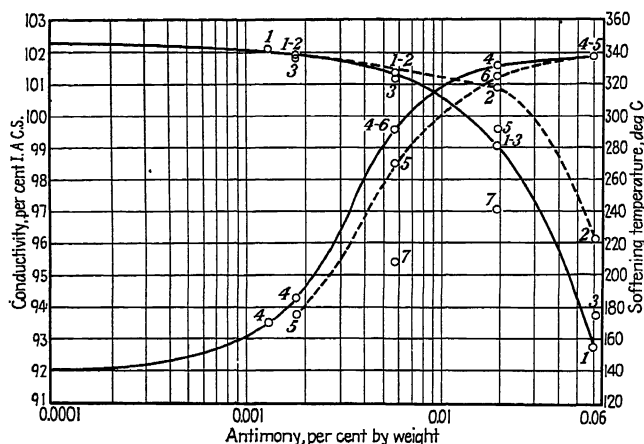


FIG. 2.—EFFECT OF ANTIMONY ON CONDUCTIVITY AND SOFTENING TEMPERATURE OF HIGH-PURITY COPPER.

Points 1, conductivity of oxygen-free alloys.

Points 2, conductivity of oxygen-bearing alloys annealed at 500°C.

Points 3, conductivity of oxygen-bearing alloys annealed at 800°C. and quenched.

Points 4, softening temperature of oxygen-free alloys.

Points 5, softening temperature of oxygen-bearing alloys; penultimate anneal $\frac{1}{2}$ hr. 600°C.

Points 6, softening temperature of oxygen-bearing alloys; penultimate anneal 1 hr. 850°C.

Points 7, softening temperature of oxygen-bearing alloys; penultimate anneal 15 hr. 500°C.

of all the impurities investigated, but the wide divergence in the occurrence of the three stages with respect to composition demands a detailed exploration of the characteristics of each impurity. For instance, it has been shown, in a previous paper of this series,² that while nickel and iron in high amounts are generally recognized as very effective in raising the softening temperature of copper, the results obtained from additions up to 0.05 per cent by weight are negligible, because these amounts are wholly within the rather large initial zones of ineffectiveness peculiar to these elements.

Several attempts were made to prepare the desired oxygen-bearing alloys by diffusion from an oxide scale in an atmosphere of nitrogen at 850°C., but the rate of penetration of oxygen as revealed by the

new alloy, containing 0.062 per cent Sb by chemical analysis, to replace the previous 0.06 per cent alloy, the quantity of which was insufficient for the work at hand. These castings were hot-rolled to $\frac{5}{16}$ in., annealed at 850°C. for 10 min., and quenched and cold-drawn to 0.162 in., where suitable lengths were cut off and drawn to 0.081-in. wire for the conductivity anneals. The conductivity measurements listed in Table 2 have been corrected for the volume effect of excess Cu_2O by adding 0.136 per cent I.A.C.S. to the measured values for each 0.01 per cent O_2 present.

In the presence of oxygen, the conductivities are no longer constant over the annealing-temperature range; they vary, approaching a maximum for the 600°C. anneal and a minimum after the 800°C. anneal. In the latter case, the results are

equivalent to those obtained from the oxygen-free samples (Fig. 2). The results obtained at the lower annealing temperatures represent rejection of antimony from solid solution. The characteristics of this reaction were studied by varying the heat-treatment.

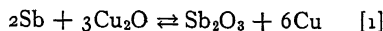
By reannealing the same wire over the temperature range 500° to 800°C., the reaction was found to be reversible, and the conductivity differences listed in Table 2 were duplicated at will from either direction. In addition, the low conductivities obtained from the anneals at 400° and 500°C. indicated that a 1-hr. annealing period at these temperatures was entirely too short for the attainment of equilibrium conditions. Accordingly, the original 500°C. wire of sample 83M was reannealed at this temperature for increasing periods of time, with the results shown in Table 3.

TABLE 3.—*Additional Annealing Treatments at 500°C., Sample 83M*

Total Hours at 500°C.	Conductivity, Per Cent I.A.C.S.	Total Hours at 500°C.	Conductivity, Per Cent I.A.C.S.
1	96.1	22	101.3
3	97.4	46	101.9
5	98.4	69	102.0
7	98.95	87	101.9

An appreciable period of time is required for completion of the reaction at 500°C., but almost all of the 0.062 per cent Sb present in this sample has been rejected from solid solution, taking into consideration the loss of conductivity due to the volume effect of the precipitate. The relative reaction rates at 500° and 800°C. can be appreciated from the fact that the conductivity of this sample when reannealed at 800°C. for 1 hr. and quenched, dropped from 101.9 to 93.7 per cent. From additional experiments, it is known that this reversal proceeds exceedingly rapidly, and for all practical purposes appears to keep pace with the rate at which the sample can be brought up to temperature.

There is no doubt that the insoluble phase is an antimony oxide, possibly Sb_2O_3 ,* which in all probability is unstable at high temperatures because of the mass effect of the excess copper, which acts as a reducing agent. The reaction may be written



In the temperature range 400° to 600°C., at a rate that is highly dependent on temperature, the reaction proceeds in the direction of Sb_2O_3 , removing antimony from solid solution. The data of Table 3 indicate that the reaction proceeds virtually to completion at 500°C. At 700°C. and above, the equilibrium rapidly shifts to the left, and antimony enters solid solution. The properties of samples quenched from these temperatures, therefore, correspond to those of their oxygen-free analogues.

Eq. 1 and its equilibrium characteristics stipulate that Sb_2O_3 may be added to molten oxygen-bearing copper and that reduction to soluble antimony will be effected. This was readily carried out in a clay crucible in the absence of all reducing elements; the alloy contained 0.20 per cent O_2 and had a conductivity of 83.5 per cent as drawn. A 1-hr. anneal at 500°C. caused sufficient precipitation to raise the conductivity to 90.6 per cent.

Likewise, it is also possible to diffuse sufficient oxygen into an oxygen-free alloy at 600°C. to precipitate the low-temperature phase. Fig. 3 illustrates the progress of the diffusion into a strip of oxygen-free pure copper containing 0.2 per cent Sb. The sample was scaled in air and allowed to remain at 600°C. for 50 days in an atmosphere of nitrogen.

In addition to the reaction of Eq. 1, which is of primary importance, a second type of precipitation is evident from the behavior of samples annealed at 800°C. or

* The oxide has not been identified, but will be referred to as Sb_2O_3 , for convenience.

higher for long periods of time. This was first noticed in the rods that had been soaked at 850°C. in an attempt to oxidize the antimony by diffusion. For instance,

If the compound precipitated at 800°C. and above is assumed to be an antimonate of general composition $\text{Cu}_x\text{Sb}_y\text{O}_z$, the process can be conveniently represented as

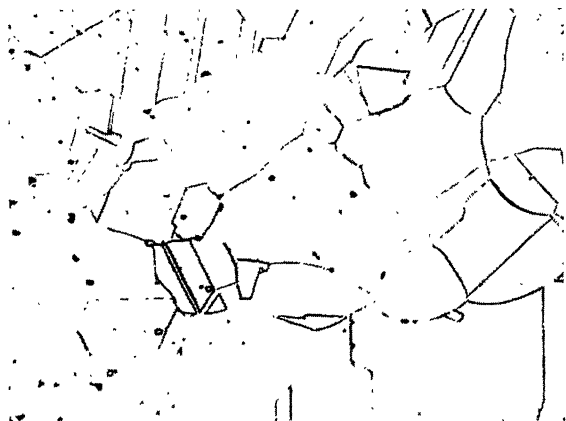


FIG. 3.—PRECIPITATE OF ANTIMONY OXIDE FORMED BY DIFFUSION OF OXYGEN AT 600°C. INTO OXYGEN-FREE COPPER CONTAINING 0.2 PER CENT ANTIMONY. $\times 150$. Etched with NH_4OH and H_2O_2 .

the conductivity of sample 75M is 92.7 per cent in the oxygen-free condition, but a wire drawn from a $\frac{3}{8}$ -in. rod soaked for 10 days at 850°C. in the presence of O_2 was found to be 94.1 per cent. Confirmatory experiments were made on wires; sample 83M, for instance, with an initial conductivity (800°C. anneal) of 93.7 per cent was reannealed for 288 hr. at 800°C. in N_2 , whereupon the conductivity increased to 97.6 per cent.

This very slow reaction is also of the reversible type, since remelting brings about the original behavior, but whether or not the reversal takes place in the solid state—i.e., just below the melting point—has not been determined. In any event, once formed at 800°C., the precipitate is stable at lower temperatures and no changes occur in samples reannealed at 500°C. This reaction explains why the oxygen-bearing conductivities obtained from samples annealed at 800°C. are always slightly higher than similar oxygen-free measurements.

a reaction between Cu_2O and the equilibrium amount of Sb_2O_3 existing at that temperature. Since the latter quantity is exceedingly small, the low rate of formation is readily understandable, despite the relatively high diffusion rates prevailing in these conditions.

While the progress of the reactions can be followed most conveniently from the large changes of properties associated with a considerable antimony content, the nature of the equilibrium is such that the relative quantities of the reactants are important. This is particularly true of the small amounts of antimony common to commercial coppers, and an estimate of the importance of the time factor in their behavior can be obtained from Table 4.

The extremely slow response of sample 76MO is of commercial interest because this shows that while antimony forms at least two oxides in tough-pitch copper under the proper thermal conditions, the time cycle and normal thermal history of commercially rolled electrolytic tough-

pitch coppers virtually ensures the retention of all the antimony in solid solution.

The principles of the reactions outlined from the conductivity data are completely substantiated by the records of softening temperature. The effects of thermal treatment have been investigated by heat-treatment of certain 0.162-in. wires before they were drawn up to 0.081-in. test size. Thus, wires annealed one hour at 850°C.

TABLE 4.—*Percentage of Conductivity vs. Time of Anneal at 500°C.*

No.	Sb, Per Cent	1 Hour	17 Hours	43 Hours
76MO	0.0018	101.8	101.8	102.0
77MO	0.0058	101.25	101.45	101.55

and quenched before drawing to 0.081 in. have softening temperatures equivalent to those obtained from oxygen-free samples (Fig. 2). If the process anneal is $\frac{1}{2}$ hr. at 600°C., sufficient precipitation of Sb_2O_3 occurs to definitely lower the values obtained in the range 0 to 0.02 per cent Sb. With higher antimony contents, the slope of the curve is so small that considerable rejection of antimony from solid solution can occur without noticeable effect on the softening temperature. Finally, the effects of proportionately large losses of antimony from solid solution, such as are obtained from a 15-hr. precipitation treatment at 500°C., are reflected in the major decreases in softening temperature indicated in Fig. 2.

Numerous experiments in the laboratory have demonstrated that the high softening temperatures of the dilute antimonial tough-pitch coppers can be exploited commercially without awkward changes in mill practice. The 800°C. quenching treatment may be carried out on either hot-rolled rods or slabs, to convert the antimony to the soluble form. These, in turn, may be process-annealed at 400°C. during cold-rolling without substantial precipitation of

Sb_2O_3 . Full-scale commercial experiments have been carried out in this manner on hot-rolled 0.150-in. slabs containing 0.007 per cent Sb. Sheets rolled to 0.030 in. using a 1-hr. 400°C. process anneal at 0.095 in., were found to have a softening temperature of 280°C., equivalent to a silver-bearing copper containing 7.6 oz. per ton Ag processed in the normal commercial manner. The maximum sacrifice in conductivity for this antimony content is but 1.2 per cent.

Owing to the considerable controversy over the effects of antimony on the hot-working properties, the behavior of the oxygen-bearing samples was carefully observed during hot-rolling. No cracking was detected in any of the samples containing 0.02 per cent Sb or less. The samples containing 0.06 per cent Sb usually developed small cracks, but only after cooling to a dull red heat. However, this can be avoided by rapid rolling to ensure complete breakdown of the cast structure before the shape cools to the dull red cracking range. Hot shortness was also successfully avoided either by increasing the temperature of the billets from 850° to 900°C., or by reheating after the first two passes.

This behavior suggests that antimony in solid solution has very little effect on the ductility, and that the difficulties that attend the rolling of tough-pitch coppers high in antimony are associated with precipitation of antimony oxide as the slab cools below 700°C. This may be minimized or eliminated by the use of a high-temperature heating furnace and sufficiently rapid handling to ensure the elimination of the cast structure before precipitation of Sb_2O_3 progresses to an appreciable extent.

EFFECT OF CADMIUM

While cadmium is widely used to produce high-conductivity high-strength wire,⁸ its effect in small amounts has received scant attention because of its absence from the normal commercial product. Blazey⁹ has

found that oxygen is present in cadmium coppers. Smith, Burkhardt¹⁰ and others have noted their high softening temperatures but have not explored the low end of the composition range.

Because of the volatility of cadmium, the alloys were prepared individually as billets, the oxygen-free samples by solidification in a tightly closed graphite crucible and the

One set of samples was prepared in the usual way, annealing for $\frac{1}{2}$ hr. at 600°C. at 0.162 in. and cold-drawing to 0.081 in. For comparison, other portions of several alloys were annealed at 850°C. for 1 hr. at 0.162 in., and quenched, before drawing to size. Table 5 and Fig. 4 indicate that the oxygen-free samples are essentially unaffected by the differences in heat-treatment,

TABLE 5.—Alloys of Cadmium and Pure Copper

Sample No.	Cd, Per Cent	O ₂ , Per Cent	Hard Drawn	Conductivity, Per Cent I.A.C.S., Annealed at						Softening Temperature, Deg. C.	
				300°C.	400°C.	500°C.	600°C.	700°C.	800°C.	1 Hour 600°C.	1 Hour 850°C.
318M	Nil	Nil	100.2	102.35	102.4	102.4	102.4	102.4	102.35	147	
328M	0.0026	Nil	100.2	102.3	102.3	102.4	102.35	102.3	102.35	197	
327M	0.0096	Nil	100.0	101.35	102.35	102.3	102.3	102.25	102.3	306	313
326M	0.044	Nil	99.25	100.65	101.95	101.95	102.05	102.05	102.0	354	353
325M	0.164	Nil	97.6	99.7	100.8	100.95	100.95	100.95	100.8	367	363
330M	0.013	0.011	99.85	101.0	102.15	102.3	102.35	102.3	102.25	290	330
331M	0.050	0.017	99.75	100.75	102.15	102.3	102.35	102.4	102.3	325	345
332M	0.168	0.017	98.45	100.05	101.45	101.65	101.75	101.75	101.95	362	363

oxygen-bearing alloys by casting through air. Oxygen absorption during hot-rolling was minimized by heating the oxygen-free alloys in closed graphite tubes. All samples were hot-rolled to $\frac{5}{16}$ -in. rod and drawn to 0.162 in.; there one portion was cut off and drawn to 0.081 in. for the conductivity anneals. Table 5 lists the data. The cadmium and oxygen contents were determined chemically.

The effect of cadmium on the conductivity is so small that at least 0.01 per cent Cd may be added without measurable change. When oxygen is present this figure approximates 0.05 per cent Cd. The addition of oxygen only partially restores the conductivity to that for pure copper (Fig. 4), and in this respect cadmium and antimony behave similarly. Anneals of short duration do not produce conductivity differences illustrative of the suspected instability of the oxide due to the small conductivity effects involved and the slow rate of precipitation. Consequently, softening temperature measurements were used to follow the behavior.

as expected. But the oxygen-bearing alloys exhibit higher softening temperatures in the 850°C. quenched condition, and these are approximately equivalent to the oxygen-free values. Thus there is little doubt that the equilibrium constant for the reaction between cadmium and cuprous oxide is highly dependent on temperature. Substantial amounts of cadmium oxide probably cannot exist in tough-pitch copper much above 700°C., and the rate of formation at 500° to 600°C. is fairly slow. All in all, the parallel between the reactions of cadmium and antimony with oxygen is pronounced.

The behavior of cadmium-bearing tough-pitch coppers also has been studied on a commercial scale. Additions ranging up to 0.06 per cent Cd had no perceptible effects on the casting of the wirebars or their behavior in hot-rolling to $\frac{1}{4}$ -in. rod. Determinations of softening temperature made after a variety of heat-treatments adequately confirmed the reversible nature of the oxide. Furthermore, it was ascertained that the loss of cadmium from solid solution during hot-rolling is moderate, and

that the rate of precipitation during a 1-hr. process anneal at 400°C. is small.

A general picture of the attractive combination of properties afforded by these

that is formed after solution of the metal in a suitable acid mixture. This has been used by Alkins and Hallows¹² as a means of identification of the ease with which

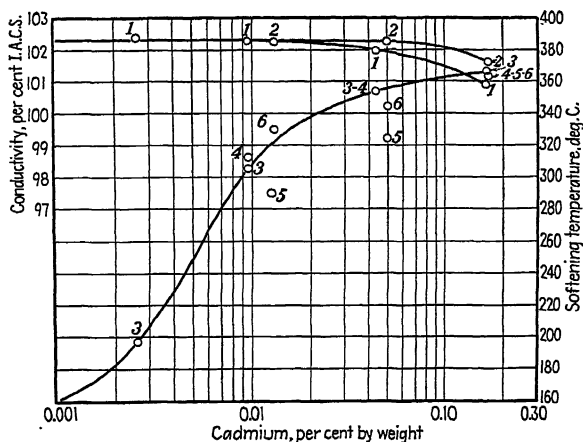


FIG. 4.—EFFECT OF CADMIUM ON CONDUCTIVITY AND SOFTENING TEMPERATURE OF HIGH-PURITY COPPER.

Points 1, conductivity of oxygen-free alloys.

Points 2, conductivity of oxygen-bearing alloys annealed at 500°C.

Points 3, softening temperature of oxygen-free alloys; penultimate anneal 1 hr. 600°C.

Points 4, softening temperature of oxygen-free alloys; penultimate anneal 1 hr. 850°C.

Points 5, softening temperature of oxygen-bearing alloys; penultimate anneal ½ hr. 600°C.

Points 6, softening temperature of oxygen-bearing alloys; penultimate anneal 1 hr. 850°C.

alloys is illustrated by the results obtained from several wirebars containing 0.032 to 0.034 per cent Cd. The conductivity as measured after a 20-min. anneal at 500°C. was 101.5 per cent. Wire cold-drawn to 0.081 in. from the ¼-in. rod in the as-rolled condition had a softening temperature of 308°C. This was raised to 345° by quenching from 850°, and when drawn using a process anneal of 1 hr. at 400° after the 850° quench, the softening temperature decreased only slightly, to 332°C.

EFFECT OF TIN

Additions of tin to oxygen-free copper result in substantial losses of conductivity, but as described by Pilling and Halliwell¹¹ and others, tin in tough-pitch copper is combined with oxygen and has little effect on this property. In discussing these results, Bassett mentions the residue of SnO₂

SnO₂ in copper is reduced by H₂ at temperatures above 550°C. The identity of the oxide has been further corroborated by Rhines¹³ by means of X-ray diffraction.

Bassett¹¹ and Burkhardt¹⁰ have reported that tin is effective in raising the softening temperature but there appears to be a lack of data on the modifications caused by very small quantities. Similarly, the conductivity data for the dilute oxygen-free alloys are in need of revision.

The present series of samples was synthesized and continuously cast in the usual way and the data determined as previously described. Table 6 and Fig. 5 indicate that in oxygen-free copper the conductivity losses due to small amounts of tin are rather moderate, being almost equivalent to those derived from nickel on a weight per cent basis. Up to 0.05 per cent, the losses are a linear function of composition

and amount to 0.09 per cent I.A.C.S. for each 0.001 per cent Sn. The addition of oxygen results in complete restoration of the conductivity, as reported previously.

nessed the slow growth of this constituent during periods of prolonged annealing at high temperature. The mechanism of the phenomenon can be represented adequately

TABLE 6.—*Alloys of Tin and Pure Copper*

Sample No.	Sn, Per Cent	O ₂ , Per Cent	Hard Drawn	Conductivity, Per Cent I.A.C.S., Annealed at						Softening Temperature, Deg. C.
				300°C.	400°C.	500°C.	600°C.	700°C.	800°C.	
191M	Nil	Nil	100.1	102.2	102.2	102.2	102.2	102.15	102.2	137
199M	0.0007	Nil	100.1	102.0	102.0	102.0	102.1	102.1	102.1	142
200M	0.0015	Nil	100.0	102.0	102.1	102.0	102.15	102.05	102.1	175
201M	0.005	Nil	99.7	100.8	101.85	101.9	101.8	101.8	101.75	277
202M	0.010	Nil	99.1	99.7	101.3	101.4	101.4	101.3	101.4	315
203M	0.050	Nil	99.55	96.4	97.7	97.7	97.7	97.7	97.7	347
191MO	Nil	0.023	100.05	102.05	102.2	102.3	102.0	102.1	102.15	138
199MO	0.0007	0.034	100.1	102.25	102.35	102.35	102.35	102.25	102.3	143
200MO	0.0015	0.027	100.2	102.15	102.3	102.05	102.25	102.3	102.25	143
201MO	0.005	0.023	100.15	102.3	102.35	102.3	102.2	102.2	102.2	137
202MO	0.010	0.025	100.05	102.25	102.35	102.35	102.35	102.3	102.3	143
203MO	0.050	0.024	100.15	102.2	102.35	102.35	102.3	102.35	102.25	141

As Fig. 5 demonstrates, tin is one of the most effective elements in raising the softening temperature. This, of course, is true only when tin is present in solid solution, since the presence of oxygen precipitates SnO_2 , which is wholly ineffective.

without resort to the awkward assumption of solubility on the part of SnO_2 , by again considering the reversible characteristics of reactions of this type:

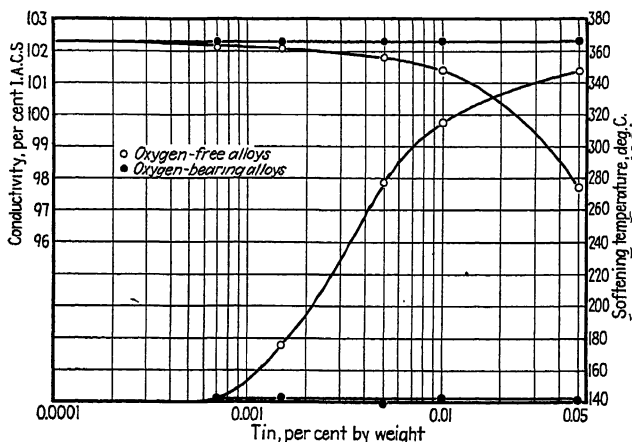
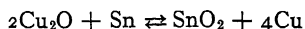


FIG. 5.—EFFECT OF TIN ON CONDUCTIVITY AND SOFTENING TEMPERATURE OF HIGH-PURITY COPPER.

However, in oxygen-free coppers tin is far more efficacious than silver if high softening temperature is the only consideration.

The instability of SnO_2 in copper has been suspected by many who have wit-

If the equilibrium shifts slightly to the left at high temperatures, some tin will enter solid solution, and coalescence of SnO_2 will proceed, since the dissociated atoms of tin and oxygen will diffuse independently to

the surface of the growing SnO_2 particle, where again they combine and precipitate.

Heat-treatments designed to retain tin in solid solution in the presence of oxygen were employed in an attempt to verify this hypothesis by means of the effect of the soluble tin on the softening temperature. Unfortunately, the results were inconclusive. This, however, merely suggests that the equilibrium amount of soluble tin that

the softening temperature are exceedingly sketchy.

The data reported in Table 7 and Fig. 6 were obtained in the usual manner; all oxygen-bearing alloys were obtained by remelting the oxygen-free rods and casting through air. The master alloy, containing 0.2 per cent Te, was found to lack the high ductility of oxygen-free copper, but the test samples, with their lower tellurium con-

TABLE 7.—*Alloys of Tellurium and Pure Copper*

Sample No.	Te, Per Cent	O ₂ , Per Cent	Hard Drawn	Conductivity, Per Cent I.A.C.S., Annealed at						Softening Temperature, Deg. C.	
				300°C.	400°C.	500°C.	600°C.	700°C.	800°C.	$\frac{1}{2}$ Hour 600°C.	1 Hour 850°C.
283M	Nil	Nil	100.3	102.4	102.3	102.3	102.3	102.35	102.3	143	
285M	0.0007	Nil	100.1	102.2	102.15	102.3	102.2	102.1	102.15	186	195
286M	0.0015	Nil	100.0	102.1	102.2	102.2	102.2	102.1	102.0	207	257
287M	0.005	Nil	99.9	101.8	101.9	101.85	102.0	101.7	101.15	227	344
288M	0.01	Nil	100.0	101.9	101.9	101.85	101.95	101.7	101.0	200	370
289M	0.05	Nil	99.65	101.2	101.4	101.65	101.75	101.4	100.7	250	385
283MO	Nil	0.034	100.15	102.35	102.4	102.4	102.4	102.4	102.35	140	
285MO	0.0007	0.035	100.05	102.15	102.25	102.35	102.3	102.25	102.15	169	198
286MO	0.0015	0.031	100.0	102.1	102.15	102.15	102.2	102.1	102.0	197	252
287MO	0.005	0.030	99.85	101.9	101.95	102.0	102.1	101.8	101.3	227	332
288MO	0.010	0.034	99.5	101.25	101.35	101.70	101.85	101.55	100.75	230	371
289MO	0.05	0.025	99.6	101.5	101.65	101.8	102.0	101.8	101.0	248	377

exists in the presence of oxygen in solid copper at high temperatures is too small for detection by either softening temperature or conductivity measurements. Both properties change significantly only after the addition of appreciable quantities (Fig. 5).

EFFECT OF TELLURIUM

The use of tellurium to promote machinability in copper alloys^{14, 15} has revived interest in the effect of this element. Traditionally, tellurium has been considered to be very harmful because of its tendency to promote hot and cold shortness. This has been reported by Addicks,¹⁶ who also mentions that tellurium is "practically insoluble in copper," and therefore has little effect on its conductivity. Skowronski has surveyed the low composition range in more detail, with similar results. The descriptions of the influence of tellurium on

tents, were hot-rolled and/or drawn without the appearance of either hot or cold shortness.

If the results of the 500°C. anneals are compared, the conductivity losses due to tellurium are indeed small, but these increase with increasing annealing temperatures and it is evident that the solid solubility of tellurium increases accordingly. Because the data for the oxygen-bearing samples are influenced by errors in correcting for the effect of the excess Cu_2O , etc., it is to be expected that some deviations will occur. Nevertheless, the influence of oxygen on the results appears to be essentially nil, and it is proposed that in this concentration range tellurium and oxygen do not combine to an appreciable extent.

Following the determinations listed in Table 7, the samples were reannealed at the same temperature for periods up to 73 hr.

No further changes were noted at 500°, 600° or 700°C., but small additional losses, some as high as 0.2 per cent I.A.C.S., were obtained from the more concentrated

little solid solubility is permitted, and the increases are appropriately modest, as demonstrated by the lower of the two curves of Fig. 6. If advantage is taken of the

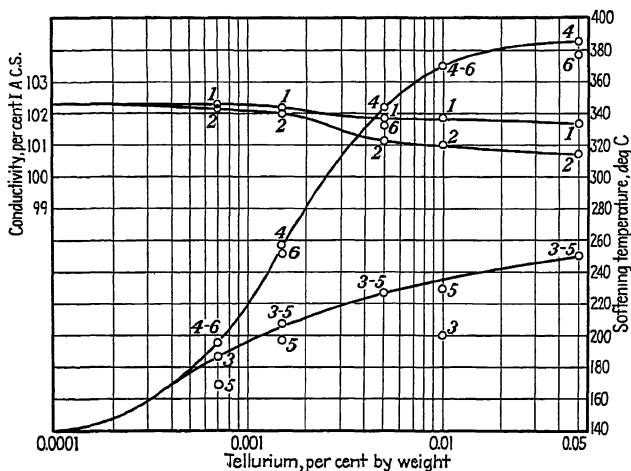


FIG. 6.—EFFECT OF TELLURIUM ON CONDUCTIVITY AND SOFTENING TEMPERATURE OF HIGH-PURITY COPPER.

Points 1, conductivity of oxygen-free alloys annealed at 500°C.

Points 2, conductivity of oxygen-free alloys annealed at 800°C.

Points 3, softening temperature of oxygen-free alloys; penultimate anneal $\frac{1}{2}$ hour 600°C.

Points 4, softening temperature of oxygen-free alloys; penultimate anneal 1 hour 850°C.

Points 5, softening temperature of oxygen-bearing alloys; penultimate anneal $\frac{1}{2}$ hour 600°C.

Points 6, softening temperature of oxygen-bearing alloys; penultimate anneal 1 hour 850°C.

alloys at 800°C. It is, of course, possible to arrive at an approximation of the solid solubility of tellurium from the detailed data. Including an appropriate allowance for the effect of excess copper telluride and other constituents, it appears that the solid solubility may be deduced as about 0.0075 per cent Te at 800°C., 0.0015 per cent Te at 700°C., about 0.0004 per cent Te at 600°C., and something less than 0.0004 per cent Te at 500°C. In any event, it is certain that a marked solubility increase occurs between 700° and 800°C. Within this limited range, tellurium lowers the conductivity about 0.23 per cent I.A.C.S. for each 0.001 per cent soluble Te.

The influence of tellurium on the softening temperature is of altogether different proportions but equally insensitive to oxygen. When a final intermediate anneal at 600°C. is used in the drawing cycle, very

solubility increase that occurs above 700°C., by using a 1-hr. anneal at 850°C. and a quench as the final intermediate anneal, the softening temperature increases at the relatively enormous rate shown in the upper curve. Of all the elements commonly found as impurities in commercial coppers, none approaches tellurium for individual effectiveness in promoting high softening temperature.

In addition, tellurium also affects the shape of the annealing curve obtained by plotting tensile strength against annealing temperature. As has been shown previously, the transition from hard to soft in pure copper is rapid, and the entire process is complete within a 25°C. temperature span. In the presence of soluble tellurium, this change may progress only halfway over a 100°C. range, and surprisingly high annealing temperatures are required to remove

completely the effects of cold-working. Consequently, if a full anneal is attained, the temperature will have been sufficiently high to precipitate a considerable portion of the tellurium from solid solution, and further cold-working will result in a correspondingly lower softening temperature.

PERIODIC RELATIONS

As previously shown for iron, cobalt and nickel, the accuracy of measurement of the increases in resistivity caused by the additions of impurities to pure copper is relatively high; this permits a rather precise mathematical treatment of the data based on the relative positions of the impurities in the periodic table. Norbury¹⁷ has demonstrated the existence of the general periodic relationship and Linde¹⁸ has shown that in some cases it is a function of valence.

Obviously, the following precautions are necessary in considering the data and many of the previous inconsistencies can be traced to one or more of these:

1. Extraneous impurities, particularly oxygen, must be absent.

2. The unit effect for each element is usually at its maximum only over a narrow concentration range of low order, and must be calculated from data obtained in this range.

3. In cases of limited solid solubility, the effect must be determined within the solubility region.

In determining the unit increases in resistivity for each 0.01 atomic per cent of the elements listed in Table 8 it was therefore necessary in some cases to calculate a theoretical effect for 0.01 per cent based on the actual effect measured from a more dilute alloy. For instance, for tellurium, the solid solubility is restricted to about 0.0075 per cent by weight at 800°C., and the result given has been derived from the conductivity of the sample containing 0.005 per cent Te by weight (0.0025 atomic per cent) annealed at 800°C. Mass resistivity is employed.

When these unit effects are plotted against $(n-1)^2$ (Fig. 7) where n is the valence of the impurity as determined by its position in the periodic system, the

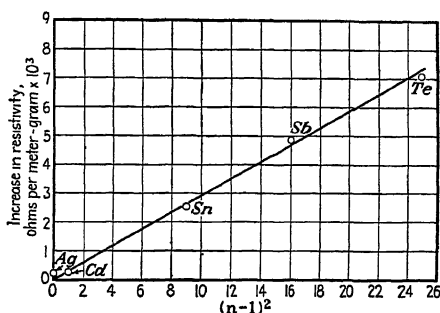


FIG. 7.—RESISTIVITY EFFECTS AS A FUNCTION OF VALENCE.

expected straight line is obtained. The deviations are well within the limits of error of the determinations.

TABLE 8.—Increases in Resistivity

Solute Element, Atomic Per Cent	Valence, n	Increase in Resistivity, Ohms per Meter-gram $\times 10^3$
0.01 Ag.....	1	0.11
0.01 Cd.....	2	0.275
0.01 Sn.....	4	2.54
0.01 Sb.....	5	4.84
0.01 Te.....	6	7.06

SUMMARY

1. Silver has a very small effect on the conductivity of copper. Up to 10 oz. per ton Ag the conductivity depression is 0.015 per cent I.A.C.S. for each ounce per ton Ag. A considerable increase in softening temperature is obtained from additions of silver, but the shape of the curve indicates that the amounts present in electrolytic coppers may be neglected as contributors to their annealing behavior. Oxygen does not combine with silver in copper.

2. Antimony enters solid solution in oxygen-free copper and lowers its conductivity linearly 0.16 per cent I.A.C.S. for each 0.001 per cent Sb, up to 0.06 per cent Sb. Major increases in softening tempera-

ture are also realized. In the presence of oxygen, antimony forms at least two oxides. The simpler in composition is precipitated below 700°C. and is unstable at higher temperatures. The more complex is formed very slowly at 800°C. and is stable at lower temperatures. Oxygen-bearing antimonial coppers may be heat-treated to retain antimony either in solid solution in its effective form or as an ineffective insoluble oxide.

3. The effect of cadmium on the conductivity of oxygen-free copper is only slightly larger than that of silver; each 0.001 per cent Cd lowers the conductivity 0.0082 per cent I.A.C.S. between 0 and 0.164 per cent Cd. Cadmium in solid solution has a pronounced influence on the softening temperature. The reaction of cadmium with oxygen is similar to that of antimony. Cadmium oxide is precipitated in appreciable amounts below 700°C.; temperature and time are important factors. Above 700°C. the oxide is unstable. Heat-treatments may be carried out to retain cadmium in either the soluble or insoluble form.

4. Tin has a moderate effect on the conductivity of oxygen-free copper (0.09 per cent I.A.C.S. per 0.001 per cent Sn) but is responsible for major increases in the softening temperature. The presence of oxygen completely nullifies these changes in properties by precipitation of SnO_2 . No evidence of the instability of the oxide at high temperatures has been obtained, but the measurements are not particularly well adapted to the detection of threshold dissociation.

5. Tellurium has a limited solid solubility in oxygen-free or oxygen-bearing copper, which increases appreciably above 700°C. Tellurium does not combine with oxygen under these conditions. Its unit effectiveness in decreasing the conductivity is high (0.23 per cent I.A.C.S. per 0.001 per cent soluble Te) but the total depression obtained from large additions is small be-

cause of its small solubility; above the solubility limit, the decreases are due only to the volume effect of Cu_2Te . Tellurium has the most pronounced influence on softening temperature of any of the impurities common to commercial coppers. Despite the solubility limitations, heat-treatments may be carried out to obtain coppers having high conductivities and extraordinary resistance to softening.

6. These five fifth-period elements increase the resistance of copper in relation to the ratio $(n - 1)^2$ where n is the valence of the solute element as determined by its position in the periodic table.

ACKNOWLEDGMENT

The authors acknowledge with pleasure their indebtedness to Dr. A. J. Phillips, director of the research program from which these data have been taken. Mr. Stephen Mikula carried out much of the experimental work. Thanks are due also to the American Smelting and Refining Co. for permission to publish the results.

REFERENCES

1. J. S. Smart, Jr., A. A. Smith, Jr. and A. J. Phillips: *Trans. A.I.M.E.* (1941) **143**, 272.
2. J. S. Smart, Jr. and A. A. Smith, Jr.: *Trans. A.I.M.E.* (1942) **147**, 48.
3. J. L. Gregg: *Arsenical and Argentiferous Copper*. New York, 1934. The Chemical Catalog Company, Inc.
4. M. Hansen: *Der Aufbau der Zweistofflegierungen*, 1936-1937.
5. J. C. Mertz and C. H. Mathewson: *Trans. A.I.M.E.* (1937) **124**, 73.
6. S. L. Archbutt and W. E. Prytherch: *Jnl. Inst. Metals* (1931) **45**, 265.
7. S. Skowronski: *Metallurgy of Copper—Hoffman and Hayward*. New York. McGraw-Hill Book Co.
8. W. C. Smith: *Chem. and Met. Eng.* (1921) **25**, 1178.
9. C. Blazey: *Metal Ind.*, London (1929) **34**.
10. A. Burkhardt: *Metallwirtschaft* (1931) **10**, 657-659.
11. N. B. Pilling and G. P. Halliwell: *Trans. A.I.M.E.* (1926) **73**, 679, 25.
12. W. E. Alkins and A. P. C. Hallowes: *Jnl. Inst. Metals* (1935) **56**, 125.
13. F. N. Rhines: *Trans. A.I.M.E.* (1940) **137**, 246.
14. H. L. Burghoff and D. E. Lawson: *Trans. A.I.M.E.* (1938) **128**, 315.

15. C. S. Smith: *Trans. A.I.M.E.* (1938) **128**, 325.
16. L. Addicks: *Trans. A.I.M.E.* (1906) **36**, 18.
17. A. L. Norbury: *Trans. Faraday Soc.* (1921) **16**, 570.
18. J. O. Linde: *Ann. Physik* (1932) **15**, 219.

DISCUSSION

(Alan Morris presiding)

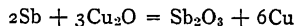
P. A. BECK,* Cleveland, Ohio.—The authors are to be congratulated on the mass of interesting information offered in their paper. I am particularly interested in the data obtained on the effect of very small additions of alloying elements on the recrystallization temperature. This effect, important as it is from a practical point of view, is very little understood in its fundamental nature. The present contribution, a result of careful and accurate work, is therefore especially valuable.

From the data presented it appears that in each alloy series there is a concentration range where the recrystallization temperature increases particularly steeply with increasing alloy concentration. Above this range the rate of increase is much lower. It is very interesting to note that the alloy concentration at which further additions become less effective—i.e., the knee of the curve—corresponds roughly to 0.01 per cent in all cases here reported, except silver.

The effect of tellurium is particularly interesting from a fundamental point of view. Tellurium appears to raise the recrystallization temperature in both the dissolved and the precipitated form (precipitate probably Cu_2Te), although the latter effect is smaller. The recrystallization retarding effect of solid solutions usually is considered to be quite different fundamentally from that of a finely dispersed second phase. The latter effect probably is largely due to growth inhibition. This is shown by the fact that a finely dispersed second phase often retards grain growth (coalescence) as well as recrystallization. Examples: the well-known effect of alumina on the coarsening of austenite, and the similar effect of CoBe on grain growth in beryllium-copper alloys. The effect of solid solution on grain growth is certainly very much smaller, whereas its effect on recrystallization is in this instance at least apparently stronger than that of a second phase.

* Cleveland Graphite Bronze Co.

The very interesting reversible reactions affecting the electrical conductivity of the ternary Cu-Sb-O alloys and the softening temperature of the ternary Cu-Cd-O alloys are well worth noting. The authors express these reactions in terms of chemical formulas, such as



Their explanation (p. 107) is that Sb_2O_3 is in all probability unstable at high temperatures, "because of the mass effect of the excess copper, which acts as a reducing agent." This leaves no doubt as to the fact that they view these reactions in the light of homogeneous equilibrium and the law of mass action. However, the observed phenomena depend on the passage of Sb from one phase to another phase and, in fact, these reactions involve three phases: the Cu solid solution, Sb_2O_3 , and Cu_2O . Obviously, in such cases the experimental facts can be much better described in terms of heterogeneous equilibria and ternary constitution diagrams.

Fig. 8 shows schematically the probable form of the Cu-Sb side of the isothermic section corresponding to 500°C. of the Cu-Sb-O diagram. It was drawn in accordance with the authors' conclusion that the Cu phase coexists with Sb_2O_3 and that practically all Sb is oxidized to Sb_2O_3 if enough oxygen is present and if the annealing time is long enough to approach equilibrium. Fig. 10 shows in more detail the Cu corner of the same isothermic section. The solubility of oxygen in Cu was taken from Baker's work as approximately 0.003 per cent. Point *T* represents the composition of the Cu-Sb-O solid solution in equilibrium with both Cu_2O and Sb_2O_3 . As seen in Fig. 10, alloys 77MO, 78MO, and 83M fall within the three-phase field $\text{Cu} + \text{Cu}_2\text{O} + \text{Sb}_2\text{O}_3$. The order of magnitude of the antimony concentration of point *T* was determined by the conductivity of alloy 83M after prolonged annealing allowed to approximate equilibrium (Table 3). After sufficiently long anneal the corrected conductivity of the other two alloys should be the same, since the composition of the copper phase must be the same (*T*) for all alloys of the three-phase field, under equilibrium conditions.

The conditions at 800°C. can also be described by an isothermic section of the ternary

diagram. The phases existing at this temperature are the copper solid solution, the liquid antimony phase containing up to approximately 75 per cent copper in solution, the solid

existence at 800°C. of a separate $\text{Cu}_x\text{Sb}_y\text{O}_z$ compound, formed by reaction between Cu_2O and Sb_2O_3 , as postulated by the authors, rather improbable. The dissolved Cu_2O apparently

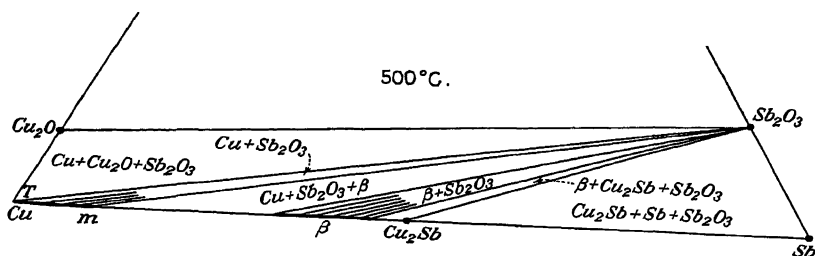


FIG. 8.

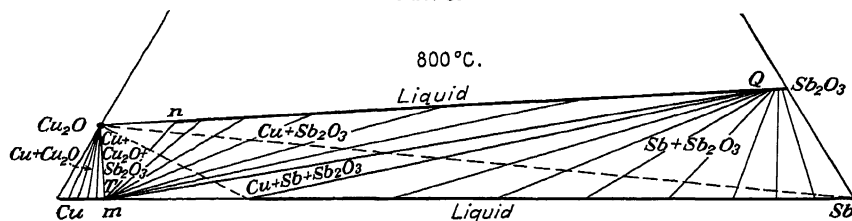


FIG. 9.

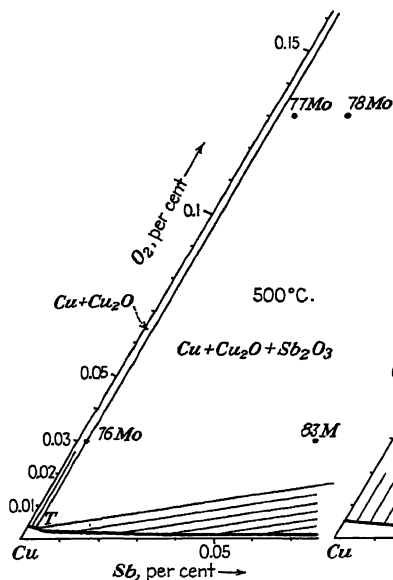


FIG. 10.

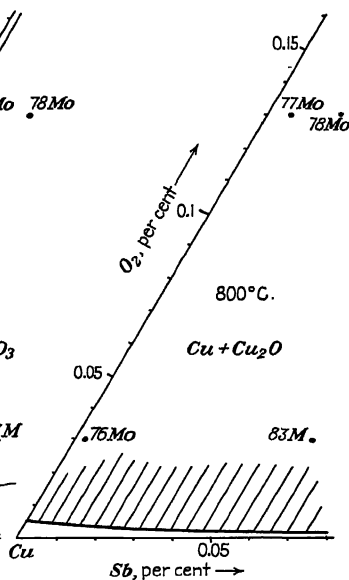


FIG. 11.

Cu_2O phase, and the liquid Sb_2O_3 phase. The latter can incorporate very large amounts of Cu_2O in liquid solution, as indicated by a few preliminary experiments. This makes the

lowers the melting point of Sb_2O_3 considerably, and possibly these two constituents form a eutectic. The possible existence of a $\text{Cu}_x\text{Sb}_y\text{O}_z$ or rather $(\text{Cu}_2\text{O})_x(\text{Sb}_2\text{O}_3)_y$ compound is,

however, not definitely excluded, and should be further investigated.

The authors' data indicate that in their ternary alloys at 800°C. copper antimony solid solutions coexist with Cu_2O , and that *unsaturated* Cu-Sb solid solutions, at least in this low concentration range, cannot coexist with Sb_2O_3 . The latter, if present, will react with the copper-rich phase to form Cu_2O and antimony, which goes into solid solution. This fact, however, does not necessitate the assumption that at this temperature copper *saturated* with antimony (point *m* in Fig. 9) will react with Sb_2O_3 to form Cu_2O and antimony. (If such a reaction should take place, the dotted tie lines in Fig. 9 should be valid.) On the contrary, it is easy to show that molten antimony will react with Cu_2O under oxidizing conditions, to form copper solid solution, copper-antimony intermetallic phases, and an antimony oxide phase. Accordingly, the tie lines in Fig. 9 were drawn to show the coexistence of the saturated copper solid solution (*m*) with liquid Sb_2O_3 solutions ($Q - n$). Point *T* corresponds to the copper-rich solid solution that coexists with both Cu_2O and the saturated Sb_2O_3 liquid *n*. Comparison of Figs. 8 and 9 shows that the major change in the copper corner, taking place between 500° and 800°C., is the displacement of point *T* toward higher Sb concentrations. This gradual shift of point *T* within this temperature range accounts for the reversible phenomena, observed by the authors, much more adequately than the change of the "equilibrium constant" referred to in the paper (p. 110).

The nature of the change occurring during very long anneals at 800°C. is obscure. The suggestion offered in the paper that it consists in the formation of a complex $\text{Cu}_x\text{Sb}_y\text{O}_z$ precipitate, resulting from the interaction between Cu_2O and Sb_2O_3 , appears very doubtful (see above). It may be that the loss of antimony is due to the gradual sublimation of Sb_2O_3 from the surface of the specimen. The vapor tension of Sb_2O_3 is relatively high even at much lower temperatures than 800°C., and sublimation readily takes place at around 600°C.

C. S. SMITH,* Washington, D. C.—The recrystallization-temperature measurements described by the authors are practically the first that have been done on materials of sufficient purity to enable a detailed discussion of the effect of composition in the very dilute alloys of greatest interest.

The authors have plotted their results against composition on a logarithmic scale. This is justifiable and, indeed, is the only recognized method of plotting results when a wide composition range must be covered without sacrifice of detail in the earlier parts of the curve. Unfortunately, logarithmic plotting distorts the curve considerably, and it is nothing but this method of plotting that enables the authors to say, as on pages 105 to 106, that "... the softening temperature is influenced only slightly by the initial additions ... followed by a limited concentration zone of high effectiveness ... terminated by a rapidly diminishing zone. This behavior is typical of all the impurities investigated." Actually, if the authors' results are plotted on a linear scale it will be seen that the first additions are—weight for weight—actually the most potent in raising recrystallization temperature, for the curves start out as a straight line followed by a progressive decrease in slope. The first zone of relative ineffectiveness is purely a result of logarithmic plotting, as can be seen by comparing the authors' figures with Fig. 12, in which the same results have been replotted on a linear scale. This figure also shows the difference between the effects of various additions on the recrystallization temperature of copper. Iron, nickel and cobalt (for which the data are taken from the authors' earlier paper) are relatively ineffective in amounts up to 0.05 per cent, while silver, cadmium, tin, antimony and tellurium produce effects increasing in the order named. Perhaps it is more than a coincidence that the initial slope of these curves is in the order of increasing valence of the added element (Ag-1, Cd-2, Sn-4, Sb-5, Te-6). If the recrystallization temperature is plotted against the product of the valence and atomic percentage of the added element, these curves become grouped quite closely together, as may be seen in Fig. 13. It must be remembered that the softening

* National Research Council.

temperatures plotted were arbitrarily selected on the basis of 50 per cent loss of tensile strength in a 60-min. anneal, and had some other criterion been selected it is likely that

temperature and valency of solute with the results just shown.

Dr. Smith has mentioned that some intermediate alloy structures, involving a transition

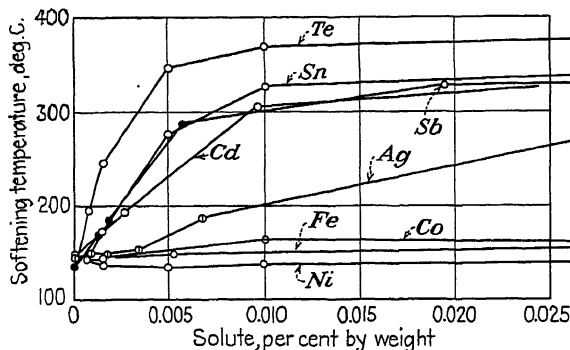


FIG. 12.

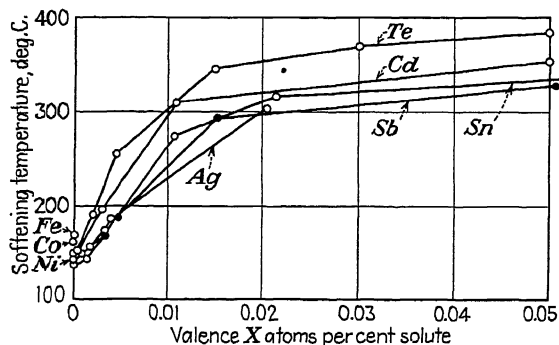


FIG. 13.

even closer grouping could be obtained. It is interesting that iron, nickel and cobalt all have very little effect on the softening temperature, and these transition elements are known to act in metallic alloy lattices as though their valence were zero. The valence effect will often be unnoticeable because of the low solubility of the elements of higher valence.

J. H. FRYE, JR.,* Bethlehem, Pa.—I wondered, while Mr. Smart was presenting his paper, if there was any connection between softening temperature and position of the solute element in the periodic table. I was very gratified, therefore, to see that Dr. Smith had investigated the relation between softening

and a B subgroup element, occur at electron-atom ratios corresponding to the Hume-Rothery rule if the transition element is assigned a valency of zero.

In addition to this evidence, that a transition element may contribute no valency electrons, there is the quite independent evidence of magnetic measurements. By these means it has been shown that additions of Ni, Pd, and Pt to Cu, Ag, and Au contribute no valency electrons as long as the electron-atom ratio is greater than 0.6.

J. S. SMART, JR. (author's reply).—The data presented in this paper provide a considerable basis for speculation, and Mr. Beck's response is gratifying. The authors have also found the effects of dispersed second phases on recrystallization and grain growth an interesting sub-

* Assistant Professor of Metallurgy, Lehigh University.

ject. Mr. Beck has noted a few of the many examples of the effectiveness of these second phases in restricting grain growth. In many such cases, precipitation occurs during recrystallization without changing the appearance of the annealing curve; i.e., the transition from hard to soft is rapid and continuous.

In others, such as the behavior of tellurium in copper, the curve is modified to the extent that the temperature interval from hard to soft at constant annealing time is greatly increased, but a continuous curve is still obtained.

In certain copper-phosphorus-iron alloys, the softening process can be observed to start at a relatively low temperature, and then to cease almost entirely for an appreciable temperature interval, owing to the effects of simultaneous precipitation, after which the softening process continues at higher temperatures and at a relatively slow rate. This produces a discontinuous or an interrupted annealing curve; it may possibly differ from the continuous type only in the degree of the effect of the precipitate.

However, there are also instances, such as Cu_2O in copper, in which the precipitate exerts a marked restricting effect on grain growth without influencing the softening process to any measurable degree. In view of this, it is rather debatable whether at this stage we can safely ascribe the effects of precipitates in retarding recrystallization simply to growth inhibition, as Mr. Beck suggests.

In presenting the data for antimony, the authors have limited themselves to a description of the general behavior of this element in oxygen-free and tough-pitch coppers and the resultant effects on the physical properties. It is freely admitted that if a comprehensive constitutional study is desired, the use of the phase diagram is essential and Mr. Beck undoubtedly has carried this as far as possible within the limited scope of the data. Unfortunately, with the data available, one is forced into speculative assumptions in rather short order. The fact that a precipitate forms at a very slow rate at 800° to 850°C. under conditions of long-time annealing has been determined, but so little else is known about it that one is almost forced into some kind of assumption even to discuss it. Therefore, it is quite under-

standable that Mr. Beck somewhat doubts the assumptions made by the authors, and quite properly so. They were intended only to provide a practical means for rationalizing the data to the point where they could be used to predict the magnitude of the changes in physical properties during heat-treatment. In any event, whatever the composition of this compound, or its mode of formation, antimony is rejected from solid solution at this temperature, but not from the copper by sublimation. This was thoroughly checked on samples treated so that more than 50 per cent of the antimony was removed from solid solution, and unquestionably the analytical methods are sufficiently accurate to detect losses in these amounts; no loss was found. In addition, it was also determined that antimony did not preferentially enter the surface oxide scale under these conditions, and thus deplete the concentration by this means.

The authors wish to express their thanks to Dr. Smith for his correction with regard to the conclusions drawn from the logarithmic plots. In addition to the deceptive general shape of the curves, those presented actually do show the concentration zone effects, and as pointed out in Dr. Smith's Fig. 12 these are simply the result of how one draws the curves through the points. The curves should have been drawn on the logarithmic plots so that they conformed to those obtained from a linear scale. As Dr. Smith points out, the initial zone of concentration then becomes the zone of greatest effectiveness on the softening temperature, with the possible exception of the curve for silver.

The correlation of softening temperature with valence is an appealing contribution, and there is much to be said for the chances of improving the agreement of the data by using some criterion of the softening temperature other than that employed by the authors. If, indeed, this correlation could be rigorously demonstrated, we might possibly arrive at a more fundamental measure of the softening temperature. There can be no question that the method we are now using is arbitrary, despite the very real and considerable practical experimental advantages to recommend it.

Internal Friction of an Alpha-brass Crystal

BY CLARENCE ZENER,* JUNIOR MEMBER A.I.M.E.

(Cleveland Meeting, October 1942)

THE internal friction of nonferrous metals vibrating at low stress amplitudes has so far always been successfully interpreted in terms of inhomogeneities of one sort or another. Examples are the fluctuation of stress across a specimen vibrating transversely,^{1,2,3} the stress inhomogeneities due to the elastic anisotropy and partial random orientation of the individual crystallites,^{4,5} localized weak regions introduced by cold-working,^{6,7} grain boundaries and possibly twinning planes.^{8,9} Perfect single crystals are, by definition, homogeneous. Actual single crystals usually, perhaps always, contains some imperfections. The present investigation was undertaken to determine whether the internal friction of single crystals may likewise be attributed to inhomogeneities.

This study was made possible through the gift of a large single crystal of 70-30 alpha brass by H. L. Burghoff, of the Chase Brass and Copper Co. The specimen, $\frac{1}{2}$ in. in diameter and 10 in. long, was similar to samples previously described by Mr. Burghoff.¹⁰

EXPERIMENTAL METHOD

The experimental method used has previously been described in Institute papers.^{5,6,9} The measure of internal friction adopted here, $1/Q$, is $(1/\pi) \times$ the logarithmic decre-

ment, a measure used by some writers, and is also $(1/2\pi) \times$ the specific damping capacity, a measure used by other writers. In all measurements the stress level was kept so low that the measurements were independent of stress level. In all measurements in which the temperature was varied, observations were made as the specimen slowly cooled from its highest temperature.

The specimen was vibrated transversely. Observations were made at the fundamental frequency and at the first overtone, of about 620 and 1710 cycles per second, respectively. No attempt was made to avoid acoustical losses.

EXPERIMENTAL RESULTS

The specimen was annealed for several hours at 450°C. The temperature dependence of the internal friction was then determined from room temperature to 400°C. As shown in Fig. 1, the internal friction increased by only a factor of 2 from room temperature to 300°C., then by a factor of 100 during the next 100° interval. These measurements are consistent with the view that the observed internal friction is the superposition of two distinct parts. One, dominant at room temperature, is nearly independent of temperature. This part may be accounted for by acoustical losses and by transverse thermal currents. It was not further investigated. The second part, when plotted in the manner of Fig. 1, lies upon a straight line. Therefore it has a heat of activation H ; i.e., it varies with temperature as

$$\text{Internal friction} \sim e^{-H/RT} \quad [1]$$

This research was supported by a grant from The Engineering Foundation and was carried on as a part of Engineering Foundation Project 77. Manuscript received at the office of the Institute Jan. 30, 1942. Issued in *METALS TECHNOLOGY*, September 1942.

* Associate Professor of Physics, Washington State College, Pullman, Washington. Now at Watertown Arsenal, Watertown, Massachusetts.

where R is the gas constant (1.986 cal. per gram mol), and T is the absolute temperature.

retical ratio of these two frequencies is 2.76.¹¹ In Fig. 2, two parallel straight lines have been passed through the two sets of

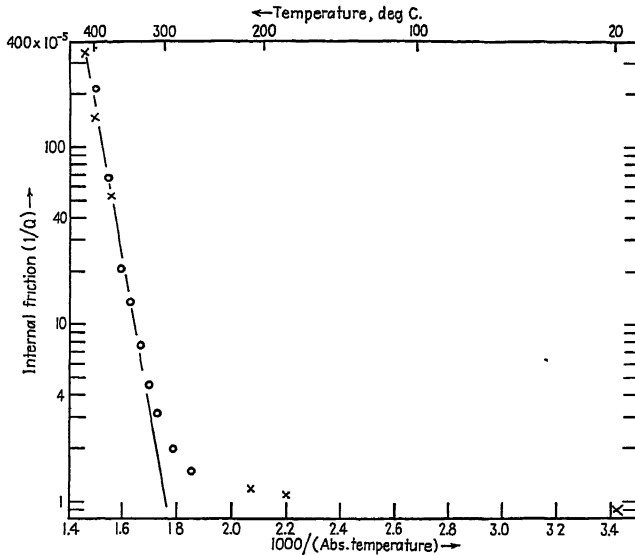


FIG. 1.—SEPARATION OF INTERNAL FRICTION INTO LOW-TEMPERATURE AND HIGH-TEMPERATURE COMPONENTS.

Circles and crosses represent observations made on two different runs, both at a frequency of 1710 cycles per second.

Internal friction may be interpreted phenomenologically as an indication of an inelastic relaxation of stresses. Eq. 1 suggests that the internal friction is proportional to the rate of this stress relaxation, the heat of activation being associated with this rate of stress relaxation. If this is true, the lower the frequency, the more relaxation will take place during a half cycle; hence the greater will be the dissipation of energy. In fact, it may readily be shown analytically that the energy dissipation per cycle, and hence the internal friction, will be inversely proportional to the frequency. The following relation, therefore, would be expected:

$$\text{Internal friction} \sim (1/f)e^{-H/RT} \quad [2]$$

This relation was tested by making measurements at two different frequencies, the fundamental and first overtone. The theo-

observations, the spacing of the two lines being determined by the theoretical ratio 2.76. It is seen that relation 2 is satisfied within experimental error.

Relaxation phenomena may be classified into two groups, denoted as limited and unlimited. In the latter group the stress associated with a given strain will become completely relaxed provided only sufficient time is allowed. In solids with unlimited relaxation, the internal friction will continue to increase indefinitely as the frequency is lowered. Such solids would not vibrate freely at low frequencies; i.e., they would be overdamped with respect to low frequencies. Amorphous substances such as pitch are good examples. In solids with only limited relaxation, only a certain fraction of the macroscopic stress associated with a given strain can become relaxed. Common examples are solids with a disperse plastic

phase, and specimens in which temperature equilibrium is upset by the application of a strain. The behavior of solids with limited relaxation has already been analyzed from

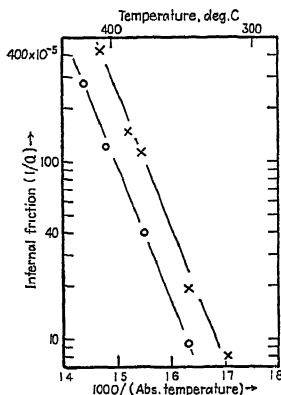


FIG. 2.—FREQUENCY DEPENDENCE OF HIGH-TEMPERATURE COMPONENT.

Crosses and circles represent observations made at 620 and 1710 cycles per second. The upper line has been displaced by the theoretical factor of (1710/620) from the lower line.

many viewpoints.^{1,7,12,13,14} In the particularly simple but important case where the stress relaxes according to an exponential law, the frequency dependence of internal friction is given by

$$\text{Internal friction} \sim 1/(\phi + \phi^{-1}) \quad [3]$$

where ϕ is a dimensionless parameter proportional to the frequency of vibration f . When $\phi \gg 1$, the internal friction is inversely proportional to ϕ ; hence varies as $1/f$. When $\phi \ll 1$, the internal friction is proportional to ϕ ; hence varies as f . If the relaxation phenomenon in our single crystal is of this simple limited type, the conditions under which the observations in Figs. 1 and 2 were taken are such that $\phi \gg 1$. Upon comparing Eq. 3 in the case $\phi \gg 1$ with Eq. 2, we see that then

$$\phi = (f/f_0)e^{H/RT} \quad [4]$$

where f_0 is as yet an undetermined constant with the dimensions of frequency.

The experimental differentiation between limited and unlimited relaxation may be obtained by making observations over a wide frequency range. In this particular

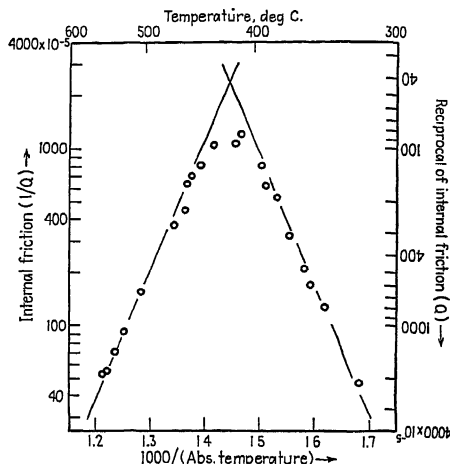


FIG. 3.—INTERNAL FRICTION IN REGION OF CRITICAL TEMPERATURE.

The straight-line asymptotes have slopes of equal magnitude but of opposite sign. When this figure is turned upside down, the observations should lie upon a curve that is the sum of the two asymptotes. Observations made at 620 cycles per second.

case, the pertinent frequency range would lie lower than the frequency used in obtaining Figs. 1 and 2. Unfortunately, our crystal has no lower natural frequencies. However, as may be seen from Eq. 2 or Eq. 4, the same effect may be obtained by raising the temperature. In preparation for this experiment, the crystal was given an 8-hr anneal at 700°C. The apparatus was then heated as hot as it was thought capable of standing, and the internal friction was measured as the specimen slowly cooled. (The apparatus, in fact, was damaged by this experiment.) The observations shown in Fig. 3 prove that the stress relaxation in our crystal is of the simple limited type.

The observations may be readily compared with the theoretical formulas of Eqs. 3 and 4, by observing that the recipro-

cal of the internal friction is the sum of two terms, one proportional to p , the other to $1/p$. Hence, when the internal friction is plotted on semilog paper against $\log p$, as in Fig. 3, a plot of the reciprocal of internal friction against $\log p^{-1}$ is obtained by turning the graph upside down. In this inverted diagram, the observations should be the sum of two straight lines whose slopes have equal magnitude but opposite sign, and this is true in the figure, within experimental error.

DISCUSSION OF EXPERIMENTAL RESULTS

From the experiments described in the previous section certain inferences have been drawn concerning the relation between very small macroscopic stresses and strains, in the crystal investigated; namely, it has been shown that when a strain is applied a certain fraction of the macroscopic stress relaxes in an exponential manner.

From the present experiment the atomistic origin of this relaxation cannot be determined. The atomistic origin thus offers an interesting subject for speculation. It is difficult to imagine a mechanism for the limited relaxation of stress in a perfect homogeneous crystal. Therefore we are led to investigate possible types of inhomogeneities.

The inhomogeneity may reside in a fluctuation in the concentration of the zinc atoms. It is possible that the free energy is not a minimum when the zinc atoms are perfectly randomly dispersed, but only when clusters form in which the concentration of zinc atoms is higher than the average concentration. The equilibrium concentration in the clusters would change with the state of strain. The readjustment that accompanies the application of a strain would result in a partial relaxation of the stress.

The inhomogeneity may reside in an imperfection in the lattice positions. The position of the imperfection may be able to move when the crystal is strained. Such

a movement, of course, would result in a stress relaxation. In accordance with our observations that the stress may be only partly relaxed, a given strain can give rise to only a definite displacement of the imperfection. Such movable imperfections are commonly called dislocations, and have been studied theoretically in considerable detail (for a summary, see reference 15).

Whatever the nature of the inhomogeneity that gives rise to our observed internal friction, it is possible to describe, by general arguments, the internal friction more completely than by Eqs. 3 and 4. The constant of proportionality in Eq. 3 has been shown,⁷ quite generally, to be the relative difference in the elastic modulus measured dynamically at high frequencies, E_∞ , and that measured quasistatically (E_0). Thus

$$\text{Internal friction} = \frac{E_\infty - E_0}{E_0} / (p + p^{-1}) \quad [5]$$

$$\text{In our crystal, } \frac{(E_\infty - E_0)}{E_0} \text{ is } 0.025.$$

The dimensionless parameter p is given by Eq. 4 in terms of two quantities, f_0 and H , which must be determined by experiment. It would be very convenient if there were a relation between these two quantities, so that only one need be obtained from experiment. Although the exact mechanism of the stress relaxation is unknown, it is reasonable to suppose that this relaxation involves some sort of atomic diffusion. In the derivation of the highly successful Dushman-Langmuir diffusion formula,¹⁶ a constant that plays much the same role as our f_0 is replaced, somewhat arbitrarily, by JH/Nh . Here J is the factor that converts the energy units in H from calories into ergs,

$$J = 4.18 \times 10^7$$

N is the factor that converts JH from ergs per gram mol to ergs per atom,

$$N = 6.03 \times 10^{23} = \text{Avogadro's number.}$$

Finally, h is Planck's constant, 6.55×10^{-27} erg sec. JH/Nh may be interpreted as the frequency with which an atom would vibrate if the difference between successive quantized energy levels were JH/N ergs. Tentatively trying this same substitution gives:

$$p = (Nh/JH)fe^{H/RT} \quad [6]$$

This equation may be checked by comparing the value of H calculated by use of this equation with the value of H calculated from the slopes of the asymptotes in Fig. 3. From Eq. 5, the internal friction is seen to be a maximum when $p = 1$. But Fig. 3 shows that this maximum occurs when f is 620 cycles per sec., and T is 690° abs. Upon substituting these values of p , f and T into Eq. 6, we obtain an equation for H . This equation gives 33,800 cal. per gram mol. From the slopes of the straight-line asymptotes, which the author drew before being prejudiced by the calculation above, is obtained 33,600 cal. per gram mol. The discrepancy between these two values is well within experimental error.

SUMMARY

An investigation of the internal friction of an alpha-brass crystal at high temperatures has yielded the following results:

1. As the crystal slowly cools from a high temperature, its internal friction rises rapidly from 550°C. to about 420°C. , then falls equally rapidly upon further cooling.

2. The observed internal friction follows a simple relaxation formula containing only a single parameter. This dimensionless parameter is a function of both the frequency and the temperature of measurement, and contains as an unknown constant only a heat of activation.

3. The observations may be interpreted as evidence of inhomogeneities of some unknown type, which give rise to a stress relaxation.

4. The heat of activation for the relaxation of stress is about 33,000 cal. per gram mol.

REFERENCES

1. K. Bennowitz and H. Rötger: *Physik. Ztsch.* (1936) 37, 578.
2. C. Zener, W. Otis and R. Nuckolls: *Phys. Rev.* (1938) 53, 100.
3. K. Bennowitz and H. Rötger: *Ztsch. teck. Physik* (1938) 19, 521.
4. R. H. Randall, F. C. Rose and C. Zener: *Phys. Rev.* (1939) 56, 343.
5. C. Zener and R. H. Randall: *Trans. A.I.M.E.* (1940) 137, 41.
6. C. Zener, H. Clarke and C. S. Smith: *Trans. A.I.M.E.* (1942) 147.
7. C. Zener: *Phys. Rev.* (1941) 60, 455.
8. A. Barnes and C. Zener: *Phys. Rev.* (1940) 58, 87.
9. C. Zener, D. Van Winkle and H. Nielsen: *Trans. A.I.M.E.* (1942) 147.
10. H. L. Burghoff and C. H. Mathewson: *Trans. A.I.M.E.* (1941) 143, 45.
11. R. V. Southwell: *Theory of Elasticity*, 214. Oxford, 1936.
12. R. Becker: *Ztsch. f. Physik* (1925) 33, 185.
13. H. Jeffreys: *Proc. Roy. Soc.* (1938) 138, 283.
14. C. Zener: *Phys. Rev.* (1938) 53, 90.
15. F. Seitz and T. A. Read: *Jnl. Applied Physics* (1941) 12, 100-118, 170-186, 470-486, 538-554.
16. S. Dushman and I. Langmuir: *Phys. Rev.* (1922) 20, 113.

Effect of Antimony on Some Properties of 70-30 Brass

By DANIEL R. HULL,* MEMBER, H. F. SILLIMAN† AND EARL W. PALMER,‡ MEMBER A.I.M.E.

(New York Meeting, February 1943)

THE brass-rolling industry has not had a great deal of experience with antimony in its product. There have been some recent excursions with antimony as a corrosion inhibitor in tubes, but in sheet brass it has been regarded with apprehension and generally avoided. This is not to say that

brass made with an antimonial brand of copper. These bars were cast $6\frac{3}{4}$ in. wide by 1 in. thick by 45 in. long. In the first pass through the rolls, 19 of the 20 split lengthwise throughout their length, while each half curved outward in a wide arc as it emerged from the rolls.



FIG. 1.—TWENTY BARS OF COMMON BRASS SPLIT LENGTHWISE IN ROLLING. Copper, 65.25 per cent; lead, 0.02; antimony, 0.007. Photo taken in 1922.

contaminations have never occurred, and probably a great many brass mill men have had their own ideas on the effect of such contamination. Our own views were based upon certain experiences some years ago with strip castings that split lengthwise in the early stages of rolling.

The nature of this splitting is shown in Fig. 1, from a photograph taken in 1922 as a record of 20 bars of 65-35 common

—Manuscript received at the office of the Institute Dec. 1, 1942. Issued in METALS TECHNOLOGY, February 1943.

* Metallurgist, The American Brass Co., Waterbury, Conn.

† Assistant Metallurgist, The American Brass Co.

‡ Assistant Research Metallurgist, The American Brass Co.

In those days, if splitting was not a frequent occurrence, it was not unfamiliar. One can recall periods of short duration when large amounts of common brass would behave in this way. There was nothing imaginary about these spells. The affected metal would split lengthwise in the breakdown rolls, and no maneuvering of mill practice made any difference. The condition would descend like a plague, demoralize the mill for several days, and disappear. It is doubtful if anyone knew the cause—however many explanations may have been current.

In 1921 a quantity of split brass was traced to the use of fired small-arms

cartridge cases and, with the help of a spectroscope, attributed to antimony. There was, in that instance, no doubt that the fired cases were responsible. A year later, the confirming experiment with antimonial copper just cited appeared to establish beyond question that antimony was the crucial ingredient.

Since that time, only occasional and minor manifestations of splitting have come to the attention of the writers. The phenomenon, as a brass-mill nightmare, has been forgotten. But wherever it has occurred, it has been associated with antimony. We came to regard splitting as a specific indication of antimony, and the source of contamination could always be discovered by tracing backward from the split bars to the material used in their making. It was frequently possible to identify the bars that were likely to split by a peculiar fracture at the shears, when the gate ends were cut. Instead of a normal shear cut, the metal would fracture in a manner suggesting brittleness (Fig. 3).

The belief that antimony was the cause of splitting seemed to be well founded, but it was only a personal view, without any verification beyond observations made in the mill. The opinion was widely held that fired cases could safely be used in cartridge brass, and evidence in support of such a view has been plentiful. Since the brass industry recently has been confronted with large quantities of fired cases, the need of further study has become apparent.

LITERATURE

A search of the literature reveals little that is pertinent to the particular subject. The only references during the past 20 years that we have found, relative to the effect of antimony on the rolling properties of brass, are in Russian. *Amsterdamskiy*¹ states that the limit is 0.004 to 0.02 per cent, dependent on the amount of zinc.

¹ References are at the end of the paper.

N. S. Severgin² mentions fired cases as a source of antimony; states that a brass of 64 per cent copper cannot be cold-worked with as much as 0.009 per cent antimony, and places the upper limit at 0.005 per cent.

Both references are within the range covered in this paper, and are in substantial agreement with the findings described herein. In the abstracts of the references that were available there was no mention of lead, which would modify any general statement.

It is not particularly surprising that the subject has not been investigated in America. Fired cases have not been a considerable item in the scrap supply and the available copper and zinc over the past 20 years have been of high purity. The wrought-brass industry has been well satisfied to let antimony be of interest by its absence.

PRELIMINARY STUDY

As a preparation for tests on a commercial scale, a preliminary study was made at the laboratory. Brass of 70-30 composition was made in a small high-frequency induction furnace, from cathode copper and electrolytic zinc, and cast into bars $1\frac{1}{4}$ in. wide by $\frac{5}{8}$ in. thick by 5 in. long. Each bar was sawed in half, and one part was used for hot-rolling and the other for cold-rolling. Hot-rolling was carried down to 0.20 in. thickness, unless failure occurred sooner. Cold-rolling was carried to 0.100 in. before the first anneal, which constituted a severe test. A small laboratory roll was used for this work. The pertinent details are presented in Table 1.

The addition agents are tabulated in the amounts used rather than the amounts found on analysis. A substantial number of analyses were made and were in close agreement with amounts added. The round numbers are used as being more convenient and just as significant. Considering the quality of the materials used, the lead may

be assumed to be less than 0.01 per cent except in alloy No. 4562, which was made of fired cases. The general scheme involves a series carrying from 0.001 to 1.0 per cent

numbers 4568, 4569, 4579 indicate that the limit is being approached. The weight of evidence indicates an antimony limit between 0.05 and 0.10 per cent. With 0.10

TABLE 1.—*Laboratory Roll Record of 70-30 Brass with Various Additions*

Alloy No.	Melting Atmosphere	Additions, Per Cent	Hot-rolling Behavior	Cold-rolling Behavior
4552	Reducing	0.001 Sb	OK	OK
4553	Reducing	0.002 Sb	OK	OK
4555	Reducing	0.004 Sb	OK	OK
4557	Reducing	0.008 Sb	OK	OK
4559	Reducing	0.015 Sb	OK	OK
4560	Reducing	0.020 Sb	OK	OK
4561	Oxidizing	0.020 Sb	Slight genl. failure	OK
4568	Oxidizing	0.02 Sb	Moderate genl. failure	Slight cracking
4569	Oxidizing	0.05 Sb	Severe genl. failure	Moderate cracking
4579	Reducing	0.05 Sb	Moderate genl. failure	Slight edge cracking
4580	Reducing	0.10 Sb	Severe genl. failure	Genl. failure first pass
4581	Reducing	0.20 Sb	Severe genl. failure	Genl. failure first pass
4582	Reducing	0.50 Sb	Severe genl. failure	Genl. failure first pass
4583	Reducing	1.0 Sb	Crumbled utterly	Crumbled first pass
4562 ^a	Reducing	Remelted cases	General failure	OK
4564	Reducing	0.03 Sb ₂ S ₃	OK	OK
4565	Reducing	0.03 Sb ₂ S ₃ + 0.02 Mg	OK	OK
4566	Reducing	0.03 Sb ₂ S ₃ + 0.05 Mn	OK	OK
4584	Reducing	0.02 Sb	Slight failure	OK
4585	Reducing	0.05 Sb	Slight failure	OK
4586	Reducing	0.10 Sb	Moderate failure	Failed first pass
4587	Reducing	0.02 Sb + 0.05 Si	Slight failure	OK
4588	Reducing	0.05 Sb + 0.05 Si	Slight failure	OK
4589	Reducing	0.10 Sb + 0.05 Si	Moderate failure	Severe cracking
4590	Reducing	0.02 Sb + 0.02 P	Slight failure	OK
4591	Reducing	0.05 Sb + 0.02 P	Moderate failure	OK
4592	Reducing	0.10 Sb + 0.02 P	Moderate failure	OK
4593	Reducing	0.02 Sb + 0.02 Mg	Slight failure	OK
4594	Reducing	0.05 Sb + 0.02 Mg	Moderate failure	OK
4595	Reducing	0.10 Sb + 0.02 Mg	Severe failure	Failed first pass
4596	Oxidizing	0.02 Sb	Moderate failure	OK
4597	Oxidizing	0.05 Sb	Severe genl. failure	OK
4598	Oxidizing	0.10 Sb	Severe genl. failure	Failed first pass
4599	Oxidizing	0.02 Sb + 0.05 Si	Moderate failure	OK
4600	Oxidizing	0.05 Sb + 0.05 Si	Moderate failure	OK
4601	Oxidizing	0.10 Sb + 0.05 Si	Severe genl. failure	Severe cracking
4602	Oxidizing	0.02 Sb + 0.02 P	Moderate failure	OK
4603	Oxidizing	0.05 Sb + 0.02 P	Moderate failure	OK
4604	Oxidizing	0.10 Sb + 0.02 P	Severe genl. failure	OK
4605	Oxidizing	0.02 Sb + 0.02 Mg	Moderate failure	OK
4606	Oxidizing	0.05 Sb + 0.02 Mg	Moderate failure	OK
4607	Oxidizing	0.10 Sb + 0.02 Mg	Severe genl. failure	Failed first pass

^a Entire charge made up of fired 0.30-caliber cases.

antimony, melted under charcoal, with three oxidized melts in the region of incipient failure; then four heats with sulphide additions; then the series 0.02 per cent, 0.05 per cent, 0.10 per cent antimony, repeated with silicon, phosphorus, and magnesium as deoxidizers, and all repeated again with oxidation of the copper during melting. The importance of antimony oxide was considered not unlikely.

The inferences to be gathered from Table 1 may be summarized briefly, as follows:

Antimony, up to 0.05 per cent, does not greatly interfere with cold-rolling but alloy

per cent antimony, or more, the brass cracks up in cold-rolling. The degree of this breaking up is shown in Fig. 2. Alloy numbers 4568 and 4569, which failed in cold-rolling at 0.02 and 0.05 per cent antimony, give the only evidence, which is slight, that antimony oxide may be more effective than metallic antimony. As this evidence is not borne out in the series 4596 to 4607, it is not given too much weight in the minds of the writers.

In the presence of phosphorus, antimony up to 0.10 per cent did not interfere with cold-rolling. Manganese, magnesium, and

silicon, as deoxidizers, were without effect in counteracting antimony.

Antimony sulphide did not accentuate the effect of antimony.

Heats No. 1 and No. 2 were made of new copper and zinc.

Heats No. 3 and No. 4 contained 45 per cent scrap from Nos. 1 and 2.



FIG. 2.—70-30 BRASS CAST AND ROLLED AT LABORATORY.

a, Sb 0.50 per cent, cold-rolled.

b, Sb 0.10 per cent, cold-rolled.

c, Sb 0.50 per cent, hot-rolled.

d, Sb 0.10 per cent, hot-rolled.

The hot-rolling limit was between 0.01 and 0.02 per cent antimony. Fig. 2 shows hot-rolling failures with 0.10 and 0.50 per cent antimony.

TESTS ON COMMERCIAL SCALE

With this laboratory work as a basis, the investigation was carried to the mill and continued on a commercial scale. The first series of tests was made by melting 600-lb. charges of cathode copper and electrolytic zinc in an Ajax-Northrup high-frequency induction furnace, under a cover of charcoal, and adding known quantities of antimony. The metal was cast into bars $1\frac{1}{8}$ by $4\frac{1}{2}$ by 85 in., five bars from each heat. (This mold is used for all the mill tests hereafter described.)

Heats No. 5 and No. 6 contained 45 per cent scrap from Nos. 3 and 4.

TABLE 2.—*Composition of Brass Containing Antimony*
PER CENT

Heat No.	Copper	Zinc (Diff.)	Iron	Lead	Antimony
1	70.06	29.91	0.01	0.0070	0.0058
2	69.45	30.52	0.01	0.0074	0.0060
3	69.68	30.29	0.01	0.0080	0.0067
4	69.56	30.41	0.01	0.0090	0.0065
5	69.39	30.59	0.005	0.0050	0.0070
6	69.75	30.22	0.005	0.0064	0.0070

The object of returning part of the scrap was to determine any possible effect from remelting. Compositions are shown in Table 2.

The 30 bars made were gated and cut in half, and the 60 half bars were rolled into strip without incident. It appeared that the antimony of itself had not affected the rolling properties.

Since there was a question whether antimony oxide might be more effective than metallic antimony, a Northrup heat was made by melting copper cathodes with very little charcoal protection, and allowing it to oxidize rather severely after melting. The antimony was then added, then the zinc. The large quantity of sludgy dross that developed on addition of the zinc was evidence of extensive oxidation. A companion heat was made in the same manner, without antimony. The compositions of these heats appear in Table 3.

TABLE 3.—*Composition of Brass Oxidized in Melting*
PER CENT

Heat No.	Copper	Zinc (Diff.)	Iron	Lead	Antimony
7	69.35	30.64	0.005	0.0072	0.000
8	68.97	31.01	0.005	0.0052	0.0058

Four bars, of the same dimensions used previously, were obtained from each heat, and rolled into strip without unusual incident. Although undoubtedly a larger percentage of antimony would have been more conclusive, the oxidation was more severe than would ever be likely to occur in routine work. To this extent, therefore, the antimony in brass melted under oxidizing conditions failed to produce any obvious effect in rolling.

Since the antimony in the metal described was about the same as that found in mixed lots of fired small-arms cartridge cases, several heats were made exclusively of such cases. (The smaller the caliber of the case, the greater the ratio of residual antimony.) This work was done in an Ajax-Wyatt furnace, pouring 10 bars per heat of the same dimensions used previously. The composition of the metal, which is repre-

sentative of mixed lots of small-arms cases, is shown in Table 4. The charge added for heat No. 11 was somewhat diluted by the residual bath in the furnace from the preceding heat.

TABLE 4.—*Composition of Brass from Remelted Fired Cases*
PER CENT

Heat No.	Copper	Zinc (Diff.)	Iron	Lead	Antimony	Sulphur
11	70.26	29.66	0.01	0.0583	0.0049	0.003
12	70.01	29.89	0.01	0.0804	0.0066	0.003
13	69.83	30.08	0.01	0.0676	0.0074	0.005
14	69.83	30.08	0.01	0.0700	0.0072	0.004

The 40 bars from these four heats were gated, cut in half, and rolled in the usual manner (1½ in. thick at start; first pass to 0.750 in.; second pass to 0.570 in.; anneal). Nearly half of them split lengthwise in the first or second pass (Table 5).

TABLE 5.—*Rolling Record of Brass from Fired Cases*

Heat No.	Number of Split Bars	Number of Bars Not Split
11	4	16
12	10	10
13	10	10
14	8	12
	32	48

The 48 bars that did not split in the breakdown passes were annealed and rolled into strip without notable incident.

It appears from this that, since antimony of the order of 0.007 per cent did not interfere with the rolling of very pure brass, the results obtained from the use of fired cases were probably caused by some combination of impurities originating in such cases. The most obvious of these is lead. Although there is nothing in Table 4 on which to base a suspicion of sulphur, the known presence of sulphide in the primer indicated that it ought not to be dismissed without a trial.

Further work, therefore, was carried out in the Ajax-Northrup furnace, pouring

four or five bars at each heat, of the same dimensions used previously. Since lead by itself, in the amount under discussion, would not interfere with cold-rolling, and the effect of antimony alone had just been

splitting virtually disappeared after electrolytic zinc came into general use for commercial grades of drawing brass. Previous to that time, high-grade zinc could be considered only for the most

TABLE 6.—70-30 Brass Containing Combinations of Antimony, Lead and Sulphur
PER CENT

Heat No.....	15	16	17	20	21	22
Copper.....	69.90	68.69	69.38	69.19	68.72	69.49
Zinc (diff.).....	30.08	31.29	30.51	30.72	31.20	30.42
Lead.....	0.0048	0.0048	0.0890	0.0749	0.0672	0.0652
Antimony.....	0.000	0.0088	0.0083	0.000	0.0088	0.0088
Sulphur.....	0.011	0.007	0.009	0.007	0.002	0.012
Impurities added.....	S	S + Sb	S + Sb + Pb	S + Pb	Sb + Pb	S + Pb + Sb

covered, there remained to be determined the effect of sulphur and the combinations of antimony plus sulphur; antimony plus lead and sulphur plus lead. The compositions of the heats made in these combinations are shown in Table 6.

This metal was made from cathode copper and electrolytic zinc, the lead and antimony were added as metal and the sulphur as pure copper sulphide. The bars were gated, cut in half, and rolled as previously, with the result shown in Table 7.

Only the bars containing both lead and antimony showed any tendency to split. The sulphur was irrelevant as far as this test was concerned. There appears little doubt that the effect observed from the use of fired cases is due to the combination of about 0.007 per cent antimony and 0.07 per cent lead, and that probably this was true also in 1921. It explains, too, why

particular purposes. The general run of nonleaded brass contained of necessity between 0.10 and 0.20 per cent lead. A slight contamination with antimony, there-

TABLE 7.—Rolling Record of Brass with Combinations of Antimony, Lead and Sulphur

Heat No.	Impurities Added	Number of Bars Split	Number of Bars Not Split
15	S	0	8
16	S + Sb	0	8
17	S + Sb + Pb	7	3
20	S + Pb	0	8
21	Sb + Pb	3	5
22	S + Pb + Sb	4	4

fore, would be critical. The metal shown in Fig. 1 is recorded as containing only 0.02 per cent lead. While it is not available for checking, a number of analyses were made and, from the history of the work, there is

TABLE 8.—Composition and Rolling Record of Brass with Additions of Antimony and Antimony plus Phosphorus

Heat No.	Composition, Per Cent					Number Bars Split in Rolling	Number Bars Rolled without Splitting
	Copper	Lead	Iron	Antimony	Phosphorus		
23	69.30	0.003	0.005	0.018		1	3
24	69.57	0.004	0.005	0.042		2	2
25	69.77	0.004	0.005	0.068		2	2
26	69.65	0.005	0.005	0.089		2	2
27	69.91	0.003	0.005	0.040	0.044	0	4
28	70.14	0.004	0.005	0.053	0.040	1	5

no reason to believe that the figure is incorrect. The inference is that much less than 0.07 per cent lead in combination with 0.007 per cent antimony would be critical.

were added—from 0.02 up to 0.09 per cent. The bars were of the same dimensions as formerly. Compositions are shown in Table 8.

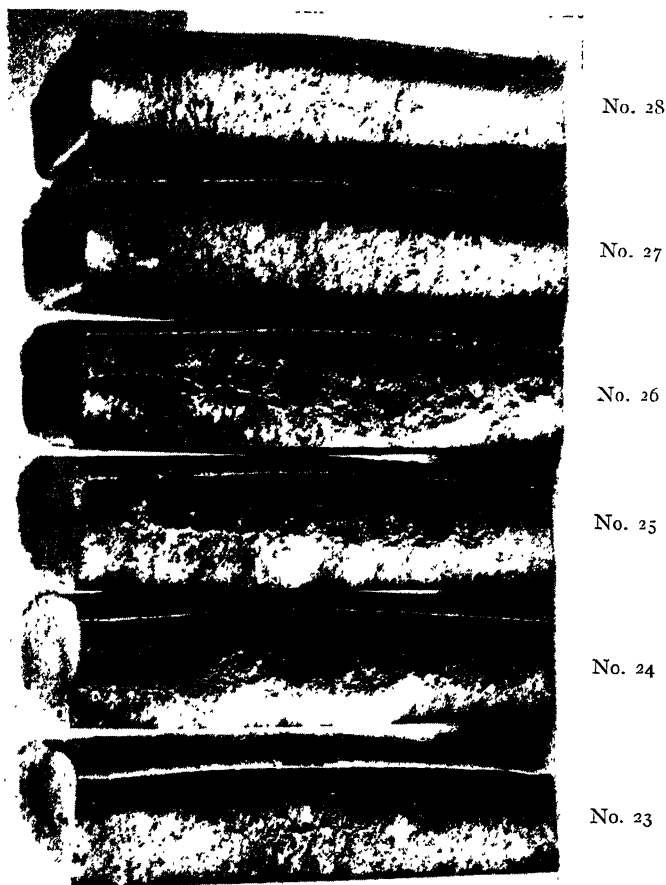


FIG. 3.—SHEARED SECTIONS OF 70-30 BRASS CASTINGS SHOWING EFFECT OF ANTIMONY.

No. 23, Sb 0.018 per cent. No. 26, Sb 0.089 per cent.

No. 24, Sb 0.042 per cent. No. 27, Sb 0.040, P 0.044.

No. 25, Sb 0.068 per cent. No. 28, Sb 0.053, P 0.040.

PERCENTAGES OF ANTIMONY

It was felt that this work would be inadequate unless amplified by determination of the quantity of antimony that can be tolerated in the absence of lead. To this end, several Northrup heats were made, using cathode copper and electrolytic zinc, to which increasing amounts of antimony

Again the cast bars were sheared in two before rolling, so that each bar in the table represents half of a casting. It was surprising that the effect in the rolling test did not increase greatly as antimony was stepped up from 0.018 to 0.089 per cent, but it is indicated that about 0.02 per cent antimony may have an effect. The addition

of phosphorus to heats 27 and 28 had a definite effect in counteracting antimony, as was indicated in the preliminary laboratory work.

The appearance of the shear cut was also indicative of the presence of antimony. This peculiar feature has already been mentioned as characteristic. Since nothing exactly like it is seen in any other connection, it has long been regarded by the writers as a specific indication of antimony. In Fig. 3 are photographs of sheared sections from the castings described in Table 8. They are consistent with the roll tests. The appearance of brittleness increases sharply from 0.018 to 0.042 per cent antimony and does not increase much more up to 0.089 per cent. But it should be remembered that neither this test nor the test by rolling is quantitative—they are qualitative, and it would be a mistake to attempt to measure specific brittleness in terms of such tests. On the addition of phosphorus, in heats 27 and 28, the shear cut is again smooth and normal, as would be expected in soft, ductile metal. This is significant and lends confirmation to the view that additions of antimony have an effect whether or not the brass splits in rolling.

It is probable that a perfectly flat bar would not split at all in rolling. None of the laboratory castings split in rolling, even when they contained so much antimony that they broke up badly. The mold that was used for the full-scale mill work is almost obsolete, but something similar to it was much used formerly, when brass slabs for flat rolling were invariably "crowned"; i.e., the castings were somewhat thicker in the center than at the edges. This mold was chosen because of its convenience, but it was a fortunate choice because it accentuates the effects that were sought.

It is also possible that with very slow rolls there would have been less splitting, even with a "crowned" casting, but any

test that brings out differences in physical properties is to the purpose.

Since the nature of the splitting and of the shear cut suggested lack of impact strength, a few qualitative tests were made, which indicated that this was true. A number of roughly made notched-bar samples from Table 8 showed that Nos. 23 to 26 (antimony 0.018, 0.042, 0.068 and 0.089 per cent) all broke sharply, under impact, with a brittle fracture, while normal brass similarly treated merely stretched and bent. It was gratifying that while this work was in progress the work of John Rae³ came to the writers' attention, as he notes the same lack of impact strength in alpha-beta brasses made from fired cases. The fractured samples from heats 23, 24, 25 and 26 (Table 8) were decidedly brown, and Rae also noted that antimony imparts a difference in color in a fracture.

Lynes⁴ also has noted an impairment of impact strength of a 70-30 brass rod, through the addition of 0.10 per cent antimony.

For quantitative impact tests, more castings were necessary and these were made in an Ajax-Wyatt furnace, using the same mold as for previous mill work. Table 9 shows the compositions studied and gives the results of Charpy impact tests not only on the cast metal but also on the same stock after one and two cycles of rolling and annealing. Specimens were taken $\frac{1}{2}$ in. from each edge and from the center of the castings, and the same system was followed with the bars resulting from the breakdown rolling. After the second rolling, the stock was so thin that smaller specimens were used, and all three specimens represent material approximately halfway between center and edge.

Referring to the castings, and starting with normal brass as a reference point, the addition of 0.005 per cent antimony has not impaired the impact strength; 0.01 per cent antimony has had an effect, particularly in the center specimen; 0.022 per

cent has had a still further effect in the center and at one edge, though the other edge is not in agreement. The bar made from

These larger amounts of antimony cause progressive impairment of the impact strength of 70-30 brass, but it is notable

TABLE 9.—*Impact Strength of 70-30 Brass*

Specimen Mark	Composition, Per Cent			Impact Strength, Ft.-lb.		
	Copper	Antimony	Lead	As cast ^a	Rolled to 0.570 In. and Annealed at 550°C. ^a	Further Rolled to 0.250 In. and Annealed at 550°C. ^b
1 Edge	68.91	0.0006	0.008	101.4	82.1	19.1
1M Middle				48.0	82.0	20.4
1 Edge				90.9	80.0	19.7
2 Edge	69.41	0.0050	0.006	106.5	87.5	21.2
2M Middle				67.6	120.4	20.8
2 Edge				101.7	84.8	22.0
3 Edge	69.42	0.010	0.012	80.2	92.4	24.3
3M Middle				37.3	111.2	21.3
3 Edge				93.2	92.5	21.1
4 Edge	69.51	0.022	0.006	106.1	85.6	19.6
4M Middle				29.2	104.7	22.3
4 Edge				74.1	85.6	22.2
18 Edge ^c	69.33	0.0072	0.058	43.4 ^d	76.0 ^d	15.9
18M Middle ^c				17.7 ^d	94.9	18.8
18 Edge ^c				35.7 ^d	77.5	17.7

^a Standard Charpy specimens, 0.394-in. square, 45° notch of 0.01-in. radius 0.079-in. deep.

^b Small Charpy type specimens, 0.250-in. square, 45° notch of 0.01-in. radius 0.083-in. deep.

^c This metal entirely from fired cases.

^d Specimen completely fractured. All others incomplete.

fired cases shows a drastic weakening in all specimens.

After the first rolling and annealing, the impact strength appears to be independent of antimony content, but the bar containing both antimony and lead (made from fired cases) has slightly impaired properties. The same is true after the second cycle of rolling and annealing. The recovery of impact strength by the center section of the cast bar after rolling and annealing is probably connected with the absorption of beta.

In order to study the effects of larger amounts of antimony on the casting, standard Charpy impact specimens were milled from a series of laboratory castings containing up to nearly 0.1 per cent antimony. These were all cut from the edges of small bars, and were tested both as cast and after annealing at 700°C. for 2 hr. For comparison, specimens of the mill bar made from fired cases were also included. The results are given in Table 10.

that considerable ductility is regained when the cast bars are annealed. Unfor-

TABLE 10.—*Impact Strength of 70-30 Brass*

Specimen Mark	Composition, Per Cent			Impact Strength, Ft.-lb. ^a	
	Copper	Antimony	Lead	As Cast	Annealed 700°C.
4865 }	70.33	0.0008	b	62.5	84.0
4865 }				59.1	85.8
4866 }				43.8 ^b	75.6
4866 }	70.25	0.020	b	49.5	85.9
4866 }				19.7 ^c	73.1
4867 }				22.6 ^c	74.9
4867 }	70.13	0.040	b	14.6 ^c	77.2
4867 }				16.0 ^c	69.7 ^c
4868 }				8.7 ^c	64.0
4869 }	70.22	0.060	b	12.7 ^c	58.9
4869 }				8.3 ^c	57.3
4870 }				8.1 ^c	60.1
4870 }	70.03	0.078	b	43.4 ^c	41.0 ^c
4870 }				15.7 ^c	48.5
18 }					
18 }	69.98	0.096	b		
18 }					
18 }					
18 }	69.33	0.0072	0.058		
18 }					
18 }					

^a Standard Charpy specimens. See Table 9.

^b Not determined. About 0.005 per cent.

^c Specimen completely fractured. All others incomplete.

tunately, as shown by bar No. 18, this is not true when lead is present as well as antimony.

Many of these impact specimens did not fracture completely, and the reliability of figures for energy absorption in such cases may be questioned. However, none of the specimens were merely bent; all were fractured to a considerable depth. The figures certainly are not absolute, but it is believed that they offer a suitable basis for comparison.

It appears from these impact studies that antimony in excess of 0.010 to 0.020 per cent markedly decreases the impact strength of cast 70-30 brass, and that if lead is present the tolerance for antimony is appreciably under 0.010 per cent. However, if the casting survives the first rolling operation, its impact strength after annealing is greatly improved.

It is notable, in the mill, that if a casting does not split in the breakdown, it never splits in later rolling, after it has been annealed. Such metal as that described in Tables 4, 6 and 8, which did not split in the first or second roll pass, has been finished into strip, blanked and cupped without notable incident, except occasionally an abnormal tendency of the strip to edge cracking.

This edge cracking has been noticed particularly in a substantial lot of 700-lb. castings (19 by 2 by 56 in. from water-cooled molds) made from a commercial collection of fired small-arms cases. These bars were flat, and did not split in rolling. They were run into strip with some annoyance from edge cracking, but were blanked and cupped and worked up into 0.30-caliber cases without any other incident. While this, in broad terms, was successful, it leaves the brass manufacturer with a sense of something less than complete satisfaction. In the ordinary routine, metal is not expected to "sawtooth" at the edges. Such a condition, if general, would be a serious handicap to the operation of a mill. But in this instance, one cannot brush aside a doubt as to whether the final product would be impaired through some

property that has not been recognized in the course of our limited experience. That may seem like an unnecessary apprehension, but less likely things have happened. Full-scale production too often has revealed deficiencies that were not apparent in preliminary, small-scale work.

Throughout the course of this work, extensive examinations of microstructure have been made. Beyond saying that no very obvious effects have been noticed in the alloys under consideration, it is felt that the question lies outside the scope of this paper. A discussion of microstructure could not be undertaken without a good deal more study. No work with antimony in hot-rolled brass has been done except in the laboratory, where the limit was found between 0.01 and 0.02 per cent. Since mixed lots of fired cases commonly carry about 0.007 per cent antimony and 0.07 per cent lead, they could not be used in alpha brass intended for hot-rolling; the lead of itself would prevent that.

CONCLUSION

Antimony affects the impact strength of 70-30 brass. Under some circumstances this is manifest in lengthwise splitting of cold-rolling bars, in edge cracking, and in a brittle shear fracture. Impairment of impact strength in the brass as cast is distinct and measurable at 0.01 per cent antimony. At about that point it begins to be apparent in rolling and 70-30 brass cannot be cold-rolled with 0.10 per cent antimony.

The presence of lead in amounts substantially less than 0.10 per cent greatly accentuates the effects of antimony.

Fired small-arms cases, when melted, may yield castings containing about 0.007 per cent antimony and 0.07 per cent lead. In such amounts these elements greatly impair the impact strength of the casting, and lead to serious difficulties in breakdown rolling. Cold-work followed by annealing

improves considerably the impact strength of such material, but it is probable that it never becomes quite as resistant to impact as normal 70-30 brass free from antimony.

ACKNOWLEDGMENTS

Acknowledgment is made to The American Brass Co. for permission to publish this paper; to Mr. John R. Freeman, Jr., Technical Manager of The American Brass Co., for assistance and encouragement, and to Mr. R. S. Baker, Technical Supervisor of the Torrington Branch of The American Brass Co., for indispensable cooperation.

REFERENCES

1. I. A. Amsterdamskiy, V. O. Gagen-Torn and B. F. Grashchenko: *Metallurg* (1934) 8, 107-113. Abstr., Chem. Abstr. (1935) 29 (22), 7919. (Original not consulted.)
2. N. S. Severgin: Abstr. *Jnl. Inst. Metals* (1931) 47, 566. (Original not consulted.)
3. J. Rae, Jr.: The Use of Fired Small Arms Cartridge Cases in the Production of Some Alpha-Beta Extrusion Brasses. *Jnl. Inst. Metals* (Oct. 1942) 311.
4. W. Lynes: *Proc. Amer. Soc. Test. Mat.* (1941) 41, 876.

DISCUSSION

(Cyril Stanley Smith presiding)

J. T. KEMP,* Washington, D. C.—The paper by Hull, Silliman and Palmer will stand as one of the remarkable contributions by the Institute of Metals Division to the TRANSACTIONS of the A.I.M.E. The authors and the company they represent have found time and mill space to investigate the irregular rolling-mill behavior of brass castings made by remelting fired cartridge cases and to clarify their long-standing beliefs regarding the influence of antimony in brass-mill rolling stock. It is to their great credit that this work has been done at a time when productive resources are taxed to the maximum.

The paper records a thoroughgoing practical study, combining both the laboratory and the mill. It has the merit of candor and literary quality. It is to be hoped that a second installment may follow eventually and a study

be presented of the metallurgical reasons for the phenomena. A suggestion is found in one of the later paragraphs that such interesting data may be obtainable from the material the authors worked with.

Undoubtedly pressure from Washington upon the brass mills to use fired cartridge cases for making new cartridge brass in greater quantities than they now do prompted the research. The paper is, therefore, very timely. It will clear discussion of much of the ambiguity that has beclouded the subject during the past several months.

The inference that 0.07 per cent lead in combination with 0.007 per cent antimony is a critical limit in brass for cold-rolling would seem to justify the further inference that lead and antimony in substantially lower concentrations would be critical in brass to be hot-rolled. It is pointed out that melts of fired cartridge cases approach the critical limit in lead and antimony (Table 4). Table 2 appears to support the theory that antimony will build up toward the critical concentration in successive furnace charges melting normal quantities of returned antimonial scrap. The trend of the leads, however, seems contradictory. Indirectly these statements become an argument against the use of fired cases in melting new cartridge brass. Taking the over-all view, however, the problem of utilizing fired cases for cartridge brass should entail a much less serious degree of contamination. The return of fired cases to commercial use of all kinds is less than 3 per cent of the monthly melt of cartridge brass. It is expected that this percentage will rise in the future, though to what extent depends upon the course of the war.

Some 2500 tons of fired cartridge cases are recovered monthly in continental United States. It is the highest grade of brass scrap. It has been contaminated by dirt, stones, shot, tramp iron and the products of combustion. Proper equipment is being set up at the several depots handling this kind of scrap to clean off the dirt, separate foreign metals, explode misfires and unfired primers. Washing machinery is under discussion but as yet the effectiveness of washing in removing the products of combustion, the source of antimony and some of the lead, is not known. It is expected that a handling procedure will be devised that will remove the objectionable contamination to

* Metals Consultant, Division of Conservation and Standardization, Services of Supply, United States Army.

such an extent that all brass mills will willingly accept fired cases as part of their allotted copper and zinc for cartridge brass. Constructive suggestions are welcomed.

THE CHAIRMAN.—Mr. Freeman, would you care to discuss this paper?

J. R. FREEMAN, JR.,* Waterbury, Conn.—I have not a great deal to add, except a word of caution.

In the first place, the fundamental purpose in presenting the paper is to bring out discussion in a technical atmosphere from technical men, since the problem of the use of fired cartridge cases is one that has to be faced by the industry. We have to do all we can to make use of fired cases in the largest possible amounts. We felt, therefore, that this work should be carried through in as complete a manner as possible, which I think the authors have done.

I think, also, that it is fair to call attention to the first picture again (Fig. 1). It really is dramatic evidence of the fear, and justifiable fear, that we have all had in making use of fired cases under edict from Washington, more or less, without first making very careful investigation to determine the effect their use might have on the quality of the type of brass being produced in which these fired cases are used or may be used.

One other point that is mentioned in the paper and I think should be considered, along with Mr. Kemp's remarks, is the quantity of fired cases that may be used in any charge; that is, in a casting shop. Mr. Kemp made a statement that at the present time fired cases represent only 3 per cent of brass production for small arms. It would not be difficult to absorb 3 per cent in any furnace charge in a mill making cartridge brass for cold-rolling, but I would like to emphasize that all of this may contain lead in quantities that prevent the use of the fired cases in brass cast for hot-rolling.

So, in considering the quantities of fired cases that may be used we must bear in mind the operations within the mills, whether we are casting bars for cold-rolling or whether we are casting bars for hot-rolling.

Now, a very large percentage of the production today, perhaps 70 per cent, is by hot-

rolling, and we must bear that fact in mind in making use of fired cases. In other words, as Mr. Hull pointed out in his closing remarks, I feel we must approach this problem with caution, if perhaps not with quite the apprehension that we have had before.

Along with these remarks we must bear in mind not only the fired cartridge cases as a source of scrap but we must also bear in mind the very large percentage of scrap that is of necessity used in the casting shops today.

The over-all scrap produced between a brass casting and a finished small-arms case is somewhere of the general order of 65 to 70 per cent including circulating mill scrap within a brass mill, and the scrap that comes back to us from the small-arms plants. Now that scrap in itself tends to build up impurities; in particular, that portion coming back to us from small-arms plants will contain iron and lead although every effort is being made at the Arsenal and in our mills to keep it clean so it can be used.

Now, if on top of the 65 or 70 per cent scrap charge we have to use today to keep ahead of the scrap that is just being formed incident to the manufacturing operations, we must add a considerable quantity of fired cases, we soon reach a point, unless very great care is taken, where our impurity content builds up beyond its permissible specification value. Thus we find ourselves between the devil and the deep sea having to meet, under conditions of increasingly heavy pressure for ever greater production, very high-quality requirements of specifications, obviously necessary, and yet make use of fired cases which cannot be classed as scrap of highest quality, although they have been called such. It can be done but the problem must be approached with reasonable caution.

M. L. WOOD,* Waterbury, Conn.—The authors have presented an interesting and timely array of facts which is now of great importance to the brass industry.

There are two separate phases of this paper; namely, the use of fired small-arms cartridge cases in the manufacture of brass, and the more general one of the effect of antimony,

* Technical Manager, American Brass Company.

* Process Metallurgist, Chase Brass and Copper Company.

either alone or with other elements, on the physical properties of the brasses.

The effect of antimony on the physical properties of copper and copper alloys is complicated, as shown by the scattered and contradictory published information. Practically nothing has been reported for alloys high in zinc, so the present paper and the one by Rae³ are most welcome.

It has been my privilege to be intimately associated with the commercial production of some millions of pounds of copper-base alloys to which antimony has been purposely added. For that reason, I can assure you that the authors are justified in their restraint in drawing conclusions. Antimony may be, but is not necessarily, harmful in mill production. Apparently there are a number of modifying effects to be considered, which are not too well defined.

In the use of fired cartridge cases, our experience has not been as unhappy as that reported by the authors. Brass made from charges consisting entirely of fired rifle cases has been hot-rolled or cold-rolled without trouble. Typical analyses of such metal are given in Table 11.

As a further check on antimony pickup, some melts were made in a laboratory high-frequency furnace. One charge was made from primer cups only, and another from cases with primers intact, taken from the same shipment. The analyses are shown in Table 11.

TABLE 11.—*Analyses at Chase Brass and Copper Company*
CHARGES ENTIRELY OF FIRED RIFLE CASES

Brass	8-in. Cases for Hot-rolling	4½ by 1½-in. Bars for Cold-rolling
Lead, per cent.....	0.015	0.02
Antimony, per cent....	0.011	0.015

MELTS IN LABORATORY HIGH-FREQUENCY FURNACE

Charge	Antimony, Per Cent	Lead, Per Cent
Primers only.....	0.063	0.14
Cases with primers.....	0.012	0.015

Some considerable production of sheet brass has been made commercially using 500 lb.

of fired cases in a 1000-lb. charge. The chief disadvantage noted was that so much light scrap was difficult to push down into the melt, and consequently melting time is longer. No trouble was experienced in rolling this metal, except in one instance where a small lot of the cases contained some antimonial lead slugs. The bars made therefrom exhibited the peculiar fracture at the shear cut noted by the authors, and some bars split in rolling. However, the antimony content was 0.05 per cent and the lead 0.28 per cent. This trouble was caught during the cropping of gates before any serious damage resulted.

The possibilities of intermetallic compounds, low solid solubility of antimony and of oxide films have been advanced at various times to explain trouble experienced with antimony. The behavior of melts made with additions of phosphorus, either under oxidizing or reducing conditions, are most interesting and perhaps present a possible clue to some variations in properties for a given antimony content.

The high impact values reported by Rae on Naval brass rod containing considerable lead are outstanding. Consideration of the heats of formation of the oxides of antimony, zinc, and tin show that there is a possibility that tin may reduce antimony oxides.

Some experiments were made recently by us on brasses melted under charcoal in which antimony was varied in the following steps: None, 0.03, 0.06, 0.12 per cent, with and without addition of 1 per cent tin and 0.1 per cent lead. The casting used was a 2-in. round to be subsequently cold-rolled. This operation is perhaps more severe than sheet rolling, but the shape was selected as giving a more uniform sample for impact testing.

The cast rods were cold-rolled in grooved rolls with three series of three passes each, the total reductions not only being great but also of a very severe type as compared with simple flat-bar rolling. The results are summarized in Table 12.

Impact tests were made on metal drawn from 5/8 to 1/2 in. Similar tests on free-turning rod are in the range of 10 to 15 ft.-lb. The values given here are comparative only among themselves, since none of the specimens fractured completely. The tests on alloy No. 1, which is low in impurities, can be taken as a reference value.

TABLE 12.—*Results on Brasses Melted under Charcoal*

Alloy No.	Analysis, Per Cent			First and Second Rolling	Third Rolling	Izod Impact, Ft.-lb.
	Anti- mony	Tin	Lead			
1	0.001		0.002	OK	OK	90
2	0.042		0.009	OK	Broke up, rejected	
3	0.056		0.009	OK	Broke up, rejected	
4	0.13		0.006	Slight cracking	Broke up, rejected	86 96 87
5	0.001	1.03	0.04	OK	OK	
6	0.043	0.92		OK	OK	
7	0.058	0.91	0.001	OK	OK	64
8	0.12	0.92	0.001	Slight cracking	Broke up, rejected	
9	0.039	0.82	0.15	OK	OK	
10	0.053	0.97	0.13	Broke up, rejected		
11	0.12	0.89	0.09	Cracking	Broke up, rejected	

Alloys 1 to 4 constitute a series with increasing antimony content, very low lead content, and no tin. The performance of these alloys was fair. Alloys 5 to 8 inclusive differ from the first four only by the inclusion of approximately 1 per cent tin. The performance was markedly better. Alloys 9 to 11 inclusive were generally similar to alloys 6 to 8, except for a moderately high lead content. These alloys as a group behaved rather poorly.

The general conclusion is drawn that increasing antimony by itself is harmful, and this effect is very much aggravated by a lead content of the order of 0.1 per cent, whereas in lead-free alloys the presence of 1 per cent tin is distinctly beneficial. The latter conclusion is borne out by our experience with production of Admiralty brass tubes containing antimony, which have been produced on a very large scale commercially over a period of some years.

In spite of the fact that we agree with the authors that the combination of lead and antimony is very serious, it is interesting to note that a fairly large experimental lot of leaded brass tubes was processed through our mills to a finished size of $1\frac{1}{16}$ -in. diameter by 0.065-in. wall thickness with individual reductions of the order of 40 per cent without particular difficulty. This particular material contained 66 per cent copper, 0.5 per cent lead, and 0.1 per cent antimony. On the other

hand, other lots of generally similar composition did give serious trouble and it was concluded that such a combination of lead and antimony was distinctly not commercial.

The tests just cited, together with other data presented here and by the authors, leads to the conclusion that general comments on harmful effects of antimony or of antimony and lead cannot always be taken too literally unless every detail of fabrication from casting right through to the finish is known. Certainly there is room for further investigation of the effect of casting conditions on the subsequent working behavior of such alloys.

T. C. MERRIMAN,* Seymour, Conn.—I might refer to considerable experience with a previous employer, not precisely on fired cases, but on "pulled down" ammunition, which amounts to the same thing. Many of the primers were "crimped in," which prevented punching them out. The "pulled down" cases were run through a gas-fired rotary furnace, but the products of combustion of the priming mixture remained in the cases to such an extent that the use of those cases when remelted into cartridge brass for rerolling caused serious trouble. The troubles were in good agreement with the findings in this paper.

Attempts to remove the products of combustion by washing the "popped" shells in dilute sulphuric acid and several other media just did not work.

J. L. KIMBERLY,† New York, N. Y.—I think there is one question that should be brought up in connection with the possible damage of antimony and lead. The major outlet for fired cases as of today is in the casting of manganese bronze for propellers. If the presence of antimony and lead together is very damaging to the impact strength, it seems to me there is a possibility that we are now producing inferior propellers; and while it may not be within the field of any of you gentlemen, it certainly would be worth while to find out whether that is true or not.

D. R. HULL.—There is one more illustration that I would like to show.

We can only speak for ourselves. If others have used this kind of metal and find no

* Seymour Manufacturing Company.

† Navy Purchasing Office.

trouble with it, that is their story and justifies the discussion. The strip shown in Fig. 4 is representative of 50,000 lb. of 70-30 brass that was made in a modern water-cooled mold about

cent antimony and 0.07 per cent lead. In such amounts these elements greatly impair the impact strength of the casting, and lead to serious difficulties in breakdown rolling."

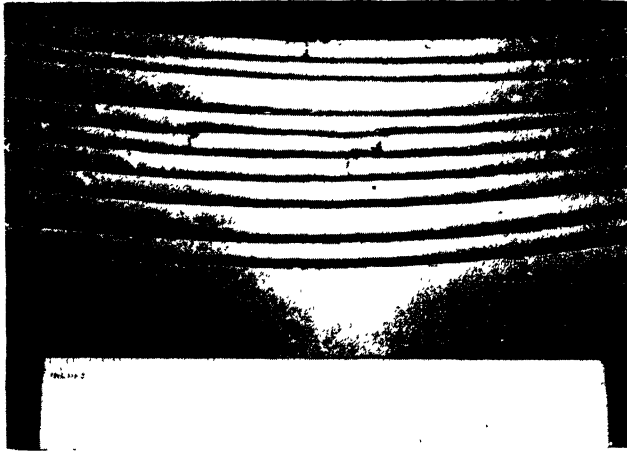


FIG. 4.—EDGE CRACKS IN 0.155-IN. GAUGE STRIP MADE FROM FIRED CARTRIDGE CASES.

2 in. thick and 19 in. wide, the bars weighing about 700 lb. The charges were composed wholly of fired small-arms cases.

Fig. 4 shows the edge of a coil in the rundown stage. It is representative of the lot as a whole and refers to every bar in it. It did not split in rolling but the edges are gone. The cracks can be sheared off, but it is not first-grade brass.

I think that the effect of antimony on brass containing beta is perhaps a separate study. It is, at any rate, outside the scope of this paper.

W. B. PRICE,* Waterbury, Conn.—It is evident that phosphorus imparts beneficial results when introduced with antimony and is analogous to the results we obtained with bismuth last year.⁵

The statements are made under Conclusions that: "The presence of lead in amounts substantially less than 0.10 per cent greatly accentuates the effects of antimony."

"Fired small-arms cases, when melted, may yield castings containing about 0.007 per

Rae, in the summary of his paper,³ says: "Results have shown that the use of fired cartridge cases should be avoided in 'Straight' copper-zinc alpha-beta brasses, especially 62:38 quality, as they have a definite embrittling effect, the properties of resistance to shock and cold riveting being most detrimentally affected. From the results obtained, it is estimated that 10-20 per cent of cases can safely be used in leaded brasses with very slight impairment of properties, provided no other antimony-bearing material is used in the mixture."

In connection with these remarks, it is interesting to note that since the end of World War I, we have made millions of pounds of pin wire using 300 lb. of fired cases to an 800-lb. charge (37.5 per cent fired cases) without experiencing any embrittling effect and without impairing the cold-heading properties. The composition of our pin wire is: copper, 60 to 63 per cent; lead, 0.07 to 0.35 per cent and zinc, balance.

D. R. HULL (author's reply).—Mr. Kemp refers to the build-up of antimony in Table 2, due to the re-use of scrap, while the lead failed to build up. Perhaps the make-up of these charges is not adequately described in the text.

* Director of Research, Scovill Manufacturing Company.

⁵ W. B. Price and R. W. Bailey: Bismuth—Its Effect on the Hot-working and Cold-working Properties of Alpha and Alpha-beta Brasses. *Trans. A.I.M.E.* (1942) 147, 136-143.

Charges 1 and 2 were of new copper and zinc plus antimony.

Charges 3 and 4 contained 45 per cent scrap from 1 and 2; balance new copper and zinc, plus antimony.

Charges 5 and 6 contained 45 per cent scrap from 3 and 4; balance new copper and zinc, plus antimony.

It is apparent that the antimony would always be diluted by the use of 55 per cent of new copper and zinc, and fresh additions would be necessary to maintain it at about 0.007 per cent, which was the purpose of the trial. At this stage of the investigation the authors were not aware of the effect of lead plus antimony. The trial run was made to determine, on a commercial scale, the effect of 0.007 per cent antimony, that being the amount found in fired cases. All the melts were commercially lead free, since something between 0.005 and 0.01 per cent is about the lowest lead that can be realized in brass made with available grades of electrolytic zinc. The test indicated that the results observed when melting fired cases were caused by something more than the antimony carried into the melt by them, and was cited for that purpose.

While on the subject of the build-up of impurities through the use of contaminated scrap, the following contribution by Dr. Cyril Stanley Smith is of interest, thus:

Let A be the fraction of the charge composed of contaminated scrap, such as fired cases.

Let B be the fraction of the charge composed of circulating scrap from previous melts.

Let n be the number of melts.

After the first charge, B will be contaminated to an increasing degree and any given melt will contain a fraction, contaminated to the same degree as A , to the amount of:

$$A(1 + B + B^2 + \dots B^{n-1}) \quad [1]$$

Since B is less than one, this series has a limiting value of:

$$\frac{A}{1 - B} \quad [2]$$

which the contamination of the melts will approach.

Table 13 shows the values of this function for various values of A and B ; i.e., for various

percentages of contaminated scrap such as fired cases, and circulating mill scrap. These figures are limiting values for an infinite number of melts, but an application of formula 1 would show that the limits are practically reached after only five or six melts.

TABLE 13

Percentage of fired cases (100A) in each charge.	3	5	10	20	30	40	50
Percentage of circulating mill scrap (100B) in each charge:							
10	3.3	5.6	11.1	22.2	33.3	44.5	55.6
20	3.8	6.2	12.5	25.0	37.5	50.0	62.5
30	4.3	7.2	14.3	28.6	42.9	52.2	71.5
40	5.0	8.3	16.7	33.3	50.0	66.7	83.3
50	6.0	10.0	20.0	40.0	60.0	80.0	100.0
60	7.5	12.5	25.0	50.0	75.0	100.0	
70	10.0	16.7	33.3	66.7	100.0		
80	15.0	25.0	50.0	100.0			
90	30.0	50.0	100.0				

From this table it is seen that with the continued use of 10 per cent fired cases and 70 per cent circulating scrap, the ultimate result would be equivalent to a melt of 33.3 per cent fired cases, balance uncontaminated stock. But 30 per cent fired cases with 70 per cent circulating scrap would, after five or six repetitions, be practically equivalent to 100 per cent fired shells.

In his experience with the use of fired cases, Mr. Wood has not found as much lead as the authors have regularly found. That would constitute a reasonable explanation for his greater success with such material. In our work, charges made entirely of fired small-arms cases have contained in the neighborhood of 0.07 per cent lead. Mr. Wood's comments relative to the effect of tin are of interest. The authors agree that there are modifying as well as confusing factors, and the subject is not exhausted.

Mr. Price has cited a long experience indicating that pin wire will tolerate a certain amount of antimony, introduced by the regular use of 37.5 per cent of fired small-arms cases in the charge. This is a matter of record and contributes to general clarification. Dr. Smith's

table indicates that the amount of circulating pin-wire scrap would have a bearing on the result, although the authors feel that an alpha beta brass of 63 per cent copper is in a different category from 70-30. It really falls in the range covered by Rae, rather than by us. Since Mr. Price does not say whether he uses a bit of phosphorus, it is assumed that he does not.

Further remarks by Mr. Price are appreciated as are also those by Mr. Kimberly and Mr. Merriman. We are in particular sympathy with Mr. Merriman's experience in washing fired cases with dilute sulphuric. A large part of the contamination seems to be in the primer cavity, to which a cleaning solution has inadequate access.

Hardness Changes Accompanying the Ordering of Beta Brass

By CYRIL STANLEY SMITH,* MEMBER A.I.M.E.

(Cleveland Meeting, October 1942)

BETA brass (consisting of approximately equal atomic proportions of copper and zinc) exists as a random solid solution at high temperatures, but at low temperatures

about 100°C. The electrical resistivity of the alloy illustrates the changes clearly (Fig. 1). This type of reaction has been a favored subject for study by physicists. An

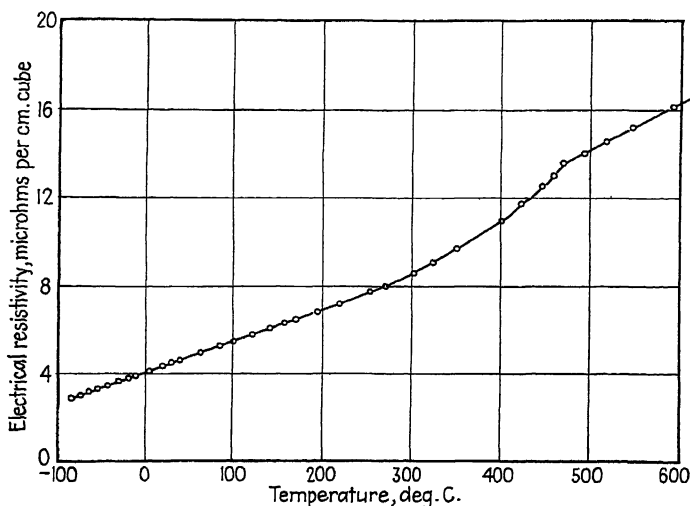


FIG. 1.—EFFECT OF TEMPERATURE ON ELECTRICAL RESISTIVITY OF BETA BRASS (51.78 PER CENT COPPER).

an ordered structure is stable, with the copper and zinc atoms occupying alternate sites on the body-centered-cubic lattice. On cooling, ordering commences at a temperature of 450° to 470°C., depending on the composition. The degree of ordering progressively increases at lower temperatures until it becomes virtually complete at

excellent summary of the theory is to be found in a paper by F. C. Nix and W. Shockley.¹

All published data on electrical conductivity, specific heat and other properties agree in indicating that the ordering reaction in beta brass takes place so rapidly that it cannot be prevented or even retarded by quenching. With most ordered alloys, cold-working induces disorder and

Manuscript received at the office of the Institute July 15, 1942. Issued in METALS TECHNOLOGY, October 1942.

* Research Metallurgist, American Brass Co., Waterbury, Conn.

¹ *Reviews of Modern Physics* (1938) 10, 2-71.

increases the resistivity very rapidly. This is not true with beta brass. A wire 0.0424 in. in diameter of an alloy containing 51.78 per cent Cu, 0.01 per cent Fe, 0.02 per cent

and immediately tested. It is to be concluded that the type of ordering responsible for conductivity changes is virtually instantaneous in its occurrence and that it

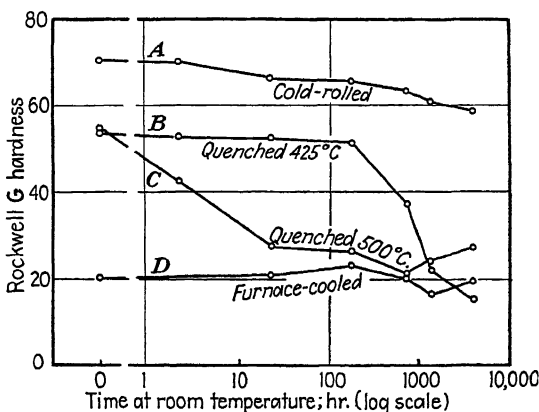


FIG. 2.—HARDNESS OF BETA BRASS AGED AT ROOM TEMPERATURES.

- A. Samples annealed at 425°C., slowly cooled to room temperature and cold-rolled 15 per cent reduction.
 B. Annealed one hour at 500°C., furnace-cooled to 425°C., held one hour at 425°C. and quenched.
 C. Annealed one hour at 500°C. and quenched.
 D. Annealed one hour at 425°C. and furnace-cooled.

Pb, balance Zn, was annealed at 400°C., furnace-cooled and then cold-drawn to 0.0404 in. (9.5 per cent reduction). The electrical conductivity in the cold-drawn condition was 39.5 per cent I.A.C.S. at 20°C. After aging for 3 days at room temperature, the conductivity was 39.8 per cent I.A.C.S., and it did not further change on annealing for one hour at 200°C., a treatment that undoubtedly reestablished almost complete order. Other tests showed the resistivity at 20°C. to remain constant within 1.5 per cent, regardless of whether the wire was quenched or furnace-cooled from 500°C., and whether it was cold-worked or aged. The temperature coefficient of resistance over the temperature range plus 20 to minus 80°C. was 0.00315 per deg. C. for slowly cooled material; 0.00310 for the same wire quenched from 500°C., and 0.00297 for the slowly cooled wire cold rolled about 12 per cent reduction

and immediately tested. It is to be concluded that the type of ordering responsible for conductivity changes is virtually instantaneous in its occurrence and that it

can not be affected either by rapid cooling or by cold-work. Hardness measurements, on the other hand, do show an effect that can be explained only in terms of some kind of ordering phenomenon. A sample of beta brass when slowly cooled is softer than when freshly quenched. However, a quenched sample loses its hardness at room temperatures very rapidly if it has been quenched from a temperature above that corresponding to complete disorder, and relatively slowly if quenched from a temperature in the range of partial ordering. Hardness changes resulting from cold-working are relatively stable. These effects can be seen in Fig. 2, in which is plotted the Rockwell G hardness* of samples of beta brass strip

* $\frac{1}{16}$ -in. ball, 150-kg load, red scale. All hardness figures reported are the averages of three readings. There was a considerable spread between individual readings (sometimes as much as 10 numbers, usually not over 5),

(51.78 per cent copper) given various preliminary treatments and then aged at room temperatures with periodic redetermination of hardness on the same samples.

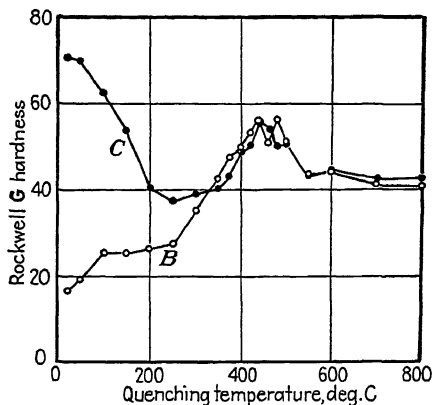


FIG. 3.—EFFECT OF QUENCHING TEMPERATURE ON HARDNESS OF BETA BRASS IMMEDIATELY AFTER QUENCHING.

Curve B. Samples furnace-cooled from 500°C. to room temperature, then reheated to temperatures indicated and quenched.

Curve C. Specimens furnace-cooled from 500°C., cold-rolled 20 per cent reduction, then reheated to temperatures indicated and quenched.

In order to show the effect of temperature more clearly, a series of samples was quenched from increasingly higher temperatures and the Rockwell hardness measured within 45 sec. of quenching, and at intervals thereafter. The alloy contained 52.24 per cent Cu, 0.007 per cent Pb, 0.002 per cent Fe, 0.002 per cent Cd, balance Zn, and was in the form of rolled strip 0.040 in. thick. Figs. 3 to 6 show the hardness immediately after quenching and of the same samples after resting for a day, a month, and four months, respectively, at room temperatures. One curve (B) in each of these figures relates to samples that had been furnace-cooled from 500°C. to room temperature prior to reheating, and the other relates to similarly furnace-cooled samples that had been cold-rolled 20 per cent probably a result of the large grain size of the samples.

cent reduction before reheating as shown. A constant, controlled, heating rate of 60°C. per hour was used, and individual samples were removed and quenched as

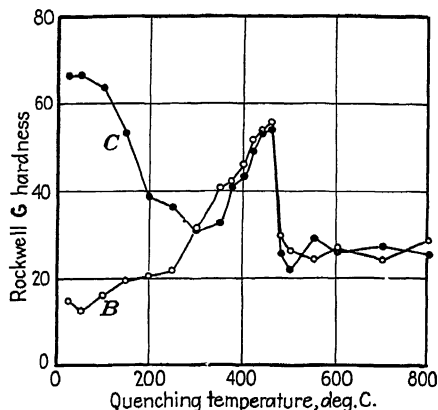


FIG. 4.—HARDNESS OF SAMPLES OF FIGURE 3 AFTER AGING FOR 24 HOURS AT ROOM TEMPERATURES.

soon as the indicated temperatures were reached, without soaking. Tests in which the critical temperatures were approached

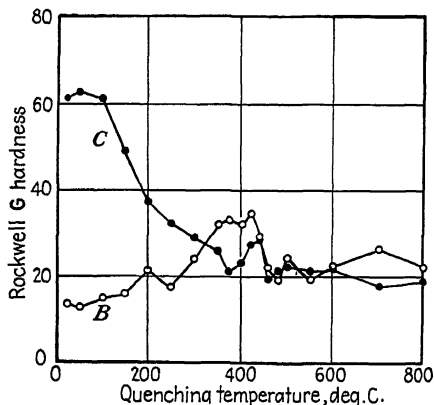


FIG. 5.—HARDNESS OF SAMPLES OF FIGURE 3 AFTER AGING FOR 32 DAYS AT ROOM TEMPERATURE.

by slow cooling gave results virtually identical with those of the furnace-cooled samples quenched during subsequent slow heating.

The effects of aging at room temperature after quenching are seen on comparing these figures. The rate of softening on room-temperature aging of a sample

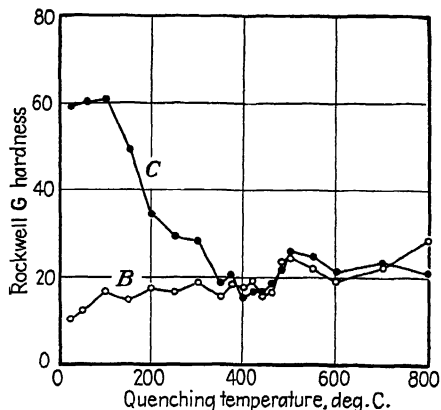


FIG. 6.—HARDNESS OF SAMPLES OF FIGURE 3 AFTER AGING FOR FOUR MONTHS AT ROOM TEMPERATURE.

quenched above the transformation point is obviously much greater than that of one quenched in the range 460° to 300°C. , where the degree of order is increasing.

specific heat curve for beta brass, though the apparent critical temperature is about 30°C. lower. The peak is much less prominent both in the freshly quenched samples and in those aged for a month at room temperature, while it is virtually absent after aging for four months. In tests on another alloy (containing 51.89 per cent Zn, 0.01 per cent Fe, 0.001 per cent Pb) the peak had disappeared after only 16 days.

If it is assumed that hardness is related to ordering, and that a completely ordered structure represents the softest condition obtainable at room temperatures, these curves suggest that the rate ordering is of greater from a completely disordered structure than it is from a partially ordered condition. This is by no means unreasonable and, indeed, finds analogy in many other types of transformation. It will be remembered that conductivity and specific heat (which are largely dependent on short distance order) do not change with quenching temperature or with aging. Hardness evidently is connected with the presence of out-of-step domains or some other disturb-

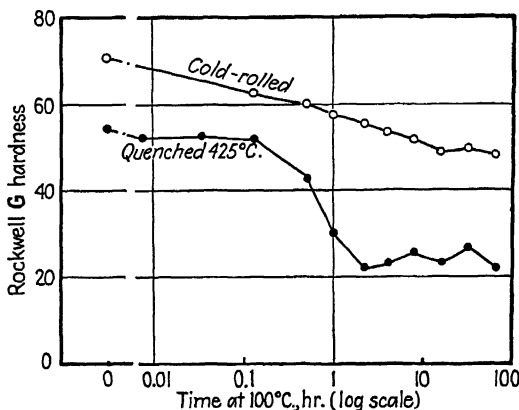


FIG. 7.—EFFECT OF AGING AT 100°C. ON HARDNESS OF QUENCHED OR COLD-ROLLED BETA BRASS (51.78 PER CENT COPPER).

Because of this difference in rate, the hardness curve for the samples tested 24 hr. after quenching (Fig. 4) has a peak and a general shape that parallels the well-known

ance of long-range order. It is easy to conceive that a series of small zones would align themselves with a growing nucleus more readily than large balanced groups

(formed where partial ordering was stable) could rearrange themselves in terms of the long-range ordering force.

A comparison of curves *B* and *C* in Fig. 3 shows that hardening effect due to cold-work is completely removed at 250°C. Fig. 2 shows that there is even some softening on prolonged aging at room temperatures, and Fig. 7 shows the expected more rapid change at 100°C. Microscopic examination reveals that loss of work hardness is associated with the disappearance of deformation markings in the grains and is not accompanied by recrystallization unless annealing temperatures exceed about 300°C. Grains may be enormously elongated yet still retain their individuality if the sample is given successive small reductions by cold-rolling followed by repeated annealings at about 200°C., and such material possesses a very high degree of preferred orientation.

ACKNOWLEDGMENT

The willing and capable assistance of Mr. I. W. Kirschbaum in making many of the heat-treatments and hardness measurements described herein is gratefully acknowledged.

DISCUSSION

(*F. N. Rhines presiding*)

R. M. BRICK,* New Haven, Conn.—Most studies of ordering in metallic solid solution alloys, as summarized in the paper of Nix and Shockley,¹ have neglected the interesting question of related alterations in mechanical properties. Nix and Shockley devote only about 0.4 per cent of the space in their long review of the subject to this aspect of the problem. Thus the present article on hardness changes accompanying ordering is indeed welcome, although it would be more valuable had the author found time to investigate changes in strength and plasticity properties.

The fact that complete ordering in binary alloys is confined to simple atomic ratios; viz., 1:1 for the body-centered cubic lattice

or 1:1 and 3:3 for the face-centered cubic lattice, has led to the usage of compound designations for ordered structures; for example, CuZn or CuAu and Cu₃Au as representatives of the lattice types just mentioned. Since most intermetallic compounds are harder and less plastic than solid solutions, it has often been assumed that ordering is accompanied by a hardening and embrittling of the structure. The β to β' brass change might have been thought to conform to this idea; while all metals soften at elevated temperatures and vice versa, the change from very soft β (at a red heat) to hard β' at room temperatures is much greater than the equivalent change in the hardness of α over the same temperature range. Nix and Shockley quote references that show that ordering of CuPt, CuPd and CuAu is accompanied by a hardening effect, similar to an age-hardening response, while Sachs and Weerts show that ordering of Cu₃Au gives first a hardening and later a softening effect.

Are ordered solid solutions generally more like pure metals in properties than the same alloys when in the disordered state, as would be indicated by most electrical resistivity measurements, or do they correspond to compounds, or is it impossible to generalize? The resistivity data given by Dr. Smith suggest that ordering in β brass is of an unusual character while his softening data seem to reveal the conflicting status of property changes accompanying ordering.

On this basis, his statement (p. 147) that "If it is assumed that . . . a completely ordered structure represents the softest condition . . ." seems unwarranted, unless it likewise is assumed that hardening data on CuAu, CuPt and CuPd represent only partial ordering—i.e., out-of-step domains—or that ordering of a face-centered and of a body-centered cubic lattice give completely different types of hardness changes.

The statement that "grains may be enormously elongated yet still retain their individuality" is not clear. What exactly is meant by "retain their individuality"?

W. M. BALDWIN, JR.,* Euclid, Ohio.—Dr. Smith has raised an interesting point in

* Hammond Metallurgical Laboratory, Yale University.

* Research Metallurgist, Midwestern Division, Chase Brass and Copper Company.

the behavior of beta brass. Some time ago, our laboratory ran some tests on beta brass wire which confirm Dr. Smith's experimental work. Brass wire (52 per cent Cu, balance Zn)

before and after annealing. The results are shown in Fig. 8. A minimum in each hardness curve is found at 300° to 350°C. and a maximum at 400° to 450°C. Photomicrographs

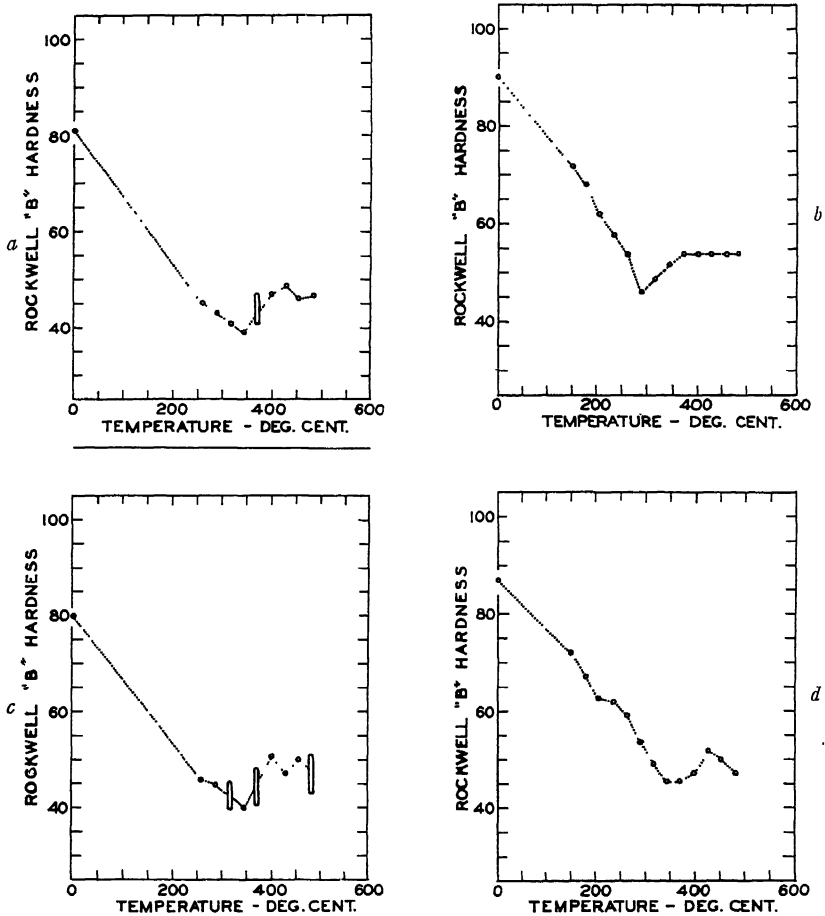


FIG. 8.—ROCKWELL B VS. ANNEALING TEMPERATURE FOR COLD-DRAWN BETA BRASS (52 PER CENT COPPER, BALANCE ZINC) WIRE.

a. Extruded 0.148 in., drawn 0.132 in., 0.126 in., 0.116 in. with $\frac{1}{2}$ hr. 850°F. intermediate anneals.

b. Extruded 0.190 in., drawn 0.174 in., 0.161 in., 0.148 in., 0.136 in., 0.125 in. with $\frac{1}{2}$ hr. 450°F. intermediate anneals.

c. Extruded 0.148 in., drawn 0.137 in., 0.126 in., 0.116 in. with $\frac{1}{2}$ hr. 450°F. intermediate anneals.

d. Extruded 0.150 in., drawn 0.134 in.

was drawn according to different schedules to diameters ranging from 0.116 to 0.134 in., then annealed at various temperatures and air-cooled. Rockwell hardness was determined

showed that the strain lines produced by cold-work disappeared at 150° to 200°C.; while recrystallization began at 260° to 290°C. and was complete at 300° to 400°C. These figures

are all in general agreement with Dr. Smith's, and we are only too glad to offer them to him in support of his own experimental findings.

C. S. BARRETT,* Pittsburgh, Pa.—Dr. Smith has found a very interesting example of a superlattice in which hardness is dependent upon the presence of pseudo grain boundaries between out-of-step domains. The role of these pseudo grain boundaries apparently is very similar to the role of ordinary grain boundaries in inhibiting plastic flow. They are accompanied by local stresses that oppose the passage of slip movements—according to current theories, the passage of “dislocations.” As the domains coalesce and the boundaries are reduced in number, these barriers are removed. There will certainly be more research in the future on the effects of these boundaries and the rates of coalescence of the domains in superlattices.

Another question of interest to metallurgists is whether in any alloy systems showing superlattices a partially ordered phase of one composition can be in equilibrium with a disordered phase of different composition, so that one can properly draw a two-phase region in the constitution diagram. This has been suggested in a theoretical treatment of Shockley's but has not been determined experimentally.

J. L. CHRISTIE,† Bridgeport, Conn.—In Fig. 2, the difference of Rockwell hardness between 25 and 55 is quite appreciable. Is it not quite unusual for such a change of hardness to take place just on standing at room temperature?

Another question: Is it not highly unusual to get sufficient softening to permit considerably more cold-work without getting the recrystallization that usually we associate with the annealing operation?

G. P. HALLIWELL,‡ Chicago, Ill.—The addition of iron, manganese and especially aluminum in sufficient amounts to an alpha-beta brass will produce an all-beta structure. Such alloys are known as high-strength manganese bronzes. They are produced commercially with a tensile of 110,000 to 115,000

lb. and an elongation of 10 to 15 per cent in the sand-cast condition. Frequently these properties are exceeded, but we are being asked for an alloy that will regularly meet 120,000 lb. tensile and 15 per cent elongation or better. It is the last 5000 lb. and the last 3 to 5 per cent elongation that is difficult to attain. Is there any information available on the effect of these metals on the degree of ordering, and can we anticipate any improvement in properties in these alloys from this source?

D. HARKER,* Schenectady, N. Y.—In this discussion there has been no mention of the difference between two kinds of ordering reactions. In one kind the crystal system does not change and the axial lengths remain almost unchanged; in the other, there is a change in crystal system.

In beta brass the atoms are always arranged on a body-centered cubic lattice, and the only change on ordering is that of replacing the random distribution of copper and zinc atoms on this lattice by an arrangement where the copper atoms are all at the cube corners and the zinc atoms are all at the cube centers. I believe no significant change in lattice constant accompanies this reaction, and Dr. Smith's work shows that there is no great change in hardness.

In a case such as that of AuCu, however, where the crystal system changes during ordering, the hardness behavior should be different. At high temperatures the atoms are arranged at random on a face-centered cubic lattice, while in the low-temperature, ordered, phase the planes parallel to a cube face of the high-temperature phase are filled alternately with gold and copper atoms. This structural change results in a tetragonal distortion of the originally cubic lattice, the distance between lattice planes in the direction perpendicular to the gold and copper layers being less than that in the other original cube edge directions. If a large single crystal of AuCu above the ordering temperature is cooled, ordering will start in several different places independently, and the different ordered regions will have their gold and copper planes oriented at random among the three possible directions. Where

* Metals Research Laboratory, Carnegie Institute of Technology.

† Handy and Harman.

‡ H. Kramer and Company.

* Research Laboratory, General Electric Company.

two regions of different orientation meet, the planes on which slip can occur will not continue smoothly across the boundary. If there are enough of these regions, it will be difficult for slip to take place, and the crystal will be much harder than it was when in the disordered state.

I believe great hardening would take place in CuPt also, where conditions similar to AuCu prevail. AuCu₃, on the other hand, has an ordering reaction similar to that of beta brass, and it shows but little difference in hardness between quenched and slowly cooled specimens.

C. S. SMITH (author's reply).—Dr. Brick rightly takes me to task for looseness of expression.

The "assumption" (p. 147) is of course that the softest condition represents the completely ordered structure and not vice versa; moreover, disorganized beta was not included in this comparison because of the unlikelihood of its being retained at room temperature for measurement. Surely it is to be expected that completely ordered beta with no out-of-step domains will be softer than beta with subboundary irregularities, whether these are out-of-step domains or ordered areas surrounded by disordered material. Dr. Harker's suggestion that the out-of-step domains will retard slip to a greater extent when a change of symmetry exists seems very reasonable.

In answer to Dr. Brick's comment on "individuality": When beta brass is cold-rolled, the grains elongate and develop deformation markings at relatively few locations. On annealing at a temperature of about 200°C., the deformation lines disappear and the hardness decreases, but the grains do not recrystallize, and the grains retain their extended shape. On further rolling the grains may be elongated still further, until eventually each originally equiaxed grain becomes a thin lath. If such a sample is treated with mercury, it is possible to separate the individual grains, which look much like blades of grass.

Mr. Christie comments upon the usual behavior of softening without recrystallization. The extent of possible cold-rolling in beta brass

is relatively small, and the crystallographic distortion can be removed by relaxation at relatively low temperatures without the formation of nuclei of different orientation. Tungsten seems to behave similarly, and it is probable that many other cases will be found. Anyone unfamiliar with metal behavior would probably expect this to happen generally.

Mr. Halliwell rightly inquires as to the practical significance of these observations. If means can be found for retaining the intermediate out-of-step structures, the resultant properties would be distinctly useful. Such hopes actually initiated the research of which a portion is described in this paper. However, in no experiments that have been done has there been any indication that partial disordering is sufficiently stable to be utilized as a practical means of hardening. In manganese-bronze castings the rate of cooling is sufficiently low so that no further changes can be expected at room temperatures. It would be anticipated, however, that considerable increase in ductility would occur on aging at room temperatures in very small castings or in castings that for some other reason have been rapidly cooled from temperatures above 300°C.

Many years ago Carpenter¹ published photomicrographs which were interpreted as showing eutectoidal decomposition of beta. It has since been shown conclusively that there is no eutectoid in this part of the copper-zinc system, but it is not impossible that Carpenter's patterns (generally dismissed as mere etching effects) were actual microscopic evidence of out-of-step domains. Definite micrographic evidence of the formation and growth of ordered nuclei has been found in the copper-aluminum beta phase,² where the particles grow in an irregular rosette shape and can be observed to impinge and eventually to merge with each other. In private conversation, I have been informed that similar structures have been seen in copper-zinc alloys, though I have never been able to develop them myself.

¹ H. C. H. Carpenter: The Structural Resolution of the Pure Copper-Zinc Beta Constituents into Alpha plus Gamma. *Jnl. Inst. Metals* (1912) 8, 51.

² C. S. Smith and W. E. Lindlie: A Micrographic Study of the Decomposition of the Beta Phase in the Copper-aluminum System. *Trans. A.I.M.E.* (1933) 104, 69.

Recent Developments in the Formation of Aluminum and Aluminum Alloys by Powder Metallurgy

By G. D. CREMER* AND J. J. CORDIANO*

(New York Meeting, February 1943)

ALUMINUM powder is a well-known article of commerce and in various forms has been marketed widely for use in paint, for pyrotechnic purposes and for exothermic mixtures. For a number of reasons, however, aluminum powder has not been employed extensively in powder metallurgy, although a great many proposals along this line have been offered.

Aluminum and aluminum-alloy powders oxidize readily upon exposure to air and the thin film of oxide (or hydroxide) thus formed is highly refractory, in that ordinary gaseous reducing agents such as hydrogen or carbon monoxide do not reduce the oxide to metal at temperatures below the melting point of aluminum. It has been thought that the presence of these films of oxide on aluminum particles would interfere markedly in powder metallurgical work and a number of suggestions have been made, either for preventing the formation of the film through the production of the powders in inert or reducing atmospheres, or for the removal of the oxide by means of powerful reducing agents, including "nascent" or atomic hydrogen released from metal hydrides.

A second and more serious difficulty in the use of aluminum and aluminum-alloy powders in powder metallurgy resides in the fact that during compression such powders tend to adhere or cold-weld to

the die walls, thus interfering with the formation and ejection of a compact.

A third difficulty, which has been encountered only with aluminum-alloy powders, is their hardness when compared with elemental aluminum. Certain of these powders are susceptible to age-hardening, which further hinders the formation of strong green compacts. These conditions are particularly true of atomized aluminum-alloy powders.

Even in the annealed condition, plastic deformation of alloy powders under pressure is low when compared with unalloyed powders. This fact, coupled with the lower corrosion resistance of the alloy powders, is probably the significant factor in our failure to obtain strong sintered pieces.

METHODS OF PRODUCING THE POWDER

Many methods have been proposed for manufacture of aluminum powder, only a few of which are used commercially. Several of the more important processes include: (1) atomization of the molten metal; (2) mechanical pulverization and other types of comminution; and (3) graining, in which molten aluminum is stirred during freezing.

For pigment and certain pyrotechnic uses aluminum flake powder is desirable, because of its greater proportion of surface to volume; and large quantities of such material are made by a procedure that involves stamping or ball milling. In making flake intended for use as pigment,

Manuscript received at the office of the Institute Dec. 1, 1942. Issued in METALS TECHNOLOGY, June 1943.

* Research Engineers, Hardy Metallurgical Co., New York, N. Y.

the flattening procedure usually is conducted in the presence of stearic acid or mineral spirits that prevent agglomeration of the flakes, and also may impart the desirable quality known as "leafing." In general, however, aluminum flake is not suitable for powder metallurgy and, in fact, except for a few special applications, all flaky metal powders are unsatisfactory in the powder metallurgy process.

Grained aluminum powders such as those customarily employed in thermit mixtures are unsatisfactory in powder metallurgy because of excessive oxide content and coarse particle size.

Mechanical pulverization methods also are unsuitable for the production of aluminum powders intended for use in powder metallurgy because of inherent work-hardening effects and the difficulties involved in producing fine-mesh powders on a commercial scale.

In the development program that is summarized here, elemental aluminum powders made by a variety of procedures were investigated, and it was found that in so far as powder metallurgy is concerned those made by atomization are most suitable. In all of the work reported hereinafter, the compacts were formed from powders made by atomizing molten aluminum in a current of hot gas, followed by a quick chilling of the spray in large quantities of air at atmospheric temperature. This procedure inevitably results in the formation of aluminum powder coated by an oxide film, but, because of the relatively smooth surface of the particles and the extremely rapid quench involved, these films are thin and highly protective. It has been our experience that oxide films of this character are not entirely objectionable and may, in some instances, be of actual value, particularly in controlling the grain size in the finished aluminum and aluminum-alloy articles. A further advantage is that this method of atomization is flexible and easily adjusted to produce a wide range of

particle sizes. Moreover, it is adapted to safe, large-scale and economical production.

LUBRICATION OF DIES

As noted, a primary difficulty, and one that has been experienced and acknowledged by earlier investigators, is the tendency of aluminum powders to "cold-weld" or adhere to the die when compacted. This cold-welding phenomenon is very serious when aluminum powder is compacted in a steel die employing the usual wall lubricants, including fatty acids, oils and graphite. In some instances, especially at relatively high briquetting pressures—say in the neighborhood of 50 tons per sq. in.—the cold-welding is so severe that the force required to eject the compact is at least half of the forming pressure. If cold-welding occurs to any substantial degree in a powder metallurgical compression operation, quality production with close tolerances and high strengths is impossible. Each time such a compact is made there is a change in the amount of aluminum accumulated on the die wall, with a resultant change in the dimensions of the ejected piece, together with nonuniform density, laminations, spalled sides, and other faults. The cold-welding tends to become progressively worse and eventually results in complete jamming of the die.

It has been proposed to admix solid lubricants directly with the aluminum powders in a manner like that employed by manufacturers of porous bushings and similar articles. The addition of a substantial portion, say 2 per cent by weight, of stearic acid powder to aluminum powder will prevent jamming of the die during compression. However, during sintering of compacts so formed, volatilization of the stearate occurs, with resultant porosity, discoloration, oxidation, and lowered strengths.

Since the primary purpose of the work described in this paper was the development of a procedure for the manufacture

of aluminum and aluminum-alloy parts of high strength and accurate configuration, it was necessary at the outset to overcome the difficulties attendant upon heretofore customary die lubricants and the methods of application, and to prevent cold-welding without introducing deleterious components into the compacts themselves. This was done by lining the dies with flat-lying overlapping metal flakes. We have found that so-called bronzing powders used in paint and ink manufacture are suitable for this purpose. These powders are in the form of fine metallic flakes of minus 300-mesh major dimension, with an average thickness of about 0.000005 in. When such fine flake powders (suspended in a volatile carrier such as carbon tetrachloride) are sprayed on the die walls, a thin, but substantially impenetrable layer is formed thereon. The lubrication quality of the flakes is due to their ability to adhere to the die wall in a flat-lying, overlapping position, and may be improved by incorporating a substantial proportion of a fatty acid (say stearic acid) or a soap (say aluminum stearate) in the carrier liquid.

In our laboratory work, the lubricant has been applied as a spray, by a hand atomizer, but it may be painted on the die wall or applied with an automatic wiper, which passes into the die bore periodically, preferably after each piece is ejected and before the die is again filled with powder.

The effect of the flake lubricant is marked. A reduction of as much as 95 per cent is effected in the pressure required for ejection and lamination is prevented. Thus, in instances in which a compressive force of 20 tons was required to eject a piece when conventional lubricants were employed, replacement of such lubricants by the metal flake has reduced ejection pressure to less than a ton, and the resulting compact has been strong, clean and to close tolerance.

The flake lubricant is not limited in its

utility to the powder metallurgy of aluminum, but may be employed advantageously with other powders, including copper, brass and iron. However, in general, such powders do not manifest as great a tendency to weld to the die wall, therefore the advantage accruing to the use of the flake lubricant is less.

PROCEDURE AND RESULTS OF LABORATORY WORK

Following the solution of the die-lubrication problem, a number of types of aluminum and aluminum-alloy powders were investigated to find those most suitable for powder metallurgy. The alloy powders, irrespective of their method of production, were relatively unsatisfactory. Specimens produced by compression and sintering of such powders were inferior to analogous wrought or cast material, the most serious deficiency being a lack of ductility. In these preliminary tests, however, several grades of atomized elemental aluminum powders responded encouragingly to powder metallurgical technique. At higher compacting pressures, properties approaching those of wrought annealed commercial aluminum were obtained. This development led to the use of these elemental aluminum powders in subsequent work for the production of aluminum and aluminum-alloy parts.

Because comparatively small proportions of alloying elements produce great changes in the properties of aluminum, the possibilities of mixing such alloying elements in powder form with elemental aluminum powder were investigated. In this way, the good "compactability" of aluminum powder was retained and the requisite alloys were formed during the sintering operation by diffusion between powder particles.

All of the sintered alloy compositions described hereinafter were produced by mixing the alloying elements as powders with atomized elemental aluminum powder.

The raw materials, die lubrication, equipment and procedure employed in the work are summarized as follows:

Raw Materials

ALUMINUM POWDER^a—Atomized, -30 Mesh
Major impurities: Fe, 0.28 per cent; Si, 0.17; Cr, 0.03; Cu, 0.01.
Screen analysis, Tyler series: -30 +100, 20.2 per cent; -100 +200, 21.8; -200 +325, 19.2; -325, 38.8.
COPPER POWDER^b: electrolytic, 99.3 per cent Cu, 99 per cent -325 mesh.
MANGANESE POWDER: electrolytic, 99.9 per cent Mn; -325 mesh.
MAGNESIUM POWDER: added as 50:50 Mg-Al alloy, -325 mesh.

Lubricant

Polished aluminum flake, -325 mesh.
Carbon tetrachloride.
Stearic acid powder.
Ratio by volume: 2:50:2.

Application

The fine aluminum flake powder suspended in a carrier of CCl_4 containing the dissolved stearic acid was sprayed directly onto the die walls by means of a bulb atomizer. As thin a film as could be applied with reasonably complete coverage was found most satisfactory. Lubrication of this type is preferably done before every filling of the die with metal powder, although under some conditions such lubrication every other time has proved adequate.

Compacting Die

A steel double-acting die was used, which produced a tensile bar compact of rectangular test cross section measuring $\frac{1}{4}$ in. by approximately $\frac{3}{16}$ in. thick. Specimens so formed were 4 in. over-all with a 1-in. gauge length. Ejection was accomplished by removing the upper punch and continuing the motion of the lower punch through the die.

Pressure was applied by a 125-ton hydraulic press with a ram moving at the rate of 10 in. per minute.

Powder fill for all the test bars produced was kept constant by maintaining a given fill cavity and striking off excess powder flush with the top surface. A supporting shim was

then removed, permitting compression to take place between parallel walls and below the slightly tapered section necessary for ejection (Fig. 1).

ELEMENTAL ALUMINUM

As shown by the chemical analysis, the atomized aluminum powder employed as the basic material in our work is low in silicon and iron. On the basis of our experience, it appears that the combined silicon and iron content of the elemental base powder should not exceed about 0.5 per cent.

Preliminary experiments with the elemental base powder were run to determine the effect of particle size and pressure. In this work the basic 30-mesh material, a portion of the material screened through 100 mesh to give a medium particle blend, and a third portion screened through 200 mesh to give a fine blend were employed. These several powders were compressed at various pressures and heat-treated as indicated in Figs. 2 and 3.

In the work summarized in these figures all specimens were sintered for 30 min. at 620°C. in air. In addition to the 30 min., the furnace time included a 15-min. heat-up period and 15-min. cooling period, during which the temperature was permitted to drop to 510°C. At this temperature specimens were quenched in cold water. The sintering time involved is relatively short, well within the limit of commercial requirements.

The results of the foregoing tests indicated that particle size has but slight effect upon tensile strength of the sintered compacts, so that Figs. 2 and 3 may be considered as representative of the results obtained with all three powder sizes.

The fact that powder size does not have an effect upon tensile strength, however, should not be taken as indicating that particle size is unimportant. In general, fine powders have poor flow characteristics and abrade the die, so that coarse blends of aluminum powders are preferred.

^a Reynolds Metals Co., Grade "PM 30 mesh."

^b American Metals Co., Ltd., grade "C."

Moreover, fine aluminum powders tend to be forced into the space between the

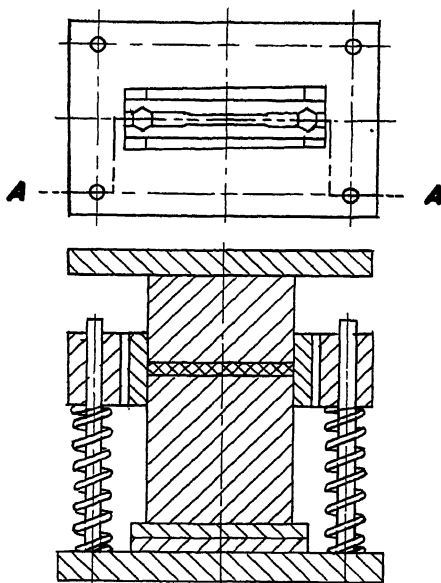


FIG. 1.—DIE ASSEMBLY.

die wall and the punch, with the resultant formation of fins.

pacts increases markedly with pressure up to 35 tons per sq. in. At this point the curve flattens out and, in general, no great increase in density is obtained with pressures greater than about 50 tons per sq. inch.

In Fig. 3, it will be observed that tensile strength increases with relative rapidity as the pressure is raised to about 40 tons per sq. in. Thereafter, the curve of tensile strength flattens off and in general increases in tensile strength are not to be expected above 60 tons per sq. in. compacting pressure. Also, the curve for elongations does not follow the tensile-strength curve and, other conditions being equal, improved ductility is obtained with increasing pressure, at least up to 60 tons per sq. inch.

In general, adequate commercial results can be obtained with compacting pressures between 40 and 60 tons per sq. in., assuming that the molds have been properly lubricated. At 60 tons per sq. in., the tensile strength obtained was 17,500 lb. per sq. in., this being accompanied by an elongation of 30 per cent in 1 in. It will be recognized that these values do not fall

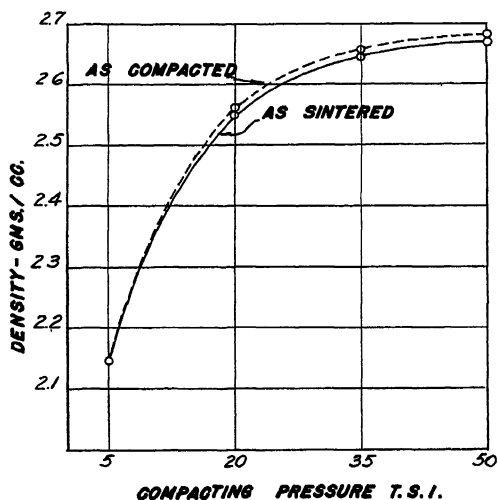


FIG. 2.—EFFECT OF COMPACTING PRESSURE ON THE PROPERTIES OF AIR-SINTERED ALUMINUM.

In Fig. 2, it will be observed that the density of the sintered aluminum com- far short of those obtained in forged aluminum. It should also be noted, in

connection with the foregoing tests, that the fatigue resistance of the material was high. A limited number of tests made on pieces compressed at 50 tons per sq. in.

MANUFACTURE OF ALUMINUM ALLOYS FROM ELEMENTAL POWDER MIXTURES

In preliminary work it was found that the foregoing conclusions with respect to

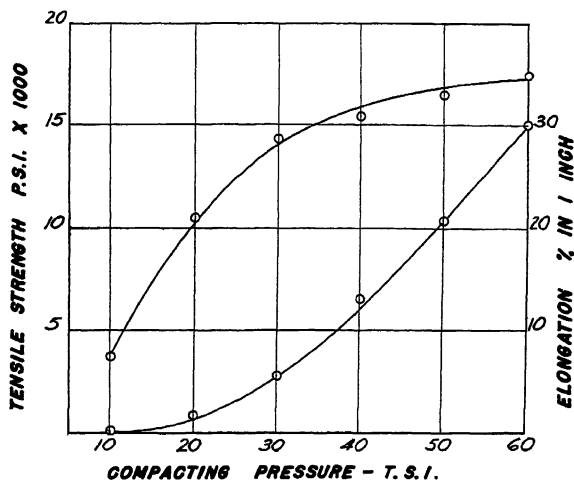


FIG. 3.—EFFECT OF COMPACTING PRESSURE ON THE PROPERTIES OF AIR-SINTERED ALUMINUM.

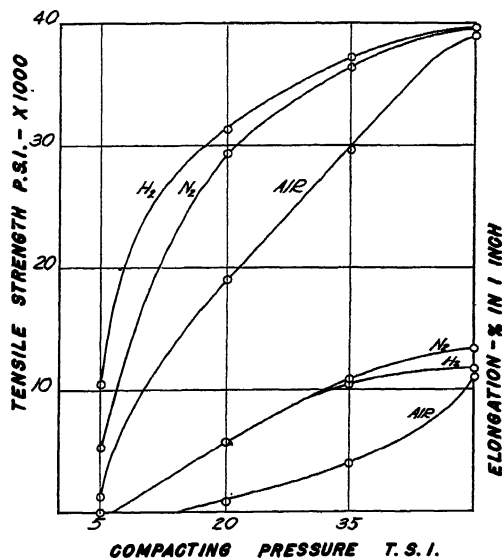


FIG. 4.—EFFECT OF SINTERING ATMOSPHERE ON PROPERTIES OF 96-4 ALUMINUM-COPPER ALLOY COMPOSITION MIXTURE.

showed a fatigue resistance of approximately 8000 lb. per sq. in. with 10^8 cycles of stress without rupture.

the effect of pressure upon the properties of the sintered aluminum compacts also held true for several simple aluminum

alloys made from mixtures of the basic aluminum powder with various alloy ingredients. Thus, the conclusions held true for 96-4 aluminum-copper; 95-4-0.5-0.5

temperature they were quenched in cold water.

The values reported on Figs. 4 and 5 are for bars in the as-quenched condition.

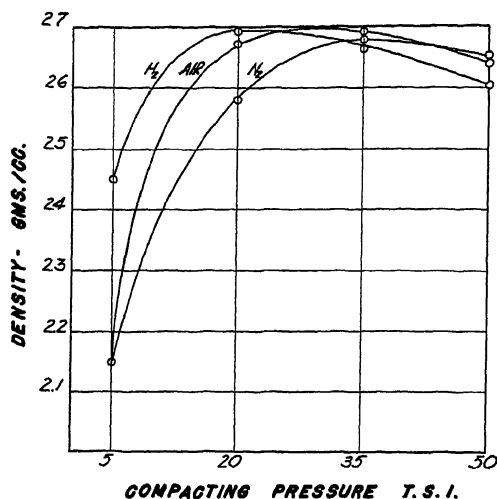


FIG. 5.—EFFECT OF SINTERING ATMOSPHERE ON PROPERTIES OF 96-4 ALUMINUM-COPPER ALLOY COMPOSITION MIXTURE.

aluminum-copper-magnesium-manganese and 97.2-2.5-0.3 aluminum-copper-magnesium. It should be noted, however, that it was found necessary to employ aluminum powder of at least minus 100-mesh in order to obtain adequate mixing of the aluminum powder with the appropriate alloy ingredients.

The results of a number of tests with sintered compacts made from the basic aluminum powder to which 4 per cent of electrolytic copper was added are summarized in Figs. 4 and 5. In all the tests reported on these figures, specimens were sintered for 30 min. at 600°C. in various atmospheres noted on the graph. As in the tests made with the basic aluminum powder alone, the specimens were in the furnace for a total of 60 min., there being a heat-up time of 15 min. and a cooling time of 15 min. During the cooling period, the temperature of the specimens was allowed to drop to 510°C., from which

On Fig. 4, it will be observed that the best tensile strengths were obtained by sintering in hydrogen. However, nitrogen is also a suitable atmosphere and even air is suitable if the compacting pressure is sufficiently high. Thus, although sintering in hydrogen gives considerably better results if the compacts were formed at a pressure of only 20 tons per sq. in., with a compacting pressure of 50 tons per sq. in. there is little to choose from among hydrogen, nitrogen and air.

The foregoing conclusions with respect to the effect of atmosphere upon tensile strength are also applicable with slight modification in regard to ductility. Thus, at low compacting pressures, both nitrogen and hydrogen are superior to air. At high compacting pressures, say 50 tons per sq. in., the best ductility was obtained in an atmosphere of nitrogen, although the ductility obtained in hydrogen and air was good.

Fig. 5 shows that the higher densities in sintered compacts were obtained with relatively low compacting pressures of 20 to 35 tons per sq. in. However, hydrogen-sintering at 600°C. of specimens formed at these lower pressures was particularly characterized by marked shrinkage and distortion. This tendency of such compacts to warp during sintering in hydrogen can be reduced substantially by sintering at a lower temperature, but only with accompanying serious loss in strength.

The sintering operation, in addition to bringing about a welding of the particles and an alloying action, also appears to act as a high-temperature solution treatment, particularly if the material is cooled to about 500°C. before quenching. This cooling from the sintering temperature to 500° or thereabouts, also tends to minimize warping.

It was discovered that the compacts formed as outlined in Figs. 4 and 5 would respond to a conventional precipitation-hardening treatment for this type of material and that by such procedure the hardness of the material could be raised to 50 Rockwell B.

Attempts to duplicate the results of Figs. 4 and 5 by sintering at lower temperatures indicated that the seemingly high sintering temperature of 600°C. is necessary to bring about adequate diffusion of the 96-4 mixture within the sintering time employed.

The microstructure of the compacts formed as outlined in Figs. 4 and 5 are shown in Fig. 6. These photomicrographs show that before sintering the copper—the large, dark, irregular particles—is present in an unalloyed condition. After sintering the copper is in large part diffused and in solution. After a precipitation treatment at 300°F. for 12 hr. in air, the copper is precipitated in a form somewhat different from the one that would be expected in an analogous alloy made by casting.

It may be interesting to compare the values obtainable in the manufacture of 96-4 aluminum-copper compositions made by powder metallurgy with those obtained by an analogous alloy by the casting technique.

As-sintered compacts made by powder metallurgy have both higher tensile strength and ductility than an analogous material as cast. Distinction also remains after solution treatment, as witness the fact that the material made by powder metallurgy has a tensile strength of 38,000 lb. per sq. in. and elongation of 10 per cent as compared with 33,000 lb. per sq. in. tensile strength and an elongation of 4 per cent for the cast solution-treated material.

In short, the physical properties of the compacts made from a mixture of 96 per cent aluminum powder and 4 per cent copper powder compared favorably with those of the commercially cast and heat-treated alloy. This is particularly true in regard to ductility, as shown by the elongation results, which are several times greater than those for equivalent cast material.

It is believed that the improved physical properties of the 96-4 alloy made by powder metallurgy may be attributed at least in part to the fine grain size obtainable. Moreover, it should be observed that pieces made by the powder metallurgy technique are substantially free from unpredictably large blowholes and inclusions, the only voids being in the form of well-distributed fine pores. Consequently, the high structural factor of safety employed for the cast material is unnecessary.

In further experiments in the manufacture of aluminum alloys, 0.5 per cent of finely divided manganese and 0.5 per cent of finely divided magnesium was incorporated in the basic 96-4 aluminum-copper mix to produce a high-strength material having some of the properties of Duralumin. In this work, the manganese was incorporated as finely ground electrolytic

manganese powder. It is difficult to obtain fine magnesium powder suitable for powder metallurgical work and instead of such powder a brittle 50-50 aluminum-mag-

nesium, it immediately became apparent that the atmosphere employed in sintering was important. As previously noted in the discussion of Figs. 4 and 5,

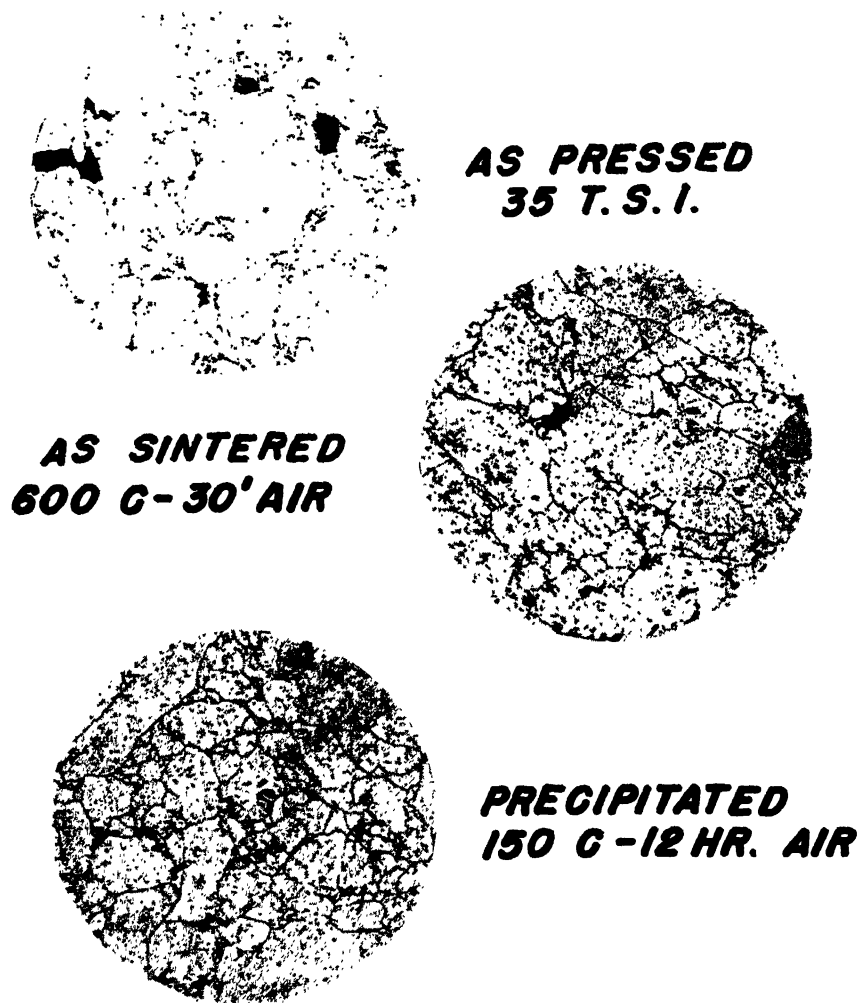


FIG. 6.—REPRESENTATIVE PHOTOMICROGRAPHS OF 96-4 ALUMINUM-COPPER SPECIMENS PRESSED AT 35 TONS PER SQUARE INCH AND SINTERED AT 600°C. FOR 30 MINUTES. $\times 200$. ETCHED.

nesium alloy was pulverized. This alloy powder gave better results than the best elemental magnesium powder we were able to obtain.

In our work with compacts containing

elemental aluminum and compacts made of mixtures of aluminum-copper powder can be sintered in a variety of atmospheres with adequate results. This is not true of compacts containing elemental magnesium

or magnesium-aluminum alloy powders. Such compacts were found to require a reducing or neutral atmosphere. In other words, air sintering does not give optimum results.

time depending upon the thickness of section of the piece. If the piece is heated above $550^{\circ}\text{C}.$, molten eutectic forms and seriously damages the structure. We have found, however, that pieces of equivalent

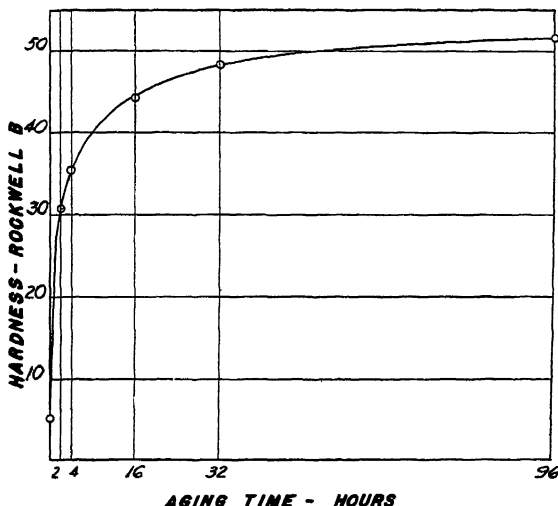


FIG. 7.—AGING PROPERTIES OF SINTERED ALLOY COMPOSITION MIXTURE.
95 per cent Al, 4 Cu, 0.5 Mg, 0.5 Mn.

A suitable technique for preparing strong pieces by powder metallurgy from a mixture of 94.5 per cent aluminum powder, 4 per cent copper powder, 0.5 per cent manganese powder and 1 per cent of a powder containing 50 per cent magnesium and 50 per cent aluminum is as follows: Compacting pressure, 50 tons per sq. in.; sintering atmosphere, dry nitrogen; sintering time, 30 min. at $580^{\circ}\text{C}.$ followed by a 15-min. cooling to $510^{\circ}\text{C}.$ and a quench in cold water. This drastic quenching procedure leaves the sintered material in a condition susceptible to age-hardening at room temperature. The increase in hardness of a compact prepared as described above is shown graphically in Fig. 7.

It will be recognized that the conventional heat-treatment for a forged alloy equivalent to the one described consists in holding the metal at a temperature not exceeding about $515^{\circ}\text{C}.$ for a length of

chemical analysis made by powder metallurgy respond differently to such solution-treating procedures. Upon the basis of the results obtained with cast materials, a logical sintering temperature for the powder mixture described would be in the neighborhood of 480° to $550^{\circ}\text{C}.$ but experiments were unproductive. In this temperature range, heat-treatment over extended periods of time does not bring about any substantial degree of strength, and, moreover, ductility is not developed. However, when the heat-treatment temperature is raised to 580° to $590^{\circ}\text{C}.$, there is a marked improvement in physical properties. For example, a compact made from the foregoing aluminum-copper-magnesium-manganese powder mixture pressed at 50 tons per sq. in., and sintered for 30 min. in nitrogen at a temperature of $580^{\circ}\text{C}.$ had initially a tensile strength of 33,000 lb. per sq. in.

and an elongation of 10 per cent. Following a room-temperature aging treatment for 4 days, the tensile strength and elongation of the material were, respectively, 50,000 lb. per sq. in. and 10 per cent.

In this connection, it will be interesting to note that when compacts were prepared under these same conditions from an aluminum-alloy powder containing copper-magnesium-manganese, exudations occurred over the entire surface of the specimens. Moreover, the pieces were brittle and porous. When compacts made from aluminum-alloy powder were sintered at relatively low temperatures, say 500°C., exudation did not occur but the pieces were weak, having a tensile strength of about 3000 lb. per sq. inch.

From the foregoing, it will be apparent that the sintering treatment of aluminum alloys made from powder mixtures requires further investigation.

Recently, experimental work has been done on a limited scale with a modified aluminum-alloy composition mixture containing 2.5 per cent copper, 0.5 per cent magnesium, balance aluminum. Various compacting pressures and sintering procedures were employed with encouraging results. Elongations of 20 per cent with tensile strengths on the order of 40,000 lb. per sq. in. were obtained with compacting pressures as low as 30 tons per sq. in., the sintering being conducted in nitrogen at a temperature of 610°C. for 30 min. This particular powder mixture holds considerable promise, because of its simplicity and particularly because of the low compressive force required.

CONCLUSIONS

Aluminum powders made by atomization may be employed to produce high-strength pieces by powder metallurgy, despite the presence of oxide films on the particles, provided that die surfaces are treated to eliminate jamming or cold-welding.

Cold-welding, which tends to be very serious in the powder metallurgy of aluminum, may be eliminated by coating the dies with a thin film of flat-lying, overlapping metal flakes.

In properly lubricated dies, elemental aluminum parts of high strength can be made satisfactorily. Under proper conditions, strengths at least as high as those encountered in equivalent cast and forged material may be obtained.

The work indicates that in the manufacture of aluminum alloys by powder metallurgy it is desirable to employ a mixture of the alloy ingredients rather than pre-alloyed powder. A number of aluminum alloys have been made by this procedure and the physical properties thereof compare favorably with those of equivalent cast and forged material, although it has not been possible as yet in all instances to equal the properties of cast and forged material.

Aluminum-alloy parts made by powder metallurgy from mixtures of powders of the elements are susceptible to age-hardening and precipitation-hardening treatment although these treatments in general may be different from those employed in the production of cast or forged material.

A technique has been developed for the manufacture of small aluminum and aluminum-alloy pieces of high strength and accurate configuration. Further advantages of the new technique reside in the economical use of material, low scrap loss, and relative low cost of operation.

DISCUSSION

(*W. A. Dean presiding*)

A. REIS,* New York, N. Y.—After paying tribute to this very interesting paper, I will limit my question to purely a scientific point of view. I would ask the authors if they can give figures as to the changes in porosity and in electrical conductivity with heat-treatment and compression during this treatment.

* Professor of Metallurgy, Cooper Union.

J. J. CORDIANO (author's reply).—In this investigation we did not collect data on the changes in electrical conductivity with changes in heat-treatment and compaction.

The effects of compaction on the porosity of the pressed piece is marked. At low pressures in the neighborhood of 20 to 25 tons per sq. in. porosity is usually of the order of 15 to 20 per cent. At high pressures (50 to 60 tons per sq. in.), the porosity is a fraction of 1 per cent.

There is a definite change in porosity with heat-treatment both for the compacts pressed at low pressures and at high pressures. There is a tendency for specimens compacted at low pressures to shrink and distort during the heat-treatment, thus decreasing the porosity. However, at high compacting pressures, there is a tendency for the specimens to expand and compacts with an initial porosity of less than 1 per cent would have a porosity of 3 to 5 per cent after heat-treating.

R. A. QUADT,* Barber, N. J.—Have you any idea what the yield strength is?

J. J. CORDIANO.—Yes, the yield strength of the aluminum alloys corresponding to 17ST varied between 32,000 and 35,000 lb. per sq. inch.

R. A. QUADT.—That is in a treated composition?

J. J. CORDIANO.—Yes, these values are for the specimens in the heat-treated condition.

R. STEINITZ,† Yonkers, N. Y.—Have you any idea of the oxide form of the powder during sintering in different atmospheres? Is it dissolved in aluminum, or what does it do?

J. J. CORDIANO.—Our idea on the subject is that the oxide surrounding the particles remains inert during the sintering operation. In order to promote sintering it would be necessary to dislodge this oxide film so that we may get clean metal to metal contact. We believe that the high compacting pressures do dislodge these films. The plastic deformation of the soft cores that occurs above 40 tons per

sq. in. compacting pressure is sufficient to disrupt the oxide films and cause clean inter-particle contact.

L. W. KEMPF,* Cleveland, Ohio.—The authors have confirmed in a positive manner that usable mechanical properties can be developed by powder-metallurgy procedures from mixtures consisting predominately of aluminum powder. I had hoped for some comments from individuals who are in the actual business of producing parts by such a process.

I have had an interest, although somewhat academic, in this field for some years, and have made some attempts to interest manufacturers in producing usable parts from aluminum powders. The tonnage of parts so manufactured in the United States today is practically nil in comparison with the quantities being produced from copper or even iron powders. There must be a very good reason for this situation, in view of the advantages that are inherent in the use of aluminum in this process. The reason is touched upon in the authors' paper.

Manufacture of parts by powder metallurgy today is based almost entirely on large-production runs of a specific part. The economics of the process are such that production must be rapid and must utilize automatic machines, or the process will not stand up against competition with die casting, or other types of fabrication. The difficulty in economical production of parts from aluminum powder lies in the tendency to weld or stick to the dies. The authors have overcome this by lubricating the die surfaces, which works entirely satisfactorily in the laboratory. There is, however, no production machine on the market today that provides for the lubrication of die surfaces in the manner described by the authors. I see no fundamental reason why such a machine could not be designed and made to operate efficiently. The fact remains that there is none.

I would just like to add that I wish the authors every success in promoting the use of such aluminum powders in powder metallurgy, even though it necessitates some changes in the fabricating procedures.

* Assistant Research Metallurgist, American Smelting and Refining Company.

† American Sintel Corporation.

* Aluminum Research Laboratories, Aluminum Company of America.

J. J. CORDIANO.—We are working with a concern in attempts to produce parts on production equipment using automatic die lubrication.

G. D. CREMER (author's reply).—With regard to die lubrication, the results of our laboratory work indicate that the properties of compacts so formed are improved to such an extent that some work should be done on devising automatic die lubrication. This is a problem for the machine designer and, knowing the ingenuity of our American engineers, we feel that it is just a matter of time before such lubrication will be used with automatic equipment.

R. P. SEELIG,* Long Island City, N. Y.—The company that I am connected with has successfully produced parts made from aluminum-base material by powder metallurgy. I want to emphasize that the technique used was somewhat different from the one described by the authors of the paper. I am merely mentioning this to prove that the manufacture of light metal parts by powder metallurgy is commercially feasible.

C. HARDY,† New York, N. Y.—Many pieces can be made and have been made from aluminum powders. Often statements have been made in connection with powder metallurgy that "It can't be done." At the present moment presses are being built that were unthought of years ago. Dies are being made that everyone said could not be made, and I believe that automatic die lubrication will follow the same course.

MEMBER.—What happens to the die lubricant?

J. J. CORDIANO.—Each successive layer wipes off.

MEMBER.—There is no build-up?

J. J. CORDIANO.—No.

MEMBER.—How many pieces have you run?

J. J. CORDIANO.—I would say that we have run about 4000 or 5000.

C. J. BIER,* West Orange, N. J.—It seems rather remarkable that the tensile strength obtained by sintering the briquettes in air, hydrogen, or nitrogen at 50 tons per sq. in. is practically the same. Work with copper alloys and many other powder alloys has shown that the sintering atmosphere is of extreme importance, especially when the powder is oxidized, as these aluminum alloys must have been, since the aluminum was atomized.

J. J. CORDIANO.—On that point it does seem remarkable at first glance that such conditions could be true, but as we have pointed out and stressed in the paper, we use elemental aluminum powders as a mixture with our alloying elements, and high compacting pressures. The elemental aluminum powder is very soft, and compacting this material under pressures of 50 tons per sq. in. results in a green density of 99 per cent or higher of corresponding wrought material of the same composition. Since the porosity is so low and the oxides of aluminum form protective coatings, there is not much chance for penetration of whatever atmospheres are used during the sintering or heat-treating process, with the result that the properties of the sintered pieces are the same, or closely so, for whatever atmospheres are used.

G. D. CREMER.—To supplement Mr. Cordiano's remarks, it has been shown that at lower compacting pressures air sintering causes an excessive drop in physical properties. These compacts pressed at lower pressures by being porous are not impervious to the sintering atmosphere and penetration of oxidizing atmospheres causes excessive internal oxidation, with resulting poor properties.

C. J. BIER.—It has been stated that the method of processing aluminum powder outlined here is entirely commercial. In view of the fact that a briquetting pressure of 30 tons per sq. in. is considered rather high in large-scale operations at the present time it would seem that since, even with the unusual methods of lubrication used by the authors, briquetting pressures of 50 tons per sq. in. were required, the techniques proposed here for processing powdered aluminum and its alloys may be

* Chief Engineer, Powder Metallurgy, Inc.

† Hardy Metallurgical Company.

* H. L. Crowley and Co., Inc.

reasonably questioned as to their being "entirely commercial."

J. J. CORDIANO.—Of course, we cannot make a blanket statement about a certain compacting pressure being commercial or not. Consideration must be given to the cost of the part being made. If a piece is relatively high priced, compacting pressures of 50 tons per sq. in. may prove commercial even though die wear is increased over the die wear for parts pressed at 30 tons per sq. in. In addition, die lubrication minimizes die wear to a much greater extent than does powder lubrication at the pressures we are discussing.

C. J. BIER.—The statement by the authors that it has been their experience that oxide films may be of value in controlling the grain size in the finished aluminum articles, is indeed unusual and one on which a clarification would be desirable.

The authors remark that particle size has but slight effect upon tensile strength of the sintered compacts. If this is so in aluminum powders, these powders are entirely different from any other type of metal powder. For it has been repeatedly demonstrated that the particle size of the powder in all other metal powders has a very large influence on the tensile strength of the sintered briquettes. In aluminum alloys the effect of particle size could be expected to be less noticeable because sintering is done in the solid solution plus liquid phase. It would be interesting to know the methods used in determining the tensile strength of the compacts. Were the tensile strengths obtained on bars as sintered, as sized, or were the bars machined after sintering and before pulling? Was the standard A.S.T.M. procedure used in pulling the tensiles? What was the method employed in obtaining the density of these briquettes?

It is indeed unfortunate that the photomicrographs given are at such a low magnification as to have little or no significance in the interpretation of the degree of sintering. One would like to see photomicrographs at about 500 diameters illustrating the sintering of aluminum as well as its alloys. Such things as oxide coatings, the disappearance of particle boundaries and the progress of the sintering processes cannot be satisfactorily observed at low magnifications. If the authors have examined the briquettes made of aluminum powders at higher magnifications, can it be said that the oxide coatings of the particles disappear or remain after "sintering"?

J. J. CORDIANO.—As indicated in our paper, we have found that the particle size of the powder has a minor influence on the tensile strength of the sintered briquettes.

The method we employed in determining the tensile strength of the compacts consisted of testing the bars in the as-sintered state without subsequent sizing or machining. The test section was rectangular in cross section and the gauge length was at least four times the square root of the cross-sectional area. Densities were determined on cylindrical briquettes as well as on sections of the test specimens. Densities were determined by measurement and checked by the water-immersion method.

Examination of photomicrographs of sintered specimens at 500 magnification reveals that the oxide coatings that had originally surrounded the particles remained after sintering and probably outlined the particle boundaries as they existed after compression. These oxide inclusions had no preferential arrangement with respect to the grain structure developed during sintering and were apparent within the grains as well as at the grain boundaries.

Rate of Precipitation of Silicon from the Solid Solution of Silicon in Aluminum

By LAWRENCE K. JETTER,* JUNIOR MEMBER, AND ROBERT F. MEHL,† MEMBER A.I.M.E.

(Cleveland Meeting, October 1942)

SOME advances have been made recently in the theory of the kinetics of precipitation from metallic solid solution despite the complexities of the problem, but there is surprisingly little quantitative information available on rates of precipitation with which to test present theory or upon which to build new theory.‡ Attempts to measure rates of precipitation have been beset with difficulties which originate both in the anomalies that attend the changes in the properties selected for measurement, as, for example, in electrical conductivity or mechanical properties, and also in the complexities in the structural changes in some systems, as in the aluminum-copper system.

If the functional relationship between the quantity of precipitate and the value of the selected property is uncertain, measurements of that property are obviously of uncertain utility in determining absolute rates of precipitation. If the precipitating system passes through one or

more transition stages, the interpretation of measured rates lacks definiteness; in such cases, it is necessary to measure the rate of reaction in each separate stage, if the rate measurements are to have any significance from the kinetic point of view.*

These difficulties cannot be wholly avoided, for at least in some measure they are characteristic of the process of precipitation from solid solution, but they can be minimized both by the selection of a simple system and by the use of a method of measurement relatively free from anomalous behavior. The present paper reports dilatometric measurements on the rate of precipitation of silicon from the aluminum-rich solid solution in the aluminum-silicon system—a study that approaches the desiderata of simplicity.

The aluminum-silicon system offers advantages from these points of view: there are no known anomalies in the property changes accompanying precipitation;^{2,3,4} there are no known transition stages; the precipitate is an element, not a compound, and both matrix and precipitate are cubic, and while the structures are not identical (the solid solution is face-centered cubic and the precipitate is diamond cubic), the system at least approaches the ideal case of a crystal precipitating from a matrix of the same crystal type—the ideal case which Becker⁵ assumed in treating the precipitation process theoretically. The dilatometric method, while not free from disturbing effects, as the subsequent dis-

This paper is taken from a thesis presented by L. K. Jetter to the Committee on Graduate Instruction of the Carnegie Institute of Technology in partial fulfillment of the degree of Doctor of Science, June 1939. Manuscript received at the office of the Institute Dec. 1, 1941; revised May 14, 1942. Issued in METALS TECHNOLOGY, September 1942.

* Research Laboratories, Aluminum Company of America, New Kensington, Pa. Formerly Aluminum Company of America Graduate Fellow, Department of Metallurgical Engineering, Carnegie Institute of Technology, Pittsburgh, Pa.

† Director, Metals Research Laboratory, and Head, Department of Metallurgical Engineering, Carnegie Institute of Technology, Pittsburgh, Pa.

‡ A review of recent advances in precipitation theory is given in reference 1. References are at the end of the paper.

* The anomalies in property change and the occurrence of transitional stages are discussed in reference 1.

cussion will show, is not so prone to give anomalous results as other methods; it is capable of a high degree of precision in measurement and gives results in terms of volume which can be converted into quantity of precipitation.

CHANGES IN SPECIFIC VOLUME DURING PRECIPITATION IN THE ALUMINUM-SILICON SYSTEM

The aluminum-silicon system is of the simple eutectiferous type, consisting of only the aluminum-rich and the silicon-rich solid phases. The solid solubility of silicon in the aluminum-rich phase is 1.65 per cent at the eutectic temperature ($577^{\circ}\text{C}.$) and decreases with decreasing temperature to 0.05 per cent at $200^{\circ}\text{C}.$ ⁶ The constituent that precipitates from the supersaturated aluminum-rich solid solution has been identified as elementary silicon.⁷

During isothermal precipitation in this type of system, changes in specific volume with time arise both from the increase in the quantity of precipitate and from the decrease in the solute concentration of the matrix solid solution. Since the atomic weight of silicon is greater than that of aluminum, and since the lattice parameter of the aluminum-rich solid solution increases with decrease in solute concentration,⁸ the specific volume of the matrix should increase with decrease in solute concentration. This has been confirmed by experiment.⁹ Furthermore, the specific volume of free silicon is greater than that of the aluminum-rich solid solution. Accordingly, since an increase in specific volume results both from an increase in the amount of precipitate and from a decrease in the solute concentration of the matrix, an over-all increase in specific volume should result upon precipitation.

In metallic systems, the specific volume relationships are generally quite simple: for solid solutions the specific volume is a linear function of the solute concentration in weight per cent; for mixtures of phases

the specific volume is equal to the sum of the specific volume of each phase times its amount in weight per cent. There is no evidence to suggest that these relationships do not hold in the aluminum-silicon system. Upon precipitation, therefore, if the solute concentration of the matrix were decreased instantaneously and uniformly to the proper value as each solute atom is transferred from the matrix phase to the precipitate phase, the specific volume during the reaction would be a linear function of the amount of the precipitate phase in weight per cent. This is shown schematically in Fig. 1. A limitation of the dilatometric method lies in the fact that the solute concentration may not decrease in this ideal manner, as we shall see later. This complexity of the precipitation process, however, affects not only the specific volume but all properties that are dependent, even in part, upon the solute concentration.

It has been suggested that a tendency toward lattice coherency between precipitate and matrix should contribute an anomalous volumetric effect.^{10,11} It is not an easy matter to determine the occurrence of lattice registry at the matrix-precipitate interface in this system, and any effect of this and the accompanying strain upon the measured changes in specific volume must remain somewhat conjectural. But such registry occurs usually when there is a possibility of good matching between the lattices of the two participating phases;¹ in the present case a careful comparison of the dimensions and atom spacings of the face-centered cubic aluminum-rich solid solution ($a_0 = 4.0413$ to $4.039\text{\AA}.$) and the diamond cubic silicon precipitate ($a_0 = 5.4173\text{\AA}.$) discloses no attractive possibility of atomic matching. This is in conformity with the fact that the system appears to be unable to develop a platelike Widmanstätten figure, for matching usually is accompanied by the formation of precipitate in plate form, the plane of the

plate being the plane along which good matching occurs.¹² Although this point admittedly is uncertain, it seems likely that any anomaly in the dilatometric

Chevenard, Portevin, and Waché,⁴ but neither have presented complete dilatation-time curves. The latter authors showed the rate of dilatation to be in remarkable agree-

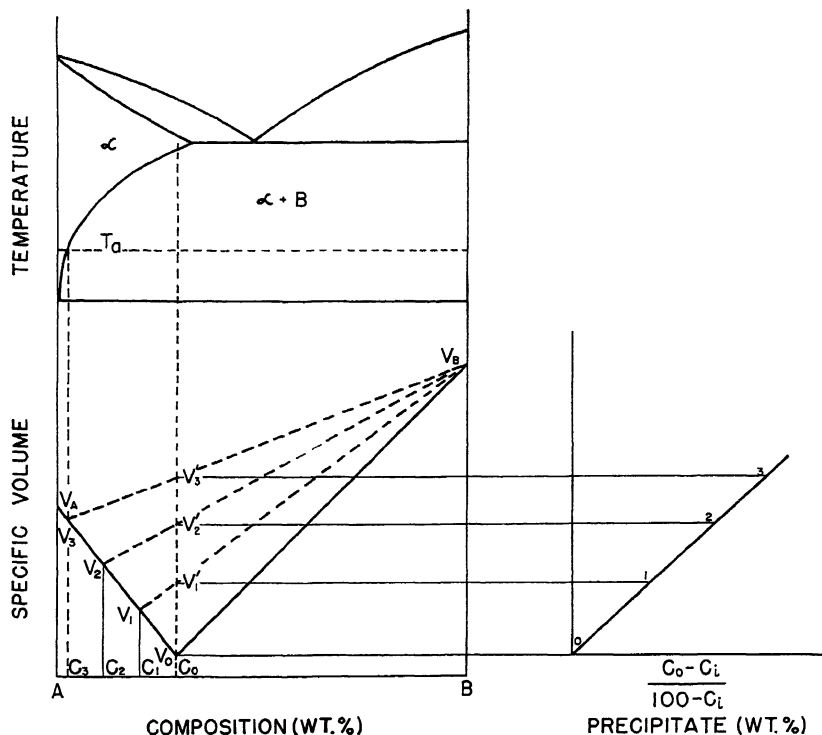


FIG. 1.—SCHEMATIC DIAGRAM SHOWING RELATIONSHIP BETWEEN SPECIFIC VOLUME AND QUANTITY OF PRECIPITATE IN AN ALLOY OF COMPOSITION C_o UPON AGING AT TEMPERATURE T_a AFTER QUENCHING FROM α REGION.

$i = 0, 1, 2, 3$, time of aging (0, as-quenched state; 3, complete reaction).

T_a , temperature of aging.

C_i , solute concentration of matrix phase.

$V_A V_i$, relationship between specific volume and composition (solute concentration) in matrix phase.

V_B , specific volume of precipitate phase.

$V_i V_B$, relationship between specific volume and composition for mixture of precipitate and matrix phases.

V_i' , specific volume of mixture of precipitate and matrix for alloy of composition C_o .

$V_i' - V_o$, change in specific volume.

$C_o - C_i$, decrease in solute concentration of matrix phase.

$\frac{C_o - C_i}{100 - C_i}$, quantity of precipitate phase (wt. per cent).

curve resulting from this type of strain must be minor in degree.

Dilatometric measurements during the aging of aluminum-silicon alloys have been reported by Kempf and Hopkins¹³ and by

ment with the rate of change of the coefficient of thermal expansion, a property that is supposed to follow the amount of precipitate very accurately in the aluminum-silicon system.¹⁴

DILATOMETRIC APPARATUS

The dilatometer employed is shown in Fig. 2. It is a differential dilatometer that employs an optical-mechanical means of amplification of differential changes in length between the test and a comparison specimen. Measurements are made with an autocollimator of the type employed in the Tuckerman optical strain gauge.¹⁵

The dilatometer consists essentially of a metal frame 8 in. long, 3 in. wide, and 8 in. high, embodying devices for the support of the specimens and of the optical system. The dilatometric specimens are channels of the following dimensions: length 6.5 in., flange 0.375 in., web 0.5 in., and thickness 0.125 in. They are held in the dilatometer in a horizontal position with their webs adjacent. Near the back they are held securely on a knife-edge and near the front they are supported by a roller. At the front a spring clamp holds them firmly against a tool-steel lozenge, which maintains a distance of 0.1 in. between them. This lozenge is a part of a device that is suspended from a projection of the frame and that supports a square-faced 45° - 45° - 90° optical glass prism so that its faces are vertical. This device is mounted on a jewel bearing and can rotate easily. Differential changes in length of the specimens impart rotation to the prism about a vertical axis by means of the lozenge. A second prism of identical type is supported on a screw through the frame. This prism is stationary with respect to changes in specimen length, but it can be rotated by means of a worm and gear for alignment of the optical system. The two prisms have a right-hand left-hand relationship and are separated by a distance of 0.5 inches.

These prisms, together with the autocollimator, compose the optical lever by means of which the length changes are amplified and measured. This optical lever is the autocollimated, double-mirror type in which the diagonal faces of the prisms serve as the mirrors. A scale at the focal

distance of the objective lens is illuminated by a lamp. The beam of light is projected upon the face of the stationary prism, internally reflected from its diagonal face upon

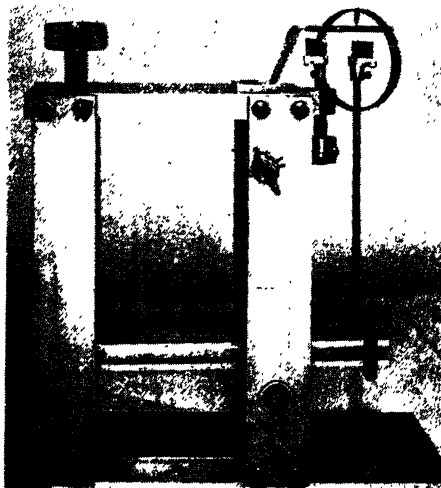


FIG. 2.—DIFFERENTIAL DILATOMETER, SIDE VIEW.

the face of the movable prism, and then internally reflected from its diagonal face back into the autocollimator upon a reticule, which also is at the focus of the objective lens. Any rotation of the movable prism results in a linear motion of the image of the illuminated scale along the reticule. The scale of the former is a vernier with respect to the latter, thus enabling very fine distinctions to be made. The quantity actually measured is the angle between the incident and the reflected light beam. It is a property of this optical lever that a reading taken in any direction in a plane perpendicular to the line of intersection of the two mirrors depends solely on the angle between the two mirrors. Deviation from the perpendicular introduces a cosine error, which is negligible for small deviations. For deviations large enough to cause considerable error, the image is thrown out of the field of view and readings cannot be made. As long as

the autocollimator is in such a position that a distinct image can be observed, the correct reading can be made. This is a great advantage over single-mirror optical levers, which require the position of the observing system to be fixed, for it enables the autocollimator to be moved and replaced without effect on the measurement. Thus one autocollimator can be used intermittently with several dilatometers.

The sensitivity of the optical system to changes in relative angular position of the prisms is 0.00001 radian. With a 5.1875-in. gauge length (distance between knife-edge and lozenge) and a 0.1-in. lozenge, this corresponds to an over-all value of 1.9×10^{-7} in. per in., a sensitivity comparable to that of an interferometer dilatometer.¹⁶

The thermostat in which the aging was carried out is a well insulated sheet-iron vessel containing a low-melting salt mixture as the heating medium. The bath is heated with an immersion heater and its temperature controlled by a mercury thermostat and appropriate relays. The temperature of the thermostat can be readily adjusted to the desired value and can be maintained constant to within 0.1°C. Thermal gradients are eliminated by agitation of the bath with a motor-driven stirrer. This temperature control is quite satisfactory for the most accurate dilatometric work.

MATERIAL AND PREPARATION OF THE ALLOYS

The aluminum used in the preparation of these alloys had a purity of 99.95+ per cent. High-purity electric-furnace silicon was used. The aluminum was melted in a plumbago crucible in an electric furnace, and the silicon added. The melt was thoroughly stirred with a graphite rod and fluxed with gaseous chlorine before casting. The metal was cast as 8-lb. ingots in a cold iron tilting mold. The ingots were heated 12 hr. at 490°C. and hot-rolled to 1.0-in. slab. The slab was annealed and

then cold-rolled to 0.375-in. plate. The plate was heat-treated at 570°C. for 1 week (168 hr.) in order to ensure complete solution and homogeneity of the silicon in the aluminum-rich solid solution, and was quenched in water at room temperature. The dilatometric specimens were machined from the as-quenched plate.

The composition of the alloys by chemical analysis is given in Table I. The total impurity varied from 0.007 to 0.014 per cent. The most serious impurity is the iron, varying from 0.004 to 0.010 per cent, which is capable of combining with silicon to form an insoluble aluminum-silicon-iron constituent.^{6,7} The amount of silicon removed from solid solution by these low percentages of iron, however, is probably small.

TABLE I.—*Composition of the Aluminum-silicon Alloys*

Alloy No.	Composition by Analysis, Weight Per Cent			
	Si	Fe	Cu	Al (by Difference)
4	0.41	0.004	0.003	99.583
6	0.58	0.006	0.008	99.406
8	0.80	0.006	0.003	99.191
10	0.94	0.006	0.006	99.048
13	1.23	0.010	0.003	98.757

An aluminum-magnesium alloy containing 1 per cent Mg was used for the comparison specimen. It was machined from 0.375-in. plate and carefully annealed in order to ensure dimensional stability. Tests showed definitely that no dilatometric effect could arise from the comparison specimen and interfere with the dilatometric curves. This alloy was used in preference to pure aluminum in order to minimize the effect of creep.

EXPERIMENTAL PROCEDURE AND RESULTS

Just prior to the aging experiment the aluminum-silicon test specimen was again heat-treated 2 hr. at 577°C. and quenched in water at the desired temperature. The

specimen was immersed vertically in order to minimize distortion. The dilatometer was then removed from the thermostat, the quenched test specimen was inserted

had reattained the desired aging temperature (3 to 4 min. later). Meanwhile the optical system was adjusted for proper measurement. Readings were taken every

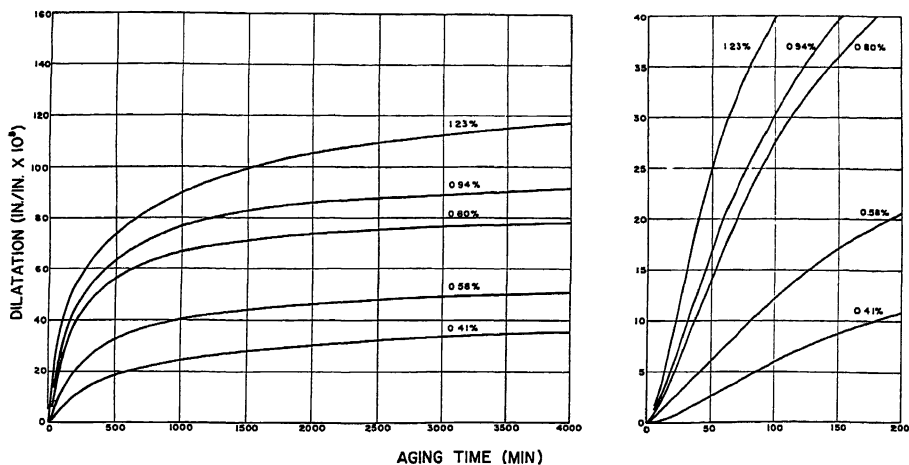


FIG. 3.—DILATATION-TIME CURVES FOR VARIOUS SOLUTE CONCENTRATIONS AT AN AGING TEMPERATURE OF 216.0°C. QUENCH, WATER AT 25°C.

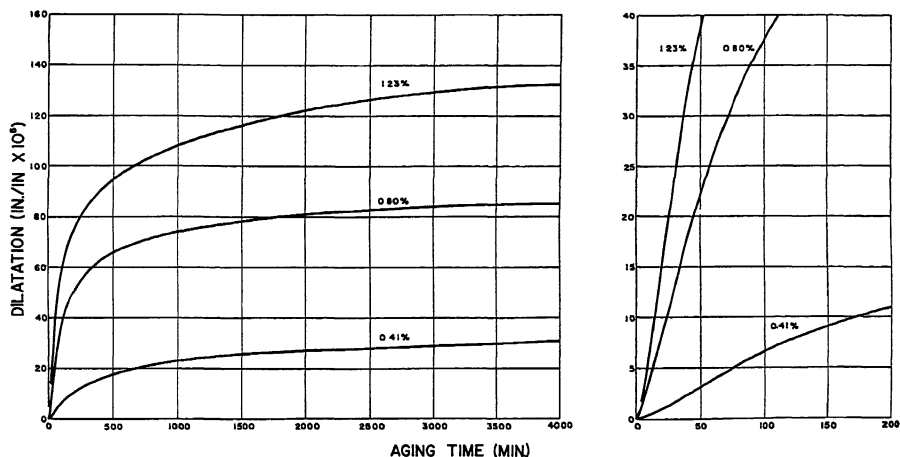


FIG. 4.—DILATATION-TIME CURVES FOR VARIOUS SOLUTE CONCENTRATIONS AT AN AGING TEMPERATURE OF 216.0°C. QUENCH, WATER AT 0°C.

and secured in the proper position, and the dilatometer was replaced. Zero time was considered to be the time when the dilatometric specimen had attained bath temperature ($\frac{1}{2}$ min. after the dilatometer was replaced), but the initial reading was not taken until the instant that the bath

minute for the first 20 min. and then at progressively longer time intervals until dilatation was complete, or nearly so. The dilatation that had occurred in the period 0 to 3 min. obviously was unknown, but graphical extrapolation served to approximate it.

The reproducibility of the dilatation-time curves is good. As an example: Curves for separate specimens of the 0.80 per cent Si alloy aged at 216°C. for 4000 min. showed a maximum difference of only 1×10^{-5} in. per in. in a total elongation of 80×10^{-5} in. per in.

Dilatation-time curves were obtained in the manner described for solute concentrations of 0.41, 0.58, 0.80, 0.94, and 1.23 weight per cent Si and for aging temperatures of 196.0, 206.0, 216.0, 226.0, and 236.0°C. on specimens re-heat-treated 2 hr. at 577°C. and quenched in water at 25°C. just prior to aging; a second set of dilatation-time curves were obtained for solute concentrations of 0.41, 0.80, and 1.23 weight per cent Si and for aging temperatures of 206.0, 216.0, 226.0°C. on specimens similarly re-heat-treated and quenched in water at 0°C. just prior to aging. These 34 curves form the basis for the subsequent discussion of rates; Figs. 3 and 4 are examples for quenches in water at 25°C. and at 0°C., respectively.*

DISCUSSION OF RESULTS

Reactions in systems in which a new phase arises from an unstable parent phase have been demonstrated to take place by the formation of nuclei and the growth of these nuclei.¹⁸ The rate of these reactions, therefore, must be determined by a rate of nucleation N and a rate of growth G . Considerable success has attended the analysis of the rate of formation of pearlite from austenite from this point of view.^{17,28}

Precipitation from supersaturated solid solution differs from eutectoid decomposition in the fact that much of the original phase is retained at the completion of the

reaction, though with diminished solute concentration, with the final amounts of the matrix and precipitate phases readily derived from the constitutional diagram by application of the lever-arm principle. This decrease in the solute concentration during the reaction complicates the analysis of the kinetics of the process in two ways: (1) true rates of precipitation are difficult to measure, for the property changes that arise from the change in solute concentration are superimposed upon those that arise from the formation of the precipitate phase; (2) N and G vary with time, for obviously they must vary with solute concentration—the time variation of solute concentration as it affects the values of N and G appears complex, and at the moment it appears impossible to make reasonable assumptions concerning it.

If the solute concentration were instantaneously and uniformly decreased as each solute atom is transferred from the matrix to the precipitate phase, it would be an easy task to analyze property changes (such as changes in specific volume) into true rates of precipitation; furthermore, under this same condition, since the time variation of solute concentration could be determined, and if N and G varied with solute concentration in a simple and predictable manner, the theoretical curve of reaction rate could be computed and applied to the analysis of the rate of reaction in a manner analogous to that for the formation of pearlite from austenite.

The precipitation process, however, is not this ideal. The formation of nuclei appears to involve no appreciable change in the solute concentration of the matrix.^{11,19} The growth of these nuclei, however, does result in a change in the solute concentration, but not uniformly throughout the matrix. The solute atoms at the nucleus-matrix interface attach themselves to the nucleus, thereby diminishing the solute concentration of the adjacent solid solution and creating a concentration gradient.

* The remainder of the curves (Figs. A to G) have been deposited with the American Documentation Institute. To obtain them, write to the American Documentation Institute, Bibliofilm Service, 1719 N St., NW., Washington, D. C., asking for Document No. 1643 and enclosing 30¢ for microfilm (images 1 in. high on standard 35-mm. motion-picture film) or 90¢ for photostat (6 by 8 in.).



FIG. 5.—MICROSTRUCTURE OF ALUMINUM + 1.23 PER CENT SILICON ALLOY AGED VARIOUS TIMES AT 216.0°C.

a. As-quenched. $\times 100$. *b.* Aged 10 minutes. $\times 100$. *c.* Aged 40 minutes. $\times 100$. *d.* Aged 145 minutes. $\times 100$. *e.* Aged 145 minutes. $\times 500$. *f.* Aged 810 minutes. $\times 100$.

Re-heat-treatment, 2 hours at 577°C. Quench, water at 25°C. Etch, 2 minutes in 0.5 per cent HF. Original magnifications given; reduced approximately $\frac{1}{2}$ in reproduction.

Other solute atoms in the matrix then diffuse into this region of low concentration, and growth continues. At first only the region in the vicinity of the growing particle is decreased in solute concentration, but as growth proceeds the concentration gradient becomes less steep and a greater extent of the matrix is affected, until the solute concentration attains a uniform value corresponding to the solubility limit. During nucleation, therefore, the solute concentration may be considered essentially unchanged at the initial value, but after growth has become appreciable and the solute concentration has been appreciably diminished, it appears impossible to assign a value to the solute concentration and therefore to note the values of N and G that it determines.

The microstructural changes that occur during the aging of aluminum-silicon alloys are shown in Fig. 5. These changes suggest that the rate of growth is very slow in these alloys and that the initial changes are almost entirely a result of nucleation. In the initial stages precipitation is evident only in the appearance of a brown or yellow stain on the surface after etching; individual precipitate particles are not resolved microscopically until the later stages and then only in restricted regions. Consideration of the extent of the stained regions compared to the volume of the precipitate phase that can exist also indicates that the precipitate is in an extremely high state of dispersion even after a relatively long aging time.

Thus, if it is assumed that nuclei generally form without appreciable change in the solute concentration of the matrix (which seems plausible), it follows that the rate of nucleation remains constant at a maximum value from the first instant through the initial period of reaction, ultimately decreasing when the solute concentration of the matrix decreases appreciably. It follows that the dilatation during the initial period is a result of nucleation only

and that the rate of dilatation is proportional to the rate of nucleation.

The dilatation-time curve, however, shows a very short initial period of increasing rate, then a period of constant maximum rate followed by a long period of continuously decreasing rate. If nucleation begins at maximum rate, and if the rate of dilatation is a measure of the rate of nucleation, it is difficult to account for this short initial period of increasing rate of dilatation; the effect, however, is minor and will be disregarded (Fig. 13).*

The microstructural changes also show that precipitation takes place at different rates in different grains and in different regions in the same grain. The regions of more rapid precipitation are presumably the regions that have suffered a greater degree of plastic deformation during quenching.^{10,20} Thus the rate of dilatation must be an average of the rates for the strained and unstrained regions. It is not easy to see how this difficulty can be avoided in studies of precipitation in systems that must be quenched rapidly for aging.

The effect of initial solute concentration upon the maximum rate of dilatation is shown in Figs. 6 and 7. At constant aging temperature the rate of dilatation increases with increase in solute concentration from zero at a value corresponding to the solubility limit at the aging temperature to probably a maximum at a value corresponding to the solubility limit at the heat-treating temperature. The increase is slow at first but becomes more rapid and then slow again. The effect of aging temperature upon the maximum rate of dilatation is shown in Figs. 8 and 9. At

* Tests have shown that the initial period of increasing rate of dilatation, though minor, is definite; it is not a result of lag in the dilatometer. It appears possible that this initial period may represent a period during which the specific volume increase caused by the plastic deformation during quenching is partially relieved; the dilatometer is sufficiently sensitive to detect such changes.

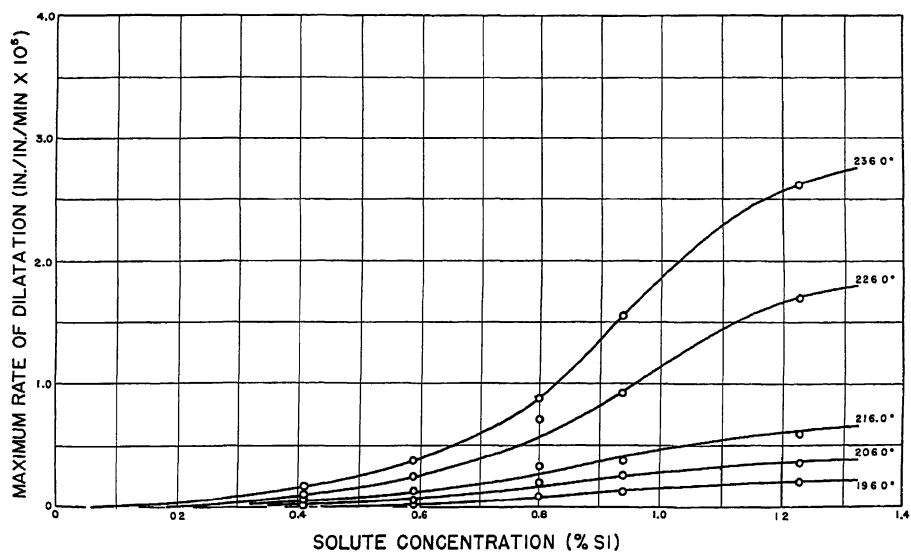


FIG. 6.—EFFECT OF SOLUTE CONCENTRATION ON MAXIMUM RATE OF DILATATION AT VARIOUS AGING TEMPERATURES. QUENCH, WATER AT 25°C.

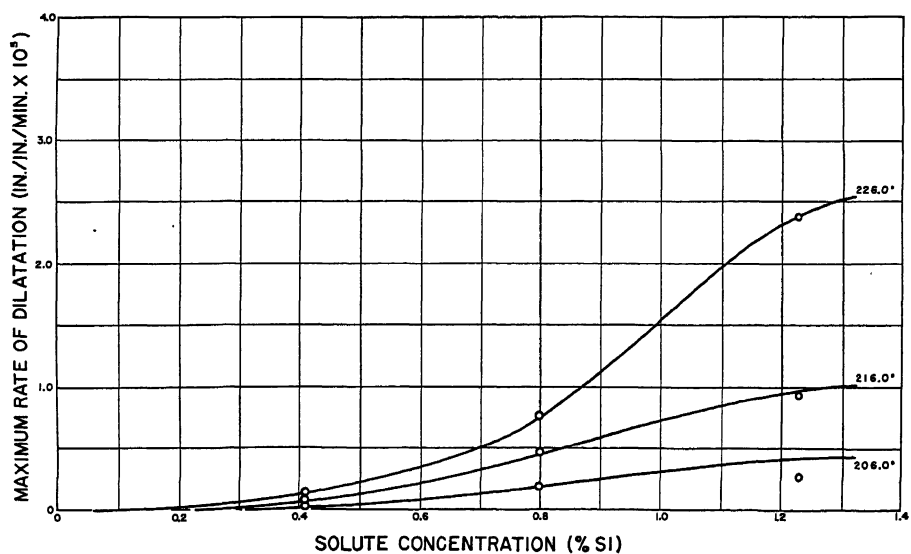


FIG. 7.—EFFECT OF SOLUTE CONCENTRATION ON MAXIMUM RATE OF DILATATION AT VARIOUS AGING TEMPERATURES. QUENCH, WATER AT 0°C.

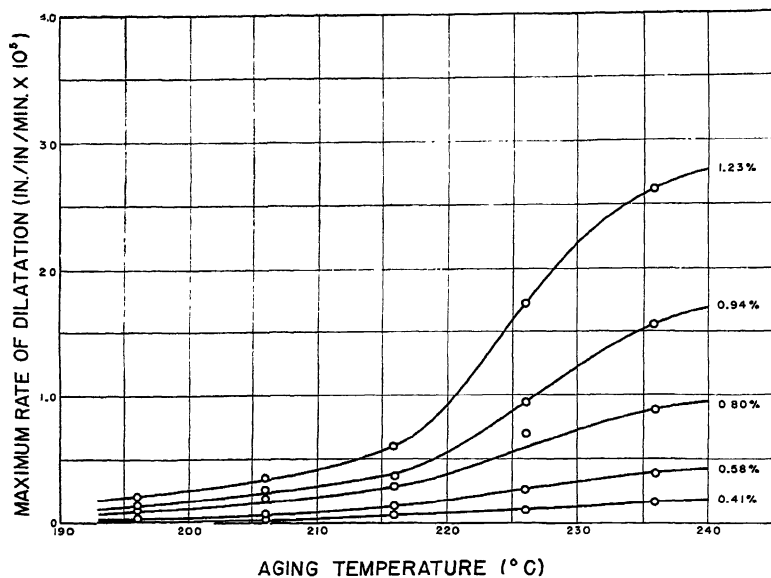


FIG. 8.—EFFECT OF AGING TEMPERATURE ON MAXIMUM RATE OF DILATATION FOR VARIOUS SOLUTE CONCENTRATIONS. QUENCH, WATER AT 25°C .

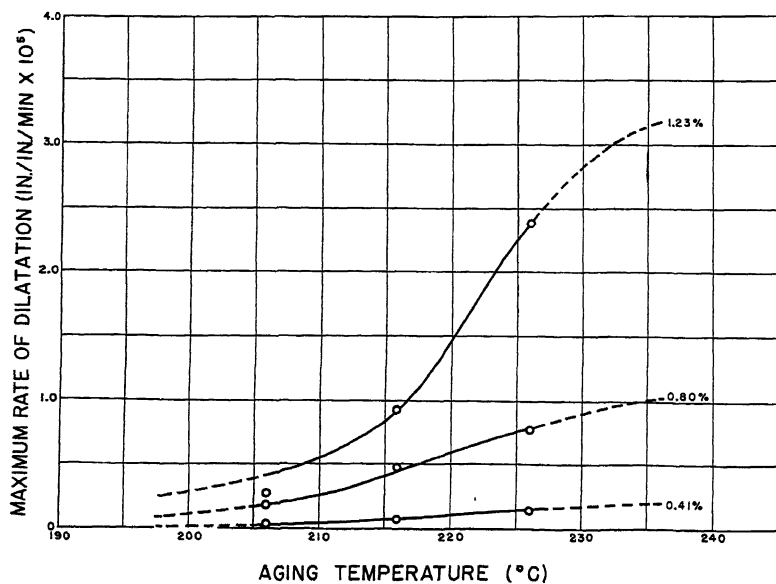


FIG. 9.—EFFECT OF AGING TEMPERATURE ON MAXIMUM RATE OF DILATATION FOR VARIOUS SOLUTE CONCENTRATIONS. QUENCH, WATER AT 0°C .

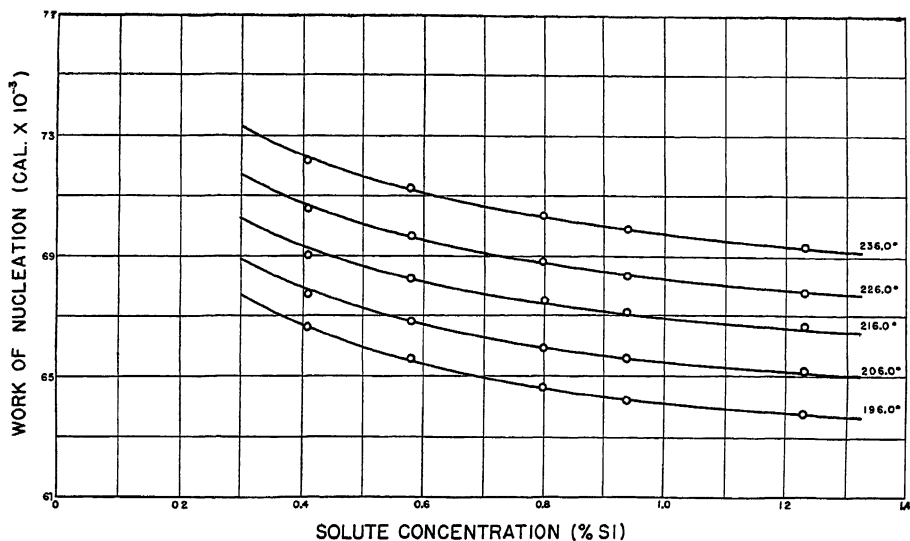


FIG. 10.—EFFECT OF SOLUTE CONCENTRATION ON WORK OF NUCLEATION AT VARIOUS AGING TEMPERATURES. QUENCH, WATER AT 25°C. POINTS DERIVED FROM CURVES IN FIG. 6.

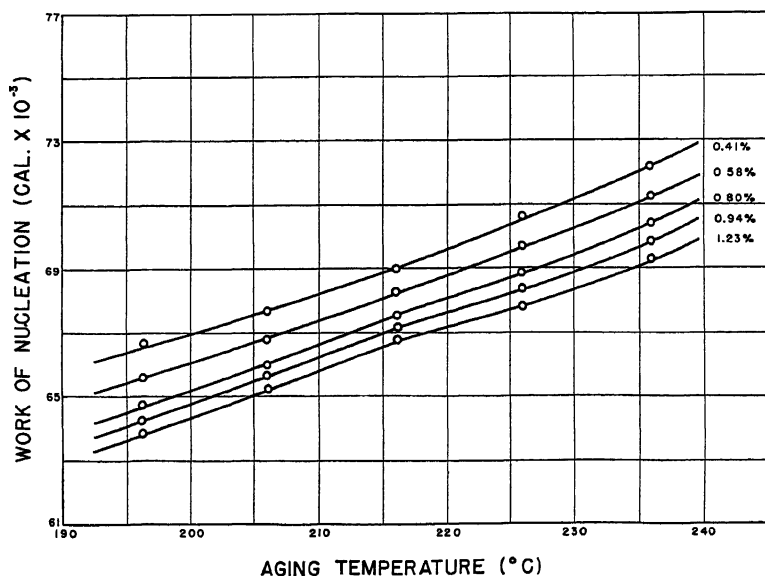


FIG. 11.—EFFECT OF AGING TEMPERATURE ON WORK OF NUCLEATION FOR VARIOUS SOLUTE CONCENTRATIONS. QUENCH, WATER AT 25°C. POINTS DERIVED FROM CURVES IN FIG. 8.

constant initial solute concentration the rate of dilatation increases with increase in aging temperature. The increase at first is slow but becomes more rapid and then

and old phases. Becker found by calculation of the energies involved that with any given aging temperature and solute concentration there is associated a critical

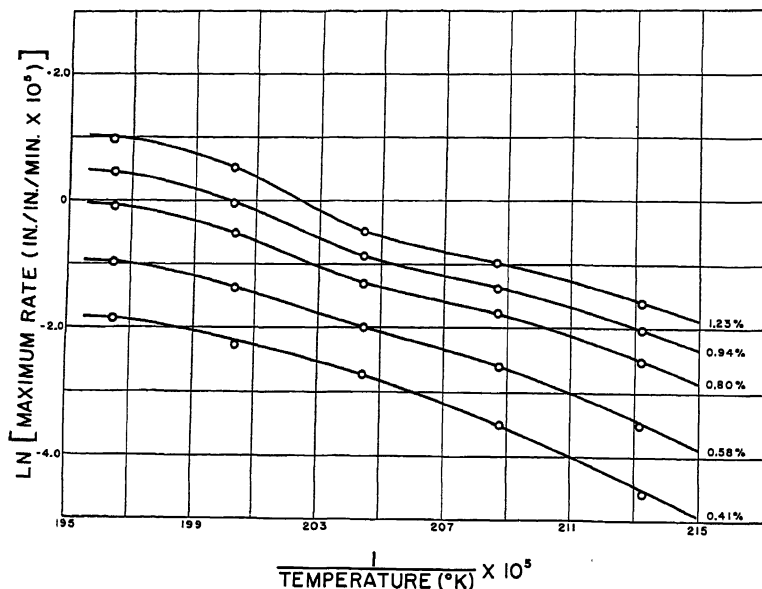


FIG. 12.—EFFECT OF AGING TEMPERATURE ON MAXIMUM RATE OF DILATATION FOR VARIOUS SOLUTE CONCENTRATIONS. $\ln N$ vs. $1/T$ PLOT. QUENCH, WATER AT 25°C. POINTS DERIVED FROM CURVES IN FIG. 8.

slow again. The shape of these curves suggests that a maximum occurs at some higher temperature, for obviously the rate must be zero at the equilibrium temperature.

The theory of nucleus formation in precipitation reactions has been reviewed recently.¹ The most comprehensive treatment has been that of Becker,⁵ who conceived nucleation as the formation of a region in the supersaturated solid solution of composition corresponding to that of the precipitate phase by chance encounters of atoms moving from point to point by diffusion. Whether a region so formed is stable with respect to the supersaturated solid solution—i.e., can proceed to grow—depends upon the energy required for the formation of the interface between the new

size above which the region becomes a stable nucleus. The critical nucleus size and the work of nucleation were found to increase with increasing temperature at constant solute concentration and to increase with decreasing solute concentration at constant temperature. Both quantities attain an infinite value at any point on the solvus curve.

For the initial rate of nucleation Becker proposed the equation

$$N = K \times e^{-\frac{Q}{RT}} \times e^{-\frac{A(T, C)}{RT}}$$

where Q is the activation heat for diffusion, A is the work of nucleation (which is a function of solute concentration and temperature), T is the absolute aging temperature, C is the solute concentration, and K

is a constant. The relationships between the initial rate of nucleation and solute concentration and aging temperature, as derived from this equation, are very similar to the relationships between the maximum rate of dilatation and these same two factors obtained experimentally. If the rate of dilatation may be taken as a measure of the rate of nucleation, the experimental results may be considered to be generally in agreement with the theory. The effect of variation of nucleus size is to make the experimental values of rate of nucleation too large at high temperatures and too low at high solute concentrations; it is believed that the correction to be made is small and would not change the general shape of the curves, since Becker has shown that the nucleus size varies markedly only at very low degrees of supersaturation.*

Exact values of A cannot be calculated from this equation because the value of K is unknown. The variation of A with solute concentration and aging temperature, however, may be obtained by assuming a value of K . The relationships obtained for a value of $Q = 31,500$ cal.²¹ and for a value of $\ln K = 100$ are shown in Figs. 10 and 11. It is obvious that these values of the work of nucleation cannot be real, for the value of K has been assumed, but the *slope* of the curves may well be approximately correct. These curves show that the work of nucleation increases with decreasing solute concentration but increases with increasing

temperature, in conformity with the relationships predicted by Becker.

Many previous investigators^{13,22-26} have reported the logarithm of the rate of precipitation, expressed in various ways, to be a linear function of the reciprocal of the

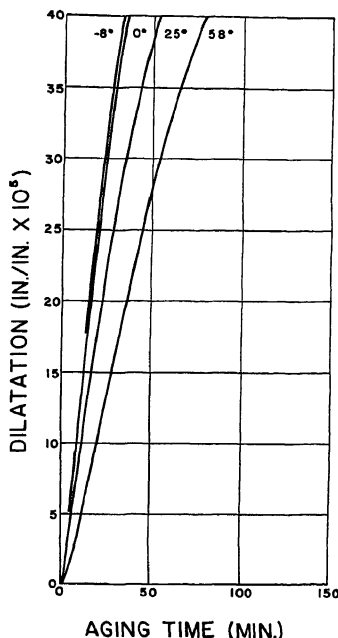


FIG. 13.—EFFECT OF RATE OF QUENCHING ON DILATATION-TIME CURVES.

Solute concentration, 0.94 per cent Si.

Re-heat-treatment, 2 hours at 577°C.

Quench, water or NaCl solution at temperatures indicated.

Aging temperature, 226.0°C.

absolute aging temperature and have attempted to express the variation in the rate of precipitation with temperature by the equation

$$V = K' \times e^{-\frac{Q'}{RT}}$$

where K' is a constant and $-\frac{Q'}{R}$ is the

slope of the $\ln V$ vs. $\frac{1}{T}$ curve. Attempts to relate Q' to the Q for diffusion showed that in all cases Q' was lower than Q .²⁷ No exactly linear relationship between $\ln V$

* The study of the kinetics of precipitation reactions of this sort is made difficult by the lack of a method to determine the rate of nucleation N ; N and G are inextricably associated, and at the moment N can only be inferred from argument. It is possible that the new work on Guinier-Preston zones^{1,29} may offer an opportunity to calculate N at least approximately. It is possible to determine the approximate sizes of these zones, which are in fact the initial precipitate particles; with this size and a dilatometric measure of the volume of the precipitate, N could be calculated but correction would have to be made for the volume anomalies originating in the strain resulting from registry at the matrix-nucleus interface.²⁹

and $\frac{1}{T}$ is predicted by the Becker equation, but it is approximated at low aging temperatures, in which case

$$Q' = Q + \left[A + \frac{1}{T} \frac{\partial I}{\partial \frac{1}{T}} \right]$$

Since A is very small and increases with increasing temperature, the quantity in the brackets is negative in sign, and therefore Q' should be less than Q . A plot of the logarithm of the maximum rate of dilatation against the reciprocal of the absolute aging temperature in the temperature range employed here does not show the linear relationship (Fig. 12).

The effect of increasing the rate of quenching upon the dilatation-time curve is shown in Fig. 13. The maximum rate of dilatation increases as the temperature of the quenching bath is lowered. The relationship between the rate of dilatation and solute concentration or aging temperature, however, is not altered—the curve is merely shifted to higher values (Figs. 6–9). Evidently an increase in the rate of quenching causes an increase in the extent of the regions suffering greater plastic deformation and exhibiting faster rate of nucleation, and thereby an over-all increase in the rate of dilatation.

SUMMARY

1. A differential dilatometer of the optical-mechanical type, with a sensitivity of 2×10^{-7} in. per in. well suited to studies of precipitation from solid solution, is described.

2. A graphical method of calculating the quantity of precipitate from the change in specific volume is presented.

3. Measurements are reported on the rate of dilatation for isothermal aging of binary aluminum-silicon alloys of five compositions up to 1.23 per cent Si at temperatures from 196° to 236°C. for two rates of quenching.

4. The rate of dilatation increases with increasing solute concentration and with increasing temperature. The rate of dilatation is increased with increase in the rate of quenching owing to the nucleating effect of quenching strain. These results are discussed in terms of the theory of nucleation.

ACKNOWLEDGMENTS

The authors are indebted to the Aluminum Company of America, whose grant of a fellowship made this study possible. The authors acknowledge the valuable suggestions of Dr. M. Gensamer for designing and constructing the dilatometer. An expression of gratitude is in order for those members of the staff of the Aluminum Research Laboratories who aided in the preparation and analysis of the alloys and who gave helpful advice and criticism of the work.

REFERENCES

1. R. F. Mehl and L. K. Jetter: The Mechanism of Precipitation from Solid Solution—The Theory of Age-Hardening. Age Hardening of Metals. Amer. Soc. Metals (1940).
2. W. Helling: Zur Frage der Aushärtung von Al-Si Legierungen. *Ztsch. Metallkunde* (Jan. 1937) 29(1), 25.
3. L. Guillet and M. Ballay: Influence of Thermal Treatment on the Electrical and Mechanical Resistance of Al-Si Alloys Containing up to 2.5 Per Cent Si. *Rev. Mët.* (1930) 27, 398–403.
4. P. A. Chevenard, A. M. Portevin and X. F. Waché: A Dilatometric Study of Some Univariant Two-phase Reactions. *Jnl. Inst. Metals* (1929) 42(2), 337–373.
5. R. Becker: Die Keimbildung bei der Ausscheidung in metallischen Mischkristallen. *Ann. Phys.* (1938) [5] 32(5), 128.
6. E. H. Dix, Jr. and A. C. Heath, Jr.: Equilibrium Relations in Al-Si and Al-Fe-Si Alloys of High Purity. *Trans. A.I.M.E.* (1928) 78, 164–194. *Proc. Inst. Met. Div.*
7. W. L. Fink and K. R. Van Horn: Constituents of Al-Fe-Si Alloys. *Trans. A.I.M.E.* (1931) 93, 383.
8. M. L. V. Gayler and G. D. Preston: The Age Hardening of Some Al Alloys. *Jnl. Inst. Metals* (1929) 41, 191.
9. J. D. Edwards: The Properties of Pure Al. *Trans. Amer. Electrochem. Soc.* (1925) 47, 287.
10. W. L. Fink and D. W. Smith: Age-hardening of Al Alloys, I—Al-Cu Alloy. *Trans. A.I.M.E.* (1936) 122, 284–293.
11. W. L. Fink and D. W. Smith: Age-hardening of Al Alloys, IV—Discussion of the

- Theory. *Trans. A.I.M.E.* (1940) **137**, 95-107.
12. R. F. Mehl and others: Studies upon the Widmanstätten Structure. *Trans. A.I.M.E.*, (1931) **93**, 78-110, and following volumes.
 13. L. Kempf and H. L. Hopkins: Density Changes in Solid Al Alloys. *Trans. A.I.M.E.* (1936) **122**, 266-281.
 14. A. Portevin and P. Chevenard: Étude dilatométrique des transformations et des traitements thermiques des alliages légers d'aluminium. *Rev. Mét.* (1930) **27**, 412.
 15. The Tuckerman Optical Strain Gauge. Amer. Instrument Co., Silver Spring, Md.
 16. C. S. Taylor, L. A. Willey, D. W. Smith and J. D. Edwards: The Properties of High Purity Al. *Metals and Alloys* (1938) **9**, 189.
 17. W. A. Johnson and R. F. Mehl: Reaction Kinetics in Processes of Nucleation and Growth. *Trans. A.I.M.E.* (1939) **135**, 416.
 18. R. F. Mehl: The Physics of Hardenability. The Mechanism and the Rate of the Decomposition of Austenite. Hardenability of Alloy Steels. Amer. Soc. Metals (1939).
 19. W. L. Fink, D. W. Smith and L. A. Willey: Precipitation-hardening of High-purity Binary and Ternary Al-Cu Alloys. Age Hardening of Metals. Amer. Soc. Metals (1940).
 20. W. L. Fink and D. W. Smith: Age-hardening of Al Alloys, III—Double Aging Peaks. *Trans. A.I.M.E.* (1938) **128**, 223-233.
 21. R. F. Mehl, F. N. Rhines and K. A. von den Steinen: Diffusion in Alpha Solid Solutions of Al. *Metals and Alloys* (Jan. 1941) **13**, 41-44.
 22. M. Cohen: Age-hardening of Duralumin. *Trans. A.I.M.E.* (1939) **133**, 95-106.
 23. A. Hone: *Rev. trimestr. can.* (1933) **19**, 396; (1934) **20**, 376.
 24. M. Cohen: Aging Phenomena in a Ag-rich Cu Alloy. *Trans. A.I.M.E.* (1937) **124**, 138-156.
 25. C. H. M. Jenkins and E. H. Bucknall: The Inter-relation of Age-hardening and Creep Performance, I—The Age-hardening of Ni-Si-Cu Alloys. With an appendix by E. H. Bucknall and C. H. M. Jenkins: The Relationship of Time, Temperature, and Concentration as Factors in Age-hardening. *Jnl. Inst. Metals* (1935) **57**(2), 141-171.
 26. P. Chevenard and A. Portevin: Emploi des méthodes physicothermiques pour l'étude des alliages légers. London Congress Int. Assn. Test. Mat. (April 1937).
 27. R. F. Mehl: Diffusion in Solid Metals. *Trans. A.I.M.E.* (1936) **122**, 11-56.
 28. R. F. Mehl: The Structure and the Rate of Formation of Pearlite. Sixteenth Campbell Memorial Lecture. *Trans. Amer. Soc. Metals* (1941) **29**, 813.
 29. C. S. Barrett, A. H. Geisler and R. F. Mehl: Mechanism of Precipitation from the Solid Solution of Silver in Aluminum. *Trans. A.I.M.E.* (1941) **143**, 134.

DISCUSSION

(Dana W. Smith presiding)

H. Y. HUNSICKER,* Cleveland, Ohio.—The authors have referred to possible effects of internal residual stresses from quenching, and I would like to ask whether the reference specimen was quenched in exactly the same manner and at the same time as the test specimen, and, if so, whether or not the effect of the strain would be balanced out by the reference specimen?

L. K. JETTER (author's reply).—The comparison, or reference, specimen was not quenched at any time. Since, by necessity, the reference specimen and the test specimen were different alloys, the residual internal stresses developed by quenching might be expected to be of different magnitude even if the two specimens were quenched in the same manner, as has been shown by the work of Kempf, Hopkins, and Ivanso.²¹ The dimensional changes resulting from the partial relief of internal stresses in the two specimens, therefore, would not be expected to be identical.

* Aluminum Research Laboratories, Aluminum Company of America.

²¹ L. W. Kempf, H. L. Hopkins and E. V. Ivanso: Internal Stresses in Quenched Aluminum and Some Aluminum Alloys. *Trans. A.I.M.E.* (1934) **111**, 158-180.

Aging in the Solid Solution of Silver in Aluminum

By A. H. GEISLER,* JUNIOR MEMBER, C. S. BARRETT† AND R. F. MEHL,‡, MEMBERS A.I.M.E.

(New York Meeting, February 1943)

THE mechanism by which the super-saturated solid solution of 20 per cent silver in aluminum decomposes has been reported in two previous publications.^{1,2} The analysis of streaks in Laue photograms showed that thin platelike particles (the so-called Guinier-Preston aggregates) form upon {111} matrix planes in the early state of decomposition.¹ The size of these particles is larger, the higher the temperature at which they form in accordance with nucleation theory;³ at all temperatures they increase in size with aging.² When they have grown thick enough to afford three-dimensional diffraction, powder X-ray photograms show that the structure is not that of the equilibrium precipitate γ but that of a transition lattice γ' . Since this is also platelike in shape and also lies upon the {111} matrix planes with the [110] direction in the matrix parallel to the [11.0] direction in γ' , it seems likely that the original platelet particles are merely γ' in an early stage

of formation, and thus finely dispersed. The atomic spacing and pattern on the (00.1) plane in γ' are identical with those on the (111) matrix plane to which it lies parallel, and since comparable directions in the two planes are parallel, the lattices are thus coherent at the interface; an analogous coherence has been found in aluminum-copper alloys.³ The structures γ' and γ are both close-packed hexagonal and are oriented alike; they differ only in interatomic distances. Consequently, γ' is regarded as γ strained from its ordinary dimensions by the lattice coherency between it and the matrix.² The lattice movements that transform the matrix to the equilibrium precipitate appear to be very simple.²

The mechanism of precipitation in this system is simpler and is more precisely known than that in any other system,^{2,4} hence the system should be a profitable one for the difficult task of correlating property changes with structural alterations.

The present report provides additional studies on powder X-ray diffraction from alloys of 10 per cent, 20 per cent and 30 per cent Ag, and presents the correlation of crystallographic changes with changes in microstructure, Brinell hardness and electrical resistivity of the three alloys.

PREPARATION OF SAMPLES AND EXPERIMENTAL PROCEDURE

The preparation of the 20.2 per cent Ag alloy has been described.² Alloys containing 9.9 and 29.7 per cent Ag were prepared from 99.97 per cent Al and 99.99+ per cent Ag using a similar procedure. Rolled

This paper represents part of a thesis submitted by A. H. Geisler to the Graduate Committee of the Carnegie Institute of Technology, Pittsburgh, Pa., in partial fulfillment of the requirements for the degree of Doctor of Science, April 1942. Manuscript received at the office of the Institute Nov. 28, 1942. Issued in METALS TECHNOLOGY, February 1943.

* Research Metallurgist, Aluminum Research Laboratories, Aluminum Company of America, New Kensington, Pa. Formerly Aluminum Company of America Graduate Fellow, Department of Metallurgical Engineering, Carnegie Institute of Technology, Pittsburgh, Pa.

† Staff Member, Metals Research Laboratory, and Associate Professor, Department of Metallurgical Engineering, Carnegie Institute of Technology, Pittsburgh, Pa.

‡ Director, Metals Research Laboratory, and Head, Department of Metallurgical Engineering, Carnegie Institute of Technology, Pittsburgh, Pa.

¹ References are at the end of the paper.

plate $\frac{1}{4}$ in. thick was used for hardness determinations while 0.028-in. wire was prepared for powder X-ray diffraction studies and electrical resistivity determinations. Microscopic examinations were made principally on the $\frac{1}{2}$ -in. long wires, which were aged without interruption for various times at 158°, 225°, 265° or 303°C.—the same wires for which powder photograms had been made. The microstructure of the hardness specimens was also studied after the runs had been completed.

The solution heat-treatment consisted in heating the as-drawn wire samples (sealed in glass) and the as-rolled hardness specimens for 1 to 5 hr. at 500° to 550°C. followed by quenching in an ice-water mixture. Upon quenching, the glass tubes into which the wire specimens had been sealed broke, thus affording an efficient quench. The aging treatments were conducted in a small salt bath controlled to $\pm 0.5^\circ\text{C}$. The hardness and electrical resistance specimens were aged in direct contact with the liquid salt while the samples for the X-ray studies were enclosed in glass (except for the very short aging times at high temperatures when the samples were in direct contact with the salt). The aging of the hardness specimens was interrupted at intervals in order to make hardness readings while electrical resistance measurements were made with the samples at temperature without interrupting the aging.

Hardness measurements were made using the Brinell tester with a 10-mm. ball and a 500-kg. load applied for 30 sec. Three indents were made for each aging time while four measurements of each indent were taken. The average of these 12 measurements was used to determine the hardness number. The electrical resistance was determined by the use of a Kelvin double bridge. Values of resistivity on 2-in. lengths of wire were determined in as short a time as 30 seconds.

ADDITIONAL X-RAY DIFFRACTION RESULTS

The significance of radial streaks in Laue photograms extending out from the center in the direction of the $\{111\}$ poles that are normal to the X-ray beam is mentioned elsewhere.¹ These streaks correspond to rods in the reciprocal lattice from (000) toward $\{111\}$ reciprocal lattice points, and immediately demonstrate that there are platelets parallel to $\{111\}$. These streaks occur only in the early stages of precipitation when the reciprocal lattice rods are large in diameter and diffuse because of small lateral platelet dimensions. The central rays are formed only when the X-ray beam is directed approximately parallel to the surface of a set of platelets (i.e., when the reciprocal lattice rods are tangent to the reflection sphere). In aluminum-silver alloys this occurs when $\{111\}$ plane normals are approximately perpendicular to the beam, thus on photograms made with the beam along $[110]$ but not those with the beam along $[100]$. The central areas of two of these photograms are reproduced in Fig. 1. In Fig. 1a the four streaks 55° from the vertical are very diffuse and extend into the center of the photogram past the angle corresponding to the minimum wavelength reflection for any of the matrix planes. Further aging results in lateral growth of the platelets, so that the streaks become sharper and the four central rays are now merely short spurs that extend slightly beyond the edge of the shadow of the lead button as shown in Fig. 1b.

When the X-ray beam is perpendicular to a set of platelets and parallel to one of the reciprocal lattice rods, a darkened ring is found about the central spot in the early stages of precipitation as shown in Fig. 1c. This likewise is caused by the diffuseness of the lattice rod resulting from the small lateral dimension of the platelets and disappears when aging is continued and larger platelets are formed.

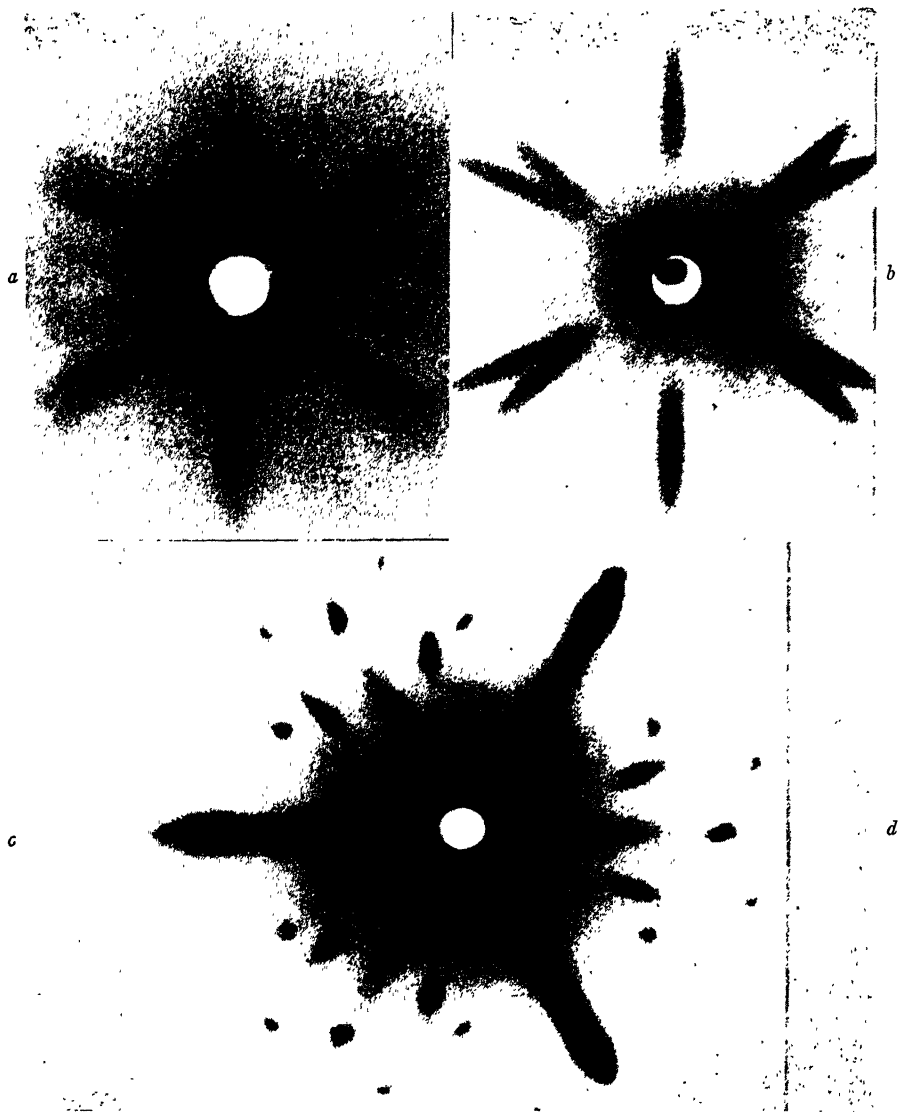


FIG. 1.—LAUE PHOTOGRAPHS FOR AN ALUMINUM + 20 PER CENT SILVER ALLOY.
a, aged 150 days at 30°C., [110] parallel to beam, 10-cm. film to specimen distance.
b, aged 104 hours at 150°C., [110] parallel to beam, 10-cm. film to specimen distance.
c, aged 81 days at 30°C., [111] parallel to beam, 5-cm. film to specimen distance.

The direction of the central rays thus identifies the plane on which plates form and confirms the previous conclusion² based on more elaborate reciprocal lattice constructions that platelets form in alu-

minum-silver alloys upon {111} planes of the matrix solid solution. The presence of central rays in the $\langle 100 \rangle$ in published photograms for aluminum-copper alloys^{1,5,22} proves that in this system the

platelets form parallel to {100}. This again is in agreement with the stereographic projection and the reciprocal lattice results. Finally, the application of this principle is made in the study of the reaction in

265°, and 303°C.), either in the as-quenched or quenched and cold-worked temper, the precipitate has the γ' structure when it has grown sufficiently in size and quantity to yield a powder pattern. The γ' precipi-

TABLE 1.—*Correlation of Microscopic and Powder X-ray Diffraction Data for Aluminum-silver Alloys*

Alteration	Time for Occurrence of Various Alterations, ^a Min.		
	10 Per Cent Ag	20 Per Cent Ag	30 Per Cent Ag
Aging temperature, 158°C.			
Grain-boundary precipitate appears.....		660-1,500	
General precipitate appears.....		3,180-3,900	
γ' pattern appears.....	8,160-9,600	3,180-3,900	1,560-2,400
Grain-boundary transformation starts.....		>14,760	
γ pattern appears.....	>15,000	>14,760	>9,600
γ and γ' patterns equal in intensity.....			
γ' pattern disappears completely.....			
Aging temperature, 225°C.			
Grain-boundary precipitate appears.....		0-10	
General precipitate appears.....		30-60	
γ' pattern appears.....	120-180	30-60	15-30
Grain-boundary transformation starts.....		9,600-14,760	
γ pattern appears.....	>43,200	36,000-57,600	14,400-21,600
γ and γ' patterns equal in intensity.....		>57,600	57,600
γ' pattern disappears completely.....			>57,600
Aging temperature, 265°C.			
Grain-boundary precipitate appears.....		0-3	
General precipitate appears.....		3-6	
γ' pattern appears.....	15-20	6-10	2-4
Grain-boundary transformation starts.....		>420	
γ pattern appears.....	>480	>420	>420
γ and γ' patterns equal in intensity.....			
γ' pattern disappears completely.....			
Aging temperature, 303°C.			
Grain-boundary precipitate appears.....	0-1	0-1½	0-½
General precipitate appears.....	1-3	1½-2	½-1
γ' pattern appears.....	2-3	1-1½	½-1
Grain-boundary transformation starts.....	100-360	100-150	10-30
γ pattern appears.....	1,500-2,760	660-1,500	230-360
γ and γ' patterns equal in intensity.....	>4,200	>5,340	2,760
γ' pattern disappears completely.....			>4,200

^a Second value represents aging time of sample in series first showing designated alteration while first value represents aging time of preceding sample of series.

aluminum-magnesium alloys,³⁴ where it is found that platelet formation occurs on 15 planes; because of the complicated nature of this reaction neither the stereographic projection nor the complete reciprocal lattice can be constructed.

The additional powder X-ray diffraction studies, the results of which are shown in Tables 1 and 2, show that in all alloys (10, 20, and 30 per cent Ag), at all the investigated temperatures (158°, 225°, 265°, and 303°C.), either in the as-quenched or quenched and cold-worked temper, the precipitate has the γ' structure when it has grown sufficiently in size and quantity to yield a powder pattern. The γ' precipi-

tate increases in amount to a maximum with aging time and then decreases to zero as γ forms at its expense. The information given in Table 1 was obtained principally for correlating crystallographic changes with microstructural, hardness and electrical resistivity changes.

The results shown in Table 2 for the aging of wire cold-drawn after the solution heat-treatment are of considerable interest. While cold-work greatly accelerates the

precipitation process, with the γ' structure appearing in $\frac{1}{3}$ to $\frac{1}{4}$ the time required for an as-quenched alloy, the amount of deformation—probably above some small critical amount—seems to have no effect, as shown by the data for reductions of 33 and 73 per cent upon aging at 155°C. It is interesting to note that when the pattern for γ' appears in photograms for worked alloys, the high-angle $K\alpha$ doublets for γ' like those from the distorted matrix are not resolved (Table 2). The large-angle lines of both patterns remain blurred until the $\gamma' \rightarrow \gamma$ transformation is well underway. At this time the diffuse γ' lines are replaced by sharp γ lines while the matrix doublets become sharp and spotty. In addition, a galaxy of small, sharp spots replaces the deformation texture diffraction in the small-angle white radiation part of the photogram that corresponds to a pinhole pattern. The latter observations for diffraction from the matrix show that the cold-worked matrix recrystallizes during the formation of γ while the presence of diffuse γ' and matrix lines might be interpreted as evidence for very strong coherency between γ' and the matrix*—that is, lattice-parameter variations in the matrix resulting from microscopic cold-work stresses may be responsible for lattice-parameter variations of γ' because of the coherency between the two.

MICROSTRUCTURE

The microstructures of all three alloys aged at 303°C. and of the 20 per cent alloy aged at the four temperatures were

* Line diffuseness might also be due to small particle size resulting from the high rate of nucleation in the cold-worked sample; however, it would be expected that the particle size of γ also would be small, since it is also nucleated at grain boundaries and along slip planes. This is not true, since the γ -line doublets are resolved from the beginning. Microscopic examination showed that the size of the γ' particles in the cold-worked and aged samples was no smaller than that in some of the as-quenched and aged samples that produced patterns with resolved γ' doublets.

examined after powder patterns had been obtained for all samples (some 150). A summary of the observations is incorporated in Table 1. The results show that

TABLE 2.—*Structural Changes Occurring in a Cold-worked 20 Per Cent Silver Alloy as Determined by the Powder X-ray Diffraction Method*

Cold Reduction by Drawing.....	Time for Occurrence of Various Alterations, Min.	
	33 Per Cent	73 Per Cent
Aging temperature, 155°C.		
γ' pattern appears...	780-1440	720-1440
γ pattern appears...	43,200-72,000	36,800-69,120
γ and γ' patterns equal in intensity..	> 72,000	95,040
Aging temperature, 221°C.		
γ' pattern appears ^a ..		15-30
γ pattern appears ^b		60-180
Recrystallization of matrix starts.....		60-180
γ and γ' patterns equal in intensity..		300
γ' pattern disappears completely.....		600-1140
Recrystallization of matrix complete...		600-1140
Last observation.....		7,200

^a Large-angle $K\alpha$ doublets for matrix and γ' blurred.

^b Large-angle $K\alpha$ doublets for γ resolved but those of matrix and γ' blurred.

a fine grain-boundary precipitate appears first, followed by general precipitation throughout the grains. The X-ray pattern for γ' is not observed until the general precipitate is present. The individual precipitate particles cannot be resolved microscopically at this early stage. Only after longer aging periods at high temperatures are the particles of the general precipitate large enough to be resolved and the Widmanstätten figure recognized, though the latter can be observed at the grain boundaries at an earlier time.

The most interesting result of the microscopic examination is the discovery of a unique reaction that nucleates at the grain boundaries of the matrix grains in which γ' has densely precipitated. The reaction is

shown in Fig. 2 for a 30 per cent alloy aged at 303°C. The first evidence is the appearance of thin, light zones at the grain boundaries of the overetched matrix grains in which the precipitation of γ' is well advanced, as shown in Fig. 2a. As the time of aging is increased, these areas of grain-boundary transformation increase in number and size, as shown in Figs. 2b to 2f. Photomicrographs at high magnifications are shown in Figs. 3 and 4, which show that these light grain-boundary areas are two-phase regions consisting of large precipitate plates in a light matrix of depleted solid solution.

The sequence of the patterns appearing in X-ray powder photograms (Table 1) shows that the grain-boundary process is directly related to the formation of the equilibrium precipitate γ . In all cases studied the pattern for γ is observed only after the reaction has progressed approximately as far as is shown in Fig. 2c. On first examination, it would seem that a considerable amount of reaction has occurred before it has been detected by the X-ray photogram; however, the second phase constitutes only a small amount of the total volume in these transformed grain-boundary areas and the amount prior to that shown in Fig. 2c is probably comparable to that of the grain-boundary precipitate which forms on first aging of the quenched alloy and which escapes detection by X-ray diffraction methods. Consequently, the conclusion can be drawn that the coarse precipitate plates in the transformed areas are γ and the discontinuous grain-boundary reaction represents the mode of transformation of $\gamma' + (\text{depleted}) \text{ matrix}$ to $\gamma + \text{depleted matrix}$.*

* The precipitate shown in Fig. 5 of reference 2 is γ' . Although the patterns of γ' and γ are visible in the powder photogram for this sample, this particular area does not show any regions of the grain-boundary transformation.

The discontinuous reaction, in which decomposition occurs at an interface advancing

Observations similar to those obtained with the small annealed wires are also found for large hardness-determination specimens and for cold-worked wires. In both of these, precipitation of γ' along the slip planes is observed in the early stages similar to that in aluminum-copper alloys that have been deformed in quenching.^{7,8} The formation of γ in the large specimens, however, occurs in the same manner as that in annealed wires, as shown in Fig. 3. The extent of transformation in these greatly overaged samples agrees well with data for small wires. On the other hand, the grain-boundary type of transformation in cold-worked wires is nucleated at slip planes as well as at the grain boundaries, so that white parallel bands of $\gamma + \text{matrix}$ appear in addition to white grain-boundary zones.

The transformation of γ' to γ is a discontinuous reaction³ similar to the apparent aging reaction in Mg-Al,⁹ Cu-Be,^{10,11} Ni-Be,¹² Cu-Ag^{13,14,30} and Ag-Cu^{13,24,25,31} alloys. From the photomicrographs, particularly Figs. 3c and 4a, it is evident that the reaction is a nucleation and growth process in which the transformed areas are nucleated at points on the original grain boundaries similar to the subcritical transformation of austenite to pearlite.¹⁵ The nodules form at points on the grain boundaries and generally grow into just one of the two grains adjacent to the boundary. The γ precipitate plates usually form in just one direction in each nodule, and the shape of the nodule probably is determined by a faster rate of edgewise growth than of growth normal to the plates, as shown in Figs. 3 and 4. Under certain conditions, plates grow from one boundary across the entire grain and stop at the opposite boundary (Fig. 4b). No more than four directions of γ plates are observed

from the grain boundaries toward the center of the grains, follows after continuous and general precipitation³ and indeed this may prove always to be true.³²

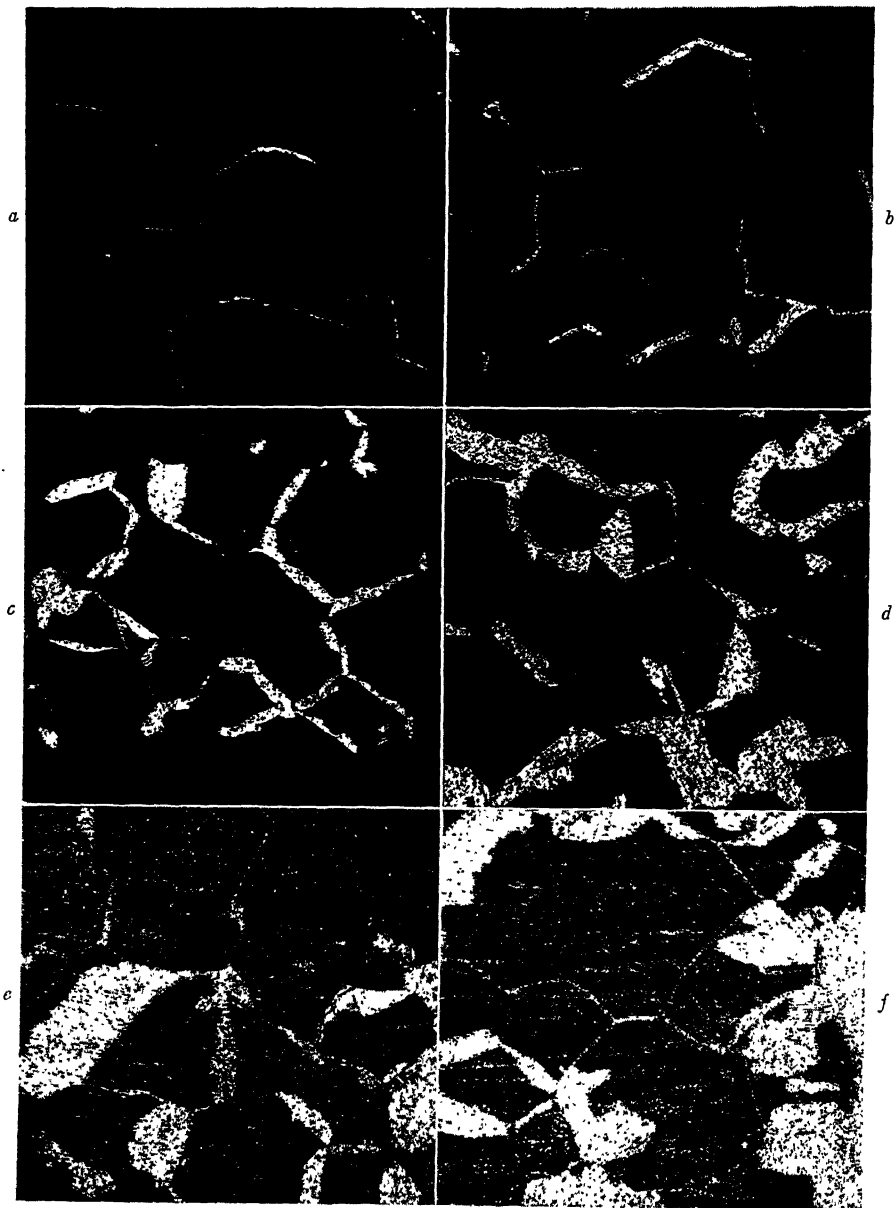


FIG. 2.—MICROSTRUCTURE OF ALUMINUM + 30 PER CENT SILVER ALLOY WIRES AGED VARIOUS TIMES AT 303°C. AND SHOWING GRAIN-BOUNDARY TRANSFORMATION OF γ' TO γ . $\times 100$. ETCHED IN 25 PER CENT HNO_3 .

a, aged 30 minutes.

c, aged 6 hours.

e, aged 25 hours.

b, aged 100 minutes.

d, aged 11 hours.

f, aged 46 hours.

γ pattern first observed in photograph for sample *c*.

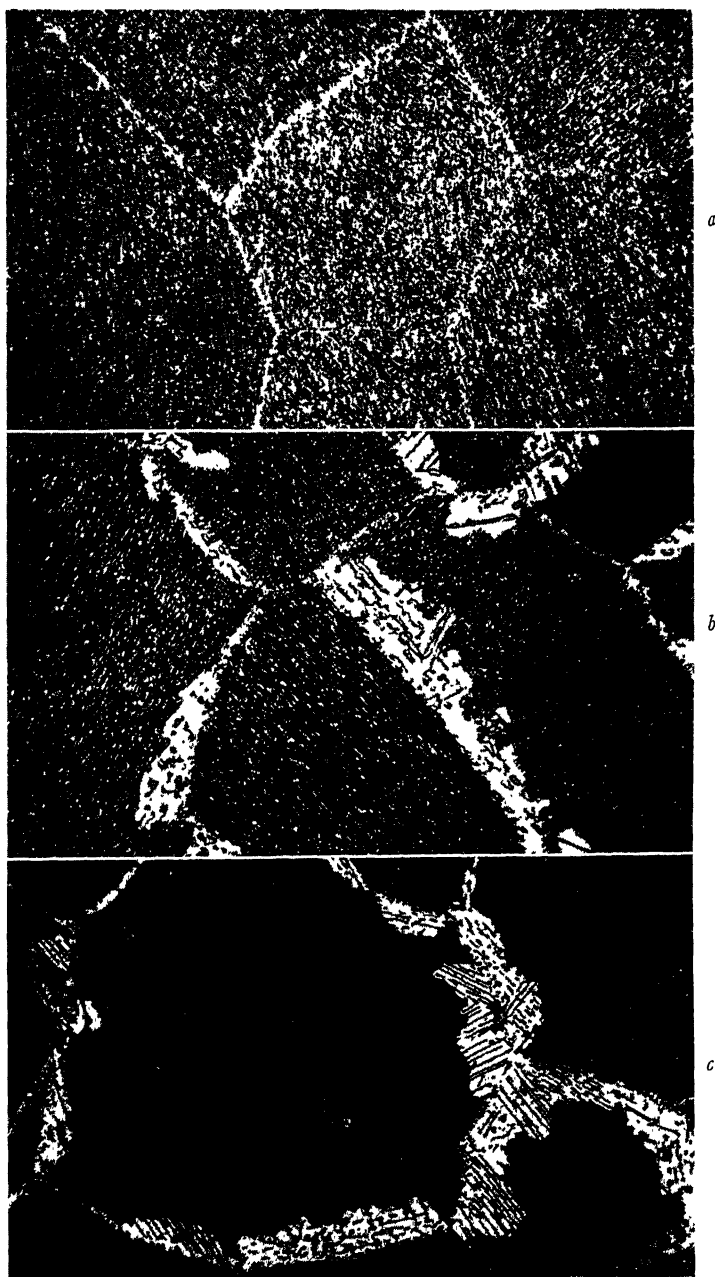


FIG. 3.—MICROSTRUCTURE OF HARDNESS DETERMINATION SPECIMENS AGED 521 HOURS AT 225°C.
× 500. ETCHED IN 25 PER CENT HNO_3 .

a, Al + 10 per cent Ag. *b*, Al + 20 per cent Ag. *c*, Al + 30 per cent Ag.

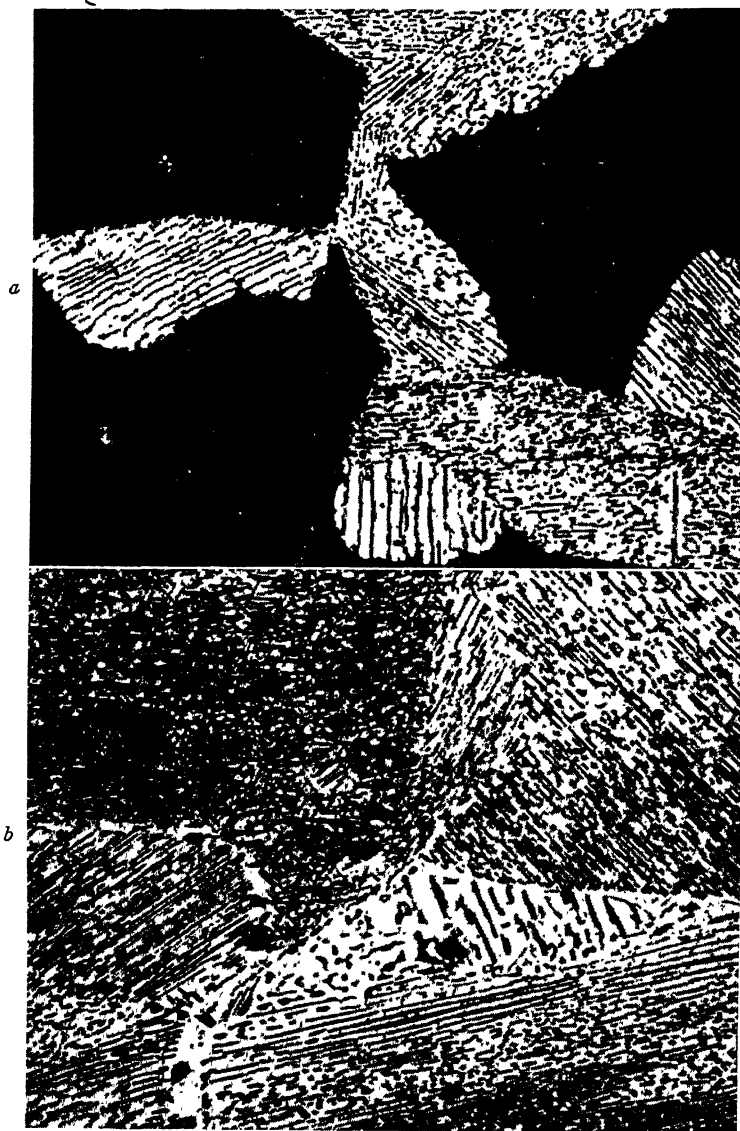


FIG. 4.—MICROSTRUCTURE OF ALUMINUM + 20 PER CENT SILVER ALLOY WIRES AGED AT 303°C. $\times 1000$. ETCHED IN 25 PER CENT HNO_3 .
a, aged 6 hours; *b*, aged 70 hours.

among a number of nodules growing into the same grain. Finally, and most important, it is found that in general the γ plates in any of the nodules growing into a given grain are not parallel to the

γ' plates within that grain.* Since the γ' -matrix and γ -matrix orientation relations are the same, this point suggests

* In Fig. 4*b* the plates in the one nodule growing into the upper left grain are definitely

that the reaction is accompanied by reorientation of the matrix grains by a process similar to recrystallization,^{13,23,32} which accompanies the formation of γ from γ' in cold-worked samples. The fact that a maximum of four plate directions exists in all nodules growing into the same grain suggests that a definite relation between the orientations of old and new matrix grains exists as in silver-copper alloys.¹³

HARDNESS

Precipitation from supersaturated aluminum-silver alloys in the early stages is accompanied by an increase in hardness and strength as in other age-hardenable alloys. The precipitation-hardening of 10, 20, and 30 per cent Ag aged at 158° and 225°C. is quite apparent from the curves shown in Fig. 5. On aging at 225°C., the hardness increases rapidly reaching a maximum in from 2 to 10 hr., depending on the silver content. After reaching this peak the hardness decreases rapidly at first and then more slowly. At 158°C. the hardness increases rapidly at first and then increases more slowly. Since the hardness specimens were found microscopically to exhibit precipitation upon slip planes resulting from deformation during quenching, two aging peaks probably should occur.⁸ Consequently, in the absence of experimental data, a primary peak has been sketched between the initial rapidly rising part and the final more slowly rising part of the curves for the 20 and 30 per cent Ag alloys at 158°C. and possible locations of primary peaks have been indicated in the curves for aging at 218° or 225°C. (Fig. 7). These data are in general consistent with earlier age-hardening data on aluminum-silver alloys;^{6,16-19} however, discrepancies may arise from differences in purity of aluminum used.⁶

not parallel to any of the four directions of γ' plates. Other photomicrographs show that when four or more nodules exist none of the directions of γ and γ plates coincide.

The correlation of hardness changes with microstructure and with X-ray diffraction data for small wires suggests that the hardening of these alloys is directly associated with the precipitation of the transition lattice γ' in a very small particle size. Evidence of precipitation is observed throughout the hardening stage, contrary to the observations of Kosaki¹⁹ and Guillet,⁶ who failed to observe precipitation until after the maximum hardness had been reached. Fig. 6 shows the change in hardness in the early stage for the three alloys aged at 225°C. As indicated by the arrow, the pattern of γ' is observed in the powder diffraction photograms before the maximum hardness is attained. Evidently, the hardening is related to the formation of platelets and the growth of these through a size large enough to give three-dimensional diffraction to a size providing maximum hardness. A similar relation exists for the hardening of the alloys at 158°C.

An initial decrease in hardness of considerable magnitude in some cases is observed frequently for 20 and 30 per cent Ag samples as shown in Fig. 7 (see also reference 16). The mechanical and thermal treatments of all these samples had been the same, so that the different behaviors may be attributed only to slight and accidental variations in the quenching practice. The softening is probably the result of re-solution of nuclei formed during quenching or retained from the solution heat-treating temperature by quenching, of a size too small to be stable at the aging temperature.³ The overaging of larger particles formed in this manner prior to general precipitation may also contribute to the softening and may be the cause of the lowered ultimate maximum hardness.

ELECTRICAL RESISTANCE

According to an earlier investigation,²⁰ the electrical resistivity of 5 to 38 per cent Ag alloys decreases in a uniform and normal

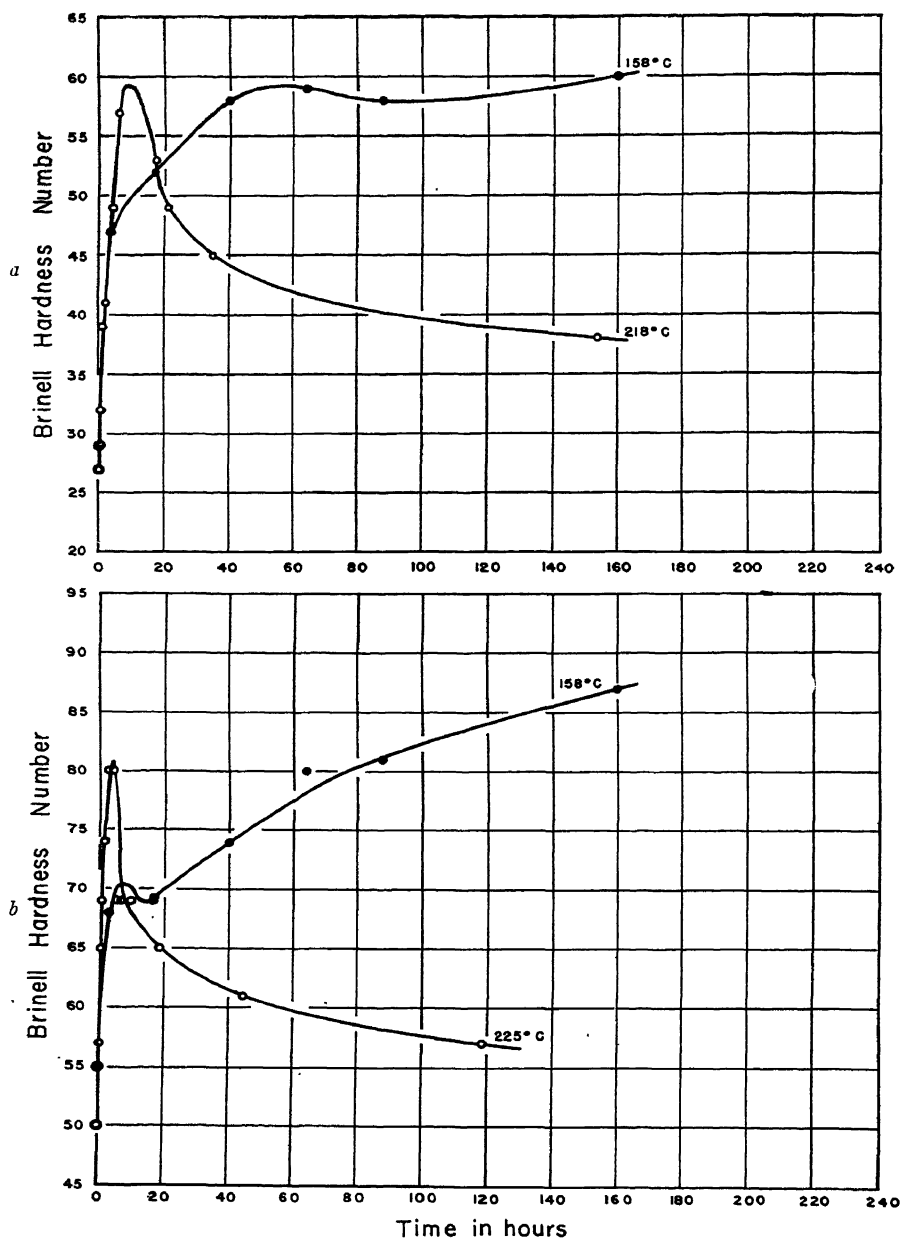


FIG. 5.—CHANGE IN HARDNESS OF ALUMINUM-SILVER ALLOYS AGED AT 158° AND 225°C.

a, Al + 10 per cent Ag.

b, Al + 20 per cent Ag.

c, Al + 30 per cent Ag.

(Fig. 5 continued on next page.)

manner during precipitation on aging at temperatures between 220° and 331°C .; however, the present research shows that the decrease is not uniform, particularly

On aging at 229°C . (Fig. 8b) a similar course of resistance change occurs except that the maxima are less prominent or appear merely as deflection points. Here again

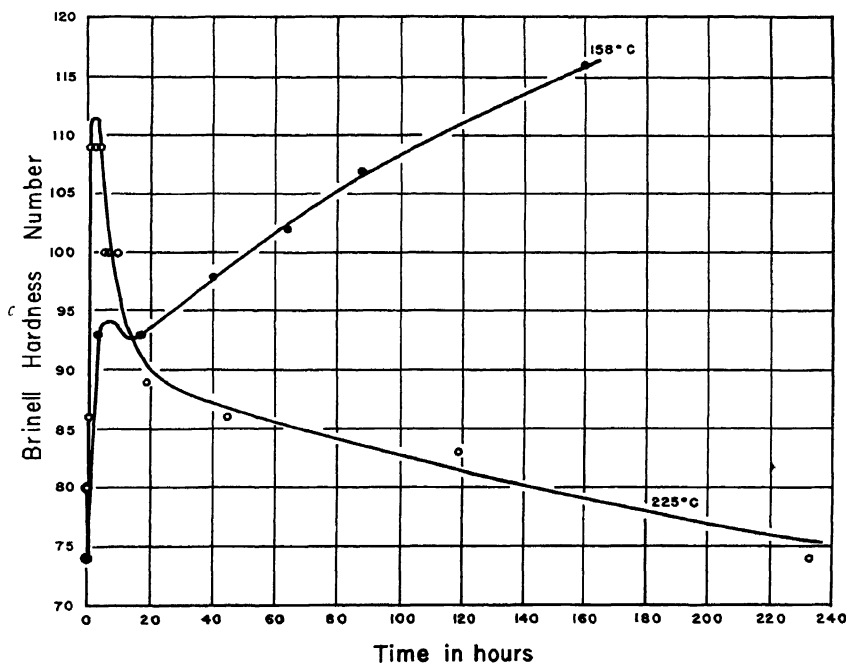


FIG. 5.—(Continued)

at the lower aging temperatures, as shown in Fig. 8. The electrical resistance of the three alloys at all temperatures decreases immediately from the first measurement ($\frac{1}{2}$ to 2 min. after placing sample in aging bath), indicating that the depletion of the matrix in silver begins at once. On aging at 158°C . (Fig. 8a) this initial decrease, which continues for a considerable length of time, dependent on the silver content, is followed by a rise of the resistance to an intermediate maximum. At the time period at which the maxima on the resistivity curves occur the pattern of γ' first appears in powder diffraction photograms made for samples of the same wire fabricated, heat-treated, quenched and aged simultaneously with the resistance measurement samples.

the γ' pattern is observed at the same time at which the maxima or deflections appear. The resistance then falls at a rate greater than the initial rate and finally (with the 20 and 30 per cent Ag alloys) the rate of decrease becomes slower. On aging at 265°C ., a maximum is found only in the curve for the 20 per cent alloy. At 265° and 303°C . (Figs. 8c and 8d), the pattern of γ' is first observed in powder photograms for samples aged for periods shortly after the beginning of the rapidly falling part of the curves.

The correlation of X-ray diffraction and microscopic observations with the resistance curves suggests that the maximum or first change in slope is directly related to the growth of the platelets to a size large

enough to afford three-dimensional diffraction and to the first appearance of the general precipitate in the microstructure.

The structural alteration at the grain

these two curves, for besides the several hardening and the later softening processes that occur in the as-quenched and aged alloy there are additional processes operat-

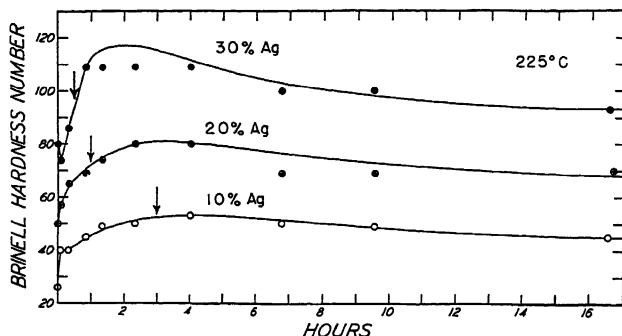


FIG. 6.—AGE-HARDENING OF ALUMINUM-SILVER ALLOYS AT 225°C. CORRELATED WITH X-RAY DIFFRACTION DATA.

Arrows indicate aging times for specimens that first exhibited the pattern for γ' in the powder photograms.

boundaries accompanying the formation of γ is not clearly evident in the resistance curves; only two of the runs were continued until after γ appears. There is no change of slope in the second gradually decreasing part of the curve for the 10 per cent Ag alloy aged at 303°C. before or after the time at which the pattern for the stable phase appears in the diffraction photogram. However, with the 30 per cent Ag alloy (Fig. 8d) a definite deflection occurs at a time between that for the first appearance of the grain-boundary reaction in the microstructure and that for the first appearance of the γ pattern in the powder photogram. Consequently, it is possible that the formation of γ from γ' is accompanied by a further decrease in resistance during aging superimposed upon the final gradual decrease resulting from depletion of the matrix in silver.

It will be observed in Fig. 9 that the maximum present on the curve for the sample that had not been cold-worked is absent in the curve for the cold-worked sample. A similar consequence is shown in curves for deformed and undeformed duralumin.³³ It is not easy to correlate

ing in the cold-worked alloy; e.g., softening from recovery of cold-worked strains. Moreover, the effect of deformation by cold-work is to accelerate the aging process as shown; and since deformation in an aggregate of grains gives a very heterogeneous distribution of strains, the rate of aging varies greatly from point to point in the deformed alloy.⁸ This heterogeneity in the rate of aging is probably responsible for the loss of the maximum, spreading the resistance increase shown in the maximum over a wide extent of the curve for the cold-worked sample, so that only alterations in slope occur but no maximum.

DISCUSSION OF RESULTS

The observation of the grain-boundary transformation in these alloys is new. It is quite possible that the sequence of structural changes observed in this system—matrix \rightarrow coherent transition lattice forming a Widmanstätten figure plus matrix of unaltered orientation \rightarrow non-coherent coalesced equilibrium lattice plus recrystallized or reoriented matrix³⁴ lattice—is general, occurring in many if not in all systems. On this view, discontinuous

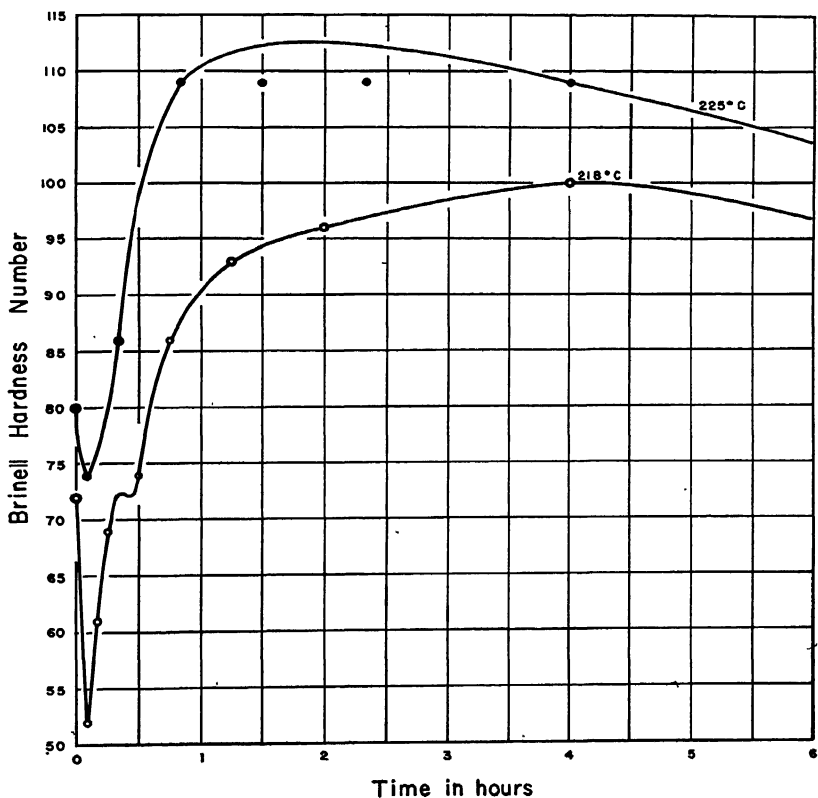
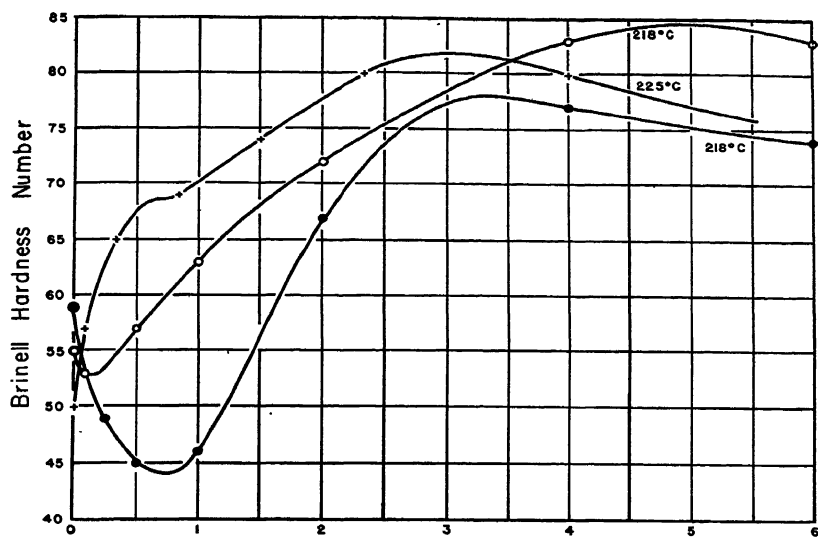


FIG. 7.—HARDNESS CURVES FOR ALUMINUM-SILVER ALLOYS SHOWING INITIAL DECREASE IN HARDNESS BEFORE AGE-HARDENING.
a, Al + 20 per cent Ag; *b*, Al + 30 per cent Ag.

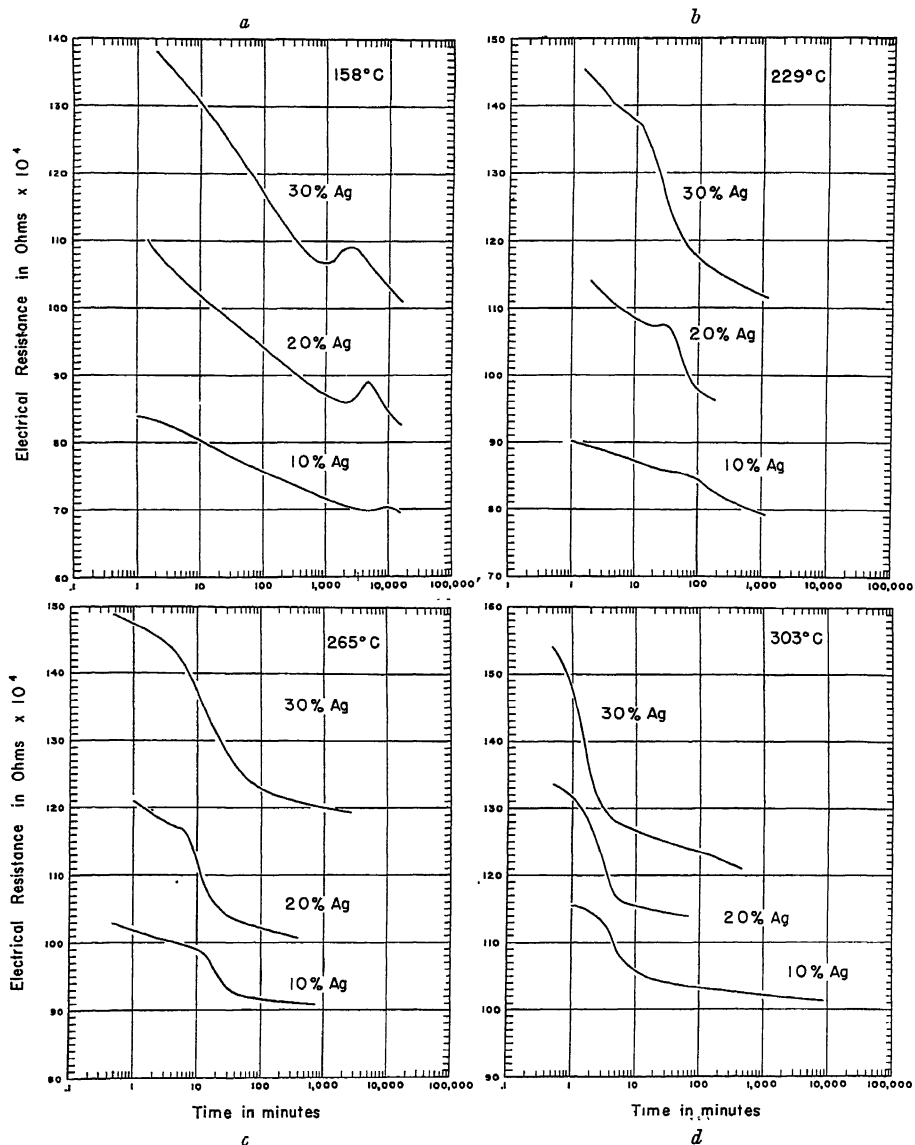


FIG. 8.—CHANGE IN ELECTRICAL RESISTANCE WITH TIME ON AGING ALUMINUM-SILVER ALLOYS AT VARIOUS TEMPERATURES.

a, aged at 158°C.
c, aged at 265°C.

b, aged at 229°C.
d, aged at 303°C.

precipitation is not a primary type of precipitation³ but a type of structural change occurring late in systems that show normal continuous precipitation. In some

systems, as in Al-Ag, the disregistry between the matrix and equilibrium phase γ is so small that the coherent γ' structure can grow to a size large enough to

be seen microscopically before it breaks away from the matrix and coalesces, with the matrix sometimes recrystallizing; this appears to be the case with Pb-Sb,²⁹

breaking away from the matrix before the particles grow to a visible size.

The mechanism by which the well-defined Widmanstätten figure of the co-

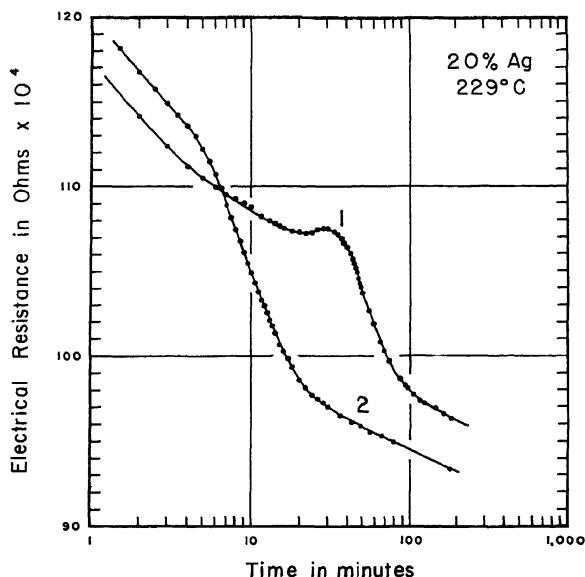


FIG. 9.—CHANGE IN ELECTRICAL RESISTANCE WITH TIME ON AGING AS-QUENCHED AND COLD-WORKED SAMPLES OF ALUMINUM + 20 PER CENT SILVER WIRE AT 229°C.

Curve 1, aged from as-quenched condition.

Curve 2, cold-drawn 33 per cent reduction of area after quenching prior to aging.

Plotted data show conformity of measurements to drawn electrical resistance curves.

Ag-Cu,^{13,31} Ni-Be¹² and, under some circumstances, Cu-Ag^{13,14,30} alloys. In other systems, of which Cu-Be is the prototype, continuous precipitation cannot be recognized but only a slight general darkening of the center of the aging grains while the readily recognized discontinuous precipitation at the grain boundaries occurs.^{3,10,11} As Bumm¹⁰ has suggested, it is quite possible that true precipitation is occurring within the grains (see discussion by C. S. Smith³²) and that the discontinuous reaction is but a secondary and later stage of precipitation. Accepting this as a theory, alloys of the Cu-Be type differ from alloys of the Al-Ag type only in that the degree of disregistry between the matrix and the equilibrium precipitate is greater, so that the strains become great enough to cause

herent transition lattice changes to the differently oriented and shaped aggregate of the equilibrium precipitate and matrix is not clear; evidently this change requires some re-solution and diffusion, which is somewhat difficult to conceive. The factors that cause some systems to exhibit precipitate coalescence without matrix recrystallization^{22,27,23} and others to show both^{29,34} are obscure, though, as Nabarro²³ points out, strain doubtless plays a part; it is possible that further research will show that matrix recrystallization is more common than now supposed.

The nature of the hardening process, though still not wholly clear, is now reasonably well understood. It is known that precipitation-hardening in Al-Ag, Al-Cu³ and Al-Mg²⁷ alloys is associated with the

formation of a transition lattice, which for the first two systems had been shown to be coherent with the matrix. Hardening has been attributed to the reaction stresses in the matrix that keep the precipitate in the strained coherent condition.³ No doubt such stresses must be appreciable to cause both subsequent recrystallization of the matrix and the electrical resistance increase observed with Al-Ag alloys and to cause the recrystallization, electrical resistance increase and diffraction line widening in Ag-Cu alloys.^{24,25} Maximum hardness probably depends on four factors: (1) hardening resulting from the stresses in the matrix that keep the precipitate in the strained coherent condition; (2) hardening resulting from the strains induced by volume changes accompanying precipitation* and from the mere presence of particles of a second noncoherent phase, which is doubtless very minor in both cases; (3) softening arising from depletion of the solid solution in solute atoms, and (4) softening arising from the release of the coherency stresses through the formation of the equilibrium precipitate frequently accompanied by recrystallization of the matrix. Although the effect of factor 1 should be the greatest with the largest plates of the coherent precipitate, the hardness of Al-Ag alloys is at a maximum when the precipitate is quite small, suggesting that factor 3 actively influences the hardening at an early stage, and the softening by factor 4 has no effect on the hardness maximum, since this reaction occurs very much later in the aging process. On the other hand, maximum hardness in the Pb-Sb alloy²⁹ is reached when general precipitation is well advanced and the grain-boundary reaction is started. Consequently, hardening occurs from factor 1 or factor 2, while softening begins when factor 4 becomes important accompanied

by factor 3. Possibly a similar hardening reaction exists for Cu-Be, Ni-Be, Cu-Ag and Ag-Cu alloys in which the diffraction pattern of the equilibrium phase may be observed before the maximum hardness is attained. This, however, may be from the second phase in the grain-boundary zones, while the continuous precipitate causing hardening³² may be coherent but may not grow thick enough to permit detection or structure determination.

The variation in resistivity with aging time in Al-Ag alloys is different from that in other alloys. The change is normal at first at 158°C. and above, then passes through an intermediate maximum (Fig. 9). The initial decrease probably originates in depletion of the matrix in solute before the coherency strains have become great enough to contribute their resistivity increase. As the coherent particles form and grow the strains increase and finally attain a magnitude that contributes an appreciable increase in resistivity superimposed on the initial gradual decrease; however, a second decrease at a faster rate soon attains prominence and the resistivity falls again. Such a phenomenon therefore should be observed only in systems where the disregistry is extremely small and the precipitate particles grow large before large strains are created; when the disregistry is great, as in Al-Zn, Cu-Ag, Ag-Cu and presumably Cu-Be, the coherency strains may produce a resistance increase from the very onset of aging.

This argument associates the increase in resistivity on aging with coherency strains, and not with particle size alone, as Mott²⁶ has done. For the present results, it hardly seems likely that the particle-size theory can hold, for this affords an increase in resistivity when the particle size is in the range of 5 to 10 Å. on a side. The resistivity maximum in Al-Ag alloys occurs when the size of the particle is much larger than this, in the neighborhood of 100 to 1000 Å. on a side. Lack of data for the low-tempera-

* The old idea that strains are set up during aging and are important in producing age-hardening is based upon this type of strain.³

ture aging (below 100°C.) of Al-Ag alloys does not preclude the possibility that an initial increase is present, which may be explained by the Mott theory;* however, when the disregistry is great both reactions may be superimposed.

Property changes accompanying aging involve the superposition of several reactions upon which the properties are dependent. The attempt has been made in this work to separate the important processes contributing to hardening and softening during aging by studying the aging process consisting of the precipitation reaction and the reaction whereby the coherent precipitate transforms to the equilibrium structure. The correlation of X-ray diffraction and metallographic data to the courses of hardness and electrical resistance change for aluminum-silver alloys was made, with the interesting results that increases in these properties occur during the formation and growth of the coherent transition lattice and are caused by the stresses induced in the matrix by holding the precipitate in the coherent condition; a subsequent decrease in these properties occurs when the solid solution depletion reaction attains prominence and more than compensates for the increase. It is concluded that the aluminum-silver alloys exhibit a typical aging sequence and that a similar mechanism should exist for all alloy systems, but that the property changes should depend on that particular reaction of the sequence of several, which is of most importance for the given alloy system.

SUMMARY

1. New Laue X-ray diffraction photographs for an Al + 20 per cent Ag alloy are presented. It is shown that the matrix planes along which platelets form in alloy

systems in general can be predicted merely by studying central radial streaks.

2. Powder X-ray diffraction data are given for alloys containing 10, 20 and 30 per cent Ag, on aging at 158°, 229°, 265° and 303°C. These show that the coherent transition lattice γ' forms on precipitation in all alloys at all temperatures and later transforms into the equilibrium phase γ .

3. Microscopic examinations show that the γ' to γ transformation is accompanied by a discontinuous type of reaction nucleated at the grain boundaries and probably involves the recrystallization of the strained matrix.

4. The correlations of microscopic and X-ray diffraction data with age-hardening curves for the three alloys suggest that hardening is caused by the precipitation of γ' and the stresses in the matrix involved in keeping the equilibrium phase in this strained condition. Softening begins when the effect of decreasing solute concentration in the matrix becomes more pronounced than the hardening reaction, and this occurs very much earlier than the γ' to γ transformation.

5. Electrical resistivity curves for the three alloys on aging at 158°, 229°, 265° and 303°C. are given. An intermediate maximum superimposed on the normal resistance decrease is attributed to the stresses induced in the matrix as the result of the matrix holding γ in the coherent γ' condition. Mott's theory of critical particle size does not apply to this maximum in the aluminum-silver alloys, since the particles at the resistance maximum are much larger than the predicted.

6. Finally, the conclusions drawn from the observations for aluminum-silver alloys are applied to published data for other alloy systems in an attempt to establish a consistent theory of aging.

ACKNOWLEDGMENTS

The authors wish to express their appreciation to the Aluminum Company of

* With an Al-Cu alloy aged at 100°C. evidence of both processes is present.²¹ Hardening occurs during a flattened part of the electrical resistance curve²¹ that may correspond to the superimposed resistance increase resulting from the development of coherency strains.

America for granting a fellowship to one of them, which made this research possible, and for supplying chemical analyses of the alloys that were investigated. They are also indebted to members of the staff of Aluminum Research Laboratories for assistance and advice generously given.

REFERENCES

1. C. S. Barrett and A. H. Geisler: Atomic Distribution in Aluminum-silver Alloys during Aging. *Jnl. Applied Physics* (1940) **11**, 733-739.
2. C. S. Barrett, A. H. Geisler and R. F. Mehl: Mechanism of Precipitation from the Solid Solution of Silver in Aluminum. *Trans. A.I.M.E.* (1941) **143**, 134-150.
3. R. F. Mehl and L. K. Jetter: The Mechanism of Precipitation from Solid Solution—The Theory of Age-hardening. Symposium on Age-hardening of Metals. Amer. Soc. Metals (1940) 342-417.
4. R. F. Mehl and C. S. Barrett: Studies upon the Widmanstätten Structure. I—Introduction. The Aluminum-silver System and the Copper-silicon System. *Trans. A.I.M.E.* (1931) **93**, 78-110.
5. G. D. Preston: Precipitation in the Solid State. *Jnl. Sci. Instruments* (1941) **18**, 154-157.
6. L. Guillet and L. Guillet, Jr.: Sur le durcissement structural des alliages aluminium-argent riches en aluminium. *Compt. rend.* (1939) **209**, 79-81.
7. W. L. Fink, D. W. Smith and L. A. Willey: Precipitation-hardening of High-purity Binary and Ternary Aluminum-copper Alloys. Symposium on Age-hardening of Metals. Amer. Soc. Metals (1940) 31-53.
8. W. L. Fink and D. W. Smith: Age-hardening of Aluminum Alloys, III—Double Aging Peaks. *Trans. A.I.M.E.* (1938) **128**, 223-233.
9. A. M. Talbot and J. T. Norton: Age-hardening of Magnesium-aluminum Alloys. *Trans. A.I.M.E.* (1936) **122**, 301-313.
10. H. Bumm: Über den Ausscheidungsverlauf bei Kupfer-beryllium-legierungen. *Zisch. Metallkunde* (1937) **29**, 30-32.
11. G. Masing and others: Beryllium. Siemenskonzern, 1932. Chemical Catalogue Co.
12. L. Graf: Mikroskopische Verfolgung der Ausscheidung in übersättigten Nickel-beryllium-legierungen. *Zisch. Metallkunde* (1938) **30**, 59-62.
13. C. S. Barrett, H. F. Kaiser and R. F. Mehl: Studies upon the Widmanstätten Structure, VII—The Copper-silver System. *Trans. A.I.M.E.* (1935) **117**, 39-57.
14. H. Bumm: Mikroskopischer Nachweis des Ausscheidungsverlaufs bei Kupfer-silber-legierungen. *Metallwirtschaft* (1935) **14**, 429-431.
15. R. F. Mehl: The Physics of Hardenability. The Mechanism and the Rate of the Decomposition of Austenite. Symposium on Hardenability of Alloy Steels. Amer. Soc. Metals (1939) 1-54.
16. R. S. Archer and L. W. Kempf: Discussion of reference 4. *Ibid.*, 114-115.
17. M. Hansen: Die Alterungshärtung der aluminiumreichen Silber-aluminium-legierungen. *Zisch. Metallkunde* (1928) **20**, 302.
18. W. Kroll: Hardening Aluminum-silver Alloys. *Metal und Erz* (1926) **23**, 555-557; *Metallurgist* (Suppl. to *Engineer*) (1927) **3**, 83-85.
19. M. Kosaki: On the Age-hardening Mechanism in Silver-aluminum Alloys. *Kinzoku no Kenkyu* (1936) **13**, 342-348.
20. A. Hone: Reactions in Solid Metallic Systems. *Rev. trimestr. can.* (1933) **19**, 396; (1934) **20**, 376-391, 766.
21. W. L. Fink and D. W. Smith: Age-hardening of Aluminum Alloys, IV—Discussion of the Theory. *Trans. A.I.M.E.* (1940) **137**, 95-107.
22. J. Calvet, P. Jacquet and A. Guinier: The Age-hardening of a Copper-aluminum Alloy of very High Purity. *Jnl. Inst. Metals* (1939) **65**, 121-137.
23. F. R. N. Nabarro: The Strains Produced by Precipitation in Alloys. *Proc. Roy. Soc.* (1940) **175-A**, 519-538.
24. W. F. Cox and C. Sykes: Precipitation in the Alloys of Copper and Silver during Age-hardening. *Jnl. Inst. Metals* (1940) **66**, 381-387.
25. N. Ageew, M. Hansen and G. Sachs: Entmischung und Eigenschaftsänderung übersättigter Silber-kupfer-legierungen. *Zisch. Phys.* (1930) **66**, 350-376.
26. N. F. Mott: Discussion of Gayler. *Jnl. Inst. Metals* (1937) **60**, 267.
27. W. L. Fink and D. W. Smith: Age-hardening of Aluminum Alloys, II—Aluminum-magnesium Alloy. *Trans. A.I.M.E.* (1937) **124**, 162-167.
28. L. K. Jetter and R. F. Mehl: Rate of Precipitation of Silicon from the Solid Solution of Silicon in Aluminum. Page 166, this volume.
29. R. S. Dean, L. Zickrick and F. C. Nix: The Lead-antimony System and Hardening of Lead Alloys. *Trans. A.I.M.E.* (1926) **73**, 505-529.
30. C. S. Smith and W. E. Lindlief: The Equilibrium Diagram of the Copper-rich Copper-silver Alloys. *Trans. A.I.M.E.* (1932) **99**, 101-114.
31. M. Cohen: Aging Phenomena in a Silver-rich Copper Alloy. *Trans. A.I.M.E.* (1937) **124**, 138-156.
32. C. S. Smith: Discussion of reference 3. *Ibid.*, 425-426.
33. R. W. Lindsay and J. T. Norton: Effect of Plastic Deformation on the Age-hardening of Duralumin. *Trans. A.I.M.E.* (1939) **133**, 111-119.
34. A. H. Geisler, C. S. Barrett, and R. F. Mehl: Mechanism of Precipitation from Solid Solutions of Zinc in Aluminum, Magnesium in Aluminum and of Some Magnesium-base Alloys. Page 201, this volume.

DISCUSSION

(See page 223.)

Mechanism of Precipitation from Solid Solutions of Zinc in Aluminum, Magnesium in Aluminum and of Some Magnesium-base Alloys

BY A. H. GEISLER,* JUNIOR MEMBER, C. S. BARRETT† AND R. F. MEHL‡, MEMBERS A.I.M.E.
(New York Meeting, February 1943)

THE studies of the mechanism of precipitation and of the resulting property changes in aluminum-silver alloys¹⁻³ have presented some new concepts of the aging reaction—concepts that may be fundamental in establishing a complete quantitative theory of age-hardening. With both aluminum-copper and aluminum-silver alloys, thin platelike aggregates form parallel to the Widmanstätten planes of precipitation.^{1,4} These platelets grow in lateral dimensions and in thickness with aging time until they are thick enough to produce an X-ray diffraction line pattern. Their structure is that of a transition lattice which is coherent with the matrix, since the atomic spacings in the matrix and the precipitate are the same on each side of their common interface.^{2,4} The equilibrium precipitate forms later from and at the expense of the transition lattice.

Since age-hardening occurs during the

This paper represents part of a thesis submitted by A. H. Geisler to the Graduate Committee of the Carnegie Institute of Technology, Pittsburgh, Pa., in partial fulfillment of the requirements for the degree of Doctor of Science, April 1942. Manuscript received at the office of the Institute Dec. 1, 1942. Issued in METALS TECHNOLOGY, February 1943.

* Research Metallurgist, Aluminum Research Laboratories, Aluminum Company of America, New Kensington, Pa. Formerly Aluminum Company of America Graduate Fellow, Department of Metallurgical Engineering, Carnegie Institute of Technology, Pittsburgh, Pa.

† Staff Member, Metals Research Laboratory, and Associate Professor, Department of Metallurgical Engineering, Carnegie Institute of Technology, Pittsburgh, Pa.

‡ Director, Metals Research Laboratory, and Head, Department of Metallurgical Engineering, Carnegie Institute of Technology, Pittsburgh, Pa.

¹ References are at the end of the paper.

formation and growth of the transition lattice, the major contributor to the hardening no doubt is the stress condition in the matrix resulting from the matrix holding the precipitate in the coherent condition. The development of these stresses also appears to be responsible for an increase in the electrical resistance superimposed on the normal decrease resulting from a change in the concentration of the matrix during aging.³

The two consecutive reactions constituting the aging process are accompanied by characteristic microstructural alterations. The initial precipitation process results in the formation of a Widmanstätten figure, while the later transformation of the transition lattice to the equilibrium lattice is accompanied by a coalescence, in the case of aluminum-copper alloys,⁵ and by the appearance of light areas at the grain boundaries with aluminum-silver alloys showing a structural rearrangement of matrix and precipitate.³ This latter reaction is similar microscopically to the so-called "discontinuous precipitation." Possibly discontinuous precipitation is a process that often if not always follows true precipitation of a coherent lattice and during which the transformation of the coherent transition lattice to the equilibrium lattice takes place accompanied by matrix recrystallization.³

EXPERIMENTAL PROCEDURE

The alloys were made using 99.97 per cent Al or distilled magnesium, with

alloying additions of high-purity metals. Weighed quantities corresponding to the added solute compositions given in Table 1 were melted together under suitable fluxes in graphite crucibles. After casting in an iron mold, the ingots were homogenized according to the treatments in Table 1. The 1-in. thick ingots of the aluminum alloys were either rolled or forged and rolled with intermediate annealing treatments to $\frac{1}{4}$ -in. plate from which specimens for hardness determinations were cut. Wire 0.028-in. in diameter was drawn from 0.1-in. sheet produced by further rolling the $\frac{1}{4}$ -in. plate. The magnesium-base alloys were hot-forged and rolled to 0.03-in. sheet from which small square wires were cut. The wire samples were used for powder X-ray diffraction studies and electrical resistance measurements. For Laue work large grains were grown in sheet samples of some of the alloys by the strain-anneal method.

The samples were heat-treated from the cold-worked temper as shown in Table 1.

electrical resistance samples of the aluminum-rich alloys were aged in direct contact with the liquid salt while the wire and single crystal samples for the X-ray diffraction studies were sealed in glass. An oil bath was used for the hardness and electrical resistance specimens of the magnesium-lead alloy. The aging treatments at 100° and 155°C. were conducted in baths of boiling water and boiling bromobenzene, respectively. The aging of the hardness and single-crystal specimens was interrupted for making observations while individual $\frac{1}{2}$ -in. long wire specimens were used for each aging time for the powder diffraction studies followed by microscopic examination. Resistance measurements were made continuously on the sample at temperature in the aging bath.

The Laue and powder photograms were made with the radiation from a tube with a cobalt target operating at 37,000 volts with exposure times varying from 2 to 12 hr. The electrical resistivity

TABLE 1.—*Solubility Characteristics, Compositions (Weight Per Cent), Solvus and Solidus Temperatures and Thermal Treatments of Alloys or Alloy Systems Investigated*

System	Solubility at Eutectic Temperature		Solubility at Low Temperature		Composition Alloys Studied		Solvus Temperature, Deg. C.	Solidus Temperature, Deg. C.	Homogenization Treatment		Solution Heat-treatment	
	Solute, Per Cent	Temperature, Deg. C.	Solute, Per Cent	Temperature, Deg. C.	Added, Per Cent	Actual, Per Cent			Time, Hr.	Temperature, Deg. C.	Time, Hr.	Temperature, Deg. C.
Al-Zn ⁷	31.6	270	5.4	125	12 Zn	11.8	215	585	48	400	1	400
Al-Mg ^{10,12}	15.1	451	4.0	200	25 Zn	22.0	245	570	50	450	1	445
					5 Mg	4.7	240	590	48	500	2	500
					10 Mg	9.1	350	530	24	450	2	445
					14 Mg		440	460	24	450	2	450
					20 Pb	21.0	340	570	19	500	9	490
Mg-Pb ¹⁹	42.0	468	3.0	100	12 Sn		320	580	19	550	2	550
Mg-Sn ¹⁹	14.8	561	0.8	250	7 Zn		330	360	48	345	7	345
Mg-Zn ²⁴	8.4	341	2.0	150								

The wire samples and the single crystals were sealed in glass. At the conclusion of the heat-treatment all samples were quickly quenched in a mixture of ice and water.

The aging treatments at temperatures above 155°C. were conducted in a salt bath controlled to $\pm \frac{1}{2}$ °C. Hardness and

measurements were made in 2-in. lengths of the 0.028-in. wire employing the Kelvin double bridge. The Brinell hardness number was determined from the average of four measurements on each of three indents made with a 10-mm. ball and a 500-kg. load applied for 30 seconds.

ALUMINUM-ZINC ALLOYS

The large decrease in solid solubility of zinc in aluminum⁷ (Table 1) makes this system very suitable for this type of

that coherent platelets form and grow in the early stages of precipitation in Al-Zn alloys. A few of the patterns are reproduced in Fig. 1. These show prin-

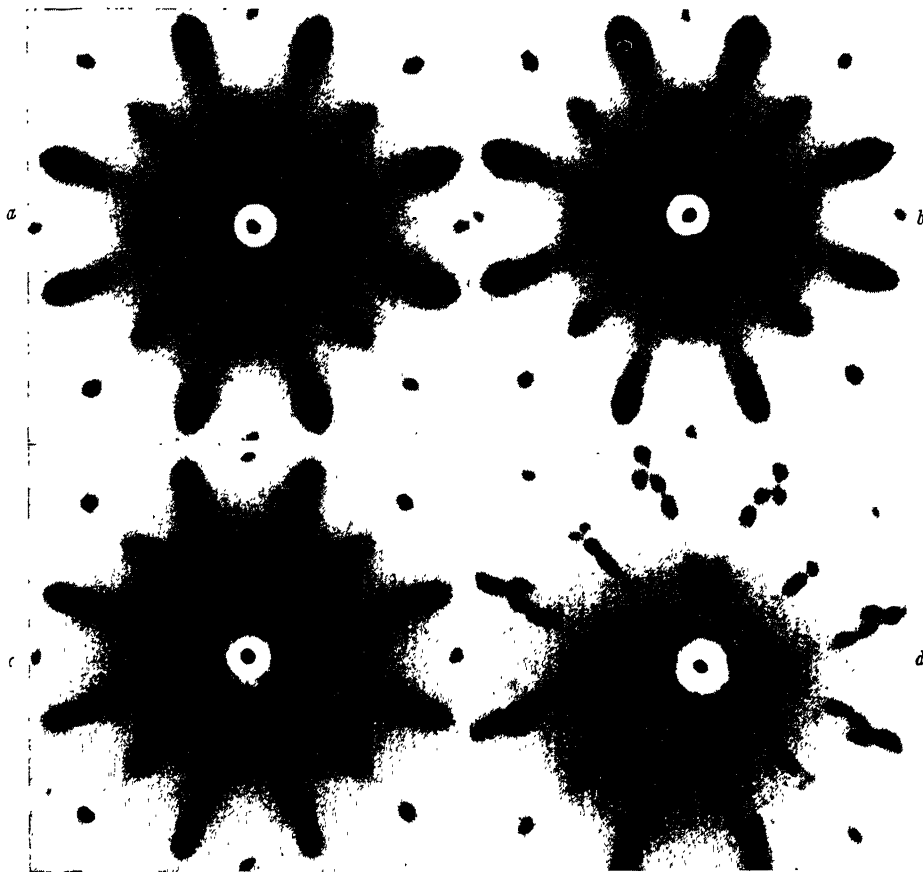


FIG. 1.—LAUE PHOTOGRAPHS FOR ALUMINUM-ZINC ALLOYS, $[001]$ PARALLEL TO BEAM.

- a, 12 per cent Zn aged 11 days at 100°C.
- b, 12 per cent Zn aged 28 days at 100°C.
- c, 12 per cent Zn aged 20 days at 155°C.
- d, 25 per cent Zn aged 1 month at 100°C.

study. The precipitation mechanism should be interesting, since a solid solution of a pure metal (Zn with 0 to 0.4 per cent Al) precipitates from the solid solution matrix.

Laue X-ray Diffraction Studies

Laue X-ray diffraction studies using single crystals of the Al-Zn alloys show

cipally the development of the normal Laue precipitate spots. In general, the streaks are very diffuse, indicating that the coherent platelets do not grow very large in either the thickness direction or laterally. The well-developed streaks, characteristic of large lateral platelet dimensions, found with Al-Ag alloys, are not

observed; orientations are found, however, in which the crystal produces streaks sufficiently well developed to permit accurate analysis. One of these patterns is reproduced in Fig. 2. The analysis

coherent to the matrix since they must have the same lateral atomic distribution and spacing as the $\{111\}$ matrix planes, but they may have a different lattice spacing normal to this plane. Coherency

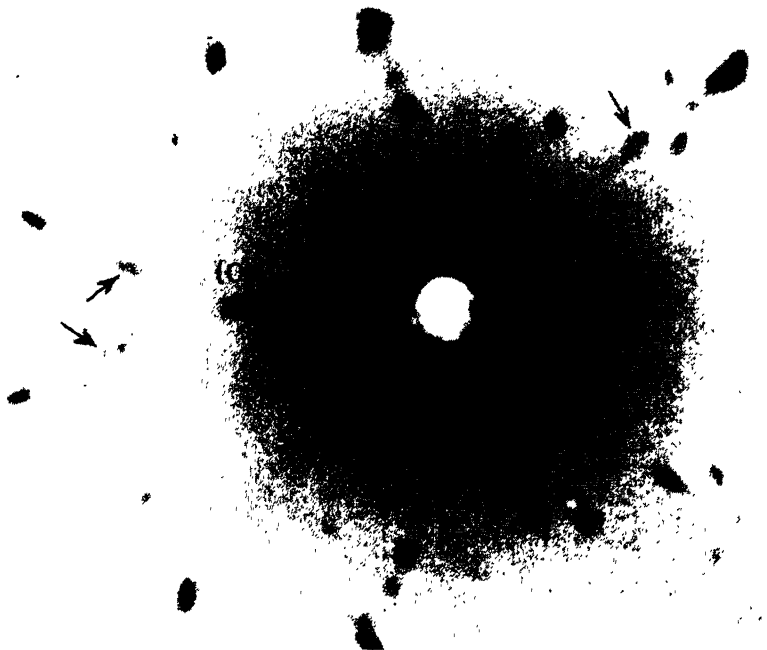


FIG. 2.—LAUE PHOTOGRAPH FOR ALUMINUM + 25 PER CENT ZINC ALLOY AGED 8.3 DAYS AT 100°C . Crystal rotated 15° about $[100]$ (vertical) from $[001]$ parallel beam.

n Fig. 3 as well as stereographic projections of other patterns shows that the streaks follow zone circles through $\{111\}$ matrix poles.* It has been shown previously that such a condition may be caused by the formation of small crystal platelets on $\{111\}$ matrix planes.¹ The platelets are

* In Fig. 3 it may appear that the streaks could be considered as occurring on zone circles through $\{100\}$ poles; however, the absence of a radial streak from the $(0\bar{1}0)$ spot corresponding to a line in the stereographic projection from $(0\bar{1}0)$ toward $(00\bar{1})$ as observed in a similar pattern for Al-Mg (Fig. 8f) and the presence of the strong and markedly zonal streaks from the $(0\bar{1}0)$ spot toward the center corresponding to the zones from $(0\bar{1}0)$ toward $(\bar{1}\bar{1}1)$ and $(11\bar{1})$ on the stereographic projection, definitely prove that the planes on which platelets form are not $\{100\}$ but $\{111\}$.

of the platelets with the matrix is demonstrated by the fact that the streaks accurately pass through matrix spots while the appearance of Laue precipitate spots slightly displaced from the zonal streaks, indicated by the arrows in Fig. 2,* proves that the precipitate is no longer in registry with the matrix when the particles have grown large enough to afford three-dimensional diffraction. This latter fact is also shown by the appearance of precipitate diffraction spots partly overlapping matrix spots; complete overlapping would have occurred if the precipitate had been coherent. It may be concluded that zinc

* The direct examination of this film and others provides somewhat better proof.

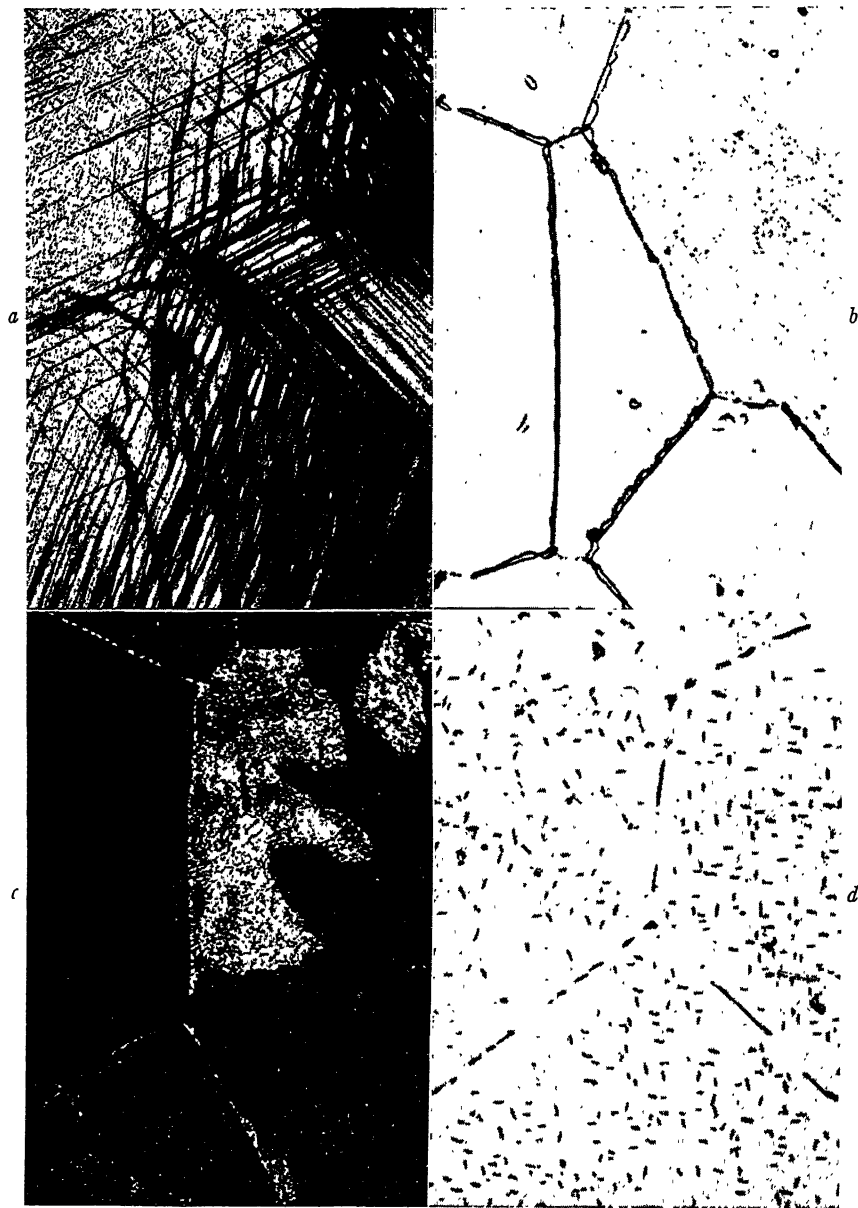


FIG. 4.—MICROSTRUCTURE OF AGED ALUMINUM-ZINC ALLOYS.

- a*, 12 per cent Zn air-cooled after homogenization treatment and aged about 2 years at 30°C. $\times 100$. Etched in HCl-HF-HNO₃.
b, 25 per cent Zn aged 3 hours at 100°C. $\times 1000$. Etched in 25 per cent HNO₃.
c, 25 per cent Zn aged 46 days at 100°C. $\times 500$. Etched in 25 per cent HNO₃.
d, 25 per cent Zn aged 370 hours at 229°C. $\times 500$. Etched in 0.5 per cent HF.

Microstructure

Typical photomicrographs of some of the samples are given in Fig. 4. Precipitation along slip planes (Fig. 4a) is observed



FIG. 5.—ENLARGED PORTION OF A POWDER PHOTOGRAPH FOR ALUMINUM + 25 PER CENT ZINC ALLOY AGED 40 DAYS AT 155°C.

1. The $\{111\}_{\text{Al}}$ K_{α} line.
2. The $(00.2)_{\text{Zn}}$ K_{α} line.
3. The $\{111\}_{\text{Al}}$ K_{β} line.
4. The $(00.2)_{\text{Zn}}$ K_{β} line.

in the samples used for hardness determinations but not with the small wire samples. Coarse grain-boundary precipitation (Fig. 4b) preceding general precipitation occurs before a change is detected in the powder diffraction pattern. General precipitation at 100° and 155°C. produces a mottled structure (Fig. 4c) in which the individual particles are difficult to resolve. Occasionally a grain-boundary effect (Fig. 4c) somewhat similar to that found for Al-Ag alloys is observed. The particles are much larger in samples aged at 229°C. and Widmanstätten figures may be found (Fig. 4d).

Widmanstätten Relations

The crystallographic orientation relationships between the face-centered cubic

matrix and the hexagonal close-packed precipitate should be those found between the same lattice types in the Al-Ag system, though in the present case the disregistry

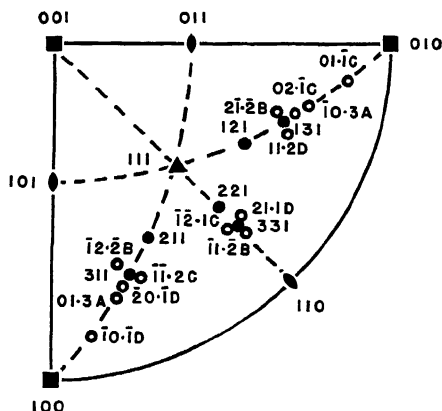


FIG. 6.—STEREOGRAPHIC PROJECTION OF ONE QUADRANT OF FIG. 1d.

Filled symbols are poles of matrix crystal while open circles are poles of the zinc crystals. A refers to crystallites on (111) matrix plane, B on $(\bar{1}\bar{1}\bar{1})$, C on $(\bar{1}\bar{1}1)$ and D on $(\bar{1}1\bar{1})$.

would be 7 per cent while in Al-Ag alloy it is only $\frac{1}{10}$ of this.² The combination of evidence from three sources shows that this prediction is correct.

Microscopic evidence indicates that the precipitate forms as plates parallel to the octahedral matrix planes, since a maximum number of four plate directions corresponding to the four planes in the $\{111\}$ family is observed in photomicrographs as shown in Fig. 4d. The examination of small-angle Debye lines in powder patterns for coarse-grained samples shows that the intensity distribution along the (111) matrix and (00.2) precipitate lines are the same, as the result of a pairing of the spots. This is seen in Fig. 5 and shows that these two planes are parallel.² Assuming that the directions of closest packing in these two planes are parallel, a standard stereographic projection for an aluminum crystal with a zinc crystal on each (111) was prepared. The comparison of this with the stereographic projection of Fig. 1d

shows that each pole in Fig. 6 accurately coincides with one on the standard projection, permitting the assignment of indices as in Fig. 6 and substantiating the assumed relationship. Consequently, it may be concluded that zinc precipitates from aluminum-rich Al-Zn alloys as plates parallel to $\{111\}$ matrix planes in such a way that the $(00.1)_{\text{Zn}}$ plane is parallel to a $(111)_{\text{Al}}$ plane and the $[11.0]_{\text{Zn}}$ directions are parallel to the $[110]_{\text{Al}}$ directions.

The Sequence

The fundamental mechanism of precipitation from supersaturated Al-Zn alloys is qualitatively identical to that obtaining for Al-Ag alloys. During the early stages the precipitate, the terminal zinc-rich solid solution, forms as coherent platelets on the octahedral matrix planes with the same atomic distribution and atomic spacing in the plane of the platelets as those of the parallel matrix planes. The platelets grow with time but break away from the matrix and assume the normal atomic spacings for the zinc-rich solid solution before they have grown large enough laterally to produce well-developed streaks and before they have become thick enough to diffract as three-dimensional gratings. Consequently, while the precipitate in the coherent platelet condition does not produce a powder pattern from which the structure can be rigorously solved, its structure is necessarily that of a strained lattice of the same lattice type as that of zinc, and it is therefore a transition lattice.

After the platelets have broken away from the matrix, with adjustment in lattice spacing, further growth occurs, and finally the powder pattern of zinc is observed; the large noncoherent precipitate particles then are oriented in respect to the matrix as already described and with the same relations as those between the matrix and the coherent platelets from which this equilibrium precipitate grows.

No doubt the atom movements required to form zinc are the same as those required to form γ in Al-Ag alloys, which have been discussed elsewhere.²

Hardness

The correlation of X-ray and microscopic information with changes in hardness shows that hardening occurs during the formation and growth of the coherent platelets in the early stages of precipitation; age-softening occurs when coherency is lost—when the precipitate particles have grown large enough to be detected by their powder pattern—and when the softening resulting from matrix depletion becomes pronounced.

The hardness curves for the 25 per cent Zn alloy are shown in Fig. 7. The hardness of the quenched alloy rapidly decreases from 87 to 75 during the first hour of aging at 229°C. and then remains constant.* The pattern for zinc was present in powder photograms for wires aged at this temperature less than 1 hr. (0.042 days). A slight increase in hardness from 87 to 93 occurs on aging for 1 hr. at 100°C. while the lattice-parameter change begins between 8 and 20½ hr. Further aging at 100°C. causes a decrease in hardness through an intermediate maximum between 5 and 10 days, with a few lines of the zinc pattern appearing in powder photograms after aging 2 to 6 days. It is very likely that the initial hardness increase is due to platelet formation at the grain boundaries while the broad intermediate maximum is the result of platelet formation occurring within the grain at a later time. The softening between the initial and intermediate maxima is probably the result of the growth of the grain-boundary platelets to large particles of noncoherent zinc (Fig. 4b)

* The low values of 60 at 1½ days and 70 at 3 days resulted from air-cooling the sample from the aging temperature. The specimen was quenched in ice water before all other measurements.

and the resulting matrix depletion; the first few weak diffraction lines of zinc observed probably originated from this after the alloy was very much overaged. The Laue patterns (Figs. 1d and 2) show the heterogeneous nature of the process.

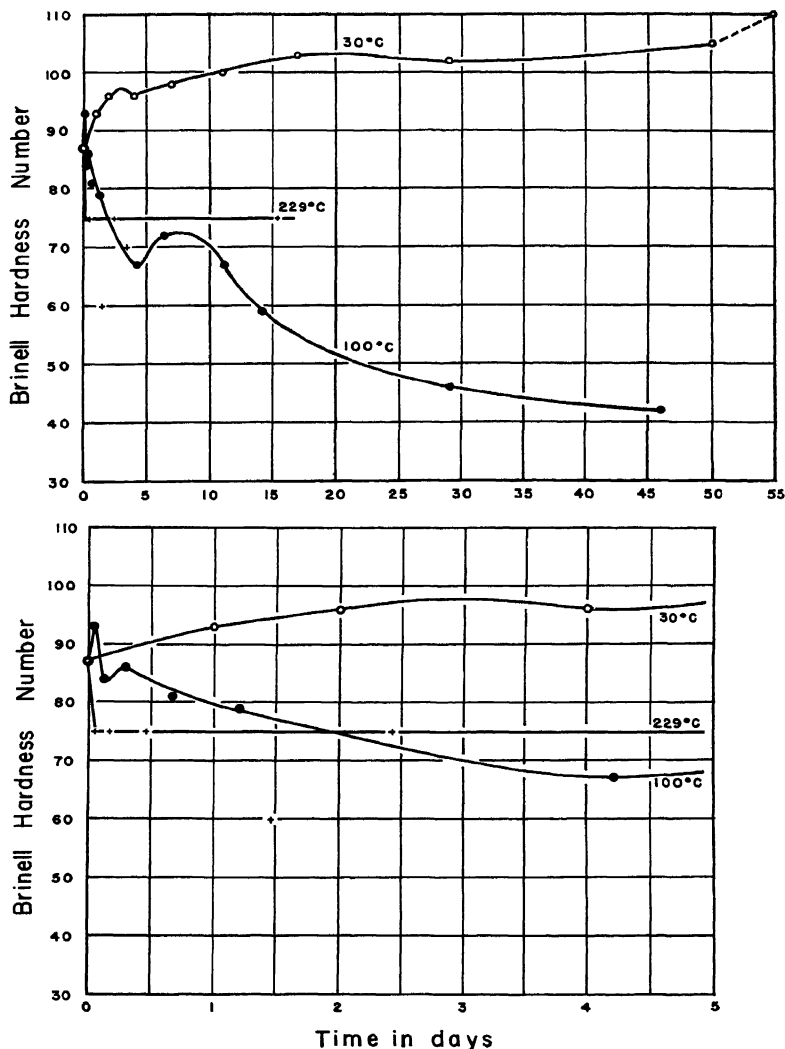


FIG. 7.—CHANGE IN HARDNESS OF ALUMINUM + 25 PER CENT ZINC ALLOY ON AGING AT VARIOUS TEMPERATURES.

grain-boundary material. The development of the zinc pattern with both the Laue and powder methods was very slow; the pattern continued to grow stronger

Faint zinc precipitate spots are present as early as 8.3 days, but while these are very strong after 30 days, platelet streaks are still present.

The hardness increases from 87 to 110 in 208 days at 30°C. without the appearance of the zinc pattern in the powder photograms. This rate of hardening is much slower than that found by other observers^{8,9} for 20 and 25 per cent Zn alloys. While most of the matrix is unaltered, evidence of localized precipitation on slip planes and at the grain boundaries is observed in areas of the microstructure, though the particles are much too small to be resolved. Streaks are present in Laue photograms for samples aged at room temperature but they are very diffuse, appearing as a general darkening near the center of the photograms, which obscures the thermal streaks for the matrix (see reference 2).

The hardening during precipitation in Al-Zn alloys is probably caused by the stresses in the matrix resulting from the matrix holding the equilibrium zinc precipitate in the strained coherent platelet condition. The absence of pronounced hardening for these alloys may be attributed to the fact that the coherent platelets break away from the matrix at a very early stage before a sufficient size and quantity have been reached to harden the entire matrix area.

Electrical Resistance

An attempt was made to study the change in electrical resistance on aging the 25 per cent Zn alloy at 229°C. Unfortunately, this temperature was probably too close to the solvus temperature, for only a very gradual decrease was observed. With the cold-worked sample a greater decrease was observed. The rapid initial increase in resistance observed with Al-Zn alloys on aging at 25°C.,⁶ which may be

caused by coherency stresses as the intermediate maximum with Al-Ag alloys,³ was probably completed before the initial resistance measurement (one minute after start of aging) could be made. The comparison of resistance measurements on aging at 100°C. with the hardness curve should be interesting.

ALUMINUM-MAGNESIUM ALLOYS

A study of the occurrence of platelet streaks in Laue photograms for Al-Mg alloys is of special interest. If the platelets are merely segregated areas of solute atoms alone upon the planes of subsequent Widmanstätten precipitation, as originally suggested by Preston⁴ and Guinier⁵ for Al-Cu alloys, and do not represent the first stage in atomic movements converting the matrix to the equilibrium precipitate,² it would be expected that streaks would not be observed for the platelets in Al-Mg, for the X-ray scattering of Al and Mg atoms are virtually the same, and it would be almost if not wholly impossible to differentiate between the matrix on one hand and the areas rich in magnesium but of the same crystal structure as the matrix on the other hand. The inability of Guinier and coworkers¹⁷ to detect central rays with Al-Mg alloys similar to those found with Al-Cu alloys suggests that platelets do not form; it will be shown, however, that rays very similar to those from Al-Cu crystals (and Al-Ag and Al-Zn) are observed, which presumably originate from true precipitate platelets.

Laue X-ray Diffraction Studies

A few of the Laue patterns obtained are shown in Fig. 8. The first evidence of precipitation is the appearance of four

FIG. 8.—LAUE PHOTOGRAMS FOR ALUMINUM-MAGNESIUM ALLOYS, [001] PARALLEL TO BEAM.

a, 10 per cent Mg aged 44 days at 100°C.

b, 10 per cent Mg aged 46 hours at 228°C.

c, 10 per cent Mg aged 330 hours at 155°C.

d, 10 per cent Mg aged 7 days at 228°C. Crystal slightly distorted.

e, 5 per cent Mg aged 93 days at 155°C.

f, 10 per cent Mg aged 49 hours at 155°C. Crystal rotated 15° about [100] (vertical) from [001] parallel beam.

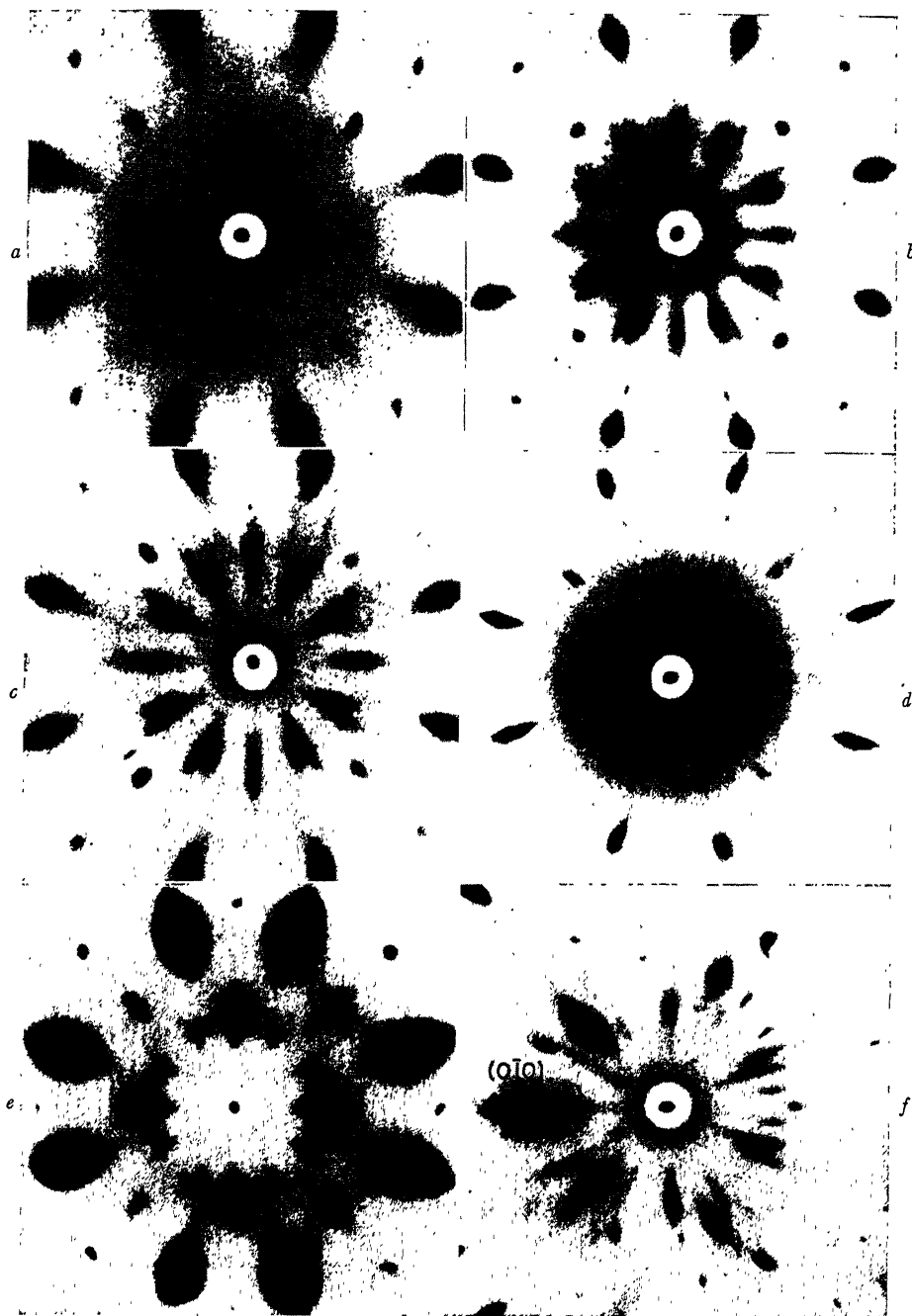


FIG. 8.—CAPTIONS ON OPPOSITE PAGE

long $\langle 100 \rangle$ streaks extending into the center of the pattern (horizontal and vertical in Fig. 8a) and a region of diffuse scattering about the direct beam. In addition, a halo appears around the direct beam about one half the distance between the center and the edge of the photogram in Fig. 8a. The next stage is the appearance of eight new radial streaks in $\langle 120 \rangle$ directions (about 27° on each side of the $\langle 100 \rangle$ streaks) shown in Figs. 8b and 8d. The initial blurred halo, therefore, is the result of the diffuse merging of the more intense parts of these 12 radial streaks. Growth of the platelets results in the intensification of these streaks and of the scattering around the direct beam, with the development of diffuse maxima on or near the streaks, as in Fig. 8b. These later develop into short intense streaks (or elongated spots) while the sections of the streaks near the direct beam and the scattering about the direct beam greatly decrease in intensity (Fig. 8c), indicating lateral growth of the platelets. Finally, normal Laue spots for the precipitate appear on the short streaks as shown in Fig. 8e.

The determination of the matrix planes along which platelets form cannot be made with certainty from the stereographic projection of the streaks, even with the pattern shown in Fig. 8f, which contains many streaks. Most of the streaks associated with the normal matrix spots show that platelets form on cube matrix planes; however, the short isolated streaks suggest platelet formation on either $\{110\}$ or $\{120\}$, but these cannot be plotted stereographically with sufficient accuracy to distinguish which of these two families of planes is used.

The determination of the matrix planes upon which the platelets form is best made by an analysis of the central rays and the scattering about the direct beam, according to a method previously developed.³ These two diffraction effects occur

when the platelets are small and when the X-ray beam is directed approximately parallel and perpendicular, respectively, to sets of platelets [i.e., when the spheres of reflection through (000) of the reciprocal lattice are tangent and normal, respectively, to diffuse platelet reciprocal lattice rods from (000) to (hkl), where (hkl) are the reciprocal lattice points of the planes on which platelets form]. Therefore, the diffuse scattering about the center and the streaks in the $[100]$ and $[010]$ directions corresponding to reciprocal lattice rods from (000) to (001), (100), and (010), respectively, suggest that platelets form parallel to $\{100\}$ of the matrix. In a like manner the rays in the $\langle 120 \rangle$ directions show that platelets form on $\{120\}$ matrix planes. It may be concluded that platelets form parallel to both $\{100\}$ and $\{120\}$ planes in the early stages of precipitation in Al-Mg alloys.

Coherency of the platelets with the matrix cannot be demonstrated conclusively by the data obtained. If platelets occur on 15 matrix planes, each matrix spot should have a large number of streaks through it. Because of this, individual streaks probably are obliterated or never strongly developed,* and the accurate passage of the streaks through the matrix spots as required for coherency cannot be confirmed. On the other hand, Guinier and coworkers¹⁷ observed that, while the precipitate Laue spots were weak at first, they often appeared as streaks joined to a spot of the matrix. The presence of the streaks joined to the matrix spots [like those in Fig. 8f for a few of the spots, particularly the (010) spot] shows that the platelets causing the streaks are coherent with the matrix while the development of precipitate Laue spots on these streaks shows that the platelets retain their coherence when they have grown to a

* The high intensity of the central rays is explained by the fact that all wave lengths in the incident X-ray beam contribute.

size sufficient to afford three-dimensional diffraction.²

Powder X-ray Diffraction Studies

A previous powder X-ray diffraction study¹¹ has shown that the precipitate may not have the normal structure of the equilibrium phase β ; unfortunately, however, the pattern for the precipitate was not observed in the photograms made in this present work.

The pattern for the equilibrium phase is weak, contains many lines and suggests that the normal β structure is complicated;* the transition lattice may also have a weak pattern and a complicated structure.

The marked decrease of lattice parameter with decreasing concentration of Al-Mg solid solutions^{12,13} may be used as an indicator of the solid solution decomposition and precipitation during aging. A summary of the results of powder diffrac-

precipitation can be detected microscopically before the lattice-parameter change is evident¹¹ (Fig. 9a). A slight initial increase in the lattice parameter before the normal decrease for magnesium depletion, and without any microstructural alterations, was observed for one series of aging treatments (14 per cent Mg aged at 155°C.). Although similar observations for 12 and 13.5 per cent Mg alloys were attributed by Lacombe and Chaudron¹⁶ to an ordering of magnesium atoms in the matrix prior to precipitation, it is not likely that this is true. The phenomenon may be related to the relief of quenching stresses¹² or to the re-resolution on aging of unstable nuclei formed at or on cooling from the solution heat-treating temperature.²⁷

Microstructure

Precipitation in these alloys is continuous.²⁷ The first evidence is localized precipitation at the grain boundaries and in some instances upon slip planes (in the specimens for hardness determinations). Localized precipitation is followed by the appearance of a general precipitate that increases in amount with aging, as shown in Figs. 9a and 9b. Further aging causes growth and coalescence of the particles (Fig. 9c). Occasionally the precipitate forms as an unresolvable maze of particles with no definite Widmanstätten figure (Fig. 9b); however, in a few instances well-defined plates in a maximum of three directions are observed (Figs. 9d and 9e) at an early stage of precipitation, showing that the precipitate forms as plates parallel to {100} matrix planes, at least in the early stages. Later, when precipitation is more extensive, it is very likely that other plate directions are also present (Fig. 9f) probably resulting from plates on {120} matrix planes.¹⁵

Hardness

Age-hardening of the 10 per cent Mg alloy at 100°, 155° and 229°C. (Fig. 10)

TABLE 3.—Powder X-ray Diffraction Results for Aluminum-magnesium Alloys

Aging Temperature, Deg. C.	Time for Occurrence of Various Alterations, Hr.			
	100	155	166	229
10 Per Cent Mg				
a_0 change begins	1,344-1,774	48-96	33-52	2-4
a_0 change ends..	>3,214	336-504	240-384	12-19
14 Per Cent Mg				
a_0 change begins	360-720	4¼-7¼	2-5	¾-½
a_0 change ends..	>720	>192	>64	2-3

tion studies for 10 per cent and 14 per cent Mg alloys on aging at temperatures between 100° and 229°C. is given in Table 3. These data will be used to correlate precipitation with hardness and resistivity changes during aging. A rather discontinuous shift of the diffraction lines occurs during precipitation, while some

* Only one reference was found in which an attempt had been made to solve the structure of the equilibrium phase, β Al-Mg¹⁴. It was found that the pattern could be assigned to a large hexagonal lattice with $a_0 = 11.38 \text{ \AA}$. and $c/a = 1.57$.

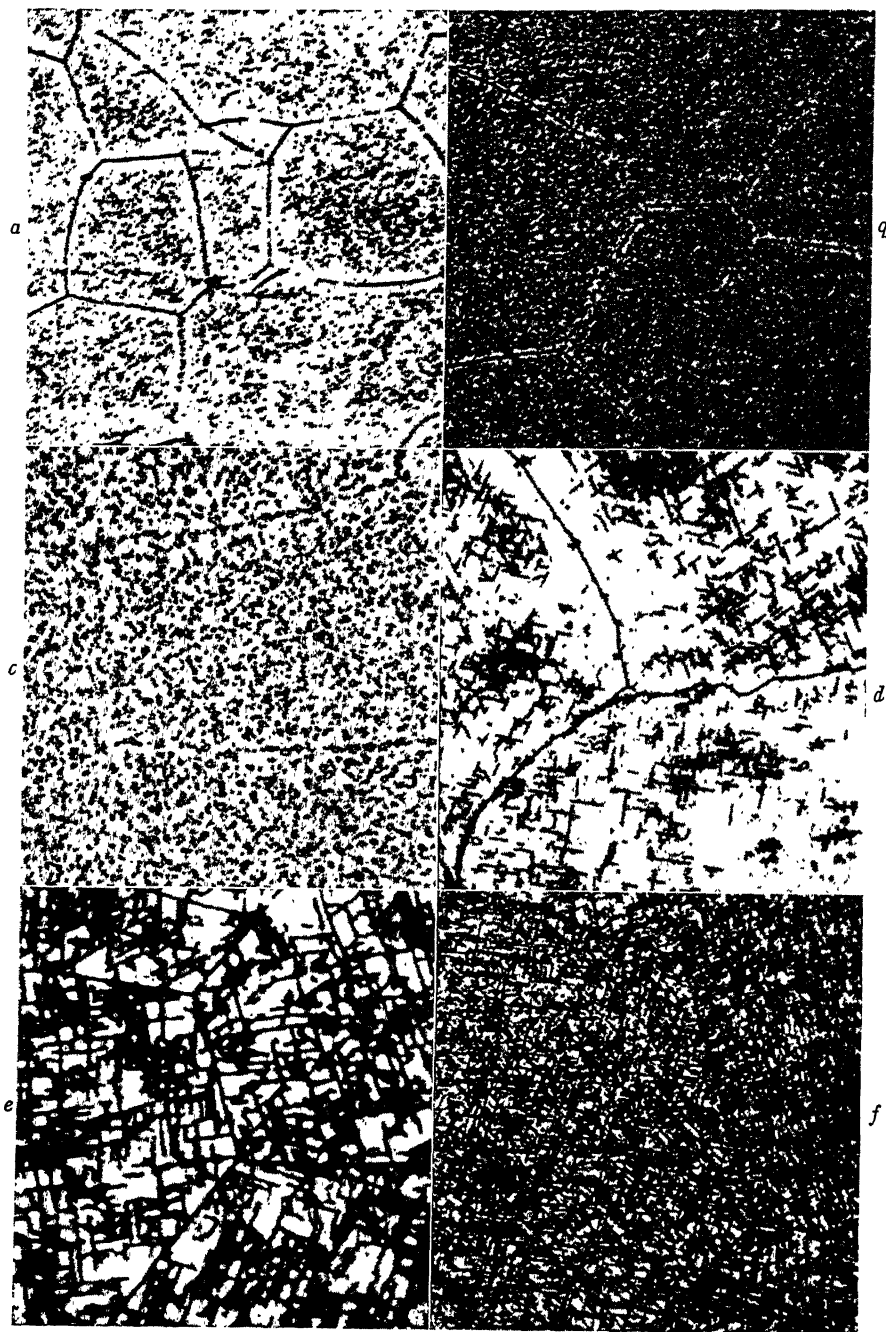


FIG. 9.—CAPTIONS ON OPPOSITE PAGE.

occurs during the formation of platelets and growth of these to microscopically visible precipitate particles of a different crystallographic structure than that of the equilibrium second phase,¹¹ while softening is accompanied by coalescence of the particles. The correlation of powder patterns for small wires shows that complete decomposition of the supersaturated quenched alloy takes place during hardening, the maximum hardness occurring slightly after the lattice-parameter shift is completed. Somewhat similar results have been reported for elongation and tensile strength.¹¹ Although the X-ray data are not complete, the precipitate causing hardening is most likely a coherent transition structure, for the Widmanstätten figure and observed hardness (and later electrical resistance) increase are characteristic of the development of large coherent particles.³ On the other hand, this alloy is distinguished from the previously studied aluminum-base alloys by the fact that hardening occurs throughout the decomposition of the matrix without the softening accompanying solute depletion attaining importance.

Electrical Resistance

The change in resistivity on the aging of the 10 per cent and the 14 per cent Mg alloys at 166° and 229°C. is shown in the curves in Fig. 11. All the curves have an initial part during which little or no change occurs. The length of this interval varies from 2 min. for the 14 per cent Mg alloy aged at 229°C. to about 400 min. for the 10 per cent Mg alloy aged at 166°C. While only a very slight increase to a broad maximum occurs for the 10 per cent alloy

at 229°C. during this period, the period is terminated by a definite maximum for the 14 per cent Mg alloy at both temperatures and this is followed by a rapid decrease. The latter, no doubt, results from depletion of the matrix in magnesium for the beginning of the lattice-parameter change (in powder photograms for wire samples treated simultaneously with the resistance specimens) is observed for specimens aged for times slightly greater than that corresponding to the beginning of the rapidly decreasing part of the curves. The curves for the 14 per cent Mg alloy are somewhat similar to those for Al-Ag alloys³; the difference lies in the slopes of the initial part of the curves. With Al-Ag alloys a gradual decrease in resistance occurs before the maximum is reached and thus the maximum is intermediate; with Al-Mg alloys the slope of the initial section of the curves is virtually zero, and the resistance increases to a true maximum with a resistance greater than that in any other portions of the curves. No doubt the correlations of microscopic and X-ray diffraction data show that in both alloys the resistance maximum is directly related to the growth of platelets to a size that can just be detected microscopically or by the powder diffraction method, and the increase probably is caused by the development of coherency stresses in the matrix before the rapid decrease for solute depletion becomes important.

MAGNESIUM-BASE ALLOYS

The precipitation reaction in a few magnesium-base alloys was followed, principally by powder X-ray diffraction studies, in a further search for coherent transition

FIG. 9.—MICROSTRUCTURE OF AGED ALUMINUM-MAGNESIUM ALLOYS.

- a, 10 per cent Mg aged 2 hours at 229°C. $\times 500$.
- b, 10 per cent Mg aged 32 hours at 229°C. $\times 500$.
- c, 10 per cent Mg aged 25 days at 229°C. $\times 500$.
- d, 10 per cent Mg aged 95 days at 100°C. $\times 1000$.
- e, 14 per cent Mg aged $\frac{1}{2}$ hour at 229°C. $\times 2000$.
- f, 14 per cent Mg aged 8 days at 155°C. $\times 1000$.

Etched in 0.5 per cent HF.

lattices of sufficient sizes to afford Bragg diffraction. The Mg-Al system was considered a good prospect, since it has been solid solution;¹⁸ however, Talbot and Norton¹⁸ found that the pattern for the precipitate could not be observed in the

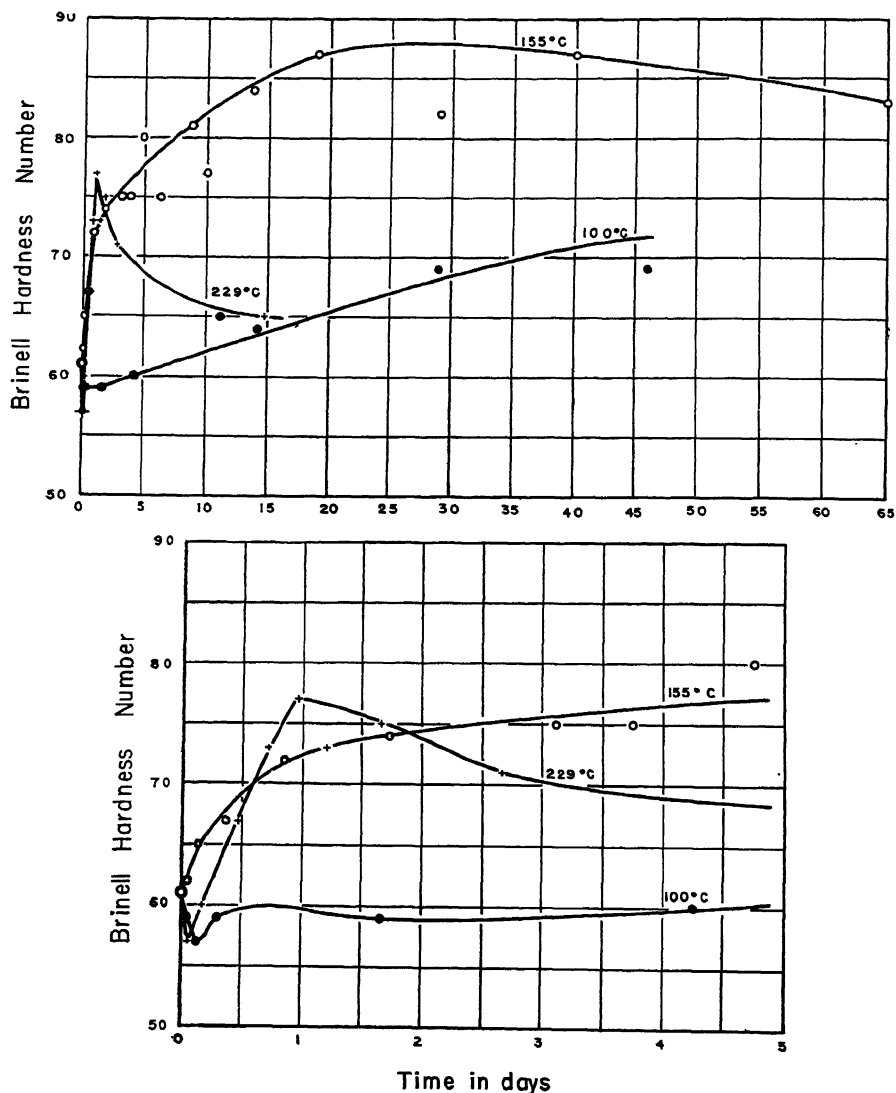


FIG. 10.—CHANGE IN HARDNESS OF ALUMINUM + 10 PER CENT MAGNESIUM ALLOY ON AGING AT VARIOUS TEMPERATURES.

shown that these alloys age-harden at elevated temperatures^{18,20,26} throughout the decomposition of the supersaturated

diffraction photograph and accordingly the structure of the precipitate could not be determined. Appreciable age-hardening

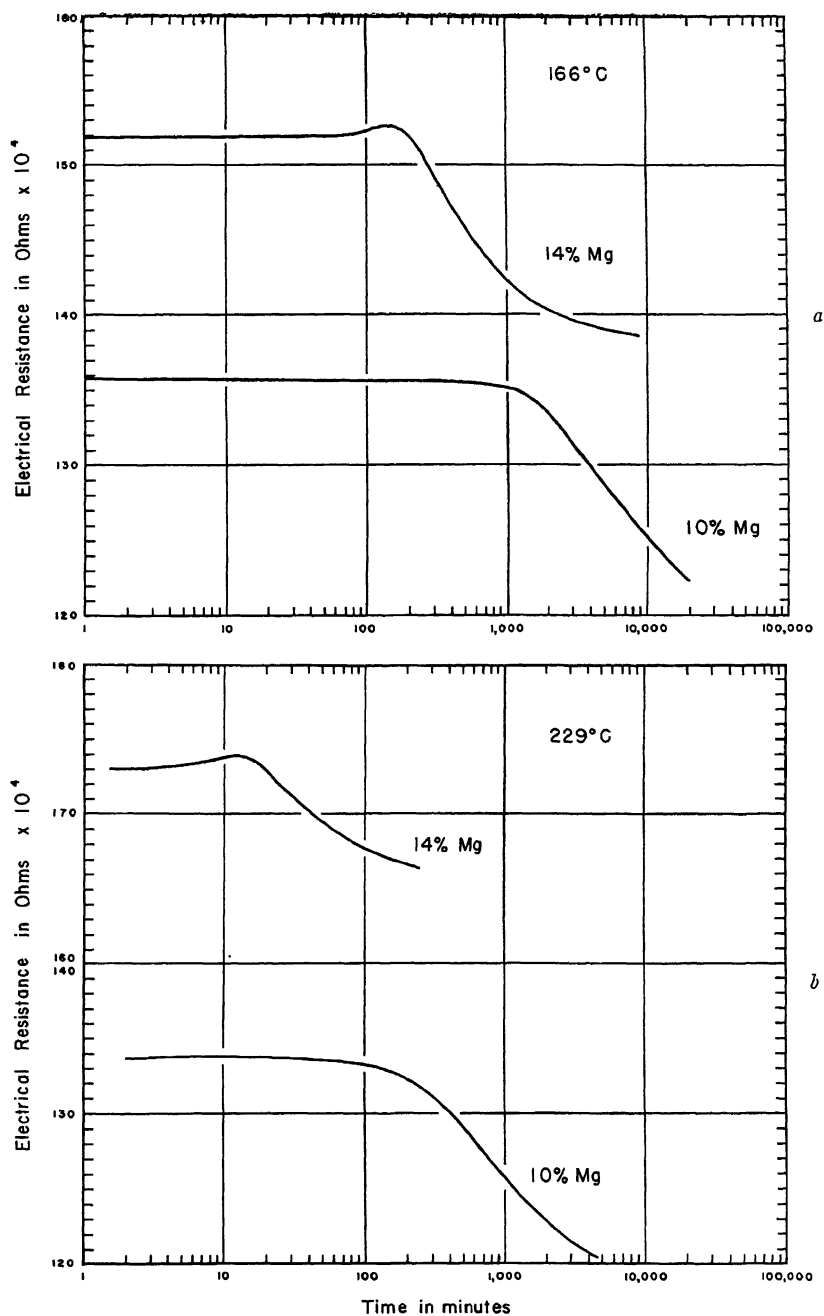


FIG. 11.—CHANGE IN ELECTRICAL RESISTANCE OF ALUMINUM-MAGNESIUM ALLOYS ON AGING.
a, aged at 166°C.; b, aged at 229°C.

occurs with Mg-Zn^{20,26} alloys while the hardening of Mg-Pb^{20,21} and Mg-Sn^{20,26} alloys is slight or absent. Since the precipitation reactions in these three alloys had not been investigated previously, they were chosen for a brief study.

X-ray Diffraction Studies

Laue photographs were made for single crystals of the 20 per cent Pb alloy after various aging treatments. No platelet streaks were observed; however, there seemed to be an additional general blackening near the central part of the pattern, which may have resulted from platelet formation on a high-order matrix plane, for after complete precipitation a galaxy of small precipitate spots was found there.

Powder X-ray diffraction photographs for the Mg-Pb and Mg-Sn alloys show that in both systems the precipitate has the structure and dimensions of the equilibrium phase when the pattern first appears, with

TABLE 4.—*Powder X-ray Diffraction Results for Magnesium-base Alloys*

Alloy	Aging Temperature, Deg. C.	Time for First Appearance of Precipitate Pattern, Hr.	Last Observation, Hr.
Mg + 20 per cent Pb.	30	> 3,144	3,144
	100	> 1,200	1,200
	155	18½–44	576
	222	¼–1½	1,152
Mg + 12 per cent Sn.	155	42–66½	720
	229	2–4	432
Mg + 7 per cent Zn..	155	Not detected	192

no change even after the longest aging time (Table 4). This is true also with aged cold-worked samples. Lattice-parameter measurements of the precipitates show that a_0 for the face-centered cubic Mg₂Pb was 6.845 Å., which is in good agreement with the value 6.836 Å. reported by Zintl and Kaiser²² but in poor agreement with Friauf's²³ value of 6.78 Å.; the parameter for the structurally analogous Mg₂Sn

with four molecules per unit cell and with the CaF₂ structure is 6.744 Å., somewhat less than the value 6.765 Å. reported by Zintl and Kaiser.²² The pattern for the precipitate formed on air-cooling or on aging the Mg-Zn alloy was not observed in the powder photographs, though microscopic examination shows that considerable precipitation had occurred. This again is unfortunate, for the extent of hardening and the development of a Widmanstätten figure in this alloy suggest that the coherent precipitate should be capable of growth to a size recognizable as a transition lattice.

The powder photographs show that with the Mg-Pb and the Mg-Sn alloys the precipitate forms on a family of matrix planes of a very high index, for there are many more orientations of precipitate particles than of matrix grains. This is shown in photographs made of stationary specimens, by the fact that full lines for the precipitate are observed when but occasional spots for the matrix appear. Studies upon the Widmanstätten structure in Mg-Sn alloys²⁵ (which probably would apply also to Mg-Pb alloys, since the structures of the precipitates in the two systems are the same with only a slight difference in a_0) show that plates form parallel to three types of matrix planes, providing a large number of precipitate orientations as observed. The discrepancy is high for all three relations, suggesting that the precipitate should be noncoherent when the particles have grown large enough to diffract as three-dimensional gratings.

Microstructure

Precipitation in the Mg-Pb and Mg-Sn alloys occurs along twin boundaries as well as at grain boundaries and on slip planes during the early stages of aging. Some particles can be seen microscopically before the pattern of the precipitate is detected in the photographs. The continuous precipitate in the Mg-Pb alloy appears as small rounded particles (Fig.

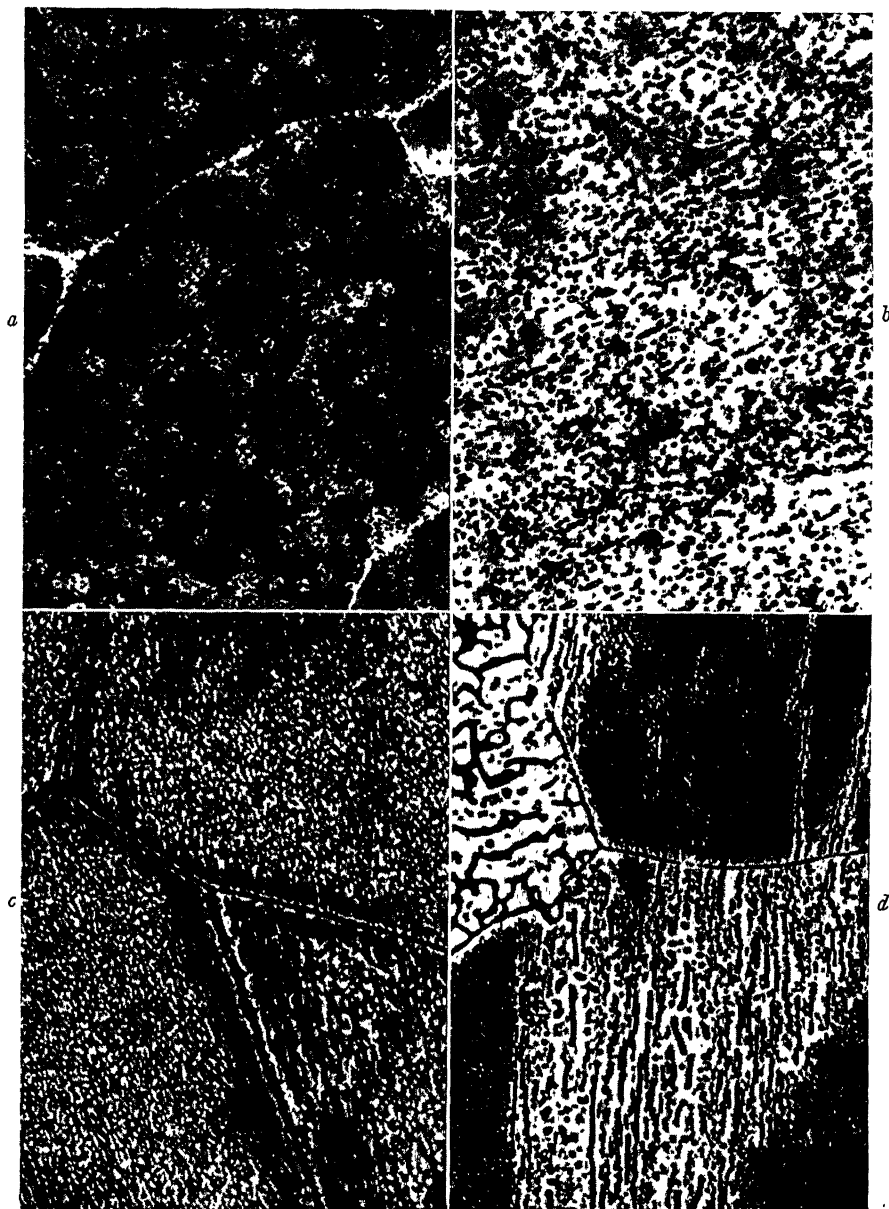


FIG. 12.—MICROSTRUCTURE OF AGED MAGNESIUM-BASE ALLOYS.

a, 20 per cent Pb aged 44 hours at 155°C. $\times 1000$.

b, 20 per cent Pb aged 48 days at 222°C. $\times 1000$.

c, 12 per cent Sn aged 6 days at 229°C. $\times 500$.

d, 12 per cent Sn aged 18 days at 229°C. $\times 500$.

a and *b* etched in 0.5 per cent HF; *c* and *d* etched in nital.

12a), which grow and coalesce into a coarse structure (Fig. 12b); no definite Widmanstätten figure is observed. Mg_2Sn precipitates continuously in Mg-Sn alloys

The electrical resistivity of the Mg-Pb alloy decreases normally during precipitation, possibly after a very slight initial increase, as shown in Fig. 13. Evidently,

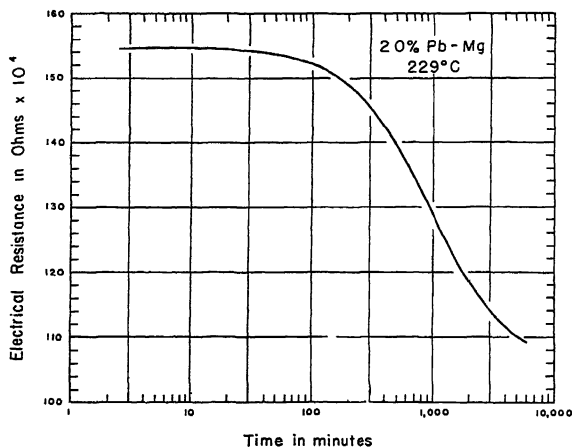


FIG. 13.—CHANGE IN ELECTRICAL RESISTANCE OF MAGNESIUM + 20 PER CENT LEAD ALLOY ON AGING AT 229°C.

as fine particles, sometimes along one direction (Fig. 12c) which may correspond to the slip plane. A coalescence process nucleated at the grain boundaries is observed also with the Mg-Sn alloy (Fig. 12d). A poorly defined Widmanstätten figure is observed for the continuous precipitate in some of the Mg-Zn samples.

Hardness and Electrical Resistance

The change in hardness and electrical resistance was determined for the Mg-Pb alloy only. The change in hardness of the 20 per cent Pb alloy is very slight, with a maximum observed increase of only nine Brinell numbers for any of the aging treatments (aging periods up to 5280 hr. at 30°C., 216 hr. at 158°C. and 167 hr. at 229°C.). The correlation with X-ray data shows that the precipitation of Mg_2Pb from Mg-Pb alloys is not accompanied by significant age-hardening; according to the literature,^{20,26} this is also true for the precipitation of Mg_2Sn from Mg-Sn alloys.

the development of coherency stresses that may cause an increase in the resistance is negligible.³

DISCUSSION OF RESULTS

It is now sufficiently clear that a theory of precipitation-hardening based upon critical dispersion is too simple. Apart from the new body of information on the crystallographic nature of the precipitation process, which has added at least one new important condition, the simple theory gives no hint as to why the extent of hardening is so different from system to system.

The first hint of a new condition came from studies of the Widmanstätten figure, studies undertaken with a view to adding to the knowledge of the age-hardening process, which demonstrated that the lattice of the matrix and the precipitate bear a fixed orientation relationship.¹⁶ The demonstration of the occurrence of coherent platelets, as shown by streaks in Laue patterns in the early stages of aging, led to the proof of lattice coherency between

matrix and precipitate and gave information on the sizes of the coherent particles. This coherency is the new condition that must be added to age-hardening theory, for it determines the extent of hardening, influences the microstructure developed, and assists in explaining the anomalous changes in electrical resistivity.^{1-5,17,27,28}

Al-Cu,^{4,5} Al-Ag¹⁻³ and Al-Mg alloys age-harden appreciably; they form a coherent transition lattice, which appears as a well-developed Widmanstätten figure when the particles grow large. On the other hand, Al-Zn, Mg-Pb and Mg-Sn alloys do not harden appreciably and the coherent particle breaks away from the matrix when very small. Apparently the degree of hardening is associated with the size that the coherent particle can attain.

This point is well illustrated by a comparison of the hardening of Al-Ag and of Al-Zn alloys. The lattice pairs involved in precipitation in each are identical in type, and in accordance with the principle the orientation relationships are identical. But the coherent particle grows to a thickness of about 3000 Å. in Al-Ag and only to 10 Å. in Al-Zn;* doubtless this is owing to the greater degree of disregistry between the matrix and the equilibrium precipitate in the latter system, amounting to 7 per cent in the latter and to 0.7 per cent in the former. Extended coherent growth appears thus to be related to this degree of disregistry, and the greater the extent of growth of the coherent particle the greater the degree of hardening appears to be. The Fe-Cu-Ni alloy investigated by Bradley and coworkers²⁹ confirms this relation between registry and extent of coherent growth; the problem in Al-Cu alloys is complicated, for the transition lattice θ' differs greatly from the equilib-

rium lattice θ and it is at present difficult to evaluate the strain.

This argument so far is built upon *size* of the coherent particle alone, proposing that the larger the platelet may grow before breaking away from the matrix, the greater the hardening. But the *number* of platelets is probably also important. Presumably a large number of small coherent particles will harden as effectively as a smaller number of larger plates, and in this sense the hardening will depend upon the degree of supersaturation, and differences in the rate of hardening will originate from differences in the rate of nucleation and the rate of growth of the precipitate. In Al-Zn alloys hardening occurs only at the lowest temperature (30°C.) when a large number of small platelets are formed; at higher temperatures the number of platelets is low and the extent of hardening is small. Evidently the rate of nucleation is low in these alloys, since precipitation occurs over a long time period; particles formed early having broken away from the matrix before other coherent particles have yet formed. Possibly Cu-Be is a system in which hardening is associated with the formation of a large number of very small platelets.

SUMMARY

1. Coherent platelets form parallel to octahedral matrix planes in the early stages of precipitation in aluminum-zinc alloys. These grow with time but break away from the matrix before they are thick enough to diffract as three-dimensional gratings. The particles have the structure and lattice parameters of the equilibrium precipitate Zn when their powder pattern is first observed. The Zn sometimes appears as plates parallel to the $\{111\}$ matrix planes; these as well as rounded particles are oriented with respect to the matrix in such a way that the (00.1) Zn plane is parallel to one of the

* Value for Al-Ag alloys was estimated from a photomicrograph (Fig. 5, ref. 2) while the value for Al-Zn alloys estimated from Laue patterns, Figs. 1 and 2, was the same as the value calculated by Nabarro's²⁸ equation (see ref. 2).

$\{111\}_{Al}$ planes with $[110]_{Zn}$ parallel $[110]_{Al}$. Age-hardening accompanies the formation and growth of the coherent platelets but softening occurs when the non-coherent zinc structure appears.

2. The first stage of precipitation in aluminum-magnesium alloys is the formation of coherent platelets on $\{100\}$ matrix planes followed by growth to a well-defined Widmanstätten figure, with the precipitate appearing as plates upon $\{100\}_{Al}$ planes. Subsequent platelet formation occurs on $\{120\}_{Al}$ planes. An increase in the electrical resistivity is observed just before the rapid decrease resulting from matrix depletion becomes predominant. Age-hardening takes place during the entire decomposition, the hardening resulting from coherency stresses fully counteracting the softening from matrix concentration change.

3. Coherent platelets may form in the early stages of precipitation in magnesium-base alloys with lead and tin but they do not grow very large because the precipitates have the structure and lattice dimensions of the equilibrium phases Mg_2Pb and Mg_3Sn when their diffraction patterns are first observed. As the result, the hardening reaction about balances the softening resulting from matrix depletion, and the age-hardening is negligible.

4. These and former observations are employed in stating a modified theory of age-hardening.

ACKNOWLEDGMENTS

The authors wish to express their appreciation to the Aluminum Company of America for granting a fellowship to one of them, which made this research possible, and for supplying chemical analyses of some of the alloys that were investigated. They are also indebted to members of the staff of Aluminum Research Laboratories for assistance and advice generously given.

REFERENCES

1. C. S. Barrett and A. H. Geisler: Atomic Distribution in Aluminum-silver Alloys during Aging. *Jnl. Applied Physics* (1940) **11**, 733-739.
2. C. S. Barrett, A. H. Geisler and R. F. Mehl: Mechanism of Precipitation from the Solid Solution of Silver in Aluminum. *Trans. A.I.M.E.* (1941) **143**, 134-150.
3. A. H. Geisler, C. S. Barrett and R. F. Mehl: Aging in the Solid Solution of Silver in Aluminum. Page 182, this volume.
4. G. D. Preston: The Diffraction of X-rays by Age-hardening Aluminum-copper Alloys. *Proc. Roy. Soc.* (1938) **167-A**, 526-538.
5. J. Calvet, P. Jacquet and A. Guinier: The Age-hardening of a Copper-aluminum Alloy of very High Purity. *Jnl. Inst. Metals* (1939) **65**, 121-137.
6. W. L. Fink and K. R. Van Horn: Equilibrium Relations in Aluminum-zinc Alloys of High Purity. *Trans. A.I.M.E.* (1932) **99**, 132-140.
7. W. L. Fink and L. A. Willey: Equilibrium Relations in Aluminum-zinc Alloys of High Purity. II. *Trans. A.I.M.E.* (1936) **122**, 244-260.
8. D. Hanson and M. L. V. Gayler: A Further Study of the Alloys of Aluminum and Zinc. *Jnl. Inst. Metals* (1922) **27**, 267-294.
9. T. Tanabe: Studies in the Aluminum-zinc System. *Jnl. Inst. Metals* (1924) **32**, 415-452.
10. E. H. Dix, Jr. and F. Keller: Equilibrium Relations in Aluminum-magnesium Alloys of High Purity. *Trans. A.I.M.E.* (1929) **83**, 351-365.
11. W. L. Fink and D. W. Smith: Age-hardening of Aluminum Alloys, II—Aluminum-magnesium Alloy. *Trans. A.I.M.E.* (1937) **124**, 162-167.
12. R. M. Brick, A. Phillips and A. J. Smith: Quenching Stresses and Precipitation Reactions in Aluminum-magnesium Alloys. *Trans. A.I.M.E.* (1935) **117**, 102-117.
13. G. Siebel and H. Vosskühler: Determination of the Solubility of Magnesium in Aluminum. *Zisch. Metallkunde* (1939) **31**, 359-362.
14. K. Riederer: The System Aluminum-magnesium-zinc. *Zisch. Metallkunde* (1936) **28**, 312-317.
15. R. F. Mehl, C. S. Barrett and F. N. Rhines: Studies upon the Widmanstätten Structure, III—The Aluminum-rich Alloys of Aluminum with Copper, and of Aluminum with Magnesium and Silicon. *Trans. A.I.M.E.* (1932) **99**, 203-229.
16. P. Lacombe and G. Chaudron: X-ray Study of the Age-hardening of the Aluminum-magnesium Solid Solution. *Compt. rend.* (1938) **207**, 860-862.
17. J. Calvet, A. Guinier, P. Jacquet and A. Silberstein: Study of the Aging of the Aluminum-magnesium Solid Solutions. *Compt. rend.* (1939) **208**, 1903-1905.
18. A. M. Talbot and J. T. Norton: Age-hardening of Magnesium-aluminum Alloys. *Trans. A.I.M.E.* (1936) **122**, 301-313.

19. G. V. Raynor: The Constitution of the Magnesium-rich Alloys in the Systems Mg-Pb, Mg-Sn, Mg-Ge and Mg-Si. *Jnl. Inst. Metals* (1940) **66**, 403-426.
20. J. C. McDonald: Tensile Properties of Rolled Magnesium Alloys, I—Binary Alloys with Al, Sb, Bi, Cd, Cu, Pb, Ni, Ag, Ti, Sn and Zn. *Trans. A.I.M.E.* (1940) **137**, 430-441.
21. W. Schmidt: Contribution to the Knowledge of the Magnesium-rich Alloys. *Zisch. Metallkunde* (1927) **19**, 452-455.
22. E. Zintl and H. Kaiser: On the Capacity of the Elements to Form Negative Ions. *Zisch. Anorg. Chem.* (1933) **211**, 113-131.
23. J. B. Friauf: The Crystal Structure of Mg₂Pb. *Jnl. Amer. Chem. Soc.* (1926) **48**, 1906-1909.
24. R. Chadwick: The Constitution of the Alloys of Magnesium and Zinc. *Jnl. Inst. Metals* (1928) **39**, 285-300.
25. G. Derge, A. R. Kommel and R. F. Mehl: Studies upon the Widmanstätten Structure, IX—The Mg-Mg₂Sn and Pb-Sb Systems. *Trans. A.I.M.E.* (1937) **124**, 367-378.
26. J. A. Gann: Treatment and Structure of Magnesium Alloys. *Trans. A.I.M.E.* (1929) **83**, 309-332.
27. R. F. Mehl and L. K. Jetter: The Mechanism of Precipitation from Solid Solution—The Theory of Age-hardening. Symposium on Age-hardening of Metals. *Amer. Soc. Metals* (1940) 342-417.
28. F. R. N. Nabarro: The Strains Produced by Precipitation in Alloys. *Proc. Roy. Soc.* (1940) **175-A**, 519-538.
29. A. J. Bradley, W. L. Bragg and C. Sykes: Researches into the Structure of Alloys. *Jnl. Iron and Steel Inst.* (1940) **141**, 63-142.

DISCUSSION

(J. D. Hanawalt presiding)

[This discussion refers also to the paper that begins on page 182]

R. S. BUSK,* Midland, Mich.—I am not quite sure to what the authors attribute hardening upon aging. Is all hardening caused by the coherency stresses? Do the authors have any idea of the critical amounts of disregistry necessary to cause hardening? One would expect a critical range, since zero disregistry could hardly cause strengthening and too much would result in complete separation.

In the Al-10 per cent Mg alloy there is reported only a very small increase in electrical resistivity. This alloy shows extensive hardening. But in the Mg-Pb alloy reported there is also no electrical resistivity increase. This alloy shows very little hardening. Can the authors explain the significance of this?

* Metallurgical Department, The Dow Chemical Company.

It is stated that there are coherency stresses in the Al-Mg system that cause hardening, but that in the Mg-Pb system there are no coherency stresses and thus there is no hardening. How do the authors know about the presence or absence of coherency stresses in these systems?

Is there a correlation between the appearance of the precipitate phase and the possibility of coherency stresses? In the magnesium-base alloys there are, in general, three elements that cause extensive age-hardening—Ag, Al, and Zn. Of these, both the Ag and Zn show the continuous type of precipitation while the Al shows the discontinuous type, with some of the continuous type also present. In the Mg-Al alloys maximum hardening is attained after complete precipitation.

A. H. GEISLER (author's reply).—The discussion by Mr. Busk is directed toward the latter part of our fourth paper of the series, for there we have included a brief study of some magnesium-base alloys. However, most of our general conclusions have been obtained primarily from observations on the precipitation in four aluminum-base alloy systems. In these systems the correlation of property changes with structural alterations shows that hardening occurs during the formation of the coherent transition state. Consequently, as mentioned in the introduction of this paper and also in two previous papers^{2,3} we have concluded that the coherency stresses are the major contributor to precipitation-hardening. Other factors that may influence the mechanical and physical properties during aging are presented on pages 194 to 199.

The amount of disregistry necessary to cause hardening is a rather indefinite quantity, for the amount of disregistry merely governs the size to which the coherent particle can grow; in this sense it is important in determining whether the coherent state can be detected by microscopic and X-ray diffraction methods. We have pointed out that the number of coherent particles is equally important in determining the extent of hardening. Thus, even with a high degree of disregistry, hardening may occur if a large number of very small coherent particles are formed. Insufficient data have been obtained to predict how small

the disregistry must be for the platelets to grow under given conditions to some arbitrary size—large enough to be detected.

The electrical-resistance change and the hardness and strength changes during aging are summations of the changes caused by various simultaneous or consecutive processes.³ While we have attributed hardness and resistance increases to the development of coherency stresses, whether or not the total change will show an increase depends upon the magnitude of the various positive and negative changes as determined by the particular alloy. In this respect, the influence of the coherency stresses on the total change should vary from one property to another.

As explained in the second paper, X-ray diffraction data show that the extent of coherent growth is high in Al-Mg alloys and low with Mg-Pb alloys. Obviously, the magnitude and influence of coherency stresses should vary likewise for an equivalent number of particles. No statement was made denying the presence of coherency stresses in Mg-Pb alloys, for it is very likely that coherent growth to a limited extent occurs in all alloys, although in many cases the particles do not grow to a sufficient size to permit detection.

In regard to Mr. Busk's last question, again we would like to refer him to page 194, where we conclude that "discontinuous precipitation" is not true precipitation but a subsequent reaction whereby a continuous coherent precipitate transforms to the noncoherent equilibrium phase. If this is generally correct, coherency stresses could be present only with a continuous precipitate and maximum hardness will occur when factor one predominates.

L. W. KEMPF,* Cleveland, Ohio.—As one who has followed the development of theories of precipitation-hardening for a number of years, this series of papers is particularly satisfying. It seems to me that a very long step now has been taken toward a rationally tenable theory of precipitation-hardening. I have long felt, and sometimes expressed, at least by implication, that a theory based on critical dispersion was too simple. There are far too many things it did not explain.

When additional data of the type reported in these papers are accumulated, I believe it will be found that a basis has been established for a really quantitative theory of precipitation-hardening.

J. D. HANAWALT,* Midland, Mich.—I should like to echo Mr. Kempf's sentiments. It is certainly very satisfying to see the progress that has taken place over the course of this series of papers.

The era of theorizing is giving way to one of experimentally observing the mechanisms of precipitation, and more fruitful results should follow. The progress is a result of experimentally observing the mechanisms of precipitation. I believe it will be very valuable if the experiments can be continued, particularly in the direction of pure quantitative measurements.

R. M. BRICK,† New Haven, Conn.—These papers, and their predecessor² constitute a most notable clarification of the age-hardening problem, although, naturally, some details remain for future research. For example, does it matter whether the matrix lattice stresses, or perhaps more appropriately, the strains associated with the coherency stage or nonequilibrium precipitate, are compressive or tensile in nature? These two possibilities exist: (1) that the atomic spacing of the equilibrium precipitate is slightly less than that of the corresponding matching plane of the matrix, in which case the nonequilibrium precipitate is in tension and the matrix in compression; or (2) the reverse case. In their previous paper,² the authors calculated a value for the maximum stress sustained by the precipitate during the coherency stage but this stress admittedly is of slight significance in the age-hardening as compared with the corresponding strain in the matrix, which perhaps could be of greater magnitude when it is compressive in nature.

A. H. GEISLER.—Dr. Brick has presented a very interesting question but the answer must await the accumulation of many more data. The best approach that we can now make

* Aluminum Research Laboratories, Aluminum Company of America.

* Director of Metallurgical Dept., The Dow Chemical Company.

† Hammond Metallurgical Laboratory, Yale University.

to the solution is in the comparison of Al-Ag and Al-Zn alloys, where the hexagonal equilibrium phases form as plates parallel to octahedral matrix planes. With the Al-Ag alloy the atomic spacings in the basal plane of the equilibrium phase are 0.73 per cent greater than those in the matrix octahedral plane, while with Al-Zn the spacings are 7.0 per cent less. Thus, the strains in the coherent Al-Ag particles are compressive while those in the coherent Al-Zn particles are tensile; however, because of the large difference in disregistry between the two systems, the major difference in hardening during precipitation quite likely originates in the difference in magnitude of the disregistry and to a much less extent in sign.

Another question of a similar type, the answer to which also must await the investigation of many additional systems before comparable conditions are found to permit the comparison, concerns the dependence of the extent of hardening on the Widmanstätten relations relative to the crystallographic slip relationships. Other factors comparable, would a coherent precipitate on cube planes harden a face-centered cubic metal as effectively or more effectively than coherent platelets on octahedral planes?

C. S. BARRETT.—A peculiar anomaly occurs when one tries to calculate the stresses in the precipitate γ^1 . Assuming certain elastic constants, calculation indicates that strong compressive stresses exist in a precipitated plate parallel to the surface of the plates.² It would appear from this calculation that the precipitate is highly stressed, yet the matrix that is coherent with it is unstressed. Obviously this is impossible.

Portions of the matrix must be stressed. But these portions probably do not contribute to the sharp diffraction lines of the matrix because the stresses change so rapidly with distance. The exact nature of the stresses in the precipitate and the stress distribution in the matrix should be calculable if the true elastic constants of the phases were known. Calculations should make clear why the strained value of the atom spacings in the surface of the precipitate match those of the unstrained matrix; whether, for example, it is possible that the only stress in a precipitated plate is a tensional stress normal to the plate surface, a stress that produces lateral contraction of the atom distances in the surface of the plate just sufficient to match the spacing of the unstressed matrix. Some calculations by Mr. Albert Guy in this laboratory indicate that the elastic constants that would produce this result are not unreasonable values.

Slip and Twinning in Magnesium Single Crystals at Elevated Temperatures

By P. W. BAKARIAN* AND C. H. MATHEWSON,† MEMBER A.I.M.E.

(New York Meeting, February 1943)

THE greater part of the literature on the plastic behavior of magnesium dates back to that active period of research in crystal mechanics immediately following the widespread preparation of isolated metallic crystals large enough for the application of conventional methods of mechanical testing. These investigations, performed on single crystals, revealed an analogy between zinc and magnesium with respect to their fundamental mode of deformation, in the operation of glide and twinning, respectively, on crystallographically similar planes.

Mathewson and Phillips (1928)¹ by

A part of a dissertation presented by P. W. Bakarian to the Faculty of the Graduate School of Yale University in partial fulfillment of the requirements for the Degree of Doctor of Philosophy. Manuscript received at the office of the Institute Dec. 1, 1942. Issued in METALS TECHNOLOGY, April 1943.

* First Lieutenant A. C. Experimental Engineering Section, Metallurgical Unit, Wright Field.

† Professor of Metallurgy, Yale University, New Haven, Conn.

¹ References are at the end of the paper.

‡ The three-index system of notation has been used throughout this paper. This is based upon two axes of equal length along close-packed directions, intersecting at an angle of 120°, and a third axis normal to the plane of the other two. To obtain the four-index system indices for planes, an additional index is supplied between the second and third indices equal to the sum of the first two with the sign changed. Directions (line indices) are given as the smallest integers proportional to coordinate differences, in terms of the above three parameters, between equivalent points lying on the line. On this basis, the line indices of a digonal axis I, normal to the plane (210) are [100]. A second digonal axis I, 60° from the first, is normal to (110) and also has the line indices [110]. Similarly, the line indices of the intermediate digonal axis II, are [210].

geometrical analysis identified the {102}‡ plane in magnesium as the twinning plane. Schiebold and Siebel (1931)² confirmed this twinning plane, established the basal plane as the plane of slip, and a digonal axis I as the slip direction. They also reported twin formation in a secondary role on the {101} plane.

Schmid (1931)³ summarized and discussed the earlier evidence and presented the results of his own experiments on the effect of temperature and small amounts of soluble elements. From X-ray studies on extended wire single crystals, he concluded that slip along the basal plane in the direction of the digonal axis I closest to the stress direction was the sole slip system operating at atmospheric temperature. This conclusion was based on experiments with crystals of many different orientations relative to the stress axis. Special attention was directed to the basal plane and the digonal axis I, as the plane and direction of greatest atomic density. Determinations of resolved shear stress at the onset of plastic yielding—i.e., the critical resolved shear stress—were also made; the average of these calculations showing 82.9 grams per sq. mm. This value varied only slightly up to 300°C. at which temperature it was found to decrease to 70.5 grams per sq. mm. The extension of his crystals at temperatures above 225°C. further disclosed the presence of new slip systems. After the origence specimens of circular section had been

transformed to flat ribbons by basal slip, the width of these ribbons was observed to decrease laterally with further extension until fracture occurred at some point. This lateral constriction, coupled with the X-ray evidence revealing a change in the direction of slip from one digonal axis to another, 60° removed, led to the prediction of a new operative slip system. Further X-ray procedure aimed at determining the new plane of slip aided only in the possible elimination of the first-order prismatic plane as the operative slip plane. The slip bands formed on the surface of the crystal at this stage were very weak, because of a faulty original surface and the closely knit basal slip bands. Schmid decided, however, that one of the pyramidal planes, either $\{101\}$ or $\{102\}$, must be responsible for this phase of the extension.

Alternating-stress fatigue tests have also been made by Schmid and Siebel⁴ using single crystals of magnesium at atmospheric temperature. As in the static tests, slip along the $\{001\}$ plane and twinning on the $\{102\}$ plane were the mechanisms of deformation, the fatigue fractures taking place along the basal plane $\{001\}$, the prismatic planes $\{100\}$, or the pyramidal planes $\{101\}$ and $\{102\}$. In like manner, the series of investigations carried out by Schmid and collaborators⁶ on the effect of solid-solution additions disclosed only a strengthening effect in the predetermined mechanisms of deformation.

While previous investigations reveal the deformational characteristics of magnesium at atmospheric temperature in considerable detail, they are found to be incomplete with respect to stressing at elevated temperature. This paper presents the results of experiments designed to supply this deficiency. The basic plan of work consisted in stressing crystals of all possible orientations at a temperature just below that at which the applied rate of stressing would cause recrystallization

of the specimen during the test. X-ray and microscopic analyses were then used in determining the mechanism of plastic deformation. Although both tension and compression stressing were used, the time available allowed comprehensive study of the latter only.

X-ray determination of the movement of the crystal axes relative to the direction of stress application was used for the indirect solution of the operative slip planes and direction. If the axis of a single-crystal specimen is plotted in a standard stereographic projection with the pole of the basal plane at center of the primitive circle, elongation by tension stressing will move this axis along the great circle through the point of origin and the crystallographically significant pole acting as the *direction* of slip; on the other hand, reduction in thickness by compression stressing will move the specimen axis along the great circle through the point of origin and the pole of the *plane* upon which slip is taking place. Supplementing this, microscopic measurements of the angular relationships existing between the markings formed on the surface of the tension specimens aided in the identification of the *planes* operating as slip planes.

A combination of X-ray and stereographic analysis was also applied in fixing the twinning elements. Owing to the difference in axial ratio, the dimensional effects of twinning in magnesium are somewhat different from those in zinc. Depending upon the orientation of the original crystal and the plane on which the twinning takes place, the length of a specimen (or dimension along the stress axis) may either increase or decrease because of twinning. The diagram in Fig. 1 shows the relation between crystal orientation and length change during $\{102\}$ twinning in a manner similar to that used by Schmid⁶ for zinc. Depending on the location of the stress axis in one or another of the triangles *A*, *B*, *C* or *D*, twinning on one of the six

possible $\{102\}$ planes (I to VI in the diagram of Fig. 1) may lead to extension or contraction as noted in the caption. If the twinning were to take place on $\{101\}$

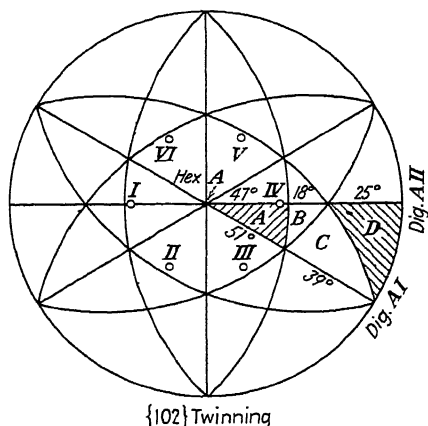


FIG. 1.—CHANGES IN LENGTH OF VARIOUS CRYSTAL DIRECTIONS CAUSED BY $\{102\}$ TWINNING IN MAGNESIUM.

I–VI are poles of twinning planes.

Area A contains all directions in which twinning on I–VI causes extension.

Area B contains directions in which twinning on II, III, V and VI cause extension; twinning on I and IV, reduction.

Area C contains directions in which twinning on II and V causes extension; twinning on I, III, IV and VI, reduction.

In area D, twinning on I–VI causes reduction in length.

planes instead of $\{102\}$ planes, the respective dimensional changes would reverse those caused by $\{102\}$ twinning, setting up a condition analogous to that found in zinc except for the slight differences in the areas of the various triangular fields.

EXPERIMENTAL PROCEDURE

The material used in the preparation of the single crystals was high-purity magnesium of the following spectrographic analysis: 99.98+ per cent Mg, 0.001 per cent Fe, 0.001 per cent Al, 0.001 per cent Si, and 0.010 per cent Pb. To maintain this degree of purity and to meet the particular

melting requirements of magnesium, a modification of the Bridgman⁷ method of casting single crystals was developed. Vacuum melting and hydrogen-atmosphere casting in a mold bored from a standard 1-in. Acheson graphite electrode were found best suited to the elimination of oxidation, possible flux contamination, porosity and excessive sublimation of the magnesium. Enclosing the mold in a special chamber constructed from standard 1-in. pipe and suitable fittings made possible the vacuum and controlled-atmosphere technique. A rate of lowering of $\frac{1}{8}$ in. per hour out of a furnace controlled to 60° above the melting point of magnesium ensured a single crystal in four out of five trials.

The back-reflection Laue method for determining crystal orientations as described by A. B. Greninger⁸ was used throughout the investigation. The angles between crystal planes in the hexagonal magnesium lattice were calculated from equations presented by Ford,⁹ using the axial ratio 1.624.¹ Using these angles and the Greninger net, the various reflections in the X-ray patterns were identified and the orientations stereographically plotted.

Compression Procedure

Extreme care was found necessary in preparing compression specimens from the cylindrical single-crystal castings. One of two procedures of cutting specimens was followed throughout. In the first, the position of the crystal axes relative to the long axis of the casting fixed the orientation of the compression specimen produced, since the cutting was perpendicular to the long axis. The cylindrical crystal was held centered inside a thin-walled brass tube having an inside diameter $\frac{3}{16}$ in. larger than that of the crystal, and molten picein poured into the annular space. On cooling, the brass tube was firmly clamped in the vise of a milling machine. With a packing of dry ice about the tube, and a slow cutter feed, small disks with parallel sides were

obtained without any deformation aside from that on the surface layers.

To cut compression specimens of particular orientations not available in the repertoire of castings, a second procedure was followed. Two properly squared blocks of soft wood, about 1 by 3 by 10 in., were nailed together and a hole of diameter slightly less than that of the casting was drilled symmetrically to the surface of contact of the blocks. A cylindrical single crystal of predetermined orientation placed in this wooden holder, and nailed firmly, could be sawed to samples of the desired thickness. Any particular orientation of the specimen could be obtained in this manner by performing the necessary rotation of the cylindrical crystal and selecting the proper angle of the cutting plane relative to the long axis. Very slow hand feeding on a low-speed band saw carrying a new blade made possible the cutting of specimens of all orientations except those in which the basal plane formed angles greater than 82° to 85° with the cut surface of the specimens. No available means of producing twin-free specimens in which the basal plane was approximately perpendicular to the surface of cutting, could be found. In the many attempts, twins were formed, passing through the entire section of the samples. When specimens other than right-angled cylinders were used, they were carefully cut and filed to rectangular sides so as to obtain a constant cross section over the entire height of each specimen. The final thickness of the specimen was usually 0.18 to 0.20 in., a thickness found to be superior by G. I. Taylor¹⁰ in his work on the effect of friction at compression surfaces.

To establish uniform distortion in the compression stressing, a compression-stressing unit built by M. R. Pickus¹¹ from a design of F. Wever¹² was used. Although originally designed for compression combined with unilateral flow, its application to the present task was made possible by

the smaller dimensions of the specimens here used. A hardened steel plunger is allowed only vertical movement, because of four constricting steel walls. This permits movement of the highly polished plunger face parallel to a similarly polished base plate located at the base of the steel walls around the plunger. In preliminary room-temperature runs, the apparatus produced a uniform distortion with minimum barreling of the cylindrical specimens. These compressions were carried out in a series of steps, with frequent lubrication of the compression surfaces with a mixture of castor oil and flake graphite.

For the runs at temperatures above atmospheric, the described compression unit was immersed in an oil bath heated by a nichrome winding. The oil was of the type employed for high-temperature heat transfer and could be used up to 340°C . without excessive fuming or breakdown. This oil served the double purpose of maintaining close temperature control and lubricating the compression surfaces. Bath temperature was controlled by an outside variable-resistance bank, and with frequent agitation of the oil a temperature accuracy of $\pm 1^\circ\text{C}$. was obtained. Under test conditions, the entire compression unit, except for one third of the plunger, was submerged in oil. After the temperature of the bath had reached the desired value, the plunger was removed and the specimen quickly placed on the platform of the unit. After the plunger had been replaced and sufficient time allowed for equilibrium, the loading was begun. Three or four loadings with intermediate removals for thickness measurements was the general procedure adopted. All loadings in compression were carried out on a Southwark-Emery hydraulic machine.

Tension Procedure

The many attempts at lathe machining of tension specimens from cylindrical single-crystal castings resulted in excessive bend-

ing strains. Search for a more appropriate method of preparation led to the development of an etching technique for producing tension test bars with a highly polished

tensile machine impractical. The tension loading equipment devised by Miller¹³ was found to satisfy the present conditions, with suitable modifications. In this equip-

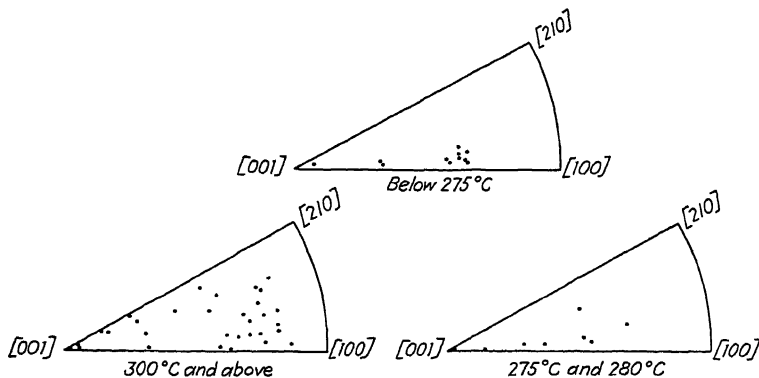


FIG. 2.—ORIGINAL ORIENTATIONS OF ALL COMPRESSION SPECIMENS BEFORE STRESSING.

surface. To obtain the best results, it was found desirable to start with a cylindrical casting as free as possible from surface roughness. To this end, hand smoothing of the surface of the casting with No. 1 emery paper was generally practiced. The cylindrical castings were then cut to length, and the end positions beyond the central gauge length covered with a layer of picein. Etching with constant agitation in a 25 per cent hydrochloric acid solution, with intermediate polishing on No. 1 paper, brought the reduced cross section to within 0.05 in. of the desired diameter. A final etch in freshly prepared 25 per cent hydrochloric acid solution, immediately followed by washing in water and drying in alcohol, resulted in a smooth and highly polished surface similar to that obtained by careful metallographic polishing techniques. Desirable, even fillets were formed at the ends of the reduced gauge length when the picein had been sharply cut away at these positions previous to the etching process.

The very small loads required in the extension of magnesium single crystals, coupled with the need for a specimen heating arrangement, made use of the standard

ment, loading was accomplished by flow of sand, at a controlled rate, into a bucket suspended directly from the specimen.

Testing temperatures of over 300°C. were attained by means of a nichrome heating coil placed around the test bar. An insulating iron shield covered on the inside with highly reflecting aluminum foil was built to enclose the heating coil. However, this insulating shield and the heating coil were designed so as to allow observation along the length of the specimen during testing. Temperature control was accomplished by variation of the power input and measurement of temperature through the use of fine thermocouples placed in contact with the test bar just outside of the reduced section.

EXPERIMENTAL RESULTS

Compression

The original orientations of the 50 specimens studied in compression are shown in Fig. 2. The conventional method of orientation notation is adhered to; that is, the pole of the basal plane [001] has been rotated to the center of the primitive circle, and the position of the normal to the compres-

TABLE 1.—*Summary of Experimental Conditions in Compression Tests*
TEMPERATURE RANGE: ATMOSPHERIC TEMPERATURE TO 238°C.

Specimen No.	Reduction No.	Reduction in Thickness, Per Cent	Total Load, Lb.	Observed, Deg.		Predicted Angle θ , Deg.	Temperature of Reduction, Deg. C.
				Angle θ	Angle η		
BR-2-1.....	0	0	0	36.0	3		Room
	1	24.2	660	26.0	3	26.5	Room
	2	25.4	3,300	18.7	3	19.3	Room
BR-2-3.....	0	0	0	34.0	3		Room
	1	20.7	350	25.5	5	26.2	Room
	2	21.2	1,850	20.5	4	20.5	Room
	3	16.9	6,000	16.5	6	16.8	Room
	4	13.9	11,200	15.0	7	16.1	Room
BR-5-1.....	0	0	0	64.0	5.5		Room
	1	20.2	2,230	46.5	5.5	48.0	Room
BR-5-2.....	0	0	0	65.5	3		Room
	1	15.6	375	52.7	4.5	50.1	Room
	2	19.9	2,050	38.7	3	39.5	Room
	3	11.1	3,970	32.0	2.5	34.3	Room
BR-1-5.....	0	0	0	8.0	12		Room
	2	4.2	1,800	8.0	12	Cleaved	Room
BR-5-3.....	0	0	0	66.0	3.5		94
	1	20.0	550	49.3	4.3	47.0	94
	2	12.7	2,400	40.0	6.0	39.7	94
BR-5-4.....	0	0	0	60.0	4.0		94
	1	14.65	310	46.5	2.5	47.7	94
	2	15.12	1,640	39.7	3.5	39.0	94
BR-5-5.....	0	0	0	53.5	5.3		200
	1	23.3	600	43.5	6.3	43.3	200
BR-5-6.....	0	0	0	60.5	3.0		200
	1	21.8	700	42.7	6.0	42.9	200
	2	31.4	2,500	31.5	5.0	27.9	200
BR-5-7.....	0	0	0	63.5	7.0		228
	1	11.0	700	} Profuse twinning			228
	2	8.4	1,500				228
BR-5-8.....	0	0	0	65.7	5.7		238
	1	20	850	49.7	7.0	46.9	238
	2	21.1	2,200	33.0	4.0	31.7	238

TABLE 2.—*Summary of Experimental Conditions in Compression Tests*
TEMPERATURE RANGE: 275° TO 280°C.

Specimen No.	Reduction No.	Reduction in Thickness, Per Cent	Total Load, Lb.	Observed, Deg.		Predicted Angle θ , Deg.	Temperature of Reduction, Deg. C.
				Angle θ	Angle η		
BR-8-2.....	0	0	0	54.7	19.0		275
	1	16.3	500	37.0	18.0	43.0	275
BR-8-1.....	0	0	0	56.5	4.0		275
	1	14.1	550	46.5	1.5	45.9	275
BR-6-3.....	0	0	0	54.5	5.7		275
	1	13.6	700	47.5	6.0	44.7	275
BR-3-1.....	0	0	0	39.0	5.0		275
	1	24.3	500	31.7	1.0	27.7	275
BR-2-10.....	0	0	0	31.7	4.5		275
	1	24	415	22.7	3.0	23.5	275
BR-6-2.....	0	0	0	14.0	2.5		275
	1	14.1	2,000	14.0	2.5	Cleaved	275
BR-2-5.....	0	0	0	0.5	3.0		280
	1	27.1	1,200	0.5	2.0	Cleaved	274
BR-6-4.....	0	0	0	67.7	8.5		Profuse twinning
	1	12.3	800	51.0	3.0	54.5	Profuse twinning

TABLE 3.—*Summary of Experimental Conditions in Compression Tests*
 TEMPERATURE RANGE: 300° to 340°C.

Specimen No.	Reduction No.	Reduction in Thickness, Per Cent	Total Load, Lb.	Observed, Deg.		Predicted Angle θ , Deg.	Temperature of Reduction, Deg. C.
				Angle θ	Angle γ		
BR-5-9.....	0	0	0	65.5	5.5		300
BR-2-8.....	1	16.0	600	50.7	3.5	49.8	300
	0	0	0	78.5	20		300
BR-6-6.....	1	13.4	690	Profuse twinning			300
	0	0	0	68.5	11.5		300
	1	14.8	700	52.5	11.3	51.6	300
	2	7.9	900	47.5	10.0	46.5	300
	3	3.7	1,200	43.0	11.3	41.5	300
BR-2-12.....	0	0	0	71.3	3.0		300
	1	15.5	400	45.0	2.0	53.3	300
BR-6-7.....	0	0	0	74.5	10.5		300
	1	9.9	600	Profuse twinning			300
	2	9.3	950				300
	3	12.4	1,400				300
BR-1-2.....	0	0	0	74.5	18.0		300
	1	9.1	1,200	55.5	20.0	61.5	300
	2	8.4	1,980	Profuse twinning			300
BR-2-9.....	0	0	0	81.5	6.5		300
	1	36.9	900	Profuse twinning			300
BR-2-6.....	0	0	0	35.0	1.3		300
	1	25.1	1,200	31.5	0.3	31.0	300
BR-2-4.....	0	0	0	62.0	2.0		300
	1	21.9	1,200	Profuse twinning			300
BR-6-1.....	0	0	0	64.0	6.3		300
	1	11.9	600	Profuse twinning			300
	2	20.5	1,500	37.5	6.0	38.7	300
BR-1-4.....	0	0	0	74.7	13.5		300
	1	6.5	400	63.0	11.0	64.5	300
	2	6.3	830	Profuse twinning			300
BR-8-3.....	0	0	0	79.0	6.3		300
	1	0	0	Profuse twinning			300
BR-1-6.....	0	0	0	71.0	5.5		300
	1	12.9	800	Profuse twinning			300
BR-11-2.....	0	0	0	78.0	6.0		300
	1	14.3	500	Profuse twinning			300
BR-C-10-III.....	0	0	0	5.5	10.0		300
	1	16.2	1,250	8.0	10.0	Cleaved	300
BR-2-11.....	0	0	0	6.0	13.0		300
	1	5.0	1,070	6.0	13.0	Cleaved	300
BR-C-10-V.....	0	0	0	59.0	26.0		300
	1	12.0	600	48.0	25.0	49.0	300
BR-C-10-VI.....	0	0	0	58.0	16.0		300
	1	15.1	550	44.0	16.0	46.1	300
BR-C-10-VII.....	0	0	0	62.0	21.0		300
	1	10.5	700	54.0	24.0	51.8	300
BR-C-10-II.....	0	0	0	29.0	30.0		300
	1	31.9	500	16.5	30.0	19.3	300
BR-C-10-XI.....	0	0	0	18.5	24.5		310
	1	38.4	1,900	11.5	23.0	11.2	310
BR-C-10-I.....	0	0	0	31.5	24.7		310
	1	22.2	500	25.0	23.3	24	310
BR-C-11-I.....	0	0	0	34.0	12.0		310
	1	19.2	500	20.0	17.6	26.3	310
BR-C-7-I.....	0	0	0	48.0	20.0		310
	1	36.4	500	27.0	20.0	28.2	310
BR-11-9.....	0	0	0	65.5	1.5		310
	1	15.8	350	49.5	2.0	49.9	310
BR-6-9.....	0	0	0	76.0	12.5		310
	1	18.7	900	Profuse twinning			310
	2	7.9	1,400				310
BR-C-10-X.....	0	0	0	16.5	26.7		315
	1	30.6	1,100	16.5	27.0	Cleaved	315
BR-11-6.....	0	0	0	72.5	10.3		320
	1	7.8	300	Profuse twinning			320
BR-11-4.....	0	0	0	74.3	6.5		320
	1	11.5	600	Profuse twinning			320
BR-1-3.....	0	0	0	75.0	19.0		320
	1	8.73	1,600	Profuse twinning			320
BR-C-10-IV.....	0	0	0	2.3			340
	1	18.6	1,010	2.3	Cleaved		340

sion surface of each specimen is represented by a heavy dot in the basic stereographic triangle formed by the directions $[001]$, $[210]$ and $[100]$. In the upper triangle are plotted the positions of the compression axis for tests at room temperature, 94°C ., 200°C ., 228°C ., and 238°C . The lower right triangle includes all specimens tested at 275°C . and one at 280°C . The remaining triangle contains the orientations of specimens stressed at 300°C . or 310°C . and the few others carried out at higher temperatures for special purposes.

The distribution of orientations in the 300°C . group is seen to cover virtually the entire triangular field except for a small area representing orientations in which the basal plane is nearly perpendicular to the surface of compression (within a range of 10°). In every attempt to prepare specimens with these orientations, profuse and deeply penetrating twins resulted. A combination of cutting-stress characteristics and ability to twin on all possible $\{102\}$ twinning planes under compression makes it very difficult to cut specimens in this particular range of orientation.

A complete tabulated summary of the experimental conditions in these compression tests is given in Tables 1, 2 and 3. The angles fixing the position of the compression axis are given as η and θ ; where η is the angle between the $[100]$ direction and the projection of the compression axis on the (001) plane, and θ the angle between the compression axis and the pole of the basal plane, $[001]$. The calculated shift of the compression surface normal relative to the crystal axes was found for each specimen, assuming that translation parallel to the basal plane was the only mechanism active during the stressing. These calculations were based on the familiar sine law⁶ adapted to compression:

$$\frac{H_1}{H_2} = \frac{\sin \theta_1}{\sin \theta_2}$$

Where H_1 and H_2 are, respectively, the heights (or thicknesses) of the specimen before and after compression; and θ_1 and θ_2 , the angles along a great circle

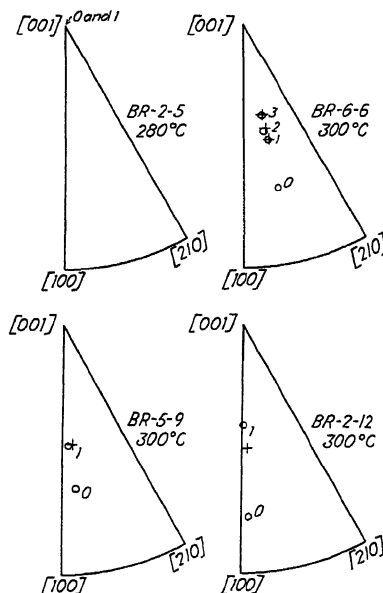


FIG. 3.—STEREOGRAPHIC DIAGRAMS SHOWING ORIENTATION CHANGES RESULTING FROM COMPRESSION STRESSING.

Open circles denote positions of axis of compression found by X-ray analyses; crosses denote predicted positions of this axis after various increments of reduction calculated by assuming translation on (001) plane as the only operative mechanism of deformation.

between the axis of compression and the normal to the slip plane, before and after compression, respectively.

These calculated positions of the compression axis relative to the $[001]$ direction are also included in the tables wherever the agreement between calculated and observed orientations indicates the prevalence of this mode of deformation.

Stereographic diagrams have been made to show the orientation changes in all the specimens. Because of lack of space only a few illustrative cases are included herein. For specimens in which twinning was not active, the shift of the compression

axis relative to the crystal axes is presented in basic triangles formed by the $\{001\}$, $\{100\}$ and $\{210\}$ directions. Fig. 3 shows the movements in specimens numbered BR-2-5, BR-6-6, BR-5-9 and BR-2-12. The orientation changes found in the specimens showing twinning, or twinning and glide combinations, are presented in basic stereographic circles in which the center of the circle represents the axis of compression. The locations of the $\{001\}$ pole and the associated zone circle containing the pole of the operative twinning plane are shown for each specimen previous to deformation, by a small solid circle and the dotted projection of a great circle, respectively. The new positions of the $\{001\}$ pole following increments of reduction, 1, 2, 3, etc., are as noted in the individual diagrams. [The pole of the twinning plane (not marked), of course, is located midway between the original and twinned $\{001\}$ poles on the dotted great circle.] Because of lack of space, only illustrative cases are included. In Figs. 4, 5, 6, 7, 8 and 9 are plotted the movements observed in specimens BR-11-6, BR-6-9, BR-2-8, BR-6-1, BR-6-4 and BR-2-9.

The results of the compression investigation may be divided into three parts according to the three means of accommodation to compressive reduction in thickness shown by the specimen. Under compressive stressing at 300°C ., these three modes of accommodation are determined by the orientation of the specimen before deformation. Depending on whether the axis of compression falls within a field of the basic triangle, 0° to 20° from $\{001\}$,* or a field, 60° to 90° from $\{001\}$,

* For simplification, the following designations will be used, subsequently:

Basal Field, or field of basal compression: Specimen orientations having the compression axis located in the field of the basic stereographic triangle included between $\theta = 0^{\circ}$ to 20° and $\eta = 0^{\circ}$ to 30° .

Prismatic Field, or field of prismatic compression: Specimen orientations having the compression axis located in the field of the basic

or in an intermediate position, the following mechanisms have been found to operate, respectively:

a. Fracture of the specimen along $\{101\}$, or $\{001\}$ slip followed by fracture along $\{101\}$.

b. Twinning on $\{102\}$, or $\{001\}$ slip and $\{102\}$ twinning, leading to crystal break-up.

c. Basal $\{001\}$ slip leading to crystal break-up.

Orientations in Central Field.—Within the central field of orientation, the absolute dominance of basal slip has been conclusively established. The series of tests made at various temperatures ranging from atmospheric temperature up to 310°C . on specimens having nearly similar original orientations, θ about 60° , η about 4° , exhibited only basal slip. These comprise 11 specimens, as follows: (data listed in the tables): BR-5-1, BR-5-2, BR-5-8, BR-5-9, BR-5-4, BR-5-3, BR-8-1, BR-11-9, BR-5-5, BR-5-6, BR-6-3. The observed shift of the compression axis is found to be in good agreement with the theoretically predicted shift in each case.

Specimens with initial orientations spread throughout this central orientation field were tested at 300°C . and 310°C ., including several at 275°C . (13 specimens in all): BR-2-10, BR-2-12, BR-C-10-VI, BR-C-10-XI, BR-3-1, BR-2-6, BR-C-10-VI, BR-C-10-I, BR-C-11-I, BR-6-6, BR-C-10-V, BR-C-10-II, BR-C-7-1. These also display basal slip without further complication, the theoretically predicted axis shift matching the observed shift within the experimental error. The logical conclusion that may be drawn, therefore, is that these experiments establish the complete dominance of basal, $\{001\}$, slip

stereographic triangle included between $\theta = 60^{\circ}$ to 90° and $\eta = 0^{\circ}$ to 30° .

Central Field: Specimen orientations having the compression axis located in the remaining intermediate field of the basic stereographic triangle.

as the only operating mechanism of deformation in the range of temperature from room up to 310°C . when the compression axis lies in the central orientation field of the basic stereographic triangle.

Orientations in Basal Field.—In specimens oriented with the compression axis within the empirically designated basal field, fracture along $\{101\}$ planes or basal slip followed by fracture along $\{101\}$ are the observed deformation mechanisms. The existence of a critical θ_f value as the boundary orientation dividing the sphere of activity of basal slip, and $\{101\}$ plane fracture has been established from the results with 8 specimens: BR-C-10-IV, BR-C-10-I, BR-2-11, BR-2-10, BR-C-11-I, BR-C-10-II, BR-C-10-III, BR-2-5.

Specimens oriented so that the θ values are less than the critical θ_f value will fracture without any previous slip; whereas, at orientations greater than θ_f , basal slip will operate to bring the orientation to θ values equal to or less than θ_f , at which condition fracture will occur. In the temperature range 275° to 315°C ., this critical θ_f value was found to lie between 11° and 16° . This angular range is probably related to the initial dimensions of the specimens. Variations in η values of initial orientation appear to have little or no effect upon the critical θ_f value; however, the number of tests carried out is not sufficient to conclusively substantiate this conclusion. Tests performed at 340°C . and at room temperature show the same fracture phenomenon and point toward its possible existence, regardless of the testing temperature. Several of the cleaved specimens displayed basal slip bands along their edges, proving the activity of basal slip prior to fracture. Here again, in this field of orientation, no evidence was observed that could point to active slip on any plane other than the basal.

Orientations in Prismatic Field.—Specimens with basal planes at angles greater than 60° to the compression surface—i.e.,

the designated prismatic field of orientation—showed profuse $\{102\}$ twinning and basal slip in tests through the temperature range 300° to 320°C . Since twinning takes place in heavy plates or large lamellae of the original specimen, any additional mechanism of deformation following the twinning, must of necessity be operative in the twins and in the interstitial regions of primary orientation occupying a much smaller volume. Such partitioning of the original single crystal into small sections, in spite of a definitely observed preference of twinning to one pair of planes only, results in the entrance of severe lattice distortion at early stages in the reduction. For this reason, a complete analysis of the mechanism of deformation in these specimens was not easily performed. Nevertheless, from the many X-ray photograms taken in regions where lattice distortion was not excessive, definite conclusions could be drawn concerning the general mode of deformation active in specimens oriented within this prismatic field.

X-ray analysis of the 16 specimens initially so oriented disclosed various combinations of $\{102\}$ twinning, basal slip in regions of original orientation and basal slip in the twinned material. The stereogram of specimen BR-11-6 (Fig. 4) shows the pole of the (001) plane in its initial orientation as a solid circle, and in its rotated $\{102\}$ twin position as a cross. The open circles denote the plotted positions of the same poles transferred from Laue photograms after the designated increment of reduction. The proximity of the $[001]$ pole of the twinned original orientation to that actually plotted from X-ray photograms taken after the effected reduction of 7.8 per cent (see Table 3) proves without doubt the presence of $\{102\}$ twinning.

The maximum reduction in thickness due to $\{102\}$ twinning in the most favorable orientation may be calculated from the Schmid and Boas formula,⁶

$$d = \frac{l_1}{l_0} = \frac{-s}{2} + \sqrt{\frac{s^2}{4} + 1}$$

and the reduction in this crystal, from the general formula for length change in the sense of compression, viz.,

$$\frac{l_0}{l_1} = \sqrt{1 + 2S \sin \chi_0 \cos \lambda_0 + S^2 \sin^2 \chi_0}^*$$

These operations give a maximum per-

whence $(90 - \chi_1) = \text{approx. } 32^\circ$, and the rotation, approximately 2° .

Thus, during the compression of this specimen an axial contraction $\left(\frac{l_1}{l_0}\right)$ of 0.946 occurs in the twin layers and this was presumably accompanied by the small hardly measurable axis shift (twinning plane towards compression plane) of about

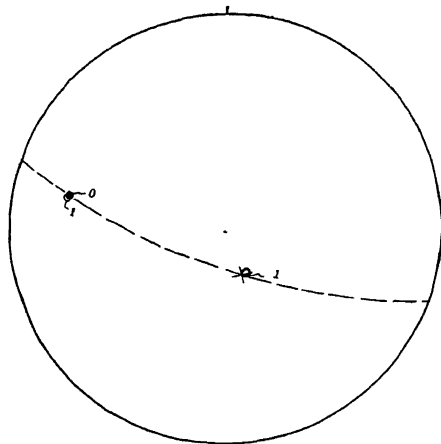


FIG. 4.

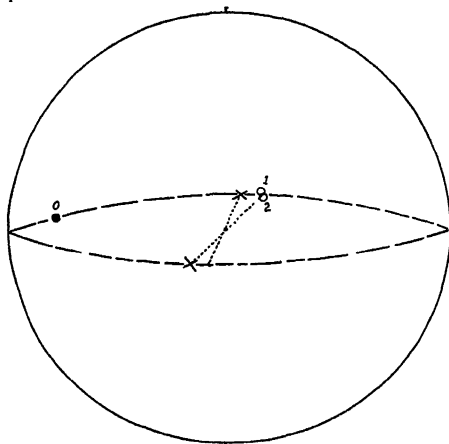


FIG. 5.

FIGS. 4 AND 5.—ORIENTATION CHANGES IN SPECIMENS BR-11-6 AND BR-6-9, RESPECTIVELY.

Compression axis at center of projections. Solid circles are original $\{001\}$; crosses are $\{001\}$ rotated from original orientation by twinning on $\{102\}$; open circles are observed $\{001\}$ after reductions.

centage reduction of approximately 6.4 and a reduction of approximately 5.4 per cent for the present crystal. The formulas give length change due to twinning without the reorientation that would be necessary to keep the compression axis normal to the surface plane of the crystal. For a given compressive length change, this change of angle is derived from the usual sine relationship: in the present case,

$$\frac{l_1}{l_0} = 0.946 = \frac{\sin (90 - \chi_1)}{\sin (90 - \chi_0)} = \frac{\sin (90 - \chi_1)}{\sin 34^\circ}$$

* In these formulas, s , the value for the amount of shear in magnesium twin gliding, is 0.1317, according to E. Schmid.³ The angles between axis and twinning plane and direction respectively, χ_0 and λ_0 , derived from the original data on this crystal (Table 3), are 56° and 61° .

2° . Since the total contraction $\frac{l_1}{l_0}$ sustained by the crystal was 0.922 (corresponding to 7.8 per cent), a final stage after twinning of $\frac{0.922}{0.946}$ (corresponding to approximately 2.5 per cent) was effected in the twin layers by some appropriate slip mechanism. Assuming this to be slip on the reorientated twin basal planes, the rotation (of these planes toward the compression plane), calculated from the sine relationship, would be approximately half a degree.*

* The angle between the axis and the reorientated basal plane of the twin is found to be 66° , whence

$$\frac{l_2}{l_1} = \frac{0.922}{0.946} = \frac{\sin (90 - \chi_2)}{\sin 24^\circ}$$

Thus $(90 - \chi_2) = 23^\circ 21'$ and the rotation = approximately half a degree.

These two calculated rotations are too small to permit any critical evaluation of the plotted points in Fig. 4, but this analysis will be of value in generally inter-

this time in spite of a very considerable compression of the specimens. The position of the original basal pole, after compression, was not determined. Doubtless it

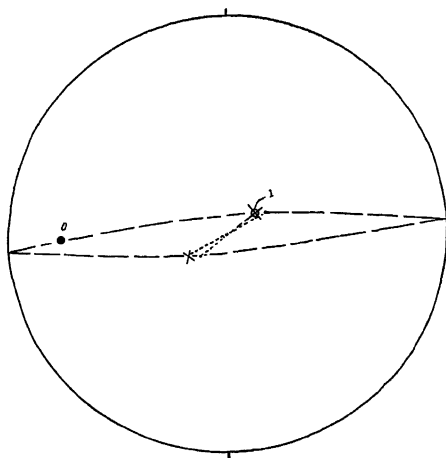


FIG. 6.

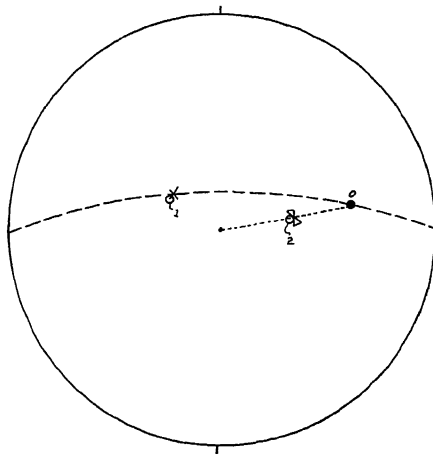


FIG. 7.

FIGS. 6 AND 7.—ORIENTATION CHANGES IN SPECIMENS BR-2-8 AND BR-6-1, RESPECTIVELY.

Compression axis at center of projections. Solid circles are original $[001]$; crosses are $[001]$ rotated from original orientation by twinning on $\{102\}$; closed crosses are predicted $[001]$ positions assuming basal glide; open circles are observed $[001]$ after reductions.

preting the results of the various experiments on prismatic compression.

Specimens BR-6-9 and BR-2-8 illustrate the differences in orientation caused by twinning on each of the two $\{102\}$ planes in the same zone. In the diagrams of Figs. 5 and 6, the relation between twins of this kind is shown by carrying the polar axis of each twinned (001) plane as a full diameter through the center of the projection to the corresponding pole on the half of the zone circle located in the opposite hemisphere. In BR-6-9, the observed orientation of the twin, plotted from the spectrograms of this specimen as noted by the open circles labeled 1 and 2, agrees quite well with the "negative" basal pole of one of the associated twins. On the other hand, the observed orientation in BR-2-8 coincides with the pole of the other twin. Here again, the twinned position of the basal plane remains sensibly constant,

shifted in normal manner toward the compression pole.

Immediate $\{102\}$ twinning, followed by basal slip and rotation in the untwinned sections are the observed deformational mechanisms operating during the compression of specimens BR-6-1, BR-1-4, BR-1-2 and BR-6-4. The stereograms of these specimens point to this conclusion, first by the proximity of the observed basal pole (open circle) to the basal pole of the original orientation in twinned position (cross on great circle), and second by the axis shift found in the untwinned regions. This is illustrated by the diagrams of specimens BR-6-1 and BR-6-4, Figs. 7 and 8. The approximate agreement between the observed and calculated twin orientations suggests their formation immediately upon stressing and offers poor evidence of a conventional axis shift due to basal slip in the twinned regions. The predicted

movement of the basal pole, based on a hypothetical assumption of basal slip in the original untwinned crystals, and evaluated from the observed reduction, is

$$\frac{l_1}{l_0} = 0.9 = \frac{\sin \theta_1}{\sin 25^\circ}$$

whence

$$\theta_1 = 22\frac{1}{3}^\circ$$

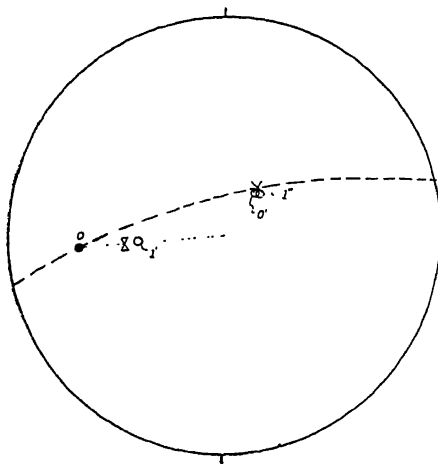


FIG. 8.

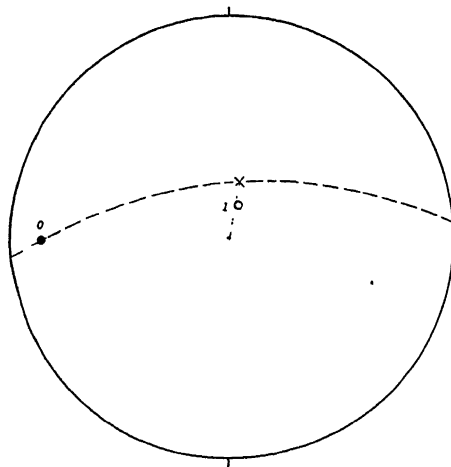


FIG. 9.

FIGS. 8 AND 9.—ORIENTATION CHANGES IN SPECIMENS BR-6-4 AND BR-2-9, RESPECTIVELY.

Compression axis at center of projections. Solid circles are original $[001]$; crosses are $[001]$ rotated from original orientation by twinning on $\{102\}$; closed cross is predicted $[001]$ assuming basal slip in original orientations; open circles are observed $[001]$ after reduction.

plotted as a closed cross on the dotted line connecting the compression axis and the basal pole of the original crystal. The agreement between this calculated shift and that observed is better than would be expected in the presence of the profuse twinning observed.

In these orientations the angle between the reoriented basal plane and the compression surface is not large enough to give clear indication in the diagrams of a conventional axis shift due to basal slip in the twin for the corresponding moderate reductions that give the best X-ray data owing to the lack of excessive lattice distortion. Thus, the sine law for length change corresponding to a reduction of 10 per cent after twinning by slip in a twin whose basal plane is inclined 25° to the compression plane shows a rotation of less than 3° :

However, as noted above, the observed locations of the reoriented basal planes are not consistent with the hypothesis of conventional slip and rotation in the twins and the possibility of basal slip in the twin, *without rotation*, therefore is suggested as a likely mechanism of adjustment between twin and original crystal during compression in a limited range of orientations.

Slip on the basal plane in the $\{102\}$ twinned regions, detected by the conventional axis shift, was a characteristic feature of the deformation in 7 of the 16 specimens oriented in the prismatic field. The most pronounced example of this condition is found in specimen BR-2-9. Twinning of the original crystal would move the basal pole to the position marked by the cross of Fig. 9, and basal slip in this twin would then move this

[001] pole along the dotted line toward the compression axis at the center of the basic circle. The observed position of the [001] pole in the twinned sections of BR-2-9 is located midway on the dotted line. A theoretical calculation of the orientation change accompanying such a deformation can be made by assuming transformation of the entire specimen volume into a single twinned orientation, and then applying the sine law, using the new angular relationships of the twinned orientation and the actual specimen heights. These calculations have been made for all seven specimens and the tabulated results are presented in Table 4. It should be emphasized that, at best, the calculated values represent only a very rough approximation to the actual existing experimental conditions.

TABLE 4.—*Observed and Predicted Angles between the Pole of the Basal Plane and the Compression Axis after Compression*

Specimen No.	Number of Reductions	Angle between [001] and Compression Axis after Basal Slip in Twin Regions, Deg.	
		Observed	Calculated
BR-2-9.....	1	17.5	17.5
BR-6-7.....	3	20.5	20.5
BR-11-4.....	1	23.0	22.6
BR-11-2.....	1	23.5	22.5
BR-1-6.....	1	25.5	25.0
BR-8-3.....	1	21.5	
BR-2-4.....	1	32.0	27.3

A basis for the extraordinary accord between observed and calculated values is derived from the metallographic observations made on these specimens during various stages of treatment. It is safe to say that in specimens having their compression axis in the prismatic field {102} twinning takes place during the first increment of reduction. Although, on further reduction, a limited increase in the number and size of the twins has been observed, this increase generally has been found to be small compared with the initial

twinning. The twins formed as heavy lamellae or thick plates, running through the entire height of the specimen. For specimens in which the basal plane closely approached parallelism with the compression axis, the volume of these twin plates or sections was greatest, in some instances taking up more than half of the specimen (for example, in BR-2-9). This observed characteristic of the twinning, coupled with the continuity of twin layers through each specimen from top to bottom, allowed greater freedom from constraints, and in consequence, a closer approach to the assumptions upon which the theoretical calculations are based.

Calculations of the resolved shear-stress factor, $\sin \chi \cos \lambda$,* for the basal plane of the original material and the basal plane of a twin orientation, were made for all specimens showing profuse twinning. The evaluations are summarized in Table 5. In each specimen, the value of $\sin \chi \cos \lambda$ is greater along the basal plane of the twin than along the same plane in its original orientation. This is significant in view of the profuse {102} twinning common to all of these specimens. A further correlation may perhaps be derived from these resolved shear-stress evaluations. In the last seven specimens of Table 5 the resolved shear stress on the basal plane of the original orientation is substantially less than that on the basal plane of the twin; the ratio of the two being considerably greater than unity. It is this group of specimens that shows definite slip on the basal planes of the twinned volumes. However, the size, shape and interacting influences of the

* The resolved shear stress on a given plane, along a given direction in that plane, is given by the equation:⁶ $S = \sigma \sin \chi \cos \lambda$, where

S = shear stress, grams per sq. mm.

σ = stress, grams per sq. mm.

χ = angle between compression direction and slip plane.

λ = angle between compression direction and slip direction.

twins doubtless exert an important influence upon any correlation of this kind.

TABLE 5.—*Comparison of Resolved Shear-stress Factor, $\sin \chi \cos \lambda$, for Basal Plane of Parent Orientation with Basal Plane of Selected Twin*
Evaluations Made for all Specimens Oriented in Prismatic Field

Specimen No.	Sin χ Cos λ along Basal Plane		Ratio S_t/S_p	Observed Deformational Mechanism
	Parent Orientation S_p	Twin Orientation S_t		
BR-5-7..	0.396	0.444	1.12	{102} twinning and basal slip in parent orientation
BR-1-3..	0.236	0.250	1.02	
BR-11-6.	0.281	0.340	1.21	
BR-6-1..	0.391	0.428	1.09	
BR-6-9..	0.229	0.302	1.32	
BR-2-8..	0.183	0.187	1.02	
BR-1-4..	0.247	0.307	1.24	
BR-1-2..	0.244	0.250	1.02	
BR-6-4..	0.349	0.407	1.17	
BR-2-9..	0.145	0.405	2.79	
BR-6-7..	0.253	0.357	1.41	{102} twinning and basal slip in twin
BR-11-4.	0.260	0.345	1.33	
BR-11-2.	0.202	0.366	1.81	
BR-1-6..	0.307	0.397	1.29	
BR-8-3..	0.186	0.346	1.86	
BR-2-4..	0.415	0.470	1.13	

In magnesium there are three pairs of twin planes, but twinning in all of these specimens took place on two planes of the same zone. It was, moreover, definitely established that the operative pair of planes is the pair for which the intersection with the basal slip plane makes an angle as near 90° with the projection of the compression axis on the same plane as is geometrically possible.

Shock Compression

Twinning on {101} planes was not detected in the observations on slowly stressed compression specimens in spite of the special attention directed to this possibility in specimens having the basal plane at an angle of less than 30° with the surface of compression. It has been stated (Fig. 1 and discussion) that under these conditions compression stressing would not allow {102} twinning, but might well cause twins to form on {101} planes.

Since the stressing rate for these specimens was low, absence of {101} twinning was thought possibly to be due to this condition. Neumann bands or deformational twins in soft iron are known to form only when the metal is subjected to deformation by shock.¹⁴ For these reasons, a series of shock-compression tests was carried out on a group of crystals having orientations theoretically adapted to {101} twin formation. Rapid compression stresses up to 450,000 lb. per sq. in. per min., at temperatures ranging from atmospheric to $300^\circ\text{C}.$, however, caused no {101} twins. The final conclusion drawn from these experiments must emphasize the rarity of {101} twin formation in magnesium even under the most favorable conditions.

Tension

From the total of nine tension-test bars prepared, one was used in a preliminary room-temperature test of the tension apparatus, two were used in room-temperature stressing for critical resolved shear-stress determinations, and six were subjected to drastic elongation at temperatures of 330° and $345^\circ\text{C}.$, respectively. The investigation of these tension specimens included determination of the active directions of slip from X-ray analysis of the axis shift, evaluation of critical resolved shear stress, and a metallographic study of surface markings after deformation.

Determinations of Critical Resolved Shear Stress.—The evaluations of critical resolved shear stress on the basal plane in the slip direction are summarized in Table 6.

These critical-shear-stress determinations were based on yield loads taken from load-elongation curves; the onset of plastic yielding being sharply defined by the rapid extension of the specimen. Comparison of the present critical-shear-stress evaluations with the results of previous determinations by Schmid⁸ show substantial agreement. The average value

of the present room-temperature determination, 77.8 grams per sq. mm., is well within the experimental spread of Schmid's values, which averaged 82.9 grams per sq. mm. for determinations at room temperature. The average of the 330°C. group is 65.5 grams per sq. mm., while the value for 345°C. is 55 grams per

TABLE 6.—*Data on Critical Resolved Shear Stress from Tension Tests at Three Temperatures*

Specimen No.	Temperature, Deg. C.	C.R.S.S., Grams per Sq. Mm.
BR-T-5.....	Room	84.3
BR-T-3.....	Room	71.3
BR-T-4.....	330	65.5
BR-T-8.....	330	68.2
BR-T-9.....	330	62.8
BR-T-7.....	345	55.0

sq. mm. Schmid gives critical-shear-stress values of 83.2 grams per sq. mm. at 250° and 70.5 grams per sq. mm. at 300°C., at the same time recording a marked change in the deformational energy between these same temperatures (from 4.75 to 2.95 cal. per gram). The values obtained in the present investigation at elevated temperature, therefore, are reasonably in line with the somewhat higher value found by Schmid, at a somewhat lower temperature. It may be noted that the critical resolved-shear-stress value for basal slip starts to decrease significantly at about 250°C., as the temperature is raised. The rate of loading is known to influence the critical shear stress,¹⁵ in the sense of lower values for a slower rate of loading. The loading rate in the present tests was about $\frac{1}{8}$ that used by Schmid, and in consequence lower values would be expected, as may be seen in a general comparison of the results.

Determination of Basal Slip Direction.—

The change in crystal orientation due to tension stressing has also been plotted in the basic stereographic triangle, the movement of the tension axis (open circles in

the diagrams) within this triangle representing the shift in orientation. According to geometrical requirements, the tension axis in this triangle must move along the

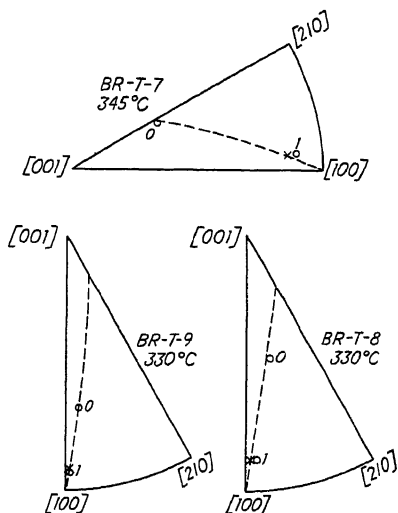


FIG. 10.—CHANGES IN ORIENTATION IN THREE TENSION BARS DEFORMED BY BASAL SLIP AT 330°C.

Original orientation designated by circle O; orientation after extension, determined by X-ray measurements, by circle I; predicted final position of tension axis, calculated on assumption of basal slip in $[100]$ slip direction, by X.

great circle connecting its original position with the operative direction of slip. Stereographic diagrams were prepared for eight of the nine specimens tested, and in each case great circles connecting the original orientation and the inferred direction of slip were constructed. The movement of the tension axis was observed in every case to follow the great circle from the original orientation toward the $[100]$ direction. Fig. 10 illustrates this in the diagrams describing tests with specimens BR-T-7, BR-T-8 and BR-T-9. The good agreement between the predicted and observed orientations, and their close proximity to the required great circle, leads to the conclusion that slip on the basal plane is along $[100]$, a digonal axis

I, or direction of greatest atomic density. This result is in agreement with Schmid's³ determination of the digonal axis I, as the direction of slip in the basal plane.

dominant activity of basal slip had transformed the entire gauge length of these bars into very thin, long ribbons.

In two of the test bars, large twins were

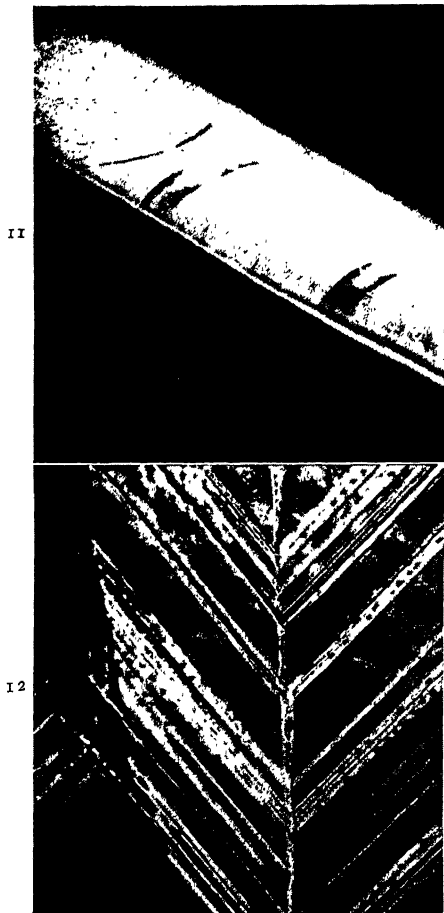


FIG. 11.—PYRAMIDAL $\{102\}$ TWINS PRODUCED IN BR-T-4 BEFORE TENSION STRESSING. $\times 4$.

FIG. 12.—BASAL SLIP BANDS IN TWIN AND PARENT REGIONS, BR-T-4. $\times 200$.

The metallographic study of the tension specimens led to several interesting observations. All but three of the specimens deformed solely by basal slip in the original crystal. The surfaces of these specimens revealed the familiar glide ellipses marking the extension of single crystals. The

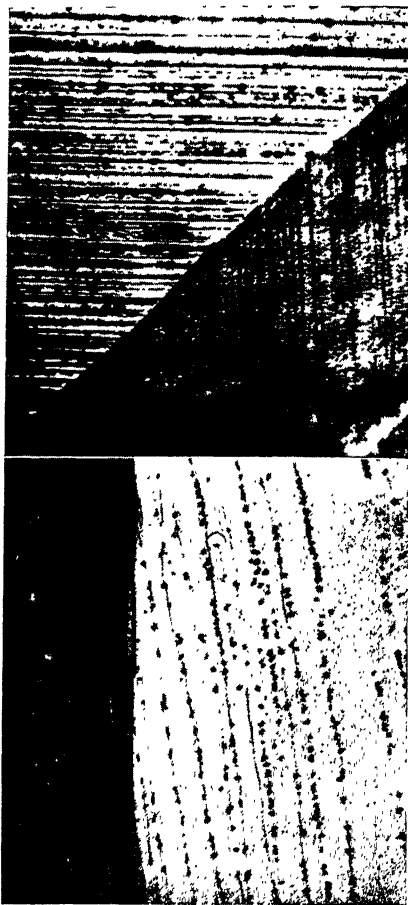


FIG. 13.—SUBLIMATION PITS ALONG BASAL SLIP BANDS IN TWIN AND PARENT REGIONS; ABSENT AT TWIN BOUNDARY, BR-T-4. $\times 250$.

FIG. 14.— $\{001\}$ SLIP BANDS IN PARENT ORIENTATION AND $\{101\}$ SLIP BANDS IN A TWIN. $\times 200$.

formed intentionally prior to the tension loading. Basal slip in both the parent and twin crystals was observed in these samples. Fig. 11 shows the twin bands in one of the tension bars prior to tension loading; Figs. 12 and 13 show basal slip bands

present in both the parent and twin volumes. It is also observed that well-defined pits follow along slip bands on the previous polished surface. This pit formation, found to be caused by localized sublimation during the stressing at elevated temperature, generally followed surface markings caused by deformation, basal slip bands in twin or parent crystal, pyramidal $\{101\}$ slip bands, and in special instances, twin boundaries.

Although virtually all the deformation was effected by the usual basal slip in the twin and original orientations, two other phenomena were also observed: (1) the presence of irregular and forked bands within and close to the boundary of one of the larger twins and (2) the forcing of basal slip at specific positions in the twins by basal slip in the parent material, acting at the twin boundary. Fig. 14 shows the irregular and forked character of the markings referred to above. Since these were found in a limited area of one twin, conclusive identification was not attempted, although they were very similar in appearance to the $\{101\}$ slip bands to be described later. Fig. 12 offers a good illustration of the second characteristic noted above. It cannot logically be assumed that this matching of the prominent slip bands of twin and parent material at their boundary position was a mere matter of chance. It was in all probability, the result of a specific type of stress interchange between the two regions, conditioned by the prior yielding along the basal plane of one region, either twin or parent orientation. The situation illustrated in Fig. 12 was observed at the boundaries of several different twins in this specimen.

Pyramidal Slip.—Specimen BR-T-6 was stressed at 330°C . in two increments, using a loading rate of 112 lb. per sq. in. per min. Previous to this loading, however, slight bending of the test bar had caused the formation of two twins at the ends of the reduced gauge length. X-ray analysis and

microscopic angular measurements identified the twins as of the $\{102\}$ type in a common zone. After the first 14 per cent elongation, examination revealed the pres-

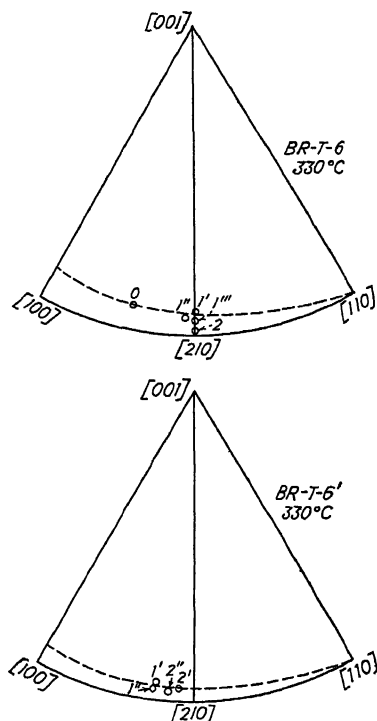


FIG. 15.—ORIENTATION CHANGES IN SPECIMEN SHOWING PYRAMIDAL $\{101\}$ SLIP.

BR-T-6 refers to main grain and BR-T-6', a small surface grain. Open circles are observed positions of tension axis.

ence of a small surface grain near the central region of the bar. A thorough microscopic and X-ray study of the specimen was made at this point, before the second extension to fracture at 26 per cent elongation. Finally, further examination and analysis were carried out.

The diagrams of Fig. 15 summarize the results of this analysis with reference to BR-T-6 as the main crystal and BR-T-6' as the small surface grain. Since the small surface grain was not detected until after stressing, its original orientation was not

known. The original orientation of the main grain placed the basal plane within $4\frac{1}{2}^\circ$ of the tension axis, the projection of the latter in the basal plane lying at an

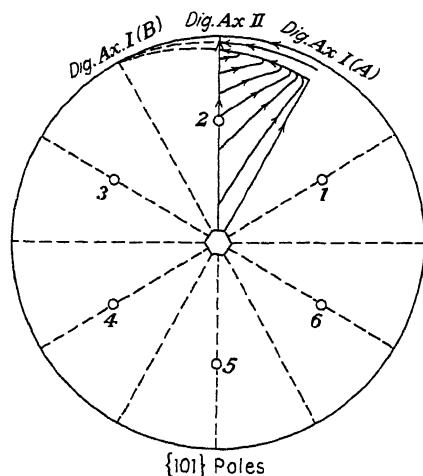


FIG. 16.—COMPOSITE DIAGRAM SHOWING DIRECTION OF TRAVEL OF TENSION AXIS IN REFERENCE TRIANGLE FOR TEMPERATURES BETWEEN 225°C . AND 330°C .

Reproduced from the results of Schmid's work and checked in present investigation.

angle of 12° to a digonal axis II. This orientation falls within the field of orientation which, according to Schmid,³ shows a change in the direction of slip as outlined in Fig. 16. The axis shift in the main grain establishes the new slip direction. In Fig. 15, open circles 1', 1'' and 1''' mark the orientations after the first extension at three different positions on the specimen. Because of the presence of previously formed $\{102\}$ twins, the elongation varied in different parts of the specimen and reached a maximum in twin-free regions. The variations in the three orientations designated by the figure one originate from X-ray determinations in regions of varying extension. The position marked 2 designates the orientation found as close to the fracture as was possible within the limits of determination fixed by the occurrence of excessive distortion. As shown by the

dashed line in the diagram, the movement of the tension axis is first along the great circle toward $[110]$, and then, on reaching a symmetry position between the $[100]$ and $[110]$ directions, the travel is along this symmetry axis toward the pole of the second-order prismatic plane, or the $[210]$ direction. From these observations, it is concluded that the $[110]$ direction is the direction of slip prevailing until $[110]$ and $[100]$ are symmetrically related to the tension axis, whereupon conjugate operation of the $[110]$ and the $[100]$ directions occurs. This is analogous to the condition found at the double slip boundary in crystals of cubic symmetry. Microscopic examination of this crystal definitely verified the presence of this conjugate slip.

The stereographic diagram presenting orientation changes in the small grain are given in BR-T-6' of Fig. 15. Although the original orientation is lacking, the movement of the tension axis during the second increment of elongation is seen to follow the great circle toward $[110]$. Thus the $[110]$ direction is again found to be the slip direction, but it may be noted that the symmetry position for conjugate slip is not attained. The disagreement between individual "1" and "2" determinations is ascribed to inhomogeneous stress conditions created by the simultaneous deformation of the main crystal. Microscopic examination of this small grain reveals only one set of slip bands (Fig. 17), as was inferred from the X-ray results. From a consideration of the orientation of the deformed grain, the axis shift toward $[110]$ during the second extension, and the absence of more than one operative slip system, it may be concluded that the original orientation placed the tension axis somewhere on the great circle shown as a dotted arc in the diagram. Doubtless it was situated at a greater angular distance from $[110]$ than was the original orientation of the main crystal; otherwise, a final orientation would have been reached

in symmetry position between $[110]$ and $[100]$. These conclusions regarding the close proximity of the two grain orientations thus accounts for the failure to detect

slip plane. Because of the restraining presence of the $\{102\}$ twins, sections of the test piece revealed only single slip; in other sections free from such restraint,

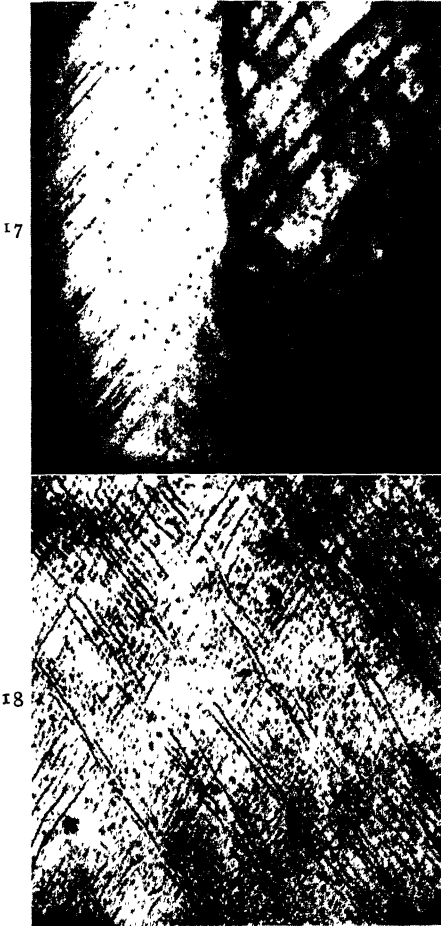


FIG. 17.—SLIP MARKINGS IN SMALL GRAIN AT LEFT AND MAIN GRAIN AT RIGHT, BR-T-6. $\times 150$.

FIG. 18.—CONJUGATE SLIP BANDS RESULTING FROM SLIP ON TWO $\{101\}$ PLANES, BR-T-6. $\times 250$.

the surface grain before stressing the test bar.

Microscopic examination and careful measurements conclusively established the first-order pyramidal plane $\{101\}$ as the

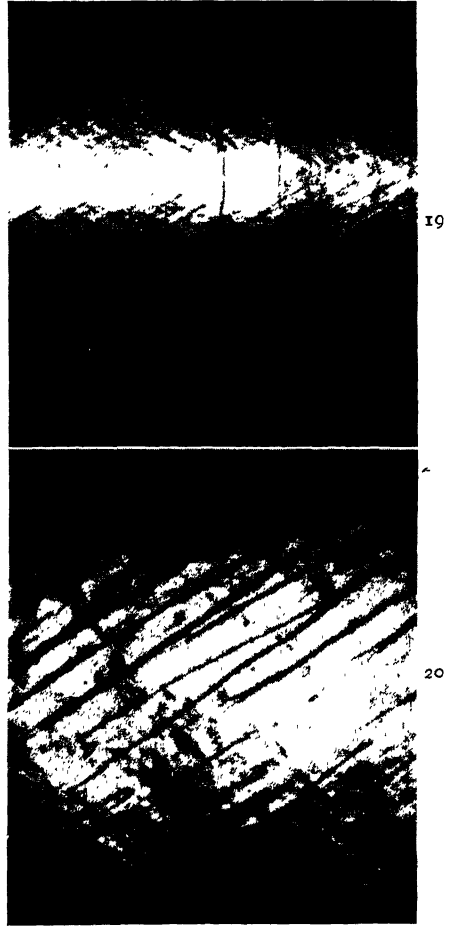
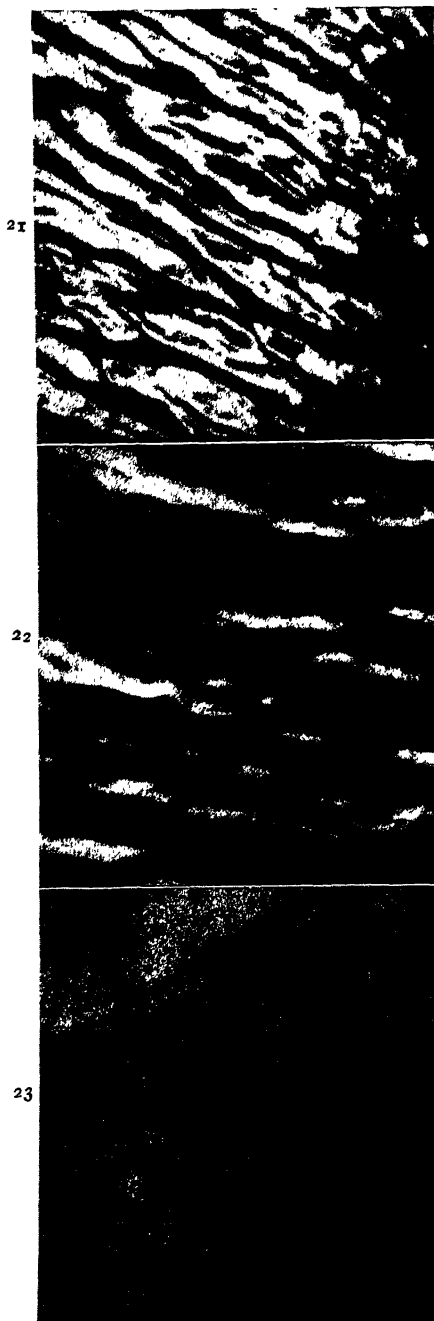


FIG. 19.—CONJUGATE SLIP BANDS AND ONE TWIN.

Bands appear to pass through the twin without change in direction, BR-T-6. $\times 40$.

FIG. 20.—INTERMEDIATE POSITION BETWEEN MINOR AND MAJOR AXES, CLOSER TO FORMER, BR-T-6. $\times 100$.

double slip was observed. The general characteristics of the surface markings or slip bands are presented in a series of photomicrographs. Unlike the sharp, straight



For legends see opposite column.

slip bands found on the polished surface of a cylindrical crystal undergoing basal translation, the slip bands produced by pyramidal slip are neither straight nor sharp in their continuity around the test bar, but rather show definite branching and the existence of heavy slip bands composed of a series of fine noncontinuous bands (Figs. 17 and 18). These slip bands are well defined in the immediate vicinity of the minor axis of the glide ellipse* (Figs. 18 and 19) but at positions one third of the way from the minor axis to the major axis the sharpness of the bands is lost, narrow surface depressions or grooves, instead, marking the position of the glide ellipse in these regions (Figs. 20 and 21). At positions close to the major axis, these narrow grooves widen, finally becoming uneven ridges at the line of intersection of the surface with the major axes of a set of glide ellipses (Fig. 22).

No twins were formed during the extension, but the $\{102\}$ twins that already were present on the test bar, in addition to yielding interesting microscopic effects, were useful in confirming the nature of the slip mechanism. Fig. 23 shows the displacement of adjacent sections through twin bands by the operation of $\{101\}$ slip across the twins. This observation was made in several places on the same specimen.

Evidence of slip along the $\{101\}$ plane was obtained in three ways. First, a Laue photogram was taken with the incident beam normal to the marked test bar, mounted vertically. From this photogram, poles of the $\{001\}$ and $\{101\}$ planes were

* Glide ellipse refers to the curve of intersection of the slip plane with the surface of the cylindrical test bar.

FIG. 21.—INTERMEDIATE POSITION BETWEEN MINOR AND MAJOR AXES, CLOSER TO LATTER, BR-T-6. $\times 100$.

FIG. 22.—POSITION OF MAJOR AXIS, BR-T-6. $\times 100$.

FIG. 23.— $\{101\}$ SLIP BANDS THROUGH TWINS, DISPLACING CUT SEGMENTS RELATIVE TO ONE ANOTHER, BR-T-6. $\times 200$.

plotted stereographically as shown in Fig. 24, where the incident beam is at center of circle and TT' represents the long axis of the test bar. Then, in turn, each of the

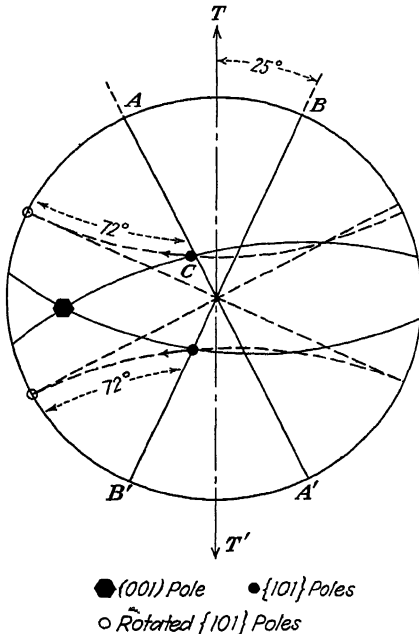


FIG. 24.—STEREOGRAM OF BR-T-6.

TT' is axis of specimen and BB' is trace of operative $\{101\}$ slip plane perpendicular to plane of projection.

$\{101\}$ poles was rotated about TT' as axis until it fell on the circumference of the primitive circle. With the pole in this position, the plane was normal to the plane of the projection, of course, and would be represented by a diameter normal to the line connecting the rotated pole with the center of the projection. In the illustrative diagram of Fig. 24, only two $\{101\}$ poles are shown, one of these, C , being the pole of a plane upon which slip had actually taken place. The necessary 72° rotation reveals the diameter BB' as the trace of the plane whose pole was originally at C . The angle between BB' and the long axis of the main crystal is measured as 25° . Now, if this particular $\{101\}$ plane is

actually the active slip plane, the specified 72° rotation about the long axis of the crystal should bring the slip band observed on the surface of the crystal to a position

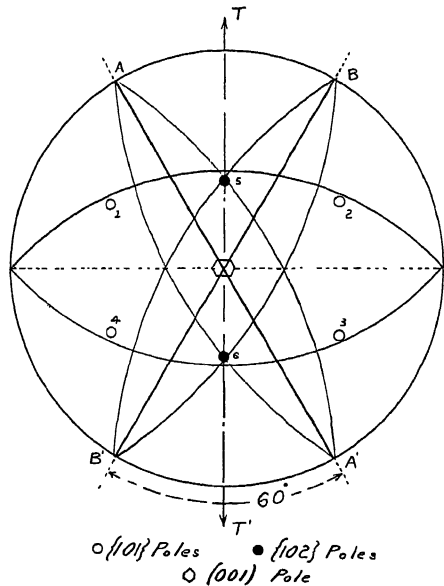


FIG. 25.—STEREOGRAM SHOWING CONDITIONS ILLUSTRATED IN PHOTOMICROGRAPH OF FIG. 19.

TT' is axis of specimen and BB' and AA' are traces of the operative $\{101\}$ planes.

making an angle of 25° with the axis of the test bar. An average of 10 such determinations, after proper rotation, gave $25\frac{1}{2}^\circ$ as the measured angle.

The second method takes advantage of the presence of $\{102\}$ twins. These twins were identified as of the form $\{102\}$ by the X-ray-microscopic method described in the previous paragraph. The tension test bar was then placed on the stage of a microscope in such position that the normal to the twinning plane, the long axis of the specimen, and the line of sight through the eyepiece, all fell in the same plane. In this position the major axis of the parallel twin lamellae will also lie in that same plane, normal to first-order prismatic planes. This condition is shown in the

photomicrograph of Fig. 19, and is stereographically plotted in Fig. 25. The lower solid circle (6) represents the pole of the $\{102\}$ twin illustrated in Fig. 19, the open circles denote the poles of $\{101\}$ planes from which the present slip bands could originate; and the pole of the basal plane, which is parallel to the long axis TT' of the crystal, is at the center of the primitive circle. The intersections of the $\{101\}$ planes with the plane of the projection are drawn as BB' and AA' . The angle between AA' and BB' is 60° . Measurement of the angle between the intersecting slip bands on the surface of the test bar corresponding approximately to the unique orientation of Fig. 19 gave an average of 63.2° in a series of separate readings. The orientation shown in the diagram of Fig. 25 is not exactly the one found in the specimen after the first extension. Fig. 15, the original plot of this specimen, shows that in reality the axis of the specimen lies about 3° from the basal plane. The correction for this very slight shift, however, is scarcely beyond the limit of accuracy of the work; so that for present purposes, the actual angle between the two operative slip planes, O_3 and O_4 , viz., (001) and $(1\bar{1}1)$, may be taken to be 60° . Since the measurements on the crystal were made on the surface of a cylinder and not on a flat section, the measured value of 63.2° is in good agreement with the theoretical value of 60° .

Prismatic planes and other pyramidal planes whose poles are in the zones O_1O_3 and O_2O_4 would also produce the traces BB' and AA' . However, only the pyramidal $\{101\}$ slip here postulated can proceed without change of direction from parent crystal through the twin as repeatedly observed (e.g., Fig. 23). This is due to the perfect interchange of the poles O_3 and O_4 by the twin rotation around the pole, 6.

The third means of identification rests upon the simple expedient of analyzing a Laue photogram with the X-ray beam normal to the plane of the glide ellipse.

The results from several photograms on both operative planes gave checks to within 5° of the required planes of form $\{101\}$.

The character of the axis shift in the diagram of Fig. 15, the presence of single $\{101\}$ slip, and the demonstration of the operation of the $(1\bar{1}1)$ and (011) planes instead of $(1\bar{1}1)$ and (101) during double slip, all serve to attest the validity of the maximum resolved shear-stress law when applied to the planes of the same form; i.e., $\{101\}$ planes in the present case. Calculations of the resolved shear stress along the first-order $\{101\}$ planes of the unextended crystal were made, using as slip direction the digonal axis I present in each plane, and as stress the value at the determined yield point. Evaluated from the standard formula, these resolved stresses for the three possible planes (1, 2, and 3 of Fig. 16) are:

	GRAMS PER SQ. MM.
Plane 1.....	400
Plane 2.....	165
Plane 3.....	244
Basal plane.....	64

The present work definitely established the operation of plane 1 prior to plane 3, no evidence of slip along 2 being found. The tabulation above shows that the resolved shear stress is at a maximum on plane 1. When the tension axis reaches the symmetry position between the two digonal axes I, the resolved shear stress in the appropriate slip directions is equal on planes 1 and 3, and much less on plane 2; therefore, at this position double slip should be operative on planes 1 and 3. These were the observed conditions.

In the evaluations given above, it is seen that the resolved stress required for initial yield along an operative $\{101\}$ plane is 400 grams per sq. mm. Since evidence of basal slip was not observed, this value may be considered to be the critical resolved shear stress for $\{101\}$ pyramidal slip. Although possibly somewhat higher than the true value, it is thought to

constitute a reasonably reliable determination, in spite of the presence of an extraneous surface grain and twin lamellae, since ample restraint-free segments of the gauge length were present for the initiation of unobstructed pyramidal slip. It may be recalled that the critical resolved shear stress for basal slip at 330°C. was found to be 65.5 grams per sq. mm. This crystal, therefore, barely escaped basal slip at the beginning of its deformation.

Importance of Slip Direction

The slip direction comes to the forefront in this investigation as the most important geometrical factor regulating the plastic deformation of magnesium. Pyramidal $\{102\}$ twinning, although found to be active to an extraordinary degree under compression stressing, is definitely confined to a limited field of orientations; and, even here the influence of the slip direction is manifest in the subsequent deformation of the twinned regions. This and the other observed mechanisms appear to operate with the common favor or disfavor of the slip direction, a first-order digonal axis, or lattice line of greatest atomic density. Whether it be slip on the basal (001) plane or a pyramidal $\{101\}$ plane, in either the parent crystal or twin, or, indeed, cleavage along a $\{101\}$ plane, it is a digonal axis I acting as the slip direction, or being incapable of so doing, which brings about the respective results. Conclusive tests have established this as the fundamental direction for basal slip from atmospheric temperature up to 330°C., and for pyramidal $\{101\}$ slip from 225°C. (according to Schmid) up to 330°C. These two slip mechanisms, along with $\{102\}$ twinning, have now been found definitely to account for the tensile or compressive deformation in all orientations except one small field. Crystals with their basal planes at an angle of less than 15° to the surface of compression invariably failed by $\{101\}$ fracture when compressed

at temperatures ranging from that of the atmosphere up to 340°C.

When it is considered that slip has been observed to operate along planes of this form during tension stressing, it seems at first glance unreasonable not to find single, double, or even triple slip operating when the basal plane in the crystal is almost parallel to the surface of compression. In these particular orientations $\{101\}$ pyramidal planes lie at angles favorable to slip (43° to 28° to stress axis). However, slip is possible only with the cooperation of slip directions in the planes, which make angles substantially less than 90° with the stress axis. A digonal axis I, the line of greatest atomic density, occurs in each of these $\{101\}$ planes (one in each plane of a pair), but these three axes are nearly parallel to the surface of compression and for this reason could not be expected to act as slip directions. Each of the $\{101\}$ planes contains two other lines of low indices, the intersections with other planes of the same form, which are favorably oriented to act as slip directions but have somewhat less than half the density of the former line. Specimens of this orientation always exhibit cleavage. This situation leads to the conclusion that only the line of closest packing, a digonal axis I, can act as the slip direction, and must itself be favorably oriented to the stress axis if slip is to operate, irrespective of the plane concerned.

Change of Slip Plane

In contrast with the condition described by Andrade and Chow¹⁸ for body-centered cubic metals, the change of slip plane in magnesium depends upon resolved shear stresses as well as upon temperature. Whereas molybdenum, potassium and sodium have been found to change their slip planes at temperatures determined by the ratio of temperature of test to melting point, irrespective of the shear stresses resolved on such planes, for magnesium

it has been established that the resolved shear stress on the pyramidal plane must reach a value about six times that on the basal plane before pyramidal slip can operate, even when tests are conducted far above $225^{\circ}\text{C}.$, the temperature originally found by Schmid to be a critical minimum for the new slip process. The effect of this six-fold shear-stress requirement for $\{101\}$ slip relative to (001) slip is to limit the field in which pyramidal slip can operate to those orientations in which $\sin \chi \cos \lambda$ values, on the most favorably oriented $\{101\}$ plane, are about six times the stress resolved on the basal plane. This condition is fulfilled when the axis of extension is within 5° of the basal plane. The precise effect of temperature above $225^{\circ}\text{C}.$ and prior basal slip on the incidence of $\{101\}$ slip has not been determined. However, the good adjustment of the present results at higher temperatures to the orientational boundaries set up by Schmid for pyramidal $\{101\}$ slip points to the absence of any marked influence by the conditions in question.

The question arises as to why the slip plane changes with temperature. Förster and Köster¹⁷ have observed a marked increase (about 200 per cent) in the damping capacity of magnesium in the range 225° to $250^{\circ}\text{C}.$, a similar but smaller increase (about 100 per cent) in aluminum at $400^{\circ}\text{C}.$, and a more gradual increase with temperature for molybdenum. Since damping capacity connotes the dissipation of energy in the lattice,^{18,19} it appears possible that the important increases in the damping capacity at the temperatures paralleling those at which new slip systems have been found to operate may perhaps be attributed to a preferential directionality of atomic vibration acting in conjunction with the potential energy due to spacing. Possibly it is significant that magnesium and aluminum, which show the marked increase in damping capacity, are both close packed, while molybdenum, which

shows only a very gradual increase, is not close packed. Andrade views the phenomenon in "analogy with the change in crystal structure that takes place with temperature in the case of certain metals, as exemplified by calcium, which is face-centered cubic at room temperature and close-packed hexagonal above $450^{\circ}\text{C}.$, or zirconium, which is close-packed hexagonal at room temperature and body-centered cubic at $862^{\circ}\text{C}.$ This change must depend upon the way in which the free energy of the different crystalline forms varies with temperature, which in its turn will mainly depend on how the energy of vibration varies with the temperature." In any case, the experimental evidence of changing plane of slip indicates that the rate of variation of strength with temperature is different on the different systems of planes in a crystal.

Surface Markings

Only a speculative suggestion can be offered in explanation of the irregularities in surface markings resulting from $\{101\}$ pyramidal slip. In comparison with pyramidal slip bands, the basal bands remain perfectly elliptical and regular throughout the range of temperature and manner of stressing. A geometrical characteristic that may be responsible for the difference in behavior of these two systems of planes is the relative nearness (as concerns parallelism) of other planes of comparable atomic density, having the common slip direction. The basal plane has an atomic surface density roughly twice (1 to 0.47) that of the $\{101\}$ plane, but if the two $\{101\}$ planes that are very close together ($d = \text{approx. } 0.44 \text{ \AA.}$), owing to the presence of the centered atom of the interpenetrating lattice, are considered as one, the ratio approximates unity (1 to 0.94). Similarly, the modified ratio of surface densities of the basal and pyramidal planes of the form $\{102\}$ is 1 to 0.73. Neither of these pyramidal planes is

close enough to modify the characteristics of basal slip. However, with respect to pyramidal $\{101\}$ slip, the associated $\{102\}$ planes lie within an angular range (18°) of possible cooperation. It is, therefore, suggested that the specified irregularities, forking and ridge formation, are the result of cooperative or accessory slip on very limited sections of those $\{102\}$ pyramidal planes having the same digonal axis I as slip direction.

The slip bands observed in alpha iron, beta brass, and mercury crystals show a close resemblance to these $\{101\}$ bands observed in magnesium. It is known that several slip systems can operate in body-centered alpha iron and beta brass. Andrade and Chow¹⁶ suggest that "Taylor's picture²⁰ of rodlike slipping can be easily explained on the basis of glide taking place on three planes at once. The non-planar glide surfaces (causing the irregular glide bands) can be built up by slip, in the $[111]$ direction, taking place on different planes in short, adjacent, parallel-sided strips." In like manner, Greenland²¹ attributed the wavy and branched slip bands in mercury to "gliding on surfaces which are not planes but are made up of glide elements having a common glide direction." It is thus seen that in the analogous cases of irregular slip bands, similar explanations have been advanced.

Although the basal slip bands in greatly extended magnesium crystals showed no particularly characteristic spacings, such an effect was indeed observed among the pyramidal slip bands. The measured spacings of the most prominent bands average 0.0046 cm. This value, which is roughly the same as the one given by Andrade and Hutchings²² (0.0053 cm.) for mercury extended at a temperature near the melting point, is of the order of 10,000 lattice spacings.

Twinning at Different Temperatures

A significant increase in individual size and total volume of twins was observed

in the compression tests at elevated temperature ($300^\circ\text{C}.$) of specimens favorably oriented for $\{102\}$ twinning. The behavior of zinc, cadmium and alpha iron, as reported by Schmid and Boas,⁶ is in direct contrast to this observed characteristic of magnesium. Thus, increase in temperature tends to suppress twinning, during the plastic extension of zinc and cadmium; while a decrease in temperature well below atmospheric is necessary in order to obtain profuse twinning in pure alpha iron. A speculative rationalization of these anomalies may be made in a manner paralleling that given for the change of slip plane with temperature. Since simple shear, or twinning, is the accepted mechanism of mechanical twin formation, the rate of variation of strength with temperature of different crystallographic planes should influence the formation of twins in a manner analogous to its effect on ordinary slip.

Kolesnikov²³ reports slip on the first-order prismatic planes of zinc at temperatures above $300^\circ\text{C}.$, although slip markings were not observed and the selection of these in favor of pyramidal planes admittedly was not conclusive. Andrade's work on body-centered cubic metals establishes the $\{112\}$ plane as the slip plane for the smallest values of the ratio temperature of test to temperature of melting (T/T_m). And, in the present experiments, the first-order pyramidal plane was found to operate in magnesium at the elevated temperatures. If a changing characteristic of vibration of the atoms is contributing to the change of slip plane, it should conceivably aid in the twinning, provided the twinning plane and the new slip plane are the same, or very nearly parallel. Assuming that the new slip plane in zinc is the first-order prism, the twinning plane $\{102\}$ is greatly inclined to it (43°) and twinning would not be favored by an increase in temperature. In the body-centered cubic metals, the $\{112\}$ plane is the twinning plane, and also the slip plane for the lowest values of T/T_m ; here,

decreased temperature would be expected to favor twinning. The first-order pyramidal plane $\{102\}$ is the twinning plane in magnesium, and its moderate inclination (less than 20°) to the $\{101\}$ pyramidal plane operating as the high-temperature slip plane indicates that increased temperature would be expected to favor twinning in this case. In connection with twinning at elevated temperatures, it may be noted that mercury has been observed to twin at temperatures closely approaching the melting point.

Selection of Twinning Planes

The compression tests have also furnished some interesting observations relative to the questions: which of the various possible twinning planes is operative, and what decides when twinning shall take place? Previous attempts to establish a criterion determining which of the various twinning planes may operate have been made by Gough²⁴ and Andrade and Hutchings.²² With zinc, for example, exhibiting three pairs of twinning planes, Gough observes that twinning takes place on the two pairs that do not contain the direction of slip. Andrade and Hutchings²² restate this rule in adaptation to their results on the twinning of mercury, as follows: "The operative planes are those for which the intersection with the glide plane makes an angle as near 90° as is geometrically possible with the glide direction. With mercury the angle is 90° ; with zinc it is 60° , as against 0° for the inoperative plane."

The results of the present investigation are in full agreement with this rule but narrow the number of operative twin planes from two pairs down to one. This conclusion was reached from the analysis of every compression test showing twinning. The rule as it applies to magnesium may be stated as follows: The operative pair of planes is the pair for which the intersection with the slip $\{001\}$ plane makes an angle as near 90° as is geometrically possible with the projection of the compression

axis on the same plane. Whether this restriction to one pair of planes is a result of temperature of test, manner of deformation, or some property of the metal, is left unanswered.

The question as to what determines the occurrence of twinning has also been considered by Andrade and Hutchings.²² From the results of their experiments on mercury, a possible condition for twinning is stated as follows: "Twinning takes place when the glide planes and direction make such angles with the direction of applied force that new glide planes formed by twinning will be just as favorably disposed for glide." In the present experiments, calculation of the ratio of $\sin \chi \cos \lambda$ in the original orientation of the slip plane to the twinned orientation of the same plane for all compression specimens displaying twinning gave values less than unity in each case. Twin formation in these specimens therefore facilitated the deformational process.

SUMMARY OF RESULTS

1. A method was described for preparing isolated crystals of magnesium from the molten metal. The procedure, based on the well-known Bridgman method, produced single crystals in the majority of attempts and ensured against possible contamination of the product.

2. The mechanism of plastic deformation in high-purity magnesium at $300^\circ\text{C}.$, and several lower temperatures, was investigated in a series of compression tests including representative orientations from all possible adjustments of the crystal relative to the stress axis. The results indicate that slip on the basal plane in the original material, twinning on the $\{102\}$ plane, slip on the basal plane of the twinned regions, and fracture (or cleavage) along the $\{101\}$ plane are the only mechanisms operating during compression stressing, prior to the entrance of general crystal break-up. The dominance of these

several mechanisms has been classified into three fields of orientation.

3. A series of shock-compression tests carried out on favorably oriented crystals at temperatures ranging from that of the atmosphere up to 300°C. was not successful in causing the {101} twin formation previously reported by Schiebold and Siebel.²

4. Tension tests were made to determine the slip plane, direction, and general characteristics of pyramidal slip, as well as the values of critical resolved shear stress. The results prove definitely that the first-order diagonal axis in the plane of slip is the slip direction, whether slip occurs on the basal plane (001) or the first-order pyramidal plane {101}. Proof of single and double slip on the first-order pyramidal planes {101} is presented, and it is concluded that slip functions on one plane until the symmetry position is reached between two equivalent slip directions, at which point double slip comes into play in a manner analogous to that found in face-centered cubic metals. Evaluations of the critical resolved shear stresses were made at two temperatures besides that of the atmosphere for basal slip, and at one temperature (330°C.) for {101} slip.

5. A unique method of preparation of highly polished tension-test specimens was described. The metallographic examination of these bars disclosed several interesting phenomena:

a. Pyramidal {101} slip bands, unlike (001) slip bands, are irregular, discontinuous and forked, resembling slip bands found in α -iron.

b. Interactivity of slip within the parent and twinned sections of crystals (illustrated and discussed).

c. Small sublimation pits formed during extension at elevated temperature are found to follow surface markings caused by the deformation, viz., basal slip bands in the twin or parent crystal, pyramidal

{101} slip bands and, in some instances, twin boundaries.

6. A discussion of the results with relation to the plastic behavior of other metals has also been included.

ACKNOWLEDGMENT

The authors wish to express most sincere thanks to Dr. J. D. Hanawalt and Dr. J. C. McDonald, of the Dow Chemical Co., who incited interest in the problem; to members of the Yale staff; and to the Dow Chemical Co. for the financial assistance that made this work possible.

REFERENCES

1. C. H. Mathewson and A. J. Phillips: *Proc. Inst. Metals Div.*, A.I.M.E. (1928) 445.
2. E. Schiebold and G. Siebel: *Ztsch. Physik.* (1931) 69, 458.
3. E. Schmid: *Ztsch. Electrochem.* (1931) 37, 447.
4. E. Schmid and G. Siebel: *Metallwirtsch.* (1934) 13, 353.
5. E. Schmid and H. Seliger: *Metallwirtsch.* (1932) 11, 409, 421.
6. E. Schmid and G. Siebel: *Metallwirtsch.* (1932) 11, 577.
7. E. Schmid and W. Boas: *Kristallplastizität*. Berlin, 1935. Julius Springer.
8. P. W. Bridgman: *Proc. Amer. Acad. Sci.* (1925) 60, 305.
9. A. B. Greninger: *Trans. A.I.M.E.* (1936) 122, 74.
10. W. E. Ford: *Dana's Textbook of Mineralogy*. New York, 1921. John Wiley and Sons.
11. G. I. Taylor and W. S. Farren: *Proc. Roy. Soc., London* (1926) 111-A, 529.
12. M. R. Pickus and C. H. Mathewson: *Trans. A.I.M.E.* (1939) 133, 161.
13. F. Wever: *Trans. A.I.M.E.* (1931) 93, 51.
14. R. F. Miller: *Trans. A.I.M.E.* (1936) 122, 176.
15. L. B. Pfeil: *Carnegie Schol. Mem., Iron and Steel Inst.* (1926) 25, 319.
16. W. Boas and E. Schmid: *Ztsch. Physik* (1930) 61, 767.
17. E. N. da C. Andrade and Y. S. Chow: *Proc. Roy. Soc., London* (1940) 175-A, 29.
18. W. Förster and W. Köster: *Ztsch. Metallkunde* (1937) 29, 116.
19. T. A. Read: *Trans. A.I.M.E.* (1941) 143, 30.
20. C. Zener: *Proc. Phys. Soc., Rept. on Internal Strains in Solids* (1940). Univ. Press, Cambridge, England.
21. G. I. Taylor and C. F. Elam: *Proc. Roy. Soc., London* (1937) 112-A, 337.
22. K. M. Greenland: *Proc. Roy. Soc., London* (1937) 163-A, 26.
23. E. N. da C. Andrade and P. J. Hutchings: *Proc. Roy. Soc., London* 148-A, 120.
24. A. F. Kolesnikov: *Jnl. Expt. and Theor. Physics* (U.S.S.R.) (1938) 8, 1030-1039.
25. H. J. Gough: *Edgar Marburg Lecture, Proc. Amer. Soc. Test. Mat.* (1933) 33, pt. II, 3.

DISCUSSION

(J. D. Hanawalt *presiding*)

J. D. HANAWALT,* Midland, Mich.—Magnesium is the only one of the structural metals that crystallizes in the hexagonal system. For castings, this fact is not of great significance, because the random orientation of the grains eliminates the effects of the anisotropy of the magnesium single crystal. In wrought magnesium, however, the grains are oriented in definite directions due to the mechanism of plastic flow, and the directional characteristics of the single crystal are to some extent carried over into the wrought metal. For example, the difference between the values of tensile and compression yield strengths in certain directions is a consequence of the twinning on (102) planes. Another observation of interest is that certain magnesium alloy extrusions at intermediate temperature are oriented as though glide on the basal planes had been in the Dig. Ax. II direction while at high temperature the direction of glide has changed to the Dig. Ax. I direction. These results are complicated, of course, by alloy composition and grain-boundary effects as well as because the stresses are not simple,

and may not be directly related to the observations on single crystals. However, the present paper provides a basis for further work along these important lines. At some future time, it may be possible to understand these more complicated situations in polycrystalline metal.

G. EDMUNDS,* Palmerton, Pa.—This paper is an excellent and authoritative piece of work on the subject. In consequence of it, we now know a great deal more about the mechanism of the deformation of magnesium as well as the plastic deformation of the other hexagonal metals.

C. H. MATHEWSON (author's reply).—Regarding the variation in textural conditions noted by Dr. Hanawalt, I do not think it is possible from a pure knowledge of the slip and twinning elements to completely determine the origin of any particular texture. It is very difficult to analyze these textures, but it does appear very necessary to know the slip and twinning elements as a part of the information required for any extended theorizing with respect to what may happen when there are conditions of restraint; due, for example, to the simultaneous presence of other crystals.

* Director of Metallurgical Dept., The Dow Chemical Company.

* New Jersey Zinc Company.

Preliminary Spectrographic and Metallographic Study of Native Gold

BY WELTON J. CROOK*

(New York Meeting, February 1939)

UNLESS present in considerable proportion, metals of the precious-metal group—other than gold and silver—are not readily detected by the methods of fire assaying usually applied to ores and metallurgical products. Platinum, when present in small quantity, will ordinarily be reported as silver unless special methods of parting are used. Other elements occurring in the gold itself are all fluxed and slagged in the assay operation and if analyses are made on bullions the melting and slagging operations to which the bullion has been subjected may eliminate most of the associated elements. On the other hand, the analysis of precipitate from the cyanide treatment of gold ores may reveal the presence of many unexpected elements, such as tungsten and molybdenum. It is uncertain, however, whether many of the elements present in the precipitate are derived from the ore gangue or from the gold itself.

No very general survey of the distribution of metallic elements in gold seems to have been made. Rose and Newman,¹ in connection with the composition of native gold, say in part as follows:

Gold is occasionally found alloyed with copper and sometimes also with iron, bismuth, lead, mercury, tin, antimony, palladium or rhodium. Rhodium gold from Mexico was found to be of the specific gravity 15.5 to 16.8 and contained 34 to 43 per cent of rhodium. The native alloy of palladium, gold, and silver from Porpez contains 85.98 per cent of gold, 9.85 per cent palladium and 4.17 per cent silver. Maldonite, from Victoria, contains gold 64.5 per cent, bismuth 35.5 per cent (Louis).

Dana² says that native gold is usually alloyed with silver in varying amounts, and that sometimes it also contains traces of copper and iron. Rare varieties contain palladium, rhodium and bismuth. Other authors, for instance Zeigler³ and Clark,⁴ give similar information. Most references on the subject agree that ordinary native golds contain, in common, the elements silver, copper and iron. After completion of the work of which this paper is a record, the conclusion is reached that all ordinary native gold probably does contain these elements and, although in certain cases other elements may be found to be present, that it is difficult to

Manuscript received at the office of the Institute June 11, 1938. Issued in METALS TECHNOLOGY, February 1939.

* Professor of Metallurgy, Stanford University, California.

¹ References are at the end of the paper.

determine whether these other elements are in the form of metallic alloys with the native gold or are present as nonmetallic inclusions analogous to the manganese sulphide that occurs in all steel.

The present study should be considered only as a general preliminary attack on the problem, directed primarily toward determinative methods. The limited number of specimens available precludes the statement of any conclusions except those having a general nature.

ANALYTICAL METHODS

Considering the small specimens generally available for the study of lode gold and the possibility of the occurrence of unusual or rare elements in these specimens, the spectrographic method of analysis seems to be particularly adapted to the problem. A grating spectrograph of large dispersion (21-ft. focal length) was employed.

The construction and general methods of manipulation of this instrument have been described.⁵ Some points related to the manipulations used in the analysis of the gold specimens, however, should be recorded.

All the specimens were subjected to a preliminary cleaning process in order to remove, as thoroughly as possible, all gangue particles adhering to the gold. This was accomplished by treating each specimen, in a platinum crucible, for from 4 to 8 hr. with a heated mixture of hydrochloric and hydrofluoric acids. The specimens were then thoroughly washed with several applications of boiling distilled water and the cleanliness of the surface was checked with the aid of a microscope. The matter of cleaning specimens is one of considerable importance because in some specimens in which preliminary microscopic examination apparently revealed only the presence of small adherent particles of quartz, the treatment with the mixed acids showed the solution of appreciable quantities of iron from the surface of the specimen. At first, the yellow coloration of the acid was attributed to some solution of the gold itself. Tests showed, however, that the color was due to iron. This phenomenon was universal, so that it may be surmised that most native gold specimens have a slight coating of iron oxide on their surfaces.

After thorough cleaning, the specimens or fragments thereof were activated in pure carbon electrodes. The amperage used was 4.0 at 220 volts direct current. The specimens were placed in small cavities drilled into the ends of the lower (positive) electrodes. The arc burned with unusual steadiness, emitting the characteristic green light of gold.

In all, the spectral region photographed lay in the ultraviolet between 2700 and 3400 Å. As a general check on the identity of the lines of gold, an attempt was made to prepare a sample of spectrographically pure gold. To this end some scrap gold, from various sources, was dissolved in aqua regia, diluted, and filtered several times to remove silver chloride.

Nitric acid was removed by continued evaporation with hydrochloric acid and the gold finally precipitated with ferrous sulphate.

The precipitated gold was boiled with dilute hydrochloric acid, to remove iron, and finally washed free from chlorides with distilled water. This purified gold was redissolved in aqua regia, and the nitric acid removed. The diluted gold chloride solution was then filtered four times through double Whatman No. 42 filter papers. The gold was precipitated with C.P. oxalic acid and thoroughly washed with hot distilled water. The re-solution and precipitation were repeated three times. The gold was then tested spectrographically for purity.

Besides the lines of gold, one line of copper and two lines of silver were still found to be present. Two more re-precipitations eliminated the copper line but the two silver lines persisted, although with a much lower intensity. It is estimated that the silver remaining in the purified gold amounted to only about 0.05 oz. per ton of gold, or about 0.0002 per cent. Rose and Newman¹ show a number of gold spectra, and state that the majority of spectra of "proof" gold show persistent lines of silver, copper and calcium. In the purified gold mentioned above, no calcium lines were observed. In the spectra of the gold "specimen" samples, both a pure iron guide spectrum and a spectrum from the purified gold were used as guides for calculations of line wave length.

ANALYSIS OF SPECIMENS OF NATIVE LODGE GOLD

1. *Specimen from Unknown Source.*—The original specimen was a dark brown quartz containing free gold. Particles of the gold were cleaned and analyzed. The specimen contained copper, gold, iron, molybdenum and silver.

2. *Specimen from Idaho-Maryland Mine, California.*—The elements found present were copper, gold, iron, aluminum and silver.

3. *Specimen from Melones Mines, California* (Fig. 1).—This sample was marked "telluride," and it contained heavy free gold. The cleaned gold contained copper, iron, lead and silver. There is some doubt as to the origin of this specimen. The gold particles used for the analysis were not entirely free from a black gangue material. Long treatment with hydrochloric and hydrofluoric acids, and finally with nitric acid, did not completely remove the foreign material. The presence of lead may be due to this residue.

4. *Specimen from Empire Mine, California* (Fig. 2).—From the 1100-ft. level. The cleaned gold showed the presence of silver, copper, iron and nickel.

5. *Specimen from Surface Discovery, Kalgoorlie, West Australia.*—Silver, iron, and copper were found in the cleaned gold.

6. *Specimen from Lake View Mine, West Australia.*—The gold from this specimen contained silver, iron, aluminum, vanadium and copper.

ANALYSES OF NATIVE PLACER GOLD

1. *Specimen of Fine Gold from Placer Juarez, Baja California.*—A sample of the cleaned gold particles gave gold, silver, copper and iron.



FIG. 1.—SPECIMEN FROM MELONES MINE. ETCHED SECTION. $\times 1000$.

2. *Klondike Nugget* (Fig. 6).—Piece cut from nugget.

3. *Trinity County, California, Nugget* (Fig. 6).

These specimens gave nearly identical spectra showing the presence of gold, silver, copper, antimony (Klondike only), iron, aluminum, and titanium.

TABLE 1.—*Summary of Analyses*[illegible]



FIG. 2.—SPECIMEN FROM EMPIRE MINE. ETCHED MACROSECTION. $\times 15$.



FIG. 3.—SPECIMEN FROM EMPIRE MINE. ETCHED SECTION. $\times 100$.

Analysis of Platinum Nugget

The specimen (Fig. 6) came from a Pacific Coast stream, Republic of Colombia. The composition is complex. The cleaned nugget contained platinum, iron, silver, osmium, rhodium, palladium, nickel, copper, iridium, ruthenium, aluminum and gold.

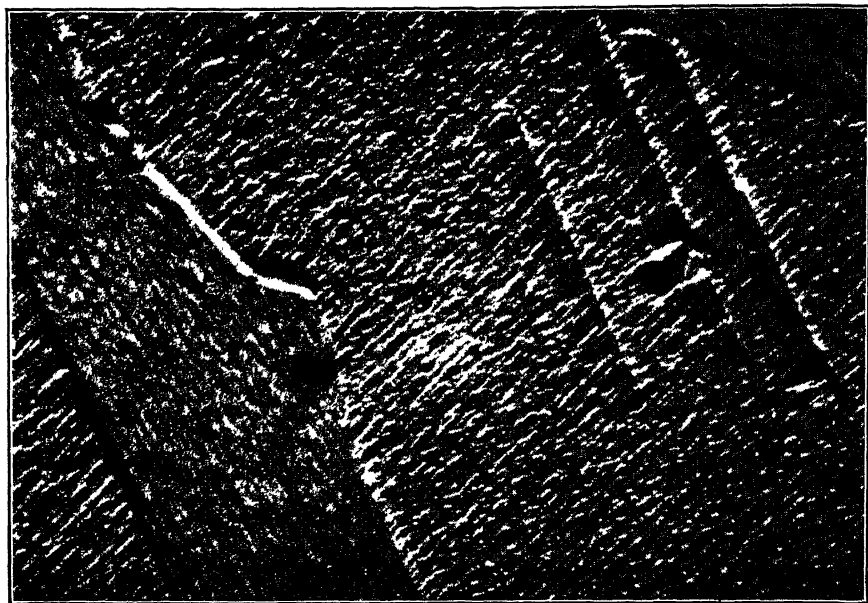


FIG. 4.—SPECIMEN FROM EMPIRE MINE. ETCHED SECTION. $\times 1000$.

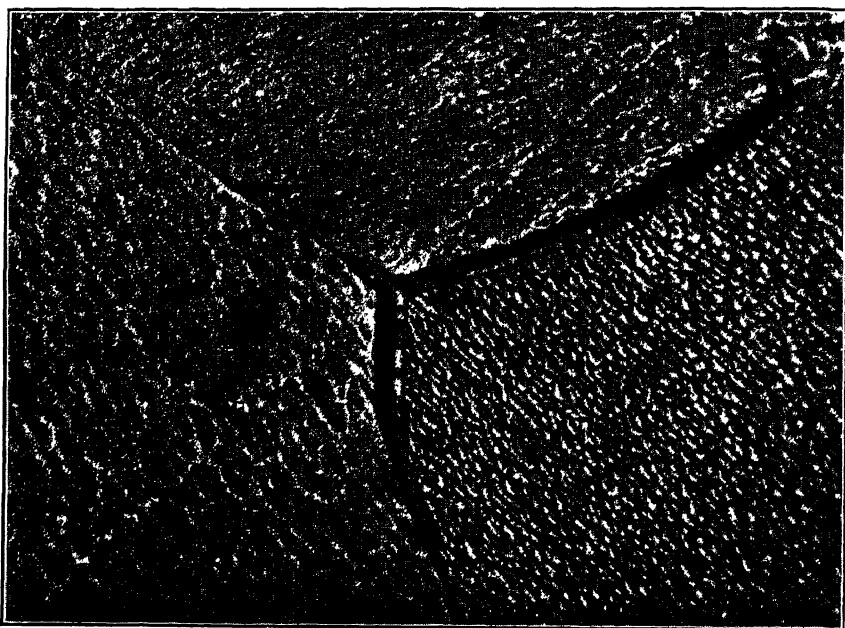


FIG. 5.—SPECIMEN FROM EMPIRE MINE. ETCHED SECTION. $\times 1000$.

DISCUSSION OF ANALYSES

The tabulated analyses show that all specimens, including the platinum nugget, contain four elements in common; viz., gold, silver, iron and copper. The question arises, however, as to the character of the occurrence of the other elements that are not common to all specimens. It is obvious that they might occur in one or all of three ways: (1) as

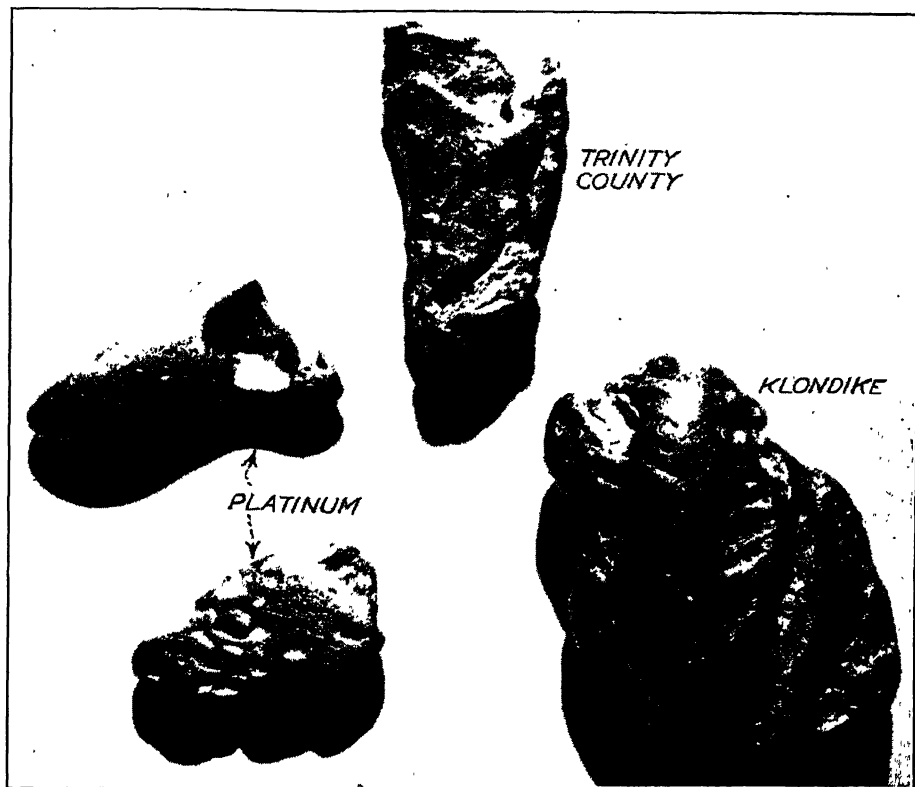


FIG. 6.—PLACER NUGGETS. $\times 4.6$.

actual alloys with the gold, (2) as adhering gangue particles on the surface of the gold, (3) as nonmetallic inclusions in the gold itself.

1. *As an Alloy: (a) Silver.*—It seems reasonable to suppose that the conditions favorable for the precipitation of gold are also favorable for silver deposition, and that the silver is deposited with the gold in elemental form. It is well known that the color of metallic gold is influenced by its silver content. Native gold containing high silver has a pale color, similar to corresponding gold-silver alloys produced by melting.

(b) *Copper*.—The same general considerations of color change may be applied to gold-copper alloys that are applied for gold and silver. Native golds of high copper content correspond in color to analogous alloys produced by melting. Native copper is a common occurrence. It might be supposed that if copper precipitates in molecular form with gold, many occasions would arise where discrete particles of metallic copper would be found associated with lode gold in quartz veins. This, however, does not seem to be true. As far as both copper and silver are concerned, the "color effect" on native gold seems to lead definitely to the conclusion that these elements occur in native gold as true alloys.



FIG. 7.—KLONDIKE NUGGET. ETCHED MACROSECTION. $\times 8$.

(c) *Iron*.—The apparently universal occurrence of the element iron in native gold is more difficult to conceive as a metallic alloy. Metallic iron is difficult to produce except by an igneous process or by electrolysis. Excluding iron of meteoric origin, the metal in elemental form is rare in nature. With very few exceptions, the published analyses of naturally occurring terrestrial metallic iron show nickel, and in all other cases the metallic iron appears to occur in connection with igneous deposits. No information is available that would indicate the possibility of the deposition of metallic iron in an ordinary gold lode deposit.

Iron sulphide, in the form of pyrite, is of course commonly associated with metallic gold. It is reasonable to suppose that the conditions favorable for the precipitation of gold are also favorable for the deposition of iron sulphide. The iron in metallic gold therefore may occur as iron

sulphide, either on the grain boundaries or in the gold molecules. In the molecules, the iron sulphide might be considered somewhat as an alloy; on the grain boundaries, as a nonmetallic inclusion.

2. *Adhering Gangue Particles*.—As previously stated, particular care was taken to remove adhering gangue particles from the surface of the specimens, by a preliminary treatment with a boiling hydrochloric and hydrofluoric acid mixture. Except on the Melones mine specimen, it is believed that a thorough cleaning was accomplished. Under these conditions, consideration of this source of elements may be eliminated.

3. *As Nonmetallic Inclusions*.—In order to study the possibilities of nonmetallic inclusions in the metallic gold itself, and to attempt to

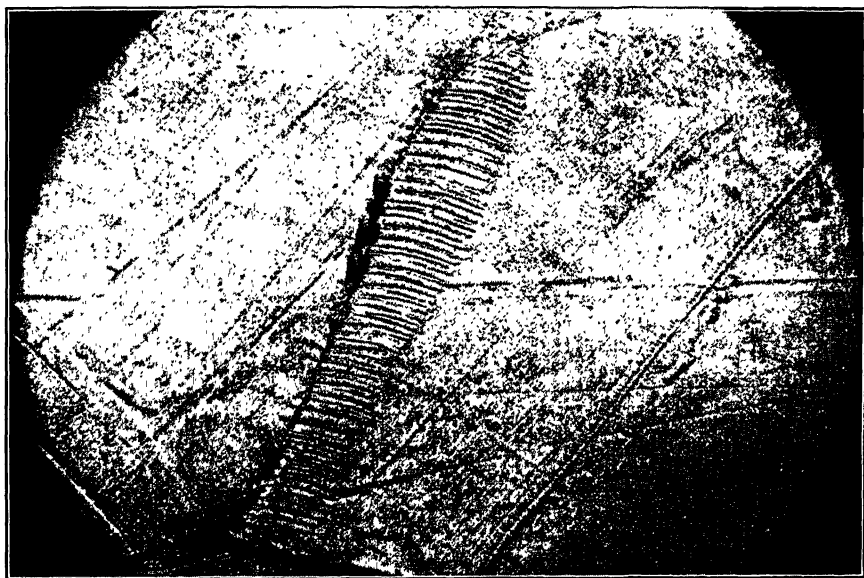


FIG. 8.—KLONDIKE NUGGET. ETCHED SECTION. $\times 400$.

account for the presence of the various elements that were found to be peculiar to different specimens, metallographic sections were prepared. To this end the gold specimens were mounted in Wood's metal, enclosed in a brass ring. Mounting in Bakelite, by means of a hot press, would have been more satisfactory, but the necessary facilities were not available at the time the work was done. On account of softness, it is somewhat difficult to produce satisfactory metallographic surfaces on gold. Polishing was done by hand on various grades of metallographic rouge papers, and the final polishing on a rotating felt-covered wheel with black iron oxide polish powder suspended in water. Various etching reagents were tried. The most satisfactory was made by mixing equal proportions of about 5 per cent aqueous solutions of potassium cyanide and ammo-

nium persulphate. Aqua regia solutions of various concentrations were tried, without obtaining satisfactory results.

In all of the specimens examined, the presence of nonmetallic inclusions was detected either as grain-boundary inclusions or as inclusions in the body of the gold crystals themselves. Photomicrographs of some of the specimens examined are included in this report. It may be stated that all the structures disclosed by microscopic examination were those that may be attributed to pure metals or solid solutions. In no case was there intimation of the presence of intermetallic compounds or eutectic alloys.

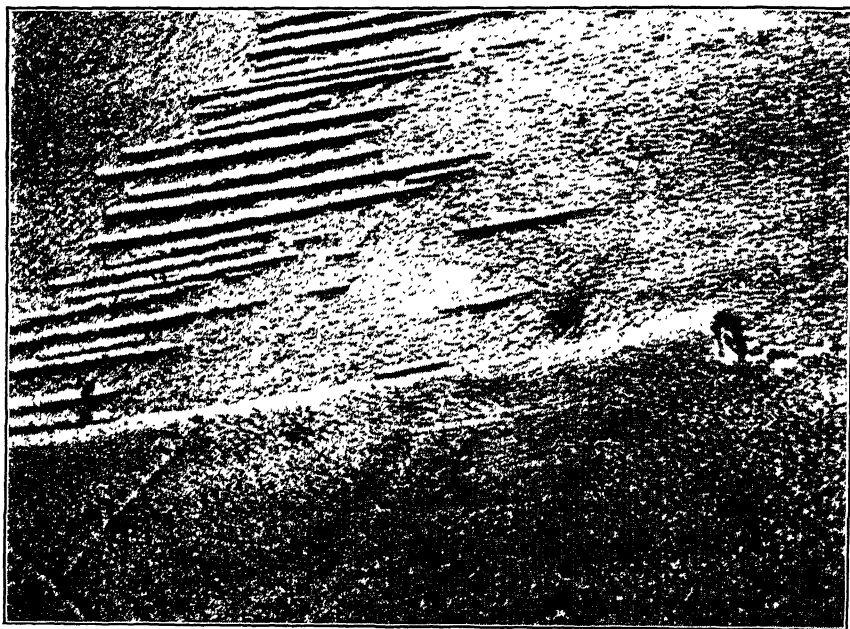


FIG. 9.—KLONDIKE NUGGET. ETCHED SECTION. $\times 1000$.

Conclusion.—From the metallographic examination, the tentative conclusion is drawn that native metallic gold ordinarily contains silver and copper only as metallic alloys; and that iron, although it may be universally present, occurs probably as iron sulphide. The many other elements that may be disclosed by the analysis of metallic lode gold and nuggets are probably present as nonmetallic inclusions which, in nuggets, may be mechanical inclusions formed by the mechanical work to which the gold has been subjected in placer deposits. In lode gold, an interesting subject of investigation would be to find whether any analogy existed between the presence of rare or unusual elements in the gold itself and in the closely adjacent gangue materials. A study might also be made

of the spectrographic analysis of nonmetallic inclusion residues obtained by electrolyzing away the metallic gold from lode and nugget specimens.

METALLOGRAPHY OF NATIVE GOLD

Lode Gold

Melones Mine Specimen.—Low-power examination of this specimen revealed little in the way of a definite structure; but the presence of inclusions was plainly discernible. At high magnification (1000 \times), a platy structure was revealed with a tendency toward cubic etch pits (Fig. 1).

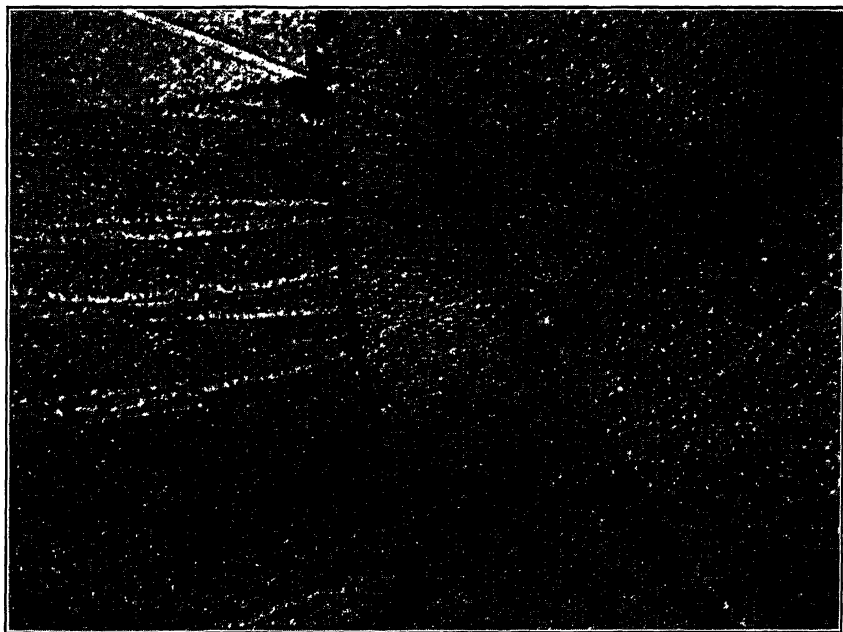


FIG. 10.—KLONDIKE NUGGET. ETCHED SECTION. $\times 1000$.

Empire Mine Specimen.—This specimen (Figs. 2-5) shows a crystalline structure that is typical of solid solutions, such as alpha brass. At higher magnifications grain-boundary inclusions and very small inclusions in the bodies of the crystals themselves were detected.

Lake View Mine Specimen.—This specimen appeared to consist of only two crystals, which exhibited a distinct difference in surface texture, owing to orientation.

Placer Gold

Juarez Placer Gold.—The specimen material consisted of extremely fine gold. The material was not examined metallographically.

Klondike Nugget.—The specimen (Figs. 7, 8, 9) was found to consist of gold crystals in which were embedded a number of nonmetallic inclusions; some voids were also present. The presence of strain lines, caused by the mechanical working of the nugget in the stream bed, were clearly indicated.

Trinity Nugget.—The surface appearance of this nugget (Figs. 11 and 12) clearly indicated that it had been subjected to considerable folding and mechanical work, so that the presence of voids and mechanical inclusions might be expected. The specimen exhibited a small crystalline structure, which extended clear to the outside surfaces. In this respect, it differed

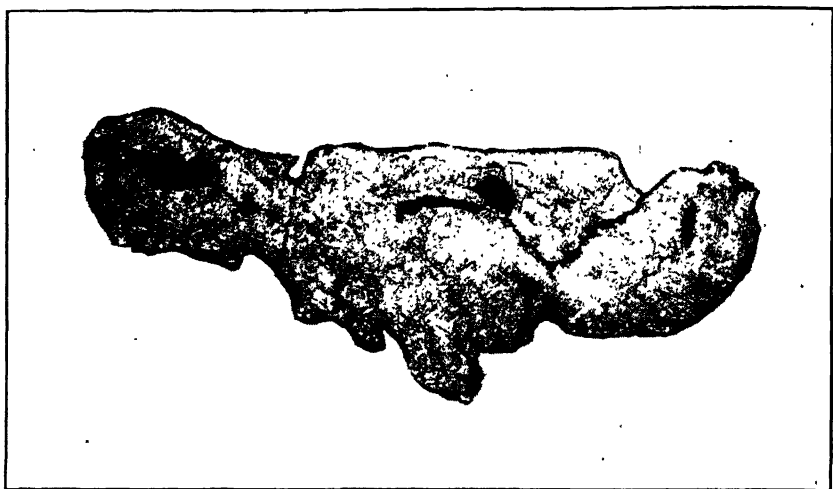


FIG. 11.—TRINITY COUNTY NUGGET. ETCHED MACROSECTION. $\times 8.5$.

materially from the Klondike nugget in that although the Trinity nugget had been subject, without doubt, to heavy mechanical work, there was a complete absence of strain lines. The absence of these lines, under these conditions, leads to the possible conclusion that the gold in the Trinity nugget had recrystallized, at ordinary temperatures, over a long period of time. Alpha brass, after severe cold-work, is well known to form "equiaxed" grains at comparatively low temperatures. The more severe the work, the lower the equiaxing temperatures. Jeffries and Archer⁶ show that the approximate lowest recrystallization temperature for gold is only 200°C . This temperature is, of course, based upon a comparatively short time factor. It seems reasonable to suppose that "time is a factor" and that when geologic time is considered, it is reasonable that severely worked gold will equiax at normal temperature. It would be interesting to study specimens of gold from "old" and "new" placers, from this point of view.

SUMMARY AND CONCLUSIONS

The small amount of specimen material available for study precludes the drawing of any but general conclusions. The observations made may be summarized as follows:

1. Ordinary native metallic gold probably consists of an alloy of gold, silver and copper. In addition, the element iron is probably always present, but possibly in the form of iron sulphide or as oxide inclusions.

2. Specimens of native metallic gold, whose surfaces have been thoroughly cleaned, may show upon analysis many and varied elements such as molybdenum, vanadium, lead, antimony, etc.; but these elements

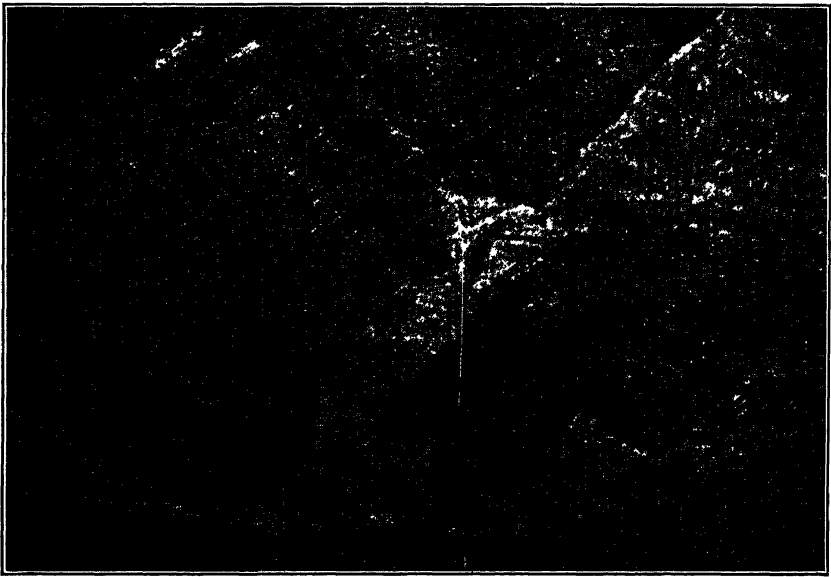


FIG. 12.—TRINITY COUNTY NUGGET. ETCHED SECTION. $\times 1000$.

are probably present in the form of nonmetallic inclusions and not alloyed with the gold itself.

3. No proof is presented for the statements 1 and 2.

4. It is not known whether or not lode gold or placer gold, from a given mine or placer, contains nonmetallic inclusions that are peculiar to the individual source.

5. The possibility exists that placer nuggets from "new" deposits show definite strain lines; while nuggets from "old" deposits, where the gold has remained at rest for long periods of time, have equiaxed at normal temperatures.

6. It is believed that a combination of spectrographic and metallographic methods may be applied readily to problems of identification of

gold from particular sources; but much labor and time must be expended on the examination of many specimens and many data accumulated before definite conclusions can be reached.

SUGGESTIONS FOR FURTHER WORK

1. A careful study of gold specimens from various levels of a number of mines, together with an attempt to correlate the analyses of gangue material with the analysis of the metallic gold, and particularly with the analysis of the inclusion material.

2. An extension of suggestion 1 to include the study of silver and copper deposits, in which the silver minerals and the copper minerals themselves are treated in the same way as the metallic gold.

ACKNOWLEDGMENTS

The encouragement given by Theodore J. Hoover, Emeritus Dean of School of Engineering, Stanford University, is gratefully acknowledged, as well as his generosity in supplying the gold specimens from Melones mine, Empire mine, Lake View mine, Kalgoorlie Surface Discovery, and the gold nuggets from Klondike and Trinity County.

The specimen material from the Idaho-Maryland mine was donated by Prof. O. E. Shepard, Department of Mining Engineering, Stanford University. The gold from the Juarez placer was furnished by Mr. Louis Moretti, Consulting Engineer, San Francisco.

REFERENCES

1. T. K. Rose and W. A. C. Newman: *The Metallurgy of Gold*, 90-91. London, 1937. Griffin & Co.
2. J. D. Dana: *System of Mineralogy*, Ed. 6. Complete with appendixes to 1915.
3. V. Zeigler: *Minerals of the Black Hills*, 48. 1914.
4. F. W. Clarke: *Data of Geochemistry*, Ed. 4, 647-649. U. S. Geol. Survey *Bull.* 695 (1920).
5. W. J. Crook: *Metallurgical Spectrum Analysis*. *Trans. Amer. Soc. Steel Treat.* (Aug. 1933) 708-732. Also Stanford Univ. Press, 1935.
6. Z. Jeffries and R. S. Archer: *The Science of Metals*, Ed. 1, 86. 1924.

Embrittlement of Silver by Oxygen and Hydrogen

By D. L. MARTIN* AND E. R. PARKER,* MEMBER A.I.M.E.

(New York Meeting, February 1943)

DURING the heat-treatment of silver specimens for tensile tests it was observed that the bars blistered and became brittle when heated in a hydrogen atmosphere.

of the tube is shown in Fig. 2. The embrittlement is extremely severe at the edge; the blisters result from the severe deformation of the surface material by large under-

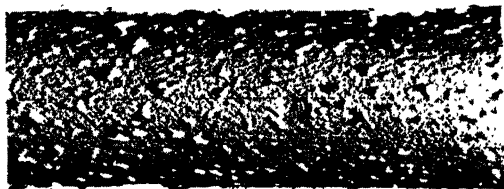


FIG. 1.—BLISTERS ON SILVER TUBE FORMED BY ANNEALING IN HYDROGEN AT 850°C . FOR ONE HOUR. $\times 3$.

FIG. 2.—MICROSTRUCTURE OF SECTION THROUGH BLISTERS SHOWN IN FIG. 1. $\times 100$. Etched with potassium bichromate followed by ammonium hydroxide-hydrogen peroxide.

To check this unexpected result, a wide variety of commercial silvers were heated in hydrogen at 850°C . Only a few of the materials developed blisters, the most severe of which is the tube pictured in Fig. 1.

The microstructure of a cross section

Manuscript received at the office of the Institute Dec. 1, 1942. Issued in METALS TECHNOLOGY, April 1943.

* Research Laboratory, General Electric Co., Schenectady, N. Y.

lying gas pockets. The effects resulting from hydrogen embrittlement of silver have been observed by numerous investigators over a long time^{1,2,3} although it was only recently that a clear explanation was offered.⁴ However, the damage resulting from hydrogen embrittlement has not been generally recognized; and it is of advantage to know more about this phe-

¹ References are at the end of the paper.

nomenon because silver is being used in increasing amounts as a substitute metal.

HISTORY

Embrittlement of oxygen-bearing copper by annealing in a hydrogen atmosphere

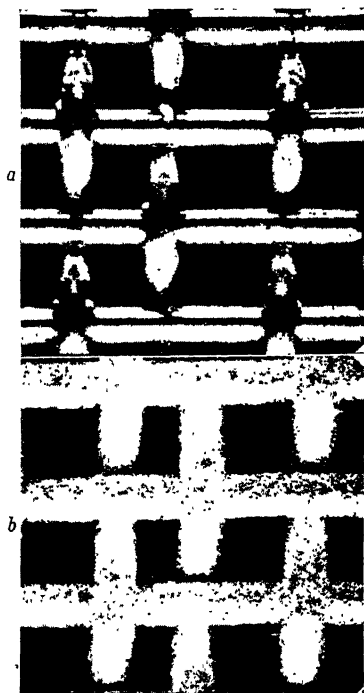


FIG. 3.—EFFECT OF HYDROGEN-OXYGEN MIXTURE ON SILVER WIRE GAUZE AS SHOWN BY BONE AND WHEELER.³

a, original appearance; *b*, gauze after air-treatment near the melting point followed by 400°C. exposure to a hydrogen-oxygen mixture.

has been thoroughly investigated.⁵⁻⁸ This effect is attributed to the formation of water vapor within the metal, by interaction of oxygen and hydrogen, with sufficient pressure to cause local rupture along grain boundaries and thus weaken the metal.

A review of the literature has revealed several examples of embrittlement of silver when heated in a hydrogen atmosphere. Graham,¹ in his experiments in 1866

on the occlusion of hydrogen by metals, found that silver acquired a beautiful frosted appearance on the surface when heated in hydrogen and by repeated heating it became brittle. Beilby and Henderson² studied the action of ammonia on metals at high temperatures. For silver, they found that at 800°C. the wire became coated with rounded blisters or bubbles, and the elasticity of the metal was greatly reduced. They attributed the change to the rapid formation and decomposition of an unstable nitride. Bone and Wheeler³ studied the catalytic action of silver on the hydrogen-oxygen reaction. They found that by heating silver in air just short of the melting point and then in a hydrogen-oxygen mixture at 400°C. "a change took place both in the outward appearance and mechanical properties." Fig. 3 illustrates very clearly the changes in the appearance of the silver gauze after this treatment. The behavior of the silver was attributed to the breaking up of a hydride.

Dornblatt⁴ briefly mentions that the formation of blisters is due to the water vapor formed within the metal by the interaction of hydrogen and oxygen.

EXPERIMENTAL RESULTS

1. The silver specimens used in the series of experiments to be described were cut from a rod of fine silver* $\frac{3}{8}$ in. in diameter, which experiments proved was not embrittled when heated only in hydrogen. However, samples of this material were made brittle by first heating in air at 850°C. and then in hydrogen at 850°C. The changes in microstructure and tensile properties are of interest. The loss of ductility and strength through hydrogen embrittlement is indeed considerable, as shown in Table 1, in which the tensile

* Fine silver contains approximately 0.05 per cent impurities. Spectrographic analysis of the silver used showed traces of Cu and Fe; Zn, Ni, Sn, Pb, Al were nil.

properties of sound and embrittled silver and copper are compared.

TABLE 1.—*Tensile Properties of Silver and Copper*

Treatment	Maximum Strength, Lb. per Sq. in.	Elongation, Per Cent in 1 in.	Reduction of Area, Per Cent
Silver			
1. Heated in N ₂ at 850°C. for 1 hr. . . .	23,250	49	70
2. Heated in air at 850°C. for 1 hr. . . .	22,750	51	67
3. Heated in air at 850°C. for 1 hr. then in H ₂ at 850°C. for 1 hr. . . .	5,600	nil	nil
Tough-pitch Copper			
1. Heated in N ₂ at 850°C. for 1 hr. . . .	33,500	39	65
2. Heated in H ₂ at 850°C. for 1 hr. . . .	24,100	6	3

The loss of strength and plasticity is clearly understood after comparison of the microstructures of the material before and after the hydrogen treatment, as illustrated in Fig. 4.

Silver forms an oxide, Ag₂O, which decomposes at about 350°C. in air. At higher temperatures oxygen exists in solution in the metal. For most treatments the specimens were maintained at temperature and the atmosphere changed from air to hydrogen. A few samples, however, were water-quenched after saturation with oxygen (by heating in air at 850°C.) and then reheated in hydrogen; no difference was noticed in the results.

When silver containing dissolved oxygen is heated in hydrogen a decline in strength and ductility results. This is in accord with the results of Rhines and Anderson⁷ on copper; they found that dissolved oxygen in copper containing no Cu₂O caused a mild susceptibility to hydrogen embrittlement.

2. The reverse of hydrogen embrittlement was also found to occur; i.e. silver containing hydrogen was embrittled by heating in air. For convenience in discussion, we have termed this effect "oxygen

embrittlement."^{*} Such embrittlement was produced by first saturating the silver with



FIG. 4.—EFFECT OF HYDROGEN ON SILVER CONTAINING OXYGEN. $\times 100$.

Etched with potassium bichromate followed by ammonium hydroxide-hydrogen peroxide.

a, heated in air at 850°C. for one hour; b, heated in air at 850°C. for one hour and then in hydrogen at 850°C. for one hour.

hydrogen at a high temperature, followed by heating in air. The resulting structure

* Strictly speaking, the terms "hydrogen embrittlement" and "oxygen embrittlement" are both misnomers, since both gases are equally necessary for the formation of water vapor. The term "water-vapor embrittlement" would be a more general and accurate description of the effect.

is shown in Fig. 5. No embrittlement was found in other samples heated only in hydrogen. To check these results, a piece of silver was degassed by heating for

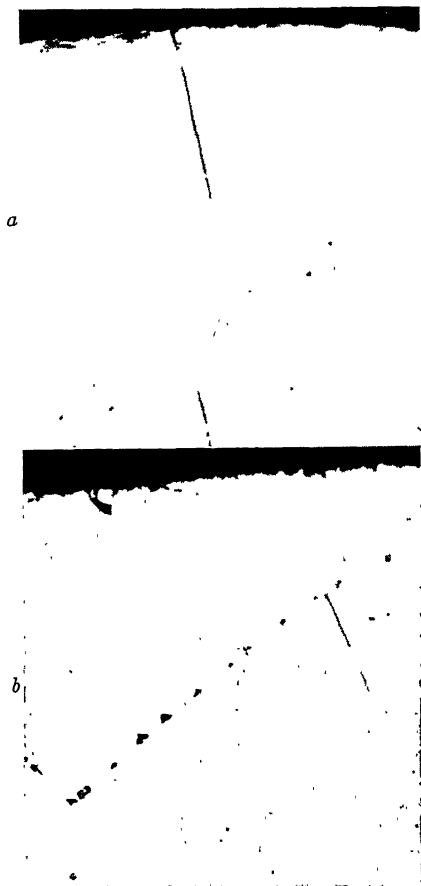


FIG. 5.—EFFECT OF OXYGEN ON SILVER CONTAINING HYDROGEN. $\times 500$.

Etched with potassium bichromate followed by ammonium hydroxide-hydrogen peroxide.

a, heated in hydrogen at 850°C . for one hour;
b, heated in hydrogen at 850°C . for one hour then in air at 850°C . for one hour.

$\frac{1}{2}$ hr. in vacuum at 850°C . The piece was cut into two samples; one was heated only in hydrogen for 1 hr. at 850°C ., the other was heated first for 1 hr. in hydrogen at 850°C ., then the atmosphere was changed

to air, without change of temperature, and held for another hour. No embrittlement was found in the sample heated only in hydrogen, but marked embrittlement resulted in the sample heated first in hydrogen then in air. However, the oxygen embrittlement was not as severe as the hydrogen embrittlement (see Fig. 4).

Oxygen embrittlement could occur only if the oxygen diffused into the silver before the hydrogen could escape. This is in accordance with the known rapid absorption of oxygen by silver.

3. The grain size at the surface of the silver specimen heated first in air (Fig. 4) is much smaller than that of the sample heated first in hydrogen (or in vacuum), Fig. 5. Rhines and Grobe¹¹ observed a similar fine-grained zone in silver and silver alloys after an oxidizing anneal.

Small amounts of soluble impurities frequently have profound effects on the annealing characteristics of the base metal,^{12,13} accordingly it was considered possible that oxygen in solution might, in this case, be responsible for the fine-grained surface zone. To check this, a sample was water-quenched from 850°C . after saturation with oxygen; cold-worked and then reheated for 1 hr. in air at 850°C . If soluble oxygen inhibited grain growth the silver sample should be fine-grained throughout. However, this was not true—the fine-grained structure was confined to the surface; hence, some other factor was responsible for the retarded grain growth.

To see whether the metal in the center of the rod behaved in the same way as the metal near the surface, a rod $\frac{5}{16}$ in. in diameter was machined to $\frac{3}{16}$ -in. diameter and then heated in air for 1 hr. at 850°C . In this sample coarse grains extended to the surface, indicating that the fine-grained structure found near the surface of the $\frac{5}{16}$ -in. bar heated in air was characteristic only of the metal near the outside of the rod. Hence it was concluded that the original bar of silver was

not homogeneous. Something inherent in the surface material, apparently introduced in the manufacturing process, caused fine grains when the metal was heated in air, but not when heated in hydrogen or vacuum.

4. To determine the minimum temperature at which silver, containing oxygen, would be embrittled by hydrogen, a series of samples was first heated in air at 850°C. for 7 hr. and then quenched; individual specimens were heated for 1 hr. in hydrogen at various temperatures ranging from 450° to 850°C. The embrittlement at lower temperatures was less severe and did not occur below 500°C.

EXPERIMENTS WITH GOLD AND PLATINUM

To be susceptible to hydrogen embrittlement, a metal must contain considerable oxygen, either combined or dissolved, which is free to react with hydrogen; thus platinum and gold, which do not form stable oxides and dissolve little or no oxygen,^{8,9} should not become embrittled in hydrogen. Samples of these metals were heated in air at a high temperature and then in hydrogen; the gold and platinum were free from grain-boundary fissures.

SUMMARY

Solid silver will dissolve sufficient oxygen at high temperatures to become embrittled if subsequently heated in a hydrogen atmosphere (above 500°C.).

In the use of silver, embrittlement can be avoided by never exposing to an atmosphere containing hydrogen material that has previously been heated in air.

Oxygen embrittlement of silver, the reverse process of hydrogen embrittlement, is also possible—the metal is first heated in hydrogen and then in air.

Samples of the original material developed fine grains near the surface when heated in air, but coarse grains throughout when heated in hydrogen or vacuum.

Gold and platinum dissolve little or no oxygen and therefore are not embrittled when heated in a hydrogen atmosphere after an air treatment.

It appears that embrittlement resulting from the union of dissolved or combined oxygen with hydrogen is common to copper and silver, and probably to any metal that contains reducible oxides or that will dissolve appreciable oxygen in the solid state. If water vapor can be formed within any metal, embrittlement is possible.

ACKNOWLEDGMENTS

The authors wish to express their appreciation to Mr. Roy Adams for conducting the heat-treatments, and to Mrs. C. B. Brodie and Miss F. E. Wiley for the photomicrographs.

REFERENCES

1. Graham: *Phil. Trans.* (1866) **156**, 435.
2. Beilby and Henderson: *Trans. Chem. Soc.* (1901) **79**, 1245.
3. Bone and Wheeler: *Phil. Trans.* (1906) **205-A**, 1.
4. Dornblatt: *Silver in Industry*, chap. 5, 180. New York. Reinhold Publishing Corporation.
5. N. B. Pilling: *Trans. A.I.M.E.* (1919) **60**, 322.
6. L. Wyman: *Trans. A.I.M.E.* (1933) **104**, 141; (1934) **111**, 305; (1940) **137**, 291.
7. F. N. Rhines and W. A. Anderson: *Trans. A.I.M.E.* (1941) **143**, 312.
8. C. E. Ransley: *Jnl. Inst. Metals* (1939) **65**, 147.
9. F. M. G. Johnson and P. Larose: *Jnl. Amer. Chem. Soc.* (1927), **49**, 312.
10. J. H. Simons: *Jnl. Phys. Chem.* (1932) **36**, 652.
11. F. N. Rhines and A. H. Grobe: *Trans. A.I.M.E.* (1942) **147**, 318.
12. O. F. Hudson, T. M. Herbert, F. C. Ball and E. H. Bucknall: *Jnl. Inst. Metals* (1929) **42**, 221.
13. R. M. Brick, D. L. Martin and R. P. Angier: *Amer. Soc. Metals Preprint No. 37* (1942).

DISCUSSION

(F. N. Rhines presiding)

J. L. CHRISTIE,* Bridgeport, Conn.—Attack by hydrogen at elevated temperatures on fine silver containing oxygen is not uncommon.

* Metallurgical Manager, Handy and Harman.

mon. It occurs in varying degrees; sometimes the surface assumes the frosty appearance referred to; sometimes the surface takes on a rash of small blisters; and occasionally, in severe cases, the entire sheet becomes a mass of blisters.

The usual way of testing silver for presence or absence of oxygen is to heat it in hydrogen. This test can be misinterpreted. The elevated temperature is likely to raise up any small blisters that originated as gas cavities in the casting, and these may be confused with blisters from the hydrogen-oxygen reaction. Also, if the specimen is heated in hydrogen, withdrawn from the furnace and allowed to cool in the air, the frosty appearance or rash of blisters may result from oxygen embrittlement of the silver that has been saturated with hydrogen. We once had a case in which surface blisters appeared on silver specimens tested in a pack because of the asbestos sheets used to separate the silver sheets to keep them from sticking to one another.

While we have not made a careful study of the matter, it is our opinion that the fine grain at the surface is related to oxygen-hydrogen embrittlement. Perhaps if the past history of the $\frac{3}{16}$ -in. and $\frac{5}{16}$ -in. rods used by the authors is known, some idea of the nature and cause of the inhomogeneity can be obtained. The stock developed the fine grain at the surface when heated in air, not when heated in hydrogen; and it did not become embrittled when heated in air. Perhaps the surface layer of the stock had taken up a small amount of hydrogen from an anneal in a slightly reducing atmosphere; not enough to cause visible rupture of the grain boundaries when subsequently heated in air, but just enough to interfere with grain growth.

There are two questions. Is the past history of the silver used in the experiments a matter of record? This might throw some light on the inhomogeneity referred to on pages 272-273.

We should be interested to know also the technique followed in changing the atmosphere in the furnace from hydrogen to air without causing an explosion.

D. L. MARTIN AND E. R. PARKER (authors' reply).—The origin of the fine-grained structure near the surface of the samples that were heated in air has been the most elusive of all

the problems we have studied in connection with this work. In an attempt to determine the origin of the fine-grained structure in samples that were heated in air, all we succeeded in doing was to find numerous conditions that would not produce the structure.

For example, the previous history of the original material was unknown to us. Some of the bars were embrittled when heated in hydrogen, and others we tested were not. We remelted some of this material in a vacuum furnace in an effort to control the history. This vacuum-melted material was cold-worked and annealed in various atmospheres to study the effect of the various gases on the structure at the surface. Samples of the cold-worked silver heated in hydrogen, nitrogen, or vacuum had coarse grains all the way out to the surface. On the other hand, samples heated in air had a layer of fine grains around the outside. Thus, it would seem that oxygen must be present to cause this structural condition, although we cannot suggest a mechanism to account for the results obtained.

In regard to the second question. We were worried about changing from air to hydrogen when we thought about trying it, but actually it was not so difficult. We have a very good technician in our laboratory, who has had about 30 years of experience, and he said it was easy, so we let him do it. He inserted an iron tube inside a regular nichrome-tube furnace. The tube had a small opening at one end to which was fastened the hydrogen or air supply; the other end had a large opening. The samples were placed in the tube and air passed over them; in changing to hydrogen, the air hose was disconnected and hydrogen was slowly let in, the flow gradually increasing. Small explosions did frequently occur but if the one end of the tube is left open no great danger is involved.

In changing from hydrogen to air the process is reversed; however, in this case the hydrogen is allowed to burn out by opening both ends.

W. A. MUDGE,* New York, N. Y.—Can the same or a similar type of embrittlement be secured with silver containing oxygen if the reducing atmosphere is carbon monoxide?

D. L. MARTIN AND E. R. PARKER.—That is a good question. We really do not know, but suspect not, because tough-pitch copper is

* International Nickel Company.

not embrittled when heated in carbon monoxide and silver containing oxygen should likewise not be affected. Carbon monoxide is essentially insoluble in both solid metals.

R. VINES,* Long Island City, N. Y.—We did some similar work on silver, palladium-silver and palladium some time ago at The International Nickel Co., and obtained similar results as far as hydrogen embrittlement is concerned. However, I would like some further information about the embrittlement produced by heating first in hydrogen and then in air. How does the degree of this embrittlement compare with that produced by air followed by hydrogen, and will it occur on silver that is undamaged by hydrogen annealing if the sample is cooled or quenched from the hydrogen anneal and then reheated in air?

D. L. MARTIN AND E. R. PARKER.—Oxygen embrittlement was produced by first heating in hydrogen and then in air (oxygen) at the same temperature without cooling the sample. We did not try quenching or slow cooling of the silver after the hydrogen treatment, so that we cannot give any actual data.

The silver might lose enough hydrogen during the cooling and reheating so that embrittlement would be very slight, if it should occur at all. The amount of embrittlement that was produced by heating first in hydrogen and then in air is very small compared with that normally found when the silver is heated first in air and then in hydrogen.

J. S. SMART, JR.,† Barber, N. J.—By way of confirmation of the effect of oxygen, I might add that we have made experiments in which we diffused oxygen into copper at 850°C., quenched the samples and then cold-worked them and observed the grain-growth characteristics. We found that the amount of oxygen precipitated from solid solution is sufficient to inhibit grain growth at 600° or 700°C. to a considerable extent. If the annealing temperature is raised to 850° or 900°C., the oxide goes back into solution, releasing the restricting effect, and the sudden grain growth that then occurs forms very large grain sizes of the so-called "abnormal" type.

* Ford Instrument Company.

† Central Research Laboratory, American Smelting and Refining Company.

D. L. MARTIN AND E. R. PARKER.—We tried to determine the effect of silver oxide on the grain growth of silver heated in air. We first heated the silver in air at 850°C. to saturate it with oxygen, and then cooled it slowly in the furnace. Examination showed a fine-grained surface zone and a coarse-grained interior. A precipitate of silver oxide was visible in the microsections.

The outer layer of fine grains was machined off and the center part cold-worked. The cold-worked samples, containing silver oxide precipitate, were reheated to 850°C. This treatment produced coarse grains in the inside and fine grains at the surface in some samples and coarse grains all the way to the surface in other specimens given the same apparent treatment. Oxygen in some form seems to be responsible for the fine-grained surface zone but as yet we have not been able to tell how it operates.

G. D. MARSHALL,* Annapolis, Md.—I have observed, in extruded oxygen-free copper rod that is just as it came from the die, that the rod will often have a layer of fine-grained material at the surface, indicating either that the material was oxidized in the heating, which appears relatively unlikely, or that the oxidation and recrystallization took place simultaneously with resultant grain refinement at the surface.

C. R. MARSLAND,† Bridgeport, Conn.—I think that situation is different from the one we have here. That is more clearly connected with the grain growth due to certain work-hardening at the surface, compared with the center. I do not think that it is a gas effect.

G. D. MARSHALL.—That type of material will blister under certain conditions when it is reheated.

C. J. BIER,‡ West Orange, N. J.—In studying the metallography of powdered metal parts, there have been many instances in which I have noted a fine-grained area on the outside of a part and a relatively coarse-grained area in the interior. Since these parts were made of powders that were coated with some oxide and then were sintered in an atmosphere

* Lieutenant, U.S.N.R., U. S. Naval Engineering Experiment Station.

† Handy and Harman.

‡ Henry L. Crowley and Co., Inc.

containing hydrogen, I have often wondered whether or not the grain-size differences noted were a result of the same oxygen-hydrogen equilibrium mentioned in this paper.

D. L. MARTIN AND E. R. PARKER.—The effects described by Mr. Bier may very well be related to a hydrogen-oxygen reaction, but we cannot say that they are, since we know so little about the factors involved.

F. H. WILSON,* Waterbury, Conn.—The results in the paper suggest that a possible reason why embrittlement resulting from oxygen anneals following the hydrogen anneals is less than in the other case might be found in the relative solubilities of oxygen and hydrogen in silver. Do the authors have any ideas as to whether or not this is a factor?

D. L. MARTIN AND E. R. PARKER.—We have decided that the difference in embrittlement is more a matter of rates of diffusion than of solubility, since the solubility of both hydrogen and oxygen in silver is fairly high. Hydrogen ordinarily diffuses much more rapidly in metals than does oxygen, and in order to have oxygen embrittlement it is necessary to get the oxygen in before the hydrogen diffuses out. That being the case, it seems that the diffusion rate of oxygen in silver must be almost as great as that of hydrogen. We intend to check the rates of diffusion of hydrogen and oxygen through silver to see whether they are of the same order of magnitude.

D. C. JILLSON,† Palmerton, Pa.—I would like to caution investigators that the tolerable oxygen or moisture content of hydrogen is quite low with some materials, although not with others, and that in discussing hydrogen atmospheres used with those materials it is very important to know the moisture content of the hydrogen. For precise work, hydrogen should be dried very carefully, and the actual moisture or oxygen content should be determined.

D. L. MARTIN AND E. R. PARKER.—We have neglected to mention that in this work we used very carefully dried hydrogen. Mois-

ture does make a difference in the results, as shown by Bone and Wheeler.³

T. M. BAINS, JR.,* Washington, D. C.—This may not be pertinent, but some of the experts present might explain something. Many gold and silver assayers remember the Cornet rolls, for gold-silver bullion assay. As the bead is taken out of the cupel, sometimes it is a good size. That is dissolved in acid, to get rid of the silver. There is no copper, understand, it is pure gold-silver. There may be platinum, but we will not consider the platinum—just gold and silver. When you start to roll the bead in Cornet rolls, what happens? After the first couple of passes through the rolls it begins to crack and gets brittle. What do you do then? You heat it in a Bunsen burner, direct, to red heat.

That Bunsen flame has hydrogen in it, hasn't it?—hydrogen and CO. As it is heated, the bead softens. Then it is run through the rolls again, and a bead the size of the end of one's fingernail will make a strip about a foot long, a thousandth of an inch thick. Then it is rolled on a match stick, to make the "cornet," and put into acid. I wonder if you could tell me exactly what happens? This is a case of annealing in hydrogen, which softens the silver, and then working it in the cold hardens it and causes it to crack.

When the bead is taken out of the furnace, you must remember, all the oxygen is out, because with a large bead you can make a "sprout." I have seen "sprouts" 4 or 5 in. high, due to the rapid expulsion of oxygen from the bead. Therefore, you take the bead out and cover it with another cupel and cool it gradually, so that probably all the oxygen is out of it, all the absorbed oxygen, before work is begun on it.

I know nothing about it, but I would like to have that explained, because I have been puzzled. Can you give me any explanation of that phenomenon? I have worked more than 40 years on that problem.

D. L. MARTIN AND E. R. PARKER.—That sounds like a pretty tough problem, and if you have been at it that long we probably cannot give you the correct answer. Probably the bead is very porous from the liberation of

* American Brass Company.

† Research Division, New Jersey Zinc Company.

* War Production Board.

oxygen and would tend to be brittle on that account. Rolling for one or two passes would tend to close the voids (although cracks might form) and reheating would tend to sinter or weld the sides of the pores together. The sintering of the cracks would make the metal more ductile.

The Bunsen flame may not contain hydrogen, since certain parts of the flame are oxidizing

in nature, therefore water-vapor embrittlement would not necessarily occur if the bead were heated in the flame.

Another possibility is that the bead may have a coarse crystal structure, typical of cast metals, which tends to crack when cold-worked; however, by reannealing after a few passes the structure is refined and the ductility increased.

Sulphides in Nickel and Nickel Alloys

By A. M. HALL*

(New York Meeting, February 1943)

SULPHUR, even in small amounts, may often be harmful to nickel and high-nickel alloys, causing impairment of mechanical strength and destruction of malleability and ductility, as shown by Merica and Waltenberg.^{1,2} It may act either in the form of nonmetallic inclusions produced in the liquid state during furnacing or as reaction products resulting from its diffusion into the solid metal.

In recognizing the action of this element, ability to identify its various forms by means of the microscope is often of considerable importance, especially when direct quantitative methods are inapplicable.

TABLE 1.—*Nominal Compositions of Alloys Investigated*

Name	Composition, Per Cent							
	Ni + Co	Cu	Cr	Fe	Mn	Si	C	S
Malleable nickel...	99.4	0.1		0.15	0.2	0.05	0.1	0.005
Monel...	67	30		1.4	1	0.1	0.15	0.01
Inconel...	79.5	0.2	13	6.5	0.25	0.25	0.08	0.015

Of the sulphur compounds associated with nickel and high-nickel alloys, the sulphides that may be found in malleable nickel, Monel† and Inconel† are an important group. These sulphides were investi-

gated by metallographic methods in order to provide descriptive data by which to identify them. The nominal compositions of malleable nickel, Monel and Inconel are given in Table 1.

The term "sulphide" is employed here in a very general sense, to designate a substance in which sulphur and one or more metallic elements are combined. The term includes any combinations of compounds and solid solutions.

METHOD OF INVESTIGATION

Three groups of small laboratory melts were made, one group to represent each of the three types of alloy under investigation. Within each group, a number of ingots with a sufficient variety of chemical analyses were prepared so that the effect of each of the elements entering the complete commercial alloy could be isolated and observed. In most cases, to facilitate metallographic study by exaggerating the number and size of the resulting sulphides, somewhat greater amounts of the minor elements were added than are present in the commercial alloys. Likewise, considerably more sulphur was added than is normal, but not enough to complicate the system.

Transverse sections were cut at a point one third of the distance from the butt to the head of each ingot, polished and examined with an inverted stage metallograph equipped with a combination polarizing-analyzing vertical illuminator. The light source was a tungsten-mercury vapor arc lamp.

Manuscript received at the office of the Institute Dec. 1, 1942. Issued in METALS TECHNOLOGY, June 1943.

* Research Metallurgist, Huntington Works Laboratory, International Nickel Co., Huntington, West Va.

¹ References are at the end of the paper.

† Reg. U. S. Pat. Office.

TABLE 2.—*Sulphides in Nickel, Monel and Inconel*

Melt No.	Chemical Analysis, Per Cent ^a							Description of Sulphide				Reaction of Sulphide to			
	Group	Cu	Cr	Fe	Mn	Zr	Mg	S	Type	Form	Appearance as Polished		Distilled Water ^e	Sulphur Printing	Nitric Acid ^d
											White Light ^b	Polarized Light, Crossed Nicols			
A-1 Nickel				0.69				0.065 } 0.066 }	Ni	Envelopes and globules	Very pale yellow	Black ^e	No effect	No print	Darkened
A-2 Nickel				0.68				0.084	Ni and Mn	For description of manganese sulphide, see B-3	Blue gray	Anomal. ^f	Removed	Print	Removed
A-3 Nickel				0.72	0.49		0.103	0.079 } 0.088 }	Mg	Small globules	Light blue	Black ^e	No effect	No print	Pitted and darkened
A-4 Nickel					0.69			0.097 }	Cu	Irregular globules	gray	Black ^e	No effect	No print	Darkened
B-1 Monel	29.26			1.01	0.88			0.088 }	Mn	Globules	Medium gray	Black ^e	No effect	Print	Darkened
B-2 Monel	29.30			1.01	0.88			0.088 }	Mn	Globules	Medium gray	Black ^e	No effect	Light print	Darkened
B-3 Monel	29.24			1.04	0.95	0.10 ^g		0.080	Mn-Zr	Globules			No effect	No print	Darkened
B-4 Monel	28.50												No effect	No print	Darkened
B-5 Monel	29.08			1.12	0.90		0.189	0.082 } 0.11 }	Mg	For description, see A-4	Pale gray ^h	Black ^e	No effect	No print	No effect
C-1 Inconel		15.20						0.10 } 0.098 }	Cr	Irregular globules			No effect	No print	No effect
C-2 Inconel			14.21	6.72				0.191 } 0.057 }	Cr ⁱ	Irregular globules	Pale gray ^h	Black ^e	No effect	No print	No effect
C-3 Inconel			14.06	7.09	0.51								No effect	No print	No effect
C-4 Inconel			14.00	6.81	0.47		0.191	0.057	Mg	For description, see A-4			No effect	No print	No effect

^a Balance, nickel.^b Tungsten-mercury vapor arc-light source, apochromatic objective, oil immersion.^c 20 minutes immersion at room temperature.^d Immersion in commercially concentrated acid at room temperature.^e Isotropic behavior.^f Some specimens appear isotropic, some show uniform coloration and some show irregular extinction. These effects are believed to be due to surface oxidation of the sulphides.^g 0.10 per cent added. Presence in melt verified qualitatively by spectrograph.^h Bluish fringe with apochromatic objective; reddish fringe with fluorite objective.ⁱ May be complex, containing iron or manganese, or both.

Identification was based on a correlation between total chemical analysis and observations made with the microscope.

PREPARATION OF MATERIAL

Melting was accomplished in an air atmosphere, using a laboratory coreless induction furnace. The heats were maintained and finished high in carbon to ensure, as far as possible, the absence of oxygen. The ingots, weighing about 200 grams each, were chill-cast to prevent precipitation of graphite or of carbides (in the Inconel group) whose presence might produce confusion.

Electrolytic nickel, electrolytic copper and silicon-reduced chromium were used. The minor elements were added either unalloyed or in the form of nickel addition alloys.

The metallographic sections were cut, ground and polished using dry methods and slow speeds to prevent any alterations in the inclusions that heat or liquids might induce.

When sulphur printing was employed, the technique standard for iron and steel was used except that a stronger acid solution was required; i.e., a 10 per cent by weight aqueous sulphuric acid solution.

When the cyanide persulphate etchant was used, as in revealing nickel sulphide in nickel, the method was to apply a few drops of 10 per cent by weight aqueous potassium cyanide solution to the surface to be etched. Then an equal volume of the solution formed upon dissolving a few crystals of ammonium persulphate in 10 ml. of water was added.

Discussion of Observations

In Table 2 the sulphides observed, together with the melts in which they were found, are listed and described. They are also illustrated in Figs. 1 to 15.

Nickel sulphide is very difficult to distinguish from nickel as polished. However, a few seconds immersion in 2 per cent

FIG. 1.—NICKEL SULPHIDE IN MELT A-1. CYANIDE-PERSULPHATE ETCH.

FIG. 2.—MANGANESE SULPHIDE IN MELT A-3 AS POLISHED.

FIG. 3.—NICKEL SULPHIDE AND MANGANESE SULPHIDE IN MELT A-3. CYANIDE-PERSULPHATE ETCH.

All oil immersion, $\times 1000$.

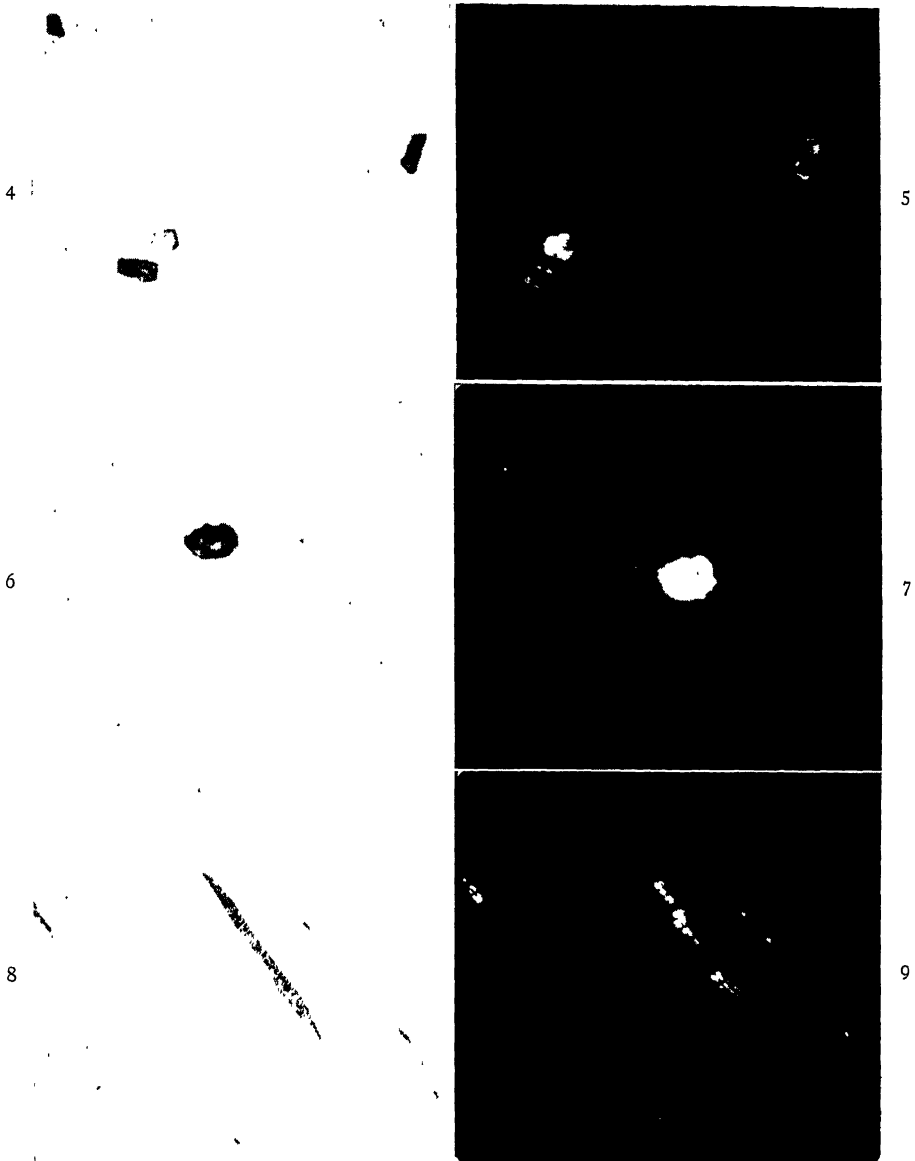


FIG. 4.—MAGNESIUM SULPHIDE IN MELT A-4, AS POLISHED. OIL IMMERSION, $\times 1500$.

FIG. 5.—SAME FIELD AS FIG. 4, POLARIZED LIGHT, CROSSED NICOLS.

Note that one specimen shows extinction, while the others show nonuniform coloration.

FIG. 6.—MAGNESIUM SULPHIDE IN COMMERCIAL MONEL, AS POLISHED. OIL IMMERSION, $\times 1500$.

FIG. 7.—SAME FIELD AS FIG. 6, POLARIZED LIGHT, CROSSED NICOLS.

FIG. 8.—MAGNESIUM SULPHIDE IN COLD-DRAWN HIGH-SULPHUR FREE-MACHINING MONEL, AS POLISHED. OIL IMMERSION, $\times 1500$.

FIG. 9.—SAME FIELD AS FIG. 8, POLARIZED LIGHT, CROSSED NICOLS.

10

11

12

13

14

15

FIG. 10.—COPPER SULPHIDE IN MELT B-1, AS POLISHED. OIL IMMERSION, $\times 1500$.

FIG. 11.—CHROMIUM SULPHIDE IN MELT C-1, AS POLISHED. OIL IMMERSION, $\times 1500$.

FIG. 12.—NICKEL SULPHIDE FORMED BY DIFFUSION OF SULPHUR INTO NICKEL AT 930°C . CYANIDE PERSULPHATE ETCH. OIL IMMERSION, $\times 1000$.

FIG. 13.—NICKEL SULPHIDE AND MANGANESE SULPHIDE FORMED BY DIFFUSION OF SULPHUR INTO HIGH-MANGANESE NICKEL AT 940°C . CYANIDE PERSULPHATE ETCH, $\times 750$.

FIG. 14.—COPPER SULPHIDE, PROBABLY COMPLEX, FORMED BY DIFFUSION OF SULPHUR INTO MONEL. $\times 750$.

FIG. 15.—CHROMIUM SULPHIDE, PROBABLY COMPLEX, FORMED BY DIFFUSION OF SULPHUR INTO INCONEL. $\times 500$.

nital reveals it very satisfactorily. The cyanide persulphate etchant also yields good results. Iron, in the amounts found in commercial nickel, does not appear to com-

sulphide³ is isometric and hence should be isotropic.

In the Monel series, iron when present in normal amounts again appears not to com-

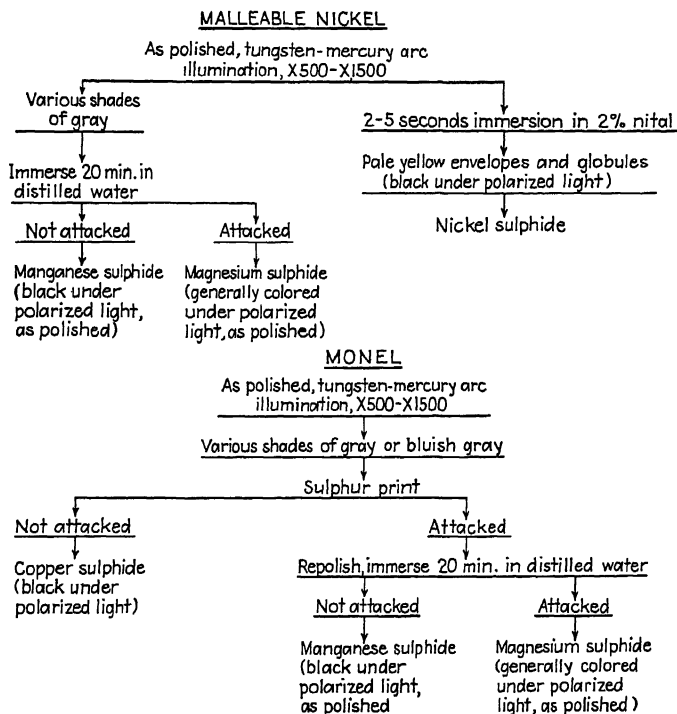


FIG. 16.—TENTATIVE SCHEMES FOR DISTINGUISHING SULPHIDES IN MALLEABLE NICKEL AND MONEL.

bine with sulphur. In melt A-3, insufficient manganese was present to combine with all the sulphur and some nickel sulphide was also observed. At higher manganese or lower sulphur contents, manganese sulphide is the only sulphide found, as shown by Merica and Waltenberg.^{1,2} The behavior of magnesium sulphide under polarized light with crossed nicols seemed anomalous. Some specimens appear isotropic, some show fairly uniform coloration in all positions of stage rotation, while others have an extinction that is spotty and uneven. These effects are believed to be due to the presence of a surface film formed on the sulphide by atmospheric oxidation, possibly aided by moisture in the air. The known magnesium

sulphide³ is isometric and hence should be isotropic. The sulphide in melt B-4 appeared in all respects similar to the manganese sulphide found in melt B-3. However, it would not yield as dense a sulphur print. In view of Urban and Chipman⁴ and Portevin and Castro⁵ it is thought that this is a manganese sulphide containing some zirconium.

The sulphide found in melt C-1 was similar to the chromium sulphide described by Urban and Chipman⁴ and Portevin and Castro.⁶ Though it appeared to be unaltered by the addition of iron and manganese (melts C-2 and C-3), it is nevertheless considered highly probable that in the presence of these elements the sulphide may become complex. It may contain chromium,

together with either or both iron and manganese.

Merica and Waltenberg^{1,2} observed that the hot and cold malleability of nickel increased as the envelopes of nickel sulphide gave way to the intercrystalline globules of manganese sulphide, and again as these were replaced by the intragranular particles of magnesium sulphide. Similarly, they observed that the change from copper sulphide to manganese sulphide and finally to magnesium sulphide improved the hot and cold malleability of Monel. This tendency of magnesium sulphide to replace manganese sulphide and of manganese sulphide to replace either nickel sulphide or copper sulphide may be seen in Table 2, wherein the data show that the dominance of magnesium sulphide also extends to the Inconel group. For these alloys, normal commercial furnace practice results in the final formation of magnesium sulphide whose intracrystalline location renders it harmless to malleability.

The data in Table 2 suggest the tentative schemes of Fig. 16 for distinguishing among the sulphides likely to be found in malleable nickel and Monel.

In the Inconel group no scheme of identification was developed, since only two types of sulphide were found. Immersion in distilled water or sulphur printing readily distinguishes between them.

SULPHIDES PRODUCED BY DIFFUSION

It is recognized that the phenomena involved in producing a nonmetallic inclusion in the liquid state of a metal or during the solidification and cooling of a metal are quite different from those resulting in a reaction product formed upon diffusion in the solid state. Nevertheless, in the sulphides associated with nickel, Monel and Inconel, the end products of these two groups of processes are often sufficiently similar so that the data in Table 2 may be used successfully to identify the general type to which belong many of the sulphides produced upon the diffusion

of sulphur into the solid metal at high temperatures. The most common of these sulphides are illustrated in Figs. 12, 13, 14, and 15.

SUMMARY

A group of sulphides that may be associated with malleable nickel, Monel and Inconel was described as they occur in small induction-furnace melts. From the data collected, tentative schemes for distinguishing among these sulphides were developed. The data may also be used to identify the general type to which belong the commonly encountered sulphides formed upon the diffusion of sulphur into the solid metal.

ACKNOWLEDGMENT

The author wishes to express his appreciation to the officials of The International Nickel Company, Inc. for permission to publish the data contained in this paper. Further, he is very grateful for the interest shown toward the work by the company, and in particular by the Development and Research Division and by the Technical Service Section of the Development and Research Division.

REFERENCES

1. Merica and Waltenberg: Malleability and Metallography of Nickel. Nat. Bur. Stds. *Tech. Paper* No. 281 (Apr. 2, 1925).
2. Merica and Waltenberg: The Malleability of Nickel. *Trans. A.I.M.E.* (1925), **71**, 799.
3. C. D. Hodgman: Handbook of Chemistry and Physics. Chemical Rubber Publishing Co., 1939.
4. Urban and Chipman: Non-Metallic Inclusions in Steel. *Trans. Amer. Soc. Metals* (1935) **23**, 645.
5. Portevin and Castro: Morphology of the Inclusions in Siderurgical Products. *Jnl. Iron and Steel Inst.* (1937) **135**, 223.
6. Portevin and Castro: Morphology of the Inclusions in Siderurgical Products. *Jnl. Iron and Steel Inst.* (1936) **134**, 213.

DISCUSSION

(F. N. Rhines presiding)

C. B. POST,* Reading, Pa.—May I ask the author by what chemical method his sulphur figures were determined?

* The Carpenter Steel Company.

A. M. HALL (author's reply).—We used the gravimetric method.

C. B. POST.—Would the author care to state at what sulphur content hot-working difficulties in 36 to 50 per cent nickel steel are encountered?

A. M. HALL.—I do not know.

C. B. POST.—It was interesting to find a confirmation of several experimental facts noted in our laboratories regarding nickel sulphides in high-nickel steels. Generally, nonmetallic inclusions can be seen at high magnifications on the specimens as polished, and for other nonmetallic constituents an outline of the films may be seen before and after etching. However, in studying the effect of sulphur and deoxidation practice in high-nickel steels (36 to 50 per cent nickel) on hot ductility, we were thrown off the track for several months because the as-polished nickel sulphide films were not visible under the microscope. Certain agents then will attack the grain boundary, with the result that experimental proof was lacking on the nature of the grain-boundary constituents.

It would be a very valuable contribution to the literature if one of the journals would show the photomicrographs in their original colors. Regarding my question on the sulphur content and hot-ductility, around 0.018 per cent sulphur seems to be the boundary for hot shortness, although the actual sulphur content depends somewhat on the chemical method used to determine it.

F. N. RHINES,* Pittsburgh, Pa.—I should be much interested in knowing the dry polishing technique that has led to such excellent polishes.

A. M. HALL.—We use a series of standard emery papers, mounted on a disk rotating in a vertical plane, to do the initial dry grinding. After grinding through grade 000 paper we take the specimen to a wheel rotating horizontally. This wheel is covered with shirt broadcloth into which levigated alumina has been rubbed.

Then we have a second horizontal wheel, covered with shirt broadcloth impregnated

with a half and half mixture of paraffin and beef tallow. This mixture is worked into the cloth to produce a smooth surface. The abrasive is again levigated alumina, but this time it is sieved through a shirt broadcloth screen to provide a finer particle size. The paraffin and tallow dressing aids in producing a finer cut.

The final polish is made on a third horizontal wheel covered with kitten's ear velvet, using as an abrasive a green chrome rouge, which has been prepared in a grease. The entire polishing procedure is carried out dry. We find that slow speeds are generally advisable in each polishing step.

F. N. RHINES.—Is the sample then washed?

A. M. HALL.—Carbontetrachloride or alcohol can be used.

G. D. MARSHALL,* Annapolis, Md.—Have you found that the addition of magnesium as a desulphurizer, or the presence of magnesium sulphide, has any particular effect on the annealing characteristics of nickel and nickel alloys?

A. M. HALL.—Differences are produced by the magnesium content. Whether it is due to the presence of magnesium sulphide, we do not know.

F. N. RHINES.—I should like to comment upon the author's statement that some of the sulphides shown were produced by diffusion in the solid state. The temperature named, I believe, was 930°C., whereas the nickel sulphide eutectic is at a considerably lower temperature. It would seem to me, therefore, that the diffusion must be one that is progressing through a liquid nickel-sulphur eutectic mixture, perhaps at the grain boundaries, and that the reason the structure looks the same in the as-cast and the diffused state is that in both cases the sulphur is present as a liquid, and then freezes at the grain boundaries in much the same way.

A. M. HALL.—I think you have a very good point there. Perhaps, at the temperatures used, there is a liquid phase present during the process which produces the sulphide end product.

* Assistant Professor of Metallurgy, Carnegie Institute of Technology.

* Lieutenant, U.S.N.R., U. S. Naval Engineering Experiment Station.

Time-to-fracture Tests on Platinum, 10 Per Cent Iridium-platinum and 10 Per Cent Rhodium-platinum Alloys

By H. E. STAUSS,* MEMBER A.I.M.E.

(Cleveland Meeting, October 1942)

THE time-to-fracture test has been applied to pure platinum and to two alloys of platinum under the special conditions of small cross-sectional area of the specimens and of a test temperature above the annealing temperature. While the results are similar in character to those secured with large specimens of steel at temperatures below the annealing temperatures, two differences are noted: (1) an upward inflection in the curves for log stress vs. log time for the alloys, and (2) a sharp break in the curve for log stress vs. log time for pure platinum when single crystals filled the wire.

The experiments showed that: (1) platinum and 10 per cent rhodium-platinum maintained their strengths at 1100°C. better than did 10 per cent iridium-platinum, and (2) the rhodium-platinum after a time exceeded the iridium-platinum in strength at 1100°C.

Platinum alloys in their service at high temperatures encounter conditions somewhat similar to those that exist in the usual form of the "time-to-fracture"¹ test with steel. This paper is intended primarily to present results obtained by a "time-to-fracture" test under conditions approximating actual service for platinum (at the temperature 1100°C. under oxidizing conditions) with three materials, pure platinum (99.99 per cent), a platinum alloy with 10

per cent iridium, and a platinum alloy with 10 per cent rhodium. The experimental procedure differed from that previously used in this type of measurement in that the samples were of small diameter (0.010 in.), were fully annealed, and were tested at a temperature definitely above their annealing points (600°C., 1000°C. and 1050°C., respectively, for 60 per cent cold reduction and 15 min. heating time^{2,3}).

The experimental arrangement was similar to that previously described,⁴ using as heating unit a small, horizontal, platinum-wound furnace, 1½ by 12 in., maintained at constant temperature by an automatic controller. The samples were 0.010-in. wires, which had been annealed at 1200°C. by drawing them slowly through the furnace. The time-to-fracture was measured electrically. Elongation was not determined because of the difficulties inherent in the experimental arrangement. Life—that is, the time-to-fracture—was considered the important property in these first tests. No attempt was made to measure the reduction in area, but the types of fracture were noted qualitatively; in the text they are referred to as (1) the normal, plastic, or necked fracture, (2) the knife-edge fracture, and (3) the brittle or intercrystalline fracture with small reduction of area.

Results for different constant applied stresses are plotted in Fig. 1. In all cases at least two trials were made for each stress, although they cannot always be indicated separately on the curves. The breaking stresses drop very rapidly to a small frac-

Manuscript received at the office of the Institute Sept. 22, 1942. Issued in METALS TECHNOLOGY, April 1943.

* Research Physicist, Baker and Co., Inc., Newark, N. J.; now Senior Industrial Specialist, War Production Board, Washington, D. C.

¹ References are at the end of the paper.

tion of their short-time values. Roughly, the long-period strengths (175,000 min.) are 420 and 700 lb. per sq. in., respectively, for platinum and the 10 per cent iridium-

was still losing strength at 175,000 min. The rhodium-platinum alloy behaved intermediately between platinum and iridium-platinum, but its curve crossed that of the

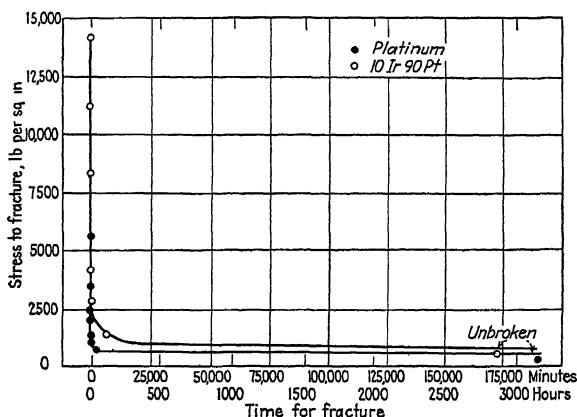


FIG. 1.—STRESS VERSUS TIME TO FRACTURE.

platinum alloy, as against 5600 and 1400 lb. per sq. in., respectively in the short-time test of 0.2 min. The ratio of the strength of the iridium-platinum wire to that of pure platinum has declined to a value of 1.7 after 175,000 min. from a value of 2.5 for a test lasting 0.2 min., or from 2.6 as determined in the short-time experiments reported earlier.⁴ This establishes that even at the temperature of 1100°C. the iridium-platinum alloy is weakened under oxidizing conditions, a phenomenon that is known to occur at higher temperatures.⁵ In their general shape these curves agree with those published for the time-to-fracture test¹ with the usual larger specimens at lower temperatures, but the time scale is much shorter.

In Fig. 2 the curves have been redrawn on a stress-log time scale. In this time-foreshortened scheme, the relative behaviors of the three materials are more clearly seen. Pure platinum appeared to have reached a practically asymptotic minimum value at 175,000 min. The iridium-platinum alloy suffered a sharp loss in strength between 5 and 10 min. and

latter at 10,000 min. While no value was secured in the neighborhood of 100,000 min. for the rhodium-platinum, it is obvious that this alloy was maintaining its strength better than was the iridium-platinum.

It is informative to plot the results of the experiment on log scales because of the linear relationship that has been observed in time-to-fracture tests with steel¹ at temperatures below those at which the specimens would be annealed in a short time. This has been done in Fig. 3. In attempting to compare these results with similar published experiments and results, it must be borne in mind that the following special conditions applied:

1. The samples were a pure metal and simple binary solid solutions, not complex alloys.
2. The small cross section of the samples made crystallographic characteristics unusually important, and readily revealed phenomena resulting from diffusion.
3. The high temperature of test eliminated secondary effects resulting from straining and recrystallization (but not grain growth), and speeded diffusion.

4. The samples were extremely, but not completely, resistant to oxidation, the resistance decreasing in the order platinum, rhodium-platinum, iridium-platinum.⁵

fracture of the wire changed from the normal, necked type of plastic rupture to a knife-edge fracture. Apparently the break in the curve was caused by the growth of

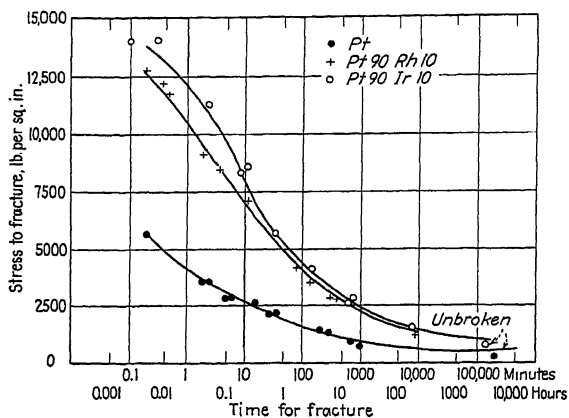


FIG. 2.—STRESS VERSUS LOG TIME TO FRACTURE.

The log-log curve for platinum is virtually a straight line up to 300 min., at which point a sharp discontinuity and rapid decline in strength occurred; yet an only

single crystals across the diameter of the wire after the longer times, and this was verified metallographically by a study of the structure of two samples on either side

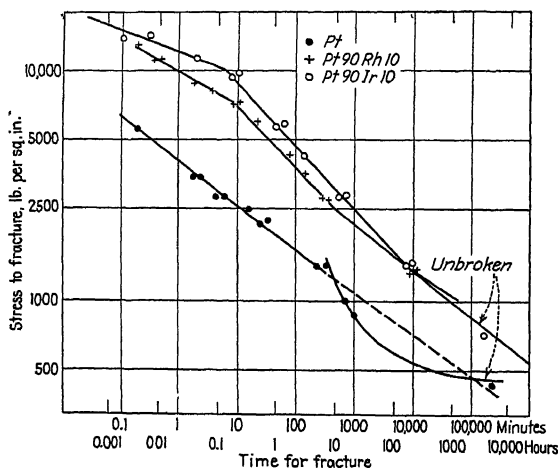


FIG. 3.—LOG STRESS VERSUS LOG TIME TO FRACTURE.

slightly smaller load (420 lb. per sq. in. as against 780) produced no break in 189,840 min., after which the test was stopped. At the discontinuity at 300 min., the type of

of the break, one stressed at 1400 lb. per sq. in. and the other at 780. Although the test temperature was far above the annealing temperature, no brittle or intercrystal-

line fracture occurred. The final test at the stress of 420 lb. per sq. in. lies above the original curve extrapolated to the same fracture time, but it must be noted that the

interpreted as the result of the increasing difficulty of penetration of the oxidation and a consequent decreased rate of weakening by oxidation. This upward inflection of



FIG. 4.—STRUCTURE OF PLATINUM WIRE FRACTURED AFTER 243 MINUTES (4 HOURS). $\times 100$.

specimen had not fractured. The type of curve obtained raises the questions whether the decrease in strength with time was the result of the slow removal of the stiffening effect of the grain boundaries as the grains grew in size, and whether a final minimum strength would be reached, which would be characteristic of the single crystal.

The curve for 10 per cent iridium-platinum shows two breaks. The first occurred at about 8 min., after which the curve fell more steeply. The type of fracture changed at this same time; for the shorter periods the fracture was the plastic, necked type, while for the longer periods it was of the brittle, intercrystalline character. This result, in keeping with the known greater propensity to oxidation of the iridium alloy, is in accordance with the conclusion of White, Clark, and Wilson¹ that the break in slope of time-to-fracture curves of steel is the result of oxidation. It is very interesting that at about 10,000 min. the curve shows an inflection upward, which can be



FIG. 5.—STRUCTURE OF PLATINUM WIRE FRACTURED AFTER 910 MINUTES (15 HOURS). $\times 100$.

the log stress-log time curve apparently has not been observed with steel samples of large cross section at temperatures below the annealing points. None of the samples of the alloy showed grains completely filling the cross section of the wire, and the curve therefore does not show the peculiar break observed with pure platinum.

The curve for 10 per cent rhodium-platinum is like that for the iridium-platinum. It becomes steeper at about 10 min. and again at this time the type of fracture changed from plastic to brittle or intercrystalline, probably indicating oxidation. With this alloy, as with the iridium alloy, the grains did not grow to the full diameter of the wire. After about 400 min., the curve shows a marked inflection upward, crossing the curve of the iridium-platinum at about 10,000 minutes.

The time-to-fracture tests at 1100°C., therefore, verify the results of practical experience at elevated temperatures, that

the 10 per cent rhodium-platinum alloy is more satisfactory than the 10 per cent iridium-platinum alloy for prolonged use under oxidizing conditions. On the basis of the results of these experiments, it is evident that these two platinum alloys under continuous stress at 1100°C. must not be loaded more than 1.5 per cent of their normal room-temperature tensile strengths as measured in the annealed conditions, or 6 per cent of their short-time strengths when tested in 0.2 min. at 1100°C.

REFERENCES

1. A. E. White, C. L. Clark, and R. L. Wilson: The Fracture of Carbon Steels at Elevated Temperatures. *Trans. Amer. Soc. Metals* (1937) 25, 863.
2. E. M. Wise and J. T. Eash: Properties of the Platinum Metals, I—*Trans. A.I.M.E.* (1935) 117, 313; II, *Trans. A.I.M.E.* (1938) 128, 282.
3. E. M. Wise and R. F. Vines: Effect of Cold-work upon Hardness and Recrystallizing Behavior of Pure Platinum. *Trans. A.I.M.E.* (1940) 137, 464.
4. H. E. Stauss: Tensile Strengths at Elevated Temperatures of Fine Wires of Some Platinum Alloys. *Trans. A.I.M.E.* (1940) 137, 474.
5. Unpublished work of the Physics Department, Baker and Co., Inc.

The Metallurgy of Fillet Wiped Soldered Joints

By E. E. SCHUMACHER* AND G. M. BOUTON,† MEMBERS A.I.M.E., AND G. S. PHIPPS†

(New York Meeting, February 1943)

THE seriousness of the present tin scarcity has stimulated large consumers of this vital metal to develop drastic conservation measures in order to extend the available supplies to cover the emergency period. By devising new soldering methods and alloys the Bell System has contributed a substantial share in the tin conservation effort. Fortunately, the changes, as far as can be determined now, have not introduced weakness into the soldered joints.

Some of the new procedures were already in the process of development at the onset of the emergency, while others were devised under its stress. In some instances, the newly developed solders were found to be more difficult to use than the alloys previously available, and would not have been introduced under normal conditions.

One major change made that previously had been under consideration will result in large savings of tin. Unless service difficulties are encountered, this modification gives promise of remaining after the emergency has passed. The change involves a reduction in the amount of solder placed on a wiped joint between the cable sheath and the sleeve. Instead of the customary full sized wiped joint, a wipe of fillet proportions is formed. Through this change, a solder saving of more than 60 per cent per joint can be realized.

Plumbers and cable splicers for many years have joined lead pipes and cable

sheath by a soldering process called "wiping." The name is an apt description of the operation. For a wiped joint, the sections to be united are heated by molten solder poured over their surfaces, and the resulting semiliquid mass is manipulated by wiping with cloth pads to a well rounded symmetrical form like the one shown in Fig. 1. The operation requires considerable skill on the part of the splicer and close control of the composition of the solder.

At first consideration, the problem of tightness in such joints seems simple but experience shows that even under the best conditions the fissures frequently found in the solder occasionally link and form a path that allows leakage to occur. In telephone cables not maintained under gas pressure, such leaks permit the entrance of water, which wets the paper-covered conductors and thereby impairs the insulation value and causes service interruptions.

By going to an extreme and wiping off all the solder in excess of a fillet, it has been found that many causes of porosity are eliminated. Figs. 2 and 3 show cross sections of joints wiped in the old and the new ways. The saving in solder, and consequently in strategic tin, is evident. The field splicing forces find that joints are easier to make by the new method and are less likely to be porous.

The metallurgical considerations that are responsible for the success of the fillet wipe are of interest. Much has been written about the wiping process of soldering cable joints and the many requirements of a good wiping solder have frequently been listed. The success of the procedure described

Manuscript received at the office of the Institute Dec. 1, 1943. Issued in METALS TECHNOLOGY, February 1943.

* Research Metallurgist, Bell Telephone Laboratories, New York, N. Y.

† Metallurgist, Bell Telephone Laboratories.

herein is dependent upon a few fundamental characteristics of lead-tin alloys in the process of freezing, which have sound metallurgical explanations.



FIG. 1.—CONVENTIONALLY WIPED JOINT BETWEEN TELEPHONE CABLE AND SLEEVE. ONE-THIRD ORIGINAL SIZE.

For an understanding of the defects possible in a soldered joint wiped in the usual manner, the simple solidification phenomena of metals may be considered.

the volume of the melt at that time; on further cooling, dendrites of lead-tin solid solution grow inward toward the center of the crucible, and at the same time many tiny new crystals form throughout the liquid. Thus there are taking place simultaneously: (1) shrinkage of metal as it becomes solid, (2) shrinkage of previously frozen solid as it cools, and (3) shrinkage of the remaining liquid as the temperature drops. The originally solidified outer cylinder adhering to the crucible walls remains essentially at its original height. The level of the semiliquid portion nearer the center of the crucible falls continuously, until the precipitated crystallites formed in the body of the melt make a loosely piled mass extending from the upper surface to the bottom of the crucible. Further shrinkage of the liquid then leaves these primary crystallites at approximately this level while the liquid recedes, leaving fissures between them. This can be beautifully observed by means of a binocular

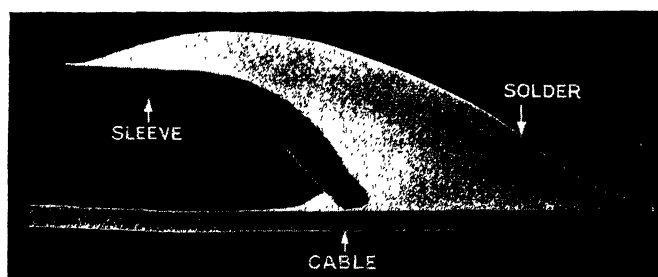


FIG. 2.—SECTION FROM JOINT WIPED CONVENTIONALLY. $\times 1\frac{1}{2}$.

As is well known, molten metal in a crucible when allowed to cool with free circulation of air will begin freezing near the walls of the vessel and, with a few exceptions, will end with a concave surface due to solidification shrinkage. Restricting the discussion to a simple lead-tin wiping solder, solidification progresses as follows: a lead-tin solid solution commences to freeze and forms a rather porous cylinder touching the crucible walls and extending to a height corresponding to

microscope focused on the surface of a solidifying crucible of wiping solder, or on the top surface of a solidifying wiped joint.

Further insight into the mechanism of solidification of wiping solder may be gained by another simple illustration. If two solder strips are cast by pouring small quantities of molten solder, one on a cold iron surface and the other on a cloth-covered board, and both are then bent cold to produce specimens like those shown in

Fig. 4, the chill-cast sample will exhibit fewer cracks resulting from shrinkage than will the slowly cooled one. In the slowly cooled sample, primary crystallites form

of the old massive-type joints, which may lose several drops by drainage after the splicer has completed his shaping operations. It is also shown by the greater

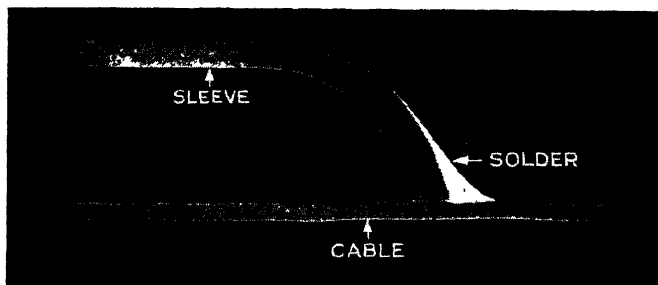


FIG. 3.—SECTION FROM JOINT WIPED BY FILLET TECHNIQUE. $\times 1\frac{1}{2}$.

throughout the solidifying mass and pack at a level above that warranted by the final volume of completely solid solder. The sample cast on the cold plate begins to freeze at its surface in contact with the iron plate and, because of the rapid extraction of heat by the cold iron, it continues to freeze in a rapidly advancing smooth front until the last liquid at the top is solid. Because of the steep temperature gradient, there is little opportunity for nucleation and dendrite formation in the upper liquid. The surface of this melt therefore is smooth and free from the fissures that are caused by the shrinkage of the eutectic away from the dendrites in the slowly cooled sample. Recession of the liquid in the slowly cooled sample leaves a multitude of shrinkage channels, which, if they occurred at the critical portion of a wiped joint, would cause leaks.

Another illustration may be useful in demonstrating the processes taking place in connection with joint wiping. Solder may be allowed to solidify in a crucible until its surface is quite firm to a probe. If, at this stage, the crucible is tilted sideways to a position shown in Fig. 5, part of the remaining eutectic may be poured out, leaving spongy regions. This loss of eutectic is observed frequently during the formation

number of pores in the top half of a joint compared with the bottom, and the somewhat grayer surface appearance of the top.

Although a solidification range in which quantities of liquid and solid metal may exist at equilibrium is an essential feature of a wiping solder, another factor of major importance is the nucleation rate of the alloy. Wiping solders having high nucleation rates will develop quickly a myriad of points or nuclei throughout the melt, from which further crystallization will proceed, while an alloy of low nucleation rate will develop relatively few of these points in the same time and consequently grow fewer and larger crystals. The alloy first mentioned will have a texture similar to fine clay, while the second will behave like coarse sand and water when subjected to wiping tests. In the fine claylike texture more solid particles are present than in the water-sand type of texture, therefore more surface is available for the retention of the liquid in the former type of semisolid mass. Drainage is thus greatly retarded, with the result that porosity is materially lessened. The type of texture determines in a large measure the ease of shaping and potential porosity of a wiping solder.

Having examined elementary forms of solidification, attention may now be

focused on the setting up of the wiped joint itself. In practice, the parts to be joined are cleaned and fluxed. Circumferential paper pasters are then applied to

by using cloth pads. When solidification has proceeded to a condition where the solder can support itself in position, manipulation is stopped. From this point on, loss

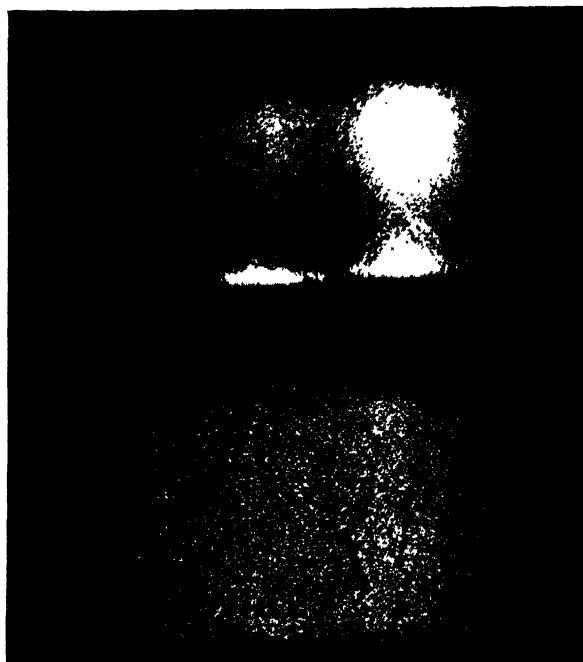


FIG. 4.—BENT STRIPS ILLUSTRATING EFFECT OF VARIATIONS IN COOLING RATE ON STRUCTURE OF WIPING SOLDERS. $\times 3$.

Upper strip was chill-cast and shows a sound ductile surface.

Lower strip, of same solder, was cooled slowly and upon bending exposes fissures between crystallites at surface.

the sheath and sleeve to restrict the spread of the solder. The splicer then pours hot solder from a ladle over the prepared parts and catches the excess in a cloth held in contact with the bottom of the joint. The caught solder is repeatedly pushed back around the cable with a wiping motion, to aid "finning" or alloying and to distribute the heat. After a few such operations, the prepared surfaces can be seen to be thoroughly wetted by the solder. At this stage a portion of the caught solder is mixed in the ladle with more hot solder, and the mass, which now has a claylike consistency, is poured on the joint and molded into place

of heat takes place by conduction away from the joint by the sheath and sleeve, by radiation, and by air convection currents at the surface of the solder. As a result of this combination of heat losses, final solidification takes place in the interior of the solder mass near the important sheath-sleeve junction. The action that causes pipes to form in castings draws the eutectic from the critical area between the sheath and the end of the sleeve. If the solder has the proper characteristics there will be a shell of solder that does not have interconnecting shrinkage cavities, drainage cavities or fissures due to the wiping

operation, and the finished joints will be gastight. If the solder is unduly coarse or has insufficient liquid eutectic at the time the mass is too rigid to manipulate further, the resultant joint may leak.

The new fillet wiping technique is similar to the old up to the step where the splicer molds the mass to shape. At this point the new technique consists in wiping the solder to a small fillet similar to that shown in Fig. 3. The resultant joint has much less solder and therefore much less total shrinkage and tendency to draw eutectic from the space between the sheath and sleeve. Also, at the temperature where wiping is discontinued there is insufficient volume of solder left by the fillet wiping technique to permit drainage drops to accumulate and fall from the bottom of the joint. Thermal conduction along the sheath and sleeve cause rapid solidification of the solder at the joint, eliminating the possibility of drainage. Experience has shown a consistently high percentage of sound joints when fillet wiping is rigidly practiced. During the development period of the fillet wiping technique, examination of the few fillet-type wiped joints that were found to leak showed quantities of solder present, much in excess of that required. Under the microscope such joints showed the telltale sponginess where the eutectic had been drawn away from the junction in the course of final solidification.

Physical tests on joints made using the fillet wipe between sections of telephone cable and sleeving have demonstrated that fillet joints similar in size to that shown in Fig. 2 made with 38 per cent tin, 0.1 per cent arsenic, balance lead wiping solder, are stronger in tensile strength, creep and fatigue than the cable itself.

The application of the new technique has gone much further toward saving tin than any known permissible change in the composition of solder. Using the old technique, a reduction of only one per cent in the nominal tin content of a lead-tin wiping

solder resulted in widespread occurrence of leaky joints, indicating that little tin could be saved by a simple change in solder specification. This observation was to be

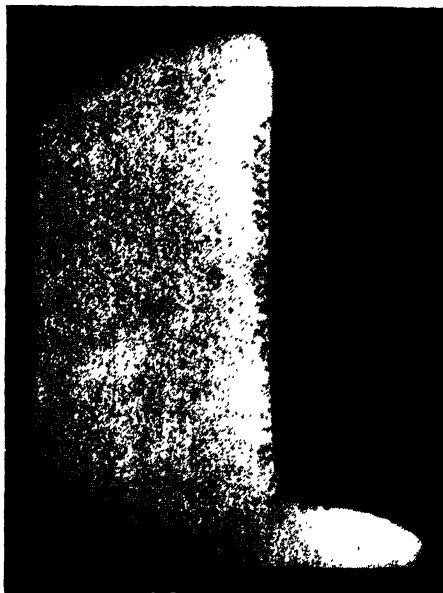


FIG. 5.—INGOT OF WIPING SOLDER THAT WAS TILTED IN THE CRUCIBLE BEFORE COMPLETELY SOLIDIFIED. $\times 1\frac{1}{2}$.

Lower lip represents eutectic drainage from partly solidified mass.

expected, since many studies had been conducted over the years to reduce the tin content in wiping solders to the minimum consistent with the production of satisfactory joints. Tin has always been much more expensive than lead and for large users of solder a reduction of one per cent in the tin content might result in savings of many thousands of dollars annually.

While the use of the fillet wipe leads to large savings in tin, other avenues for conserving this strategic metal are available, such as the substitution of ternary and quaternary alloys containing less tin than that required by the binary lead-tin wiping solders. A satisfactory alloy of this type was developed, which contains 13 per cent

tin, 23 per cent bismuth, 0.1 per cent arsenic, balance lead. Though readily available a short time ago, bismuth now has become too restricted to be used extensively in solders. A wiping solder is now being introduced into service, in which through the inclusion of a small quantity of antimony it has been possible to reduce the tin content. This material appears suitable for fillet wiping, although it requires somewhat more skill to use than the 38 per cent tin, 0.1 per cent arsenic, balance lead, wiping solder. Other compositions may be usable that contain less tin than is ordinarily used but on the whole the savings accomplished by modifications in composition will be small compared with those produced by the new wiping technique that has been described.

IN SUMMATION

By virtue of its small solder volume, the fillet wipe reduces tin consumption and produces joints less liable to leakage than the conventional wiped joints. The reasons for the success of this type of joint are based on the sound metallurgical principles herein described. The use of the fillet wipe promises to survive the period of restricted tin consumption.

DISCUSSION

(B. W. Gonser *presiding*)

B. W. GONSER,* Columbus, Ohio.—Could you give us some statement about the present limitations of composition in wiping solder? I know the War Production Board has been cutting down on the tin content of solder for most applications but do not remember just what the last ruling has been on wiping solders.

G. M. BOUTON (author's reply).—The limitation on solders is 20 per cent tin. However, in wiping solders it has been found necessary to use 32 per cent tin. This is recognized and is permitted by the most recent W.P.B. order. Our original composition, which we preferred in the Bell System and would use now if we could, is 38.25 per cent tin, 0.1

per cent arsenic, and the balance lead, possibly with a small amount of antimony in it. By adding 2 per cent antimony, a solder can be produced that is workable with 32 per cent tin.

Reduction to 30 per cent tin, even with 2 per cent antimony present, showed a marked increase in difficulty in handling in practical tests, and a large increase in the percentage of leaky joints produced. The joints cannot be wiped as tightly, so that more solder is left on them, thereby consuming more tin than would be used with a solder having higher content of tin.

T. M. BAINS, JR.,* Washington, D. C.—Have you had any experience with the silver solders?

G. M. BOUTON.—We have worked with a number of lead-tin solders containing silver. The handling properties, as expressed by the splicers, do not seem to show any noticeable improvement with the silver present. Sound joints, however, can be produced with them.

T. M. BAINS, JR.—What proportion?

G. M. BOUTON.—Using lead-tin solder, somewhere around 30 per cent tin and 1 or 2 per cent of silver.

T. M. BAINS, JR.—How about cutting out all the tin?

G. M. BOUTON.—That would not make a wipeable solder. The melting point of the lead-silver solder, 304°C., would be higher than the melting point of the sheath now used in the Bell System when nonequilibrium conditions of solidification are taken into consideration.

MEMBER.—How far can you deviate from the proportion of arsenic? Is 0.08 all right, or 0.12?

G. M. BOUTON.—You cannot put very much more than 0.1 per cent arsenic in lead-tin solder because it will dross out, probably as a tin-arsenic compound; probably 0.08 per cent would be satisfactory.

A. M. HALL,† Huntington, W. Va.—What is the virtue of the arsenic?

G. M. BOUTON.—The arsenic seems to give a considerably finer grain size in solders, and in practical wiping tests the splicers have repeatedly expressed their opinion that it makes the solder smoother.

* Battelle Memorial Institute.

* War Production Board.

† International Nickel Company.

T. M. BAINS, JR.—Have you tried sodium? Sodium, you know, is piling up in the manufacture of tetraethyl lead.

G. M. BOUTON.—No, we have not tried sodium in solder. Lead-sodium alloys, as a whole, have a great disadvantage. When exposed to the air they become coated with moisture and probably would be poor from the corrosion standpoint.

C. E. SWARTZ,* Cleveland, Ohio.—There were just two things I was thinking about while the paper was being given. One is the matter of joints made other than with solder. In some instances, I have been told, lead burning has been used instead of soldered joints, in joining lead and lead alloys. I presume that would be a disadvantage in this particular case, because of the temperatures involved, at least.

The other was the matter of tin-free solders, which has been touched upon. Some work has been done at the University of Minnesota recently, in which tin-free solders have been the subject of investigation. I would be interested to know of any work that has been done in other laboratories, especially in the Bell Telephone laboratories.

G. M. BOUTON.—Probably lead burning could be used for joining cables. On the other hand, it is an art that requires a very large program of training, and we have a large number of splicers. Also, there is some objection to taking open flames into the manholes because of the hazards involved and there is some objection to taking open flames in the air. Probably in a very breezy location considerable difficulty would be experienced, and with a canvas tent over the splicing operation there would be some hazard from the flame.

As far as tin-free solders are concerned, there are several that should work for specific purposes. The antimony solder, from the University of Minnesota, should be quite satisfactory on ferrous materials. On brass and copper we have not had very much success with it; even arsenic in ordinary solders causes difficulty in soldering to brass parts, and I would think this antimony-arsenic solder would not be suitable for that. As a matter of fact, the sponsors do not say it is satisfactory

for brass. Concerning wiping solders, I do not know of any that are entirely tin-free that work satisfactorily.

B. W. GONSER.—I might comment, Dr. Swartz, that we make a practice of testing the various substitute solders that are suggested from time to time, and have casually examined the sodium-lead and the antimony-arsenic-lead tin-free solders. It is advisable for everyone interested in solders to examine substitute compositions, since out of innumerable applications a limited scope may be found for most of them. Superficial testing for adherence, flowability, and joint strength does not take long. Even though relatively poor results may be secured under one set of conditions, the solder should not be hastily condemned, since with experience a technique may be developed that does make the solder work on some joints.

In our limited tests, the antimony-arsenic-lead solder seemed to be quite brittle. A bar of the solder, for example, could be bent one way but would fracture readily on any reverse bending. It was somewhat difficult to handle and joint penetration by capillary flow was poor, we thought. As a general purpose solder it was not in the same class as tin-lead solders, but it might be entirely satisfactory where soldering conditions were not difficult and particularly where torch soldering could be used.

The sodium-lead solder did not flow very well on tarnished copper or steel when using normal acid fluxes, and corrosion in a moist atmosphere was rather disturbing. We have been informed since that a sodium hydroxide flux is preferable for use with this solder on steel. Have any of you other people had experience on which you would care to comment?

C. J. SNYDER,* Hastings-on-Hudson, N. Y.—We have used commercially a straight bismuth-lead wiping solder to some extent, about 29.5 per cent bismuth and the remainder lead. Adding small amounts of tin did not seem to improve it very much.

This solder is not good for joints involving one or more copper numbers; also it is not easy to apply to complicated joints, although it does not seem to be very difficult on straight joints, and it makes a nice, tight joint.

* Chief Metallurgist, Cleveland Graphite Bronze Company.

* Anaconda Wire and Cable Company.

New Electrolytic Zinc Plant of the American Zinc Company of Illinois

By L. P. DAVIDSON, MEMBER A.I.M.E.

(New York Meeting, February 1942)

THE new electrolytic zinc plant of the American Zinc Company of Illinois commenced operation in April 1941. The simple flowsheet using the standard current density and the economic reasons that dictated it are given herewith.

The Evans-Wallower Zinc Co. built an electrolytic zinc plant at Monsanto, Ill., in 1929 and operated it for about two years. The plant stood idle from 1932 and was purchased by the American Zinc Co. in 1940. Because of the condition of the equipment, excepting the motor generator set, a complete rebuilding was necessary.

The Fairmont City plant of the American Zinc Co. could treat the leach residues, the purification cake and the skimmings from the melting furnace in its various plants. This possibility permitted a simple flowsheet with good economic results.

The flowsheet is shown in Fig. 1. The calcined concentrates are leached in mechanically agitated tanks with spent electrolyte and such ferric iron solution as necessary. When the acid has been neutralized and the iron coagulated, the fluid is discharged to settling tanks. The underflow from these thickeners is filtered on a Moore filter; the filter cake leaves the plant for retreatment and the filtrate joins the thickener overflow.

Zinc dust is added to this solution until the copper and cadmium are precipitated. The pulp is filtered through Shriver presses, which deliver the purified solution to stor-

age tanks, and the copper-cadmium-zinc cake is shipped for retreatment and recovery of these three metals.

The purified solution is electrolyzed; the regenerated acid is returned for use in the leaching plant and the cathode zinc, after stripping, goes to the melting furnace, from which it is cast in slabs. The skimmings from the melting furnace are shipped to the Fairmont City plant for reduction to metal in the retort furnaces.

The choice of this simple flowsheet was made possible only because of the facilities of the Fairmont City plant. The long leaching period, with high acid content and high temperature which characterize the high-density process, gives a higher zinc extraction but also dissolves more impurities, which must be removed. The same is true to a lesser degree of the multi-step leaching of the western low-density plants. By the sacrifice of some initial extraction, solutions can be obtained that are relatively easy to purify and give good ampere efficiency. This loss in initial extraction is made up in the retreatment of the residues in the Waelz plant. The impurities that accompany the zinc thus extracted are inconsequential when the Waelz product is treated in a distillation plant.

It was recognized that this flowsheet would require a somewhat greater amount of sulphuric acid—either as acid or as sulphate sulphur in the calcine—because of poorer washing. The sulphuric acid plant at Fairmont City could deliver 60° Bé. acid to compensate for the sulphate loss and the cost would be less than the cost of more intensive washing.

Manuscript received at the office of the Institute Feb. 11, 1942. Issued in METALS TECHNOLOGY, August 1942.

* General Superintendent, Electrolytic Division, American Zinc Company of Illinois, Monsanto, Illinois.

The retreatment of the purification cake for copper and cadmium recovery was facilitated by the existence of the cadmium plant. The distillation of the skimmings results in a greater production of net slabs for a given electrolyzing capacity, provided that this material is treated by itself. This possibility exists at Fairmont City and also permits of a very simple handling of the skimmings at the electrolytic plant.

To make consistently Special High Grade Zinc, the electrolyzing cells were equipped with anodes of the lead-silver alloy developed by U. C. Tainton, and ample cooling facilities were provided. In this way the lead content of the zinc produced has been satisfactory.

It is believed that the choice of this flowsheet offered the following advantages over the retention of the high-density flowsheet formerly used in the plant:

1. Cheaper and faster separation of the leach residue from the neutral zinc sulphate solution.
2. Less equipment for the production of the same amount of zinc.
3. Cheaper zinc-dust purification.
4. No necessity for process steam.
5. Greater flexibility in treating various calcines.
6. Lower maintenance costs.
7. Less cooling water.
8. Less labor.

EQUIPMENT

The flowsheet (Fig. 1) and the layout of the equipment (Fig. 2) show the flow of the material through the plant.

The equipment is standard and only the less usual features will be described.

The incoming calcine is unloaded pneumatically and delivered to storage bins. From the bins it is drawn into a feeding car of 5000-lb. capacity, which, after weighing, is spotted at the desired leaching tank. A screw conveyor will empty this car in less than five minutes.

Coarse residue is removed from the neutral pulp by an Allen cone in closed circuit with a Dorr classifier.

All piping is either lead or copper up to the Shriver presses. The lines for purified solution are either rubber hose or steel pipe.

No process steam is used, the heat of reaction being sufficient for adequate solution of zinc oxide and temperature of purification. The temperature in the leaching tanks, at the time of discharge, is about 75°C., with a temperature of 45° to 50°C. in the purification tanks during the addition of zinc dust.

The cell room has 180 lead-lined reinforced-concrete cells arranged in 15 cascades of 12 cells each. The cells are 8 ft. by 4 ft. 10 in. by 2 ft. 10 in. inside dimensions. They are arranged in cascades, six cells in a row, the difference in height being 4 in. Each of the upper five cells has two lead cooling coils set in either end. The bottom cell has one coil only set in the upper end.

The water piping is so arranged that one valve controls the water to four coils. The discharged water flows through a rubber hose onto the basement floor and into the sewer. This protects the concrete floor from acid spills and permits good temperature control. The inlet temperature is about 17°C., and with 1500 gal. per min. for the entire cell room, gives an average cell temperature of 38° to 40°C.

Electrical Substation

Primary power is delivered at 13,200 volts from the Cahokia plant of the Union Electric Co. A part is transformed to 440 volts for auxiliary power, the rest being used at the line voltage by the 8400-hp. synchronous motor for the generation of the electrolyzing current. Two generators of 5000 amp. at 600 volts are operated from the synchronous motor, and, running in parallel, deliver 10,000 amp. of current to the cell room.

The limiting voltage of the generators made it necessary to use very large bus bars for the cells. The average cross section of these bars is 33 sq. in. While at first

trates is as follows: Zn, 51.46 per cent; Fe, 4.12; Pb, 3.23; CaO, 0.52; MgO, 0.26; Al_2O_3 , 0.86; Cu, 1.25; Cd, 0.22; Sb, 0.024; Ba, 2.53; SiO_2 , 0.99.

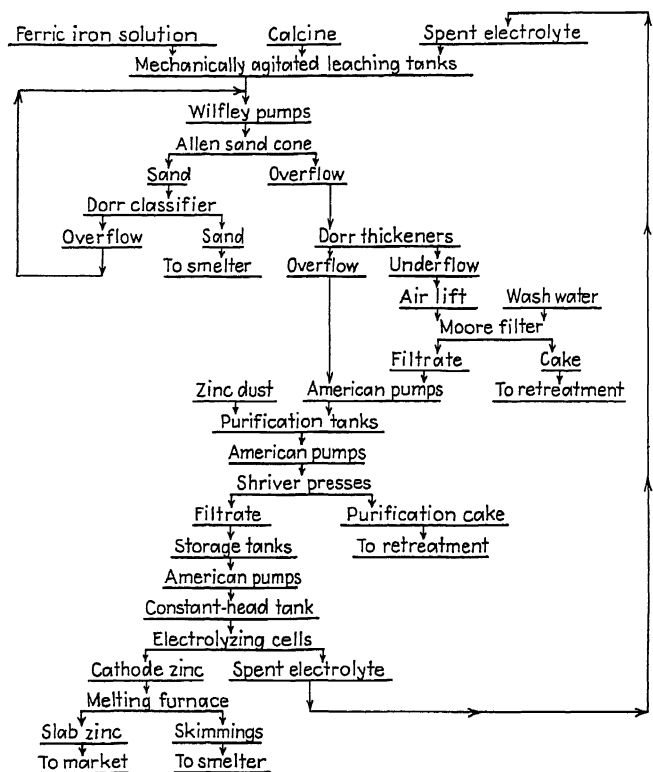


FIG. 1.—FLOWSHEET, ELECTROLYTIC ZINC PLANT, AMERICAN ZINC COMPANY OF ILLINOIS.

glance this appears to be excessively large, the economic and operating results have amply justified it.

METALLURGY

The plant was designed to treat, during the first two years of operation, a large tonnage of concentrates from the Buchans mine in Newfoundland. These concentrates are to be roasted in a flash roaster at the titanium oxide plant of the National Lead Co. at St. Louis, where the sulphur will be utilized for the manufacture of sulphuric acid. An average analysis of these concen-

Because of the late starting of this plant, the feed that has been available for the electrolytic plant has not been primarily from the Buchans concentrates, and to date has not been flash-roasted. In general, the operating procedure has been as planned, but wide variations in the zinc content of the calcines treated have made it difficult to attain the expected metallurgical results.

The leaching is done in batches. About 30 volume tons of spent electrolyte is neutralized with calcine. The acid content of the spent electrolyte is about 13.5 per cent and enough ferric iron solution is added to give 0.5 grams per liter Fe in the

head acid. The actual time of leaching is about 2 hr., and filling and discharging of the tanks takes an additional hour.

The zinc-dust purification has been made

per liter; Co, 0.5 to 1.8 mg. per liter and Ge, 0.4 to 1.8 mg. pre liter. There is little MgO and it has shown no sign of building up in the circuit.

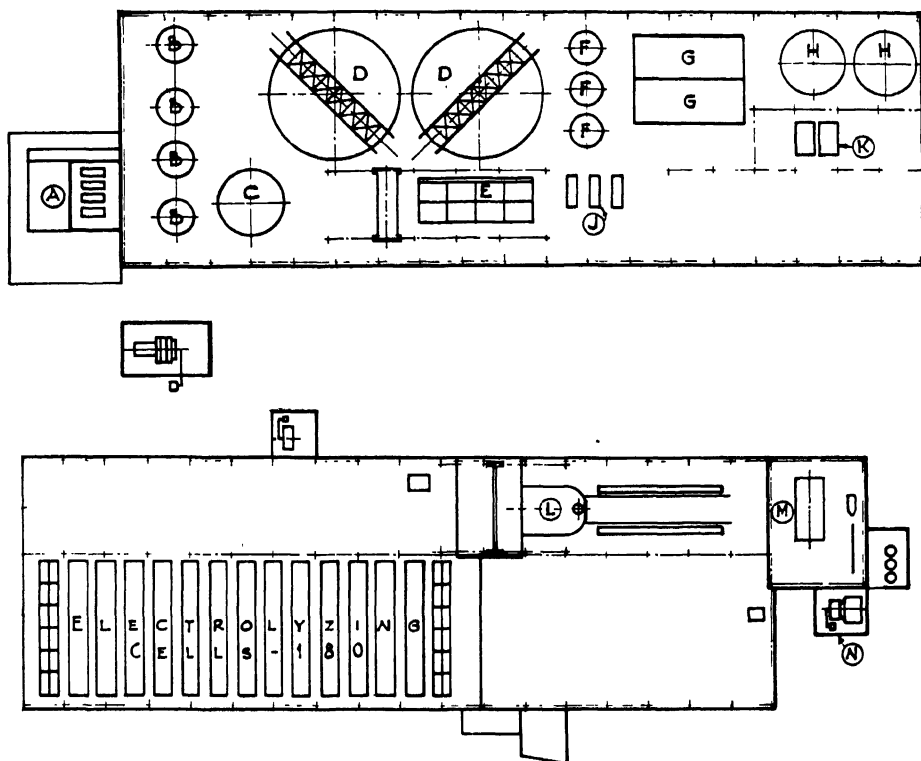


FIG. 2.—LAYOUT OF EQUIPMENT.

- A, iron dissolving cells
- B, three leaching tanks, one oxidizing tank
- C, high acid storage tank
- D, 50-ft. thickeners
- E, Moore filter
- F, three mechanically agitated purification tanks

- G, spent-electrolyte storage
- H, purified solution storage
- J, three Shriver presses
- K, heating plant
- L, melting furnace
- M, motor-generator set
- N, air-cooling for motor-generator set

with about 3.0 per cent zinc dust, based on cathodes produced. At times copper sulphate has been used as an addition agent but, in general, better solution has been made without its use.

The purified solution usually contains about 135 grams per liter of zinc, with impurities as follows: Fe, 20 mg. per liter; As, trace; Cd, 1.5 mg. per liter; Cu, 0.4 mg.

In the electrolysis, the acid content of the upper five cells of the cascade is held at 10.0 to 11.0 per cent H_2SO_4 , that of the bottom cell being about 2.0 per cent higher. The zinc depletion is about 80 grams per liter and the zinc content of the cell acid about 55 grams per liter.

Goulac is used as an addition agent in the amount of 1.1 lb. per cascade per day.

It is added to the feed line to the cell room rather than to the individual cells.

Operation of the casting furnace has been very simple and surprisingly efficient. The casting crew works only five days a

TABLE I.—*Data for December 1941*

Tons feed treated.....	2,919
Zn, per cent.....	64.16
Pb, per cent.....	1.59
Tons zinc dust used.....	51.2
Based on cathodes, per cent.....	3.32
Tons 60° H ₂ SO ₄ used.....	319
Tons classifier sand.....	107
H ₂ O, per cent.....	16.1
Zn, per cent.....	41.6
Pb, per cent.....	1.16
Tons purification cake.....	159
H ₂ O, per cent.....	25.0
Zn, per cent.....	45.1
Cd, per cent.....	6.4
Cu, per cent.....	5.2
Tons cathodes stripped.....	1,540
Average amperes.....	9,601
Ampere efficiency, per cent.....	88.52
Power consumption, kw-hr. per lb. cathodes, d.c.....	1.419
Load factor.....	93.34
Tons cathodes melted.....	1,608
Tons slabs cast.....	1,550
Ratio slabs to cathodes.....	0.964
Slab assay, per cent:	
Zn (difference).....	99.9950
Pb.....	0.0026
Cd.....	0.0012
Fe.....	0.0009
Cu.....	0.0003
Tons dross produced dry.....	79.3
Zn, per cent.....	84.4
Dross to cathodes melted, per cent.....	4.2
Labor, shifts per ton slabs.....	1.80
NH ₄ Cl used, lb. per ton slabs.....	1.55

week. Slabs are cast on the afternoon and night shifts and the furnace is skimmed on the day shift. The dross is worked with a small amount of salammoniack and raked into steel concrete buggies. These are dumped and such liquated metal as is present runs through and freezes on the concrete floor. The metal is picked from the skimmings and returned to the melting furnace. The lumps of skimmings are broken up and screened on a ½-in. square-mesh sand screen. The undersize is shipped to the retort plant and oversized metallics are returned to the furnace.

With no further treatment than that described above, the ratio of slabs to

cathodes has been 95.5 per cent. The zinc content of the skimmings varies between 84 and 87 per cent with less than 0.1 per cent of the cathode zinc unaccountable.

The data in Table I are those of December 1941, and are typical of the operation. They are not ideal but they show what has been accomplished in eight months of operation.

DISCUSSION

(Herbert R. Hanley presiding)

A. A. CENTER,* San Francisco, Calif.—Mr. Davidson and the American Zinc Co. have taken full advantage of having near by a retort zinc plant (with a Waelz department) to which products from the electrolytic zinc plant can be sent. The transfer of leached calcine would normally be made when further extraction of zinc from it in the electrolytic plant would mean disproportionate trouble from harmful impurities dissolved with the additional zinc. The paper does not specifically mention treating Tri-State zinc concentrate. However, it can be said that this material can be treated to much better advantage with the facilities described than in the original plant at the site. The writer tried electrolytic zinc treatment of Tri-State concentrate at Great Falls, Mont., some years prior to the building of the earlier plant at Monsanto. Zinc extractions were high but electrolytic results were poor. It was found that the current efficiency could be raised to a considerable extent, and without undue purification, by not carrying the extraction of zinc in the leaching too far. Such practice was not practical, of course, at the time. A setup like that described in this paper permits operation to be varied in accord with prevailing market conditions; i.e., in accordance with the kind of zinc-bearing materials it seems best to buy at any given time.

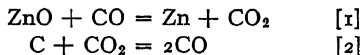
* Consulting Engineer.

Relative Rates of Reactions Involved in Reduction of Zinc Ores

BY E. C. TRUESDALE* AND R. K. WARING,* MEMBER, A.I.M.E. †

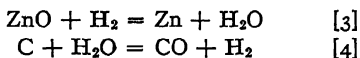
(New York Meeting, February 1941)

THE Research Division of The New Jersey Zinc Company (of Pa.) has conducted, over a period of years, numerous tests of the reducibility of various zinc ores and the reactivity of various kinds of coal, using a number of different experimental methods. Most of these tests have involved the reduction of mixtures of ore and coal. In such cases the following simultaneous reactions are believed to be mainly responsible for the production of zinc, as was shown by Bodenstein¹ some years ago:



Each of these reactions is dependent upon the other for the supply of CO and CO₂, respectively, and the over-all rate of formation of zinc vapor will be determined by the slower of these two reactions.

An analogous pair of reactions sometimes of importance is:



While it is possible to obtain an indication of the relative reducibility of various ores, or of a fine versus a coarse ore, by testing them with a given coal, and while coal reactivities may be measured in a corresponding manner, a more direct

determination of relative reaction rates is possible by carrying out the desired reactions, such as 1 and 2, separately and under reproducible conditions. It is one purpose of this paper to present some of the results that have been obtained by the latter method.

C. G. Maier² discusses the relative rates of reactions 1 and 2 and concludes that while at relatively low temperatures reaction 1 is faster than reaction 2, this difference becomes less with increasing temperatures, although at smelting temperatures reaction 1 is still the faster. He also says (p. 48), "At temperatures . . . between 1100° and 1300°C., . . . the zinc oxide reduction reaction is intrinsically more rapid than its physical limitations; that is, it is limited by gas diffusion rates."

In the course of numerous reactivity tests involving the separate use of reactions 1 and 2, we have obtained data that show by direct experiment, we believe for the first time, the correctness of Maier's statements concerning these reactions. We also include data on the relative rate of reaction 3, involving reduction by hydrogen. Finally, some interesting results obtained by carrying out the reduction of a zinc ore-coal briquet in streaming atmospheres of nitrogen, carbon monoxide and hydrogen, respectively, are presented.*

Manuscript received at the office of the Institute Nov. 30, 1940. Issued in METALS TECHNOLOGY, April 1941.

* Research Division, The New Jersey Zinc Company (of Pa.), Palmerton, Pa.

† References are at the end of the paper.

* The method described in this paper for measuring gaseous reaction rates has also been modified to obtain equilibrium data for the ZnO-CO reaction, and the results will appear in the *Journal of American Chemical Society*.

EXPERIMENTAL PROCEDURE

Experimental Method.—The experimental method adopted for the determination of the respective reaction rates was to pass a stream of the desired gas at a known rate through a vertical furnace tube, which was maintained at the desired temperature and in which a small briquet of the desired solid reactant was freely suspended from one arm of an analytical balance. By determining the rate of loss in weight of the briquet for successive brief intervals the course of the reaction could readily be depicted by plotting this reaction rate, in mols per minute, against time. The use of standard rates of gas flow and of briquet size permitted the determination of the effect on the reaction rate of changes in gas composition, temperature, and the character of the solid reactant; these standardized experimental conditions also permitted a direct comparison of the rates of the various chemical reactions. These rates, as usual in reactions involving solids, are influenced by the effective specific surface of the materials. The effective specific surface depends not only on the measured area of the briquet but also on factors such as particle size and porosity. The relative rates reported in this paper, therefore, apply quantitatively only to the particular materials used. It is believed, however, that they give a rough measure of what is to be expected with other materials of a similar nature.

Apparatus.—The furnace used was a compensated wound laboratory furnace, 17 in. long by 12 in. in diameter, provided with a silica reaction tube $1\frac{1}{4}$ in. in diameter and 30 in. long, the bottom end of this vertical tube projecting 6 in. below the lower end of the furnace. Immediately above the upper end of the furnace a $\frac{3}{4}$ -in. diam. silica side tube was sealed onto the reaction tube, wound with resistance wire for heating, and insulated. The purpose of this auxiliary heating was to keep the exit

gases hot, thus preventing the condensation of zinc or excessive formation of rock oxide. A hydrogen flame was usually kept at the mouth of this tube. The furnace was mounted on a small truck to facilitate alignment with the balance so that the briquet would be freely suspended.

Fig. 1 shows the arrangement of the reaction tube assembly and the location of the experimental briquet. Unimportant sections of the tube have been omitted from the figure, in order to permit reproduction of the essential features of the assembly. The system of tubes, held in place by rubber stoppers, *C*, which were thermally insulated by plugs *D*, was arranged so that by passing a stream of purified nitrogen into the upper side arm *B* a downward current of inert gas was created, which prevented any of the gaseous reaction products from leaving the furnace except through the heated side tube *F*. This arrangement was necessary to prevent condensation of zinc or zinc oxide on the $\frac{1}{16}$ -in. silica rod *A*, by which the specimen briquet *H* was suspended from the overhead balance. *K* was a baffle used to spread the incoming reducing gas, and *J* was the refractory protection tube for the platinum-platinum-rhodium thermocouple.

Composition of Materials.—The composition of the zinc-bearing materials used in

TABLE I.—Composition of Ore Samples Used for Reduction Tests

Material	Composition, Per Cent						
	Zn	Fe	Mn	Pb	S	CaO	SiO ₂
Roasted flotation concentrate.....	68.1	2.35		3.3	1.5		
Selected willemite ^a	50.7	0.3	6.2			0.22	26.6
Pigment zinc oxide.....	80+	0.015		0.02	0.03 (as SO ₃)		

^a The composition of pure willemite is theoretically 58.7 per cent Zn, 26.8 per cent SiO₂. The selected willemite must, therefore, have contained some tephroite, Mn₂SiO₄.

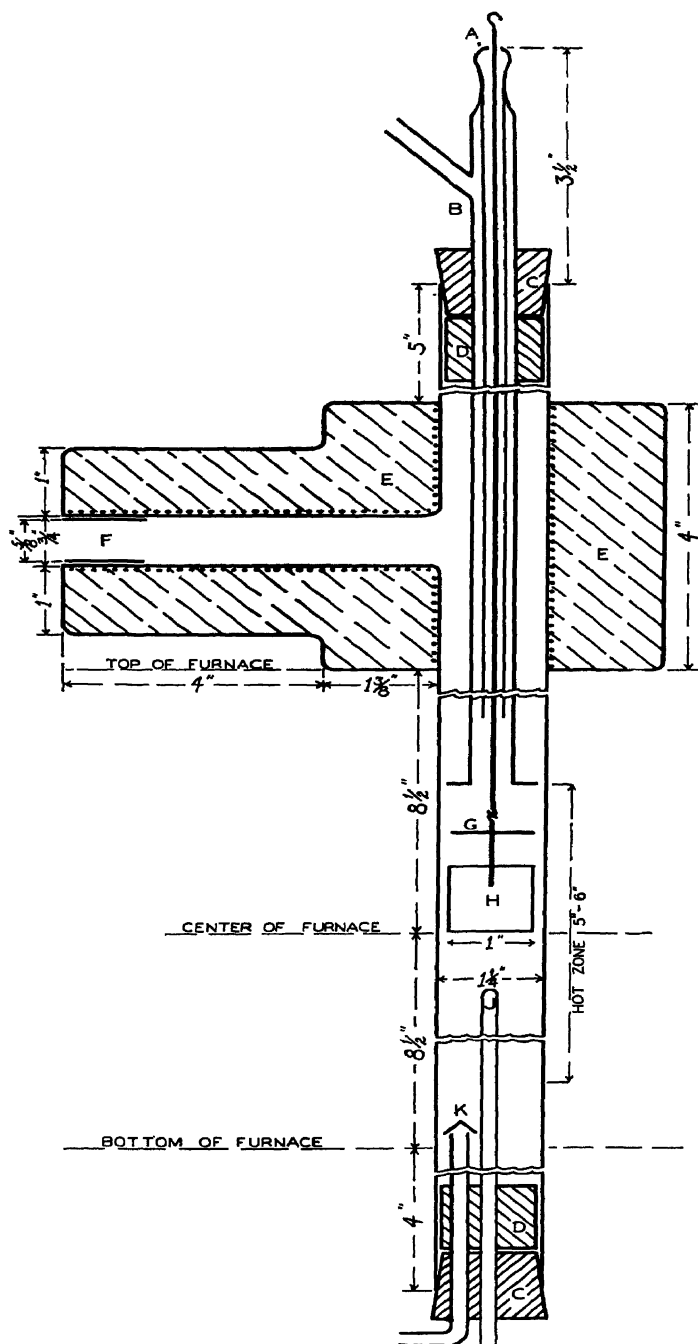


FIG. 1.—FURNACE TUBE FOR GASEOUS REDUCTION TESTS.

these tests is given in Table 1. The first ore was a commercially roasted flotation concentrate, crushed to pass 200 mesh. The second ore consisted of hand-picked

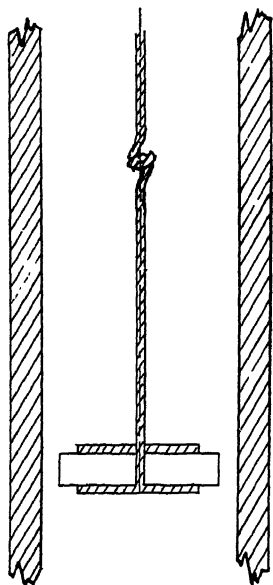


FIG. 2.—ARRANGEMENT OF $\frac{1}{4}$ -INCH BRIQUETS IN FURNACE.

crystals of willemite obtained from the Franklin, N. J., mine, and was also crushed to pass 200 mesh. The third material was a relatively coarse, ceramic-grade pigment oxide, which was selected instead of purer oxides because it underwent negligible shrinkage when heated in briquetted form.

The bituminous coal that was used was coked before being crushed to pass 100 mesh and made into briquets. The coked material contained 15.7 per cent ash, and 3.2 per cent sulphur. A complete ash analysis was not made, but the total alkali metal content, reported as Na, was about 0.2 per cent for the briquetted and recoked material. The ash analysis is important in connection with the catalytic effect of alkali metal compounds on the rate of the carbon-carbon dioxide reaction.

The Acheson graphite used came from

coarse-grained commercial rods. Its use was abandoned when results obtained at one or two temperatures indicated that constituents of widely different reactivities were present. A pure variety of graphite would undoubtedly have indicated a smaller reactivity.

The activated charcoal with which experiments were made at only two temperatures was a commercial variety made by the pyrolysis of waste solutions of cellulose; it was said to contain more than 98 per cent carbon and to have a very low ash content.

Purification of Gases.—The gases used in the investigation were carefully purified and dried by conventional means. Particular attention had to be paid to removal of sulphur present as carbonyl sulphide in the carbon monoxide. This was because carbonyl sulphide tended to form a film of zinc sulphide on the briquet.

The rates of gas flow were measured by means of carefully calibrated capillary flow meters.

Preparation of Briquets.—All briquets were made on a small laboratory press. Water was a suitable liquid to add in pressing the ore briquets, but with the carbon briquets a dilute honey solution was found to work more satisfactorily as a binder. All briquets were dried and then heated at 1000°C. for one hour; this served to harden them to the necessary degree and with the coal also served to drive off additional volatile matter. Ore briquets were heated in air, carbon briquets in purified nitrogen. Graphite pieces were machined to the standard briquet size.

Some of the first experiments were done with the 1-in. briquets shown in Fig. 1, and longer ones were used on occasion, but it was soon found that the reaction rates were too rapid for convenient measurement, and that the reaction was being slowed down by its close approach to equilibrium. Accordingly, the length of the 1-in. dia. briquet was reduced from 1 in. to $\frac{1}{4}$ in. and the

disk thus formed was mounted between two circular silica plates approximately $\frac{7}{8}$ in. in diameter, thus exposing a ring of the briquet $\frac{1}{4}$ in. thick and $\frac{1}{8}$ in. wide to the reacting gas. A rapid gas flow was thus maintained in the $\frac{1}{8}$ -in. annular space separating the briquet from the furnace tube. This arrangement is illustrated in Fig. 2. Unless otherwise mentioned, all data refer to the $\frac{1}{4}$ -in. briquets. The apparent exposed area of these briquets was 7.5 sq. cm. and the "time of contact" of the hot gas and briquet was of the order of 0.01 sec. The reproducibility of the reaction-rate measurements with these $\frac{1}{4}$ -in. thick briquets was about 5 per cent in most cases.

Description of a Typical Experiment.—The furnace was surveyed and the temperature adjusted before the beginning of a series of experiments, so as to give a zone of uniform temperature about 5 in. long, the center of which was slightly above the center of the furnace. The experimental briquet was suspended as nearly as possible in the middle of this zone. Temperatures were measured by a carefully calibrated platinum-platinum-rhodium thermocouple inserted from the bottom of the furnace to a point about 1 in. below the briquet, as at *J*, Fig. 1, and the furnace temperature was maintained constant to $\pm 1^\circ$ by an automatic controller. The temperatures thus measured were higher by a few degrees than the temperature of the reacting surface of the briquet, since the reactions being studied were strongly endothermic. A few experiments were made to determine this temperature difference and will be described later.

In starting an experiment, the briquet was suspended in the furnace until it attained a constant temperature and an approximately constant weight. During this time, a stream of 2000 c.c. per minute of purified nitrogen was passed through the furnace, and an equal flow of nitrogen into the upper end of the reaction tube was

maintained throughout an experiment. Ore briquets quickly reached a constant weight while coke briquets, because of further loss of volatile, required about $\frac{1}{2}$ hr. to attain a weight loss as low as 1 or 2 mg. per min., which usually was negligible in comparison with the reaction rate to be measured.

With the briquet and suspension balanced, the experiment was finally begun by shutting off the flow of nitrogen at the bottom of the furnace and admitting the desired gas. The rate of weight loss was determined by successively removing fractional gram weights from the balance and then determining, with a stop watch, the times at which the pointer passed the zero mark. The record of a typical experiment is given in Table 2, in which the rate of weight loss, measured in grams per minute, has been expressed in mols per minute in order that the results obtained with different materials may be directly comparable.

TABLE 2.—*Typical Experiment*

Briquet of roasted flotation concentrate reduced at 1000°C., using CO at the rate of 2000 c.c. per min. Weights removed from balance pan in steps of 0.2 gram each. Gas contained 99.5 per cent CO, 0.5 per cent N₂.

Total Time, Min.	Time Intervals, Min.	Reaction Rate, Mols per Min.
0.0		
0.57		
1.30	0.73	0.0034
2.10	0.80	0.0031
2.97	0.87	0.0028
3.87	0.90	0.0027
4.82	0.95	0.0026
5.80	0.98	0.0025
6.83	1.03	0.0024
7.89	1.06	0.0023
9.00	1.11	0.0022
10.12	1.12	0.0022
11.30	1.18	0.0021
12.55	1.25	0.0020
13.87	1.32	0.0019
15.22	1.35	0.0018
16.67	1.45	0.0017

Estimation of Reaction Temperatures.—

It was realized that the temperature of the briquet surface would drop rapidly following the start of an experiment, and probably would become fairly constant at some lower value within a few minutes. This

drop in temperature should be greater, the more highly endothermic the reaction, the more reactive the substance being tested, and the higher the experimental temper-

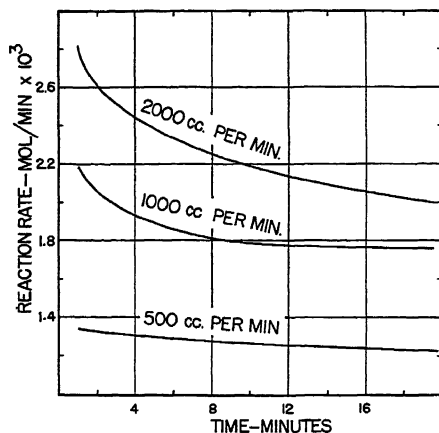


FIG. 3.—RATE OF REDUCTION OF ZINC OXIDE BY CARBON MONOXIDE AT 900°C.
Briquet diameter, 1 inch; length, 0.8 inch.

ature. This uncertainty concerning briquet temperature was probably the most serious one encountered in the course of the work.

The small size of the $\frac{3}{4}$ -in. test briquets precluded any measurement of briquet temperature under test conditions, but some tests were made on longer, unshielded zinc-ore briquets which served to show the order of magnitude of the temperature drop occurring during the reduction of zinc ores. A platinum-platinum-rhodium thermocouple in a $\frac{3}{16}$ -in. silica protection tube was embedded along the axis of a briquet so that the couple junction was $\frac{1}{2}$ in. from the bottom of the briquet. Nitrogen was run through the furnace until this couple and the control couple below the briquet reached the same temperature. Carbon monoxide was then run through the furnace until a constant temperature difference was indicated by the two couples; this required from 10 to 20 minutes.

Results obtained with pure willemite briquets 1 in. long showed a drop in

briquet temperature of 3° at 1000°C. and of 6° at 1100°, and the same results were obtained whether the carbon monoxide flowed at 200 or 2000 c.c. per min. This independence of rate of gas flow would be expected of a slowly reacting material.

Results obtained with zinc oxide briquets were as follows: At 1000°C., 1-in. briquets showed temperature drops of 12° and 27°, respectively, when the rate of gas flow was 200 and 2000 c.c. per min. At 1100°C., briquets $1\frac{3}{4}$ in. long showed temperature drop of 8° and 24°, respectively, when the rates of gas flow were 200 and 2000 c.c. per min. No tests were made with the remaining zinc ores, but the drop in briquet temperature undoubtedly would be proportional to the reactivity of the materials. Similar proportional decreases in briquet temperature would be expected for the carbonaceous materials, since the heat requirement of the CO-CO₂ reaction is of the same order of magnitude as that of the ZnO-CO reaction.

Since the reaction rates will be shown to be approximately doubled for a 100° rise in temperature, it is obvious that the decrease in briquet temperature that must have occurred during the first 10 or 15 min. of an experiment would be accompanied by an appreciable decrease in reaction rate, and that the more reactive materials would be more severely penalized in this respect. It is for this reason that, in the majority of cases, *initial* rates, obtained while the briquets were still at the nominal furnace temperatures, were used in determining relative reaction rates.

EXPERIMENTAL RESULTS

Effect of Rate of Gas Flow.—The effect of the rate of gas flow on the reaction rate is shown in Fig. 3. These results were consecutively obtained with a briquet 0.8 in. long, the curves being shifted for convenience to a common time origin, and show clearly that with so large an exposed surface a significant approach to equilibrium

had occurred, so that a satisfactory approach to a maximum reaction rate could not be obtained at permissible gas velocities. This is a consideration frequently

partly because with this ore an inert residue remained through which the gas must diffuse to get at the unreduced ore. Formation of a porous residue should be even

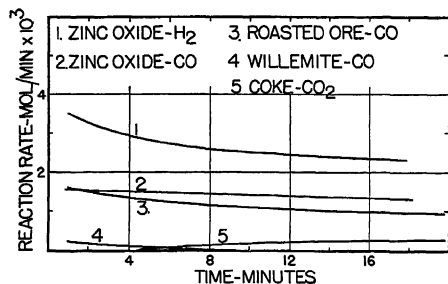


FIG. 4.—RATES OF REACTION AT 900°C. OF $\frac{1}{4}$ -INCH BRIQUETS IN A GAS STREAM FLOWING AT 2000 CUBIC CENTIMETERS PER MINUTE.

overlooked in reaction-rate measurements. The curves also show that the decrease with time of the initial reaction rate was much greater with a faster gas flow. This decrease in rate must be largely ascribed to the decrease in briquet temperature following the start of the reaction, but it is also due in part to the progressive decrease in the size of the briquets, and in part to the formation of gas films at the briquet surface through which counter-diffusion must occur.

In the remaining data to be presented on gaseous reduction rates, the $\frac{1}{4}$ -in. briquets of Fig. 2 were used, and the rate of gas flow was held at 2000 c.c. per minute.

Effect of Temperature on Reaction Rate.—Figs. 4, 5 and 6 show the curves of reaction rate versus time for some of the materials at furnace temperatures of 900°, 1000° and 1100°C., respectively, all plotted to the same scale. Each curve is the average of two or more experiments.

There are several points of interest in these curves. The initial rates for zinc oxide and the roasted flotation concentrate were nearly identical; but the latter decreased with time more rapidly, partly because the initial rate for the latter material was too high as a result of the rapid reduction of lead and iron oxides, and

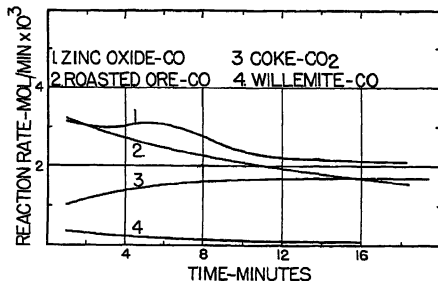


FIG. 5.—RATES OF REACTION AT 1000°C. OF $\frac{1}{4}$ -INCH BRIQUETS IN A GAS STREAM FLOWING AT 2000 CUBIC CENTIMETERS PER MINUTE.

more serious in the reduction of willemite, and the fact that the decrease in rate with time was not there more pronounced probably indicates that the inherent reaction

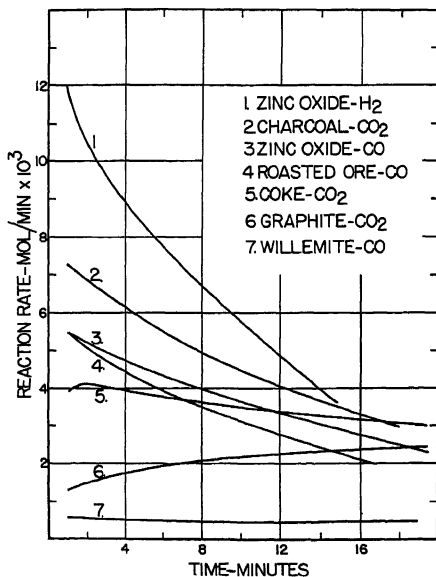


FIG. 6.—RATES OF REACTION AT 1100°C. OF $\frac{1}{4}$ -INCH BRIQUETS IN A GAS STREAM FLOWING AT 2000 CUBIC CENTIMETERS PER MINUTE.

rate of willemite was not greater than the gaseous diffusion rates.

The peculiar kink in the zinc oxide curve at 1000° was observed in all five of the ex-

periments made at this temperature, but no explanation of this phenomenon has been found.

The rate of reduction of carbon dioxide

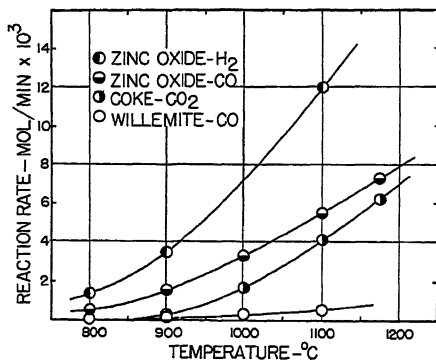


FIG. 7.—MAXIMUM REACTIVITY AS A FUNCTION OF TEMPERATURE.

by coke increased with time at the two lower temperatures, but decreased with time at 1100°. The first result is believed to be due to the catalytic effect of the coke ash in promoting the reaction, while the reverse effect at 1100° indicates that diffusion phenomena were controlling the rate of even the catalyzed reaction.

From the apparent equality of the rates for the roasted ore and for coke, which was attained in about 15 min. at 1000° and in an even shorter time at 1100°, one might conclude that a similar equality of rates would hold in a "steady-state" condition in a commercial retort. But such a conclusion is not necessarily correct, since only the initial rates are measured under comparable conditions, and since there is no assurance that equal surface areas of ore and coal are available in a commercial retort charge.

The curves of Figs. 4, 5 and 6 show clearly the great difference in reactivity between charcoal, coke and graphite, between an oxide type ore and a silicate ore, and between hydrogen and carbon monoxide.

From the curves of Figs. 4, 5 and 6, and similar curves obtained at 800° and 1175°

for some of the materials, the initial rates taken 1 min. after the start of the reaction and the rates after 15 min. (representing an approach to a steady state) were read off and are recorded in Tables 3 and 4, together with the temperature coefficients for each 100° interval. These data are used in Table 5 to show the relative maximum reaction rates, with the rate for the reduction of zinc oxide by carbon monoxide being taken as unity at each temperature. In this table, the maximum rates are initial rates except that the 15-min. rates were used for the coke-carbon dioxide reaction at 900° and 1000°.

Fig. 7 shows the maximum reactivity of the coke and the three zinc-bearing materials plotted as functions of temperature, the data being taken from Tables 3 and 4.

TABLE 3.—Rate of Reduction of Zinc-ore Briquets

Rate of gas flow, 2000 c.c. per min. Initial exposed area of briquet, 7.5 sq. cm. Time of contact about 0.01 second.

Material	Temperature, Deg. C.	Average Reduction Rate, Mols per Min. of ZnO		Temperature Coefficient for Each 100° Interval	
		Initial	15 Min.	Initial	15 Min.
REDUCTION BY CARBON MONOXIDE					
Zinc oxide....	800	0.0006	0.0005		
Zinc oxide....	900	0.0016	0.0014	2.7	2.8
Zinc oxide....	1000	0.0031	0.0021	1.9	1.6
Zinc oxide....	1100	0.0055	0.0031	1.8	1.5
Zinc oxide....	1175	0.0073	0.0032	1.5 ^a	1.2 ^a
Roasted flotation concentrate.....	900	0.0016	0.0010		
Roasted flotation concentrate.....	1000	0.0032	0.0018	2.0	1.8
Roasted flotation concentrate.....	1100	0.0055	0.0023	1.7	1.3
Willemite....	900	0.0002	0.00004		
Willemite....	1000	0.0003	0.0002	1.5	5.0
Willemite....	1100	0.0006	0.0005	2.0	2.5
REDUCTION BY HYDROGEN					
Zinc oxide....	800	0.0014	0.0011		
Zinc oxide....	900	0.0035	0.0024	2.5	2.2
Zinc oxide....	1100	0.0120	0.0035	1.7 ^b	0.7 ^b

* Estimated from the 75° temperature interval.

^b Average 100° temperature coefficient over 200° temperature interval.

TABLE 4.—*Rate of Reaction of Carbon with Carbon Dioxide*

Rate of gas flow, 2000 c.c. per min. Initial exposed area of briquet, 7.5 sq. cm. Time of contact about 0.01 second.

Material	Temperature, Deg. C.	Average Reaction Rate, Mols per Minute of Carbon		Temperature Coefficient for Each 100° Interval	
		Initial	Maximum	Initial	Maximum
Bituminous coal,	800	0.00005 ^a	0.00005		
Bituminous coal,	900	0.00012 ^b	0.0003	(2.4)	6.0
Bituminous coal,	1000	0.0010	0.0017	8.3	5.7
Bituminous coal,	1100	0.0039	0.0041	3.9	2.4
Bituminous coal,	1175	0.0063	0.0063	1.6	1.5
Graphite,	1000	0.0003	0.0004		
Graphite,	1100	0.0014	0.0025	4.7	6.2
Activated charcoal, . .	900	0.0011	0.0011		
Activated charcoal, . .	1100	0.0073	0.0073	(2.6) ^c	

^a First reading obtained about 15 min. after start of reaction.

^b First reading obtained about 8 min. after start of reaction.

^c Average 100° temperature coefficient over 200° interval.

TABLE 5.—*Relative Reaction Rates of Materials Used in Zinc Reduction*

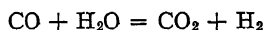
Material	Reacting with	Maximum Reaction Rate Relative to Zinc Oxide				
		Temperature, Deg. C.				
		800	900	1000	1100	1175
Zinc oxide,	H ₂	2.33	2.19		2.18	
Zinc oxide,	CO	1.00	1.00	1.00	1.00	1.00
Roasted flotation concentrate,	CO		1.00	1.03	1.00	
Willamette,	CO		0.13	0.10	0.11	
Activated charcoal	CO ₂		0.69		1.33	
Coked bituminous coal,	CO ₂	0.08	0.19	0.55	0.75	0.86
Graphite,	CO ₂		0.05 ^a	0.13	0.45	

^a Estimated from preliminary data on larger briquets.

Effect of Gas Composition on Reaction Rate.—Space will not permit more than a brief description of experiments done to demonstrate the effect of gas composition on the rate of reduction of zinc oxide by carbon monoxide. Under reaction conditions far removed from equilibrium, nitro-

gen would be expected to act primarily as a diluent, and experiments at 1100° showed that with nitrogen additions up to 12 per cent, the reaction rate was decreased by approximately 2 per cent for each per cent of nitrogen added. Carbon dioxide, being one of the reaction products as well as a diluent, would be expected to be a more effective inhibitor, and experiments at 1100° showed that additions of up to 11 per cent of carbon dioxide were approximately twice as effective as comparable amounts of nitrogen in decreasing the reaction rate.

The effect of water vapor on the reaction rate was studied by alternately passing dry and moist carbon monoxide over a zinc oxide briquet under the standard test conditions. The vapor pressure of the gas was thus quickly and repeatedly varied from 0.8 to 18 mm., and it was found that the moist gas consistently reduced the reaction rate by from 10 to 18 per cent. This effect cannot be explained by assuming the gases to react to form carbon dioxide before reaching the briquet according to the equation:



since this reaction would not occur sufficiently at 1100°. No other explanation of the effect of water vapor has been found.

Discussion of Heterogeneous Reaction Rates.—The rate of a gas-solid reaction is determined by the number of reactant molecules striking unit surface per second and, since only a small fraction of such collisions are fruitful, by the efficiency of the collision process.* According to the collision theory, only those collisions are fruitful in which the sum of the available energies (kinetic, vibrational, etc.) of the colliding molecules exceeds the average molecular energy by an amount called the energy of activation, *E*. Since activation energies are usually very much larger

* An extensive exposition of this theory is given by Hinshelwood.²

than the average molecular energy, these are customarily lumped together and the reaction is assumed to be carried on by molecules having energy equal to or greater

absolute temperature:

$$N_E = N_0 \times e^{-E/RT}$$

Hence, the fraction N_E/N_0 , having such energy at a temperature T , is found by solving the equation:

$$\log N_E/N_0 = -0.4343E/RT$$

For a given value of E , the value of the fraction N_E/N_0 , may be computed at temperatures of interest, and the ratio of the values of this fraction at two temperatures gives the relative number of activated molecules at these temperatures, and this ratio should also equal the temperature coefficient of the reaction rate for the interval in question. The larger the value of E , the greater is the temperature coefficient of the reaction rate.

By plotting the logarithm of N_E/N_0 , or the logarithm of the reaction rate against $1/T$, a straight line should be obtained whose slope depends on the value of E . Three curves, corresponding to different values of E , are shown in Fig. 8, in which the lines have been arbitrarily shifted to have a common origin corresponding to 800°C. , and in which the relative values of the fraction N_E/N_0 are expressed as relative reaction rates. In the same figure, the logarithms of the experimentally observed reaction rates, taken from Figs. 4, 5 and 6 are plotted in order to permit comparison of the slopes of the various curves.

The production of a straight line on such a plot indicates that some one reaction mechanism is controlling the reaction rate. It happens frequently that a reaction proceeds by one mechanism in one temperature range and by another mechanism, requiring a different value of E , in a different range. In this case two straight lines of different slope should be obtained, curving into each other in the intermediate range where the two mechanisms are competing with each other. The curvature, at the higher temperatures, of the line representing the zinc oxide-carbon monoxide reaction,

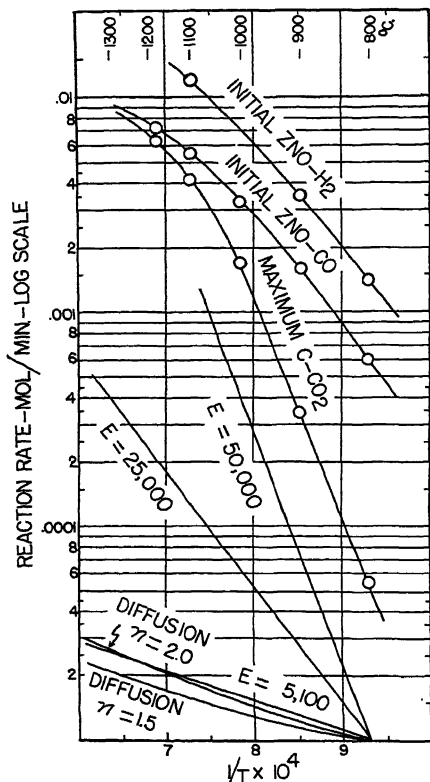


FIG. 8.—LOGARITHMIC PLOT OF REACTION RATES AGAINST THE RECIPROCAL OF THE ABSOLUTE TEMPERATURE.

than E calories per mol. The increase in reaction rate with increasing temperature, commonly called the temperature coefficient of the rate, is, therefore, a measure of the increase with temperature of the number of activated molecules. Thus, if the temperature coefficient is known, the value of E may be calculated, and *vice versa*.

The number of molecules, N_E , out of a total number, N_0 , having energies greater than E calories per mol is given approximately by the following equation where R is the molar gas constant and T is the

and of that representing the carbon-carbon dioxide reaction, is taken to mean that the molecular reaction mechanisms governing the respective reaction rates at low temperatures are being superseded by some other process requiring a lower energy of activation and having, therefore, a smaller temperature coefficient.

It is believed that this superseding mechanism is the relatively slow process of the diffusion of the reacting gas to the briquet surface through a film of counter-diffusing reaction products. The temperature coefficient of the diffusion rate of a gas may be given approximately by the expression:

$$D_2 = D_1(T_2/T_1)^n$$

where D is the diffusion coefficient, T is the absolute temperature, and the constant, n , varies from 1.5 for an ideal gas to about 2.0 for actual gases at high temperature. Calculation of relative diffusion rates from this equation for temperatures of present interest shows them to behave as though a process were occurring that required an activation energy of about 5100 cal. per mol; that is, an activation energy approximately equal to the average energy of a diatomic gas at 800°C. These curves are shown at the lower left of Fig. 8. If the assumption is correct that the experimental reaction rates are being limited by diffusion at high temperatures, the latter curves may be considered as representing the limiting slope that curves for the chemical reactions would approach at still higher experimental temperatures. It is of particular interest to note that the curve for the reduction of zinc oxide by hydrogen, a gas noted for its rapid diffusion characteristics, has not yet acquired a pronounced curvature at 1100°; in other words, the diffusion rate is still so rapid that it is not limiting the inherent chemical reaction rate.

Effect of Gases on the Reduction of Ore-coal Briquets.—The fact that gaseous diffu-

sion rates are a limiting factor in the reduction of zinc ores is nicely shown by some experiments in which briquets 1 in. in diameter and 1 in. long, composed of 50 per

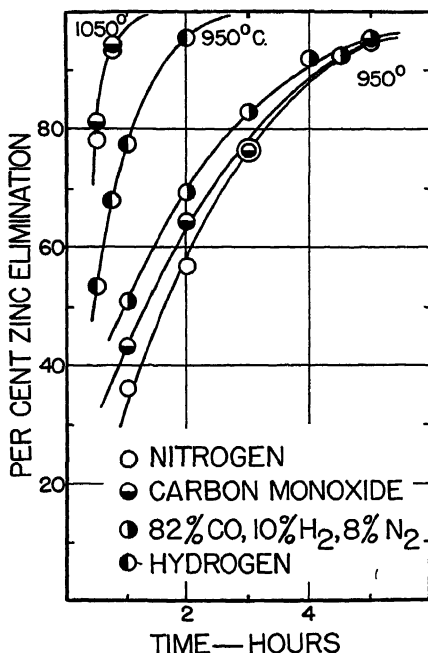


FIG. 9.—EFFECT OF FURNACE ATMOSPHERE ON REDUCTION OF BRIQUETS OF ZINC ORE AND COAL.

cent zinc oxide, 35 per cent crushed bituminous coal and 15 per cent anthracite dust were first coked at 600° to 900° in nitrogen and then reduced at various temperatures in flowing atmospheres of nitrogen, carbon monoxide and hydrogen, respectively. The furnace tube was 1¼ in. in diameter and the gases flowed at a rate of 1000 c.c. per min. Fig. 9 shows the curves of percentage of zinc elimination, based on chemical analysis, versus time, and Fig. 10 shows the relationship between zinc elimination and weight loss.

These experiments show that a stream of carbon monoxide is not more effective than a stream of nitrogen in the tests at 1050°, and that while carbon monoxide does increase the reduction rate at 950°, it is

effective only during the early stages of reduction. Carbon monoxide containing only 10 per cent of hydrogen is much more effective at 950°, and the effect on the

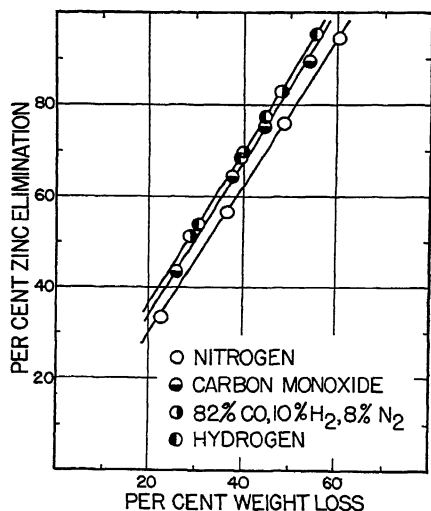
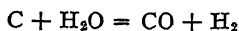


FIG. 10.—ZINC ELIMINATION VERSUS WEIGHT LOSS FOR THE REDUCTION DATA OF FIG. 9.

reduction rate persists until reduction is nearly complete. Pure hydrogen at 950° speeds up the reduction in a very striking manner, and remains effective until elimination of zinc is complete.

In a normal reduction process, the weight loss of the briquet is due to the disappearance of zinc oxide and carbon. If some reduction is due to added reducing gases, less carbon will be used and the weight loss for a given zinc elimination will be less (Fig. 10). While it is obvious from Fig. 9 that much of the reduction was due to hydrogen when this gas alone was used, the weight loss was not decreased in anything like the same proportion. This suggests that carbon was being used in some other reaction, and it is believed that the most likely reaction is the following, the water vapor coming from the reduction of zinc oxide by hydrogen:



These results indicate that carbon monoxide, a relatively slowly diffusing gas, when externally supplied aids the reduction of ore-coal briquets only at temperatures at which the diffusion rate is faster than the normal reduction rate, and even then only so long as reduction is occurring near the outer surface of the briquet where extensive diffusion is not required. Hydrogen, on the other hand, diffuses so rapidly that even the thickness of the almost completely reduced briquet offers very little resistance to its passage.

DISCUSSION OF RESULTS

Two general facts shown by the present experiments, that hydrogen is more reactive than carbon monoxide and that charcoal, coke and graphite are progressively less reactive forms of carbon, have, of course, been common knowledge for a long time, and the reasons for not employing charcoal and hydrogen in commercial zinc smelting are economic ones. Unfortunately, it is not feasible to employ hydrogen in a divided process in which hydrogen is used to reduce zinc oxide in one retort and is regenerated by the reduction of water vapor by coke in a second retort, since in each cycle the hydrogen would be diluted with an ever-increasing volume of carbon monoxide by virtue of the water-gas and producer-gas reactions.

Since the carbon-carbon dioxide reaction has been shown to be the slower of the two reduction reactions at low temperatures, any effort to speed up zinc reduction early in the smelting cycle should be directed toward acceleration of this reaction. At the higher temperatures existing toward the close of a cycle, the rates of both reactions are nearly equal and both are limited by diffusion, so that it is the diffusion processes that then need to be accelerated.

Numerous data in the literature show that substances such as sodium carbonate catalyze the carbon-carbon dioxide reaction

at relatively low temperatures, but the effect decreases with increasing temperature and is negligible at normal zinc-smelting temperatures. The use of a catalyst does not alter the equilibrium requirements of the system, so that the maintenance of an abnormally low temperature throughout a smelting cycle in order to benefit from a catalyzed charge would probably result in a lowered concentration of zinc vapor and in increased condensation difficulties.

The possibility of accelerating the diffusion rates of carbon monoxide and dioxide at normal smelting temperatures appears to be remote. A less nebulous but still impractical remedy for the diffusion limitation would be the substitution of reactive and rapidly diffusible hydrogen in place of carbon monoxide, as previously mentioned.

A word of caution should be offered in connection with the possible interpretation of the data given in this paper. The experiments were done in a thin-walled silica tube, and the furnace represented an almost instantly available source of heat supplied at the experimental temperature. Such conditions do not hold in commercial retorts, where the heat required for the endothermic reactions must be transmitted through a relatively thick retort wall and, on the average, through a considerable thickness of charge. Thus, while it is still true that the rate of the carbon-carbon

dioxide reaction limits the over-all rate of zinc production, this is in commercial practice a secondary limitation dependent primarily upon the rate at which heat can be transferred to the charge.

ACKNOWLEDGMENT

The authors gratefully acknowledge the assistance of other members of the Research Division of The New Jersey Zinc Co. in this work, particularly that of Mr. Dale M. Smith, who performed many of the experiments.

REFERENCES

1. M. Bodenstein: *Trans. Amer. Electrochem. Soc.* (1927) 51, 449.
2. C. G. Maier: *U. S. Bur. Mines Bull.* 324 (1930) 48-50.
3. Hinshelwood: *The Kinetics of Chemical Change in Gaseous Reactions*, Oxford Univ. Press, 1933.

DISCUSSION

(*Herbert R. Hanley presiding*)

O. C. RALSTON,* Washington, D. C.—This paper is an important addition to the literature on reaction kinetics of zinc reduction. The scientific literature on zinc reduction in the past concerns itself mainly with equilibrium data, established as the ideal criteria when unlimited time is available to reach equilibrium. This paper adds very considerably to an understanding of the various reaction rates involved and points out the steps that seem to be the slowest or limiting steps.

* U. S. Bureau of Mines.

Direct Production of Metallic Zinc by the Electrothermic Process

By GEORGE F. WEATON,* MEMBER, AND CARLETON C. LONG,† JUNIOR MEMBER
A.I.M.E.

(New York Meeting, February 1939)

Two years ago the general features of the St. Joseph Lead Company's zinc-smelting process were described.¹ At that time the discussion was limited to a description of the production of high-purity electrothermic zinc oxide. The present paper will describe the commercial production of electrothermic zinc metal. Since a fairly complete description of the plant of the Josephtown smelter was given in the earlier paper, the brief recapitulation given here will be limited to mention of additional equipment recently installed and a bare outline of the preparatory process.

The raw material is zinc sulphide concentrate received from the company's mines in St. Lawrence County, New York. An average dry-weight analysis of this material is: Zn, 58.28 per cent; Pb, 0.56; insoluble, 1.6; SiO₂, 1.12; Fe, 6.4; CaO, 0.47; MgO, 0.27; S, 31.9; Cd, 0.1; Cu, 0.06; Mn, 0.24. Moisture content is usually about 3 per cent. Three 21-ft. 6-in. diameter, 12-hearth Nichols-Herreshoff furnaces roast the concentrate to a calcine of average composition (first 10 months of 1938): Zn, 67.69 per cent; Pb, 0.06; insoluble, 1.75; SiO₂, 1.26; Fe, 7.24; CaO, 0.47; MgO, 0.36; S, 1.88; Cd, 0.1; Cu, 0.07; Mn, 0.27. The sulphur dioxide gas, after passing through a waste-heat boiler, proceeds through a recently redesigned low-resistance gas-purification assembly to the contact sulphuric acid plant, of which the capacity is 200 tons of concentrates per day.

The calcine is mixed with a portion of returned furnace residues and sintered on 42-in. by 44-ft. Dwight-Lloyd sintering machines, gas-fired. Wind-box gases pass through air coolers before filtering in a 1440-bag Dracco unit, and thence to stack. The Dracco fume is mixed with Cottrell dust, from roaster gas cleaning, and sent to the leach plant, where it is roasted (SO₂ to acid plant) and leached with sulphuric acid to recover, as end products, lead sulphate, zinc sulphate and cadmium.

Manuscript received at the office of the Institute Dec. 1, 1938. Issued in METALS TECHNOLOGY, February 1939.

* Manager, St. Joseph Lead Company of Pennsylvania, Josephtown, Beaver County, Pa.

† Director, Plant Research Department, St. Joseph Lead Company of Pennsylvania.

¹ References are at the end of the paper.

From the sinter-sizing circuit the portion of the sinter encompassed within the $-\frac{3}{4} + \frac{1}{4}$ -in. size range is screened out, mixed with return sinter from the residue-treatment system, and sent to the feed bins at the furnace plant. This sinter has a hard, open, lacelike structure, and has an average analysis (first 10 months, 1938) of Zn, 58.94 per cent; Pb, 0.03; insoluble, 9.48; SiO₂, 8.62; Fe, 9.02; Al₂O₃, 1.3; CaO, 1.1; MgO, 0.6; Mn, 0.39; Cu, 0.11; Cd, 0.005; S, 0.23; loss on ignition, 1.1.

By-product coke, similarly sized, comprises the other portion of the furnace feed. An average proximate analysis of this material is: ash, 12.8 per cent; volatile matter, 0.6; fixed carbon, 86.6; Cl, 0.018; S, 0.94. The residue discharged from the bottom of the furnace is separated into its components by magnetic, air and screen separation. The removed coke returns to the furnaces, as does the reclaimed sinter. A portion of the low-zinc material, depending upon the amount of iron to be eliminated from the system, is discarded, the remainder being returned to the sintering machines.

THE FURNACE

A general layout of the furnace and condensing equipment is displayed in Fig. 1. The coke and sinter bins discharge on constant-weight belt feeders, which in turn empty into a rotary, gas-fired, brick-lined kiln preheater. The preheater product drops through a neck connecting with the rotating distributor top. The charge distributor is lined with refractory brick on the under side. The furnace shaft is built up in sections, not more than 6 ft. high, independently supported on steel skewback rings. Interpolated between the sections are sealed expansion joints. The bottom section rests on a steel water ring. A slowly rotating, convex-topped, brick-covered table closes the bottom of the furnace shaft. Spent charge works toward the periphery of the table and drops into a trough, which discharges into a pan conveyor leading to the residue-recovery system.

The furnaces are about 37 ft. over-all in height, and have an inside diameter of from 57 to 69 in., the more recently constructed furnaces being of the larger bore. The refractories, a more detailed description of which has been given elsewhere,² are of high-grade, low-alumina, low-porosity firebrick (Walsh S).

An annular gap is provided in the furnace wall at a position roughly one-third of the distance between the two sets of electrodes down from the top set. This gap, or passageway, is encircled by a brick-lined chamber termed a "vapor ring." The vapor ring communicates with the condenser.

ELECTRICAL SYSTEM

The furnace is of the charge-resistor type, the charge serving as the current-carrying medium. Current is supplied through two sets of three

electrodes spaced 24 ft. apart vertically, and at 120° to each other horizontally. Pitch-impregnated, low-porosity carbon electrodes 12 in. square by 60 or 72 in. long are employed. They dip into the charge at a small angle and are set diamondwise so as to offer the least resistance to the passing charge. Electrical connection between the electrode and the 6 by $\frac{1}{4}$ -in. copper bus bar is afforded by a bronze water-cooled electrode

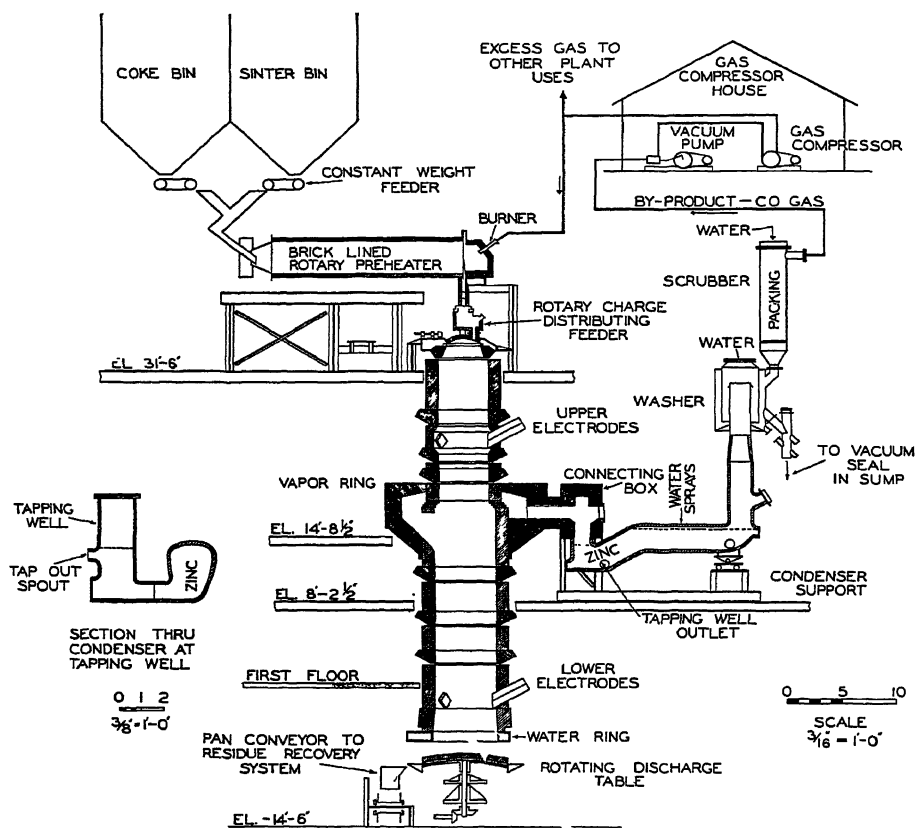


FIG. 1.—FURNACE AND CONDENSING EQUIPMENT.

clamp. Electrode consumption for the first 10 months of 1938 has been about 5 lb. per ton of metal produced.

Each of the three electrode pairs is served by a 2300/360/160-volt, 1800-amp. single-phase transformer. Close adjustment of power input is provided by an induction regulator in series with the primary circuit of the transformer. Each electrode circuit draws 1800 to 2000 amp. at 275 to 250 volts; the total power input to the furnace is carried at about 1500 kw. Control of power input may be either manual or automatic, the general practice being to employ manual regulation during periods of

wide adjustment, such as starting a furnace, and to turn the furnace over on automatic control for routine operation.

THE CONDENSER

The Josephtown condenser* is a unique metallurgical development permitting continuous one-step condensation to coherent metal of large quantities of metal vapor irrespective of its dilution by accompanying gases. Briefly, the incoming gases are bubbled through a bath of molten metal, the effect being much the same as that of a jet condenser. The condenser is disposed in the form of a U-tube with one arm, the outgoing branch, slanting upward at an angle of 30° from the horizontal. Vacuum applied to the outgoing branch displaces the metal so that a bubble of gas is drawn down the incoming branch and around the bend. The bubble now rushes up the outgoing branch, where it slightly releases the vacuum, allowing the metal to fall back a bit. This constant sloshing back and forth of the metal bath efficiently scrubs the gas and condenses the metal vapor therefrom.

Many interesting problems were met in the design of the condenser. Since it was desired to produce high-grade zinc, choice of materials of construction was limited to the few substances that are not attacked by zinc in the region of its boiling point. The condenser is lined with silicon carbide refractories (Carbofrax A or D) specially tamped to secure the maximum possible density and minimum porosity. Between the cast-steel shell and the refractories, there is placed a three-ply lining of high-temperature mica, which affords some protection to the steel in the event of a zinc leak through the brick.

The over-all length of the condenser is roughly 14 ft. An entrance tube 16 in. in diameter opens into an upward slanting ovate cavity, which contains the major portion of the zinc. This cavity is roughly 34 in. high and 23 in. wide at the widest part of the cross section. The exit tube is 23 in. in diameter. The wetted area at 18 in. of mercury vacuum is 120.3 sq. ft. The metal bath weighs approximately 11 tons, occupying a volume of about 51 cu. feet.

The exit gases from the condenser pass through a washer provided with sprays and a deckle-edge skirt forcing the gases to bubble through water. The gases then pass to a specially designed scrub tower packed with ½-in. Berl saddles and operated under flooding conditions at a constant pressure differential.

The clean gas is exhausted by single-stage reciprocating dry vacuum pumps discharging at atmospheric pressure to a single-stage gas compressor of conventional design, which returns the carbon monoxide at 30 lb. per sq. in. to the gas mains.

* G. F. Weaton and H. K. Najarian: U. S. Patent 2070101.

OPERATION

The furnace charge issues from the storage bins over constant-weight feeders. The normal rate of feeding is 36 lb. of sinter and 16 lb. of coke per minute. Stoichiometrically only about $4\frac{1}{2}$ lb. of coke per minute is required to reduce the zinc oxide; it is the provision of this large excess of coke that confers electrical stability to the system.

Before being fed to the furnace, the coke-sinter charge is preheated in a rotating kiln fired with a portion of the carbon monoxide gas recovered later in the system. The preheating temperature is carried as high as possible without volatilization of any appreciable quantity of zinc. Recent studies have shown that this temperature may be safely carried to about 850° C. High preheat temperatures are desirable because the carbon monoxide is a by-product offering heat at a cost very much lower than that obtained from the electric current once the charge enters the furnace proper.

The hot charge is fed into the top of the furnace shaft by means of a distributor top rotating in a horizontal plane. This distributor lays down the charge in such a way that a controlled segregation is obtained. The controlling of distribution of the furnace charge is a nice art; in general, it may be said that most of the larger sizes of coke are thrown toward the center of the shaft, so as to form a central "core," which will stabilize the path of the electric current. Temperatures of 1400° C. have been measured in this core; the temperature in the main body of the charge varies within wide limits but in general is about 1200° C.

As the granular charge passes downward through the furnace, the evolved zinc vapor and carbon monoxide gas pass through the annular gap in the furnace wall into the encircling vapor ring, and thence into the condenser. The gas temperature at this point is about 850° C., the dew point about 830° C.

At the start-up the vapor ring and condenser are preheated with gas burners. The furnace proper is brought into production by first charging with coke, applying power, then gradually increasing the sinter-coke ratio until normal operating conditions are established. This takes roughly a day. Initially the condenser is primed by pouring some 9 tons of molten zinc into the tapping well. The bath is then built up by subsequently condensed zinc vapor.

The condensation of zinc vapor is a continuous process, while tapping and casting, as will be described below, is a batch process. An idea of the efficiency of the condenser may be obtained by measuring the amount of zinc vapor remaining uncondensed in the exit gases and comparing this amount with the amount to be expected on the basis of the vapor pressure of zinc at the temperature of the bath of metal in the condenser. This determination has been carried out at bath temperatures of 580° and

650° C., and the results have been found to be essentially identical with those predicted from Maier's equation* for the vapor pressure of zinc as a function of temperature.

The exit gases from the condenser in passing through the washer are abruptly cooled from the temperature obtaining above the metal bath (about 550° C.) to room temperature. This shock cooling precipitates the remaining zinc vapor in the form of a finely divided metallic powder ("blue powder"). Approximately 90 per cent of the blue powder flows away with the washer water; the remaining solids are removed by the scrub tower. A portion of the cleaned and compressed gas is burned, as mentioned above, in preheating the charge; the remainder is used throughout the plant where needed. The gas has a net heating value of about 265 B.t.u. per cubic foot; a typical analysis is CO, 82 per cent; CO₂, 1.6; O₂, 1.4; N₂, 15.

The blue powder recovered in the washer and scrub towers is recovered in settling ponds. After drying, this material is returned directly to the furnaces. The blue powder formed in this process is a function of the vapor pressure of a bath of molten metal and is not related to the peculiarities of the process or of the condenser except as they may affect the temperature of the metal bath in the condenser. Control of condenser temperature may be had by adjustment of water sprays on the exterior surface. To provide leeway when the power is off the furnace (as in changing electrodes), the condenser temperature is ordinarily not allowed to fall below 550° C.

The vacuum pumps maintain a vacuum of 26 in. of mercury (barometer, 29.2 in. Hg at Josephtown) at the pumps. From 16 to 18 in. of mercury vacuum is carried on the exit side of the condenser. The pressure in the vapor ring is just negative with respect to the atmosphere. As zinc vapor is condensed, the metal level in the condenser rises, requiring an increase in the vacuum to pull the gas bubbles through. By noting this reading on an appropriately positioned gauge, the operator knows when to tap the condenser.

The lower portion of the condenser communicates with a tapping well from which the zinc is drawn periodically into a ladle. By means of a crawler hoist the ladle is transported to the casting bench, where the commercial slabs are poured. Tapping takes place without interruption of the operation of the condenser. The ladle holds approximately 1400 lb. of zinc, and this constitutes a "lot" or batch, which is indicated by numbers stamped on each slab. With each lot there is cast a pallet upon

* It may be worth while to call attention to an error in this equation.³ The same error has also appeared in this equation as quoted in the estimable work of Butts.⁴ The correct version of the equation when the pressure is expressed in millimeters of mercury is:

$$\log p = -6789.5/T - 1.051 \log T - 0.0001255T + 12.0181$$

which the slabs are piled. An electric fork truck carries the loaded pallets to storage or into the car to be loaded. For customers that wish to unload with fork trucks, the pallets are steel-strapped so as to preserve their identity during shipment.

The metal tapped from the condensers is ordinarily of "high grade" specification, containing not over 0.007 per cent Fe or 0.025 per cent Pb. With the present process it is not feasible to reduce the iron content much below 0.005 per cent. By slightly altering the preparation of the calcine and sinter and employing selected concentrates, it is possible to bring the lead down to about 0.01 per cent. Lower grades of metal containing considerably more lead are easily made by increasing the lead content of the furnace feed. This could be done by making a high-lead sinter, but as high lead may not be wanted on all of the furnaces the lead-containing material, suitably Cottrell dust from the roasting operations, is added directly to the furnace desired. By an auxiliary opening near the top of the furnace, the modifying material is charged directly into the high-temperature region of the central core, which ensures complete volatilization, so that the residues, part of which return to the furnaces in the form of coke or sinter, are not "salted."

The metal thus produced is of controlled quality; as contrasted with Prime Western zinc, made by adding lead and other ingredients to electrolytic zinc. Rather, the electrothermically produced Prime Western metal has a nascence not differing intrinsically from that of retort-block metal.

A furnace campaign lasts from six to twelve weeks, after which time it is expedient to shut down for routine repairs of the furnace refractory and to remove accretions that may have built up in the interior of the vapor ring. During regular operation the vapor ring is opened every third day for removal of any debris that may have been carried out from the descending charge in the furnace shaft.

Compared with the surface type of condensers usually employed in zinc metallurgy, the capacity of the Josephtown internal condenser is impressive. Over 15 tons of zinc per day have been tapped from one of these condensers, and during an entire furnace campaign the daily production averages over 13 tons. Some 23,000,000 B.t.u. must be dissipated during the condensing and cooling of 13 tons of zinc vapor and the accompanying noncondensable gases. The rate of heat dissipation is approximately 132 B.t.u. per min. per sq. ft. of internal wetted surface, giving an over-all heat transfer coefficient of 0.13 B.t.u. per min. per sq. ft. per deg. F. temperature difference.

The constant heaving and slopping of the molten metal mass, together with the temperature changes incident to starting up and shutting down, impose a severe strain on the refractories of the condenser lining. Notwithstanding this, the linings have given surprisingly satisfactory service. For the first 10 months of 1938 the total materials cost for refractories consumed in production of zinc metal is \$1.39 per ton of finished metal.

Of this \$0.37 represents repairs to the condenser lining, while the balance refers to repairs and replacements in the furnace and vapor ring.

Of the eight electric furnaces at Josephtown, four are equipped with condensers, while a fifth furnace will soon be so equipped. Normally, one furnace is down for repairs while the others are operating. With four furnaces operating, the production rate is approximately 55 tons of slab zinc per day. Requirements for operating labor in the furnace plant are approximately 5.5 man-hours per ton of slab zinc produced.

Three years of development work preceded the installation of the first semi-commercial condenser late in 1935. The present style of condenser was brought into regular commercial production in 1936. A new shape of condenser has been designed recently and is soon to be installed. This condenser is larger than the present style and is somewhat simpler in construction, in that a circular rather than an ovate cross section is employed. The decreased area-to-volume ratio suffered by the change from ovate to circular shape is more than counterbalanced by extension or lengthening of the lower bend of the U-tube.

DISCUSSION OF RESULTS

Approximately 40 tons of charge enters the furnace daily. The zinc elimination is 70 to 73 per cent for one pass through the furnace. Since most of the zinc in the residue finds its way, via sinter, back to the furnace, the total zinc recovery is higher than this. For the first 10 months of 1938 the over-all plant recovery of zinc (zinc in salable products divided by zinc in concentrates) is 92.62 per cent. Of the approximately 7 per cent zinc not recovered, about 4 per cent is represented by zinc in the discarded residues, while the other 3 per cent represents miscellaneous handling losses.

Power requirements for the furnaces for the first 10 months of 1938 are 2564 kw-hr. per ton of zinc or zinc equivalent. (There is no essential difference in the ratio between power and product for the oxide furnaces and for the metal furnaces.) The furnace load constitutes 81 to 82 per cent of the power load of the entire plant. The latter item includes the lighting load for office building, clubhouse, etc., in addition to the regular plant power load. The furnace power referred back to the incoming zinc concentrates (nominal 57.5 per cent Zn) and noting that the expected recovery is 92.62 per cent, gives an equivalent of 1365 kw-hr. per ton of concentrate received. Local power rates are considerably higher than in the West, but this disadvantage is offset by the geographical proximity of the market and by the favorable power-product ratio.

It is interesting to examine briefly possible factors differentiating this process from older, less successful attempts. The history of electro-thermic zinc smelting is too well known to warrant references here. In general, it may be remarked that former difficulties were largely connected with: (1) the furnace charge, and (2) the condenser. In the Josephtown

furnaces the amount of coke added is determined not by the amount of reducing agent required but, rather, by the physical requirements for a stable electrical circuit. The sinter is more or less incidental to the charge, though it is true that it influences considerably (and beneficially) the course of the electric current. With an all-coke charge, the current exhibits a tendency to concentrate in a narrow streak. Two objections may be advanced against formation of a fluid slag; one, the heat of fusion requires extra power; two, it is difficult to reclaim the excess coke. Many of the earlier experiments were made with arc furnaces, giving high local temperatures. Extremely high temperatures are not required for the reduction and volatilization of zinc. The charge resistance furnace distributes the heat throughout the charge in the locations where it is wanted.

Earlier difficulties in condensation may be traced partly to disregard of the physical chemical principles involved and partly to the use of surface condensers. This type of condenser is capable of effective use when all conditions are under exact control, but leads to excessive formation of blue powder when subjected to the vagaries attendant upon the experimental stage of electrothermic furnace development. The internal condenser is free from these restrictions.

In connection with the internal condenser, while the entering gas usually contains by volume about 55 per cent diatomic gases and 45 per cent zinc vapor, there have been extraordinary occasions when air was pulled into the furnace shaft, which diluted the condenser gases to 40 per cent and less of zinc vapor. No detrimental effect was observed at the condenser; the decreased heating value of the by-product gas, however, manifested itself in a rather compelling manner at the preheater burners.

From time to time in the literature⁵ there has appeared the suggestion that production of metallic zinc by an electrothermic process would probably be an intermittent, or, at best, a two-stage process. It is interesting in this respect to note that the Josephtown furnaces have been successfully operated, in lieu of sinter, on pellet and briquette charges compounded from calcine or other zinc oxide materials. We have, then, a clear example—from the gross or over-all viewpoint—of continuous, single-step electrothermic smelting of zinc-containing raw material to marketable metal.

Further improvements and refinements now under development appear promising.

REFERENCES

1. G. F. Weaton: *Trans. A.I.M.E.* (1936) **121**, 599-609.
2. W. B. MacBride: *Bull. Amer. Ceramic Soc.* (1935) **14**, 389-393.
3. C. G. Maier: *U. S. Bur. Mines Bull.* 324 (1930) 40.
4. A. Butts: *Textbook of Metallurgical Problems*, 378. New York, 1932. McGraw-Hill Book Co.
5. W. R. Ingalls: *Trans. A.I.M.E.* (1936) **121**, 367.

DISCUSSION

(*Francis P. Sinn presiding*)

W. R. INGALLS.* New York, N. Y.—This paper describes with much detail and with perfect frankness the features of a new and unique metallurgical process. If there are omissions, I am sure that they are in respect of matters overlooked by the authors, and in no wise intentional.

The authors speak of a preheater, in which the temperature is carried as high as possible without volatilization of any appreciable quantity of zinc, as being used simply as the cheapest way of bringing the temperature of the charge up to the most desirable figure prior to its introduction into the electrothermic distilling furnaces. I think that there may be something else of a desirable nature, such as preliminary reactions, occurring in the preheater. We should also like to have more details in respect of the movement of gas and zinc vapor through the charge in the furnace shaft. Also, in respect of the quantity and run-around of the blue-powder production.

The idea of distilling zinc ore in vertical retorts was one that early engaged the attention of zinc metallurgists, but one of the difficulties that prevented such an accomplishment was the inability of the gas and vapor to get through a column of fine ore and coal. Even in our ordinary horizontal (so-called) retorts the charge has to be "spieased," i.e., channeled at the top by the insertion of a rod; and sometimes when that has not been done properly there may be an accumulation of internal pressure that may blow out the whole charge. Of course I am conscious that at Josephstown the sintered ore is carefully screened and sized. Fine ore makes an excellent gas seal.

This brings to my mind that when I was associated with some primitive electrothermic zinc distilling work, about 30 years ago, we were quite fearful in respect of the danger of explosion of the great volume of zinc vapor in furnaces of substantial size, overlooking that we were bound to have a plus-pressure inside the furnace. We soon learned, however, that when we had leakages around the electrodes, or elsewhere, we did not have air sucked in but had zinc flames spitting out. A shovelful of

fine ore would always stop such leaks. We never had any furnace explosions but we did have some terrifying condenser explosions, which we had not foreseen.

I am led to criticize the intimation in this paper that earlier attempts at electrothermic zinc smelting were unsuccessful, and I offer this criticism without any disparagement of the fine work of Messrs. Weaton and Long in making a shaft furnace with internal heating by electricity operate continuously; or of their ingenuity in designing a method of condensing zinc vapor as spelter that is certainly unique. We should not overlook that at Trollhattan there was practically uninterrupted operation of large electrothermic furnaces from 1909 to 1931 and that from 1916 through 1930 there was produced there more than 50,000 metric tons of spelter.

I have no thought of making any comprehensive comparison between the practices at Josephstown and at Trollhattan (and elsewhere). I shall confine myself to just one thought; viz., that the earlier electrothermic metallurgists tried to combine zinc smelting and lead smelting in one furnace in one operation, although the metallurgical conditions are quite different. When in the earlier days it was tried to run off the gangue as an easy-running singulo-silicate, iron slag there was a great entry of zinc into it, just as there is in ordinary lead smelting. When the metallurgists at Trollhattan changed to a bisilicate, limy slag, the zinc kept out of it, but there were other complications introduced. Either way a large part of the consumption of electric energy was in fusing the slag. At Josephstown there is the first electrothermic, commercial practice, so far as I know, of treating a zinc ore just as a zinc ore in a retort and not trying to tap off slag, or matte, or pig lead. Consequently we should expect the use of energy at Josephstown to be less than in the other practice. Messrs. Weaton and Long figure 1365 kw-hr. as the furnace power per ton of concentrate of rather high grade. This is much lower than the furnace power at Trollhattan in 1921, when I had an association with Trollhattan Electrothermiska Aktiebolag, besides which there was in its process a substantial use of power for retreating blue powder and refining crude spelter.

* Consulting Engineer.

This brings us to the most interesting consideration of the Josephtown process; i.e., its economics. The over-all plant recovery of zinc in salable products is high, and compares favorably with what is realized in good practice with the other three processes for obtaining spelter. The use of energy is low and compares favorably with what is used in the electrolytic process of zinc extraction. The ratio of furnace power load to total plant load is about the same. The requirement for operating labor in the furnace plant, given as approximately 5.5 man-hours per ton of zinc produced, is surprisingly low, and likewise the figure of \$1.39 per ton of finished metal as the cost for refractories. The use of reducing coal is higher than in good practice in ordinary distilling. These comparisons are only suggestive, for obviously a good many essential data are missing, but they excite interest in the Josephtown process.

R. LEPSOE,* Trail, B. C.—Until about 15 years ago the mechanism of thermic zinc reduction was little understood. I believe it was Bodenstein⁶ who first proved that the reduction of zinc oxide by carbon essentially was the result of two consecutive reactions involving carbon monoxide as the carrier of reduction. Then came Maier's work on the reaction equilibria and finally the investigations by Dony-Henault⁷ on reduction kinetics.

It is evident, therefore, that the older, less successful attempts at electrothermic zinc reduction were handicapped on account of a too empirical conception of the chemistry of zinc smelting. The older methods used a slag bath, heated by electrodes. Incidentally, this method has one advantage in that complex ores could be treated for the simultaneous production of zinc, matte and lead bullion, but, on the other hand, it excluded the use of excess coke in the charge and the reduction was confined to narrow and highly heated zones around the electrodes. The ZnO-CO reaction was predominating and, owing to its reversion in the cooler parts of the system, copious quan-

tities of oxide and blue powder were formed. From an operating standpoint a cold condenser was better than the hot and, incidentally, the abrupt cooling of the zinc vapor resulted in less reoxidation. In this case, however, all the zinc was recovered as blue powder, necessitating a second treatment. As regards the efficiency of "shock" cooling, I have examples showing condenser exit gas containing 6 to 10 per cent CO₂ and only 5 per cent of the zinc in the blue powder oxidized.

The difference between the older and the Josephtown process is conspicuous. In the latter the furnace comprises an internally heated retort to which is charged a mixture of ZnO and an excess of about 350 per cent of coke. The rate of zinc reduction is obviously

$$d(\text{Zn})/dt = kX$$

where $X = (\text{CO}_2)_{\text{equi.}} - (\text{CO}_2)$

i.e., the rate is proportional to the departure from the state of equilibrium and dependent on k , which in turn depends on the length of the gas-diffusion path; hence, the more intimate the contact is between ZnO and C, the faster is the reaction. The rate of reaction also depends on the time of contact between C and CO₂ and between ZnO and CO. At Josephtown the time of contact between C and CO₂ is evidently $3\frac{1}{2}$ times greater than with the older electrothermic methods and in addition the temperature of the central coke core is several hundred degrees higher than the surrounding charge. It is thus probable that under these conditions the producer-gas reaction is the fastest reaction and that therefore the gas mixture leaving the Josephtown furnace contains very little CO₂. Even with an ordinary surface condenser there should thus be no difficulty in condensing the zinc from this gas.

The Josephtown condenser operates on the principle of a jet condenser; the formation of metallic mist is thus averted, with the result that only 1 per cent blue powder is formed, whereas if a surface condenser had been used the amount of blue powder might have been 8 per cent.⁸

According to the data submitted in the paper by Messrs. Weaton and Long, it appears that

⁸ Bunce and Handwerk: New Jersey Zinc Company Vertical Retort Process. *Trans. A.I.M.E.* (1936) 121, 439.

* Electrochemical Engineer, The Consolidated Mining and Smelting Company of Canada, Limited.

⁶ Bodenstein: The Mechanism of the Metallurgical Production of Zinc. *Trans. Amer. Electrochemical Soc.* (1927) 51, 365.

⁷ Dony-Henault: La Métallurgie Thermique du Zinc. Liège, 1938.

from a commercial standpoint also an electro-thermic zinc process has been successfully developed at last. Further application of this unique and interesting process will depend on its adaptability to the treatment of other types of ore than that being used at present.

G. F. WEATON AND C. C. LONG (authors' reply).—We shall discuss the various points raised in the order of their presentation.

The function of the preheater is to make use of a relatively inexpensive source of heat to bring the charge temperature up to a point where conductance of the coke is sufficient to carry the necessary electric power at a reasonable potential difference. Operating furnaces have, on occasion, been charged directly from the top with cold sinter and coke.

There appears to be little more to say regarding movement of gas and vapors through the charge. Probe measurements have indicated pressure heads of up to 0.4 in. of water in the most active portion of the central core. The gases simply pass through the interstices of the charge.

In practical operation, the only significant variable affecting the quantity of blue powder produced is the temperature of the metal bath in the condenser. At the now normal operating temperatures of 510° to 520°C., with 16-in. Hg vacuum, the production of blue powder amounts to approximately 1 per cent of the slab zinc produced. Such blue powder as is produced is returned to the furnaces after separation from the washer water and drying.

We do not wish to labor the point of what constitutes a successful or commercial process, as these terms are, of course, a matter of personal definition. We will merely note in passing that general metallurgical opinion, in so far as it has been expressed to us, is adequately

epitomized by the last paragraph of Mr. Lepsoe's discussion.

As the individual furnace units become larger, and as the output per unit increases, it is reasonable to expect a decrease in the power-product ratio. So far this year the ratio is about 2.5 per cent under the figure given in the paper. With the 96-in. diameter furnaces now in, or coming into production, the unit refractory costs will be much less than indicated in the paper.

Several of the new type of condensers with circular cross section mentioned in the paper have now been brought into production. The present day's production record (small furnace) is 18.6 tons of slab zinc. Another satisfactory development has been the incorporation of four single-phase circuits in the smaller (69-in. diameter) furnaces whereby a 16 to 17-ton daily production average is realized without excessive electrode consumption.

Mr. Lepsoe's conclusion that the producer-gas reaction is the faster of the two is interesting. A factor entering into this picture is the possible catalytic activity of the environment where firebrick, iron oxides, and even reduced iron are present. Several years ago during the earlier development of vapor ring and connecting box design, trouble was occasionally experienced with plug-ups due to oxide. This formation of oxide occurred in spite of infinite care and diligence in sealing possible atmospheric leaks. Increased temperature, secured by better insulation, minimized the trouble, presumably by decreasing the concentration of CO₂ in the reaction.



Gases from the Josephtown furnaces have been condensed in surface condensers. The advantages of the internal condenser, however, are quite obvious.

Adherence of Electrodeposited Zinc to Aluminum Cathodes

BY H. R. HANLEY* AND CHARLES Y. CLAYTON,† MEMBERS A.I.M.E.

(New York Meeting, February 1938)

ONE of the most important contributions to the art of electrolytic zinc production has been the aluminum cathode. This has been used in all major production since its commercial development in 1916. The literature is replete with important contributions, some of which may have been replaced by better ones, but thus far there appears no other metal to take the place of aluminum as cathode material. Credit for this innovation goes to Sherard Cowper Coles, of England. When experimenting on the extraction of zinc from Broken Hill ore at Hayle, Cornwall, in 1893, he introduced the aluminum cathode, and in 1895 obtained British Patent No. 20073.

The reason for this dominant position of aluminum as cathode material in zinc sulphate electrolytes is its unique surface, to which electrodeposited metals usually do not tightly adhere. The metal must be of high purity for best results.

It is possible to develop a starting-sheet method by which thin electrodeposited sheets of cathode zinc are made and stripped from a smooth aluminum plate. Such thin sheets of cathode zinc may be used as are the copper sheets in standard electrolytic copper-refinery practice. However, complications arise because of extreme warping of the zinc starting sheet after a few hours of deposition, and thus special arrangements must be made to compensate for this abnormality.

Reasons advanced for the ease with which deposits may be stripped from the aluminum surface are: (1) presence of a permanent oxide coating on the metal, (2) failure of aluminum to alloy with the deposit, (3) differences in coefficient of expansion, (4) high position of aluminum in the electromotive series of metals. Of these reasons for nonadherence, which may have some application in general deposition, probably the oxide coating has the greatest bearing on the subject of zinc deposition.

Adherence of zinc deposits has occasionally had serious effect on tonnage and production costs. Opinions have differed as to the specific

Manuscript received at the office of the Institute Jan. 14; revised May 18, 1938. Issued in METALS TECHNOLOGY, October 1938.

* Professor of Metallurgy, School of Mines and Metallurgy, University of Missouri, Rolla, Mo.

† Professor of Metallurgical Engineering and Ore Dressing, School of Mines and Metallurgy, University of Missouri.

cause of this adherence, but most of the ideas on this subject are associated with some degree of corrosion. Experimental work was undertaken by the authors, to confirm or establish several of the causes and to express this tendency to adhere in a relative, quantitative manner. This experimental work, which is the basis of this paper, was done during the years 1934 and 1935, but the actual writing of a report has been delayed until the present time.

An excellent account of adherence of deposits is given by Stimmel, Hannay and McBean,¹ which deals with the subject on a plant scale. Corrosion of the aluminum plate due to a small amount of hydrofluoric acid in the electrolyte was believed to be the chief cause of this adherence, although other causes of corrosion had a modified effect. Several methods were developed at this plant for control of the adherence; for example, application of a slurry of ground anode scale to the aluminum plates, and also a short immersion interval of the aluminum plates in the electrolyte before electrical contact was made.

When a new rolled aluminum plate is used as a cathode, there is generally a lack of adherence until sufficient roughness has been developed on the surface. When adherence does occur, usually it is after the aluminum plate has been in service for a period of time. Thus the subject of age is pertinent to this problem.

In order to measure quantitatively the effort required to pull zinc deposits from aluminum surfaces having various degrees of abnormality, the following method was used: The aluminum surface was covered with chlorinated rubber except for a strip $\frac{3}{8}$ in. wide by 2.8 in. long, which received the deposit. After deposition, one end of the deposit was loosened and the plate anchored face down in a horizontal position. The loose end of the deposit was clamped to a small receptacle into which test lead was poured until the load was sufficient to pull off the deposit. The weight of the receptacle plus the test load represents the stripping load. A similar method of detaching deposits is described by P. A. Jacquet² in his work on the adhesion of copper deposits.

It may be deduced that the complete loss of oxide from the aluminum cathode surface is not likely to occur in regular electrolytic zinc practice because of exposure to air and other oxidizing environment. Theodore Ledin³ and Harold K. Work⁴ have described high-metal dip solutions used to condition aluminum for reception of permanent electroplates. These effective dip solutions contain hydrochloric acid and iron, or hydrochloric acid and cadmium. When the aluminum plate is dipped into either of these solutions the acid dissolves the oxide coating and either the iron or the cadmium is plated securely to the aluminum by the immersion. The aluminum surface is thereby sealed from oxygen attack. Regular deposi-

¹ References are at the end of the paper.

tion thus is made on this strike. In customary zinc practice, the opposite conditions exist as previously noted, hence such cause of adherence must be at a minimum.

There are, however, at least two causes of adherence: viz., partial sealing off of the aluminum surface by impurities and etching of a roughened surface.

EFFECT OF IMPURITIES

Three aluminum plates $\frac{1}{8}$ in. thick, 3 in. wide, 4 in. long of varying degrees of hardness (60, 80 and 115 Rockwell B, no load) were used. Chlorinated rubber covered the surfaces except for a strip $\frac{3}{8}$ by 2.8 in., as previously noted. All plates were conditioned as follows: Cathodically cleaned 5 min. in caustic soda and sodium cyanide solution (15 grams per liter NaOH, 15 grams per liter NaCN), etched for 15 sec. in HF plus HCl solution (300 c.c. 52 per cent HF, 50 c.c. 39 per cent HCl, 300 c.c. distilled water) washed, steel-brushed in running water and immersed in water until the start of electrolysis.

The electrolytic deposition was standardized to 15 hr. operation at 35 amp. per sq. ft., temperature 30° C. The electrolyte contained 80 grams H_2SO_4 ; and 46 grams Zn per liter, as $ZnSO_4$, but no addition agents. Consistent checks in the stripping load for each of the various tempers of aluminum plates were not anticipated, but there was a fairly uniform trend in this load which decreased with increase in hardness of plate.

An aluminum plate that permits easy stripping of the deposit will show a load of 25 to 125 grams for the strip in question. Increases in this load, particularly large increases, demonstrate that the aluminum surface has become abnormal.

After the first conditioning, the average stripping loads were: 75 grams, 50 grams and 40 grams for the soft, medium, and full hard plates, respectively. Several check operations confirm these figures.

Following these series of experiments in commercially pure solution, copper sulphate was added to the electrolyte to give a concentration of 0.011 grams Cu per liter. With this addition, the stripping loads for the second cycle of electrolysis increased to the following average load in grams: 225; 120; 80. Several check operations gave slightly higher loads.

The aluminum plates were then exposed to a copper strike in a copper cyanide solution, 5 min. at 10 amp. per sq. ft., followed by the zinc deposition solution containing 0.011 grams per liter Cu. The average stripping loads were as follows, in grams: soft aluminum plates, 350; medium tempered plate, 350; full hard plate, 210.

A similar experiment was made substituting acid copper sulphate for the cyanide. The results were as follows, in grams: soft aluminum plate, 909; medium tempered plate, 1015; full hard plate, 620.

The stripped deposits contained all of the original copper strike, which was plainly visible on the zinc. The aluminum plates showed no copper by the H_2S test.

The influence of fine copper wire, attached to the aluminum plates just above the level of the electrolyte, was tested in the electrolysis of a commercially pure acid zinc sulphate solution. This "copper wire" test was planned to check observations made several years ago in an electrolytic zinc plant, the high-acid cells of which operated under unusual conditions. In these cells the zinc concentration was 14 grams per liter Zn, and the acid 125 grams per liter H_2SO_4 . The only exposed copper in the cathode assembly was two rivets. Directly below these rivets, extending down for about one-third of the immersed cathodes, there were corrosion areas on the aluminum plate to which the zinc deposits adhered tightly. There is a greater volume of spray from the surface of this solution, and the latter is more active chemically than the usual zinc sulphate electrolytes. Although copper is permissible above the electrolyte in some plants, there are conditions when it becomes adverse, and can cause adherence. The problem was solved by encasing the copper rivets with lead. This copper wire was exposed to the atomized electrolyte. The stripping loads for the second deposition under this condition was approximately the same as the previous high loads stated.

The aluminum surfaces were cleaned with a bristle brush in running water and retested in commercially pure zinc sulphate electrolyte. The average stripping loads under this condition were as follows (grams): soft aluminum plate, 125; medium aluminum plate, 107; full hard aluminum plate, 85.

The increased stripping loads in detaching the zinc deposits obtained by electrolysis of commercially pure solutions are caused by the slightly increased roughness of the aluminum surfaces developed by frequent stripping during the previous tests.

The influence of cadmium on stripping loads was next investigated. A 5-min. cadmium strike deposit was applied in an acid cadmium sulphate solution followed by the usual zinc deposition. The stripping loads were not as great as in the copper strike. However, they were much greater than the loads required to detach zinc deposits obtained from commercially pure solution. Examples of the influence of cadmium show the following stripping loads: soft aluminum plate, 130 grams, 267 grams, 445 and 410; medium tempered aluminum plate, 140 grams, 167 grams, 372 and 155; full hard tempered aluminum plate, 90 grams, 50 grams, 197 and 140.

In nearly all cases the aluminum plates after stripping showed the presence of cadmium by the H_2S test.

The aluminum plates were tested in regular acid zinc electrolyte to which 0.05 gram Cd per liter had been added, but without the cadmium

strike. The average stripping loads were as follows for the second cycle of electrolysis (grams): soft aluminum plate, 250 and 350; medium tempered aluminum plate, 155 and 275; full hard tempered aluminum plate, 140 and 190.

The aluminum plates were then cleaned from all adhering cadmium by immersing in sulphuric acid solution, 70 grams per liter H_2SO_4 , bristle-brushed in running water and again tested in commercially pure acid zinc electrolyte. The average stripping loads were as follows (grams): soft aluminum plate, 142; medium tempered aluminum plate, 125; full hard tempered aluminum plate, 112.

Although the influence of cadmium does not appear decidedly adverse, it does cause irregular and greater stripping loads than occur with the commercially pure solution.

The presence of copper and cadmium in conventional electrolytic operation is so minute that the cause of adherence cannot be ascribed to these metals. Under abnormal conditions, which cause the resolution of the zinc, the aluminum cathode may become etched, and ultimately the surface may develop adherence.

Silver and mercury-strike coats on aluminum plates, followed by regular zinc deposition, also cause adherence. These metals are irrelevant to the subject because they are not present in the solution. However, it appears that some metals, other than copper and cadmium, adversely affect stripping.

ADHERENCE OF DEPOSITS CAUSED BY ETCHING OF ALUMINUM PLATE

The surfaces of the plates were conditioned as follows: Cathodically cleaned in caustic soda and sodium cyanide solution (15 grams per liter NaOH , 15 NaCN), etched 15 sec. in HF plus HCl solution (300 c.c. 52 per cent HF , 50 c.c. 39 per cent HCl , 300 c.c. distilled water), washed, steel-brushed in running water and kept immersed in water until the start of the etching and electrolysis. The plating conditions were the same as stated before. Four new aluminum plates were used for each etching test. The following etching reagents were used: caustic soda (75 NaOH per liter), ammonium zinc cyanide (ZnO , 22.5 grams per liter, NaCN , 37.5; NH_4OH , 33.0; sp. gr., 0.90), zinc-sulphuric acid solution (100 grams per liter H_2SO_4 , 30 Zn).

Table 1 shows the average stripping load per plate for various etchings. Aluminum plates No. 2SH; 113 Rockwell hardness; room temperature; four new plates used for each test. Before etching, the average stripping loads were approximately 10 grams, 30 grams, 12 and 60 grams.

Progressive etching of the plates used in tests IX and X finally produced surfaces from which the deposits could hardly be removed. This procedure is equivalent to the etching of an "old" plate.

A special etching solution of HF and HCl was prepared as follows: 300 c.c. of 52 per cent HF, 50 c.c. of 39 per cent HCl, 300 c.c. of water. Two new No. 2SO aluminum plates, conditioned as previously stated, were dipped into this special etching solution for two minutes, washed and bristle-brushed in running water. The average stripping loads detaching the deposit of zinc were irregular, amounting to 225 and 125. Two more complete etching and plating operations in this solution were applied to these plates, resulting in a stripping load of practically zero.

TABLE 1.—Average Stripping Load per Plate

Test No.	Etchant	Time of Etching	Average Stripping Loads after Etching, Grams			
I	NaOH	20 min.	12	35	10	75
II	NaOH	3 hr.	630	950	985	1100
III	Ammonium cyanide	4.5 hr.	935	700	825	1000
IV	Acid zinc sulphate	9 hr.	842	710	810	690
V	Acid zinc sulphate	11 hr.	800	830	720	750
VI	Acid zinc sulphate	11 hr.	990	970	1120	1025
VII	Acid zinc sulphate	11 hr.	1100	1200	1150	1250
VIII	Acid zinc sulphate	11 hr.	1050	1100	1250	1270
IX	Acid zinc sulphate ^a		1300	1350	1325	1400
X	Acid zinc sulphate ^b		1400	1450	1500	1450

^a Represents plates used in test VIII etched 3 hr. longer.

^b Represents plates used in test IX etched 3 hr. longer.

A vigorous etching does not appear to be as effective as a prolonged mild attack on the aluminum plate.

A straight sulphuric acid etching of an aluminum plate without previous roughening of the surface does not produce adherence of the deposit. The adherence of deposits to the plates is most favored by a slow etching of the *roughened surface*. A small amount of hydrofluoric acid in the acid zinc sulphate electrolyte is particularly harmful.

After a plate has reached the stage when the adherence of deposits has reached a maximum, there are myriads of angular pits, ridges, sharp longitudinal troughs and similar abnormality of texture upon which the deposit can more effectively secure definite anchorage. This abnormality is experienced occasionally in practice when old aluminum plates are exposed for a long time to the action of acid electrolyte. Short periods of deposition at moderately high current density and high current efficiency are favorable factors in nonadherence of the zinc deposit to the aluminum plate.

It was found that the aluminum plates that had developed great adherence would lose most of this adherence if the surface was polished with steel wool. The wool apparently cuts down the aluminum surface and minimizes or removes the angular pits, channels, etc., and gives to

the surface a mirrorlike texture. The steel-wool fibers that were broken during this polishing were removed from the plate. It was found, also, that if the abnormal aluminum surfaces were rubbed with fine carborundum powder the surfaces were greatly altered and deposits made upon these new surfaces had much greater adherence than before. Examples of these features are given in Table 2.

TABLE 2.—*Adherence after Treatment*

Plate No.*	Stripping Load, Grams	Polished with Steel Wool. New Deposit Stripping Load, Grams	Rubbed with Fine Car- borundum. New De- posit Stripping Load, Grams
1	800	265	
2	830	50	
3	720		1140
4	750		1125

* Aluminum plates made adherent by etching (No. 2SH).

Examples of this nature show that if an impurity on the plate is of such character that it will be retained by the plate after the latter has been rubbed, the normal aluminum surface becomes altered, and the stripping characteristics then are influenced by a new surface developed by this impurity.

A variation in the method of conditioning the plates will occasion a variation in stripping load, and frequently a wide variation in results. For example, if a plate is reasonably normal as to texture, the stripping load will be less if the plate is thoroughly dried before being placed in contact with the electrolyte in the cell. There is a pronounced indication that high current density is favorable to nonadherence.

SUMMARY

Although some impurities in the solution, which are plated with the zinc, may increase the stripping load for the removal of deposits, this feature is not regarded as pertinent to the subject of adherence because the purification system will prevent the presence of these toxic substances.

Impurities in solution that promote resolution of the deposited zinc in the acid electrolyte, as well as abnormal etching of the aluminum cathode, maybe the starting point of adverse roughening of the aluminum plate. This roughened surface becomes more etched and hastens the time when the zinc deposit starts to adhere more tightly. The exposure of an old (and usually roughened) aluminum plate to the attack of acid, aided by the absence of zinc, definitely etches it. The partial cathodic zinc protection of the aluminum plate is not sufficient to prevent the development of the adverse surface. The aluminum plates that are hardest develop adverse surfaces at a slower rate.

Mild etching of a smooth aluminum plate does not produce great adherence of deposits. Steel brushing or scratching alone produces a similar effect. Etching of a steel-brushed plate, or etching of a roughened plate caused by prolonged use as a cathode, develops a surface to which zinc deposits will tightly adhere.

Numerous photomicrographs of the aluminum surfaces and cross sections, showing the basic metal and deposit, were made. These show the expected order of the work, do not add to the written description, and therefore have been omitted from the paper.

REFERENCES

1. B. A. Stimmel, W. H. Hannay and K. D. McBean: Electrolytic Zinc Plant of the Consolidated Mining and Smelting Company of Canada, Limited. *Trans. A.I.M.E.* (1936) **121**, 540.
2. P. A. Jacquet: Adhesion of Electrolytic Copper Deposits. *Trans. Electrochem. Soc.* (1934) **66**, 393.
3. T. Ledin: *Metal Ind.* (New York) (1922) **20**, 351.
4. H. K. Work: *Trans. Electrochem. Soc.* (1928) **53**, 361.

An Investigation into Anode-furnace Refining of High-nickel Blister Copper

BY FREDERIC BENARD,* MEMBER A.I.M.E.

(New York Meeting, February 1938)

THIS paper constitutes a preliminary report on experimental work done to date on the anode-furnace treatment of blister copper containing relatively high percentages of nickel. The investigation has not been completed but results obtained to date are considered of sufficient interest to warrant publication.

Blister copper treated by the Ontario Refining Co. originates from the Copper Cliff smelter of The International Nickel Company of Canada, of which the former is a wholly-owned subsidiary. The blister as received contains from 0.50 to 1.50 per cent Ni, and in this respect differs from that treated by other refineries on this continent. During the anode-furnace treatment, only a portion of the nickel content is removed, and of the amount remaining in the anodes a varying percentage is found in the anode slimes. This necessitates a more extensive treatment than ordinary nickel-free material. Sometimes it is necessary to repeat roasting and leaching operations several times before the nickel content is low enough to permit the slimes to proceed to the doré furnace. This, besides increasing treatment charges, causes greater selenium stack losses and involves a longer tie-up of precious-metal values. Therefore this investigation was undertaken with the aim of determining the factors influencing the diversion of nickel into the anode sludge.

From experience it was known that by keeping the nickel content of anodes at 0.55 to 0.60 per cent maximum a relatively satisfactory slime resulted. One avenue of attack therefore was developing improved elimination in the anode-furnace treatment so that the anode content mentioned above was not exceeded. Another angle was to improve the solubility, during electrolysis, of the nickel constituent in the anodes, thus decreasing the percentage diverted to slimes. It may be mentioned here that nickel dissolving electrochemically and entering the electrolyte presents no difficulty from a treatment standpoint.

Both of these approaches were studied and are discussed separately below.

Manuscript received at the office of the Institute Dec. 18, 1937. Issued in METALS TECHNOLOGY, February 1938.

* Plant Manager, Ontario Refining Co., Ltd., Copper Cliff, Ont.

ELIMINATION OF NICKEL IN THE ANODE FURNACE

Fire-refining methods, as far as is known, have not been successful in eliminating more than small quantities of nickel from copper. Schnabel¹ mentions cases of fairly complete elimination in the slag formed by repeated oxidation and reduction of the bath. Stahl² has proposed the addition of iron scale to the bath, resulting in the formation of nickel ferrite, which is slagged off. Such procedures are not practical even if capable of accomplishment.

Although possessing similar values for heats of formation of their respective oxides, nickel and iron are entirely unlike in regard to their formation of slags. This leads to a belief that in ordinary furnace refining a nickel-oxygen compound is formed, which is soluble in copper and therefore does not rise to the surface and enter the slag. Observations made in the work described below all tended to confirm this view.

Two types of blister are received by the refinery; one obtained from converter treatment of copper sulphide separated from nickel by the Orford process, the other resulting from the treatment of a high-grade copper concentrate. The former is designated locally as O.P. copper, the latter as N.P. (New Process).

As described elsewhere,³ all copper is now transferred from the smelter converter department to the refinery anode furnaces in the molten state. O.P. copper carries from 0.65 to 1.50 per cent Ni, and N.P. from 0.50 to 1.00 per cent. In general, the converter treatment provides the desired oxygen content of 0.90 per cent and further flapping is unnecessary except to blow down the slag. The latter is skimmed off, the bath is covered with coke and poled to a flat set. This results in the elimination of virtually all sulphur and from 15 to 20 per cent of the nickel. A series of experiments was first carried out to determine whether the percentage of nickel slagged off could be increased by continuing oxidation up to the point of 1.00 per cent oxygen. Only a small increase in slag quantity resulted, and the actual improvement in nickel removed was too slight to be of economic benefit.

Further trials were made over a considerable period, during which the bath of anode copper was saturated with cuprous oxide at a temperature of about 2300° F. and then allowed to cool to approximately 2100° F. This drop in temperature caused a precipitation of molten cuprous oxide, which carried with it 10 to 15 per cent of the total nickel present. This quantity again was not great enough to warrant spending the additional time required to carry out the procedure.

Prior to and during all experimental work on nickel elimination, careful records had been accumulated on the behavior of various lots of anodes during electrolysis. In tabulating these data, two general observations became apparent: (1) the proportion of the anode nickel content

¹ References are at the end of the paper.

diverted to slimes increased sharply with rising percentages of nickel in anodes; (2) although this was true for the great majority of cases, there were frequent isolated exceptions. The general relationship between nickel in anodes and slimes produced is shown in Table 1.

TABLE 1.—*Nickel in Anodes and Slimes*

Production No.	Nickel, Per Cent		Per Cent of Total Nickel in Slimes	Pounds Nickel in Slimes per Ton Corroded Metal
	In Anodes	In Slimes		
187	0.46	3.2	2.6	0.24
199	0.56	15.7	8.3	0.93
367	0.62	22.6	11.3	1.39
160	0.77	31.2	21.7	3.34

The exceptions referred to indicated some variable which under certain conditions greatly improved the electrolytic solution of the nickel constituent. This appeared worthy of investigation and as tank-house operating conditions are very uniform it was logical to look first for compositional variations in the anodes themselves. Spectroscopic, microscopic and chemical analyses were made, which revealed little or no segregation of metallic constituents but offered a lead from the standpoint of oxygen content.

The next step was to prepare small experimental anodes from regular furnace productions with the further step of chemical deoxidation. The anodes so produced were corroded under conditions identical with those obtaining in regular practice and the slimes resulting were examined for nickel. The results are shown in Table 2.

TABLE 2.—*Deoxidized Anodes*

Lot No.	Nickel, Per Cent		Per Cent of Total Nickel in Slimes	Deoxidant
	In Anodes	In Slimes		
1	0.46	0.38	0.50	Phosphorus
2	0.80	1.07	0.60	Phosphorus
3	0.48	2.22	1.80	Silicon

The exceptionally low nickel content of the slimes tended to confirm the theory that this was related to the oxygen content of the anode. Small amounts of residual deoxidant were found in the slimes but there was no evidence that the increased solubility of nickel was due to formation of compounds with the former. At this time a series of oxygen determinations was made on regular anode productions cast from charges poled to the normal flat set as indicated by the block sample taken before casting. The oxygen was determined on drillings by igniting in hydrogen and applying corrections for sulphur, selenium and tellurium. Slight

errors may have been introduced but the accuracy was satisfactory for the purpose involved. The results showed that the oxygen content of regularly cast anodes varied between 0.10 and 0.30 per cent.

The cause for such wide variation in the oxygen of anodes all poled to a standard "set" is unknown at this time but is thought to be due to the variable effects of poling produced by the impurities in the charge.

Several experiments were next made to examine the effect of varying oxygen content in full-sized anodes in regular tank-house operation, the range covered being 0.04 to 0.26 per cent. Unfortunately, it was not feasible at this time to secure a constant percentage of nickel but in general the observed trend was supported. The lower range oxygens were secured by carrying the poling operation past the flat-set stage to a high or medium crown set, as indicated by the control-block sample. Anodes from these charges were afforded additional protection in that the launder and ladle were well covered with charcoal.

Poling the charge to a medium crown set did not appreciably affect the set on the anodes. However, when poling was prolonged to the point of a high crown set, it was observed that high set areas from 2 to 6 in. in diameter occurred in the anodes toward the last of the casting period.

The high range oxygens were produced either by blowing air on the launder stream or casting before the normal poling operation was completed.

Full tanks of the various anodes so produced were charged to the tank house, the slimes collected separately for weight and analysis. The results are summarized in Table 3.

TABLE 3.—*Effects of Oxygen and Poling on Anode Nickel Entering Slimes*

Production No.	Treatment	Anode Nickel, Per Cent	Anode Oxygen, Per Cent	Slimes, Lb. per Ton Corroded Anode	Slimes Nickel, Per Cent	Per Cent of Total Nickel in Slimes	Slimes, Lb. of Nickel per Ton Corroded Anode
288-2	Air on launder	0.71	0.23	10.4	30.0	22.0	3.12
288-1	Poled to flat set	0.68	0.14	8.7	20.7	13.3	1.81
158-1	Poled to low set	0.54	0.26	8.9	18.3	15.1	1.62
158-2	Poled to medium crown set	0.55	0.04	7.6	7.2	5.0	0.55
298	Poled to high crown set	0.61	0.06	12.0	2.6	2.6	0.31
203	Poled to medium crown set	0.65	0.07	8.3	10.2	6.4	0.84

CONCLUSION

After operation for several months on low-oxygen anodes, experimental results have been satisfactorily confirmed. In addition to the

effect on slimes composition, the amount of copper chemically dissolved in the tank house has been reduced to a point where inside liberator tanks are no longer required, and in general the uniformity of corrosion has been materially improved.

While it is felt that the data are insufficient to permit an exact explanation at this time, it would appear that the oxygen content of high-nickel copper anodes has an important bearing on subsequent behavior during electrolysis with particular reference to slimes composition and electrolytic solution. It is along this line that the investigation is being continued.

ACKNOWLEDGMENT

Acknowledgment is made to the members of the staff that aided in the preparation of this paper.

REFERENCES

1. Schnabel: Handbook of Metallurgy, Ed. 3, 1, 275. Translated by Henry Louis.
2. W. Stahl: Slagging of Nickel in Copper Refining with Formation of Ferrites. Translated from *Metal und Erz* (1931) No. 3.
3. F. Benard: Transportation of Molten Blister Copper by Rail from Smelter to Refinery. A.I.M.E. *Tech. Pub.* 909 (1938).

Recovery of Selenium and Tellurium at Copper Cliff, Ontario

By FREDERIC BENARD,* MEMBER A.I.M.E.

(New York Meeting, February 1938)

RECOVERY of selenium and tellurium at Copper Cliff by the Ontario Refining Co. has been previously described by the writer.¹ During 1935 a new building was erected to house this operation and description of the new plant and process form the subject of this paper.

The building, of modern steel and tile construction, covers an area of 5900 sq. ft. with a volume of approximately 165,000 cu. ft. The large monitored center bay is flanked by two smaller outside bays, one of which is devoted to the tellurium section. All equipment, ceilings and upper walls, are treated with aluminum paint, giving good illumination and facilitating good housekeeping, essential from a health standpoint in handling material of this nature.

EQUIPMENT

Layout and type of equipment conforms to the requirements of the process as described below. In the selenium section, storage tanks, neutralizing tanks and precipitators are of steel construction, lead-lined and arranged for gravity flow (Fig. 1). The neutralizing tanks are equipped with water-cooled lead coils for controlling solution temperature, agitation being accomplished with compressed air. The precipitators are provided with mechanical agitators, and sulphur dioxide is introduced into the solution through $\frac{1}{2}$ -in. lead pipes leading from a manifold attached to the cover of the precipitator. Each precipitator has internal cooling coils and an air-jet exhaustor to carry off fumes. Neutralized solutions are filtered in a 29-plate wooden filter press using heavy cotton duck as a filter medium, forced feed being maintained by a Welmet centrifugal pump. Dilute solutions are concentrated by evaporation in a vacuum evaporator, constructed of cast hard lead. Heat is supplied by an outside steam chest operating under 15 lb. steam pressure. The solution is circulated through the steam chest by a pump of antimonial lead at a rate approximating 400 cu. ft. per min. The evaporator is evacuated by a water-jet condenser that creates a vacuum of 26 in. of mercury under normal operating conditions. The capacity of the vessel is 60 cu. ft. and the rate of evaporation 25 cu. ft. per hour.

Manuscript received at the office of the Institute Dec. 23, 1937. Issued in METALS TECHNOLOGY, February 1938.

* Plant Manager, Ontario Refining Co., Ltd., Copper Cliff, Ont.

¹ *Trans. A.I.M.E.* (1933) **106**, 391.

The grinding room (Fig. 2) is equipped with a 16-in. rod mill, 5 ft. long, charged with casehardened steel rods. The mill is fed by a mechanical screw feeder and discharges into a 27-in. supported centrifuge provided for the purpose of washing and dewatering. Final drying is carried out in two steam-heated drying cabinets at 180° to 190° F.

In the screening room, two motor-driven Rotex screens are used for screening the final product through 200-mesh phosphor-bronze wire cloth. Each screen is equipped with a variable-speed mechanical feeder and handles approximately 50 lb. per hour. Steel boxes are provided for storing the final product.



FIG. 1.—SELENIUM SECTION.

Equipment used in the recovery of tellurium (Fig. 3) includes four rectangular V-bottomed steel tanks for leaching and purifying. Filtration is effected by a four-leaf suction filter acting under 20 in. of vacuum supplied by a Hytor vacuum pump. In addition, two suction-box filters are provided for handling precipitated oxide. Drying is accomplished in an insulated, steel drying cabinet heated with low-pressure steam.

In the reduction of oxide to metallic tellurium an oil-fired tilting crucible furnace is used, fumes being thoroughly taken care of by an exhaust fan of ample capacity. Pulverizing and mechanical screening equipment sizes the product to market requirements.

PLANT FEED

All feed to the combined sections is received in the form of solutions derived from treatment of the various by-products of silver-refinery

processes in which selenium and tellurium are concentrated (Fig. 4). The principal sources of these solutions are described briefly as follows:

Niter Slag.—The selenium content of slimes and sludges composing a doré charge is partly recovered in niter slag during the refining period. Water-leaching of this material yields a basic solution containing selenium and tellurium as selenites and tellurites.

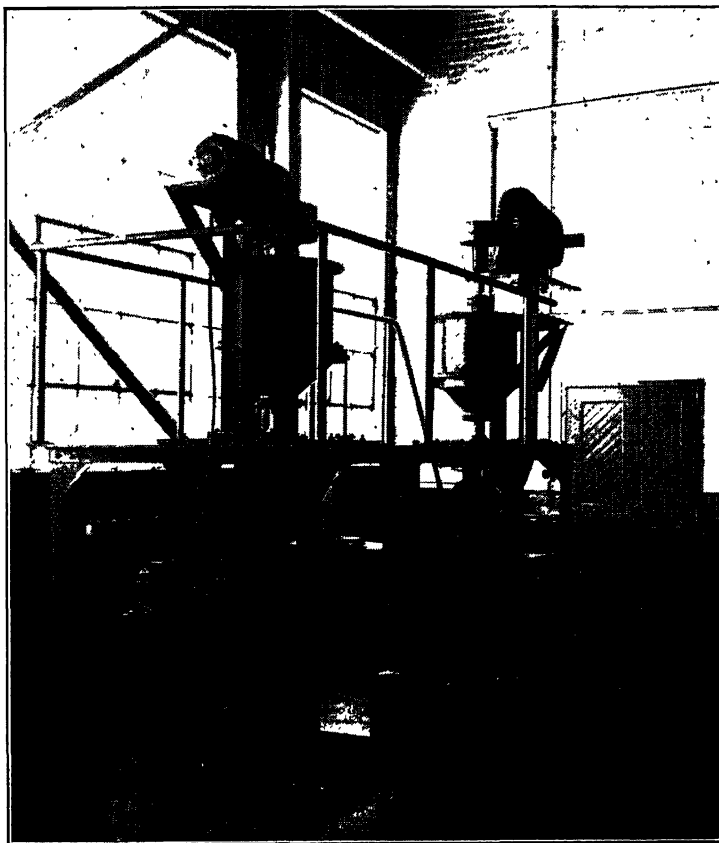


FIG. 2.—GRINDING ROOM.

Selenium Whiskers.—Each furnace operation unavoidably volatilizes an appreciable quantity of selenium. Part of this is oxidized to selenium dioxide which, on cooling, crystallizes in chambers provided in the flue system for this purpose. A mat of needlelike crystals is formed, containing roughly 55 per cent selenium, which is readily soluble in water, forming selenious acid.

Scrubber and Cottrell Solutions.—The silver-refinery flue gases are treated in a water-spray scrubber and a wet Cottrell for the recovery of

valuable constituents. Soluble selenium and tellurium entering this system are recovered in solutions, which are filter-pressed and pumped directly to the selenium plant. Assays of Cottrell solutions average 33.8 grams per liter Se and 2.4 grams per liter Te, and scrubber solution 21.8 grams per liter Se, and 1.0 grams per liter Te.

Cementation Slimes.—Leach liquors from the slimes-leaching treatment are freed of selenium and tellurium by cementation with copper sludge. This process concentrates tellurium in the cementation slimes, which, from time to time, may be profitably submitted to special treat-



FIG. 3.—EQUIPMENT FOR RECOVERY OF TELLURIUM.

ment for quick extraction of tellurium. Oxidation of the cementation slimes by roasting with caustic soda renders the tellurium soluble as sodium tellurite. The roasted product is extracted with water leaches and the liquor pumped to the selenium plant.

SELENIUM PROCESS

The selenium process consists of removing base metals and tellurium from the feed solutions by neutralizing and filter-pressing the neutral solution. The resultant press sludge comprises the feed to the tellurium plant, while the effluent liquor is charged in batches to precipitators. After being made up to 12 per cent H_2SO_4 by volume, it is gassed with sulphur dioxide to precipitate selenium. The granular product is water-washed free of acid, pulverized in a rod mill, dried, screened through 200 mesh and blended to market specifications.

Incoming feed solutions from the silver refinery are received in the storage tanks and held until sufficient quantity is on hand to make up a batch. At the start of a batch, solutions from the storage tanks are run into one of the neutralizing tanks, acid and basic solutions being blended in this operation to approximate neutrality. The solution is then sam-

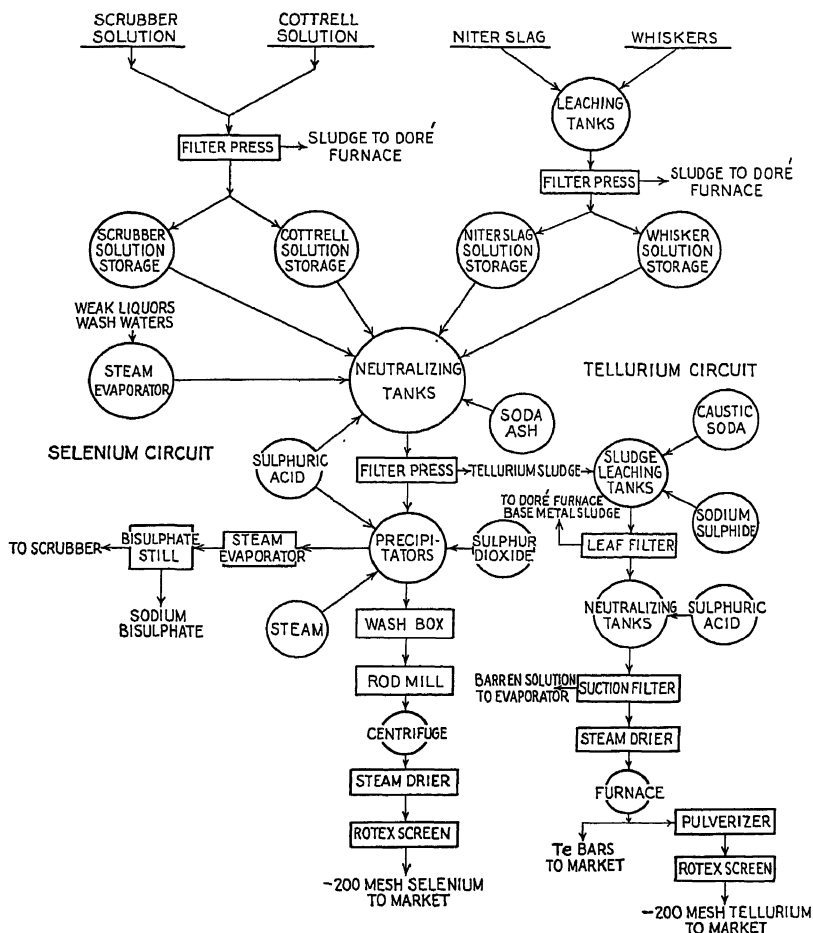


FIG. 4.—FLOWSHEET OF SELENIUM AND TELLURIUM PLANTS.

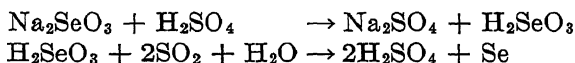
pled and a rough determination of the selenium content is made. The desired concentration of selenium is 120 to 140 grams per liter, since any tellurium and base metals not completely removed by neutralization will appear in reduced percentages in the final product if the selenium content of each batch is high. Solutions containing less than 120 grams per liter Se are filter-pressed and concentrated in the evaporator to the required strength and then returned to the neutralizing tank.

Since the purity of the final product depends principally on the removal of impurities by neutralization, this operation is carried out with care. The solution is first made distinctly acid to litmus by adding sulphuric acid, and then brought back to the neutral point by mixing in soda ash solution until the batch solution shows no effect on red and blue litmus. This ensures precipitation of the base metals, particularly lead and copper as carbonates.

After thorough agitation, a sample of the solution is filtered and divided into two portions. One drop of dilute sulphuric acid is added to one portion and one drop of dilute soda solution to the other portion. If both solutions remain clear, this test indicates that tellurium has been removed as far as possible and the neutralization is considered complete. This control test is necessitated by the fact that tellurium is soluble on either side of the neutral point and is regarded as conclusive. Other methods of testing, based on hydrogen-ion reaction with colorimetric indicators, have been tried but failed because of oxidation of the indicator dyes by selenious acid.

The neutralized solution is filter-pressed into a storage tank, from which it is charged to the precipitators in 60-cu. ft. batches. A typical analysis of the solution after filter-pressing is 125 grams per liter Se and 0.75 grams per liter Te. The filter-press cake, containing the base-metal impurities and tellurium, is water-washed and sent to the tellurium plant.

In the precipitators, selenious acid and sodium selenite are reduced to metallic selenium by the action of sulphur dioxide gas in acid solution, according to the following reactions:



Selenium present in the higher state of oxidation as selenic acid or sodium selenate is not precipitated by sulphur dioxide in sulphuric acid but may be reduced in hydrochloric acid solutions. The small quantity of selenate present in the solutions treated does not warrant the installation of the necessary equipment for handling strong hydrochloric acid.

The batch in the precipitator is made up to 12 per cent H_2SO_4 by running in the required amount of commercial acid. The heat generated by the reaction is carried away by circulating water through the cooling coils. When the temperature of the solution has been reduced to 90° F., slow gassing is started and maintained for about six hours. At this stage the solution appears bright red, because of the precipitation of amorphous selenium. The gas flow is then increased and the solution heated to 180° F. by introduction of live steam.* After approximately 20-hr.

* Canadian Patent No. 303480.

treatment under these conditions the amorphous precipitate has been converted by the heat to gray crystalline selenium, which settles to the bottom of the precipitator. The reaction is considered complete when a filtered sample shows only a faint pink shade on heating and gassing with sulphur dioxide.

Precipitation of selenium is not complete at this point, 5 to 7 grams per liter Se remaining in solution, but additional gassing tends to precipitate tellurium. A typical assay of the spent solution shows 5 grams per liter Se, 0.4 grams per liter Te, and 380 grams per liter H_2SO_4 . Fig. 5 shows the rate of precipitation of the selenium during the gassing cycle.

The contents of the precipitator are agitated for 2 to 3 hr. after completion of the gassing, then allowed to settle. The spent solution is siphoned off and the precipitated selenium washed with one 5 per cent acid wash followed by three hot-water washes. The spent solution is pumped to the silver refinery, evaporated to 50° Bé and charged to a cast-iron still, where the selenium and acid are driven off and recovered in the scrubber and Cottrell system. The molten residual sodium bisulphate is cast into slabs and sent to the smelter. Wash waters are used in the slimes-leaching process in the silver refinery.

The washed selenium is dumped from the precipitator into a suction filter box, where washing is continued with hot, filtered steam condensate until the effluent wash water tests free of acid. A few pounds of soda ash is then mixed with the selenium to ensure neutralization of any occluded acid freed by grinding and the mixture is charged to the rod mill at a rate of 150 lb. per hour. Fines are washed out of the mill by a stream of water into the centrifuge, where the ground product is water-washed until free of soda ash. After this final washing the selenium is shoveled into enamelware pans and dried in the drying cabinets for 24 hours.

The dried selenium, which now appears as a black amorphous powder, is screened through 200 mesh and the oversize is returned to the mill. Undersize material is carefully sampled and stored in steel boxes until the assay is received. A typical assay of the finished product is: Se, 99.70 per cent; Te, 0.12; ash, 0.13; Cu, 0.001; Fe, 0.01.

Selenium is shipped to the market in 8-gal. kegs holding 100 lb., and 20-gal. kegs holding 300 lb. A small quantity is supplied to consumers in 10-lb. tins.

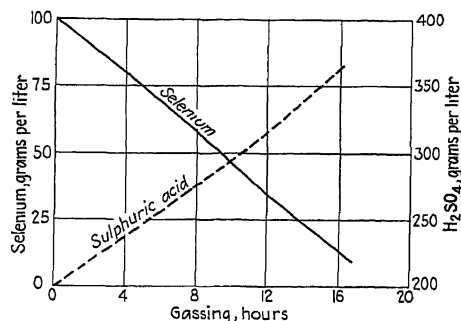


FIG. 5.—RATE OF PRECIPITATION OF SELENIUM DURING GASSING CYCLE.

TELLURIUM PROCESS

The crude tellurium sludge from the selenium process is charged in lots of 2000 lb. to a dissolving tank. About 100 cu. ft. of cold water is added and the mixture agitated with an air jet to ensure suspension. Flake caustic soda is added in small increments with continuous agitation, until the color of the suspended solids changes from gray to dark brown. This darkening of the mixture is caused by the dissolving of the light colored tellurium oxide, which leaves dark base-metal hydroxides in suspension.

The sludge of base-metal hydroxides is filtered out of the liquor on the leaf filter and the clear filtrate, containing tellurium as sodium tellurite, is discharged into a neutralizing tank. The base-metal sludge is returned to a dissolving tank where it is again leached with strong caustic to remove any tellurium residue. The sludge is again filtered out and returned to the silver refinery doré furnace. The filtrate from this second leach is used in the make-up of subsequent batches.

In the neutralizing tank, the filtered caustic liquor is neutralized by addition of dilute sulphuric acid. This operation precipitates tellurium oxide, leaving selenium in solution. Lead sulphate and some silica are also precipitated. After settling, the barren solution is decanted and sent to the selenium plant, where it is evaporated and the selenium recovered. The precipitated oxide is given four water washes by decantation and then redissolved in caustic solution.

In redissolving the oxide, care is taken to avoid a large excess of caustic soda. This precaution leaves the silica undissolved, tellurium and lead entering the solution. Sodium sulphide solution is cautiously added, to avoid excess, and precipitates lead as lead sulphide. Any excess of sulphide in solution precipitates a mixture of tellurium and sulphur.

The lead-free caustic solution is filtered through a suction box into the second neutralizing tank, where it is heated to 180° F. and again neutralized with dilute sulphuric acid. This precipitates substantially pure oxide, which is thoroughly water-washed by decantation, dewatered in a suction box and placed in enamelware pans in the drying cabinet. The dry oxide is rolled to a powder, mixed and sampled. A typical assay of this product is: Te, 77 per cent; Se, 0.03; Pb, nil; SiO₂, 0.02.

Tellurium oxide is reduced to the metal by mixing with flour and borax and heating in a covered crucible in the tilting furnace. The usual charge consists of 110 lb. of tellurium oxide, 24 lb. of grain flour, and 13 lb. of borax. The oxide, flour and 10 lb. of borax are thoroughly mixed by rolling and then charged to the crucible. The additional 3 lb. of borax is spread over the top of the charge as a cover.

As heating of the charge progresses, reduction of the metal begins at a comparatively low temperature and is complete at a dull red heat. Dur-

ing the reduction, white fumes of oxide are continually given off. When reduction is complete, the molten bath of metal is entirely covered by the borax slag and the fuming ceases. When this point is reached, the melt is cast into an iron mold. In casting the melt, some slag is first poured into the mold, to protect the latter from the action of the hot metallic tellurium, which readily combines with iron. During casting, dense fumes are evolved, necessitating the use of a gas mask by the operator.

When cool, the bar is dumped out of the mold and adhering slag is chipped off. The metal is sampled by making four saw cuts in the bar. Each melt yields about 80 lb. of metal, which assays as follows: Te, 99.75 per cent; Se, 0.04; Pb, trace.

Tellurium is shipped to the market as bars, lump metal and pulverized metal. Bars and lump metal are shipped in boxes. When pulverized tellurium is required, the metal is ground in the Mikro pulverizer, screened to specifications, and shipped in kegs holding 200 pounds.

ACKNOWLEDGMENT

The writer wishes to express his thanks for assistance rendered in the preparation of this paper by R. H. Waddington, assistant plant manager, and H. A. MacDougall, in charge of technical control, Ontario Refining Co., Copper Cliff, Ontario.

DISCUSSION

(See page 372.)

Recovery of Precious Metals and Production of Selenium and Tellurium at Montreal East

By C. W. CLARK* AND J. H. SCHLOEN,† MEMBERS A.I.M.E.

(New York Meeting, February 1938)

Two papers have been written previously concerning operations at the Montreal East plant of Canadian Copper Refiners Limited. The first one,¹ written in 1932, described silver-refinery operations at the time for producing silver and gold bullion from tankhouse anode slimes; the second,² published in 1933, consisted of a description of the entire plant. Since publication of these papers the refinery has become the world's largest producer of refined selenium. The first selenium was produced in August 1934. Tellurium production on a commercial scale followed in October 1935. This paper will deal with selenium and tellurium production and also with present operations in the silver refinery.

Blister cakes from Hudson Bay Mining and Smelting Co., Flin Flon, Manitoba, and commercial anodes from Noranda Mines Limited, Noranda, Quebec, are refined at Montreal East. Both these bullions have unusually high gold, selenium and tellurium content. The average assay of raw slimes produced from domestic and Noranda anodes is about 40 per cent Cu, 3600 oz. per ton Ag, 800 oz. per ton Au, 22 per cent Se and 3.7 per cent Te.

EARLY SILVER-REFINERY OPERATIONS

From the start of operations in 1931 until July 1934, the raw slimes were oxidize-roasted at 700° F. in a Nichols-Herreshoff furnace, acid-leached with tankhouse discarded foul electrolyte (20 per cent H₂SO₄), filtered and charged directly to the doré furnace for refining to doré metal.

This is the customary method for treating tankhouse anode slimes but was not suitable at the Montreal East plant because of the high selenium and tellurium content of our slimes.

In the acid-leaching process about 50 per cent of the selenium and tellurium in the roasted slimes was dissolved in the electrolyte. These elements were recovered with the copper as a sludge in a small electrolytic

Manuscript received at the office of the Institute Jan. 6, 1938. Issued in *METALS TECHNOLOGY*, October 1938.

* Assistant Works Manager, Canadian Copper Refiners Ltd., Montreal East, P. Q.

† Metallurgist, Canadian Copper Refiners Ltd., Montreal East, P. Q.

¹ C. W. Clark and A. A. Heimrod: *Trans. Electrochem. Soc.* (1932) 61.

² H. S. McKnight: *Trans. A.I.M.E.* (1933) 106.

purification system, which used lead cathodes and lead anodes. Lead cathodes were necessary because copper cathodes redissolved in the electrolyte and cemented selenium and tellurium from the solution. After electrolytic deposition the leach liquor was passed over scrap iron to recover the remaining copper, selenium and tellurium as a cementation mud, which was re-treated in the copper-anode furnace. The deposit from the purification system contained about 45 per cent Cu, 35 per cent Se and 6 per cent Te, and was known as "liberator mud." This mud was stored and now is being re-treated for recovery of metal.

The selenium and tellurium remaining in the acid-leached slimes were eliminated from the plant cycle by discard of doré-furnace soda-slag leach liquors and doré scrubber-system solutions.

For a short time in 1931 the oxidized, or roasted, slimes were treated with caustic potash solutions prior to acid leaching to eliminate selenium and tellurium from the slimes as potassium selenites and tellurites. This step was discarded from the original silver-refinery flowsheet, for two reasons: (1) poor selenium and tellurium elimination and consequent high cost of caustic per pound of selenium eliminated; (2) difficulty in filtering the caustic-leached slimes.

To summarize, prior to August 1934, selenium and tellurium were eliminated from the refinery cycle at five points in the flowsheet:

1. In caustic-leach liquors from treating roasted slimes. This was an outlet for a short time only.
2. In doré-furnace soda-slag leach solutions to sewer.
3. In scrubber solutions to sewer.
4. In cementation liquors to sewer.
5. In liberator mud, which was recovered and stored for re-treatment.

PRESENT SILVER-REFINERY OPERATIONS

The present processing of tankhouse slimes can be divided into eight steps as follows (Figs. 1 and 2):

1. Drying and roasting slimes with sulphuric acid for selenium elimination and conversion of metallic and oxide copper to water-soluble sulphate.
2. Water leaching of roasted slimes to remove soluble copper.
3. Caustic-soda leaching of water-leached slimes to remove tellurium.
4. Refining of caustic-leached slimes to doré bullion.
5. Separation of gold and silver by Moebius system.
6. Production and refining of selenium.
7. Production and refining of tellurium.
8. Recovery of acid from slimes water-leach liquors and discarded tankhouse electrolyte.

Raw slimes are pumped from the tankhouse to the silver-refinery surge tank, from which they are delivered at a uniform rate by Dorreo

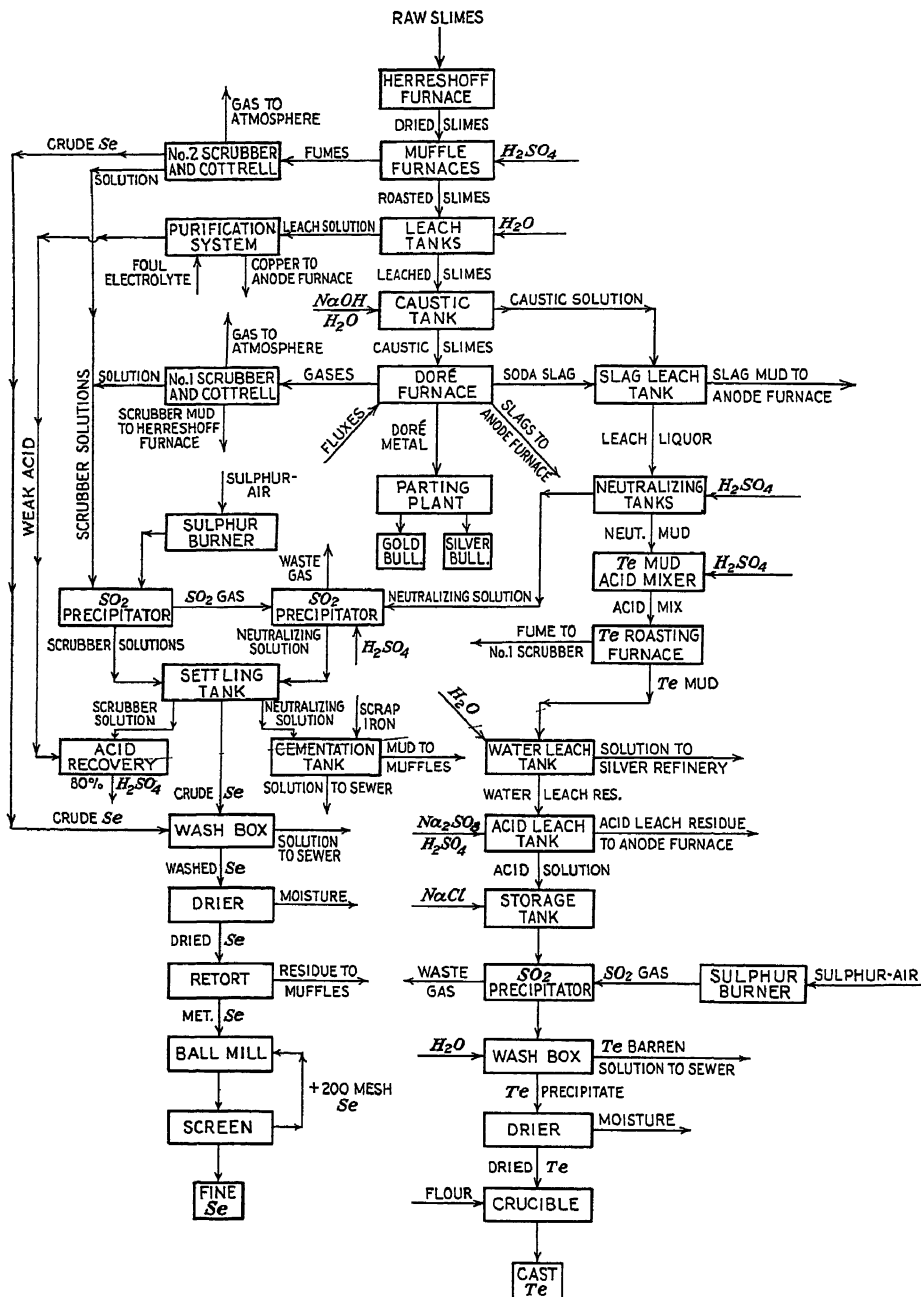


FIG. 1.—FLOWSHEET OF SILVER REFINERY WITH SELENIUM AND TELLURIUM DEPARTMENTS.

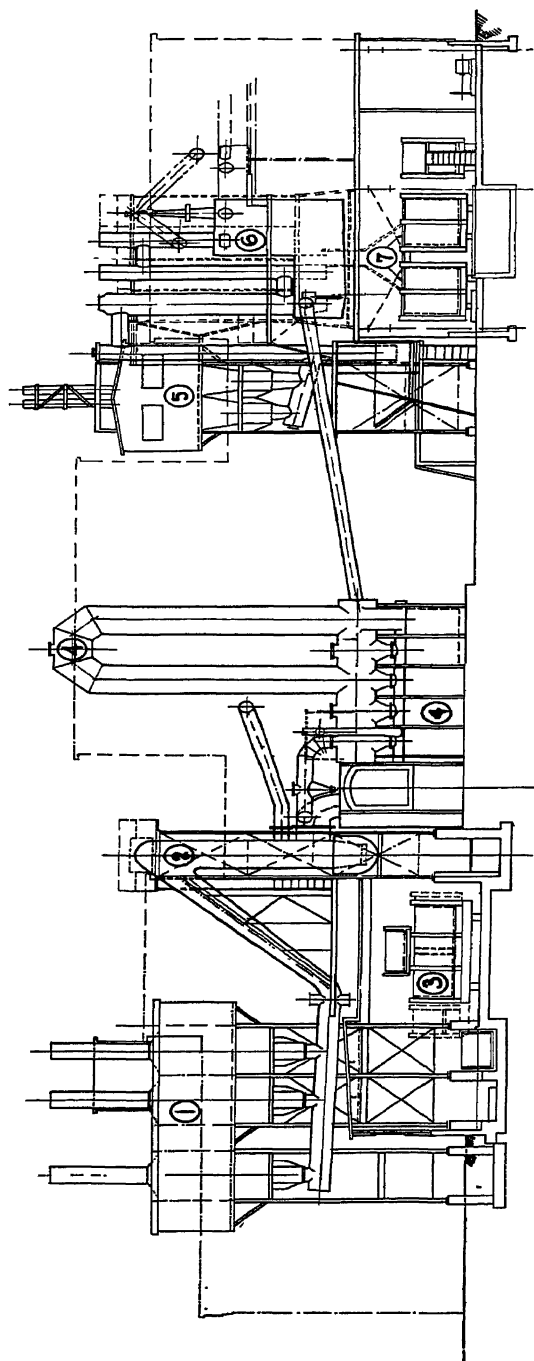


FIG. 2.—SECTION OF EASTERN SIDE OF SILVER REFINERY.

- | | |
|--|--|
| 1. No. 1 Cottrell precipitator. | 5. No. 2 Cottrell precipitator. |
| 2. No. 1 scrubber system for doré furnace gases. | 6. No. 2 scrubber system for muffle-furnace fumes. |
| 3. No. 1 scrubber-solution settling tanks. | 7. No. 2 scrubber-solution settling tanks. |
| 4. Doré furnace flue system. | |

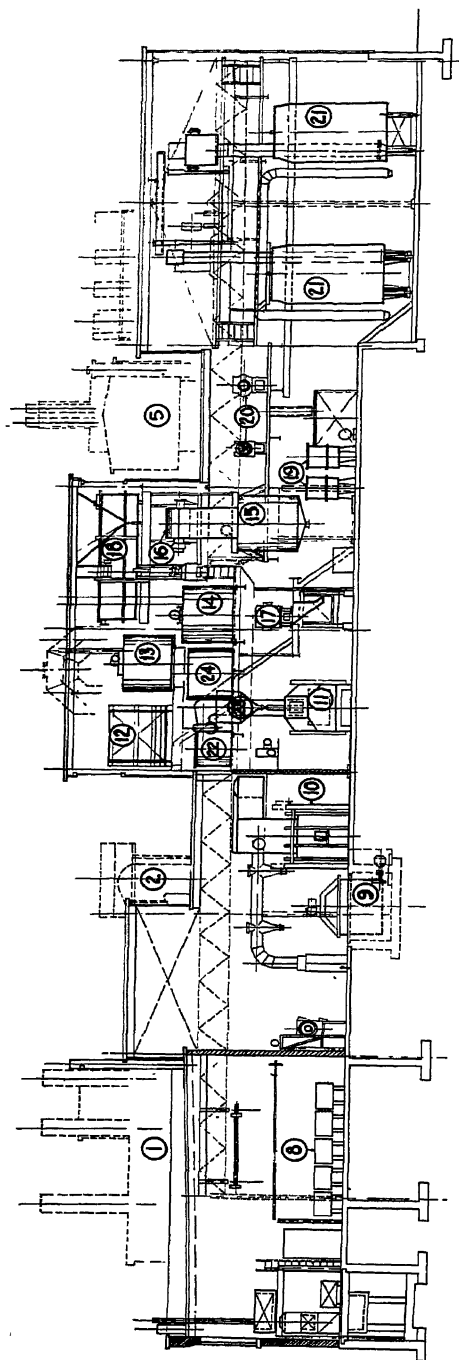


FIG. 2.—(Continued.)

- | | |
|--|---|
| 8. Moebius cells in parting plant. | 17. Filter press for caustic-leached slimes. |
| 9. Soda-slag leach tank. | 18. Storage tank for caustic leach solution. |
| 10. Doré furnace. | 19. Caustic-leach filtrate tanks. |
| 11. Furnace for roasting tellurium mud. | 20. Filter presses for scrubber mud and slag leach mud. |
| 12. Storage tanks for slimes water-leach solution. | 21. Muffle furnaces |
| 13. Slimes water-leach tanks. | 22. Wash-water storage, parting plant. |
| 14. Holding tanks for water-leached slimes. | 23. Tellurium mud-acid mixer. |
| 15. Slimes caustic-leach tank. | 24. Scrubber-solution storage. |
| 16. Oliver continuous filter for water-leached slimes. | |

diaphragm pump to a 10-ft. diameter Dorr thickener. The thickened slimes are discharged from the thickener to a 3 by 4-ft. Oliver continuous filter. The thickener overflow and Oliver filtrate are returned to the tankhouse storage tanks from a settling tank in the silver refinery.

The filtered slimes, containing 25 to 30 per cent moisture, discharge from the filter directly to the top hearth of an 8-ft. diameter six-hearth Nichols-Herreshoff furnace. The furnace dries the slimes at 250° to 300° F. down to 10 per cent moisture only. This moisture helps to prevent dusting during subsequent handling, which is an important consideration in treating such high-grade material.

The heating medium on the Nichols-Herreshoff furnace is bunker C fuel oil fired in a Dutch oven. Combustion gases from the furnace are exhausted to doré furnace flue and scrubber system.

Acid Roasting of Slimes

The Nichols-Herreshoff furnace discharge, known as dried slimes, is hoisted to the muffle-furnace platform, where the slime is mixed mechanically with about 75 per cent its weight of 60° Bé. recovered sulphuric acid before it is fed to the roasting furnaces. Certain silver-refinery and selenium-plant by-products, such as flue dust, scrubber mud and retort residue, are also acid-roasted in the muffle furnaces. The purpose of acid roasting is twofold: (1) from 80 to 95 per cent of the selenium content of the furnace feed is volatilized to the scrubber system; (2) 95 per cent of the copper content is converted to water-soluble sulphate for removal by water leaching.

There are two muffle furnaces of essentially the same design (Fig. 3). Each is of cast-iron construction, 8 ft. 0 in. in diameter, with eight roasting hearths, an equal number of combustion hearths and a top drying hearth. The furnaces are of the split type, to facilitate major repairs. All hearth connections to combustion-gas manifolds and acid-fumes manifolds are made on the stationary halves of the furnaces. There are three inspection doors on each roasting hearth and one on each combustion hearth. The roasting-hearth doors are large enough to pass a rabble arm fitted with teeth. Rabble teeth on acid hearths are made of stainless steel, while those on all other hearths are made of cast iron.

In addition to the acid mixed with the dried slimes before they are charged to the furnaces, acid is added through sprays on the third and fifth roasting hearths. In all, 2.2 to 2.5 lb. 60° Bé. sulphuric acid is used per pound of dried slimes.

The heating of the furnaces is accomplished by four 1¼-in. diameter burners set radially 90° apart on each combustion hearth. Vaporized light fuel oil, produced by a No. 9 Vapofier for each furnace, is fired through these burners. Both furnaces are lagged with 2 in. of Eagle No. 66 insulating cement. Roasting temperatures are maintained at

700° to 800° F. A permanent record of individual hearth temperatures is kept on Foxboro multipoint recorders.

The furnace shafts make one revolution every 50 sec. At this shaft speed the average roasting time for slimes is approximately 3 hr. The

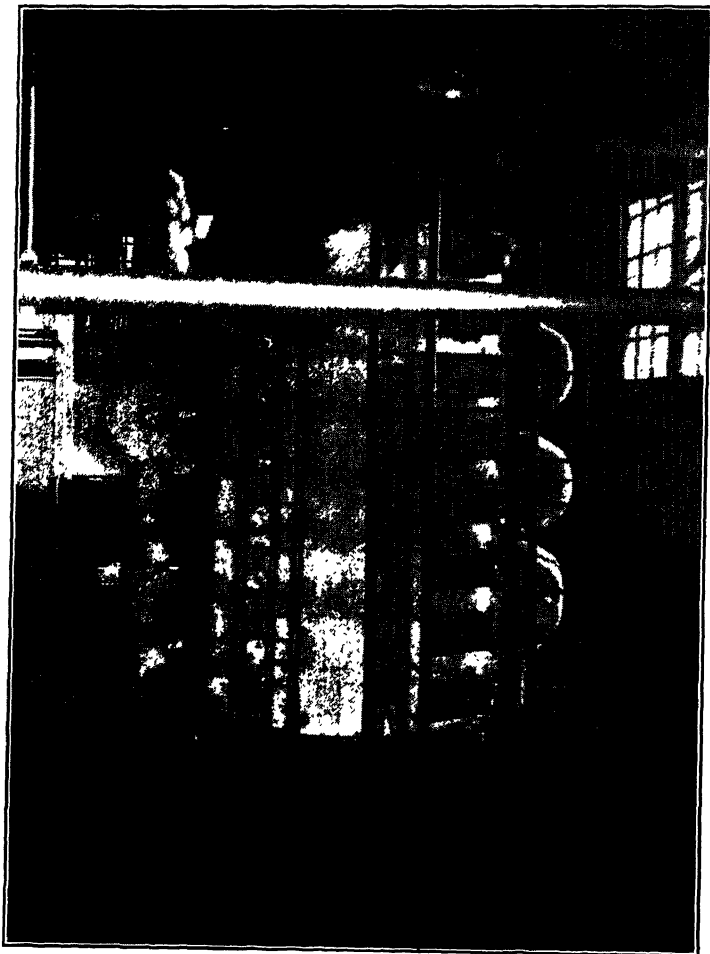


FIG. 3.—No. 2 MUFFLE FURNACE, SHOWING COMBUSTION GAS MANIFOLD AND TWO SETS OF SLIMES HEARTH INSPECTION DOORS. TEMPERATURE RECORDERS IN BACKGROUND.

combined production from the two muffle furnaces is 205,000 lb. of roasted slimes per month.

The furnaces are built on the muffle principle, combustion gases and acid fumes being handled separately. The combustion gases are exhausted by fan to the doré furnace flue and scrubber system as an insurance against possible metal loss.

Selenium Scrubber System

The acid fumes and gases from the roasting hearths of the muffle furnace are drawn through a lead-lined fumes manifold, where they are cooled with circulating scrubber solution. The cooled gases are exhausted by Corrosiron fan to a four-tower scrubber system. Each tower is equipped with lead sprays supplied with scrubber solution, which circulates through the towers, scrubber seal (or "bathtub"), settling tanks, pump tank and return. The scrubber system conditions the gas prior to Cottrell precipitation and, in addition, recovers the greater part of the selenium, selenium dioxide and acid content of the gas. A total volume of approximately 800 gal. per min. is supplied by six centrifugal pumps to the rain plates of the fumes manifold and the scrubber-tower sprays.

The products from the scrubber system are crude selenium and scrubber solution. Crude selenium is cleaned from the system daily. Scrubber solution is treated for selenium only when the selenium content has built up to one pound per cubic foot of solution. Both crude selenium and scrubber solution are treated in the selenium plant as explained later.

The Cottrell treater consists of two pipe units in parallel. Each unit has eight 8-in. diameter pipes and one 11-in. diameter pipe with the stiffener electrode. The entire Cottrell and scrubber system is constructed of lead and lead-covered steel, to resist the acid content of the gases being treated. The Cottrell treats 1800 cu. ft. per min. at 95° F., with an average daily stack loss of 2 lb. of selenium.

Both units of the Cottrell are cleaned down three times daily, once on each shift. Selenium collected in the Cottrell is processed in the same way as selenium from the scrubber system.

Water Leaching of Roasted Slimes

Roasted slimes discharged from the muffle furnaces assay about as follows: total Cu, 26 per cent; water-insoluble Cu, 1 per cent; Se, 3 per cent; Te, 2.4 per cent; Ag, 2340 oz. per ton; Au, 520 oz. per ton. This assay indicates an 80 per cent elimination of selenium during roasting. Actually, when straight slimes are handled through the muffle furnaces, 95 per cent Se eliminations are common, but this figure is considerably lower when residues of high selenium content are re-treated in furnaces.

The roasted slimes are hoisted, in buggies containing 1200 lb., to the leach-tank platform for charging in 3500-lb. batches to the lead-lined tanks. A counter-current system of leaching and decantation is employed. Second and third leach liquors from the previous batch are used for first and second leaching, respectively. Fresh water is used for final leaching. Direct steam is used for heating. No acid is used in

the leaching. If the leach liquor shows silver in solution, this is precipitated in leach tanks by means of copper scale from wire mill or high copper residues from the tankhouse. Excess copper additions are guarded against.

First leach liquors are decanted through a filter box to the purification system for copper recovery and acid regeneration. The weak acid from the purification cells is sent to the acid-recovery system for concentration to 60° Bé. prior to re-use in muffle furnaces.

At the conclusion of decantation of the third leach liquor, the water-leached slime is discharged from the leach tank to a holding tank. After four leached batches are accumulated in this tank the leached slimes are fed at a uniform rate by Dorco diaphragm pump to a 3 by 4-ft. Oliver continuous vacuum filter. The Oliver filtrate is pumped back to water-leach liquor-storage tank for use in subsequent leaches.

There is approximately 80 per cent reduction in the weight of roasted slimes during the leaching process, so that the grade of water-leached slimes is about as follows: Cu, 4 per cent; Ag, 11,700 oz. per ton; Au, 2600 oz. per ton; Se, 15 per cent; Te, 11 per cent.

Caustic Leaching of Slimes

The leached slime is discharged from the Oliver filter directly into the caustic treatment tank, which contains 150 cu. ft. of 10 per cent caustic soda solution. The purpose of this caustic leach is to remove the greater portion of the tellurium content of the leached slimes and thereby reduce the doré-furnace flue products—dusts and scrubber mud. About 85 per cent of the tellurium is removed by the caustic treatment.

At the conclusion of the leach the slimes and liquor are pumped through a 28-plate, 36 by 36-in. Shriver iron-plate filter press of the open discharge type. Two filtrate tanks are provided. Filtrate is run to the first tank until the solution is completely clear. This first filtrate is siphoned back to the caustic-treatment tank. The clear filtrate runs to the second tank, from which it is pumped to storage. As required, this caustic solution is used for leaching doré soda slags. In this way two sources of selenium and tellurium are combined and an appreciable reduction in volumes to be handled is effected. The caustic-leached slimes are retained in the filter press until they have been well washed with hot water, this water being returned to caustic-treatment tank to be used as make-up for the following batch. After washing, the slimes are blown with compressed air to aid moisture removal and are then dumped to a furnace buggy.

Caustic-leached slimes are handled in 3500-lb. batches containing 30 per cent H₂O and assaying: Cu, 4 per cent; Ag, 12,000 oz. per ton; Au, 2700 oz. per ton; Se, 14 per cent; Te, 1.5 per cent.

It is to be understood that all analyses given up to this point are to be taken as present averages and will, naturally, vary with the grade of material received at the refinery.

Caustic-leached slimes are charged to the doré furnace for refining to metal for Moebius-cell parting.

Doré-furnace Practice

The doré furnace is built on the reverberatory type and is fired with bunker C fuel oil. The hearth is built of 12-in. Lofero magnesite brick in the form of an inverted arch with a spring of $4\frac{15}{16}$ in. The hearth bricks were soaked in light fuel oil and set in a mortar of Lofero cement and fuel oil. This type of hearth absorbs much less metal than either the ordinary burned or unburned magnesite. The hearth area is $34\frac{1}{2}$ sq. ft. Under the hearth is set $2\frac{1}{2}$ in. of firebrick, a $\frac{1}{2}$ -in. steel plate and 4 in. of concrete, all of which is supported by 2 by 6-in. channels resting on concrete piers 12 in. above floor level.

The furnace side walls up to 1 ft. $10\frac{1}{4}$ in. above the hearth are constructed of 12-in. Lofero magnesite brick similar to the hearth. The upper side walls are made of fire-clay brick. The furnace roof is built of fire-clay brick and is 6 ft. 8 in. above floor level at the burner end and 5 ft. 0 in. above floor level at verb. The verb is constructed of steel-cased unburned magnesite brick supported on stainless-steel hangers, which rest on a water-cooled pipe. The bridge wall of the furnace is faced with a $4\frac{1}{2}$ -in. course of carborundum brick. The uptake, which has an area of $5\frac{1}{2}$ sq. ft., is built of steel-cased unburned magnesite brick at its lower end.

The furnace is charged through a door in the side wall and is skimmed from the front. A charge consisting of 10,000 to 12,000 lb. of slimes, containing 30 per cent moisture, is well mixed with fine soda and silica before charging. This mixture is charged to the doré furnace in 500-lb. additions. Besides the slimes, certain silver-refinery by-products are also charged to the doré furnace, and the furnace is then sealed. When the charge is completely molten the furnace is opened and the No. 1, or scoria, slag is skimmed off. This slag, which contains most of the lead, arsenic, antimony and iron, is crushed and returned to the copper-anode furnace.

(In passing, we may say, because of the high grade of material being treated and the lack of a secondaries smelting furnace in the plant, we are forced to re-treat a large tonnage of by-products in the anode furnace.)

The doré charge is next blown with air, fused soda ash being used for a flux. The soda slag formed contains most of the selenium and tellurium from the charge. This slag is leached with caustic liquor from the slimes treatment. The residue from the slag leach is returned to the anode furnace, while the filtrate is treated for recovery of selenium

TABLE 1.—*Typical Log of a Doré Furnace*

Operation	Elapsed Time, Hr.	
	Without Iron	With Iron
Charging.....	15.7	15.7
Melting.....	6.7	6.7
Skimming No. 1 slag.....	1.5	1.5
Blowing with soda and skimming soda slag.....	17.0	} 18.8
Refining with niter and skimming copper slag.....	11.4	
Casting.....	3.6	3.6
Total time.....	55.9	46.3

Fluxes Used	Pounds	
Soda.....	852	852
Purite.....	2,590	1,650
Niter.....	2,450	1,460
Silica.....	410	410
Scrap iron.....	0	800

Slag Produced	Pounds
No. 1 slag.....	4,740
No. 2 slag.....	3,890
Copper slag.....	2,740

Metal Produced	Troy Ounces
Doré metal.....	46,429
Silver content of doré.....	38,129
Gold content of doré.....	7,654

Typical Analyses for Doré-furnace Products

	Cu, Per Cent	Ag, Oz. per Ton	Au, Oz. per Ton	Se, Per Cent	Te, Per Cent
No. 1 slag.....	1.43	170	17.6	0.75	0.52
No. 2 slag.....	2.45	264	7.8	17.51	5.72
Copper slag.....	16.00	1300	25.1	6.15	0.50
Flue dust.....	5.71	810	120.1	32.06	2.55
Scrubber mud.....	0.40	1049	43.2	28.82	0.91

and tellurium. Recently scrap iron has been used in addition to the soda for breaking down the selenium matte into bullion and soda slag. When iron is used no blowing is required. The iron addition has materially reduced the amount of chemicals required per ounce of doré metal produced and the time required to process a charge through the furnace. About 40 per cent of the former chemical cost is saved and 10 hr. are cut off each furnace charge. No new iron is bought for fluxing, as sufficient scrap rabble teeth and similar material is always available in the silver refinery.

The final stage of furnace refining is the removal of the copper content by rabbling the charge with niter. The copper slag skimmed off is crushed and returned to the anode furnace for re-treatment.

Just prior to casting, the doré metal is cleaned up with Portland cement. The slag from this cleaning is recharged to the furnace with subsequent charge. The doré metal is ladled into water-cooled molds by hand. Anodes are 6 by 9 by $\frac{1}{2}$ in., weigh approximately 150 Troy ounces each and assay 845 parts fine silver, 150 parts fine gold and 5 parts copper. The average production of the doré furnace is 45,000 Troy ounces per charge, or 225,000 oz. per month. A typical doré furnace log, for a charge of 10,000 lb. of wet caustic-leached slimes (30 per cent H_2O) and 2000 to 3000 lb. of sundry material such as return slag, is given in Table 1. The effect of iron addition during the soda-slag period is clearly shown.

Doré-furnace Flue, Scrubber and Cottrell System

The gases leave the doré furnace at 2500° F. and pass through a brick flue and a steel flue for cooling and removal of considerable flue dust. The gases then pass through the exhaust fan and enter the scrubber system at 400° F. In addition to the doré-furnace gases, all gases from the Herreshoff furnace, tellurium-mud roasting furnace and combustion hearths of muffle furnaces are also exhausted through the scrubber system for conditioning prior to Cottrell precipitation.

In passing through the three-tower scrubber system, the gases are completely saturated with water by sprays and rain plates and about 90 per cent of the remaining dust is precipitated as a scrubber mud. A total volume of approximately 450 gal. per min. is supplied by three centrifugal pumps to the doré-furnace scrubber-tower rain plates and sprays. Scrubber mud and solution is filtered through a 24 by 24-in. Sperry lead-plate filter press. The mud is returned to the Nichols-Herreshoff furnace for re-treatment. The scrubber solution is pumped to the selenium plant for recovery of selenium and acid.

The gases leave the scrubber at 125° F. and pass to a three-unit Cottrell precipitator of the pipe type. Each unit consists of eighteen 8-in. diameter pipes and two 11-in. diameter pipes, all 12 ft. long. The

entire precipitator and scrubber system is constructed of antimonial lead and lead-covered steel.

Each Cottrell unit has a damper for control of gas volume and a switch for cutting the unit out of circuit for maintenance and repair. The pipes are cleaned with a scraper at the end of each doré charge and the alignment of electrodes is checked at the same time. The Cottrell handles a total gas volume of 8000 cu. ft. per min. at 95° F., the average daily metal losses from the Cottrell stacks being: 1.5 oz. Ag, 0.027 oz. Au, 1.7 lb. Se, 0.2 lb. Te. Continuous 24-hr. sampling tests are run on gases from this Cottrell as well as on the muffle-furnace Cottrell.

Power for Cottrells

Incoming power from the Montreal Light, Heat & Power Consolidated is supplied at 12,000 volts, three phase, 60 cycles. This voltage is stepped down to 550 volts and then by means of a 15-kva. transformer is boosted to 45,000 to 65,000 volts. This high-voltage current is rectified by a synchronously driven mechanical rectifier. The unidirectional current is supplied to the Cottrell units. Voltage on the precipitators is controlled in three ways: (1) low-voltage rheostat on primary side of incoming alternating current; (2) high-voltage resistance; (3) taps on high-voltage transformer. There are two complete rectifier units in the main powerhouse. The two rectifiers are arranged so that either or both can be used on either or both of the Cottrells. This provides complete flexibility of control. A private telephone system connects both Cottrell units with the powerhouse.

Parting Plant

The anodes from the doré furnace are taken to the parting plant for parting into silver and gold by the Moebius system. There are 10 rubber-lined concrete Moebius cells arranged in two groups of five cells each. The cells measure 2 ft. 5½ in. by 2 ft. 9½ in. by 1 ft. 10¾ in. inside rubber lining. Fifteen doré anodes are suspended in each cell, so that 150 anodes, weighing approximately 22,000 Troy ounces, are contained in the newly loaded cells.

The electrolyte in the cells at present assays: Ag, 50 grams per liter; Cu, 15 grams per liter; and free HNO₃, 2 grams per liter.

There are two motor-generator sets in the powerhouse, each one supplying the current for one set of five Moebius cells. The average power requirements for five cells is 13 volts and 475 amp. Since the cells are in series, with the anodes and cathodes in each cell in parallel, the current density is 28 amp. per sq. ft. of cathode area. Each set of three anodes in parallel is enclosed in a filter duck bag, to retain the gold residue from the electrolytic deposition of silver crystals on rolled silver

cathodes. Cathodes when new measure 12 by 20 by $\frac{1}{16}$ in. thick. Bakelite is used for the gold-bag frames.

In each cell is suspended a wooden frame basket having a filter-cloth bottom. Continually reciprocating wooden scrapers brush the silver crystals from the cathodes into the basket filter bottom. The baskets are withdrawn from the cells once every 24 hr. for removal of the silver crystals. These silver crystals are washed with water in a filter-bottom stoneware cart, to remove all traces of electrolyte. The silver sand is dried and melted in a graphite retort, 14,000 oz. at a time. Silver bullion is cast in bars weighing 1000 Troy ounces and assaying 999+ fine.

The average life of 150-oz. anodes containing 15 per cent gold is 36 hr. When necessary, scrappy anodes are replaced in cells by new ones. Once every four days all anodes are removed from the cells and scraped. The gold mud from the anodes is combined with that from the filter bags, washed with water and leached with boiling concentrated sulphuric acid, to remove most of the silver. After being leached, the gold sand is washed well with water and drained on filtros blocks. The sand is melted in a graphite crucible and cast into bars weighing 750 Troy ounces each and assaying 995+ fine gold. Gold bullion is shipped directly to the Royal Canadian Mint at Ottawa.

Anode scrap, after being scraped clean, is remelted in a graphite crucible and cast into doré anodes for parting. With anodes assaying 150 parts fine gold, the weight of scrap averages about 12 per cent of the loading.

Silver from all parting-plant wash solutions and gold-boiling acids is recovered by cementation with scrap copper and is re-treated in the doré furnace or used for make-up material for parting-plant electrolyte.

SELENIUM PLANT

The selenium, tellurium and acid-recovery departments are in a 60 by 60-ft. self-contained building, about 200 ft. from the silver refinery. The building is composed of three 20 by 60-ft. bays. As far as possible each of the three departments is built entirely within one bay, to facilitate handling materials and to minimize contamination of refined products.

Three classes of material are received at the selenium plant for processing: crude selenium from the muffle-furnace scrubber, neutralized

TABLE 2.—*Typical Assays of Materials Received at Selenium Plant*

Materials	Se, Grams per Liter	Te, Grams per Liter	H ₂ SO ₄ , Grams per Liter
Doré scrubber solution.....	45	4.50	180
Muffle-furnace scrubber solution.....	18	0.15	200
Neutralized slag-leach solution.....	20	0.25	0
Crude selenium, per cent.....	97.5		

slag-leach solution and scrubber solutions. Typical assays of the three materials are given in Table 2.

Precipitation of Selenium from Scrubber Solutions

All solutions are pumped from the silver refinery through an underground tunnel to the storage tanks at the selenium plant. Solutions are drawn from storage to the precipitators as required.

The precipitation of selenium from selenious acid solutions is based on this equation:



which shows that for every pound of selenium precipitated approximately $2\frac{1}{2}$ lb. of sulphuric acid is generated.

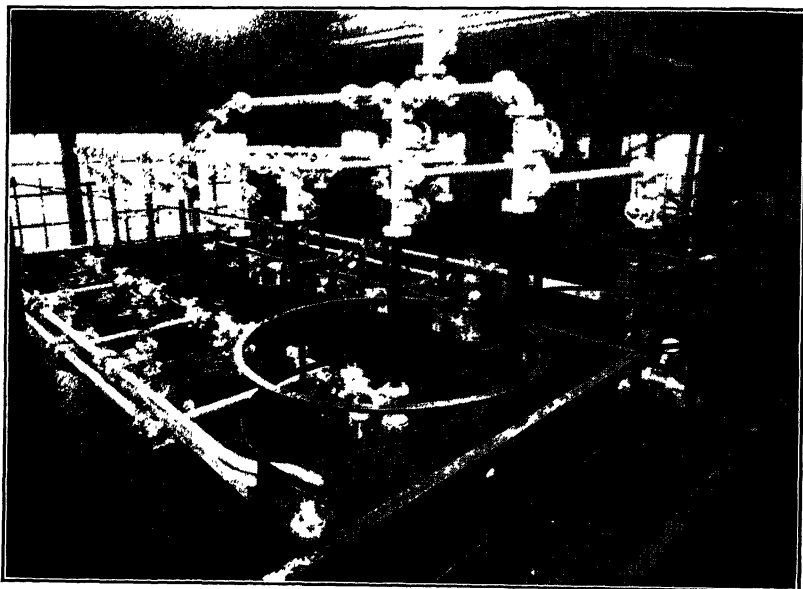


FIG. 4.—SULPHUR DIOXIDE PRECIPITATORS.

The precipitators (Fig. 4), of which there are six in series, are lead-lined dished-end tanks, 5 ft. 0 in. in diameter by 8 ft. 6 in. high. Each precipitator has an inlet and an outlet for sulphur dioxide gas, an outlet for waste gas, a manhole for inspection, a solution inlet and a bottom discharge for solutions after precipitation is complete. Besides, a thermometer, pressure gauge and sampling cock are provided on each precipitator for control purposes. Each precipitator has a cooling coil to maintain the temperature of the solution between 60° and 90° F. during precipitation. Above 100° F., selenium precipitates become

plastic and are difficult to clean from the precipitator, while below 60° F. too great a quantity of sulphur dioxide gas is required to saturate the solution.

The six precipitators are connected in series in a closed circuit, so that, by means of valves, any one of the six tanks can be the first one in series or can be removed from the circuit at any time. Series precipitation under pressure aids greatly in securing effective recovery of selenium with the minimum amount of sulphur dioxide gas. At the refinery, for every pound of sulphur burned an equal amount of selenium is precipitated, which indicates an efficiency of 80 per cent according to the

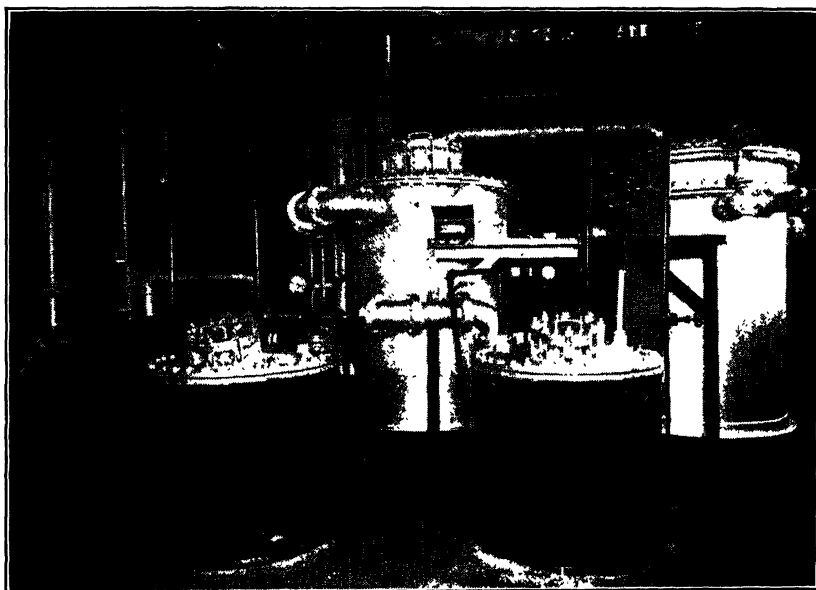


FIG. 5.—EQUIPMENT FOR GENERATING SULPHUR DIOXIDE GAS.

equation given above. This figure is possible only if four or more of the six precipitators are in service all the time.

The time required for precipitation varies directly with the concentration of selenium in the solution treated, the average being about 5 hr. per tank. When a sample from a precipitator shows completion of precipitation, that tank is cut out of circuit. The precipitator is vented carefully to remove excess sulphur dioxide, after which the manhole cover is removed and the spent solution with selenium precipitate is washed through the bottom discharge to the settling tank.

In the settling tank the solutions are boiled to remove the last traces of sulphur dioxide gas. The selenium is allowed to settle, after which the solution is decanted and pumped to the acid-recovery storage tanks.

It is impossible to precipitate selenium completely from straight sulphuric acid solutions, so that spent scrubber solution assays about 0.5 gram per liter Se and 0.2 gram per liter Te. Most of this selenium is recirculated in the acid produced from concentrating these spent solutions.

The crude selenium from the settling tank is washed with water through a $\frac{1}{4}$ -in. screen and is filtered in a vacuum wash box. From this point in the selenium process all materials entering the plant are treated alike.

Precipitation of Selenium from Neutral Slag-leach Solutions

Neutral slag-leach solutions are acidified with 10 per cent their weight of 66° Bé. sulphuric acid before they are gassed with sulphur dioxide. As regards the actual precipitation, the same procedure is followed for scrubber solutions and neutral slag-leach solutions, but the disposal of the spent solutions is different.

Because of their high content of sodium salt, spent slag-leach solutions cannot be treated for acid recovery. These solutions, after being boiled in the settling tank for removal of sulphur dioxide, are pumped to a cementation tank, where a considerable amount of the selenium is recovered on scrap iron before the solution is discarded to sewer.

Of the total selenium production, about 50 per cent comes directly from muffle-furnace scrubber crude selenium; the remaining 50 per cent comes from precipitation of scrubber solution and neutral slag solutions.

Generation of Sulphur Dioxide Gas

The sulphur dioxide gas is generated by burning elemental sulphur in a water-jacketed brick-lined steel tank, 2 ft. 9 in. in diameter by 3 ft. 2 in. high. Air under pressure is introduced above the surface of the molten sulphur. The burner with six precipitators in circuit operates at a pressure of 20 lb. per sq. in. and a temperature of 400° F. Under these conditions it is possible to burn 20 lb. of sulphur per hour, which will precipitate an equal weight of selenium. (Fig. 5.)

The gas discharges from the sulphur burner into a steel expansion tank 4 ft. 0 in. in diameter by 6 ft. 0 in. high. The purpose of this tank is to settle elemental sulphur sublimed over from the burner and to cool gases to 250° F. before they pass on to a lead-lined water scrubber tank of the same size as the expansion tank.

Sulphur dioxide gas passes from the scrubber at 17 lb. per sq. in. and 100° F. to the first precipitator in series on the floor above.

Refining Crude Selenium

After the crude selenium is washed in the filter box, it is dried in an oven.

Crude selenium assays from 0.01 to 0.30 per cent Te, depending on the source of the material. Charges of 1000 lb. to retorts are blended so that the average grade is 0.10 per cent Te.

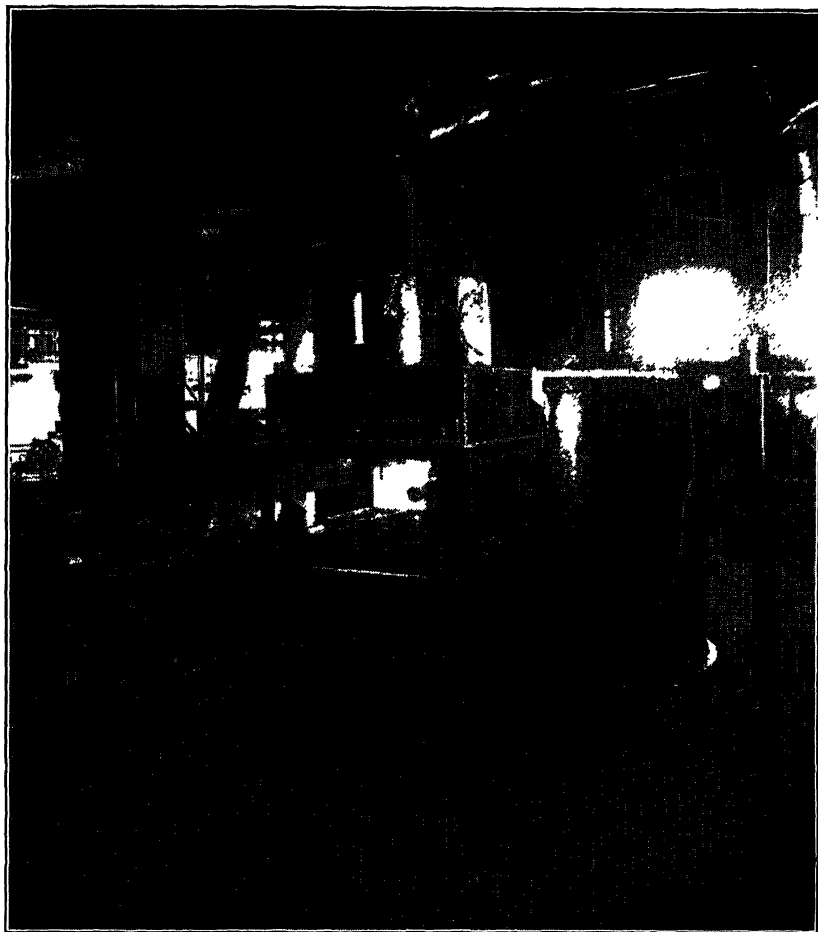


FIG. 6.—SELENIUM RETORT IN OPERATION.

Retorting crude selenium serves two purposes: it reduces the tellurium content to less than 0.10 per cent and it recovers in the residue any silver and gold that may have been in the crude selenium.

The retort bowls are made in gooseneck style of cast iron. Retort covers are made of cast iron containing 1 per cent Ni. After every second charge the retort bowl and cover are cooled, removed from the furnace and cleaned of any accumulated residue. The residue, after being ground and screened, is re-treated in the muffle furnaces at the silver refinery.

The bowls are heated in an oil-burning furnace at a temperature just sufficient to distill the selenium. Temperature control is maintained by a thermocouple indicator set in the retort cover. The retort distillate is collected in steel pans, which hold 15 lb. of selenium each. These selenium blocks are allowed to cool slowly in order to obtain the gray metallic variety. (Fig. 6.)

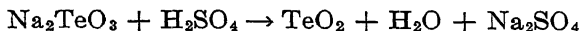
In this step, and in all others throughout the entire selenium and tellurium plants, careful control is maintained by properly prepared samples of intermediate as well as end products.

The metallic selenium blocks are held until analysis shows them to be of proper quality. Retorted selenium that contains over 0.10 per cent Te is retorted a second time. Then the blocks are broken in a small jaw crusher and ground in batches of 400 lb. each in a Patterson pebble mill. The ground selenium is screened mechanically through 150 mesh and is then ready for market. Any plus 150-mesh material is reground. Screen analysis of fine ground selenium is as follows: +200, 2.31 per cent; -200 to +300, 19.76; -300, 77.93; total, 100 per cent.

Fine selenium is packed in tins containing 5 kg., 10 lb. or 100 lb. each. The assay of fine ground selenium is 99.85 per cent Se, 0.08 per cent Te, 0.015 per cent Fe, 0.002 per cent Cu, 0.006 per cent Pb, which totals 99.953 per cent.

TELLURIUM PLANT

The precipitate formed on neutralizing, with sulphuric acid, the solution from caustic-leaching doré-furnace soda slag is the raw material for tellurium production. The principle of the neutralization is that, while sodium selenite is soluble in neutral solution tellurium dioxide is not, therefore the latter precipitates according to the equation:



Some selenium is carried down mechanically with the flocculent TeO_2 , so that this precipitate must be treated for removal of selenium before it can be used for production of tellurium. The mud is filtered through a 14-plate, 24 by 24-in. lead-plate and frame Shriver filter press. The filtrate from the neutralization is treated for recovery of selenium as described.

The TeO_2 precipitate, or "neutralized mud" as it is called, assays about as follows: Cu, 2.0 per cent; Se, 6.5 per cent; Te, 32.0 per cent, with small varying amounts of silver and gold. This mud is mixed in 900-lb. batches with sulphuric acid and is charged to a reverberatory roasting furnace. There the mud is hand-rabbled for about 8 hr., during which time very nearly all of the selenium in the mud is volatilized to the doré-furnace scrubber system for recovery. In addition, the copper in the roasted mud is converted to the water-soluble sulphate. The acid

roasting is the first step in both slimes treatment and tellurium treatment. Up to this point the tellurium mud is processed in the silver refinery.

Roasted tellurium mud assays 1.8 per cent Cu, 0.25 per cent Se, 30 per cent Te. The roasted mud is ground in a small jaw crusher, screened through $\frac{1}{4}$ -in. mesh and shipped to the tellurium plant in drums containing 450 lb. each.

Leaching Tellurium Muds

To guarantee a good quality of final tellurium product, the copper is water-leached from the roasted tellurium mud. Batches charged to the lead-lined leach tanks weigh about 900 lb. The water-leached residue is filtered through a lead-plate and frame filter press. The filtrate is returned to the silver refinery for water-leaching slimes.

The water-leached residue, containing 0.15 per cent Cu, 0.35 per cent Se, 37.0 per cent Te, is hoisted from the filter-press platform back to the leach tanks, where it is boiled with 30 per cent H_2SO_4 to dissolve the tellurium. Some selenium is also dissolved from the mud but this is immediately precipitated by the addition of sodium sulphite directly to the leach in the tank.

At the completion of the leach the undissolved residue and acid leach solution are filtered through the same press used for filtering the water-leached mud.

The acid-leached residue is barreled and returned to the anode furnace for re-treatment. In this way any silver and gold that may have been in the original neutralized mud are recovered.

The acid leach solution (200 cu. ft. in volume) is pumped to a brick and rubber-lined storage tank for conditioning with common rock salt prior to sulphur dioxide precipitation of the tellurium. From this point to the final washing of tellurium precipitate, all processing equipment is rubber-lined, to withstand the hydrochloric acid in the solutions. The acid leach solution when ready for precipitation analyses about: Cu, 0.20 gram per liter; Se, trace; Te, 20.0 grams per liter; H_2SO_4 , 350 grams per liter and NaCl, 30 grams per liter. Unlike selenium, tellurium cannot be precipitated quantitatively from 30 per cent straight sulphuric acid solutions. However, the addition of 2 per cent of salt is sufficient to carry the reaction.



nearly to completion. The solution after sulphur dioxide precipitation assays less than 0.25 gram per liter Te.

Tellurium Precipitation

The equipment for sulphur dioxide precipitation of tellurium consists of two rubber-lined precipitators, 5 ft. 0 in. in diameter by 8 ft. 6 in.

high, a water-jacketed brick-lined steel gas generator 2 ft. 9 in. in diameter by 3 ft. 0 in. high and a lead-lined water-filled gas scrubber. This equipment is entirely independent of that used on selenium production, in order to guard against contamination of final products. The burner is operated at 350° F. and 8 lb. per sq. in. pressure.

After both tankfuls of acid leach solution have been completely precipitated, they are dumped to a vented rubber-lined vacuum filter box for thorough washing with water. The filtrate from this box drains through a tile pipe to the sewer. Because of the hydrochloric acid in the barren solution, it is deemed inadvisable to attempt acid recovery from this material.

After the precipitate is washed, it is dried and melted down with flour in a graphite retort. The molten tellurium is cast in bars weighing 50 lb. each and assaying as follows: 99.7 per cent Te; 0.07 per cent Se; 0.03 per cent Cu.

ACID-RECOVERY PLANT

Weak acid that is concentrated in the acid-recovery plant comes from three sources: slimes-leach liquors, tankhouse foul electrolyte after copper deposition in the purification system, and spent scrubber solutions after selenium precipitation. Sufficient storage space is provided with six 7-ft. 6½-in. diameter by 11-ft. 6-in. deep lead-lined wooden tanks to hold a complete concentrator charge of 18 per cent H_2SO_4 .

The concentrator is a Simonson-Mantius unit (Fig. 7) with a guaranteed capacity to produce in 24 hr. 20 tons of 80 per cent H_2SO_4 from 18.6 per cent acid at 125° F. The concentrator requires per ton of 80 per cent acid produced 9300 lb. of steam at 100 lb. per sq. in. and 40,000 U. S. gal. of water at 70° F. and 25 lb. pressure at floor level. The concentrator is operated only during intervals of maximum waste-heat steam production, which is during the anode and wirebar furnace melting, skimming and poling periods, from 6.00 p.m. to 7.00 a.m. daily, except Sunday.

A concentrator batch is 15 tons of 80 per cent H_2SO_4 . At the completion of concentration the batch is dumped to the outside storage tanks for cooling and settling of the sludge. The clear acid is decanted from the outside storage to the inside storage tanks, from which it is pumped by Corrosiron piston pump as required. Most of this recovered acid is used in the muffle furnaces for roasting slimes and in the neutralization of slag-leach liquors. Because of its selenium and tellurium content, no recovered acid is used in the tankhouse for electrolyte make-up, in the acid leaching of tellurium muds or in the acid boiling of gold muds in the parting plant.

Most of the sludge produced from concentrating the weak acids is accumulated in the outside storage tanks, from which it is filtered over a

vacuum filtros-block filter. The acid filtrate is recovered in a receiver and is blown by air to the inside acid-storage tanks. The concentrated acid sludge is discarded to sewer.

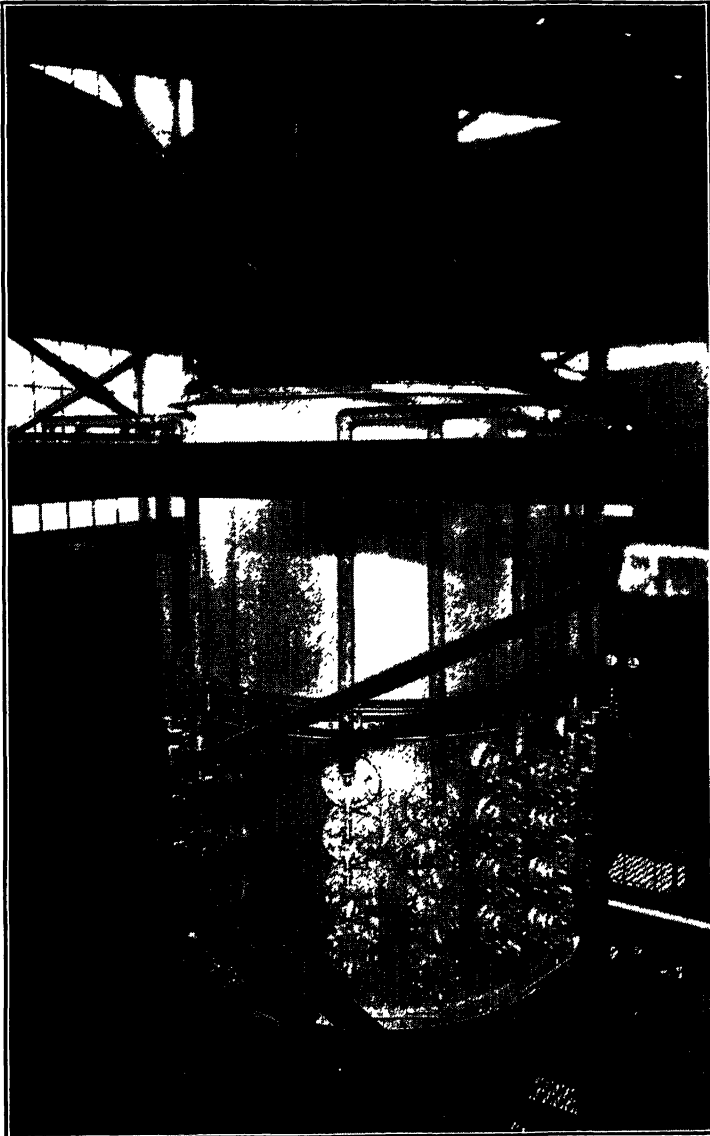


FIG. 7.—SIMONSON-MANTIUS ACID CONCENTRATOR.

Normally, between 100 and 150 tons of concentrated acid is produced per month.

DISCUSSION

(E. W. Rouse, Jr., presiding)

G. BAUMAN,* Laurel Hill, N. Y.—May I ask what the over-all recovery of selenium is—I mean, how much of the selenium present in the slime is recovered as compared with other methods used?

J. H. SCHLOEN (author's reply).—From June 1 to Nov. 30, 1937—that is the first six months of the present inventory period (we take an inventory every year)—we have lost 5.25 per cent of all the selenium we have treated. That includes all selenium lost, except about 2.5 per cent that goes back to the mine in the anode-furnace refinery slag. In other words, we have an over-all recovery of 92 per cent on the selenium coming into the plant. The summary of selenium losses for the period June 1 to Nov. 30, 1937, is given in Table 3.

TABLE 3.—Summary of Selenium Losses

Losses	Percentage of Material Treated	Percentage of Total Loss
Anode-furnace stack.....	1.23	17.2
In shapes produced.....	0.37	5.2
In cathodes shipped.....	0.10	1.4
Concentrated acid sludge discarded.....	0.24	3.4
No. 1 (Doré furnace) Cottrell.....	0.24	3.4
No. 2 (selenium) Cottrell.....	0.15	2.1
Selenium solution to sewer.....	2.81	39.0
Tellurium wash water to sewer.....	0.12	1.7
Returned to smelter in refinery slag.....	5.26	73.4
	1.91	26.6
	7.17	100.0
Over-all selenium recovery, per cent..... 92.83		

E. W. ROUSE, JR.,† New York, N. Y.—I might contribute my own part by saying that I have been able to figure pretty high selenium recoveries at times, but at the end of the month or the end of the year it was usually about 60 per cent.

D. P. WILKES,‡ Barber, N. J.—On page 344 (Mr. Benard's paper) there is the statement: "The roasted product is extracted with water leaches and the liquor pumped to the selenium

plant." I was under the impression that sodium tellurite was insoluble in water. Here is the statement: "Oxidation of the cementation slimes by roasting with caustic soda renders the tellurium soluble as sodium tellurite."

J. H. SCHLOEN.—Sodium tellurite and sodium selenite are both soluble in water solutions.

MEMBER.—In regard to recovery at Montreal East, I would like to add that this is based on the fact that there is no accumulation in the inventory in that period.

J. H. SCHLOEN.—After all, the question of metal inventories does not affect the percentage recoveries, since recoveries, as stated earlier, are based solely on amount of selenium actually treated in plant. However, metal inventories do show whether the refinery had any unaccounted-for metal loss.

H. M. SHEPARD,* Baltimore, Md.—If we do 65 per cent we consider that we are doing very well. Actually our recovery is usually slightly under 60 per cent. There have been times when we really have been scraping for selenium to meet orders and as a result a great deal of attention has been given to the recovery attained. In view of this, I am inclined to agree with the figure of 60 per cent.

E. W. ROUSE, JR.—Mr. Schloen reports that prior to some date they were throwing the selenium in the sewer.

J. H. SCHLOEN.—That's right, absolutely, 50 per cent of it. As mentioned early in our paper (pp. 350 and 351) prior to August 1934, 50 per cent of the selenium treated was recovered in the form of liberator mud and the other 50 per cent was discarded to sewer in doré-furnace soda-slag leach solutions and in scrubber solutions.

D. L. OGDEN,† Carteret, N.J.): We at the plant have studied the question of the selenium recovery continuously. We have taken definite inventories of selenium the same as we take copper, silver and gold throughout the refinery. I think it is pretty definite that the higher the

* Nichols Copper Company.

† Metallurgical Engineer.

‡ American Smelting & Refining Company.

* American Smelting and Refining Company.

† U. S. Metals Refining Company.

grade of the selenium in the incoming material, the higher the recovery will be.

There are certain definite losses of selenium throughout the plant that are constant regardless of the amount of selenium coming into the plant, and I think that has a lot to do with the percentage recovery. In other words, the loss at Montreal would probably be constant whether they had 14 per cent selenium coming into the plant in slimes, or 22 per cent; consequently, the loss or rather the percentage loss would be much greater with the lower percentage of incoming selenium. That has been true in our case, I know.

E. W. ROUSE, JR.—When you give the statement about Cottrell, does that include the water scrubbers, or does it mean Cottrell alone?

J. H. SCHLOEN.—The recovery is for scrubber and Cottrell combined. About 85 per cent of the selenium is recovered in scrubber and the remainder in Cottrell. I did not speak of Cottrell efficiency. I spoke of Cottrell loss. What the input is, I do not know, because the flue system is peculiar for gas tests. We have run them; we have obtained 95 per cent efficiency of selenium recovery on the Cottrell from the inlet to the outlet of Cottrell, but we are suspicious of the results because, as I say, the flue system is not suitable for proper gas sampling at the inlet. At the Cottrell outlet we have extended the stacks and we are able to run proper Pitot-tube traverses, and I think the outlet figures are correct.

As regards this loss, however, we take a good deal of trouble to have a complete metal inventory every year. We even tear down the entire flue system and doré furnace. It is an expensive procedure but at least we have a certain amount of satisfaction that we are doing as well as possible in accounting for all materials that we are receiving. Yearly metal inventories are especially important to our refinery, since we handle such high-grade material. All metal losses are based on actual analyses from samples taken at point of loss.

MEMBER.—Will you explain the sampling procedure?

J. H. SCHLOEN.—On the new Cottrell, that is the selenium Cottrell, taking the gases

from only the muffle furnaces, we have two Cottrell units. The gas volume from one of these is only about 900 cu. ft. per minute, so we have combined the two stacks in order to obtain satisfactory Pitot-tube readings.

The distance from Cottrell units to gas-sampling point in the 15-in. diameter stack is about 12 ft. or so. We have taken the Pitot-tube traverses about 3 ft. from the top of the stack. Here we have fairly uniform motion of gas and we have determined a point of average velocity in the stack, at which point our sampling tube is inserted. This procedure does not differ from that recommended by the Western Precipitation Company.

We use a glass sampling tube. From the tube the gas is drawn through a series of four glass funnels and condensate bottles. Each funnel supports a perforated porcelain disk inside it. On the disk are packed a 2-in. thickness of glass wool, a $\frac{1}{8}$ -in. bed of asbestos fiber and a second 2-in. thickness of glass wool. As soon as the third filter shows any trace of color, a fresh filter is placed at tail end of the train and the first filter is removed. As necessary, condensate bottles are replaced. The gas from the fourth filter is passed to a drip bottle and then to a Sprague gas meter, and so to the exhaust jet.

Hourly readings are taken of meter volume, meter pressure, meter temperature, stack temperature and stack-gas velocity. Collections are changed weekly. We have tried bubbling the gas from the last filter through stannous chloride which, as far as I can find out, is about the best reducer to detect any traces of selenium dioxide. In every case the stannous chloride showed negative results, so we feel quite sure that the selenium loss as reported at the new Cottrell is as shown. Much the same procedure is used to determine selenium and other metal losses from the doré-furnace Cottrell stacks. The losses from the doré-furnace Cottrell are somewhat higher than those from the selenium Cottrell, but, as far as these losses go, they are small. Our main loss is in selenium solution to sewer. Say we lose 5 per cent of all the selenium being treated around the plant and then besides that the 2.5 per cent of selenium going back to the smelter, for which we are not paid. How much of this selenium the smelter loses we do not know. But the main loss of selenium around the plant

is in the discarded solution. Of the 5 per cent we lose, 55 per cent is in selenium solutions to sewer, or about 3 per cent of all the selenium we treat. Actually, from our gas tests we show a loss from Cottrell stacks of only 0.4 of 1 per cent of all the selenium treated in plant, so, if our gas-testing method is accurate to, say, 50 per cent, we feel quite content, and I am sure it is much more accurate than 50 per cent. The accuracy of the method is probably plus or minus 10 per cent.

C. H. ALDRICH,* Carteret, N. J.—We have made a great many tests trying to find just where the losses of selenium occur. It is quite easy to determine losses that occur in solution, going to sewer and residue, and things that can be collected and then accurately sampled, but we have never been entirely satisfied with the results on our gases going from the Cottrell.

We have used methods like those described by Mr. Schloen, but we have always had the feeling that something was getting away which was not recovered by the ordinary methods of filtration and separation of fumes such as he has described.

We do not know exactly what it is, but we have had a feeling that there was some sort of fixed gas in the selenium which was escaping, because that seemed to be the only place that we could not determine and prove with any degree of certainty. I hoped Mr. Schloen was going to have something more definite on that phase of it.

D. L. OGDEN.—I might enlarge a little on Mr. Aldrich's statement. We used practically the same method that Mr. Schloen described. We were using an American Meter Company's dry meter, and had to dry the gas before sending it through the meter. We found that we obtained more selenium in the sulphuric acid than we did in the filter medium. This led us to believe that there was some gas, hydrogen selenide, or something of that sort, that was going through the entire system and being picked up by the sulphuric acid. We had no way of determining it, since if we put two bottles of sulphuric acid in the train, we would get selenium in both bottles, so it has always been our opinion that the losses on

the Cottrell were rather large, and we were never definitely able to pin them down. We know that there is a certain vapor tension of selenium dioxide in air and that this is increased by the quantity of water vapor in the air. Mr. Bauman at that time was working at the plant and did considerable work on it, in connection with volatilizing selenium dioxide and actually determining the vapor tension in the gas after collecting whatever selenium dioxide could be collected, but in spite of that we feel that there is some gas carrying selenium that is not collectible by the ordinary methods.

E. W. ROUSE, JR.—I wonder whether there is any question of very high recoveries at one place and relatively lower recoveries at some place else. There may be a question of assays of the incoming materials.

J. H. SCHLOEN.—All incoming material, every piece of material we receive, that contains selenium, either blister or anodes, is sampled 100 per cent. We do not use percentage sampling. On blister we use a half template; on anodes, a quarter template. We have our splitting limits on selenium assays. Our assays agree within the splitting limits. What more can anyone want?

E. W. ROUSE, JR.—As a shipper I would be very happy to have a 95 per cent recovery. It might depend on whether you are buying or selling.

J. H. SCHLOEN.—You can look over the figures, but I believe that the reason for our high recovery is definitely the type of scrubber employed, plus the fact that we eliminate the large portion of our selenium during the first step in our flowsheet. We have tried the rain plates on scrubber and there was a lot of trouble. We had losses, yes, when we started up; we did not have a well equipped scrubber and we did not have any Cottrell. It took very nearly two years to solve the problem until the Cottrell was built. Now, regardless of whether our losses on the attacks are 50 per cent, or even 75 per cent out (and we do agree on the material assays as it is shipped in), we account for everything every year. I do not see where the argument lies.

* U. S. Metals Refining Company.

E. W. ROUSE, JR.—I would like to ask a further question. The waste selenium is selenate selenium?

J. H. SCHLOEN.—Yes.

E. W. ROUSE, JR.—Are any special means taken to be sure that the selenium in your later slags is selenite and not selenate?

J. H. SCHLOEN.—No.

E. W. ROUSE, JR.—They just happen to be good.

J. H. SCHLOEN.—No, not that. We do not use niter until we have practically all the

selenium out of our matte in the doré furnace. You could possibly remove all selenium from matte by using soda and air but you cannot do it within a reasonable time. By adding niter you get a much faster reaction, but you get some selenate selenium which is not reduced by SO_2 in sulphuric acid solution later on. Blowing with soda does not produce sodium selenate. If you precipitate selenium from a hydrochloric acid solution, you can recover selenate selenium. But since we precipitate, using a straight sulphuric acid solution, we keep the niter out of doré furnace as long as we can.

INDEX

(NOTE: In this index the names of authors of papers and discussions and of men referred to are printed in SMALL CAPITALS, and the titles of papers in *italics*.)

A

- Age-hardening: aluminum-silver alloys. *See* Aluminum-silver.
- discontinuous precipitation, 201
- effects resulting from formation of both a precipitate phase and a superlattice: 14-carat gold alloys, 94
- mechanism of precipitation: brief bibliography, 222
- solid solution: brief bibliography, 200
- theory, 220, 224
- typical aging sequence, 199
- ALDRICH, C. H.: *Discussion on Recovery of Selenium and Tellurium*, 374
- Aluminum: formation of parts by powder metallurgy: cold-welding in die prevented by lubrication, 153
- elemental powder mixtures, 157
- production of powder: processes, 152
- powders most suitable, 154
- Aluminum alloys: formation by powder metallurgy. *See* Aluminum.
- Aluminum-magnesium alloys: solid solutions: mechanism of precipitation, 201, 210
- X-ray diffraction studies, 201, 210
- Aluminum-silicon alloys: aluminum-rich solid solution: precipitation of silicon: rate: dilatometric measurements, 166
- Aluminum-silver alloys: solid solution: aging: typical sequence, 199
- X-ray diffraction studies, 182
- Aluminum-zinc alloys: solid solutions: mechanism of precipitation, 201, 203
- X-ray diffraction studies, 201, 203
- American Brass Co.: study of effect of antimony on some properties of 70-30 brass, 127
- study of hardness changes accompanying the ordering of beta brass, 144
- American Smelting and Refining Co.: study of effect of certain fifth-period elements on some properties of high-purity copper, 103
- American Zinc Co. of Illinois: new electrolytic zinc plant, 298
- ANDERSEN, A. G. H. AND KINGSBURY, A. W.: *Phase Diagram of the Copper-iron-silicon System from 90 to 100 Per Cent Copper*, 38
- Anode furnace: refining of high-nickel blister copper, 336
- Antimony: amounts present in fired small-arms cartridge cases, 127

- Antimony: effect on properties of 70-30 brass, 127
- effect on some properties of high-purity copper, 105, 117

B

- BAINS, T. M. JR.: *Discussions: on Embrittlement of Silver by Oxygen*, 276
- Metallurgy of Fillet Wiped Soldered Joints*, 296
- BAKARIAN, P. W. AND MATHEWSON, C. H.: *Slip and Twinning in Magnesium Single Crystals at Elevated Temperatures*, 226; discussion, 254
- Baker and Co.: time-to-fracture tests on platinum, 10 per cent iridium-platinum and 10 per cent rhodium-platinum alloys, 286
- BALDWIN, W. M. JR.: *Discussion on Hardness Changes Accompanying the Ordering of Beta Brass*, 148
- BARRETT, C. S.: *Discussions: on Hardness and Lattice Stress in Solid Solutions*, 91
- on Hardness Changes Accompanying the Ordering of Beta Brass*, 150
- on Mechanism of Precipitation from Solid Solutions*, 225
- BARRETT, C. S., GEISLER, A. H. AND MEHL, R. F.: *Aging in the Solid Solution of Silver in Aluminum*, 182
- Mechanism of Precipitation from Solid Solutions of Zinc in Aluminum, Magnesium in Aluminum and of Some Magnesium-base Alloys*, 201
- BAUMAN, G.: *Discussion on Recovery of Selenium and Tellurium*, 372
- BECK, P. A.: *Discussion on Effect of Certain Fifth-period Elements on Some Properties of High-purity Copper*, 117
- Bell Telephone Laboratories: fillet wiped soldered joints, 291
- BENARD, F.: *An Investigation into Anode-furnace Refining of High-nickel Blister Copper*, 336
- Recovery of Selenium and Tellurium at Copper Cliff, Ontario*, 341
- BIER, C. J.: *Discussions: on Embrittlement of Silver by Oxygen and Hydrogen*, 275
- on Formation of Aluminum and Aluminum Alloys by Powder Metallurgy*, 164, 165
- BOUTON, G. M. AND SCHUMACHER, E. E.: *Discussion on Constitution of Lead-rich Lead-antimony Alloys*, 71
- BOUTON, G. M., SCHUMACHER, E. E. AND PHIPPS, G. S.: *The Metallurgy of Fillet Wiped Soldered Joints*, 291; discussion, 296, 297

- Brass: alpha: single crystal: internal friction: attributed to inhomogeneities, 122
 beta: definition, 144
 hardness changes accompanying ordering, 144
 70-30: effect of scrap composed of fired small-arms cartridge cases, 127
 properties: effect of antimony, 127
- BRICK, R. M.: *Discussions: on Constitution of the Iron-rich Iron-nickel-silicon Alloys at 600°C.*, 63
on Hardness Changes Accompanying the Ordering of Beta Brass, 148
- BUSK, R. S.: *Discussion on Mechanism of Precipitation from Solid Solutions*, 223
- C
- Cable splicing: objections to lead burning, 297
- Cadmium: effect on some properties of high-purity copper, 109, 117
- Canadian Copper Refiners Ltd.: recovery of precious metals and production of selenium and tellurium at Montreal East, 350
- Carnegie Institute of Technology: study of aging in solid solution of silver in aluminum, 182
 study of constitution of lead-rich lead-antimony alloys, 65
 study of mechanism of precipitation from solid solutions, 201
 study of rate of precipitation of silicon from solid solution of silicon in aluminum, 166
- CARTER, F. E.: *Discussions: on Hardening Effects Resulting from the Formation of Both a Precipitate Phase and a Superlattice*, 101
on Hardness and Lattice Stress in Solid Solutions, 90
- Cartridge cases: fired: amounts of antimony present, 127
 effect when used as scrap in manufacturing brass, 127
- CAUM, J. W. AND FRYE, J. H. JR.: *The Hardness of Certain Primary Copper Solid Solutions*, 75
- CAUM, J. W., FRYE, J. H. JR. AND TRECO, R. M.: *Hardness and Lattice Stress in Solid Solutions*, 83
- CENTER, A. A.: *Discussion on New Electrolytic Zinc Plant of American Zinc Company of Illinois*, 302
- CHRISTIE, J. L.: *Discussions: on Embrittlement of Silver by Oxygen and Hydrogen*, 273
on Hardness Changes Accompanying the Ordering of Beta Brass, 150
- CLARK, C. W. AND SCHLOEN, J. H.: *Recovery of Precious Metals and Production of Selenium and Tellurium at Montreal East*, 350
- CLAYTON, C. Y. AND HANLEY, H. R.: *Adherence of Electrodeposited Zinc to Aluminum Cathodes*, 328
- Columbia University: study of constitution of iron-rich iron-nickel-silicon alloys at 600°C., 48
- Copper: blister: high-nickel: elimination of nickel in anode furnace, 336
 refining in anode furnace, 336
 high-purity: properties: effect of antimony, 105, 117
 Copper: high-purity: properties: effect of cadmium, 109, 117
 effect of some fifth-period elements, 103
 effect of certain fifth-period elements: brief bibliography, 116
 effect of silver, 103
 effect of tellurium, 113, 117
 effect of tin, 111
 Copper alloys: primary substitutional solid solutions of zinc, gallium, germanium, and arsenic: hardness, 75
 Copper Cliff. See Ontario Refining Co.
 Copper-iron-silicon alloys: copper 90-100 per cent: phase diagram, 38
 Copper refining: high-nickel blister: anode-furnace treatment, 336
 selenium recovery, 341, 350
 silver recovery, 350
 tellurium recovery, 341, 350
 Copper-zinc alloys: solid solution: relation between hardness and lattice stress: zinc replaced by gallium, germanium or arsenic, 83
- CORDIANO, J. J. and CREMER, G. D.: *Recent Developments in the Formation of Aluminum and Aluminum Alloys by Powder Metallurgy*, 152; discussion, 163, 164, 165
- CREMER, G. D. AND CORDIANO, J. J.: *Recent Developments in the Formation of Aluminum and Aluminum Alloys by Powder Metallurgy*, 152; discussion, 163, 164, 165
- CROOK, W. J.: *Preliminary Spectrographic and Metallographic Study of Native Gold*, 255
- Crystals, magnesium: single: preparation, 228
 slip and twinning at elevated temperatures, 226
 tensile-test specimens: preparation, 230
- Crystals, metallic: internal friction: attributed to inhomogeneities, 122
 slip and twinning: brief bibliography, 253
 tensile-test specimens: preparation of highly polished bars, 230
- D
- DAVIDSON, L. P.: *New Electrolytic Zinc Plant of the American Zinc Company of Illinois*, 298
- Dilatometer: optical-mechanical type: for studies of precipitation from solid solution, 169
- E
- EASH, J. T.: *Discussion on Hardening Effects Resulting from the Formation of Both a Precipitate Phase and a Superlattice*, 100
- EDMUNDS, G.: *Discussions: on Constitution of Lead-rich Lead-antimony Alloys*, 73
on Hardness and Lattice Stress in Solid Solutions, 91
on Slip and Twinning in Magnesium Single Crystals at Elevated Temperatures, 254
- Electrolytic zinc: adherence to aluminum cathodes: causes, 328
 plant of American Zinc Co. of Illinois, 298
- Electron microscope: metallurgical applications, 22
 replicas for observation: formvar process, 24
 polystyrene-silica method, 24
 silver-collision process, 23

- Electron microscope: replicas for observation: types, 24
scanning method, 28
- Electrothermic process: direct production of metallic zinc, St. Joseph Lead Co.: condenser, 319
electrical system, 317
furnace, 317
operation, 320
zinc recovery, 323, 326
- Engineering Foundation: project 77: study of internal friction of an alpha-brass crystal, 122
- F
- Fifth-period elements: effect on some properties of high-purity copper, 103
- FREEMAN, J. R. JR.: *Discussion on Effect of Antimony on Some Properties of 70-30 Brass*, 138
- FRYE, J. H. JR.: *Discussion on Effect of Certain Fifth-period Elements on Some Properties of High-purity Copper*, 120
- FRYE, J. H. JR. AND CAUM, J. W.: *The Hardness of Certain Primary Copper Solid Solutions*, 75
- FRYE, J. H. JR., CAUM, J. W. AND TRECO, R. M.: *Hardness and Lattice Stress in Solid Solutions*, 83; discussion, 90, 91, 92
- G
- GEISLER, A. H., BARRETT, C. S. AND MEHL, R. F.: *Aging in the Solid Solution of Silver in Aluminum*, 182
Mechanism of Precipitation from Solid Solutions of Zinc in Aluminum, Magnesium in Aluminum, and of Some Magnesium-base Alloys, 201; discussion, 223, 224
- General Electric Co.: study of embrittlement of silver by oxygen and hydrogen, 269
- Gold: native: spectrographic and metallographic study, 255
- Gold alloys: 14-carat. *See* Gold-silver-copper.
- Gold-silver-copper alloys: age-hardening: effects resulting from formation of both a precipitate phase and a superlattice, 94
cooling rate: relation to age-hardening, 94
14-carat: age-hardening: relation to rate of cooling, 94
- GONSER, B. W.: *Discussion on Metallurgy of Fillet Wiped Soldered Joints*, 296, 297
- GREINER, E. S. AND JETTE, E. R.: *Constitution of the Iron-rich Iron-nickel-silicon Alloys at 600°C.*, 48; discussion, 63
- H
- HALL, A. M.: *Sulphides in Nickel and Nickel Alloys*, 278; discussion, 285
Discussion on Metallurgy of Fillet Wiped Soldered Joints, 296
- HALLIWELL, G. P.: *Discussion on Hardness Changes Accompanying the Ordering of Beta Brass*, 150
- HANAWALT, J. D.: *Discussions: on Mechanism of Precipitation from Solid Solutions*, 224
on Slip and Twinning in Magnesium Single Crystals at Elevated Temperatures, 254
- HANLEY, H. R. AND CLAYTON, C. Y.: *Adherence of Electrodeposited Zinc to Aluminum Cathodes*, 328
- Hardness of metals: measurements: Meyer analysis: advantages, 76, 93
disadvantages, 93
solid solutions. *See* Solid Solutions.
variables affecting: ionic overlap, 83
- HARDY, C.: *Discussion on Formation of Aluminum and Aluminum Alloys by Powder Metallurgy*, 164
- Hardy Metallurgical Co.: formation of aluminum and aluminum alloys by powder metallurgy, 152
- HARKER, D.: *Discussion on Hardness Changes Accompanying the Ordering of Beta Brass*, 150
- Homer, C. E. and Plummer, H.: technique for locating solidus curves, 65
- HOYT, S. L.: *Discussion on Hardness and Lattice Stress in Solid Solutions*, 92
- HULL, D. R., SILLIMAN, H. F. AND PALMER, E. W.: *Effect of Antimony on Some Properties of 70-30 Brass*, 127; discussion, 140, 141
- HUNSICKER, H. Y.: *Discussion on Rate of Precipitation of Silicon from the Solid Solution of Silicon in Aluminum*, 181
- I
- Inconel: sulphide content: distinguishing, 278
- INGALLS, W. R.: *Discussion on Direct Production of Metallic Zinc by the Electrothermic Process*, 325
- International Nickel Co.: study of sulphides in nickel and nickel alloys, 278
- Iron-nickel-silicon alloys: iron-rich: constitution at 600°C., 48
- J
- JETTE, E. R. AND GREINER, E. S.: *Constitution of the Iron-rich Iron-nickel-silicon Alloys at 600°C.*, 48; discussion, 63
- JETTER, L. K. AND MEHL, R. F.: *Rate of Precipitation of Silicon from the Solid Solution of Silicon in Aluminum*, 166; discussion, 181
- JILLSON, D. C.: *Discussion on Embrittlement of Silver by Oxygen and Hydrogen*, 276
- K
- KEMP, J. T.: *Discussion on Effect of Antimony on Some Properties of 70-30 Brass*, 137
- KEMPF, L. W.: *Discussions: on Formation of Aluminum and Aluminum Alloys by Powder Metallurgy*, 163
on Mechanism of Precipitation from Solid Solutions, 224
- KIMBERLY, J. L.: *Discussion on Effect of Antimony on Some Properties of 70-30 Brass*, 140
- KINGSBURY, A. W. AND ANDERSEN, A. G. H.: *Phase Diagram of the Copper-iron-silicon System from 90 to 100 Per Cent Copper*, 38

L

- Lead-antimony alloys: lead-rich: constitution: improved apparatus for determining, 65
redetermination of solidus and eutectic temperatures by observation of temperature at which rupture occurs when a slightly loaded specimen is slowly heated, 65
- Lehigh University: study of hardness and lattice stress in solid solutions, 83
study of hardness of certain primary copper solid solutions, 75
- LEPSOE, R.: *Discussion on Direct Production of Metallic Zinc by the Electrothermic Process*, 326
- LONG, C. C. AND WEATON, G. F.: *Direct Production of Metallic Zinc, Electrothermic Process*, 316; *discussion*, 327

M

- Magnesium: high-purity: plastic deformation, 201
- Magnesium crystals. *See* Crystals.
- Magnesium-lead alloys: solid solutions: mechanism of precipitation, 201, 215
X-ray diffraction studies, 201, 215
- Magnesium-tin alloys: solid solutions: mechanism of precipitation, 201, 215
X-ray diffraction studies, 201, 215
- MARSHALL, G. D.: *Discussions on Embrittlement of Silver by Oxygen and Hydrogen*, 275
on Sulphides in Nickel and Nickel Alloys, 285
- MARSLAND, C. R.: *Discussion on Embrittlement of Silver by Oxygen and Hydrogen*, 275
- MARTIN, D. L. AND PARKER, E. R.: *Embrittlement of Silver by Oxygen and Hydrogen*, 269; *discussion*, 274 et seq.
- MATHEWSON, C. H. AND BAKARIAN, P. W.: *Slip and Twinning in Magnesium Single Crystals at Elevated Temperatures*, 226; *discussion*, 254
- MEHL, R. F.: *Discussion on Hardness and Lattice Stress in Solid Solutions*, 89, 90
- MEHL, R. F. AND JETTER, L. K.: *Role of Precipitation of Silicon from the Solid Solution of Silicon in Aluminum*, 166
- MEHL, R. F., GEISLER, A. H. AND BARRETT, C. S.: *Aging in the Solid Solution of Silver in Aluminum*, 182
Mechanism of Precipitation from Solid Solutions of Zinc in Aluminum, Magnesium in Aluminum and of Some Magnesium-base Alloys, 201
- MERRIMAN, T. C.: *Discussion on Effect of Antimony on Some Properties of 70-30 Brass*, 140
- Meyer analysis: hardness measurements: advantages, 76, 93
disadvantages, 92
- Monel metal: sulphide content: distinguishing, 278
- Montreal East. *See* Canadian Copper Refiners.
- MUDGE, W. A.: *Discussion on Embrittlement of Silver by Oxygen and Hydrogen*, 274

N

- New Jersey Zinc Co.: research on relative rates of reactions involved in reduction of zinc ores, 303

- Nickel: sulphide content: distinguishing, 278
- NORTON, J. T.: *Discussion on Hardness and Lattice Stress in Solid Solutions*, 90

O

- OGDEN, D. L.: *Discussion on Recovery of Selenium and Tellurium*, 372, 374
- Ontario Refining Co.: anode-furnace refining of high-nickel blister copper, 336
recovery of selenium and tellurium, 341

P

- PALMER, E. W., HULL, H. F. AND SILLIMAN, H. F.: *Effect of Antimony on Some Properties of 70-30 Brass*, 127
- PARKER, E. R. AND MARTIN, D. L.: *Embrittlement of Silver by Oxygen and Hydrogen*, 269; *discussion*, 274 et seq.
- Parker Pen Co.: investigation of hardening effects resulting from formation of both a precipitate phase and a superlattice in 14-carat alloys, 94
- PELLINI, W. S. AND RHINES, F. N.: *Constitution of Lead-rich Lead-antimony Alloys*, 65
- Phelps Dodge Corporation: phase diagram of the copper-iron-silicon system from 90 to 100 per cent copper, 38
- PHIPPS, G. S., SCHUMACHER, E. E. AND BOUTON, G. M.: *The Metallurgy of Fillet Wiped Soldered Joints*, 291
- PICKUS, I. W. AND PICKUS, M. R.: *Hardening Effects Resulting from the Formation of Both a Precipitate Phase and a Superlattice*, 94; *discussion*, 102
- Platinum: time-to-fracture tests, 286
- Platinum-iridium alloys: 10 per cent iridium: time-to-fracture tests, 286
- Platinum-rhodium alloys: 10 per cent rhodium: time-to-fracture tests, 286
- Plummer, H. *See* Homer, C. E.
- P. M. G. alloys. *See* Copper-iron-silicon Alloys.
- POST, C. B.: *Discussion on Sulphides in Nickel and Nickel Alloys*, 284, 285
- Powder metallurgy: formation of aluminum and aluminum alloys. *See* Aluminum.
- Precipitation-hardening. *See* Age-hardening.
- PRICE, W. B.: *Discussion on Effect of Antimony on Some Properties of 70-30 Brass*, 141

Q

- QUADT, R. A.: *Discussion on Formation of Aluminum and Aluminum Alloys by Powder Metallurgy*, 163

R

- RALSTON, O. C.: *Discussion on Relative Rates of Reactions Involved in Reduction of Zinc Ores*, 315
- RCA Laboratories: applications of the electron microscope in metallurgy, 13
- REIS, A.: *Discussion on Formation of Aluminum and Aluminum Alloys by Powder Metallurgy*, 162

- RHINES, F. N.: *Discussion on Sulphides in Nickel and Nickel Alloys*, 285
- RHINES, F. N. AND PELLINI, W. S.: *Constitution of Lead-rich Lead-antimony Alloys*, 65; *discussion*, 73
- ROUSE, E. W. JR.: *Discussion on Recovery of Selenium and Tellurium*, 372 et seq.

S

- St. Joseph Lead Co. of Pennsylvania: direct production of metallic zinc by the electrothermic process, 316
- SCHLOEN, J. H. AND CLARK, C. W.: *Recovery of Precious Metals and Production of Selenium and Tellurium at Montreal East*, 350; *discussion*, 372 et seq.
- SCHUMACHER, E. E. AND BOUTON, G. M.: *Discussion on Constitution of Lead-rich Lead-antimony Alloys*, 71
- SCHUMACHER, E. E., BOUTON, G. M. AND PHIPPS, G. S.: *The Metallurgy of Fillet Wiped Soldered Joints*, 291
- SEELIG, R. P.: *Discussion on Formation of Aluminum and Aluminum Alloys by Powder Metallurgy*, 164
- Selenium: recovery: at Copper Cliff refinery, 341
at Montreal East, 363, 372
- SHEPARD, H. M.: *Discussion on Recovery of Selenium and Tellurium*, 372
- Silicon. *See* Aluminum-silicon.
- SILLIMAN, H. F., HULL, D. R. AND PALMER, E. W.: *Effect of Antimony on Some Properties of 70-30 Brass*, 127
- Silver: effect on some properties of high-purity copper, 103
embrittlement by oxygen and hydrogen, 269
- Silver-cadmium alloys: solid solution: relation between hardness and lattice stress: cadmium replaced by indium, tin or antimony, 83
- Silver refining: Montreal East, 350
selenium recovery at Copper Cliff, 341
Montreal East, 363, 372
tellurium recovery at Copper Cliff, 341
Montreal East, 368
- SMART, J. S. JR.: *Discussion on Embrittlement of Silver by Oxygen and Hydrogen*, 275
- SMART, J. S. JR. AND SMITH, A. A. JR.: *Effect of Certain Fifth-period Elements on Some Properties of High-purity Copper*, 103; *discussion*, 120
- SMITH, A. A. JR. AND SMART, J. S. JR.: *Effect of Certain Fifth-period Elements on Some Properties of High-purity Copper*, 103; *discussion*, 120
- SMITH, C. S.: *Hardness Changes Accompanying the Ordering of Beta Brass*, 144; *discussion*, 151
Discussion on Effect of Certain Fifth-period Elements on Some Properties of High-purity Copper, 119
- SNYDER, C. J.: *Discussion on Metallurgy of Fillet Wiped Soldered Joints*, 297
- Solder: tin-free: satisfactory for some uses, 297
wiping: arsenic content, 296

- Solder: wiping: composition, 296
silver no special benefit, 296
tin necessary, 296
WPB limitations, 296
- Soldered joints: fillet wiped: metallurgy, 291
method of wiping, 294
saving of tin, 291
- Solid solutions: aluminum-magnesium alloys. *See* Aluminum-magnesium.
- aluminum-zinc alloys. *See* Aluminum-zinc.
- copper. *See* Copper Alloys.
- hardness: and lattice stress: relation, 83
reasons for, 83, 89
variables affecting: ionic overlap, 83
lattice stress and hardness: relation, 83
magnesium-base alloys. *See* Magnesium-lead and Magnesium-tin.
- precipitation from: brief bibliography, 180
primary substitutional: zinc, gallium, germanium and arsenic in copper: hardness, 75
silicon in aluminum. *See* Aluminum-silicon.
- silver. *See* Silver Alloys.
- Stanford University: preliminary spectrographic and metallographic study of native gold, 255
- STAUSS, H. E.: *Time-to-fracture Tests on Platinum, 10 Per Cent Iridium-platinum and 10 Per Cent Rhodium-platinum Alloys*, 286
- STEINITZ, R.: *Discussion on Formation of Aluminum and Aluminum Alloys by Powder Metallurgy*, 163
- Sulphur: compounds associated with nickel and high-nickel alloys: distinguishing, 278
- SWARTZ, C. E.: *Discussion on Metallurgy of Fillet Wiped Soldered Joints*, 297

T

- Tellurium: effect on some properties of high-purity copper, 113, 117
recovery: at Copper Cliff refinery, 341
at Montreal East, 368
- Tin: effect on some properties of high-purity copper, 111
- TRECO, R. M., FRYE, J. H. JR. AND CAUM, J. W.: *Hardness and Lattice Stress in Solid Solutions*, 83
- TRUESDALE, E. C. AND WARING, R. K.: *Relative Rates of Reactions Involved in Reduction of Zinc Ores*, 303

V

- VINES, R.: *Discussions: on Embrittlement of Silver by Oxygen and Hydrogen*, 275
on Hardening Effects Resulting from the Formation of Both a Precipitate Phase and a Superlattice, 101

W

- WALTERS, F. M.: *Discussion on Constitution of the Iron-rich Iron-nickel-silicon Alloys at 600°C.*, 63

WARING, R. K. AND TRUESDALE, E. C.: *Relative Rates of Reactions Involved in Reduction of Zinc Ores*, 303

WEATON, G. F. AND LONG, C. C.: *Direct Production of Metallic Zinc by the Electrothermic Process*, 316; *discussion*, 327

WILKES, D. P.: *Discussion on Recovery of Selenium and Tellurium*, 372

WILSON, F. H.: *Discussion on Embrittlement of Silver by Oxygen and Hydrogen*, 276

WOOD, M. L.: *Discussion on Effect of Antimony on Some Properties of 70-30 Brass*, 138

Y

Yale University: study of slip and twinning in magnesium single crystals at elevated temperatures, 226

Z

ZENER, C.: *Internal Friction of an Alpha-brass Crystal*, 122

Zinc: metal: direct production. *See* Electrothermic Process.

Zinc ores: reduction: relative rates of reactions, 303

ZWORYKIN, V. K.: *Applications of the Electron Microscope in Metallurgy*, 13

Iron and Steel

VOLUME 154, TRANSACTIONS A.I.M.E., 1943

CONTENTS

Howe Memorial Lecture

The Development of Research and Quality Control in the Modern Steel Plant. By LEO F. REIN-ARTZ. (*Metals Technology*, April 1943)

Blast Furnace and Raw Materials

Essential Considerations in the Design of Blast Furnaces. By A. L. FOELL. (*Metals Technology*, December 1942)

Results Obtained from Surveys of Gas at Furnace Tops. By JAMES M. STAPLETON. (*Metals Technology*, January 1943)

Physical Aspects of the Dust Catcher, Gas Washer and Precipitator on No. 3 Furnace at Carrie. By C. P. CLINGERMAN and C. J. FLEISCH. (*Metals Technology*, January 1943)

Slag Control by Introduction of Flux through Blast-furnace Tuyeres. By CARL G. HOGBERG (*Metals Technology*, January 1943)

The Electrical Conductivity of Molten Blast-furnace Slags. By A. E. MARTIN and GERHARD DERGE. (*Metals Technology*, August 1943)

Some Physical Characteristics of By-product Coke for Blast Furnaces. By CHARLES C. RUSSELL and MICHAEL PERCH. (*Metals Technology*, December 1942)

Pyrometry at the Coke Oven. By ROBERT B. SOSMAN. (*Metals Technology*, December 1942)

Calcination Rates and Sizing of Blast-furnace Flux. By T. L. JOSEPH, H. M. BEATTY and GUST BITSIANES. (*Metals Technology*, December 1942)

The Low-temperature Gaseous Reduction of a Magnetite. By M. C. UDY and C. H. LORIG. (*Metals Technology*, October 1942)

Steelmaking

Problems of Total Operation in Steelmaking. By WILLIAM C. MARSHALL and FRANK G. NORRIS. (*Metals Technology*, April 1943)

Silicon-oxygen Equilibria in Liquid Iron, By C. A. ZAPFFE and C. E. SIMS. (*Metals Technology*, September 1942)

Equilibria of Liquid Iron and Simple Basic and Acid Slags in a Rotating Induction Furnace. By C. R. TAYLOR and JOHN CHIPMAN. (*Metals Technology*, September 1942)

Rapid Analysis of Oxygen in Molten Iron and Steel. By GERHARD DERGE. (*Metals Technology*, January 1943)

Silver Chloride as a Medium for Study of Ingot Structures. By KARL L. FETTERS and MARGARET DIENES. (*Metals Technology*, August 1943)

The Origin, Definition and Prevention of Scabs. By T. J. WOODS. (*Metals Technology*, Sept. 1943)

The Cause of Bleeding in Ferrous Castings. By C. A. ZAPFFE. (*Metals Technology*, October 1942)

Constitution and Thermal Treatment

Quantitative Determination of Retained Austenite by X-rays. By FRANK S. GARDNER, MORRIS COHEN and DARA P. ANTIA. (*Metals Technology*, February 1943)

Effect of Inhomogeneity in Austenite on the Rate of the Austenite-pearlite Reaction in Plain Carbon Steels. By GEORGE A. ROBERTS and ROBERT F. MEHL. (*Metals Technology*, June 1943)

A Micrographic Study of the Cleavage of Hydrogenized Ferrite. By CARL A. ZAPFFE and GEORGE A. MOORE. (*Metals Technology*, February 1943)

Constitution of the Iron-rich Iron-nickel-silicon Alloys at 600°C. By EARL S. GREINER and ERIC R. JETTE. Abstract. (*Metals Technology*, April 1943 and Volume 152)

Carbides in Low Chromium-molybdenum Steels. By WALTER CRAFTS and C. M. OFFENHAUER. (*Metals Technology*, February 1943)

Properties

Effects of Tin on the Properties of Plain Carbon Steel. By J. W. HALLEY. (*Metals Technology*, September 1942)

The Effect of Silicon on Hardenability. By WALTER CRAFTS and JOHN L. LAMONT. (*Metals Technology*, January 1943)

Calculated Hardenability and Weldability of Carbon and Low-alloy Steels. By C. E. JACKSON and G. G. LUTHER. (*Metals Technology*, October 1942)

Effects of Eight Complex Deoxidizers on Some 0.40 Per Cent Carbon Forging Steels. (By G. F. COMSTOCK, Vol. 150.) Discussion by Walter Crafts.

Calculation of the Tensile Strength of Normalized Steels from Chemical Composition. By F. M. WALTERS, JR. (*Metals Technology*, October 1942)

Chromizing of Steel. By IRVIN R. KRAMER and ROBERT H. HAFNER. (*Metals Technology*, October 1942)

True Stress-strain Relations at High Temperatures by the Two-load Method. By C. W. MACGREGOR and L. E. WELCH. (*Metals Technology*, September 1942)

